Université de Montréal

Design, Synthesis, Pericyclic Chemistry and Biomedical Applications of Azopeptides

By

Mr. Ramesh Maruthi Chingle

Département de Chimie

Université de Montréal

Thesis presented to Faculté des études supérieures et postdoctorales to obtain

Doctor of Philosophy (Ph. D.) in Chemistry

February 2018

Université de Montréal

Faculté des études supérieures et postdoctorales

This Thesis entitled:

Design, Synthesis, Pericyclic Chemistry and Biomedical Applications of Azopeptides

Presented by:

Mr. Ramesh Maruti Chingle

Thesis was evaluated by a jury composed of the following persons:

Prof. Shawn Collins, President of jury

Prof. Yvan Guindon, Member of jury

Prof. André Charette, Member of jury

Prof. William D. Lubell, Research director

Prof. Scott Miller, External examiner

Prof. David London, Representative of the Dean

Résumé

Les azapeptides sont des peptidomimétiques dans lesquels le carbone alpha d'un ou plusieurs acides aminés a été remplacé par un atome d'azote. L'objectif principal de cette étude doctorale a été de développer une nouvelle méthodologie de synthèse d'azapeptides, par l'utilisation d'azopeptides, qui sont des analogues azodicarbonylés possédant une fonction imino-urée. L'oxydation des résidus d'aza-glycine s'est avérée efficace pour l'obtention d'azopeptides, qui ont ensuite été utilisés pour effectuer des réaction péricycliques et examinés par cristallographie aux rayons X. Les réactions de Diels-Alder et d'Alder-ene sur les azopeptides ont respectivement permis d'accéder aux résidus aza-pipécolyle et aza-allylglycinyle contraints. L'analyse aux rayons X d'un azopeptide à l'état solide a fourni un aperçu de la configuration de l'imino-urée (Chapitre 2). En employant les produits, issues de la chimie des azopeptides, comme analogues contraints de la valine, des mimes de la séquence Ala-Val-Pro-Ile de la seconde protéine activatrice de caspases des mitochondries (Smac) ont été synthétisés et leur capacité à induire l'apoptose dans les cellules mammaires cancéreuses a été démontré (Chapitre 3).

Dans le but de poursuivre le développement des méthodes pour synthétiser des azopeptides une approche en phase solide a été conçue sur résine Rink Amide et pourrais être utiliser pour générer des chimiothèques de composés en utilisant la chimie combinatoire. Cette étude a été ciblée sur la synthèse d'analogues azapeptides des opioïdes morphiceptine et endomorphine ainsi que le peptide de libération de l'hormone de croissance (GHRP-6, H-His-D-Trp-Ala-Trp-D-Phe-Lys-NH_2) se liant aux récepteur du cluster de différenciation 36 (CD36). Les premiers peptides ont été examinés en raison de leur importance en tant qu'agonistes sélectifs des sous-types de récepteurs opioïdes ayant le potentiel de développer de nouveaux analgésiques. Le dernier exemple d'analogue avait pour but de poursuivre le développement de modulateurs sélectifs de CD36 ayant un potentiel thérapeutique pour le traitement de maladies comprenant une inflammation entraînée par les macrophages, y compris la dégénérescence maculaire liée à l'âge et l'athérosclérose. Douze aza-opioïdes ont été synthétisés en remplaçant la proline à la position deux des ligands peptidiques respectifs par différents résidus d'aza-pipécolate. De même, cinq analogues d'aza-pipécolyle GHRP6

ont été synthétisés en utilisant la méthode en phase solide pour remplacer respectivement les résidus Ala^3 et Trp^4 (chapitre 4). Les aza-opioïdes ont été examiné comme inhibiteur des contractions induites électriquement sur l'iléon de cobaye et du canal déférent de souris, et les analogues aza-GHRP-6 pour leurs capacités à diminuer la surproduction d'oxyde nitrique induite par CD36 après traitement avec l'agoniste lipopeptide fibroblastes des récepteurs, tous deux ont démontré l'utilité de la méthodologie de l'aza-pipécolate pour étudier l'influence de la conformation sur l'activité et la sélectivité des peptides.

Les nouvelles méthodologies de synthèse des azopeptides en solution et sur support solide décrites dans cette thèse sont conçues pour permettre leur utilisation dans des études de relations structure-activité avec différents peptides biologiquement actifs. A cet égard, des azopeptides ont été utilisés dans ces recherches pour fabriquer des ligands des facteurs inhibiteurs du mélanocyte-1 (MIF-1), Smac, opioïde et du récepteur CD36. Considérant l'efficacité des méthodes de synthèse et les applications potentielles des azopeptides, les résultats de cette thèse offrent un fort potentiel pour l'avancement de la science des peptides dans le contexte de la chimie médicinale et de la biologie chimique.

Mots-clés: Azapeptides, peptidomimétique, tour β, semicarbazone, aza-valine, semicarbazide, azopeptide, aza-Diels Alder, Alder-ene, péricyclique, GHRP-6, récepteur GHS-R1a, récepteur CD36.

Abstract

The azapeptides are peptide mimics in which the alpha carbon of one or more amino acids has been replaced with a nitrogen atom. The primary goal of this doctorate study was to develop a new method for the synthesis of azapeptides by the application of azopeptides, which are azodicarbonyl analogs that possess an imino urea component. Oxidation of aza-glycine residues proved effective for making azopeptides, which were employed in pericyclic chemistry and examined by X-ray crystallography. Diels−Alder cyclization and Alder−ene reactions on azopeptides enabled respectively access to constrained aza-pipecolyl and aza-allylglycinyl residues. X-ray analysis of an azopeptide in the solid state provided insight into imino urea configuration (Chapter 2). Employing the products from azopeptide chemistry as constrained valine analogs, mimics of the Ala-Val-Pro-Ile sequence from the second mitochondria derived activator of caspases (Smac) protein were synthesized and demonstrated ability to induce apoptosis in breast cancer cells (Chapter 3).

Following the development of a method to synthesize azopeptides in solution, a solid-phase approach was conceived to prepare azopeptides on Rink amide resin and may be amenable to combinatorial chemistry for library generation. This study was targeted on the synthesis of aza-analogs of the opioid peptides morphiceptin and endomorphins as well as the Cluster of Differentiation 36 receptor (CD36) ligand Growth Hormone Releasing Peptide-6 (GHRP-6, His-D-Trp-Ala-Trp-D-Phe-Lys-NH_2). The former were examined due to their importance as opioid receptor subtype selective agonists with potential for developing novel analgesics. The latter was targeted in pursuit of selective CD36 modulators with therapeutic potential for treating diseases featuring macrophage-driven inflammation including age-related macular degeneration and atherosclerosis. Twelve aza-opioids were synthesized by replacing proline at the two position of the respective peptide ligands with different aza-pipecolate residues. Similarly, five aza-pipecolyl GHRP-6 analogs were synthesized using the solid-phase method to replace respectively the Ala^3 and Trp^4 residues (Chapter 4). Examination of the aza-opioids for inhibitory potency on electrically induced contractions of the guinea pig ileum and mouse vas deferens, and the aza-GHRP-6 analogs for capacity to diminish CD36-mediated overproduction of nitric oxide in macrophage cells

after treatment with the Toll-like receptor-2-agonist fibroblast-stimulating lipopeptide, both demonstrated the utility of the aza-pipecolate methodology for studying the influence of conformation on peptide activity and selectivity.

The novel methods for the synthesis of azopeptides in solution and on solid support described in this thesis are designed to enable their use in studies of structure-activity relationships with different biologically active peptides. In this respect, azopeptides have been applied in this research to make ligands of the melanocyte-inhibiting factor-1 (MIF-1), Smac, opioid and CD36 receptors. Considering the effectiveness of the synthetic methods and the potential applications of azopeptides, the findings of this thesis offer strong potential for the advancement of peptide science in the context of medicinal chemistry and chemical biology.

Keywords : Azapeptides, peptide mimicry, β-turn, semicarbazone, aza-valine, semicarbazide, azopeptide, aza-Diels Alder, Alder-ene, pericyclic, GHRP-6, CD36, receptor.

Note

This thesis describes my research on the synthesis, pericyclic chemistry and biomedical applications of azopeptides. The thesis has been written employing published articles. I specify herein my contributions to each of the chapters. The introduction (Chapter 1), and unless specified otherwise below, the following chapters, all were written by myself and edited by Professor William D. Lubell. Parts of the introduction were inspired by an Accounts of Chemical Research publication that I wrote together with Professors Caroline Proulx and Lubell.

The article in chapter 2 entitled "Azopeptides: Synthesis and Pericyclic Chemistry" describes my original syntheses, isolation and characterization of the first azopeptides by oxidation of aza-glycine analogs, and their pericyclic chemistry in Diels-Alder cyclization and Alder-ene reactions to provide respectively constrained aza-pipecolyl and aza-allylglycine analogs. In addition to their characterization by NMR spectroscopy, I obtained crystals of one azopeptide and two azapeptide analogs that were characterized by X-ray analyses that were performed by Ms. Francine Bélanger at the regional centre for X-ray crystallography of the Université de Montréal.

The article in chapter 3 entitled "Application of Constrained aza-Valine Analogs for Smac Mimicry" and the Proceeding of the 24th American Peptide Symposium entitled "Peptide Coupling Challenges to Aza-Pipecolyl Smac Mimetic" describe my original syntheses, isolation and characterization of aza-pipecolyl, aza-methanopipecolyl and aza-cyclohexylglycinyl analogs of the Smac tetra-peptide Ala-Val-Pro-Ile. The biological examination of these Smac analogs on MCF-7 breast cancer cells was performed in the Department of Pharmacology, Universite de Montreal by Ms. Sara Ratni under the supervision of Professor Audrey Claing, who wrote the description of the biological experiments.

The manuscript in Chapter 4 entitled "Identification of Active Peptide Conformations by Application of aza-Pipecolyl Residue Insertion Using Solid-Phase Azopeptide Diels-Alder Chemistry" presents the solid-supported synthesis of peptides bearing aza-pipecolyl

residues for studies of two biologically relevant targets. Azopeptide construction and Diels-Alder chemistry using a solid-phase synthesis strategy introduced aza-pipecolyl residues into opioid and cluster of differentiation 36 receptor (CD36) ligands. The idea of introducing aza-pipecolyl residues into opioid ligands was conceived in collaboration with Professor Steven Ballet at the Research Group of Organic Chemistry, Vrije Universiteit Brussel, Brussels, Belgium. Twelve aza-pipecolyl opioid analogs were synthesized by me and tested for biological activity in the lab of Professor Peter W. Schiller by his students Nga N. Chung and Thi M.-D Nguyen at the laboratory of Chemical Biology and Peptide Research, Clinical Research Institute of Montreal, Canada. Five aza-pipecolyl GHRP-6 analogs were examined by Dr. Mukandila Mulumba under the supervision of Professor Huy Ong at the Faculté de Pharmacie Université de Montréal, Canada. In its present form, the manuscript and chapter were written by me employing texts from earlier publications in which the biological studies were previously described, and the documents were subsequently edited by Professor Lubell.

In Chapter 5, I have written the conclusion and perspectives of this thesis.

Table of Contents:

Contents

Article 4

Chingle, R.; Mulumba, M.; Chung, N. N.; Nguyen, T. M.-D.; Ong, H.; Ballet, S.; Schiller, P. W.; Lubell, W. D. "Active Peptide Conformer Identification by aza-Pipecolyl Residue Insertion with Solid-Phase Azopeptide Diels-Alder Chemistry" *In Preperation*, **2018**.

List of Figures

List of Schemes

List of Tables

List of abbreviations

[α]	Specific rotation in (deg * mL / g * dm)
Aid	*N*-aminoimidazolidin-2-one
AMD	Age-related macular degeneration
Boc	*tert*-butoxycarbonyl
BSA	Bovine serum albumin
Bt	Benzotriazole
BTC	bis-(trichloromethyl)carbonate
°C	Degree Celsius
Cbz	Benzyloxycarbonyl
CD36	Cluster of differentiation 36
COSY	Correlation spectroscopy
d	Doublet
DABCO	1,4-diazabicyclo[2.2.2]octane
DAN	2,3-diaminonaphthalene
DCM	Dichloromethane
DEAD	Diethyl azodicarboxylate
deg	Degree
DIC	*N*,*N*-Diisopropylcarbodiimide
DEA	Diethylamine
DIEA	*N*,*N*-Diisopropylethylamine
DMF	*N*,*N*-Dimethylformamide
DMSO	Dimethyl sulfoxide
Dmt	2,6-dimethyltyrosine
DOP	Delta opioid
DSC	*N*,*N*′-disuccinimidyl carbonate
ESI	Electrospray ionization
Et	Ethyl
eq	Equivalent
FA	Formic acid

FESP	Faculté des études supérieures et postdoctorales
Fmoc	Fluorenylmethyloxycarbonyl
FSL	Fibroblast-stimulating lipopeptide
GHRP-6	Growth hormone releasing peptide 6
GnRH	Gonadotropin-releasing hormone
GPI	Guinea pig ileum
h	Hours
HAV	Hepatitis A virus
Hmb	Hydroxy-4-methoxybenzyl
HMBC	Heteronuclear Multiple Bond Correlation
[^{3}H]NPA	Tritiated *N*-propylnorapomorphine
HPLC	High performance liquid chromatography
HRMS	High resolution mass spectrometry
HRV	Human rhinovirus
IAP	Inhibitors of apoptosis proteins
iPr	iso-Propyl
IR	Infrared
J	Coupling constant (in NMR)
L	Liter
LCMS	Liquid chromatography mass spectrometry
m	Multiplet (in NMR)
Me	Methyl
MEM	Minimum Essential medium
MIF-1	Melanocyte-inhibiting factor-1
MHz	Megahertz (in NMR)
MOP	mu opioid
mp	Melting point
MVD	Mouse vas deferens
NBS	*N*-bromosuccinimide
NMR	Nuclear magnetic resonance
NO	Nitric oxide

Pin1	Protein interacting with Never in Mitosis A
Pip	Pipecolic acid
ppm	Parts per million (in NMR)
PyBOP	Benzotriazol-1-yloxytripyrrolidinophosphonium hexafluorophosphate
R_f	Retention factor (in chromatography)
RP	Reverse phase
RT	Retention time
rt	Room temperature
s	Singlet (in NMR)
SAR	Structure−activity relationship
SFC	Super critical fluid chromatography
SMAC	Second mitochondria-derive activator of caspase
SPSS	Solid Phase peptide synthesis
t	Triplet (in NMR)
TFA	Trifluoracetic acid
THF	Tetrahydrofuran
TLC	Thin layer chromatography
TLR-2	Toll-like receptor-2
TRH	Thyrotropin-releasing hormone

To my parents.

Acknowledgement

First and foremost, I would like to thank my research supervisor, Professor William D. Lubell, for having accepted me into his group in 2013 and for his support throughout my doctorate studies. Bill, I thank you sincerely for being a great mentor and always encouraging me to do my best and work at my full potential. Without your continuous support, I probably will not have completed this project. I also thank you for encouraging me to participate in the many conferences, where I was able to present my research work and interact with the academic and industrial community.

I would like to thank my thesis committee, Professor Shawn Collins and Professor Yvan Guindon for their encouragement and guidance. I would like to thank you both for being a part of my thesis committee and for being available to discuss research and for your support during my Ph.D.

I would like to thank former group members Dr. Stephen Turcotte, Dr. Jinqiang Zhang, Dr. Yésica Garcia-Ramos, Dr. Mariam Traoré, and Dr. Ngoc-Duc Doan for their support and for creating a dynamic friendly and supportive work environment in the Lubell group when I first arrived at UdeM. I would like to thank members both past and present with whom I have had the pleasure to work with during my studies. I also would like to thank Antoine Douchez for helping me write the French abstract.

I would like to thank Dr. Alexandra Fürtos, Karine Venne, Marie-Christine Tang and Simon Comtoi-Marotte and Louiza Mahrouche from the mass spectrometry center for HRMS and LCMS analyses, Pedro Aguiar, Sylvie Bilodeau, Antoine Hamel and Cédric Malveau for their help in the NMR analyses, and Françine Bélanger at the X-ray diffraction laboratory for her help in obtaining X-ray structures. I would also like to thank Professors André B. Charette and Stephen Hanessian groups for the occasional loan of chemicals.

I am very grateful to the scholarship awarded by the Ministry of Education, Québec for the exemption of out-of-country tuition fees and the Faculté des études supérieures et postdoctorales (FESP), for financial support during my graduate studies.

I thank my parents, “Aai” (Shanta Chingle) and “Baba” (Maruthi Chingle), my brothers, Krishna, Vishnu and Mahesh and my loving sister Anjana for their continuous support, encouragement and patience throughout my studies towards a doctorate degree.

Chapter 1: Introduction

1.1. Peptides and their mimics in drug discovery

Peptides and proteins play crucial roles in the transmission of information in biological systems. The first assembly of simple peptides by Emil Fischer and Theodor Curtius was achieved more than a century ago;[1] however, the preparation of oxytocin fifty years later by Du Vigneaud illuminated the potential of peptides as pharmaceuticals, as recognized by the Nobel Prize in Chemistry in 1955 for the synthesis and elucidation of the first peptide hormone.[2] Technical progress in the field of peptide synthesis has now rendered production of all sizes and complexity possible, with specific cases being scaled-up to metric ton levels. Among important developments, the solid-phase peptide synthesis (SPPS) method described by Merrifield in 1963 revolutionized the field by accelerating the procurement of analogs for research and discovery.[3] Moreover, with newer and more efficient expression, purification and protein analysis techniques, new classes of therapeutic molecules began to emerge in this century.[4] Among peptide analogs used as therapeutics, examples include insulin for diabetes,[5] Zoladex (goserelin) for the treatment of breast and prostate cancer,[6] octreotide for acromegaly and cancer,[7] bortezomib for multiple myeloma,[8] Avastin for colorectal cancer, and Herceptin for breast cancer, LCL-161 for aggressive solid tumors.[9]

Peptide mimicry entails the design, conception and study of molecules (so-called peptidomimetics) that can replicate the form and function of peptides.[10] Peptide mimics may retain desired activities such as high potency and low toxicity yet eliminate undesirable characteristics associated with natural peptide structures, such as rapid metabolism, lack of receptor selectivity, and poor bioavailability.[10a] Peptide mimics may also enhance ability to interact selectively with a specific receptor. Mimicry of natural peptide conformations is often used to improve stability, binding affinity, and receptor specificity. In recent years, numerous modifications of amino acid side chain and peptide backbone structures have proven promising for the development of peptide mimics with enhanced utility.[11]

Peptide secondary structures are defined by their backbone ϕ (phi), ψ (psi) and ω (omega) dihedral angles.[12] Side chain geometry is defined by χ (chi) space (Figure 1.1).[13] Among the common secondary structures, the α-helix, β-strand, and β-turns have received

significant attention in the design of peptidomimetics for studying chemical biology and medicinal chemistry.[9b,14]

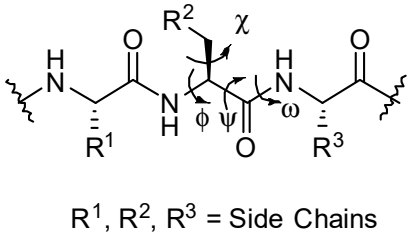

Figure 1.1. Representative peptide structure showing backbone ϕ, ψ and ω dihedral angles and side chain χ torsion angle.

1.2. Peptide β-turn conformations

The β-turn is the most common type of peptide turn and a well-studied motif in protein and peptide science.[15] The β-turn is the third most important secondary structure after helices and β-strands.[15] Implicated as a recognition site in many biological interactions,[16] the β-turn consists of four sequential residues, which are designated as *i*, *i* + 1, *i* + 2, and *i* + 3, and which change the direction of peptide chain by 180° positioning the α-carbons of the first and fourth residues at a distance ≤ 7Å and been historically classified according to the ϕ and ψ dihedral angles of the loop-region $\phi_{(i+1)}$, $\psi_{(i+1)}$ and $\phi_{(i+2)}$, $\psi_{(i+2)}$ (Figure 1.2).[15,17] Several types of β-turns have been defined based on their backbone torsion angles ϕ and ψ. A deviation of ± 30° is allowed for the three of the dihedral angles, whereas the fourth dihedral angle can deviate by ± 45°.[15b] Venkatachalam,[18] and later Hutchinson and Thornton[17b] defined nine types of β-turns, namely type I, I', II, II', VIa1,VIa2, VIb, VIII and IV β-folds (Table 1.1).[17-19] In certain turns, an internal ten-membered hydrogen bond may be formed between the carbonyl oxygen of the *i* and amide NH of the *i* + 3 residues.[15d,20] Such β-turns can initiate protein folding.[21] The type I and II and their corresponding mirror image types, I', II' β-turns have been considered to be most frequently observed in natural structures;[18] however, the type IV β-turn, which was previously considered a class of miscellaneous structures, has recently been shown to have conformers that represent about a third of all known β-turn residues.[19b] Brevern has classified type IV β-turns into sub-types denoted IV_1,

IV_2, IV_3 and IV_4, which collectively represent half of the type IV β-turns, and in many cases occur more frequently than certain classical types.[19b]

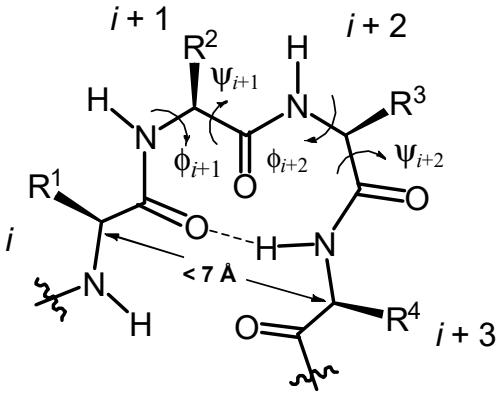

Figure 1.2. β-turn in peptide structure.[15,17]

Table 1.1. Ideal ϕ and ψ backbone torsional angles (in degrees) for type β-turns.[17-19]

Type of β-turns	ϕ_{i+1}	ψ_{i+1}	ϕ_{i+2}	ψ_{i+2}
I	−60	−30	−90	0
II	−60	120	80	0
VIII	−60	−30	−120	120
I’	60	30	90	0
II’	60	−120	−80	0
VIa1	−60	120	−90	0
VIa2	−120	120	−60	0
VIb	−135	135	−75	160
IV	−61	10	−53	−17

The type VI β-turn is a relatively rare secondary structure that features uniquely an amide cis isomer *N*-terminal to a proline residue situated at the *i* + 2 position of the peptide bond[15a,17a,22] Type VI *β*-turns are classified into two sub-types based on the dihedral angle values of their central *i* + 1 and *i* + 2 residues.[22] In the type VIa β-turn, proline *ψ*-dihedral angle is equal to 0° with a 10-membered intramolecular hydrogen bond exists between the carbonyl oxygen of the *i* residue and the amide hydrogen of the *i* + 3 residue. In the VIb β-

turn, the proline ψ-dihedral angle value is around 150° and no turn-stabilizing hydrogen bond is formed.[22]

Considerable effort has focused on mimicry of peptide backbone geometry, intramolecular hydrogen bonding, and side-chain orientations in secondary structures.[19a,23] Among such designs, the use of modified prolines has led to successful surrogates due in part to the pyrrolidine heterocycle,[20,22] which can restrict ϕ and ω dihedral angles to favor backbone geometry found in the central residues of β-turn conformations.[24] The local constraint induced by such backbone dihedral angle restrictions may have significant consequences on the conformation of the entire peptide. For example, proline residue that favor turn geometry can promote alignment of the amide bonds of distant amino acid residues in the peptide chain to form ordered hairpin and β-sheet conformations. Systematic replacement of each amino acid within a peptide sequence by proline, a "proline-scan", has thus been used to study the relevance of peptide backbone folding for molecular recognition.[25]

Constrained prolines (e.g., **1**) have been synthesized to study binding affinity and activity.[26] For example, sterically bulky 5-position substituents have been employed to favor prolyl *cis* isomer conformation.[26c,26f] Inspired by proline, other heterocycles have been used to restrict the geometry of single amino acid residues and dipeptides in efforts to nucleate peptide folding and replicate secondary structures,[27] such as β-turns,[28] β-sheets[29] and α-helices.[30] For example, "Freidinger" lactams (α-amino γ-lactams, **2**) have been used to constrain peptide ψ and ω dihedral angle geometry in studies to enhance biological activity through mimicry of biologically active turn conformers (Figure 1.3).[31] Bicyclic dipeptide mimics (**3**) that combine characteristics of proline and α-amino lactam structures,[23,32] as well as spirolactams (**4**),[33] and benzodiazepines (**5**),[34] all have similarly served as heterocycle motifs to control and mimic backbone folding.

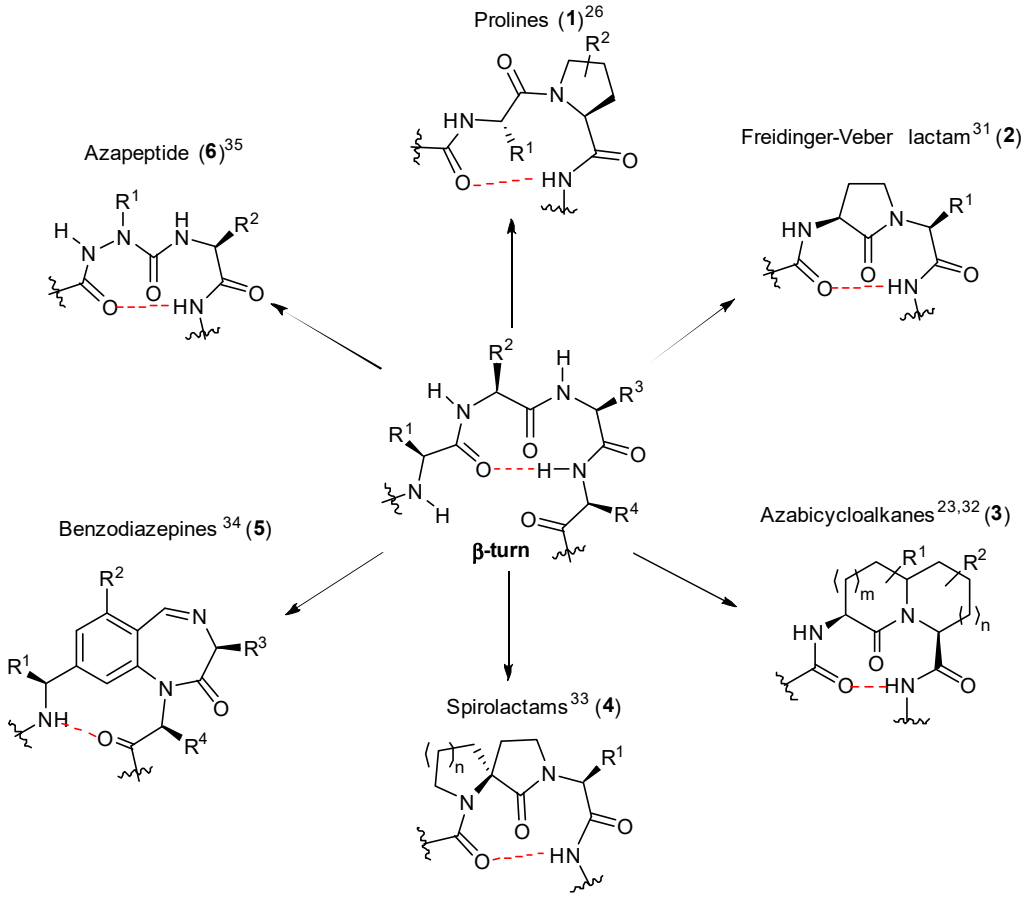

Figure 1.3. Electronic and covalent constraint to favor β-turn conformers.[23,26,31-35]

To improve peptide metabolic stability, attention has been also turned towards a development of a backbone modifications by replacement of the α-carbons of amino acid residues with nitrogen in so-called azapeptides (**6**).[35]

1.3. Azapeptides

Azapeptides are peptidomimetics in which the *α*-carbon of one or more amino acid residue is substituted by nitrogen (Figure 1.4).[35] Similar to heterocycle constraints, aza-residues can cause profound effects on the conformation of the peptide backbone. For example, the semicarbazide of an azapeptide can reinforce β-turn conformation through the combination of urea planarity and hydrazine nitrogen lone pair−lone pair repulsion,[36] as demonstrated by computational analysis,[37] X-ray crystallography,[38] and spectroscopy.[35b] Incorporation of aza-amino acids into peptides has been shown to favor type I, type II, and

type VI β-turn geometry in which the aza-residue is situated at the *i* + 1 or *i* + 2 position (Figure 1.5).[37,39]

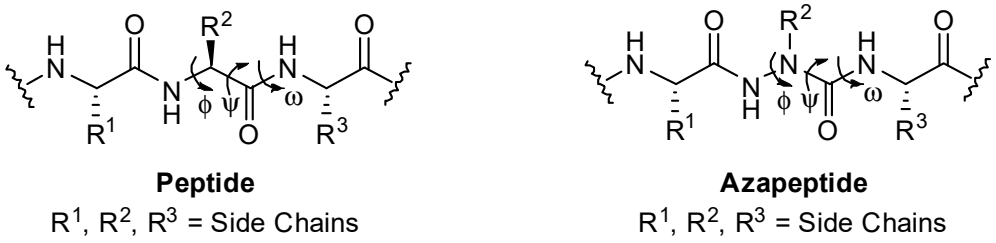

Figure 1.4. Comparison of peptide and azapeptide structure

Substitution of a semicarbazide for an amino amide residue in an azapeptide can also alter physical characteristics to improve metabolic stability without affecting the desired biological activity of the parent peptide.[40] Replacement of the amide by a urea in the azapeptide enhances stability against chemical and protease degradation and may prolong peptide activity.[41 ,42] For example, in spite lower potency, [azaVal^3]angiotensin-II (bovine) [**1.1**, H-Asp-Arg-azaVal-Tyr-Val-His-Pro-Phe-OH]

exhibited longer duration of action relative to the parent peptide (Figure 1.5).[43] Azapeptides possess thus interesting potential for peptide-based drug development.

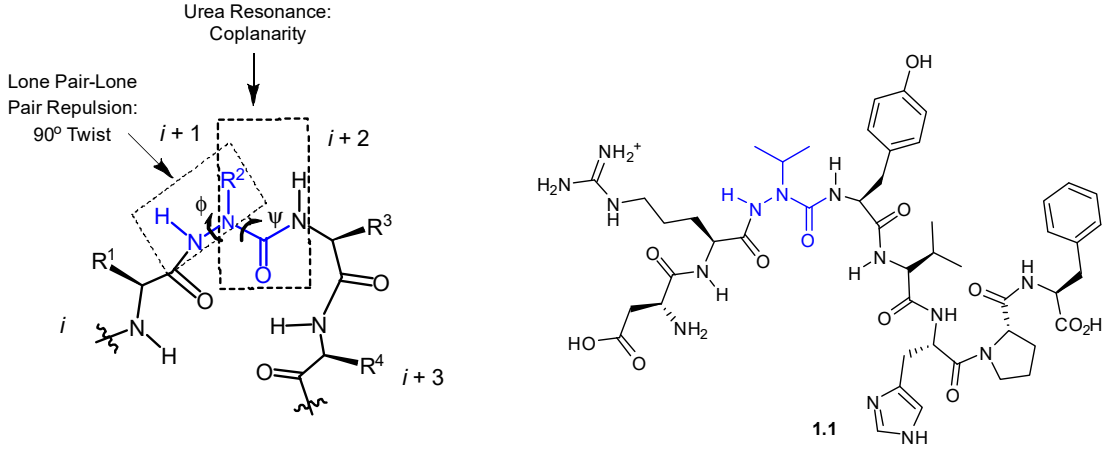

Figure 1.5. a) Schematic representation of a β-turn in an azapeptide structure;[35] (b) first biologically active azapeptide example: [azaVal^3] angiotensin-II (bovine) **1.1**.[43]

The therapeutic utility of the azapeptides was first demonstrated by FDA approval of the anti-cancer drug Goserelin, [D-Ser(*t*-Bu)^6, azaGly^{10}]-gonadotropin-releasing hormone (GnRH, **1.2**, Figure 1.6).[40,44] The aza-glycinamide analogue is a potent long-acting agonist of the GnRH receptor that is currently used in the clinic for the treatment of prostate and breast cancer.[40,44] In Goserelin, the aza-glycinamide residue has been shown to enhance metabolic stability, likely due to blocking degradation by C-terminal proteases.[40]

Moreover, azapeptides have found applications as receptor ligands, enzyme inhibitors, prodrugs, probes, and imaging agents. Although semicarbazide oligomers, "azatides", have been synthesized, they exhibited reduced receptor affinities in binding assays.[45,46] On the other hand, single C_α to N_α substitution at the P1 position of peptide substrates has enabled synthesis of serine and cysteine protease inhibitors,[12–14] and aza-residue scanning of peptide ligands has identified analogs with improved receptor binding affinity and selectivity.[35c]

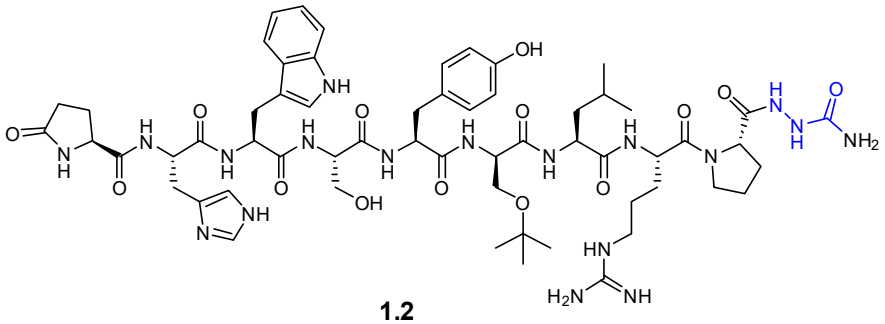

1.2

Figure 1.6. Chemical structure of Goserelin [D-Ser(*O*-*t*Bu)^6, azaGly^{10}]GnRH (Zoladex®, **1.2**). [6,40,44]

Numerous aza-analogues have been made to study and to improve the pharmacological properties of various biologically active peptides: oxytocin,[47] eledoisin,[48] enkephalin,[49] thyrotropin-releasing hormone (TRH),[50] and somatostatin.[35c,51] Interest to explore the effects of the semicarbazide on backbone folding and biological activity drives the synthesis and study of azapeptide receptor ligands and enzyme inhibitors. For the application of azapeptides in medicinal chemistry, however, synthetic methods must surmount the challenges of combining hydrazine and peptide chemistry.

1.3.1. Conformational analysis of azapeptides

Their distinctive properties make aza-amino acids attractive tools for stabilizing and studying particular secondary structures.[52] The diacyl hydrazine and urea components of the aza-amino acid residue combine to influence the backbone geometry of the azapeptide.[36a] The perpendicular orientation of the nitrogen electron lone pairs in the diacyl hydrazine has been studied in model systems.[36a] For example, high-level ab initio calculations were used to determine the minimum energy structures of *N*,*N*'-diformyl hydrazine (Figure 1.7). Among three prominent conformations, the most stable conformer rotated the dihedral angle about the hydrazine nitrogen to values between 90-101°, likely to minimize electronic repulsion (Figure 1.7). The calculations show that the global minimum is a nonplanar structure in which the nitrogen lone pairs are essentially perpendicular to one another. The second highest energy conformer rotated the dihedral angle to 180° due in part to favored intramolecular interactions between the N-H hydrogens and the carbonyl oxygens.[36a]

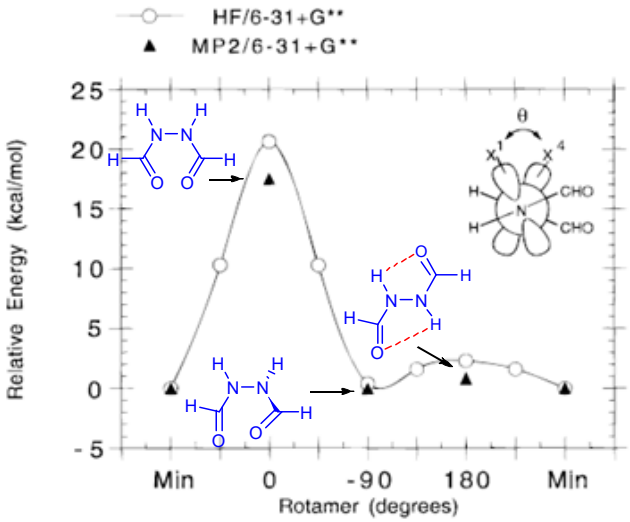

Figure 1.7. Calculated potential energy surface for rotation about the nitrogen-nitrogen bond in diformylhydrazine.[36a]

The diacyl hydrazine twist mentioned above combines with the planar urea to restrict the backbone torsion angles to 90° for ϕ, and 0° or 180° for ψ as predicted based on computational analyses, which have shown that the aza-residue is favored to adopt the central

i+1 and *i*+2 residues of type I and type II' β-turns.[52] X-ray crystallographic analysis and spectroscopic study of azapeptides have provided additional support for the turn geometry of the semicarbazide residue in azapeptides.[35a,35b] Furthermore, in chapter 2, the X-ray structure of aza-cyclohexadienylglycine peptide **1.3** demonstrated that the aza-residue adopted the *i*+1 position of a type I β-turn with an intramolecular 10-membered hydrogen bond between the carbamate carbonyl and benzhydrylamine NH which replaces the *i* and *i*+3 residues (Figure 1.8).[53]

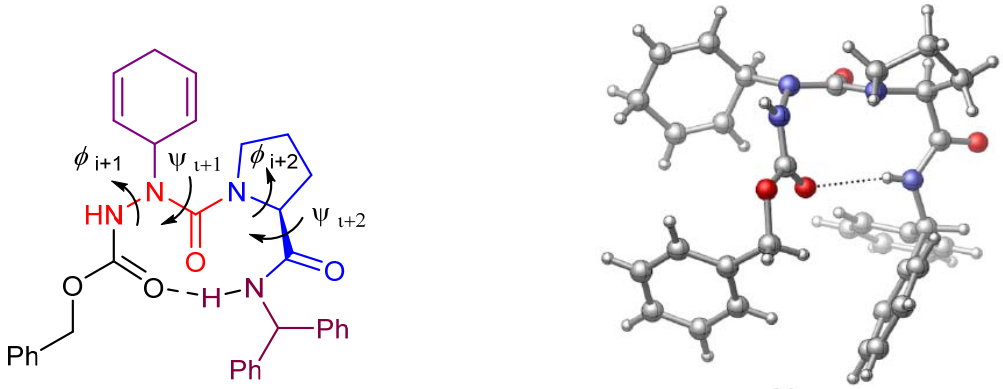

Ideal type I β-turn *i*+1 and *i*+2 residue ϕ and ψ dihedral angles: –60; –30; –90; 0

Aza-cyclohexyl glycyl peptide **1.3**: –61; –33; –79; –14

Figure 1.8. Molecular and crystal structures of aza-cyclohexyl glycine model peptide **1.3**. The intramolecular hydrogen bond is indicated by a broken line.[53]

1.3.2. Methods to synthesize azapeptides

A combination of hydrazine and peptide chemistry is necessary to synthesize an azapeptide (Figure 1.9). Hydrazine chemistry has the inherent challenge to differentiate the two nitrogens. The peptide chemistry to insert an aza-residue into a sequence must surmount issues of activation of the hydrazine for coupling to the growing chain and subsequent amino acylation of the semicarbazide residue which is known to be less nucleophilic that a natural amino amide. Once the aza-amino acid residue is inserted into the sequence, more conventional peptide chemistry can be used to elongate the sequence to obtain the final azapeptide.

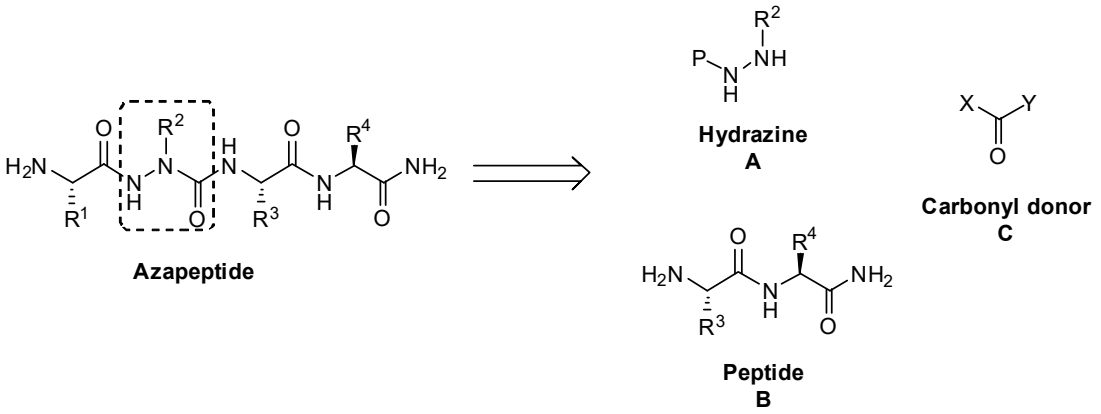

Figure 1.9. Retrosynthetic pathway for azapeptide synthesis.[35]

A variety of methods have been devised to introduce aza-amino acids into peptide analogues of varying length by solution- and solid-phase methods.[35,54] For example, aza-peptides have been prepared on solid support by conversion of the *N*-terminal amino group of the growing peptide chain **1.4** into isocyanate **1.6**,[55] or active carbamate **1.7**,[56] followed by nucleophilic attack with *N*'-alkyl carbazate **1.10** or hydrazide **1.11** (Figure 1.10). Chain termination by hydantoin formation plagues the method giving rise to impure product and reduced yield. Hydantoin **1.9** arises from intramolecular nucleophilic attack onto the activated intermediate by the secondary nitrogen of the preceding *C*-terminal amide (Strategy A, Figure 1.10). Reversible *N*-protection of the secondary amide may eliminate the side reaction. For example, *N*-2-hydroxy-4-methoxybenzyl (Hmb) protection has enabled preparation of hydantoin free aza-peptides with the inconvenience of two additional synthetic steps. [57,58]

In a second approach for azapeptide synthesis, activation and reaction of *N*'-alkyl carbazates with a phosgene equivalent provides an activated aza-amino acid equivalent **1.12** for coupling to the peptide on resin (Strategy B, Figure 1.10). For example, activation of *N′*-alkyl *N*-(Fmoc)hydrazines with phosgene in solution was used to scan several peptides by systematic amino acid replacement with aza- residues.[59] The aza-scan involves three steps: solution-phase synthesis of the *N′*-alkyl fluoren- 9-ylmethyl carbazate, *in situ* activation with phosgene in solution and coupling to peptide anchored on Rink amide resin. Removal of the

Fmoc protection and acylation of the resulting semicarbazide followed by elongation of the peptide chain delivers the final azapeptide.[54a]

Solution-phase synthetic routes for selective hydrazine functionalization have encumbered the preparation of *N*′-alkyl carbazate building blocks for azapeptide synthesis. Moreover, formation of oxadiazalone **1.13** is a troublesome side reaction during coupling of *N*-Fmoc-aza-amino acid chlorides. In the interest of performing structure−activity relationships (SARs) with a variety of aza-residues, and to avoid formation of oxadiazalones, a hydrazone/ semicarbazone protection strategy was explored.[60] Inspired by applications of Schiff-base amine protection for the modification of the α-carbon of glycine esters and dipeptides,[61] a so-called "submonomer" approach was developed in which an aza-glycine residue was first installed onto the peptide and then alkylated to add the side chain (Strategy C, Figure 1.10).[62] Activation of a hydrazone with a phosgene equivalent and coupling to the peptide chain installed a semicarbazone residue, which was *N*-alkylated, and then converted to the corresponding semicarbazide by orthogonal deprotection.[62a] Amino acylation of the resulting semicarbazide **1.15** and peptide elongation gave desired azapeptide **1.8**. A variety of side chains may be added onto the semicarbazone to construct diverse azapeptide libraries by solution and solid-phase chemistry.[58a,62a ,60a,63] In addition, semicarbazone protection of activated aza-glycine avoids oxadiazalone formation.[60a]

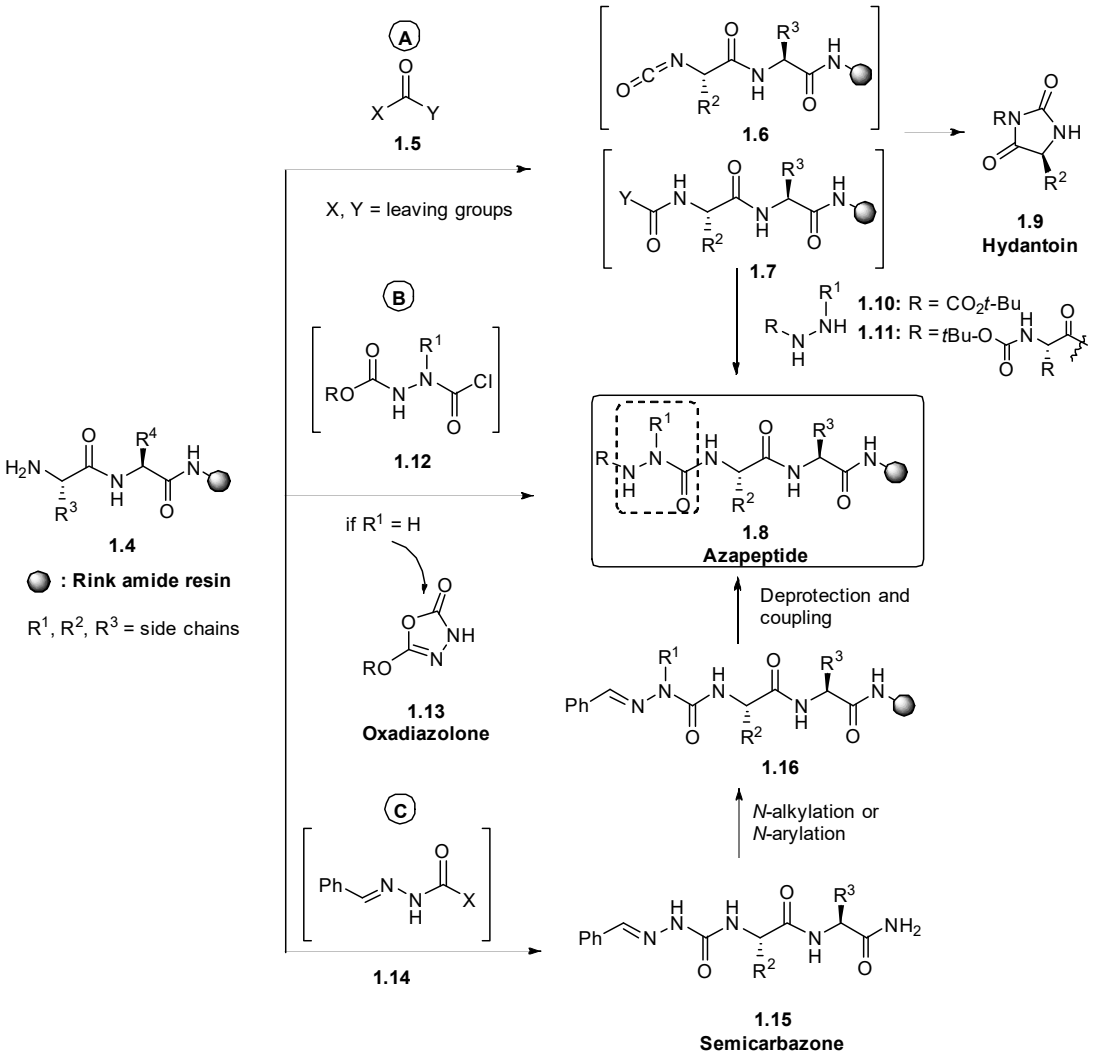

Figure 1.10. Possible pathways for azapeptide synthesis.[35]

1.4. Azopeptides

Azodicarboxylates, such as diethyl azodicarboxylate (DEAD), have many uses in organic chemistry,[64] serving as reagents in the Mitsunobu reaction,[65] electrophilic amination[66] and pericyclic processes, such as the Diels-Alder[67] and Alder-ene reactions.[67b,68] The related azodicarboxamides have been used as templates in the assembly of azo-functionalized rotaxanes,[69] reagents for diastereoselective amination of enolates,[66b] and components of cysteine proteinase inhibitors against enzymes of Hepatitis A virus (HAV) 3C and human rhinovirus (HRV) 3C.[70]

The rich chemistry of azodicarboxylate derivatives is inherent in their capacity to perform in radical, nucleophilic and electrophilic chemistry (Figure 1.11). For example, cycloadditions of azodicarboxylates with dienes were notably described by Diels to produce cycloaddition products (e.g., **1.17**).[67] Azodicarboxylate ene-reactions have given allyl hydrazine analogs (e.g., **1.18**).[71] Ene-hydrazines (e.g., **1.19**) have been prepared from azodicarboxylates, vinyl ketones and DABCO (1,4-diazabicyclo[2.2.2]octane) as a catalyst under Baylis–Hillman reaction conditions.[72] Radical mediated addition of relatively unreactive hydrocarbons to azodicarboxylates has been achieved using tetrabutylammonium decatungstate under irradiation with light to form *N*-alkyl hydrazines **1.20**.[73] Fluoroalkyl hydrazines **1.21** have been made by Lewis acid mediated reaction of azodicarboxylate with difluoroenolsilanes.[74] Moreover, 1,2,4-triazoles (e.g., **1.22**) have been synthesized using photo-redox catalysis to react 2*H*-azirines and azodicarboxylates (Figure 1.11).[75]

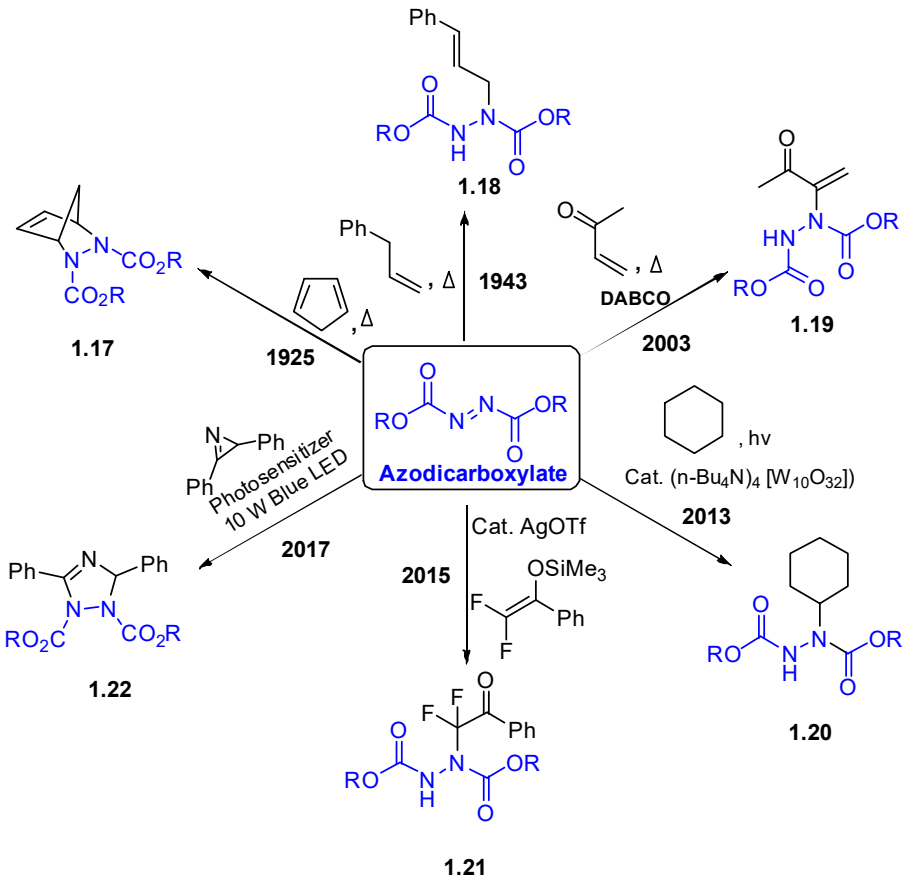

Figure 1.11. Azodicarboxylate reactivity with various substrate.[67,71-75]

Opening opportunity for pericyclic chemistry in a peptide framework, we have synthesized azopeptides **1.23** and explored their Diels−Alder and Alder−ene chemistry to synthesize aza-pipecolyl and aza-allylglycine residues (Chapter 2).[53] Notably, azapeptides bearing such cyclic and unsaturated residues offer utility for studying biologically important targets, because of their enhanced conformational rigidity and chemical reactivity, respectively.[76] Cyclic aza-amino acid synthesis is challenging requiring multiple step synthesis, due to issues to cyclize and differentiate the hydrazine nitrogen in the heterocycle prior to peptide coupling. The importance of proline and pipecolate in peptides and the conformational effects of their respective aza counterparts motivate development of effective methods to make azapeptides bearing such analogs.[76]

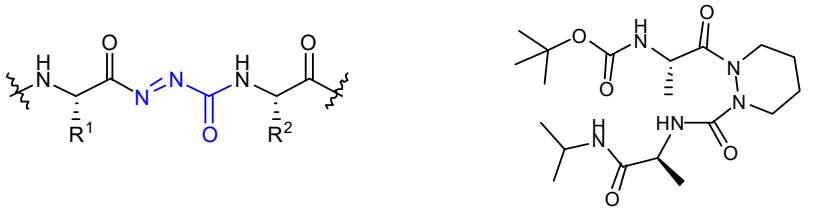

1.23
Azo-glycyl-peptide

1.24
Boc-Ala-AzaPip-Ala-NH *i*Pr

Figure 1.12. Representative azopeptide structure[53] and examples of azapeptides possessing cyclic aza-residues.[76a]

The substitution of nitrogen at the α-carbon of the pyrrolidine ring in proline to study biologically active peptides was pioneered by Dutta and Morley.[77] The resulting aza-proline was later shown to induce a type VI β-turn conformation featuring a *N*-terminal amide *cis*-isomer (e.g., **1.24**, Figure 1.12). Several azaPro peptides have been synthesized to study the importance of prolyl *cis*-amide bonds in different receptor ligands as well as to make enzyme inhibitors.[59,78] On the other hand, only a few applications of aza-pipecolate have been made to study peptide folding. In particular, the aza-tripeptide Boc-Ala-azaPip-Ala-NH*i*Pr (**1.24**, azaPip = aza-pipecolyl residue) was synthesized in seven steps using solution-phase chemistry employing benzyl *N*-Boc-aza-pipecolate, and demonstrated to adopt a type VI β-turn conformation by X-ray crystallographic analysis.[76a] Considering the challenges to make aza-pipecolyl peptides, their applications have been limited, and to the best of our knowledge, no examples of biologically active aza-Pip analogs have been reported.

1.5. Azopeptide synthesis, pericyclic chemistry and applications

Azopeptides are imino urea analogs. Chapter 2 of the thesis describes the first syntheses of azopeptides, and their pericyclic chemistry in Diels-Alder cyclizations and Alder-ene reactions in solution to provide respectively constrained aza-pipecolyl and aza-allylglycine residues.[53] Azopeptides were synthesized in solution by oxidation of *N*-Cbz- and Boc-aza-glycine residues. Aza-glycine peptides were prepared with minimal oxadiazole formation by activation of carbazates using DSC and coupling to amino and peptide esters in solution.[79] Diels-Alder cyclizations on azopeptides using various dienes was explored to provide Δ^4-aza-dehydropipecolates. Furthemore, Alder−ene chemistry with three different alkenes gave different α- and β-aza-allylglycine analogues. Finally, the conformations of select azopeptides and azapeptide products were assigned based on spectroscopic analyses and X-ray crystallographic studies.[53]

The utility of the solution-phase azopeptide methodology was first demonstrated by the synthesis of aza-pipecolyl analogues of melanocyte-stimulating hormone release inhibiting factor-1 (MIF-1, H-Pro-Leu-Gly-NH_2) as discussed in Chapter 2.[53] Subsequently, in Chapter 3, azopeptides were employed to make a series of conformationally constrained second mitochondria-derive activator of caspase (Smac) mimetics that exhibited promising apoptosis-inducing activity in breast cancer cells.[80] In particular, the pericyclic chemistry of azopeptides in solution was employed to prepare a set of constrained aza-valine analogs, which were introduced into the Smac mimetics by routes featuring the development of coupling conditions to acylate bulky and electron deficient semicarbazides.[80]

Finally, in Chapter 4, solid-phase azopeptide chemistry was developed featuring Diels-Alder reactions to insert aza-pipecolyl residues into two classes of biologically active peptide.[81] The mu selective opioid ligands morphiceptin and the endomorphins, and the cluster of differentiation 36 receptor (CD36) ligand growth hormone releasing peptide-6 (GHRP-6) were respectively examined using aza-pipecolic acid to explore the importance of prolyl amide *cis* isomers and turn conformers for receptor selectivity and activity. Seventeen aza-pipecolyl peptides were synthesized employing the solid-phase approach and examined

for biological activity to provide respectively insight for developing new antinociceptive and ant-inflammatory agents.[81]

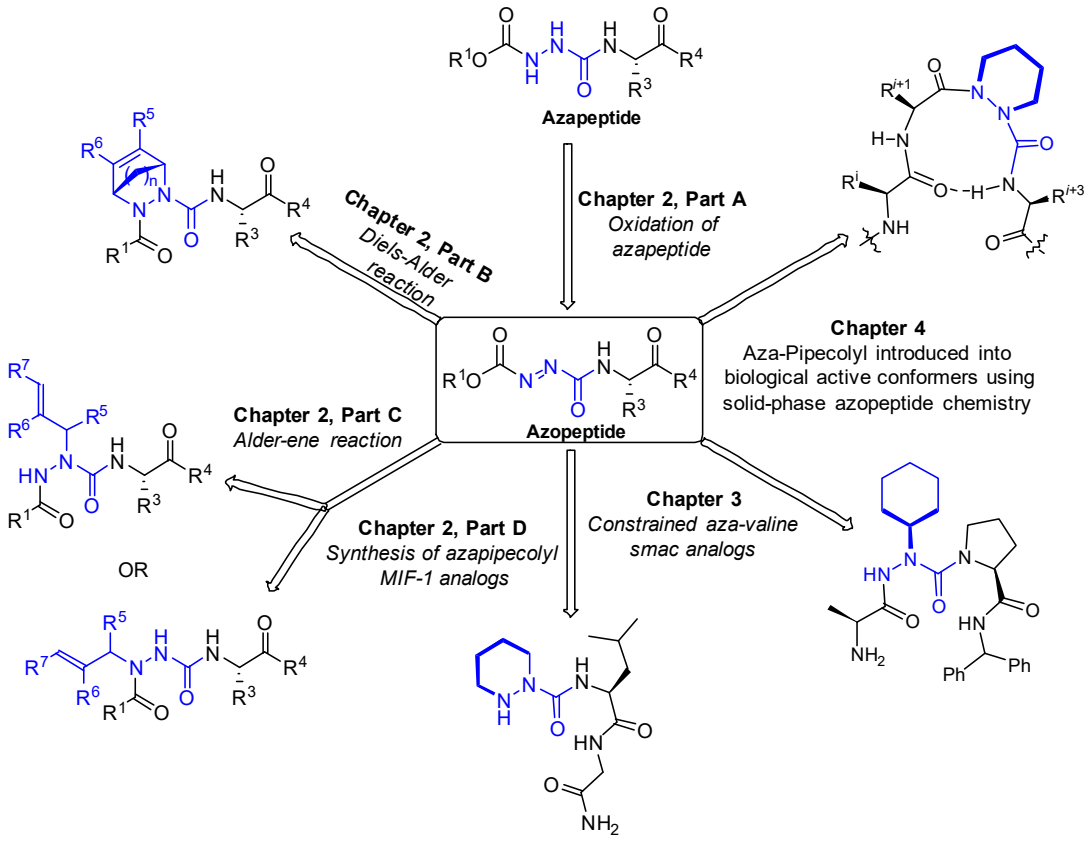

Figure 1.13. Schematic summary of chapters 2-6 of the thesis.

As concluded in Chapter 5, azopeptides have proven effective intermediates for making two classess of aza-amino acid residues to study a broad range of biological targets. Aza-pipecolic acid and aza-allylglycine residues were effectively introduced into peptides by Diels-Alder and Alder-ene chemistry on azopeptides using solid- and solution-phase chemistry to prepare four different types of biologically relevant ligands: MIF-1, Smac mimetics, opioids and GHRP-6 (Figure 1.13). Information gleaned from examination of the resulting azapeptide analogs has indicated the importance of backbone and side-chain conformational requirements for activity and receptor selectivity. In summary, this thesis has

advanced both the fundamental study of azodicarboxylates as well as the applied medicinal chemistry of azapeptides in studies of peptide chemical-biology.

References

(1) (a) Fisher, E.; Fourneau, E., Ueber einige derivate des glykokolls. *Ber. Dtsch. Chem. Ges* **1901**, *34*, 2868-2879. (b) Curtius, T., Ueber einige neue der Hippursäure analog constituirte, synthetisch dargestellte Amidosäuren. *J. Prakt. Chemie.* **1882**, *26*, 145-208.

(2) du Vigneaud, V.; Ressler, C.; Swan, J. M.; Roberts, C. W.; Katsoyannis, P. G., The synthesis of oxytocin1. *J. Am. Chem. Soc.* **1954**, *76*, 3115-3121.

(3) Merrifield, R. B., Solid phase peptide synthesis. I. The synthesis of a tetrapeptide. *J. Am. Chem. Soc.* **1963**, *85*, 2149-2154.

(4) Craik, D. J.; Fairlie, D. P.; Liras, S.; Price, D., The future of peptide-based drugs. *Chem. Biol. Drug Des.* **2013**, *81*, 136-147.

(5) Wang, F.; Carabino, J. M.; Vergara, C. M., Insulin glargine: a systematic review of a long-acting insulin analogue. *Clinical therapeutics* **2003**, *25*, 1541-1577.

(6) Miller, R.; Frank, R., Zoladex®(goserelin) in the treatment of benign gynaecological disorders: an overview of safety and efficacy. *BJOG: An Int. J. Obstetrics & Gynaecology* **1992**, *99*, 37-41.

(7) Arnold, R.; Neuhaus, C.; Benning, R.; Schwerk, W. B.; Trautmann, M. E.; Joseph, K.; Bruns, C., Somatostatin analog sandostatin and inhibition of tumor growth in patients with metastatic endocrine gastroenteropancreatic tumors. *World journal of surgery* **1993**, *17*, 511-519.

(8) Adams, J.; Kauffman, M., Development of the proteasome inhibitor Velcade™(Bortezomib). *Cancer Invest.* **2004**, *22*, 304-311.

(9) (a) Chen, K.-F.; Lin, J.-P.; Shiau, C.-W.; Tai, W.-T.; Liu, C.-Y.; Yu, H.-C.; Chen, P.-J.; Cheng, A.-L., Inhibition of Bcl-2 improves effect of LCL161, a SMAC mimetic, in hepatocellular carcinoma cells. *Biochem. Pharmacol.* **2012**, *84*, 268-277. (b) Chingle, R.; Mohammadpour, F.; Douchez, A.; Geranurimi, A.; Possi, K. C.; Lubell, W. D., Peptides in drug discovery. *Chimica Oggi/Chemistry Today (Pharma Horizon-Focus on Therapeutic Oligos and Peptides)* **2017**, *12*, 24-28.

(10) (a) Marshall, G. R., A hierarchical approach to peptidomimetic design. *Tetrahedron* **1993**, *49*, 3547-3558. (b) Ko, E.; Liu, J.; Burgess, K., Minimalist and universal peptidomimetics. *Chem. Soc. Rev.* **2011**, *40*, 4411-4421.

(11) Gante, J., Peptidomimetics—tailored enzyme inhibitors. *Angew. Chem. Int. Ed.* **1994**, *33*, 1699-1720.

(12) Ramachandran, G. N.; Ramakrishnan, C.; Sasisekharan, V., Stereochemistry of polypeptide chain configurations. *J. Mol. Bio.* **1963**, *7*, 95-99.

(13) Rizo, J.; Gierasch, L. M., Constrained peptides: models of bioactive peptides and protein substructures. *Ann. Rev. Biochem.* **1992**, *61*, 387-416.

(14) (a) Hirschmann, R., Medicinal chemistry in the golden age of biology: lessons from steroid and peptide research. *Angew. Chem., Int. Ed.* **1991**, *30*, 1278-1301. (b) Fosgerau, K.; Hoffmann, T., Peptide therapeutics: current status and future directions. *Drug discovery today* **2015**, *20*, 122-128.

(15) (a) Rose, G. D.; Glerasch, L. M.; Smith, J. A.: Turns in peptides and proteins. In *Adv. Protein Chem.*; Elsevier, 1985; Vol. 37; pp 1-109. (b) Richardson, J. S.: The anatomy and taxonomy of protein structure. In *Adv. Protein chem.*; Elsevier, 1981; Vol. 34; pp 167-339. (c) Wilmot, C.; Thornton, J., β-Turns and their distortions: a proposed new nomenclature. *Protein Eng., Design and Selection* **1990**, *3*, 479-493. (d) Lewis, P. N.; Momany, F. A.; Scheraga, H. A., Chain reversals in proteins. *Biochimica et Biophysica Acta (BBA)-Protein Structure* **1973**, *303*, 211-229.

(16) (a) Marshall, G. R., Three-dimensional structure of peptide—protein complexes: implications for recognition. *Curr. Opinion in Str. Biol.* **1992**, *2*, 904-919. (b) Marshall, G. R., Peptide interactions with G-protein coupled receptors. *Biopolymers* **2001**, *60*, 246-277.

(17) (a) Wilmot, C.; Thornton, J., Analysis and prediction of the different types of β-turn in proteins. *J. Mol. Bio.* **1988**, *203*, 221-232. (b) Hutchinson, E. G.; Thornton, J. M., A revised set of potentials for beta-turn formation in proteins. *Protein Sci* **1994**, *3*, 2207-2216.

(18) Venkatachalam, C. M., Stereochemical criteria for polypeptides and proteins. V. Conformation of a system of three linked peptide units. *Biopolymers* **1968**, *6*, 1425-1436.

(19) (a) Gillespie, P.; Cicariello, J.; Olson, G. L., Conformational analysis of dipeptide mimetics. *Peptide Science* **1997**, *43*, 191-217. (b) De Brevern, A. G., Extension of the classical classification of β-turns. *Scientific reports* **2016**, *6*, 33191.

(20) Venkatachalam, C., Stereochemical criteria for polypeptides and proteins. V. Conformation of a system of three linked peptide units. *Biopolymers* **1968**, *6*, 1425-1436.

(21) (a) Marcelino, A. M. C.; Gierasch, L. M., Roles of β-turns in protein folding: From peptide models to protein engineering. *Biopolymers* **2008**, *89*, 380-391. (b) Fischer, G., Peptidyl-prolyl cis/trans isomerases and their effectors. *Angew. Chem., Int. Ed.* **1994**, *33*, 1415-1436.

(22) Müller, G.; Gurrath, M.; Kurz, M.; Kessler, H., βVI turns in peptides and proteins: A model peptide mimicry. *Proteins: Structure, Function, and Bioinformatics* **1993**, *15*, 235-251.

(23) Hanessian, S.; McNaughton-Smith, G.; Lombart, H.-G.; Lubell, W. D., Design and synthesis of conformationally constrained amino acids as versatile scaffolds and peptide mimetics. *Tetrahedron* **1997**, *53*, 12789-12854.

(24) Lombart, H.-G.; Lubell, W. D., Synthesis of Enantiopure α,ω-Diamino Dicarboxylates and Azabicycloalkane Amino Acids by Claisen Condensation of α-[N-(Phenylfluorenyl)amino] Dicarboxylates. *J. Org. Chem.* **1994**, *59*, 6147-6149.

(25) Jamieson, A. G.; Boutard, N.; Sabatino, D.; Lubell, W. D., Peptide scanning for studying structure-activity relationships in drug discovery. *Chem. Biol. Drug Des.* **2013**, *81*, 148-165.

(26) (a) Juvvadi, P.; Dooley, D. J.; Humblet, C. C.; Lu, G. H.; Lunney, E. A.; Panek, R. L.; Skeean, R.; Marshall, G. R., Bradykinin and angiotensin II analogs containing a conformationally constrained proline analog. *Int. J. Pept. Protein Res.* **1992**, *40*, 163-170. (b) Lenman, M. M.; Ingham, S. L.; Gani, D., Syntheis and structure of cis-peptidyl prolinamide mimetics based upon 1, 2, 5-triazepine-3, 6-diones. *Chem. Comm.* **1996**, 85-87. (c) Beausoleil, E.; Lubell, W. D., Steric Effects on the Amide Isomer Equilibrium of Prolyl Peptides. Synthesis and Conformational Analysis of N-Acetyl-5-tert-butylproline N'-Methylamides. *J. Am. Chem. Soc.* **1996**, *118*, 12902-12908. (d) Bélec, L.; Slaninova, J.; Lubell, W. D., A study of the relationship between biological activity and prolyl amide isomer geometry in oxytocin using 5-tert-butylproline to augment the Cys6-Pro7 amide cis-isomer population. *J. Med. Chem.* **2000**, *43*, 1448-1455. (e) Halab, L.; Lubell, W. D., Effect of Sequence on Peptide Geometry in 5-tert-Butylprolyl Type VI β-Turn Mimics. *J. Am. Chem. Soc.* **2002**, *124*, 2474-2484. (f) Halab, L.; Lubell, W. D., Use of Steric

Interactions To Control Peptide Turn Geometry. Synthesis of Type VI β-Turn Mimics with 5-tert-Butylproline. *J. Org. Chem.* **1999**, *64*, 3312-3321. (g) Halab, L.; Lubell, W. D., Influence of N-terminal residue stereochemistry on the prolyl amide geometry and the conformation of 5-tert-butylproline type VI β-turn mimics. *J. Pept. Sci.* **2001**, *7*, 92-104.

(27) Kemp, D. S., Peptidomimetics and the template approach to nucleation of β-sheets and α-helices in peptides. *Trends in Biotech.* **1990**, *8*, 249-255.

(28) Feigel, M., 2, 8-Dimethyl-4-(carboxymethyl)-6-(aminomethyl) phenoxathiin S-dioxide: an organic substitute for the. beta.-turn in peptides? *J. Am. Chem. Soc.* **1986**, *108*, 181-182.

(29) (a) Kemp, D. S., Peptidomimetics and the template approach to nucleation of β-sheets and α-helices in peptides. *Trends in biotechnology* **1990**, *8*, 249-255. (b) Kemp, D.; Bowen, B. R., Synthesis of peptide-functionalized diacylaminoepindolidiones as templates for β-sheet formation. *Tetrahedron Lett.* **1988**, *29*, 5077-5080.

(30) Kemp, D.; Curran, T. P., (2S, 5S, 8S, 11S)-1-Acetyl-1, 4-diaza-3-keto-5-carboxy-10-thia-tricyclo-[2.8. 04, 8]-tridecane, 1 synthesis of prolyl-proline-derived, peptide-functionalized templates for α-helix formation. *Tetrahedron Lett.* **1988**, *29*, 4931-4934.

(31) (a) Freidinger, R. M.; Veber, D. F.; Perlow, D. S.; Saperstein, R., Bioactive conformation of luteinizing hormone-releasing hormone: evidence from a conformationally constrained analog. *Science* **1980**, *210*, 656-658. (b) Freidinger, R. M., Synthesis of. gamma.-lactam-constrained tryptophyl-lysine derivatives. *J. Org. Chem.* **1985**, *50*, 3631-3633. (c) Jamieson, A. G.; Boutard, N.; Beauregard, K.; Bodas, M. S.; Ong, H.; Quiniou, C.; Chemtob, S.; Lubell, W. D., Positional scanning for peptide secondary structure by systematic solid-phase synthesis of amino lactam peptides. *J. Am. Chem. Soc.* **2009**, *131*, 7917-7927. (d) Boutard, N.; Jamieson, A. G.; Ong, H.; Lubell, W. D., Structure–Activity Analysis of the Growth Hormone Secretagogue GHRP-6 by α-and β-Amino γ-Lactam Positional Scanning. *Chem. Biol. Drug Des.* **2010**, *75*, 40-50.

(32) (a) Cluzeau, J.; Lubell, W. D., Design, synthesis, and application of azabicyclo [XY 0] alkanone amino acids as constrained dipeptide surrogates and peptide mimics. *Peptide Science* **2005**, *80*, 98-150. (b) Atmuri, N. P.; Lubell, W. D., Insight into Transannular Cyclization Reactions To Synthesize Azabicyclo [XY Z] alkanone Amino Acid

Derivatives from 8-, 9-, and 10-Membered Macrocyclic Dipeptide Lactams. *J. Org. Chem.* **2015**, *80*, 4904-4918.

(33) Genin, M. J.; Gleason, W. B.; Johnson, R. L., Design, synthesis, and x-ray crystallographic analysis of two novel spirolactam systems as. beta.-turn mimics. *J. Org. Chem.* **1993**, *58*, 860-866.

(34) (a) Hata, M.; Marshall, G. R., Do benzodiazepines mimic reverse-turn structures? *J. Computer-aided Mol. Des.* **2006**, *20*, 321-331. (b) Dörr, A. l. A.; Lubell, W. D., γ-Turn mimicry with benzodiazepinones and pyrrolobenzodiazepinones synthesized from a common amino ketone intermediate. *Org. Lett.* **2015**, *17*, 3592-3595. (c) Douchez, A.; Lubell, W. D., Chemoselective alkylation for diversity-oriented synthesis of 1,3,4-benzotriazepin-2-ones and pyrrolo[1,2][1,3,4]benzotriazepin-6-ones, potential turn surrogates. *Org. Lett.* **2015**, *17*, 6046-6049.

(35) (a) Chingle, R.; Proulx, C.; Lubell, W. D., Azapeptide Synthesis Methods for Expanding Side-Chain Diversity for Biomedical Applications. *Acc. Chem. Res.* **2017**. (b) Proulx, C.; Sabatino, D.; Hopewell, R.; Spiegel, J.; Garcia, R. Y.; Lubell, W. D., Azapeptides and their therapeutic potential. *Future Med. Chem.* **2011**, *3*, 1139-1164. (c) Gante, J., Azapeptides. *Synthesis* **1989**, 405-413.

(36) (a) Reynolds, C. H.; Hormann, R. E., Theoretical study of the structure and rotational flexibility of diacylhydrazines: Implications for the structure of nonsteroidal ecdysone agonists and azapeptides. *J. Am. Chem. Soc.* **1996**, *118*, 9395-9401. (b) Lee, H.-J.; Lee, M.-H.; Choi, Y.-S.; Park, H.-M.; Lee, K.-B., NBO approach to evaluate origin of rotational barrier of diformylhydrazine. *J. Mol. Str.: THEOCHEM* **2003**, *631*, 101-110.

(37) Lee, H. J.; Choi, K. H.; Ahn, I. A.; Ro, S.; Jang, H. G.; Choi, Y. S.; Lee, K. B., The β-turn preferential solution conformation of a tetrapeptide containing an azaamino acid residue. *J. Mol. Struct.* **2001**, *569*, 43-54.

(38) Zouikri, M.; Vicherat, A.; Aubry, A.; Marraud, M.; Boussard, G., Azaproline as a β-turn-inducer residue opposed to proline. *J. Pept. Res.* **1998**, *52*, 19-26.

(39) (a) Lee, H. J.; Ahn, I. A.; Ro, S.; Choi, K. H.; Choi, Y. S.; Lee, K. B., Role of azaamino acid residue in β-turn formation and stability in designed peptide. *J. Pept. Res.* **2000**, *56*, 35-46. (b) Thormann, M.; Hofmann, H.-J., Conformational properties of azapeptides. *J. Mol. Struct.: Theochem* **1999**, *469*, 63-76. (c) Lee, H.-J.; Song, J.-W.; Choi, Y.-S.; Park,

H.-M.; Lee, K.-B., A Theoretical Study of Conformational Properties of N-Methyl Azapeptide Derivatives. *J. Am. Chem. Soc.* **2002**, *124*, 11881-11893.

(40) Dutta, A. S.; Furr, B. J.; Giles, M. B., Polypeptides. Part 15. Synthesis and biological activity of α-aza-analogues of luliberin modified in positions 6 and 10. *J. Chem. Soc., Perkin Trans. 1* **1979**, 379-388.

(41) (a) Gassman, J. M.; Magrath, J., An active-site titrant for chymotrypsin, and evidence that azapeptide esters are less susceptible to nucleophilic attack than ordinary esters. *Bioorg. Med. Chem. Lett.* **1996**, *6*, 1771-1774. (b) Wipf, P.; Li, W.; Adeyeye, C. M.; Rusnak, J. M.; Lazo, J. S., Synthesis of chemoreversible prodrugs of ara-C with variable time-release profiles. Biological evaluation of their apoptotic activity. *Bioorg. Med. Chem. Lett.* **1996**, *4*, 1585-1596.

(42) (a) Dugave, C.; Demange, L., Synthesis of pseudopeptides containing aza-phenylalanine surrogates of the Phe-pNA motif: Influence on the binding to the human cyclophilin hCyp-18. *Lett. Pept. Sci.* **2003**, *10*, 1-9. (b) Tal-Gan, Y.; Freeman, N. S.; Klein, S.; Levitzki, A.; Gilon, C., Metabolic Stability of Peptidomimetics: N-Methyl and Aza Heptapeptide Analogs of a PKB/Akt Inhibitor. *Chem. Biol. Drug Des.* **2011**, *78*, 887-892.

(43) Hess, H.-J.; Moreland, W. T.; Laubach, G. D., N-[2-Isopropyl-3-(L-aspartyl-L-arginyl)-carbazoyl]-L-tyrosyl-L-valyl-L-histidyl-L-prolyl-L-phenylalanine, 1 an Isostere of Bovine Angiotensin II. *J. Am. Chem. Soc.* **1963**, *85*, 4040-4041.

(44) Dutta, A. S.; Furr, B. J.; Giles, M. B.; Valcaccia, B., Synthesis and biological activity of highly active. alpha.-aza analogs of luliberin. *J. Med. Chem.* **1978**, *21*, 1018-1024.

(45) Gante, J., Peptidähnliche Systeme, VII. Über neue Möglichkeiten bei der Synthese von Azapeptiden. *Eur. J. Inorg. Chem.* **1965**, *98*, 3340-3344.

(46) (a) Gante, J.; Krug, M.; Lauterbach, G.; Weitzel, R.; Hiller, W., Synthesis and properties of the first all-aza analogue of a biologically active peptide. *J. Pept. Sci.* **1995**, *1*, 201-206. (b) Han, H.; Janda, K. D., Azatides: Solution and Liquid Phase Syntheses of a New Peptidomimetic. *J. Am. Chem. Soc.* **1996**, *118*, 2539-2544. (c) Han, H.; Yoon, J.; Janda, K. D., Investigations of azapeptides as mimetics of Leu-enkephalin. *Bioorg. Med. Chem. Lett.* **1998**, *8*, 117-120.

(47) Gimpl, G.; Fahrenholz, F., The oxytocin receptor system: structure, function, and regulation. *Physiol. Rev.* **2001**, *81*, 629-683.

(48) (a) Niedrich, H.; Oehme, C., Hydrazinverbindungen als Heterobestandteile in Peptiden. XV. Synthese von Eledoisin-Octapeptiden mit den Carbazylresten Azaglycin und α-Azaasparagin statt Glycin und Asparagin. *Adv. Syn. Catalysis* **1972**, *314*, 759-768. (b) Oehme, P.; Bergmann, J.; Falck, M.; Reich, J.; Vogt, W.; Niedrich, H.; Pirrwitz, J.; Berseck, C.; Jung, F., Pharmacology of hydrazino carbonic acids, hydrazino peptides and other hydrazine derivatives. Structure-action studies in heterologeous eledoisin octapeptide sequences. *Acta biologica et medica Germanica* **1972**, *28*, 109. (c) Oehme, P.; Bergmann, J.; Niedrich, H.; Jung, F.; Menzel, G., Pharmacology of hydrazine-carbonic acids, hydrazine peptides and other hydrazine derivatives. VII. Pharmacologic studies on heterologous eledoisine sequences. *Acta biologica et medica Germanica* **1970**, *25*, 613-625.

(49) (a) Han, H.; Yoon, J.; Janda, K. D., Investigations of azapeptides as mimetics of Leu-enkephalin. *Bioorg. Med. Chem. lett.* **1998**, *8*, 117-120. (b) Dutta, A.; Gormley, J.; Hayward, C.; Morley, J.; Shaw, J.; Stacey, G.; Turnbull, M., Enkephalin analogues eliciting analgesia after intravenous injection. *Life sciences* **1977**, *21*, 559-562. (c) Bélanger, P. C.; Dufresne, C., Preparation of exo-6-benzyl-exo-2-(m-hydroxyphenyl)-1-dimethylaminomethylbicyclo [2.2. 2.] octane. A non-peptide mimic of enkephalins. *Can. J. chem.* **1986**, *64*, 1514-1520.

(50) Zhang, W.-J.; Berglund, A.; Kao, J. L.-F.; Couty, J.-P.; Gershengorn, M. C.; Marshall, G. R., Impact of azaproline on amide cis− trans isomerism: conformational analyses and NMR studies of model peptides including TRH analogues. *J. Am. Chem. Soc.* **2003**, *125*, 1221-1235.

(51) (a) von Roedern, E. G.; Kessler, H., A sugar amino acid as a novel peptidomimetic. *Angew. Chem., Int. Ed.* **1994**, *33*, 687-689. (b) Hirschmann, R.; Nicolaou, K.; Pietranico, S.; Salvino, J.; Leahy, E. M.; Sprengeler, P. A.; Furst, G.; Strader, C. D.; Smith III, A. B., Nonpeptidal peptidomimetics with. beta.-D-glucose scaffolding. A partial somatostatin agonist bearing a close structural relationship to a potent, selective substance P antagonist. *J. Am. Chem. Soc.* **1992**, *114*, 9217-9218.

(52) Thormann, M.; Hofmann, H.-J., Conformational properties of azapeptides. *J. Mol. Str.: THEOCHEM* **1999**, *469*, 63-76.

(53) Chingle, R.; Lubell, W. D., Azopeptides: Synthesis and Pericyclic Chemistry. *Org. Lett.* **2015**, *17*, 5400-5403.

(54) (a) Boeglin, D.; Lubell, W. D., Aza-Amino Acid Scanning of Secondary Structure Suited for Solid-Phase Peptide Synthesis with Fmoc Chemistry and Aza-Amino Acids with Heteroatomic Side Chains. *J. Comb. Chem.* **2005**, *7*, 864-878. (b) Sabatino, D.; Proulx, C.; Pohankova, P.; Ong, H.; Lubell, W. D., Structure-activity relationships of GHRP-6 azapeptide ligands of the CD36 scavenger receptor by solid-phase submonomer azapeptide synthesis. *J Am Chem Soc* **2011**, *133*, 12493-12506.

(55) (a) Limal, D.; Semetey, V.; Dalbon, P.; Jolivet, M.; Briand, J.-P., Solid-phase synthesis of N, N′-unsymmetrically substituted ureas: application to the synthesis of carbaza peptides. *Tetrahedron Lett.* **1999**, *40*, 2749-2752. (b) Chong, P. Y.; Petillo, P. A., Solid phase urea synthesis: An efficient and direct conversion of Fmoc-protected amines to ureas. *Tetrahedron Lett.* **1999**, *40*, 4501-4504.

(56) Quibell, M.; Turnell, W. G.; Johnson, T., Synthesis of azapeptides by the Fmoc/tert-butyl/polyamide technique. *J. Chem. Soc., Perkin Trans. 1* **1993**, 2843-2849.

(57) Johnson, T.; Quibell, M.; Owen, D.; Sheppard, R., A reversible protecting group for the amide bond in peptides. Use in the synthesis of 'difficult sequences'. *J. Chem. Soc., Chem. Comm.* **1993**, 369-372.

(58) Liley, M.; Johnson, T., Solid phase synthesis of azapeptides utilising reversible amide bond protection to prevent hydantoin formation. *Tetrahedron Lett.* **2000**, *41*, 3983-3985.

(59) Melendez, R. E.; Lubell, W. D., Aza-Amino Acid Scan for Rapid Identification of Secondary Structure Based on the Application of N-Boc-Aza1-Dipeptides in Peptide Synthesis. *J. Am. Chem. Soc.* **2004**, *126*, 6759-6764.

(60) (a) Bourguet, C. B.; Proulx, C.; Klocek, S.; Sabatino, D.; Lubell, W. D., Solution-phase submonomer diversification of aza-dipeptide building blocks and their application in aza-peptide and aza-DKP synthesis. *J. Pept. Sci.* **2010**, *16*, 284-296. (b) Bourguet, C. B.; Sabatino, D.; Lubell, W. D., Benzophenone semicarbazone protection strategy for synthesis of aza-glycine containing aza-peptides. *Biopolymers* **2008**, *90*, 824-831.

(61) O'Donnell, M. J.; Zhou, C.; Scott, W. L., Solid-phase unnatural peptide synthesis (UPS). *J. Am. Chem. Soc.* **1996**, *118*, 6070-6071.

(62) (a) Sabatino, D.; Proulx, C.; Klocek, S.; Bourguet, C. B.; Boeglin, D.; Ong, H.; Lubell, W. D., Exploring side-chain diversity by submonomer solid-phase aza-peptide synthesis. *Org. Lett.* **2009**, *11*, 3650-3653. (b) Sabatino, D.; Proulx, C.; Pohankova, P.; Ong, H.; Lubell, W. D., Structure-Activity Relationships of GHRP-6 Azapeptide Ligands of the CD36 Scavenger Receptor by Solid-Phase Submonomer Azapeptide Synthesis. *J. Am. Chem. Soc.* **2011**, *133*, 12493-12506.

(63) Bourguet, C. B.; Sabatino, D.; Lubell, W. D., Benzophenone semicarbazone protection strategy for synthesis of aza-glycine containing aza-peptides. *Biopolymers* **2008**, *90*, 824-831.

(64) (a) Fahr, E.; Lind, H., The Chemistry of α-Carbonyl Azo Compounds. *Angew. Chem., Int. Ed.* **1966**, *5*, 372-384. (b) Tsunoda, T.; Otsuka, J.; Yamamiya, Y.; Itô, S., N, N, N′, N′-Tetramethylazodicarboxamide (TMAD), a new versatile reagent for mitsunobu reaction. Its Application to synthesis of secondary amines. *Chem. Lett.* **1994**, *23*, 539-542.

(65) (a) Mitsunobu, O., The use of diethyl azodicarboxylate and triphenylphosphine in synthesis and transformation of natural products. *Synthesis* **1981**, *1981*, 1-28. (b) Hughes, D. L., Progress in the Mitsunobu reaction. A review. *Org. Prep. Proc. Int.* **1996**, *28*, 127-164.

(66) (a) Trimble, L. A.; Vederas, J. C., Amination of chiral enolates by dialkyl azodiformates. Synthesis of. alpha.-hydrazino acids and. alpha.-amino acids. *J. Am. Chem. Soc.* **1986**, *108*, 6397-6399. (b) Harris, J. M.; McDonald, R.; Vederas, J. C., Synthesis of a chiral azodicarboxamide containing a bridging binaphthyl moiety: electrophilic amination reactions of achiral ester enolates. *J. Chem. Soc., Perkin Trans. 1* **1996**, 2669-2674.

(67) (a) Diels, O.; Blom, J. H.; Koll, W., Über das aus Cyclopentadien und Azoester entstehende Endomethylen-piperidazin und seine Überführung in 1, 3-Diamino-cyclopentan. *Eur. J. Org. Chem.* **1925**, *443*, 242-262. (b) Diels, O.; Alder, K., Über die Ursachen der „Azoesterreaktion" . *Eur. J. Org. Chem.* **1926**, *450*, 237-254. (c) Diels, O.; Alder, K., Synthesen in der hydroaromatischen Reihe. *Eur. J. Org. Chem.* **1928**, *460*, 98-122. (d) Jenner, G.; Salem, R. B., Anatomy of ene and Diels–Alder reactions between cyclohexadienes and azodicarboxylates. *J. Chem. Soc., Perkin Trans. 2* **1990**, 1961-1964.

(68) Desimoni, G.; Faita, G.; Righetti, P.; Sfulcini, A.; Tsyganov, D., Solvent effect in pericyclic reactions. IX. The ene reaction. *Tetrahedron* **1994**, *50*, 1821-1832.

(69) Berná, J.; Alajarín, M.; Orenes, R. l.-A., Azodicarboxamides as template binding motifs for the building of hydrogen-bonded molecular shuttles. *J. Am. Chem. Soc.* **2010**, *132*, 10741-10747.

(70) Hill, R. D.; Vederas, J. C., Azodicarboxamides: A new class of cysteine proteinase inhibitor for hepatitis A virus and human rhinovirus 3C enzymes. *J. Org. Chem.* **1999**, *64*, 9538-9546.

(71) Alder, K.; Pascher, F.; Schmitz, A., Über die Anlagerung von Maleinsäure-anhydrid und Azodicarbonsäure-ester an einfach ungesättigte Koh an einfach ungesättigte Kohlenwasserstoffe. Zur Kenntnis von Substitutionsvorgängen in der Allyl-Stellung. *Eur. J. Inorg. Chem.* **1943**, *76*, 27-53.

(72) (a) Kamimura, A.; Gunjigake, Y.; Mitsudera, H.; Yokoyama, S., A facile preparation of α-hydrazino-α, β-unsaturated ketones via aza-Baylis-Hillman reaction. *Tetrahedron Lett.* **1998**, *39*, 7323-7324. (b) Shi, M.; Zhao, G.-L., Aza-Baylis–Hillman reactions of diisopropyl azodicarboxylate or diethyl azodicarboxylate with acrylates and acrylonitrile. *Tetrahedron* **2004**, *60*, 2083-2089.

(73) Ryu, I.; Tani, A.; Fukuyama, T.; Ravelli, D.; Montanaro, S.; Fagnoni, M., Efficient C–H/C–N and C–H/C–CO–N Conversion via Decatungstate-Photoinduced Alkylation of Diisopropyl Azodicarboxylate. *Org. Lett.* **2013**, *15*, 2554-2557.

(74) Mamone, M.; Morvan, E.; Milcent, T.; Ongeri, S.; Crousse, B., Electrophilic Amination of Fluoroalkyl Groups on Azodicarboxylate Derivatives. *J. Org. Chem.* **2015**, *80*, 1964-1971.

(75) Wang, H.; Ren, Y.; Wang, K.; Man, Y.; Xiang, Y.; Li, N.; Tang, B., Visible light-induced cyclization reactions for the synthesis of 1, 2, 4-triazolines and 1, 2, 4-triazoles. *Chem. Comm.* **2017**, *53*, 9644-9647.

(76) (a) Hemmerlin, C.; Cung, M. T.; Boussard, G., Synthesis and conformational preferences in solution and crystalline states of an aza-tripeptide. *Tetrahedron Lett.* **2001**, *42*, 5009-5012. (b) Wilkinson, D. E.; Thomas, B. E.; Limburg, D. C.; Holmes, A.; Sauer, H.; Ross, D. T.; Soni, R.; Chen, Y.; Guo, H.; Howorth, P., Synthesis, molecular modeling and biological evaluation of aza-proline and aza-pipecolic derivatives as FKBP12 ligands and their in vivo neuroprotective effects. *Bioorg. Med. Chem.* **2003**, *11*, 4815-4825.

(77) Dutta, A. S.; Morley, J. S., Polypeptides. Part XIII. Preparation of α-aza-amino-acid (carbazic acid) derivatives and intermediates for the preparation of α-aza-peptides. *J. Chem. Soc., Perkin Trans. 1* **1975**, 1712-1720.

(78) (a) Zhang, W.-J.; Berglund, A.; Kao, J. L.-F.; Couty, J.-P.; Gershengorn, M. C.; Marshall, G. R., Impact of azaproline on amide cis− trans isomerism: conformational analyses and NMR studies of model peptides including TRH analogues. *J. Am. Chem. Soc.* **2003**, *125*, 1221-1235. (b) Zhang, Y.; Malamakal, R. M.; Chenoweth, D. M., A Single Stereodynamic Center Modulates the Rate of Self-Assembly in a Biomolecular System. *Angew. Chem., Int. Ed.* **2015**, *54*, 10826-10832. (c) Bac, A.; Rivoal, K.; Cung, M. T.; Boussard, G.; Marraud, M.; Soudan, B.; Tetaert, D.; Degand, P., Conformational disturbance induced by AzPro/Pro substitution in peptides. *Lett. Pep. Sci.* **1997**, *4*, 251-258. (d) Freeman, N. S.; Tal-Gan, Y.; Klein, S.; Levitzki, A.; Gilon, C., Microwave-assisted solid-phase aza-peptide synthesis: aza scan of a PKB/Akt inhibitor using aza-arginine and aza-proline precursors. *J. org. chem.* **2011**, *76*, 3078-3085. (e) Borloo, M.; Augustyns, K.; Belyaev, A.; de Meester, I.; Lambeir, A.-M.; Goossens, F.; Bollaert, W.; Rajan, P.; Scharpé, S.; Haemers, A., Synthesis and evaluation of azaproline peptides as potential inhibitors of dipeptidyl peptidase IV and prolyl oligopeptidase. *Lett. Pep. Sci.* **1995**, *2*, 198-202.

(79) Garcia-Ramos, Y.; Lubell, W. D., Synthesis and alkylation of aza-glycinyl dipeptide building blocks. *J. Pept. Sci.* **2013**, *19*, 725-729.

(80) (a) Chingle, R.; Ratni, S.; Claing, A.; Lubell, W. D., Application of constrained aza-valine analogs for Smac mimicry. *Biopolymers* **2016**, *106*, 235-244. (b) Chingle, R.; Lubell, W. D., Peptide coupling challenges in azopeptide route to aza-pipecolyl Smac mimetic. *Proceeding of the 24th Am. Pept. Symp., Ved Srivastava, Andrei Yudin, and Michal Lebl (Editors) Am. Pept. Soc.* **2015**, 172-173.

(81) Chingle, R.; Mulumba, M.; Chung, N. N.; Ong, H.; Ballet, S.; Schiller, P. W.; Lubell, W. D., Identification of Active Peptide Conformations by Application of aza-Pipecolyl Residue Insertion Using Solid-Phase Azopeptide Diels-Alder Chemistry. *In Preparation* **2018**.

Chapter 2: Design, Synthesis and Pericyclic Chemistry of Azopeptides

2.1. Context

Azodicarboxylates have many uses in organic chemistry. They are reagents for the Mitsunobu reaction,[1] electrophilic amination[2] and pericyclic reactions.[3] In the Chapter, the chemistry of azodicarbonyl molecules and peptides are merged by the conception of so called "azopeptides". Azopeptides feature an imino urea component that serves as an amino amide surrogate. Azopeptides were synthesized in solution by oxidation of *N*-Boc- and Cbz-aza-glycine residues. The structure of the azopeptides was validated by spectroscopic and crystallographic methods. The pericyclic chemistry of azopeptides was explored next in Diels-Alder cyclizations and Alder-ene reactions to provide respectively constrained aza-pipecolic acid and aza-allylglycine residues.[4] The latter were shown by X-ray diffraction to have similar geometry to that of ideal type I and VI β-turns.[4]

Azopeptides were synthesized by oxidation of aza-glycine residues using *N*-bromosuccinimide (NBS) and pyridine in dichloromethane at −78 °C to room temperature.[5] As discussed in Chapter 1, the introduction of aza-glycine into peptides is challenging because of potential side reactions leading to the formation of undesired products such as oxadiazalones and symmetric ureas. Semicarbazone protection of the aza-glycine building blocks has facilitated their introduction and use in peptides.[6] Notably herein, azaglycine residues were introduced into peptides by solution-phase chemistry by activation of the *tert*-butyl and benzyl carbazates with DSC and coupling the reactive carbazate to amino ester and peptide without oxadiazalone side product.[4a]

IR spectroscopy, NMR spectroscopy and X-ray crystallographic analyses were performed on the azopeptide to provided insight into the imino urea configuration.[4a] Azopeptides were latter examined as dienophiles in Diels−Alder reactions with various dienes to provided quantitatively aza-pipecolate and aza-methanopipecolate analogs. Alkenes such as 1,3-cyclohexadiene, cycloheptatriene, and isobutylene, all reacted with the azopeptides under two different conditions to produce aza-allylglycine analogs. The regiochemistry of the Alder−ene products was determined by a combination of NMR spectroscopy, MS experiments, and X-ray analyses.[4a]

The utility of the azopeptide method was demonstrated further by the synthesis of analogs of the neuropeptide melanocyte-stimulating hormone release inhibiting factor-1 (MIF-1, H-Pro-Leu-Gly-NH_2, PLG, **2.42**), which has been shown to be a positive allosteric modulator of the dopamine D_2 receptor.[7] Structure-activity studies in which the ϕ and ψ dihedral angles of PLG were constrained have suggested that the bioactive conformation of PLG features a type II β-turn. Moreover, the pharmacological profile of PLG offers potential for treating neurological diseases such as Parkinson's disease and tardive dyskinesia; however, the peptide nature of PLG limits potential for drug conception and has spurred design of peptidomimetic analogues.[8]

Two PLG analogues were synthesized by replacing proline with aza-pipecolyl residues. In solution, Δ^4-aza-dehydropipecolyl- and aza-pipecolylleucylglycinamide (**2.40** and **2.41)** were synthesized to study the influence of the cyclic semicarbazide moiety on biological activity in efforts to further elucidate the structural requirements for modulation of dopaminergic neurotransmission (Figure 2.1).[4a]

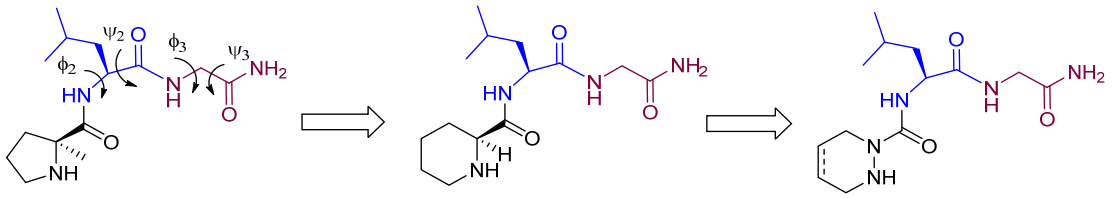

Figure 2.1. Conceptual transformation of the structure of melanocyte-stimulating hormone release inhibiting factor-1 (MIF-1, **2.42**), into [Pip^1]MIF-1 (**2.43**), to [Δ^4-azaPip^1]MIF-1 (**2.40**) and [azaPip^1]MIF-1 (**2.41**).[4a,7]

Aza-pipecolylleucylglycinamide (**2.41)** was synthesized by hydrogenations of [(Δ^4)-azaPip]MIF-1 **2.40** using palladium-on-carbon (10 wt%) in methanol under a balloon of hydrogen (1 atm). Saturated [azaPip^1]MIF-1 (**2.41**) was isolated by removal of the catalyst on filtration over Celite™. After washing with methanol, and evaporation of the combined filtrate and washings, the residue was freeze-dried to furnish azapeptide as off-white solid, that was analyzed by RP-HPLC to assess purity (See experimental section for chapter 2).

Both [Δ^4-azaPip^1]MIF-1 (**2.40**) and [azaPip^1]MIF-1 (**2.41**) were sent to Professor Ram Mishra (Department of Psychiatry and Behavioural Neurosciences, McMaster University) to evaluate their activity as potential allosteric modulators of the dopamine D2 receptors. The PLG peptidomimetics **2.40** and **2.41** were evaluated for their ability to increase or decrease the binding of tritiated *N*-propylnorapomorphine ([^{3}H]NPA) on bovine striatal dopamine D_2 receptors.[7e] The percentage change in total specific [^{3}H]NPA binding was measured across various concentrations (10^{-2} -10^{-10} M) of each peptidomimetic (Figure 2.2).[7]

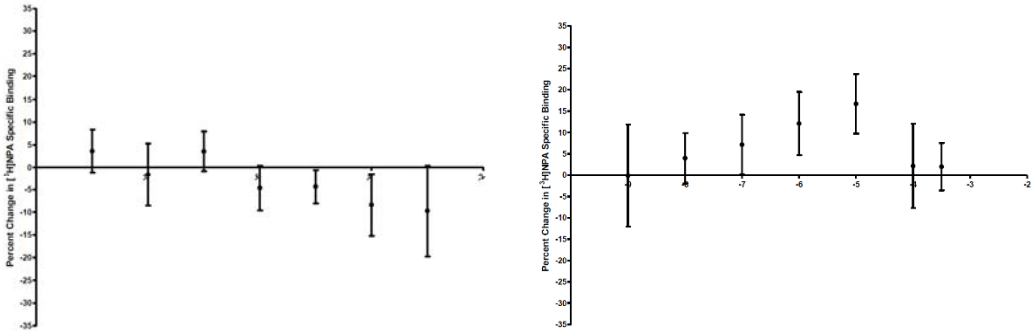

Figure 2.2. No modulation of [^{3}H]NPA binding to dopamine D_2 receptors was exhibited by analogs **2.41** and **2.42**. Data represent the percent change in specific [^{3}H]NPA binding relative to the control value when the indicated concentration of compounds **2.41** and **2.42** was added directly to the assay buffer. Results are the mean ± SEM of 3 separate experiments carried out in triplicate.

Triplicate analysis of peptidomimetics **2.40** and **2.41** showed minimal or negative modulatory effects in ability to affect [^{3}H]NPA binding to isolated dopamine D_2 receptors. At none of the tested concentrations did **2.40** and **2.41** exhibit significant effect in contrast to PLG as a positive control.[7a] The aza-pipecolic acid analogs of MIF-1 were inactive, likely due to the reduced basicity of the semicarbazide of the azaPip residues relative to the secondary amine of the parent proline.

In the chapter, solution phase synthesis featuring the preparation and oxidation of aza-glycine peptides has provided the first examples of azopeptides.[4a] Pericyclic chemistry of azopeptides using Diels-Alder cyclization and Alder-ene reactions have enabled respectively

construction of constrained aza-pipecolyl residues and assembly of aza-allylglycines possessing substituents on the α- and β-nitrogen of the semicarbazide. X-ray crystallographic analysis provided insight respectively into the azopeptide configuration and influence on conformation of substitution at the semicarbazide α- and β-nitrogen of azapeptides which were shown to adopt geometry similar to ideal type I and VI β-turns. Azopeptides intermediates were used to synthesize aza-pipecolyl analogues of melanocyte-stimulating hormone release inhibiting factor-1 (MIF-1) without classic hydrazine chemistry using ionic intermediates. Although the MIF-1 analogs were inactive, the potential for using the method to explore biologically relevant peptides was established paving the way for studies of other targets described in the following chapters.

Article 1

Chingle, R.; Lubell, W. D. Azopeptides: Synthesis and Pericyclic Chemistry. *Org. Lett.* **2015**, *17*, 5400-5403.

DOI: 10.1021/acs.orglett.5b02723

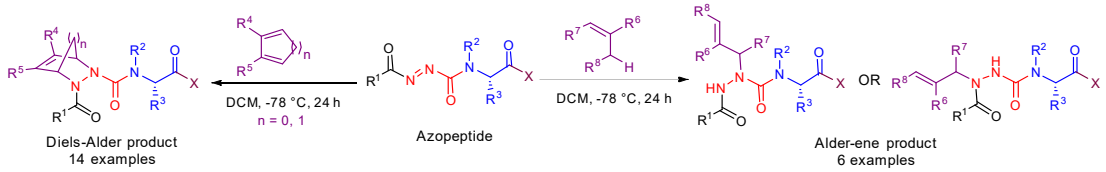

All synthetic work for this article has been done by myself.

The article is written by myself and edited by Professor William D. Lubell.

I obtained crystals of one azopeptide and two azapeptide analogs that were characterized by X-ray analyses that were performed by Ms. Francine Bélanger at the regional centre for X-ray crystallography of the Université de Montréal.

Azopeptides: Synthesis and Pericyclic Chemistry

Ramesh Chingle and William D. Lubell*

Department of Chemistry, University of Montreal, C.P. 6128,

Succursale Centre-Ville, Montréal, Québec, H3C 3J7

E-mail: william.lubell@umontreal.ca

Abstract

Azopeptides possess an imino urea as an amino amide surrogate in the sequence. Azopeptides were synthesized by oxidation of aza-glycine residues and employed in pericyclic chemistry. Diels−Alder cyclizations and Alder−ene reactions on azopeptides enabled construction of constrained aza-pipecolyl and reactive aza-allylglycyl residues. X-ray crystallographic analyses of azopeptide **2.16a** and azapeptides **2.30a** and **2.35a** provided insight into imino urea configuration and conformational affects of cycloalkane side chains at the semicarbazide α- and β-nitrogen, respectively.

Keywords

Pericyclic, Azopeptides, Diels−Alder, Alder−ene, aza-pipecolyl, aza-allylglycyl, azapeptide, Peptidomimetics.

Introduction

In the study of biologically active molecules, conformational constraint provides fundamental insight for designing enzyme inhibitors and receptor modulators.[9] In particular, the application of semicarbazides as amino acid surrogates in azapeptides (e.g., **2.1**, Figure 2.3) can restrict backbone geometry to enhance selectivity, and stability.[10]

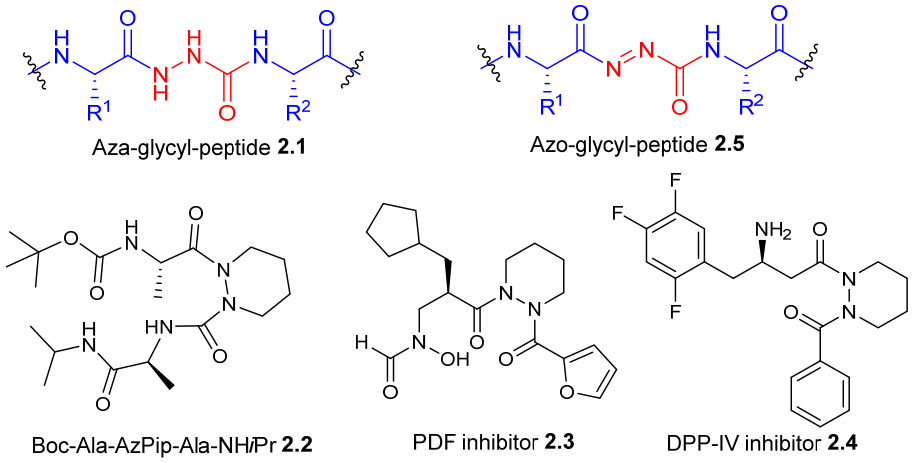

Figure 2.3. Aza- and azopeptides and aza-pipecolyl analogues.

Azapeptides bearing cyclic and unsaturated residues are consequently important targets, respectively, because of their enhanced conformational rigidity and notable reactivity.[11,12] For example, aza-pipecolyl peptidomimetics (e.g., **2.2**-**2.4**) have displayed antibacterial and anti-diabetic activities, because of their inhibitory activity on peptide deformylase and dipeptidyl peptidase IV.[11b,13,14]

The introduction of cyclic and unsaturated aza-residues is however challenging, due to the need to selectively differentiate neighboring nitrogen, and accomplished typically by lengthy hydrazine chemistry using ionic intermediates.[2a] In contrast, pericyclic chemistry offers atom economical access to cyclic and unsaturated systems. Azopeptides **2.5** possessing N=N bonds offer potential for pericyclic reactions with diene and ene systems, which have typically been performed using simple azodicarboxylates,[15] carbamoyl diazine carboxylates[16], *N*-alkyl triazole diones,[17] and phthalazinedione.[18,19] Azo-bridges between aromatic peptide side chains have been made,[20] and used to photo-regulate dynamics of side chain and backbone conformation.[21]

Results and Discussion

To open potential for pericyclic chemistry in peptide frameworks, we have now created azopeptides **2.5** and studied their Diels−Alder and Alder−ene chemistry to synthesize aza-pipecolyl and aza allylglycine residues.

Aza-glycine analogues **2.6-2.12** were synthesized using protocols featuring acylation of the peptide chain with activated methylidene or alkyl carbazates, prior to deprotection and chain elongation [see Supporting Information (SI)].[22,23,24] Azopeptides were then produced by oxidation of the aza-glycine residues using *N*-bromo succinimide (NBS, Scheme 2.1) and pyridine in CH_2Cl_2 at −78 °C to room temperature.[5,11d]

Scheme 2.1. Synthesis of Azopeptides **2.13**−**2.17**.

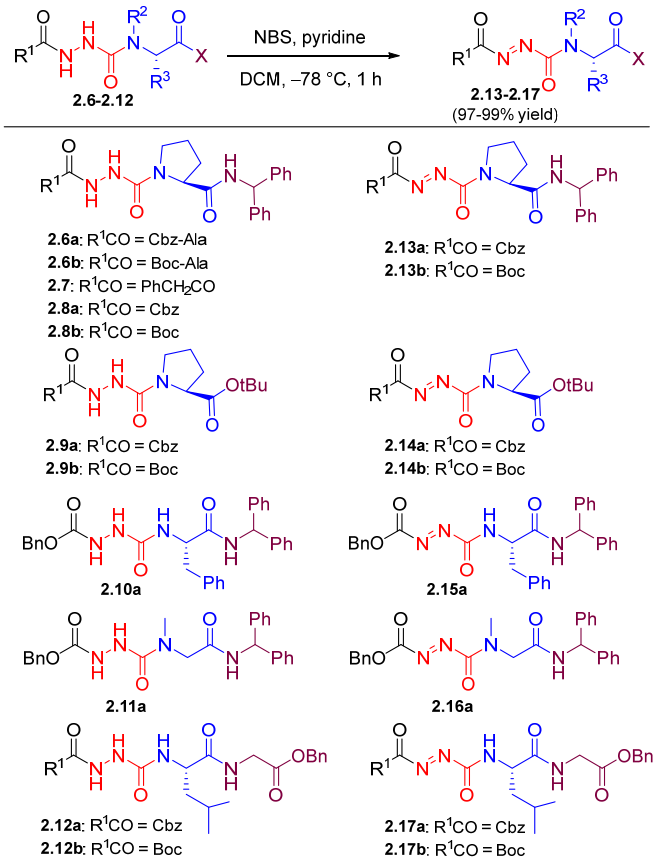

Carbamates **2.8**−**2.12** were converted, respectively, to azopeptides **2.13**−**2.17** using the NBS/pyridine conditions, as indicated by the change of the reaction solution color to pale

yellow and observation of a new relatively nonpolar bright yellow spot on the TLC plate. Suitably pure azopeptides for subsequent chemistry were isolated in 97−99% yields after concentration of the reaction mixture, partitioning between aqueous sodium bicarbonate and ethyl acetate, and evaporation of the organic phase. In the IR spectra, azopeptides exhibited a band between 1700 to 1765 cm^{-1} indicative of the N=N stretching vibration.[25] Azopeptides **2.13**−**2.17** were used without further purification because they were relatively unstable and decomposed over time, as observed by the appearance of additional spots on TLC. Certain azopeptides (e.g., **2.14** and **2.16**) could be studied by NMR spectroscopy. Moreover, crystals of sarcosine analogue **2.16a** were isolated and characterized by X-ray diffraction (Figure 2.4).

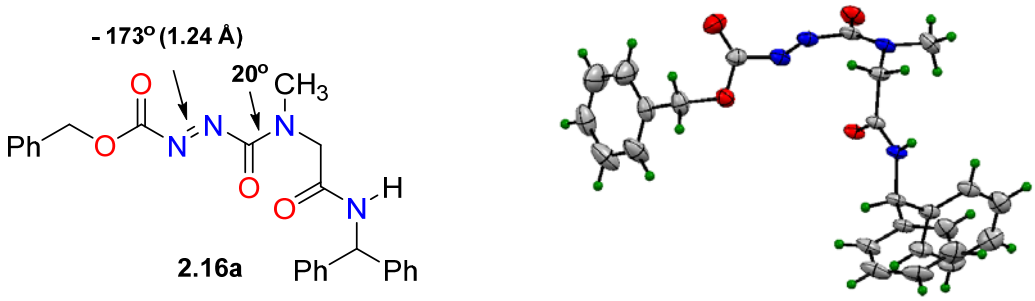

Figure 2.4. Crystal structure of azopeptide **2.16a** with bond lengths and dihedral angles. (C = Grey, H = Green, N = Blue, O = Red).

A structure search of the Cambridge Crystallographic Data Center found only ethyl (*N*-phenylcarbamoyl)azoformate (**2.18**) as a simple diacyl diazine to compare with **2.16a**.[26] Azopeptide **2.16a** and azoformate **2.18** exhibited similar N=N bond lengths (~1.24 Å) and E-diazine configuration; the former was slightly distorted from planarity with a dihedral angle value of −173°. Ureas **2.16a** and **2.18** differed in their respective E and Z conformations. Torsion angles for **16a** and **18** were, respectively, 20° and −177°, indicative of greater twisting in the tertiary urea. Azopeptide **2.16a** adopted a bent conformation; however, in spite of their relative proximity, no seven-, eight-, or 10-membered hydrogen bonds were observed between the amide NH group and either diacyl diazine nitrogen or carbonyl groups. In the crystal lattice, azopeptides **2.16a** stacked antiparallel to each other forming intermolecular hydrogen bonds between the benzhydrylamide NH proton and sarcosine carbonyl oxygen.

In CD_3OD, the NMR spectrum of **2.16a** exhibited a 1:1 isomeric mixture. Isomer assignment to the diazine or tertiary urea was not possible, but evidence for isomerization of diazine **2.15a** was obtained by NMR spectroscopy, which indicated a 1:3 mixture of azo-isomers in $CDCl_3$.

Switching the N-terminal residue from carbamate to amide in aza-glycyl peptides **2.6** and **2.7** possessing alanyl and phenylacetyl residues, respectively, destabilized the oxidation product. Although the characteristic azopeptide yellow spot was observed by TLC analysis after treatment of **2.6b** with NBS at −78 °C for 10 min, the color was pale and other products were present. Attempts to trap the diazine with butadiene and isobutylene produced complex mixtures observed using LCMS, albeit minor peaks corresponded to the masses of the Diels−Alder and Alder−ene adducts. Attempts failed to make azopeptide using (diacetoxyiodo)benzene and lead tetraacetate to oxidize azaglycines **2.6** and **2.7**.

Azopeptides **2.13**−**2.17** were examined as dienophiles in Diels−Alder reactions with butadiene, 2,3-dimethylbutadiene, cyclopentadiene, and cyclohexadiene. Butadiene was used in a sealed tube. Azopeptides **2.13**−**2.17** reacted smoothly with the butadienes and cyclopentadiene in dichloromethane at −78 °C to rt over 24 h to give the aza-pipecolyl analogues **2.19**−**2.29** in 92−99% yields after purification by silica gel chromatography (Scheme 2.2). 2- Methyl-1,3-butadiene reacted with azopeptide **2.13a** to give a 1:1 regioisomeric mixture of Diels−Alder adducts **2.21a** in 92% yield (see the SI). Cycloadditions with cyclopentadiene gave 1:1−4:1 diastereomeric mixtures measured using super critical fluid chromatography (SFC). The NMR spectra of Diels−Alder adducts from butadiene and 2,3-dimethylbutadiene were recorded at 100−120 °C to resolve broad signals due to tertiary urea isomers.

Scheme 2.2. Aza-pipecolyl Peptide Synthesis from Diels–Alder Reactions of Azopeptides **2.13**–**2.17**.

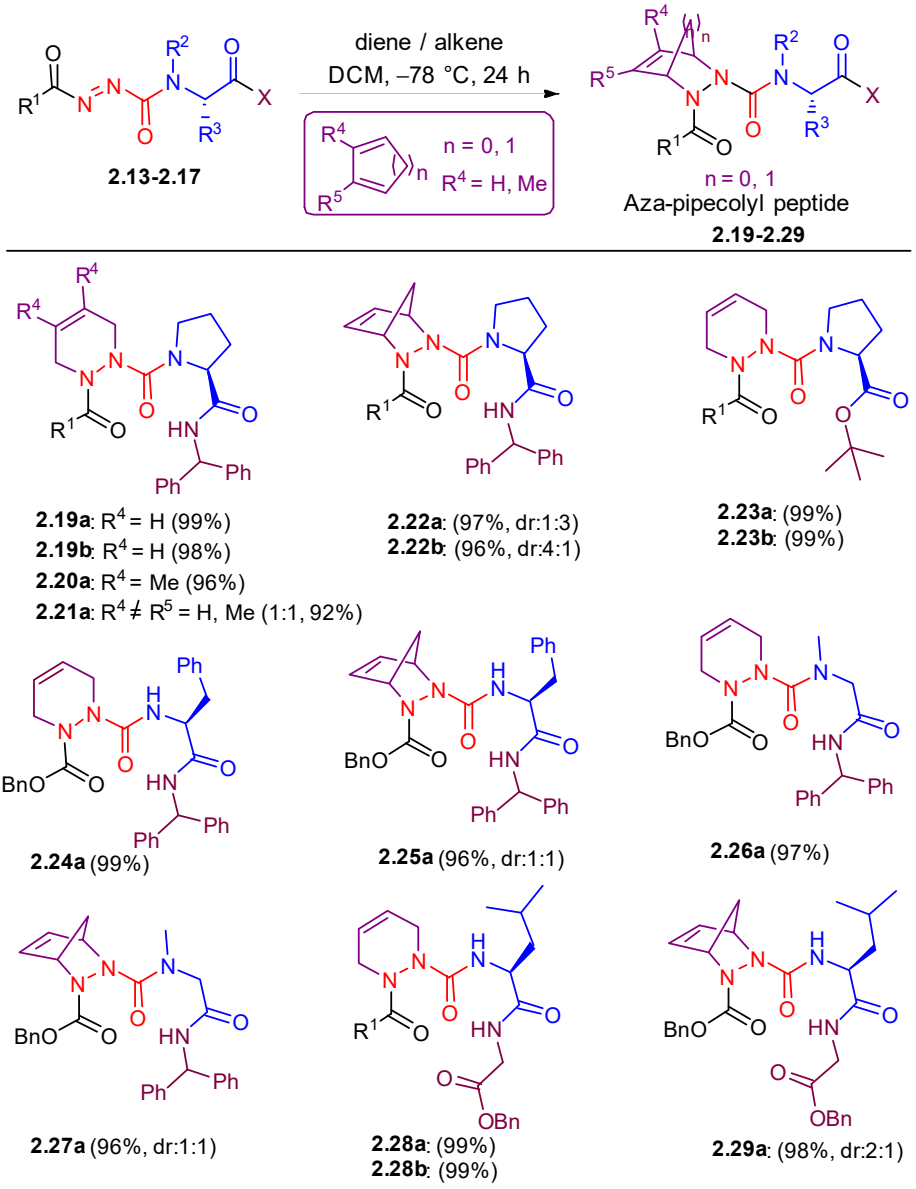

Molecular ions characteristic of Diels–Alder adducts were observed from reactions between cyclohexadiene and azopeptide (e.g., **2.13a**); however, their NMR spectra exhibited an additional set of downfield vinyl protons indicative of Alder–ene reaction products (Scheme 2.3; see SI).[27]

Alder–ene reactions were examined with two different conditions using azopeptides **2.13a** and **2.15a**–**2.16a** and three olefins: 1,3-cyclohexadiene, cycloheptatriene, and

isobutylene. Aza-allylglycines **2.30a**–**2.32a** and **2.34a** were, respectively, obtained using cyclohexadiene and isobutylene in CH_2Cl_2 at −78 °C to rt overnight. Isobutylene was used in a sealed tube. Under these conditions, no product was isolated from the reaction of cycloheptatriene and azopeptide **2.13a**. In contrast, cycloheptatriene and isobutylene reacted, respectively, with azopeptide **2.13a** in the presence of NBS and pyridine at −78 °C in CH_2Cl_2 to give *β*-substituted analogues **2.35a** and **2.33a** in 28% and 52% yield. Azaglycine **2.8a** was isolated with **2.35a** by chromatography of the reaction mixture of azopeptide **2.13a**, likely due to loss of cycloheptatrienyl cation and protonation on silica gel. The Alder–ene reaction typically provided *α*-substituted product under both conditions A and B (e.g., **2.30a** and **2.34a**); however, in cases where no reaction was observed with conditions A, *β*-substituted product was obtained using conditions B.

Scheme 2.3. Aza-allylglycine Synthesis by Alder–Ene Reactions.

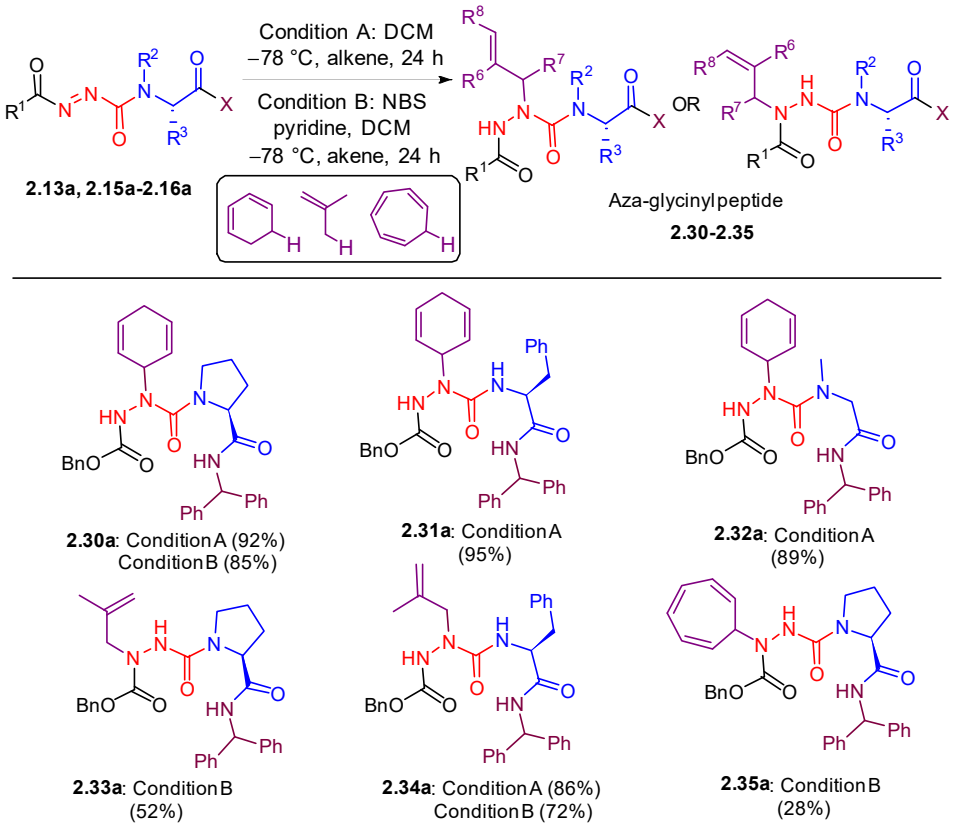

Alder–ene regiochemistry was determined by a combination of NMR spectroscopy, MS experiments, and X-ray analyses (see the SI). Azapeptides **2.33a** and **2.34a** were

examined by heteronuclear multiple-bond correlation (HMBC) NMR spectroscopy using nonuniform sampling at 120 °C, which resolved the proton signals at distinct chemical shifts (Figure 2.5; see the SI).

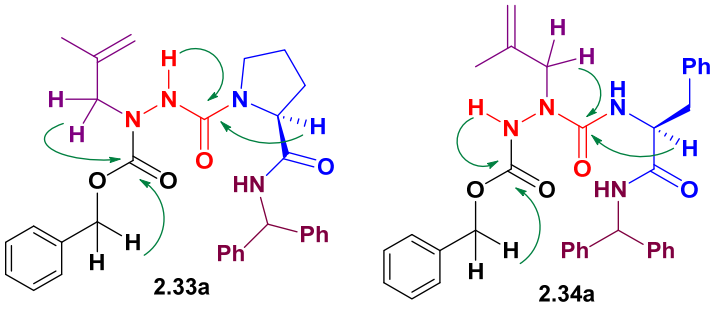

Figure 2.5. HMBC correlations used to assign the regiochemistry of the ene adducts **2.33a** and **2.34a**.

The *α*-position of the cyclohexadiene ring in azapeptides **2.31a** and **2.32a** was determined by hydrogenation with Raney nickel as catalyst, which cleaved the N–N bond giving products with molecular ion peaks of m/z $[M + H]^+$ 456 and 380, respectively, corresponding to fragments **2.36** and **2.37** (Scheme 2.4).

Scheme 2.4. Hydrogenolytic Cleavage and Mass Spectrometry to Confirm Regioselectivity of Aza-allylglycines **2.31a** and **2.32a**.

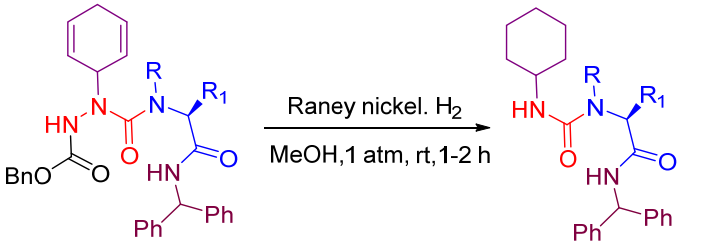

Alder–ene products from reactions of azopeptide **2.13a** with cyclohexadiene and cycloheptatriene crystallized from EtOAc on diffusion of hexane vapors. X-ray diffraction indicated *α*- and *β*- substituted semicarbazides **2.30a** and **2.35a**, respectively (Figure 2.6). In the solid state, *α*-cyclohexadienyl azapeptide **2.30a** adopted dihedral angle values indicative

of a type I β-turn with intramolecular 10-membered hydrogen bond between residues *i* and *i* + 3 (Table 2.1). On the other hand, the torsion angles of β- substituted azaglycine **2.35a** were indicative of a type VIa-like β- turn, albeit the urea ω-dihedral angle *N*-terminal to proline was −169.7°. The ϕ and ψ dihedral angles of the X-ray structures for **2.30a** and **2.35a** are compared in Table 2.1 with ideal turn geometry and the crystal structure of Boc-azaAla-Pro-NH*i*Pr **2.38**, which also adopted a type-I β-turn geometry (Table 2.1).[28] Aza-residue substituent position influenced turn geometry, offering intriguing potential as a design element for controlling peptide and peptoid conformation.

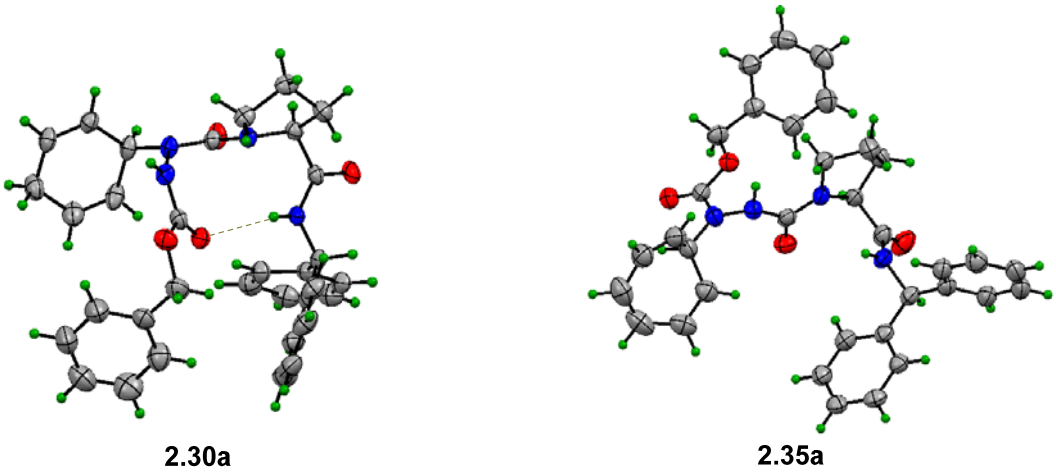

Figure 2.6. X-ray structures of **2.30a** and **2.35a**: broken lines represent inferred hydrogen bonds.

Table 2.1. Structures and ϕ and ψ dihedral angles (in degrees) from crystal analyses and ideal turns.

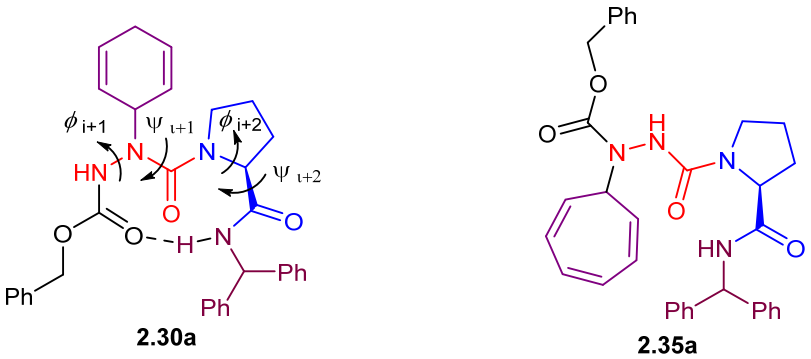

Entry	ϕ^{i+1}	ψ^{i+1}	ϕ^{i+2}	ψ^{i+2}
type I β-turn[28e]	−60	−30	−90	0
2.30a	−60.9	−33.0	−79.0	−14.2
Boc-azaAla-Pro-NH*i*Pr (**2.38**)[28a]	−58.1	−24.7	−66.7	−17.7
type VIa β-turn[28e]	−60	120	−90	0
2.35a	−65.0	153.7	−81.9	−17.8

The practical utility of this method was demonstrated by the synthesis of aza-pipecolyl analogues of melanocyte-stimulating hormone release inhibiting factor-1 (MIF-1, Pro-Leu-Gly- NH^2).[29] A bioactive *β*-turn conformation has been proposed for the positive allosteric modulator activity of this endogenous neuropeptide on the D2 and D4 dopamine receptor subtype subtypes,[30,31] inspiring MIF-1 analogue synthesis to develop therapeutics to treat Parkinson's disease and depression.

Scheme 2.5. Synthesis of aza-pipecolyl-leucyl-glycinamide **2.40**.

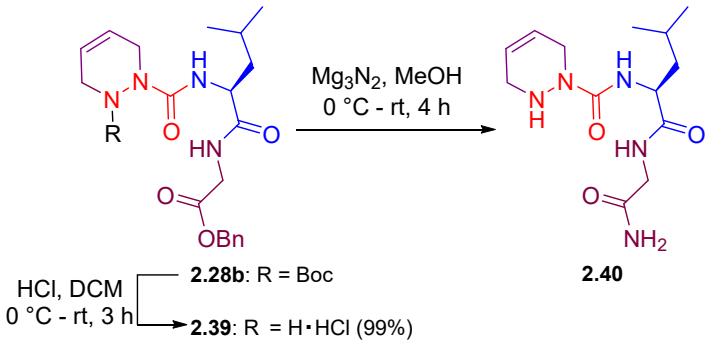

Azapipecolyl MIF-1 analogue **2.40** was synthesized to study the influence of conformational restriction of the prolyl residue on biological activity by removal of the Boc group from **2.28b** with HCl gas in dichloromethane and aminolysis of ester **2.39** with magnesium nitride in methanol (Scheme 2.5).[32]

Conclusion

Pericyclic chemistry of azopeptides has provided effective entry to azapeptides bearing aza-pipecolyl and aza-allylglycyl residues without hydrazine chemistry using ionic intermediates. Oxidation of carbamate protected aza-glycyl peptides followed by Diels−Alder and Alder−ene chemistry on the resulting diazine gave access to diverse azapeptides adopting type I and VI β-turns. The azopeptide approach offers thus a promising means for synthesizing restrained mimics to study the conformations of biologically active peptide sequences in pursuit of enzyme inhibitors and receptor modulators.

Experimental Section

The Supporting Information is available free of charge on the ACS Publications website at DOI: 10.1021/acs.orglett.5b02723.

Experimental procedures, compound characterization data, and NMR spectra for all new compounds (PDF). X-ray data for **2.16a** (CIF), X-ray data for **2.30a** (CIF), X-ray data for **2.35a** (CIF).

Acknowledgments

This research was supported by the Natural Sciences and Engineering Research Council of Canada (NSERC). We thank M. C. Tang, Sylvie Bilodeau, and Francine Belanger of the Université de Montréal centers for HR-MS analysis, NMR spectroscopy, and X-ray crystallography, respectively.

Reference

(1) (a) Mitsunobu, O., The use of diethyl azodicarboxylate and triphenylphosphine in synthesis and transformation of natural products. *Synthesis* **1981**, *1981*, 1-28. (b) Hughes, D. L., Progress in the Mitsunobu reaction. A review. *Org. Prep. Proc. Int.* **1996**, *28*, 127-164.

(2) (a) Trimble, L. A.; Vederas, J. C., Amination of chiral enolates by dialkyl azodiformates. Synthesis of. alpha.-hydrazino acids and. alpha.-amino acids. *J. Am. Chem. Soc.* **1986**, *108*, 6397-6399. (b) Harris, J. M.; McDonald, R.; Vederas, J. C., Synthesis of a chiral azodicarboxamide containing a bridging binaphthyl moiety: electrophilic amination reactions of achiral ester enolates. *J. Chem. Soc., Perkin Trans. 1* **1996**, 2669-2674.

(3) (a) Jenner, G.; Salem, R. B., Anatomy of ene and Diels–Alder reactions between cyclohexadienes and azodicarboxylates. *J. Chem. Soc., Perkin Trans. 2* **1990**, 1961-1964. (b) Desimoni, G.; Faita, G.; Righetti, P.; Sfulcini, A.; Tsyganov, D., Solvent effect in pericyclic reactions. IX. The ene reaction. *Tetrahedron* **1994**, *50*, 1821-1832. (c) Diels, O.; Blom, J. H.; Koll, W., Über das aus Cyclopentadien und Azoester entstehende Endomethylen-piperidazin und seine Überführung in 1, 3-Diamino-cyclopentan. *Eur. J. Org. Chem.* **1925**, *443*, 242-262. (d) Diels, O.; Alder, K., Über die Ursachen der „Azoesterreaktion" . *Eur. J. Org. Chem.* **1926**, *450*, 237-254. (e) Diels, O.; Alder, K., Synthesen in der hydroaromatischen Reihe. *Eur. J. Org. Chem.* **1928**, *460*, 98-122.

(4) (a) Chingle, R.; Lubell, W. D., Azopeptides: Synthesis and Pericyclic Chemistry. *Org. Lett.* **2015**, *17*, 5400-5403. (b) Chingle, R.; Proulx, C.; Lubell, W. D., Azapeptide Synthesis Methods for Expanding Side-Chain Diversity for Biomedical Applications. *Acc. Chem. Res.* **2017**.

(5) lu Wang, Y.; Wang, X. Y.; Ping Li, J.; Ma, D. I.; Wang, H., Using N-Bromosuccinimide and Pyridine as the Oxidation System to Prepare Carbonyl and Aryl Azo Compounds. *Synth. Commun.* **1997**, *27*, 1737-1742.

(6) (a) Bourguet, C. B.; Sabatino, D.; Lubell, W. D., Benzophenone semicarbazone protection strategy for synthesis of aza-glycine containing aza-peptides. *Biopolymers* **2008**, *90*, 824-831. (b) Garcia-Ramos, Y.; Lubell, W. D., Synthesis and alkylation of aza-glycinyl dipeptide building blocks. *J. Pept. Sci.* **2013**, *19*, 725-729.

(7) (a) Johnson, R. L.; Rajakumar, G.; Yu, K. L.; Mishra, R. K., Synthesis of Pro-Leu-Gly-NH2 analogs modified at the prolyl residue and evaluation of their effects on the receptor binding activity of the central dopamine receptor agonist, ADTN. *J. Med. Chem.* **1986**, *29*, 2104-2107. (b) Bhagwanth, S.; Mishra, R. K.; Johnson, R. L., Development of peptidomimetic ligands of Pro-Leu-Gly-NH2 as allosteric modulators of the dopamine D2 receptor. *Beilstein J. Org. Chem.* **2013**, *9*, 204-214, No. 224. (c) Raghavan, B.; Skoblenick, K. J.; Bhagwanth, S.; Argintaru, N.; Mishra, R. K.; Johnson, R. L., Allosteric Modulation of the Dopamine D2 Receptor by Pro-Leu-Gly-NH2 Peptidomimetics Constrained in Either a Polyproline II Helix or a Type II β-Turn Conformation. *J. Med. Chem.* **2009**, *52*, 2043-2051. (d) Mann, A.; Verma, V.; Basu, D.; Skoblenick, K. J.; Beyaert, M. G. R.; Fisher, A.; Thomas, N.; Johnson, R. L.; Mishra, R. K., Specific binding of photoaffinity-labeling peptidomimetics of Pro-Leu-Gly-NH2 to the dopamine D2L receptor: Evidence for the allosteric modulation of the dopamine receptor. *Eur. J. Pharmacol.* **2010**, *641*, 96-101. (e) Bhagwanth, S.; Mishra, S.; Daya, R.; Mah, J.; Mishra, R. K.; Johnson, R. L., Transformation of Pro-Leu-Gly-NH2 peptidomimetic positive allosteric modulators of the dopamine D2 receptor into negative modulators. *ACS Chem. Neurosci.* **2012**, *3*, 274-284.

(8) (a) Ehrensing, R.; Kastin, A.; Larsons, P.; Bishop, G., Melanocyte-stimulating-hormone release-inhibiting factor-I and tardive dyskinesia. *Diseases of the nervous system* **1977**, *38*, 303. (b) Mishra, R.; Chiu, S.; Singh, A.; Kazmi, S.; Rajakumar, A.; Johnson, R., l-Prolyl-l-leucyl-glycinamide (PLG) and its analogues: clinical implications in extrapyramidal motor disorders and depression. *Drugs Future* **1986**, *11*, 203-207.

(9) (a) Khashper, A.; Lubell, W. D., Design, synthesis, conformational analysis and application of indolizidin-2-one dipeptide mimics. *Org. Biomol. Chem.* **2014**, *12*, 5052-5070. (b) Jamieson, A. G.; Boutard, N.; Sabatino, D.; Lubell, W. D., Peptide Scanning for Studying Structure-Activity Relationships in Drug Discovery. *Chem. Biol. Drug Des.* **2013**, *81*, 148-165. (c) Hanessian, S.; McNaughton-Smith, G.; Lombart, H.-G.; Lubell, W. D., Design and synthesis of conformationally constrained amino acids as versatile scaffolds and peptide mimetics. *Tetrahedron* **1997**, *53*, 12789-12854. (d) Somu, R. V.; Johnson, R. L., Synthesis of pipecolic acid-based spiro bicyclic lactam scaffolds as β-turn mimics. *J. Org. Chem.* **2005**, *70*, 5954-5963. (e) Godina, T. A.; Lubell, W. D., Mimics of

Peptide Turn Backbone and Side-Chain Geometry by a General Approach for Modifying Azabicyclo [5.3. 0] alkanone Amino Acids. *J. Org. Chem.* **2011**, *76*, 5846-5849.

(10) (a) Proulx, C.; Sabatino, D.; Hopewell, R.; Spiegel, J.; García Ramos, Y.; Lubell, W. D., Azapeptides and their therapeutic potential. *Future Med. Chem.* **2011**, *3*, 1139-1164. (b) Doan, N. D.; Zhang, J.; Traoré, M.; Kamdem, W.; Lubell, W. D., Solid-phase synthesis of C-terminal azapeptides. *J. Pept. Sci.* **2014**. (c) Turcotte, S.; Bouayad-Gervais, S. H.; Lubell, W. D., N-Aminosulfamide peptide mimic synthesis by alkylation of aza-sulfurylglycinyl peptides. *Org. Lett.* **2012**, *14*, 1318-1321.

(11) (a) Didierjean, C.; Aubry, A.; Wyckaert, F.; Boussard, G., Structural features of thePip/AzPip couple in the crystalline state: influence of the relative AzPip location in an azadipeptide sequence upon the induced chirality and conformational characteristics. *J. Pept. Res.* **2000**, *55*, 308-317. (b) Hemmerlin, C.; Cung, M. T.; Boussard, G., Synthesis and conformational preferences in solution and crystalline states of an aza-tripeptide. *Tetrahedron Lett.* **2001**, *42*, 5009-5012. (c) Chakraborty, T. K.; Ghosh, A.; Sankar, A. R.; Kunwar, A. C., Development of 2, 3-diazabicyclo [2.2. 1] heptane as a constrained azapeptide template and its uses in peptidomimetic studies. *Tetrahedron Lett.* **2002**, *43*, 5551-5554. (d) Toya, T.; Yamaguchi, K.; Endo, Y., Cyclic dibenzoylhydrazines reproducing the conformation of ecdysone agonists, RH-5849. *Bioorg. Med. Chem.* **2002**, *10*, 953-961.

(12) (a) Boeglin, D.; Lubell, W. D., Aza-amino acid scanning of secondary structure suited for solid-phase peptide synthesis with Fmoc chemistry and aza-amino acids with heteroatomic side chains. *J. Comb. Chem.* **2005**, *7*, 864-878. (b) Kumar, A.; Ye, G.; Wang, Y.; Lin, X.; Sun, G.; Parang, K., Synthesis and structure-activity relationships of linear and conformationally constrained peptide analogues of CIYKYY as Src tyrosine kinase inhibitors. *J. Med. Chem.* **2006**, *49*, 3395-3401. (c) Bourguet, C. B.; Proulx, C.; Klocek, S.; Sabatino, D.; Lubell, W. D., Solution-phase submonomer diversification of aza-dipeptide building blocks and their application in aza-peptide and aza-DKP synthesis. *J. Pept. Sci.* **2010**, *16*, 284-296. (d) Proulx, C.; Lubell, W. D., Copper-catalyzed N-arylation of semicarbazones for the synthesis of aza-arylglycine-containing aza-peptides. *Org. Lett.* **2010**, *12*, 2916-2919.

(13) East, S. P.; Ayscough, A.; Toogood-Johnson, I.; Taylor, S.; Thomas, W., Peptidomimetic inhibitors of bacterial peptide deformylase. *Bioorg. Med. Chem. Lett.* **2011**, *21*, 4032-4035.

(14) Ahn, J. H.; Shin, M. S.; Jun, M. A.; Jung, S. H.; Kang, S. K.; Kim, K. R.; Dal Rhee, S.; Kang, N. S.; Kim, S. Y.; Sohn, S.-K., Synthesis, biological evaluation and structural determination of β-aminoacyl-containing cyclic hydrazine derivatives as dipeptidyl peptidase IV (DPP-IV) inhibitors. *Bioorg. Med. Chem. Lett.* **2007**, *17*, 2622-2628.

(15) (a) Aburel, P. S.; Zhuang, W.; Hazell, R. G.; Jørgensen, K. A., Catalytic and enantioselective aza-ene and hetero-Diels–Alder reactions of alkenes and dienes with azodicarboxylates. *Org. Biomol. Chem.* **2005**, *3*, 2344-2349. (b) Pérez Luna, A.; Ceschi, M.-A.; Bonin, M.; Micouin, L.; Husson, H.-P.; Gougeon, S.; Estenne-Bouhtou, G.; Marabout, B.; Sevrin, M.; George, P., Enantioselective desymmetrization of meso bicyclic hydrazines: a novel approach to the asymmetric synthesis of polysubstituted amino cyclopentanic cores. *J. Org. Chem.* **2002**, *67*, 3522-3524. (c) Ryu, I.; Tani, A.; Fukuyama, T.; Ravelli, D.; Montanaro, S.; Fagnoni, M., Efficient C–H/C–N and C–H/C–CO–N Conversion via Decatungstate-Photoinduced Alkylation of Diisopropyl Azodicarboxylate. *Org. Lett.* **2013**, *15*, 2554-2557. (d) Shi, M.; Zhao, G.-L., Aza-Baylis–Hillman reactions of diisopropyl azodicarboxylate or diethyl azodicarboxylate with acrylates and acrylonitrile. *Tetrahedron* **2004**, *60*, 2083-2089. (e) Nair, V.; Mathew, S. C.; Biju, A. T.; Suresh, E., A Novel Reaction of the "Huisgen Zwitterion" with Chalcones and Dienones: An Efficient Strategy for the Synthesis of Pyrazoline and Pyrazolopyridazine Derivatives. *Angew. Chem., Int. Ed.* **2007**, *119*, 2116-2119.

(16) (a) Liu, B.; Li, K.-N.; Luo, S.-W.; Huang, J.-Z.; Pang, H.; Gong, L.-Z., Chiral Gold Complex-Catalyzed Hetero-Diels–Alder Reaction of Diazenes: Highly Enantioselective and General for Dienes. *J. Am. Chem. Soc.* **2013**, *135*, 3323-3326. (b) Liu, B.; Liu, T.-Y.; Luo, S.-W.; Gong, L.-Z., Asymmetric Hetero-Diels–Alder Reaction of Diazenes Catalyzed by Chiral Silver Phosphate: Water Participates in the Catalysis and Stereocontrol. *Org. Lett.* **2014**, *16*, 6164-6167. (c) Crouillebois, L.; Pantaine, L.; Marrot, J.; Coeffard, V.; Moreau, X.; Greck, C., Solvent-and Catalyst-Free Synthesis of Nitrogen-Containing Bicycles through Hemiaminal Formation/Diastereoselective Hetero-Diels–Alder Reaction with Diazenes. *J. Org. Chem.* **2014**, *80*, 595-601.

(17) (a) Mathew, J.; Farber, K.; Nakanishi, H.; Qabar, M., Asymmetric synthesis and conformational analysis of the two enantiomers of the saturated analog of the potent thrombin inhibitor MOL-376. *Tetrahedron Lett.* **2003**, *44*, 583-586. (b) Ban, H.; Gavrilyuk, J.; Barbas III, C. F., Tyrosine bioconjugation through aqueous ene-type reactions: a click-like reaction for tyrosine. *J. Am. Chem. Soc.* **2010**, *132*, 1523-1525.

(18) Bevan, K.; Davies, J.; Hassall, C.; Morton, R.; Phillips, D., Amino-acids and peptides. Part X. Characterisation of the monamycins, members of a new family of cyclodepsipeptide antibiotics. *J. Chem. Soc. C* **1971**, 514-522.

(19) (a) Hoffmann, H., The ene reaction. *Angew. Chem. Int. Ed. Engl.* **1969**, *8*, 556-577. (b) Niu, D.; Hoye, T. R., The aromatic ene reaction. *Nature Chemistry* **2014**, *6*, 34-40.

(20) Fridkin, G.; Gilon, C., Azo cyclization: peptide cyclization via azo bridge formation. *J. Pept Res.* **2002**, *60*, 104-111.

(21) (a) Renner, C.; Kusebauch, U.; Löweneck, M.; Milbradt, A.; Moroder, L., Azobenzene as photoresponsive conformational switch in cyclic peptides*. *J. Pept. Res.* **2005**, *65*, 4-14. (b) Beharry, A. A.; Woolley, G. A., Azobenzene photoswitches for biomolecules. *Chem. Soc. Rev.* **2011**, *40*, 4422-4437. (c) Goodman, M.; Kossoy, A., Conformational Aspects of Polypeptide Structure. XIX. Azoaromatic Side-Chain Effects1, 2. *J. Am. Chem. Soc.* **1966**, *88*, 5010-5015. (d) Ulysse, L.; Cubillos, J.; Chmielewski, J., Photoregulation of cyclic peptide conformation. *J. Am. Chem. Soc.* **1995**, *117*, 8466-8467. (e) Behrendt, R.; Renner, C.; Schenk, M.; Wang, F.; Wachtveitl, J.; Oesterhelt, D.; Moroder, L., Photomodulation of the conformation of cyclic peptides with azobenzene moieties in the peptide backbone. *Angew. Chem., Int. Ed.* **1999**, *38*, 2771-2774.

(22) Bourguet, C. B.; Sabatino, D.; Lubell, W. D., Benzophenone semicarbazone protection strategy for synthesis of aza-glycine containing aza-peptides. *Peptide Science* **2008**, *90*, 824-831.

(23) Jlalia, I.; Lensen, N.; Chaume, G.; Dzhambazova, E.; Astasidi, L.; Hadjiolova, R.; Bocheva, A.; Brigaud, T., Synthesis of an MIF-1 analogue containing enantiopure (S)-α-trifluoromethyl-proline and biological evaluation on nociception. *Eur. J. Med. Chem.* **2013**, *62*, 122-129.

(24) (a) Mhidia, R.; Vallin, A.; Ollivier, N.; Blanpain, A.; Shi, G.; Christiano, R.; Johannes, L.; Melnyk, O., Synthesis of Peptide− Protein Conjugates Using N-Succinimidyl

Carbamate Chemistry. *Bioconj. Chem.* **2010**, *21*, 219-228. (b) Garcia-Ramos, Y.; Lubell, W. D., Synthesis and alkylation of aza-glycinyl dipeptide building blocks. *J. Pept. Sci.* **2013**, *19*, 725-729.

(25) (a) Fahr, E.; Lind, H., The Chemistry of α-Carbonyl Azo Compounds. *Angew. Chem. Int. Ed. Engl.* **1966**, *5*, 372-384. (b) Mohammed, I. A.; Mustapha, A., Synthesis of new azo compounds based on N-(4-hydroxypheneyl) maleimide and N-(4-methylpheneyl) maleimide. *Molecules* **2010**, *15*, 7498-7508.

(26) Small, R., Ethyl (N-phenylcarbamoyl) azoformate. *Acta Crystallogr. Section C: Cryst. Str. Comm.* **1990**, *46*, 1977-1978.

(27) (a) Franzus, B.; Surridge, J. H., The Reaction of Ethyl Azodicarboxylate with 1, 3-and 1, 4-Cyclohexadienes. *J. Org. Chem.* **1962**, *27*, 1951-1957. (b) Franzus, B., The Mechanism of Azo Ester Addition—Abstraction Reactions with Cyclic Dienes. *J. Org. Chem.* **1963**, *28*, 2954-2960. (c) Jenner, G.; Ben Salem, R., Anatomy of ene and Diels–Alder reactions between cyclohexadienes and azodicarboxylates. *J. Chem. Soc., Perkin Transactions 2* **1990**, 1961-1964. (d) Jacobson, B. M.; Feldstein, A. C.; Smallwood, J. I., Ene reactions of conjugated dienes. Rate enhancements in cyclic 1, 3-dienes and dependence of the ene adduct: Diels-Alder adduct ratio on enophile structure. *J. Org. Chem.* **1977**, *42*, 2849-2853.

(28) (a) Andre, F.; Boussard, G.; Bayeul, D.; Didierjean, C.; Aubry, A.; Marraud, M., Aza-peptides II. X-Ray structures of aza-alanine and aza-asparagine-containing peptides. *J. Pept. Res.* **1997**, *49*, 556-562. (b) Baures, P. W.; Ojala, W. H.; Gleason, W. B.; Mishra, R. K.; Johnson, R. L., Design, Synthesis, X-ray Analysis, and Dopamine Receptor-Modulating Activity of Mimics of the" C5" Hydrogen-Bonded Conformation in the Peptidomimetic 2-Oxo-3 (R)-[(2 (S)-pyrrolidinylcarbonyl) amino]-1-pyrrolidineacetamide. *J. Med. Chem.* **1994**, *37*, 3677-3683. (c) St-Cyr, D. J.; Maris, T.; Lubell, W. D., Crystal-State Structural Analysis of β-Hydroxy-γ-lactam Constrained Ser/Thr Peptidomimetics. *Heterocycles* **2010**, *82*, 729-737. (d) Venkatachalam, C., Stereochemical criteria for polypeptides and proteins. V. Conformation of a system of three linked peptide units. *Biopolymers* **1968**, *6*, 1425-1436. (e) Hutchinson, E. G.; Thornton, J. M., A revised set of potentials for beta-turn formation in proteins. *Protein Sci.* **1994**, *3*, 2207.

(29) (a) Bhagwanth, S.; Mishra, R. K.; Johnson, R. L., Development of peptidomimetic ligands of Pro-Leu-Gly-NH2 as allosteric modulators of the dopamine D2 receptor. *Beilstein J. Org. Chem.* **2013**, *9*, 204-214. (b) Raghavan, B.; Skoblenick, K. J.; Bhagwanth, S.; Argintaru, N.; Mishra, R. K.; Johnson, R. L., Allosteric modulation of the dopamine D2 receptor by pro-leu-gly-NH2 peptidomimetics constrained in either a polyproline II helix or a type II β-turn conformation. *J. Med. Chem.* **2009**, *52*, 2043-2051. (c) Mann, A.; Verma, V.; Basu, D.; Skoblenick, K. J.; Beyaert, M. G.; Fisher, A.; Thomas, N.; Johnson, R. L.; Mishra, R. K., Specific binding of photoaffinity-labeling peptidomimetics of Pro-Leu-Gly-NH 2 to the dopamine D 2L receptor: Evidence for the allosteric modulation of the dopamine receptor. *Eur. J. Pharmacol.* **2010**, *641*, 96-101.

(30) Srivastava, L. K.; Bajwa, S. B.; Johnson, R. L.; Mishra, R. K., Interaction of l-Prolyl-l-Leucyl Glycinamide with Dopamine D2 Receptor: Evidence for Modulation of Agonist Affinity States in Bovine Striatal Membranes. *J. Neurochem.* **1988**, *50*, 960-968.

(31) Genin, M. J.; Mishra, R. K.; Johnson, R. L., Dopamine receptor modulation by a highly rigid spiro bicyclic peptidomimetic of Pro-Leu-Gly-NH2. *J. Med. Chem.* **1993**, *36*, 3481-3483.

(32) (a) Veitch, G. E.; Bridgwood, K. L.; Ley, S. V., Magnesium nitride as a convenient source of ammonia: Preparation of primary amides. *Org. Lett.* **2008**, *10*, 3623-3625. (b) Bridgwood, K. L.; Veitch, G. E.; Ley, S. V., Magnesium nitride as a convenient source of ammonia: preparation of dihydropyridines. *Org. Lett.* **2008**, *10*, 3627-3629.

Chapter 3: Design Biomedical Application of Azopeptides in the synthesis of potent Smac analogs

3.1. Context

With the goal of enhancing potency, receptor affinity and selectivity, various backbone modifications have been used to lock bioactive peptides in active conformers.[1] Valine is a relatively abundant, β-branched amino acid with a preference for β-sheet conformation;[2] however, valanyl residues are observed in the turn positions of several biologically active peptides.[3] In particular, valine has been suggested to sit at the *i*+1 position of a β-turn in the active conformer of the second mitochondria-derived activator of caspase (Smac)/direct inhibitor of apoptosis-binding protein sequence (H-Ala-Val-Pro-Ile-NH_2, AVPI, **3.3**). Combining interests in the application of aza-residues to control backbone conformation and the development of novel therapeutic prototypes to treat cancer, the chapter explores the synthesis and application of a set of constrained aza-valine analogs in Smac mimics.

Constrained valine residues have been embedded in various heterocyles. For example, enantiomerically pure α-amino β-methyl γ-lactam-bridged dipeptide analogues of Val-Ala have been synthesized starting from L-aspartic acid.[4] Similarly, β-methyl and β,β-dimethylprolines have been conceived as proline-valine chimeras to explore relationships between side chain and backbone conformation in peptides.[5]

In the interest to explore the importance of valine orientation for binding and activity of AVPI (**3.3**), a series of aza-valine Smac mimics were designed, synthesized and examined for capacity to induce apoptosis in breast cancer cell lines.[6] Smac promotes apoptosis in cells by binding to certain inhibitors of apoptosis proteins (IAP) and blocking their interactions with caspases. The *N*-terminal four residue peptide sequence AVPI in Smac has been demonstrated to play a central role in disruption of the IAP-caspase interaction to promote apoptosis. Crystal and NMR solution structures have revealed that the *N*-terminal Smac sequence binds to a surface groove on the IAP (Figure 3.1).[7] The turn conformation has inspired conception of constrained analogs, such as indolizidinone **3.5** (Figure 3.2), to rigidify the Val-Pro dipeptide and enhance potency.[8,7] Moreover, replacement of the valine residue of AVPI by aza-glycine and aza-phenylalanine residues **3.6** has respectively provided

Smac analogs that induce apoptosis in breast cancer cells by a mechanism that implicates caspase 9.[9]

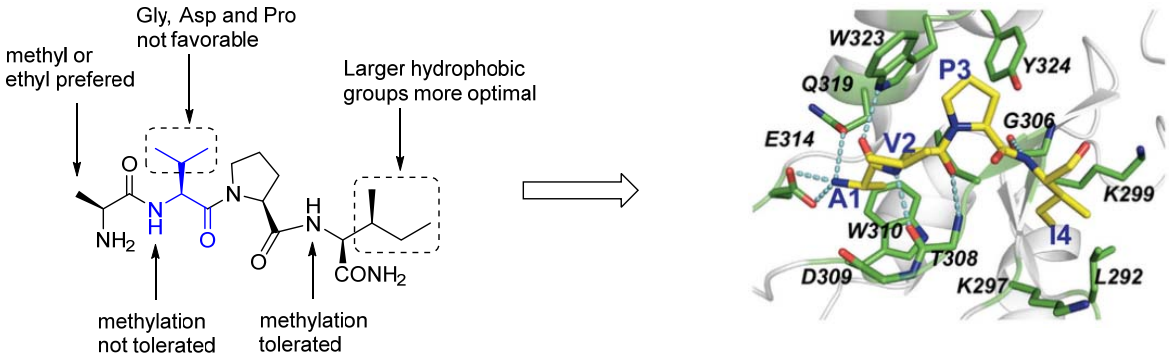

Figure 3.1. Structure-activity relationship (SAR) of Smac based peptides to IAP and detailed interactions between the AVPI binding motif and IAPs residues.[7]

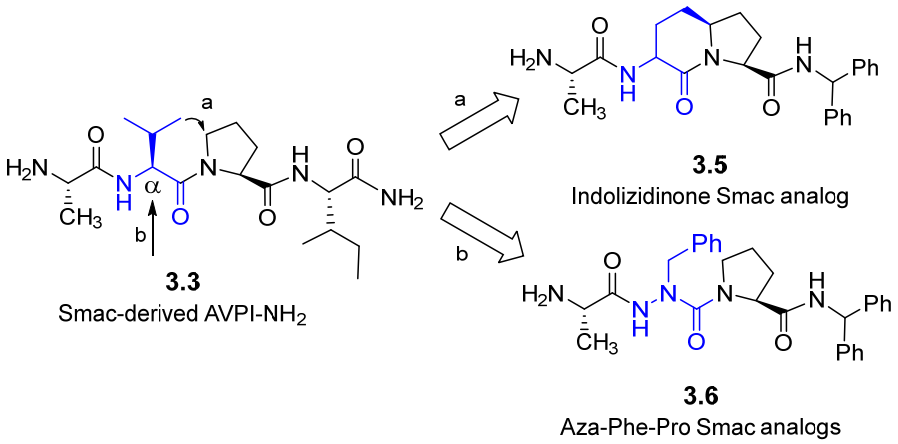

Figure 3.2. Designs of constrained Smac mimetics.[7,9]

In the context of research towards anticancer drugs, in the chapter which is composed of two publications, a set of constrained aza-valine analogs were inserted into AVPI by an approach featuring azopeptide chemistry. Diels-Alder chemistry on azopeptides in solution were used to prepare aza-pipecolate and aza-methanopipecolate peptides. Moreover, the Alder-ene reaction with cyclohexadiene was used to install an aza-cyclohexylglycine residue into the Smac peptide. Elongation from the aza-residue proved challenging and was surmounted using different coupling reagents.[6,10] Finally, the set of constrained aza-valine Smac mimics were examined for ability to induce apoptosis in MCF-7 breast cancer cells.

Among the Smac mimics, aza-cyclohexylglycine **3.11** proved particularly active. The activity of aza-cyclohexylglycine **3.11** paralleled activity of advanced Smac mimics which possess cyclohexylglycine residues, including LBW242, which sensitizes ovarian cancer cells to the antitumor effects of anticancer drugs commonly used in clinic,[11] and LCL-161 which has exhibited effectiveness against various types of cancer.[12] The application of azopeptides in pericyclic chemistry to make constrained aza-valine analogs has thus proven effective for introducing conformational control to generate analogs with promising activity for treating of cancer.

Article 2

Chingle, R.; Ratni, S.; Claing, A.; Lubell, W. D. "Application of Constrained aza-Valine Analogs for Smac Mimicry" *Biopolymers (Pept. Sci.)* **2016**, *106*, 235-244.

DOI: 10.1002/bip.22851

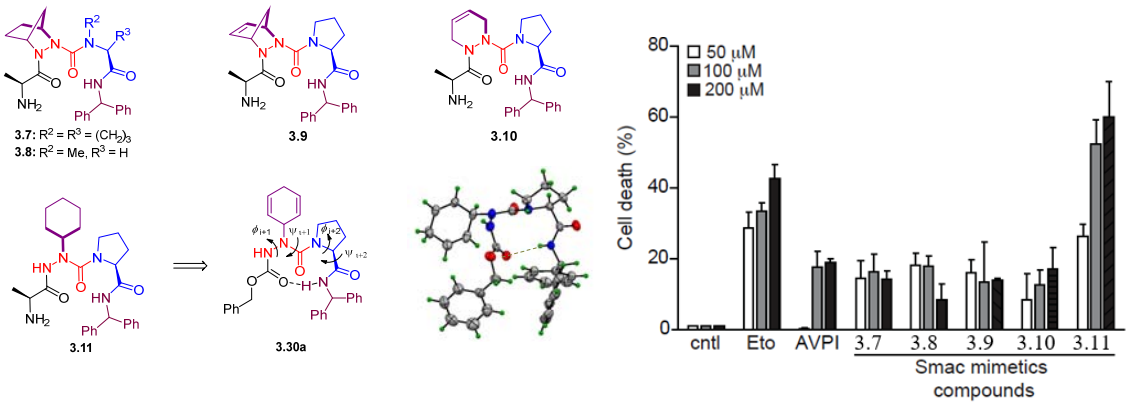

All synthetic work for this article has been done by myself.

The article is written by myself and edited by Professor William D. Lubell.

The biological examination of these Smac analogs on MCF-7 breast cancer cells was performed in the Department of Pharmacology, Universite de Montreal by Ms. Sara Ratni under the supervision of Professor Audrey Claing, who wrote the description of the biological experiments.

Application of Constrained aza-Valine Analogs for Smac Mimicry

Ramesh Chingle,[1] Sara Ratni,[2] Audrey Claing,[2] and William D. Lubell*

Département of Chemistry,[1] Département of Pharmacology,[2] Universite of Montréal, C.P. 6128, Succursale Centre-Ville, Montréal, Québec, H3C 3J7, Canada

E-mail: william.lubell@umontreal.ca

Abstract

Constrained azapeptides were designed based on the Ala-Val-Pro-Ile sequence from the second mitochondria derived activator of caspases (Smac) protein and tested for ability to induce apoptosis in cancer cells. Diels–Alder cyclizations and Alder-ene reactions on azopeptides enabled construction of a set of constrained aza-valine dipeptide building blocks, that were introduced into mimics using effective coupling conditions to acylate bulky semicarbazide residues. Evaluation of azapeptides **3.7**–**3.11** in MCF-7 breast cancer cells indicated azacyclohexanylglycyine analog **3.11** induced cell death more efficiently than the parent tetrapeptide likely by a caspase-9 mediated apoptotic pathway.

Keywords

Apoptosis; aza-valine; semicarbazide; azopeptide; aza-Diels Alder.

Introduction

Azapeptides possess a semicarbazide as an amino amide surrogate in which the α-CH is replaced by nitrogen (e.g., **3.1**, Figure 3.3).[13] Inside peptides, the aza-amino acid residue rigidifies backbone dihedral angle geometry, due to the planar urea and lone pair repulsion between adjacent hydrazine nitrogen.[14] Computation,[15] spectroscopy,[16] and x-ray crystallography,[17] all have shown that azapeptides favor turn geometry, which may facilitate receptor recognition.

Programmed cell death (apoptosis) permits the elimination of aging and abnormal cells to maintain normal tissue development, organism integrity and homeostasis.[18] During cancer, apoptosis is inhibited and cells develop and divide indefinitely.[19] Suppression of

inhibitor-of-apoptosis (IAP) proteins may prevent cell death by inhibiting the activity of caspases.[20] The second mitochondria-derived activator of caspases (Smac) is a potent pro-apoptotic protein released from mitochondria in response to apoptosis stimuli.[21] Smac promotes apoptosis in cells by binding to IAP proteins via its *N*-terminal four residue sequence (Ala-Val-Pro-Ile, **3.3**, Figure 3.3).[22,23] Mimics based on tetra-peptide **3.3** have been targeted to induce apoptosis.[7] For example, the Smac mimetic LCL-161 (**3.4**) is under investigation for the treatment of hepatocellular carcinoma, which is one of the most aggressive and widespread solid tumors.[24]

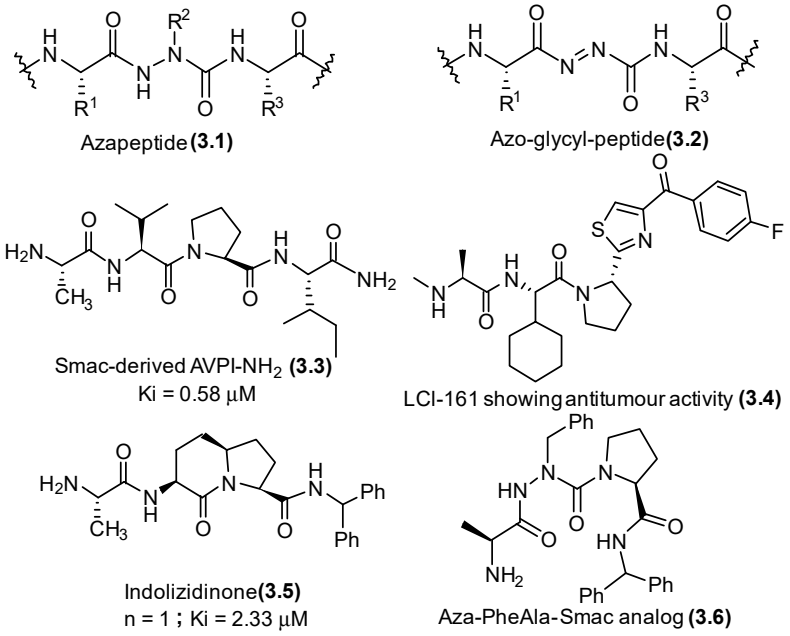

Figure 3.3. Comparison of aza-peptide **3.1** and azo-peptide **3.2**, examples of biologically active Smac mimics **3.3–3.6**.

The purported turn conformation adopted by peptide **3.3** in the biologically relevant protein-protein interaction has led to the synthesis of constrained analogs, such as indolizidinone **3.5**, to rigidify the Val-Pro dipeptide and enhance potency.[10,25] Such bicyclic amino acid analogs serve effectively as Smac mimetics, but demand multiple steps for their synthesis. Recently, aza-amino acyl proline analogs, such as aza-phenylalanine analogue **3.6**, have been assembled relatively efficiently by submonomer synthesis,[26] and shown to induce cell death by a caspase-9 mediated apoptotic pathway,[27] likely due to the greater capacity for

the aza-residue to adopt a turn geometry relative to the native peptide at the binding site in which the valine residue is accommodated.

With interest to restrict further the conformation of the aza-amino acid residue, we have now targeted aza-valine mimics featuring aza-methano-pipecolate, aza-pipecolate, and aza-cyclohexylglycine residues (**3.7**–**3.11**, Figure 3.4).

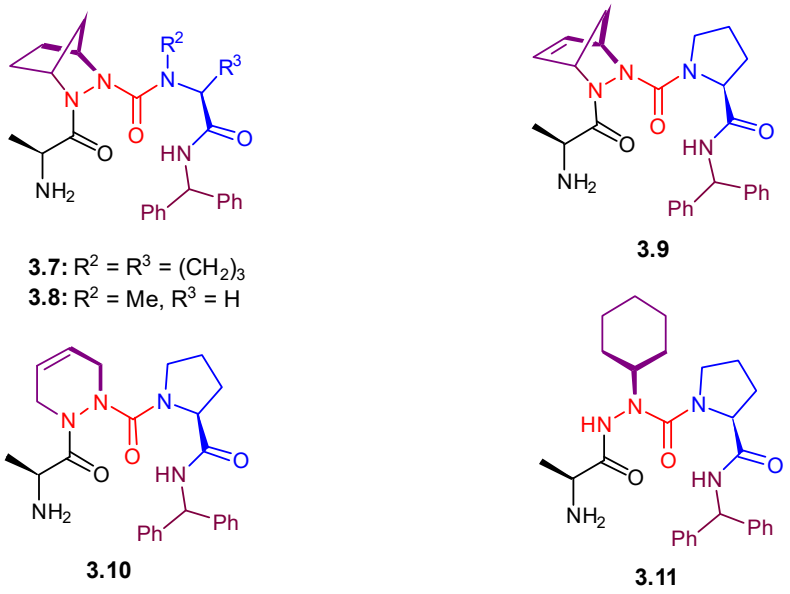

Figure 3.4. Constrained aza-Valine analogs **3.7**–**3.11** (valine side chain highlighted in bold).

Analogs **3.7**–**3.11** were pursued using pericyclic chemistry on the diazo dicarbonyl moiety of azopeptides (e.g., **3.2**).[28] For example, azopeptides **3.12** and **3.13** underwent Diels–Alder reactions respectively with cyclopentadiene and butadiene to give aza-methano-pipecolate and aza-pipecolate dipeptides **3.14**–**3.16**.[28] On the other hand, aza-cyclohexadienyl glycines **3.17a** and **3.17b** were obtained from Alder-ene reactions on azopeptide **3.13** (Scheme 3.1).[28] For example, herein we report that aza-cyclohexadienylglycine **3.17b** was obtained in 93% yield from the reaction of azopeptide **3.13b** and cyclohexadiene in dichloromethane at 78 °C. Elaboration of constrained valine dipeptides **3.14**–**3.17** into Smac mimetics **3.7**–**3.11** has now been achieved by development of effective means to couple amino acids onto bulky semicarbazides.

Scheme 3.1. Synthesis of constrained aza-valine dipeptides **3.14**–**3.17** by Diels–Alder and Alder-ene reactions.

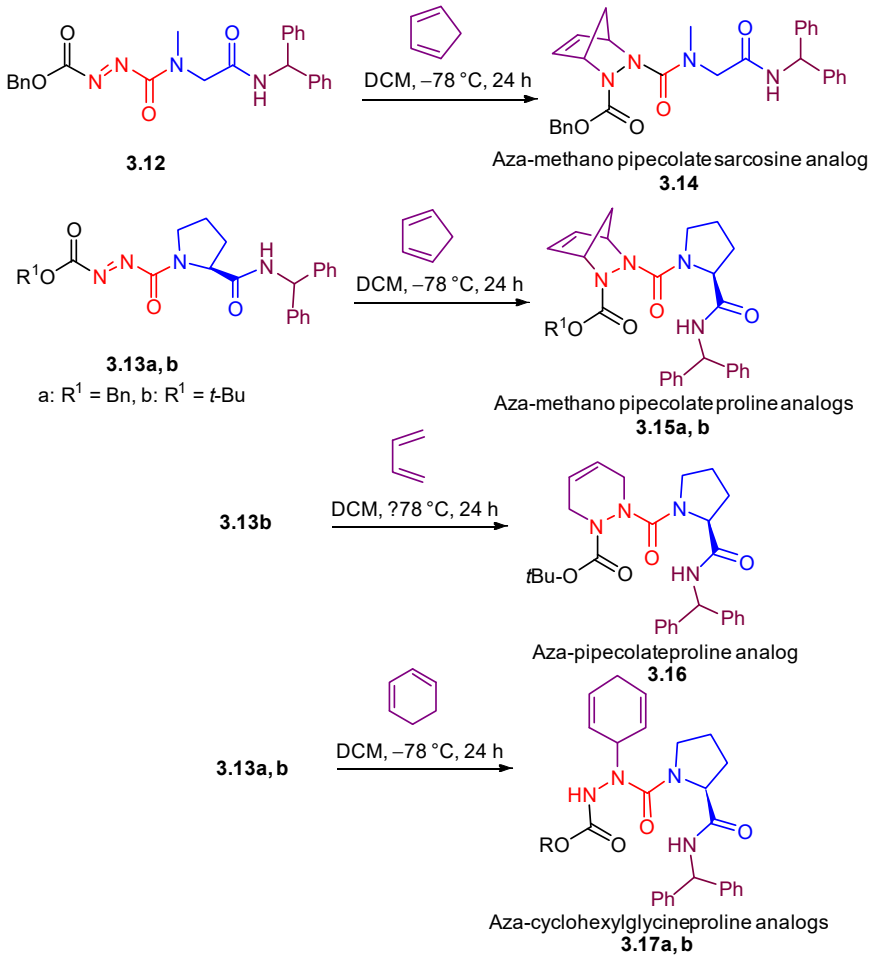

Results and Discussion

With constrained aza-dipeptide amides **3.14**–**3.17** in hand, the syntheses of AVPI analogs entailed protecting group removals, olefin reductions and couplings onto the relatively sterically hindered semicarbazides. Hydrogenation of aza-Diels–Alder adducts **3.15a** and **3.14**, and Alder-ene product **3.17a** removed the Cbz group and reduced the olefins to provide respectively bicyclic semicarbazides **3.18** and **3.19**, and aza-cyclohexylglycine **3.25** (Schemes 3.2 and 3.5). Alternatively, removal of the Boc protecting group from aza-Diels–Alder adducts **3.15b** and **3.16** without double bond reduction was performed with dry HCl gas in dichloromethane (Scheme 3.3 and 3.4). Attempts to remove the Boc group from aza-cyclohexadienylglycine **3.17b** using HCl gas resulted however in loss of the

cyclohexadiene ring and recovery of a product with molecular ion corresponding to the aza-glycine dipeptide (m/z [M + H] = 339). Under the acid conditions, elimination of the semicarbazide with formation of benzene may likely account for the loss of the side chain.

The reduced nucleophilicity of the semicarbazide residue necessitated an effective coupling method to attach the subsequent amino acid to the aza-residue.[29,30] Since the first synthesis of a biologically active azapeptide,[31] in which dicyclohexylcarbodiimide was employed to link *N*-(Cbz)-*N*-nitro-L-arginine to aza-valanyl-*O*-(benzoyl)-tyrosine ethyl ester in solution, a variety of approaches have been employed to acylate aza-amino acid derivatives. For example, more reactive activating reagents have been used in the coupling step, including TBTU,[29c] HATU,[32] and amino acid chlorides generated *in situ* with triphosgene activation.[30,33] Moreover, symmetric anhydrides have been successfully used to couple to the semi-carbazide residue linked to a solid support.[29a] Moreover, microwave irradiation has been employed to facilite coupling onto aza residues in less than an hour at 75 °C, using the HATU and *N*-(Fmoc)amino acid chloride procedures.[29d]

In the case of semicarbazides **3.18**, **3.19**, **3.22**, and **3.24**, acylation proved particularly challenging, presumably because of the combination of steric hindrance and electronic deactivation. For example, attempts to couple *N*-(Boc)alanine to semicarbazide **3.18** was examined with a variety of conditions with minimal success: TBTU/HOBT,[34] EDCl/HOBT,[35] and DIC/AtOH.[36] Efforts were similarly unsuccessful using the mixed anhydride generated from *N*-(Boc)alanine, *iso*-butyl chloroformate and *N*-methylmorpholine.[37] After examination of a variety of previously reported conditions, the combination of benzotriazol-1-yloxytripyrrolidinophosphonium hexafluorophosphate (PyBOP) and di-*iso*-propyl ethyl amine (DIEA) proved effective for the coupling of *N*-(Boc)alanine to semicarbazides **3.18** and **3.19** giving respectively aza-tripeptides **3.20** and **3.21** in 75% and 44% yields.[38] To the best of our knowledge, PyBOP had not previously been used in the acylation of semicarbazides.

Scheme 3.2. Synthesis of aza-methano-pipecolates **3.7** and **3.8**.

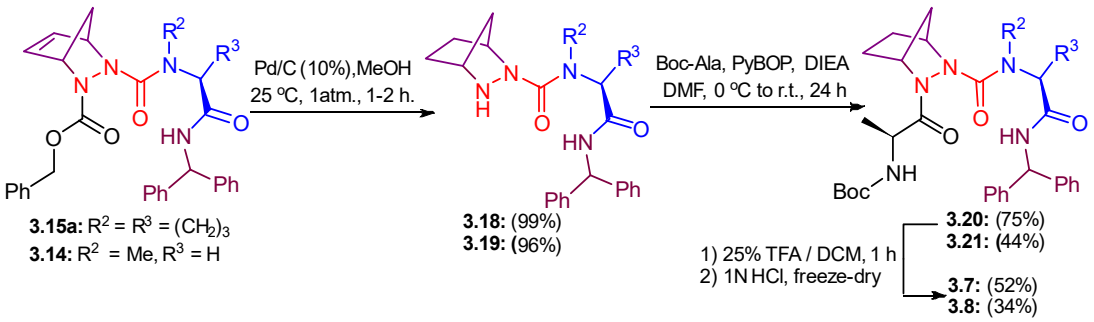

Scheme 3.3. Synthesis of aza-methano-pipecolate **3.9**.

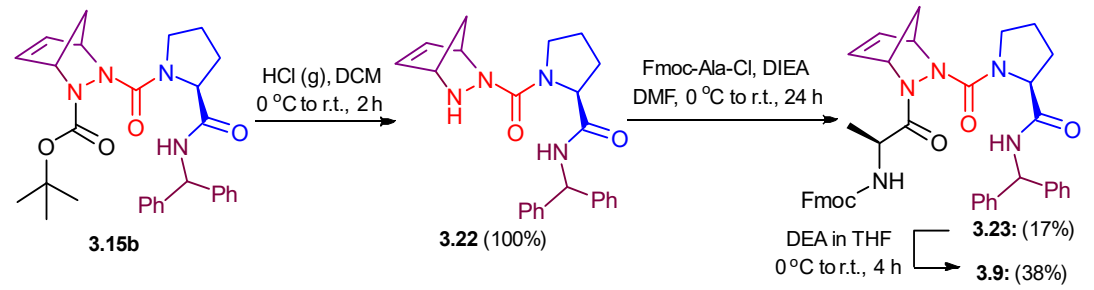

Scheme 3.4. Synthesis of aza-pipecolate **3.10**.

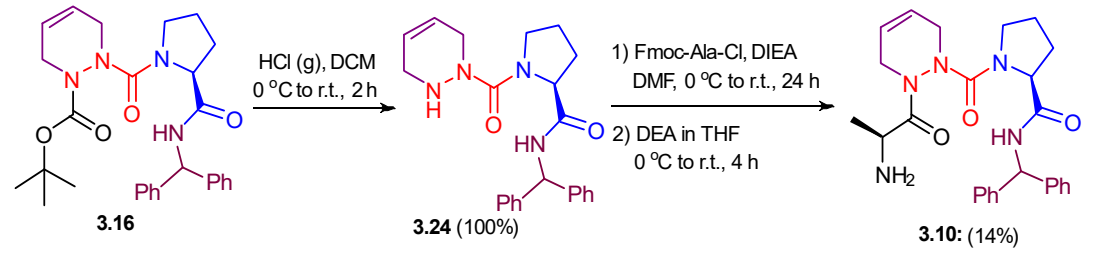

In contrast, attempts to employ the PyBOP and DIEA conditions in couplings onto unsaturated aza-methanopipecolate **3.22** and aza-pipecolate **3.24**, both were unsuccessful, perhaps due to added ring strain from the olefin reducing the nucleophilicity of the semicarbazide nitrogen.[39] After examination of a variety of other coupling conditions, acylation was best achieved using *N*-Fmoc-amino acid chlorides. The acid chloride prepared from *N*-(Fmoc)alanine acylated effectively semicarbazide **3.22** in the presence of DIEA to give the azatripeptide **3.23**, albeit in 17% yield.[40] Moreover acylation of semicarbazide **3.24** was performed using *N*-(Fmoc)alanine chloride and DIEA to provide *N*-(Fmoc)-alaninyl-

aza-dehydropipecolyl prolinamide in 39% conversion as assessed by LCMS analysis. In comparison, alaninyl-aza-cyclohexyglycine analog **3.26** was synthesized by acylation of semicarbazide **3.25** with *N*-(Fmoc)alanine acid chloride in 44% yield.

Removal of the Boc group from **3.20** and **3.21** with 25% TFA in dichloromethane, salt exchange using 1N HCl, followed by HPLC purification and freeze-drying afforded compounds **3.7** and **3.8** in 52 and 34% yields. Removal of the Fmoc group from **3.23** and **3.26** was performed using a solution of diethyl amine (DEA) in THF, which yielded azapeptides **3.9** and **3.11** in 38, and 42% yields, respectively, after purification using preparative HPLC (Schemes 3.2–3.5, see Supporting Information).

Scheme 3.5. Synthesis of aza-cyclohexylglycine **3.11**.

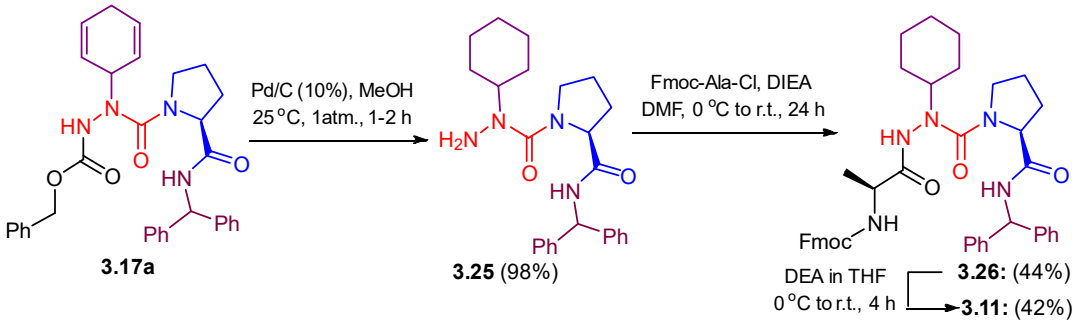

Without further purification, the alaninyl-aza-dehydropipecolyl prolinamide was treated with a solution of DEA in THF and purified by preparative reverse-phase HPLC to afford **3.10** in 14% yield over two steps from the corresponding analog **3.24**.

In addition, Ala-Val-Pro-Ile-NH_2 was prepared as a positive control by standard Fmoc-based solid-phase peptide synthesis on Rink amide resin as described previously.[27] The proapoptotic potential of Smac mimics **3.7**–**3.11** was examined in MCF-7 breast cancer cells at three different concentrations: 50, 100, and 200 μM (Figure 3.5).

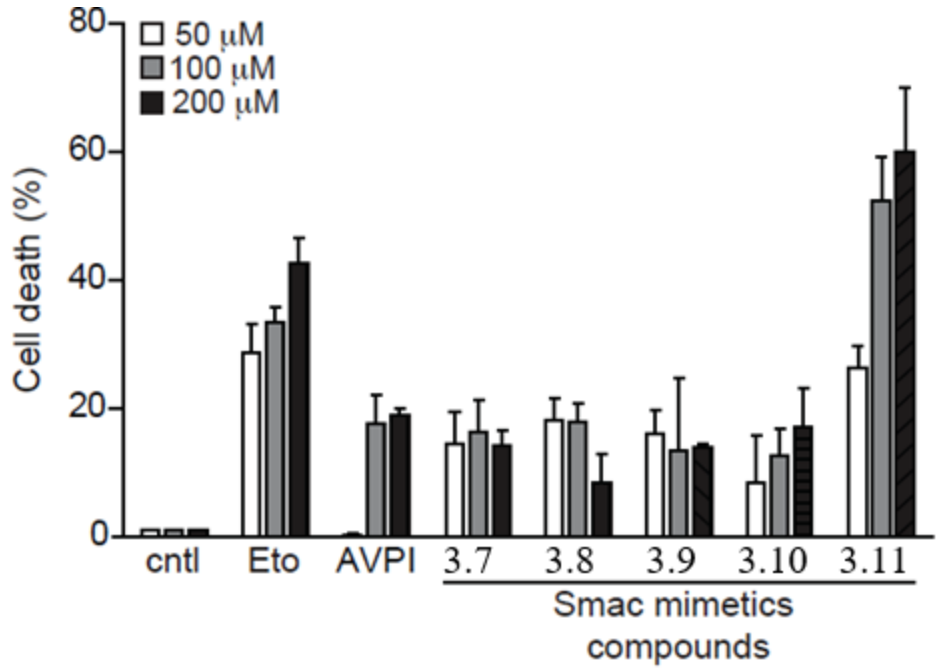

Figure 3.5. Smac mimetics induced cell death in the MCF-7 breast cancer cell line. Serum-starved cells were treated with DMSO, etoposide (Eto), AVPI or different Smac mimetic compounds for 72h at the indicated concentrations. Cell death was determined by the Trypan blue exclusion assay. All experiments were performed in triplicate and data are mean ± SEM of three independent experiments.

At these concentrations, compared to vehicle (DMSO), AVPI-NH_2 and Smac mimics **3.7**–**3.10**, all induced cell death at levels as high as ~20%, inferior to the topoisomerase II inhibitor Etoposide, which blocks DNA replication.[21] On the other hand, azacyclohexylglycine mimic **3.11** induced cell death similar to Etoposide at 50 μM (~30%), and superior to Etoposide at 100 and 200 μM, up to 60% relative to vehicle. Considering AVPI (**3.3**) as well as aza-phenylalanine analog **3.6** were previously shown to increase levels of caspase-9 using Western blot assays, aza-cyclohexylglycine analog **3.11** is expected to function by a similar mechanism of action.[27] In addition, evidence to support the possibility that mimic **3.11** may adopt a turn centered on the aza-cyclohexylglycinyl-proline sequence comes from X-ray crystallographic analysis of its precursor azapeptide **3.17a**.[28]

Conclusion

In conclusion, we have disclosed the synthesis and incorporation of novel constrained valine analogs into azapeptide Smac mimetics. Selective choice of amine protection with Cbz and Boc groups empowered respectively synthesis of saturated and unsaturated valine mimics. Chain elongation by acylation of the N-terminal of the aza-residue proved however particularly challenging and was surmounted respectively using PyBOP and *N*-(Fmoc)amino acid chlorides to deliver Smac mimics **3.7**–**3.11** after final removal of the amine protection. Analysis of the constrained valine Smac mimics indicated that best potency was obtained with aza-cyclohexylglycine analog **3.11**, which induced up to 60% cell death relative to vehicle in a breast cancer cell assay. Towards the development of improved therapy for treating cancer, the application of azopeptides in pericyclic chemistry to make constrained aza-valine analogs has proven a powerful method for introducing conformational control as well as for generating analogs with promising activity.

Experimental Section

General Methods:

Unless specified, all non-aqueous reactions were run under an inert argon atmosphere. All glassware was stored in the oven or flame-dried and let cool under an inert atmosphere prior to use. Anhydrous solvents (THF, DCM, and DMF) were obtained by passage through solvent filtration systems (GlassContour, Irvine, CA). Visualization of the developed chromatogram was performed by UV absorbance or staining with ceric ammonium molybdate or potassium permanganate solutions. Silica gel chromatography as performed using 230-400 mesh silica gel (Silicycle), and TLC was on glass-backed silica plates.[41] . Melting points were obtained on a Buchi melting point B-540 apparatus and are uncorrected. Specific rotations, $[\alpha]_D$ values, were calculated from optical rotations measured at 20 °C in $CHCl_3$ or MeOH at the specified concentrations (c in g/100 ml) using a 1-dm cell length (l) on a Perkin-Elmer Polarimeter 241 at 589 nm, using the general formula: $[\alpha]_D^{20} = (100 \times \alpha)/(l \times c)$. Nuclear magnetic resonance spectra (^1H, ^{13}C, HMBC) were recorded on Bruker AV 400, AV III 400 and AV 500 spectrometers. ^1H NMR spectra were referenced to $CDCl_3$ (7.26 ppm), CD_3OD (3.31 ppm), DMSO-d_6 (2.50 ppm) or $(CD_3)_2CO$ (2.05 ppm) and ^{13}C

NMR spectra were measured in $CDCl_3$ (77.16 ppm), CD_3OD (49.0 ppm), DMSO-d_6 (39.52 ppm), or $(CD_3)_2CO$ (29.84 ppm) as specified below. Coupling constants, *J* values were measured in Hertz (Hz) and chemical shift values in parts per million (ppm). NMR experiments at high temperature (120 °C) were used to enhance resolution of proton signals of urea isomers.[42] In cases of isomers of conformation, the minor isomer ^1H and ^{13}C NMR data are reported in brackets and parentheses respectively. Infrared spectra were recorded in the neat on a Perkin Elmer Spectrum One FTIR instrument and are reported in reciprocal centimetres (cm^{-1}). Accurate mass measurements were performed on a LC-MSD instrument from Agilent technologies in positive electrospray ionisation (ESI) mode at the Université de Montréal Mass Spectrometry facility. Sodium adducts $[M+Na]^+$ were used for empirical formula confirmation.

Reagents used: Palladium-on-carbon (10 wt%), *N*-Boc alanine, *N*-Fmoc-alanine, *N*-Bromo succinimide (NBS), pyridine, cyclohexadiene, diisopropyl ethyl amine (DIEA) and diethyl amine (DEA), all were purchased from Aldrich or Alfa Aesar and used without further purification. *N*-Fmoc-Alanine acid chloride was synthesized according to the literature method.[40] Benzotriazol-1-yl-oxytripyrrolidinophosphonium hexafluorophosphate (PyBop) was purchased from GL Biochem™ and recrystallized prior to use from dry CH_2Cl_2/Et_2O (melting point, 156 °C) and stored in the dark.

EXPERIMENTAL PROCEDURES

N-Boc-Aza-1,4-cyclohexadienylglycinyl-L-proline Benzhydrylamide (3.17b)

A stirred solution of azopeptide **3.13b** (1 eq., 0.19 g, 0.435 mmol, synthesized according to reference 17) in DCM (20 mL) at –78 °C was treated with cyclohexadiene (10 eq., 0.349 g, 0.406 mL, 4.35 mmol). The bath was removed. The reaction mixture was allowed to warm to room temperature and stirred overnight. The volatiles were removed under vacuum and the residue was purified by silica gel chromatography using 80% ethyl acetate in hexane to give azapeptide **3.17b** (0.21 g, 0.406 mmol, 93 %) as white solid: Rf 0.42 (1:4 hexane:EtOAc); mp 86−87 °C; $[\alpha]_D^{20}$ 106.5° (c 0.34, $CHCl_3$); ^1H NMR (400 MHz, $(CD_3)_2CO$) δ 8.38 – 8.20 (br s, 2H), 7.57 – 7.13 (m, 10H), 6.36 (d, 1H), 6.13 – 5.99 (m, 1H), 5.99 – 5.80 (m, 2H), 5.70 – 5.52 (m, 1H), 5.45 – 5.29 (br s, 1H), 4.63 – 4.34 (m, 1H), 3.73 –

3.50 (m, 1H), 3.50 – 3.30 (m, 1H), 2.74 – 2.52 (m, 2H), 2.38 – 2.19 (m, 1H), 1.97 – 1.74 (m, 2H), 1.74 – 1.56 (m, 1H), 1.22 (s, 9H); ^{13}C NMR (100 MHz, $(CD_3)_2CO$) δ 171.8, 159.6, 156.4, 144.0, 143.3, 130.5, (129.28), (129.25), 129.15, 128.8, 128.7, (128.6), (128.2), 127.7, 127.4, 125.4, 125.3, 81.1, 64.0, 56.6, 53.2, 50.9, 31.2, 28.3, 26.6, 26.5; IR (neat) ν_{max}/cm^{-1} 3029, 2979, 1710, 1643, 1523, 1410, 1282, 1154; HRMS m/z calculated for $C_{30}H_{36}N_4NaO_4$ $[M+Na]^+$ 539.2629, found 539.2635.

Aza-3,6-methano-pipecolyl-L-proline Benzhydrylamide (3.18)

To a solution of azapeptide **3.15a** (1 eq., 0.3 g, 0.559 mmol, 1:3 diastereomeric ratio, synthesized according to reference 17) in methanol (6 mL), 10 wt% palladium-on-carbon (0.5 eq., 0.03 g, 0.282 mmol) was added carefully under a stream of argon and the resulting suspension was placed under hydrogen atmosphere (1 atm), and stirred under a balloon of hydrogen at room temperature for the 1-2 h. The mixture was filtered through Celite™, which was washed with methanol, and the filtrate and washings were combined and concentrated to furnish amine **3.18** (0.225 g, 0.556 mmol, 99 %) as pale yellow solid: mp 167−168 °C (the white solid turned dark orange at 167 °C and melted); ^{1}H NMR (400 MHz, DMSO-d_6, 120 °C) δ 8.06 – 7.85 (m, 1H), 7.40 – 7.12 (m, 10H), 6.08 (d, J = 8.3 Hz, 1H), 4.97 – 4.57 (br, 1H), 4.57 – 4.39 (m, 1H), 4.30 – 4.15 (m, 1H), 3.64 – 3.54 (m, 1H), 3.54 – 3.36 (m, 2H), 2.11 – 1.95 (m, 1H), 1.95 – 1.61 (m, 4H), 1.61 – 1.25 (m, 5H); ^{13}C NMR (100 MHz, DMSO-d_6, 120 °C) δ 170.9, 160.6, 141.81, 141.77, 127.61, 127.58, (127.56), (126.54), 126.51, 126.47, 126.24, 126.19, (126.16), 60.4, (60.3), 57.2, 56.9, (56.7), (56.64), 55.6, 48.1, (47.7), 37.1, (36.5), (28.9), (28.7), 28.3, 27.9, 27.1, (27.0), 23.6, (23.1); HRMS *m/z* calculated for $C_{24}H_{28}N_4NaO_2$ $[M+Na]^+$ 427.2105; found 427.2112.

***N*-Boc-Alaninyl-aza-3,6-methano-pipecolyl-L-proline Benzhydrylamide (3.20)**

A solution of azapeptide **3.18** (1 eq., 0.15 g, 0.371 mmol) and DIEA (2 eq., 0.0959 g, 0.123 mL, 0.742 mmol) was added to a solution of *N*-(*tert*-butoxycarbonyl)-L-alanine (1.2 eq., 0.0842 g, 0.445 mmol) and PyBOP (1.5 eq., 0.289 g, 0.556 mmol) in DMF (5 mL), and stirred overnight. The volatiles were removed under vacuum. The residue was dissolved in EtOAc (20 mL), washed with 5 mL of saturated aqueous $NaHCO_3$, followed by brine (20 mL), dried over Na_2SO_4, filtered and evaporated. The residue was purified by column

chromatography using 1:4 hexane:EtOAc as eluant to give azapeptide **3.20** (0.16 g, 0.278 mmol, 75 %) as white solid: Rf 0.4 (1:4 hexane:EtOAc); mp 93−95 °C; ^{1}H NMR (400 MHz, $CDCl_3$) δ 7.54 – 7.10 (m, 10H), 6.34 – 6.08 (m, 1H), 5.58 – 4.91 (m, 1H), 4.81 – 4.53 (m, 2H), 4.53 – 4.36 (m, 1H), 4.30 – 3.98 (m, 2H), 3.91 – 3.40 (m, 1H), 2.62 – 2.26 (br, 1H), 2.26 – 2.02 (m, 2H), 2.02 – 1.56 (m, 7H), 1.50 – 1.37 (m, 9H), 1.37 – 1.21 (m, 3H).; ^{13}C NMR (100 MHz, $CDCl_3$) δ 172.1, 170.4, (170.2), 162.3, (155.2), 155.1, (154.8), 141.8, (141.6), 141.4, (141.3), 128.8, 128.7, 128.5, (128.0), (127.6), 127.5, 127.45, (127.42), 127.3, 79.8, (79.3), 64.9, 63.1, 60.5, (57.7), 57.2, 49.3, (48.1), (36.7), 35.0, 31.1, 29.8, 29.0, (28.53), 28.48, (27.2), 27.1, 25.8, 17.7; HRMS *m/z* calculated for $C_{32}H_{41}N_5NaO_5$ $[M+Na]^+$ 598.2999; found 598.3003.

Alaninyl-aza-3,6-methano-pipecolyl-L-proline Benzhydrylamide (3.7)

N-Boc-Azapeptide **3.20** (1 eq., 0.042 g, 0.073 mmol) was dissolved in a 25% solution of TFA in dichloromethane (5 mL), and stirred for 1 h, at which point complete disappearance of starting material **3.20** was observed by TLC (Rf 0.4, 1:4 hexane:EtOAc). The volatiles were removed under vacuum. The residue was dissolved in CH_2Cl_2 and the solution was evaporated. The residue was suspended in 5 mL of 1N HCl, stirred for 30 min, and freeze-dried to give the hydrochloride salt as off white solid, that was further purified using preparative HPLC on a Waters™ PrepLC instrument with a reverse-phase Gemini™ C18 column (250 × 21.2 mm, 5 μm), UV detection at 214 nm and a binary solvent system consisting of MeOH (0.1% FA) in H_2O (0.1% FA) at a flow rate of 10.0 mL/min. Fractions containing pure peptide were combined, and freeze-dried to afford azapeptide **3.7** (0.018 g, 0.0378 mmol, 52 %) as white solid: ^{1}H NMR (500 MHz, MeOD) δ 7.42 – 7.13 (m, 10H), 6.26 – 6.05 (m, 1H), 4.73 – 4.66 (m, 1H), 4.66 – 4.40 (m, 2H), 3.90 – 3.42 (m, 3H), 2.58 – 2.30 (m, 1H), 2.15 – 1.66 (m, 8H), 1.65 – 1.38 (m, 3H), 0.99 – 0.82 (m, 1H); ^{13}C NMR (125 MHz, MeOD) δ 173.2, (172.3), (162.5), 160.6, (159.9), 159.4, (143.1), 142.9, 142.7, 129.7, (129.59), (129.48), (129.46), 129.42, (128.8), 128.7, (128.65), 128.59, 128.5, (128.37), (128.34), 128.29, 64.8, (64.6), 63.62, 62.8, (62.7), (62.4), (61.2), (61.0), 60.8, (58.4), 58.3, 50.3, (50.2), 38.3, (37.8), 36.7, (36.1), (31.3), 29.9, (28.97), (28.86), 28.0, 25.8, 16.3, (16.1); HRMS *m/z* calculated for $C_{27}H_{34}N_5O_3$ $[M+H]^+$ 476.2656; found 476.2663.

Aza-3,6-methano-pipecolyl-sarcosine Benzhydrylamide (3.19)

Employing the protocol described for the synthesis of azapeptide **3.18**, a solution of *N*-Cbz-azapeptide **3.14** (1 eq., 0.12 g, 0.235 mmol, 1:1 diastereomeric ratio, prepared according to reference 17) in methanol (3 mL) was reacted with 10 wt% palladium-on-carbon (0.5 eq., 0.0125 g, 0.118 mmol) at room temperature for 1-2 h. After filtration through Celite™ and washing, the filtrate and washings were concentrated to yield the amine **3.19** (0.085 g, 0.226 mmol, 96 %) as dark orange solid: ^{1}H NMR (500 MHz, MeOD) δ 7.90 (s, 1H), 7.37 – 7.21 (m, 10H), 6.19 (d, *J* = 3.2 Hz, 1H), 4.13 – 3.95 (m, 2H), 3.04 – 2.89 (m, 3H), 2.48 – 2.33 (m, 1H), 2.07 – 1.96 (m, 1H), 1.94 – 1.78 (m, 2H), 1.76 – 1.57 (m, 4H); ^{13}C NMR (125 MHz, MeOD) δ (171.2), 170.6, (164.7), 160.4, 142.94, 142.86, (142.84), 129.6, 129.5, 128.6, 128.58, (128.57), 128.42, 128.36, 79.5, (61.9), (59.7), 58.23, (58.2), 54.0, (52.7), 52.3, (51.9), (38.4), 38.1, 36.2, (30.9), 30.3, 28.8, (28.5); HRMS *m/z* calculated for $C_{22}H_{26}N_4NaO_2$ $[M+Na]^+$ 401.1948; found 401.1935.

_N_-Boc-Alaninyl-aza-3,6-methano-pipecolyl-sarcosine Benzhydrylamide (3.21)

Employing the protocol described for the synthesis of *N*-Boc-azapeptide **3.20**, amine **3.19** (1 eq., 0.06 g, 0.159 mmol) in DIEA (2 eq., 0.041 g, 0.0524 mL, 0.317 mmol) was added to a solution of *N*-Boc-L-alanine (1.2 eq., 0.036 g, 0.19 mmol) and PyBOP (1.5 eq., 0.124 g, 0.238 mmol) in DMF (2 mL). The residue was purified by column chromatography using 3:7 hexane:EtOAc as eluant to give *N*-Boc-azapeptide **3.21** (0.038 g, 0.0691 mmol, 44 %) as white solid: Rf 0.44 (1:4 hexane:EtOAc); ^{1}H NMR (500 MHz, MeOD) δ 7.37 – 7.21 (m, 10H), 6.22 (s, 1H), 4.73 – 4.56 (m, 1H), 4.47 – 4.28 (m, 2H), 4.26 – 4.01 (m, 2H), 3.27 – 2.93 (m, 3H), 2.10 – 1.50 (m, 6H), 1.50 – 1.37 (m, 9H), 1.35 – 1.17 (m, 3H); ^{13}C NMR (125 MHz, MeOD) δ (170.2), 170.0, 165.0, (164.5), 162.9, (162.6), (157.5), 157.4, (143.0), 142.9, (142.79), 142.75, 129.57, (129.55), (129.53), 128.8, 128.7, 128.6, 128.43, 128.38, (80.5), 80.4, 80.1, (79.53), 79.45, 79.26, (79.0), (66.23), 64.7, (60.9), 59.9, 59.3, 58.4, 37.5, (36.3), (31.4), 29.6, 28.7, (27.5), 18.5, (17.2); HRMS *m/z* calculated for $C_{30}H_{39}N_5NaO_5$ $[M+Na]^+$ 572.2843; found 572.2839.

Alaninyl-aza-3,6-methano-pipecolyl-sarcosine Benzhydrylamide (3.8)

Employing the protocol described for the synthesis of azapeptide **7**, *N*-Boc-azapeptide **3.21** (1 eq., 0.015 g, 0.0273 mmol) was reacted with a 25% solution of TFA in

dichloromethane (2 mL) for 1 h, at which point complete disappearance of **3.21** was observed by TLC (Rf 0.44, 1:4 hexane:EtOAc). The volatiles were removed to furnish the hydrochloride salt as off white solid, that was purified using preparative HPLC on a Waters™ PrepLC instrument with a reverse-phase Gemini™ C18 column (250 × 21.2 mm, 5 μm), UV detection at 214 nm and a binary solvent system consisting of MeOH (0.1% FA) in H_2O (0.1% FA) at a flow rate of 10.0 mL/min. Fractions containing pure peptide were combined, and freeze-dried to afford azapeptide **3.8** (0.0042 g, 0.00934 mmol, 34 %) as white solid; ^{1}H NMR (700 MHz, DMSO) δ 8.30 (s, 1H), 7.43 – 7.15 (m, 10H), 6.13 (d, *J* = 8.2 Hz, 1H), 4.53 – 4.42 (m, 1H), 4.30 – 4.01 (m, 2H), 3.69 – 3.41 (m, 2H), 3.31 – 3.16 (m, 2H), 3.13 – 2.82 (m, 3H), 1.87 – 1.42 (m, 4H), 1.38 – 1.19 (m, 2H), 1.17 – 0.91 (m, 3H); ^{13}C NMR (175 MHz, DMSO) δ 174.7, 164.2, 164.5, 142.3, 129.6, 128.41, 128.36, 127.33, (127.27), 127.24, (127.20), 127.15, (127.05), (127.01), 126.98, 56.99, 56.08, 46.97, 35.1, 34.4, (34.2), (28.7), (28.6), (28.4), 28.2, (26.59), (26.55), 26.52, 25.1, 22.1, 19.1; HRMS *m/z* calculated for $C_{25}H_{31}N_5NaO_3$ $[M+Na]^+$ 472.2342; found 472.2341.

Aza-3,6-methano-Δ^4-dehydropipecolyl-L-proline Benzhydrylamide (3.22)

Dry HCl gas was bubbled into a stirred solution of *N*-Boc-azapeptide **3.15b** (1 eq., 0.1 g, 0.199 mmol, 4:1 diastereomeric ratio, prepared according to reference 17). Consumption of starting material was observed by TLC after 2 h, R*f* 0.24 (1:4 hexane:EtOAc). The resulting solution was concentrated under reduced pressure to yield amine **3.22** (0.0801 g, 0.199 mmol, 100 %) as light brown solid: 1H NMR (500 MHz, MeOD) δ 7.40 – 7.16 (m, 10H), 6.44 – 6.24 (m, 1H), 6.16 (s, 1H), 6.08 – 5.88 (m, 1H), 5.18 – 4.97 (m, 1H), 4.69 – 4.35 (m, 2H), 3.58 – 3.39 (m, 2H), 3.08 – 2.93 (m, 1H), 2.39 – 2.17 (m, 2H), 2.14 – 1.83 (m, 3H); 13C NMR (125 MHz, MeOD) δ 173.7, (156.1), 156.0, 142.97, 142.73, (142.3), (142.1), 141.96, 130.1, 129.6, 129.5, 129.3, 128.7, 128.5, 128.3, 67.8, 62.1, (61.6), 61.4, 58.4, 47.2, 36.9, (36.8), 31.2, 25.7; HRMS *m/z* calculated for $C_{24}H_{26}N_4NaO_2$ $[M+H]^+$ 425.1948; found 425.1938.

_N_-Fmoc-Alaninyl-aza-3,6-methano-Δ^4-dehydropipecolyl-L-proline Benzhydrylamide (3.23)

A solution of *N*-Fmoc-L-alanine acid chloride (4 eq., 0.131 g, 0.398 mmol, prepared freshly according to reference 29) in dry CH_2Cl_2 (2 mL) was added dropwise to a 0 °C solution of azapeptide **3.22** (1 eq., 0.04 g, 0.0994 mmol) and DIEA (2 eq., 0.0257 g, 0.0329 mL, 0.199 mmol) in dry CH_2Cl_2 (3 mL). The yellow colour solution was stirred at room temperature overnight. After stirring 24 h, the mixture turned colourless. The volatiles were removed under vacuum. The residue was dissolved in EtOAc (10 mL), washed with 5 mL of saturated aqueous $NaHCO_3$, followed by brine (10 mL), dried over Na_2SO_4, filtered and evaporated. The residue was purified by column chromatography using 1:4 hexane:EtOAc as eluant to give azapeptide **3.23** (0.012 g, 0.0172 mmol, 17 %) as pale yellow solid: Rf 0.52 (1:4 hexane:EtOAc); ^{1}H NMR (500 MHz, $CDCl_3$) δ 7.81 – 7.70 (m, 3H), 7.69 – 7.47 (m, Hz, 4H), 7.45 – 7.35 (m, 3H), 7.35 – 7.09 (m, 10H), 6.17 (d, *J* = 8.1 Hz, 1H), 6.07 – 5.95 (m, 1H), 5.63 – 5.50 (m, 1H), 5.46 – 5.09 (m, 2H), 4.59 (d, *J* = 7.5 Hz, 1H), 4.45 – 4.24 (m, 4H), 4.22 – 4.16 (m, 2H), 3.58 – 3.24 (m, 1H), 2.51 – 2.27 (m, 1H), 2.02 – 1.88 (m, 1H), 1.49 – 1.32 (m, 3H), 1.32 – 1.20 (m, 3H); ^{13}C NMR (125 MHz, $CDCl_3$) δ 174.8, (172.8), (171.3), 170.9, 157.3, 156.6, (155.7), 143.8, 143.7, (143.6), 141.7, 141.4, 135.6, 133.2, 128.8, 128.7, 128.0, 127.9, 127.51, 127.48, 127.38, 127.34, 127.24, (127.21), 125.13, (125.06), 120.23, (120.16), 78.7, 67.5, (67.2), (61.0), 60.5, (60.3), 57.2, (49.8), 47.3, (47.1), 46.3, (46.2), (35.0), (31.0), 29.8, (28.9), (28.0), 25.3, 21.2, 18.7, 17.2, 14.3; LCMS *m/z* detected molecular ion for $C_{42}H_{41}N_5NaO_5$ $[M+Na]^+$ m/z 714, R.T. = 10 min [20%-90% MeOH (0.1% FA) in water (0.1% FA) for 8 min, followed by 90% MeOH (0.1% FA) in water (0.1% FA) for 2.0 min].

Alanine-aza-3,6-methano-Δ^4-dehydropipecolyl-L-proline Benzhydrylamide (3.9)

N-Fmoc-Azapeptide **3.23** (1 eq., 0.012 g, 0.0172 mmol) was dissolved in dry THF (1 mL), treated with DEA (4 eq., 0.00505 g, 0.00711 mL, 0.069 mmol) and stirred for 4h, at which point complete disappearance of starting material **3.23** was observed by TLC (Rf 0.52, 1:4 hexane:EtOAc). The volatiles were removed under vacuum. The residue was dissolved in CH_2Cl_2, evaporated and freeze-dried to give a pale yellow solid, which was purified using preparative HPLC on a Waters™ PrepLC instrument with a reverse-phase Gemini™ C18

column (250 × 21.2 mm, 5 μm), UV detection at 214 nm, and a binary solvent system consisting of MeOH (0.1% FA) in H_2O (0.1% FA), at a flow rate of 10.0 mL/min. Fractions containing pure peptide were combined, and freeze-dried to afford azapeptide **3.9** (0.0031 g, 0.00655 mmol, 38 %) as white solid: ^{1}H NMR (700 MHz, MeOD) δ 8.53 (br s, 1H), 7.43 – 7.17 (m, 10H), 6.15 – 6.08 (m, 1H), 6.08 – 5.99 (m, 2H), 5.69 – 5.58 (m, 1H), 5.58 – 5.42 (m, 1H), 4.52 (d, 1H), 4.10 (d, 1H), 3.68 – 3.39 (m, 2H), 2.94 – 2.72 (m, 1H), 2.30 – 2.20 (m, 1H), 2.17 – 1.82 (m, 3H), 1.62 – 1.41 (m, 3H), 1.31 – 1.21 (m, 1H); ^{13}C NMR (175 MHz, MeOD) δ 174.3, (174.2), (173.9), 169.6, 157.3, 142.99, (142.93), (142.8), 142.6, (135.9), 135.8, 134.3, (134.1), (131.9), (131.6), 129.8, 129.7, 129.6, 129.4, 128.8, (128.72), 128.65, (128.57), (128.51), (128.44), (128.2), 80.8, (80.5), 75.5, (74.7), 62.6, (62.0), 58.8, (58.5), 49.8, 47.5, 35.5, (31.0), 30.4, 25.9, (17.2), 16.8, (16.4); HRMS *m/z* calculated for $C_{27}H_{32}N_5O_3$ $[M+H]^+$ 474.2499; found 474.2507.

Aza-Δ^4-dehydropipecolyl-L-proline Benzhydrylamide (3.24)

Employing the protocol described for the synthesis of azapeptide **3.22**, Dry HCl gas was bubbled into a stirred solution of azapeptide **3.16** (1 eq., 0.05 g, 0.102 mmol, synthesized according to reference 17). The resulting solution was concentrated under reduced pressure to yield amine **3.24** (0.04 g, 0.101 mmol, 100 %) as colourless viscous liquid: ^{1}H NMR (500 MHz, $CDCl_3$) δ 8.73 – 8.38 (br s, 1H), 7.69 – 7.57 (br, 1H), 7.34 – 7.05 (m, 10H), 6.11 (d, *J* = 8.4 Hz, 1H), 5.85 – 5.53 (m, 2H), 4.64 – 4.45 (m, 1H), 3.95 – 3.82 (m, 1H), 3.80 – 3.56 (m, 2H), 3.51 – 3.39 (m, 2H), 3.39 – 3.29 (m, 1H), 2.28 – 2.03 (m, 2H), 2.03 – 1.71 (m, 2H); ^{13}C NMR (125 MHz, $CDCl_3$) δ 165.0, 154.4, 141.2, 141.0, 136.7, 129.1, 128.9, 128.8, (128.7), 127.43, 127.36, 122.12, 120.8, 58.95, (57.18), 56.92, 45.1, 43.7, 43.2, 27.1, 23.2; HRMS *m/z* calculated for $C_{23}H_{26}N_4NaO_2$ $[M+Na]^+$ 413.1948; found 413.1941.

Alaninyl-aza-Δ^4-dehydropipecolyl-L-proline Benzhydrylamide (3.10)

Employing the protocol described for the synthesis of azapeptide **3.23**, *N*-Fmoc-L-alanine acid chloride (1.5 eq., 0.032 g, 0.096 mmol) was added to a 0 °C solution of azapeptide **3.24** (1 eq., 0.025 g, 0.064 mmol) and DIEA (2 eq., 0.0165 g, 0.0212 mL, 0.128 mmol) in dry CH_2Cl_2 (3 mL). Analysis of the residue by LCMS after concentration indicated 39% conversion {$C_{41}H_{41}N_5NaO_5$ *m/z* $[M+Na]^+$ 706, R.T. = 9.3 min [20%-90% MeOH (0.1%

FA) in water (0.1% FA) for 8 min, followed by 90% MeOH (0.1% FA) in water (0.1% FA) for 2.0 min].

Without further purification, the residue was dissolved in dry THF (2 mL), treated with DEA (10 eq., 0.0468 g, 0.066 mL, 0.64 mmol) and stirred for 4h. The volatiles were removed under vacuum. The residue was dissolved in CH_2Cl_2, evaporated and freeze-dried to give a light brown solid, which was purified using preparative HPLC on a Waters™ PrepLC instrument with a reverse-phase Gemini™ C18 column (250 × 21.2 mm, 5 μm), UV detection at 214 nm and a binary solvent system consisting of MeOH (0.1% FA) in H_2O (0.1% FA), at a flow rate of 10.0 mL/min. Fractions containing pure peptide were combined and freeze-dried to afford azapeptide **3.10** (0.0042 g, 0.0091 mmol, 14 %) as white solid: $[\alpha]_D^{20}$ −7.1° (*c* 0.056, MeOH); ^{1}H NMR (700 MHz, MeOD) δ 8.52 (s, 1H), 7.39 – 7.15 (m, 10H), 6.20 – 6.08 (m, 1H), 5.95 – 5.75 (m, 2H), 4.68 – 4.28 (m, 3H), 4.28 – 4.18 (m, 1H), 4.17 – 3.95 (m, 2H), 3.73 – 3.45 (m, 2H), 2.42 – 2.12 (m, 1H), 2.12 – 1.79 (m, 3H), 1.51 – 1.12 (m, 3H); ^{13}C NMR (175 MHz, MeOD) δ (173.9), 173.5, 161.9, 161.5, (143.2), 143.0, (142.8), 142.6, (129.64), 129.62, 129.5, 129.4, 128.9, 128.74, (128.66), 128.62, (128.48), (128.43), (124.17), 123.7, 123.6, (123.2), 63.2, 62.9, 58.3, (58.2), 51.1, 42.3, 41.5, 31.1, 25.1, 17.16, (17.01); HRMS *m/z* calculated for $C_{26}H_{31}N_5NaO_3$ $[M+Na]^+$ 484.2319; found 484.2337.

Aza-cyclohexaneglycinyl-L-proline Benzhydrylamide (3.25)

Employing the protocol described for the synthesis of azapeptide **3.18**, azapeptide **3.17a** (1 eq., 0.1 g, 0.182 mmol, synthesized according to reference 17) was reacted with 10 wt% palladium-on-carbon (0.5 eq., 0.00966 g, 0.0908 mmol) at room temperature, stirred for 1-2 h, and filtered over Celite™. The filtrate and washings were combined and concentrated to yield the amine **3.25** (0.075 g, 0.178 mmol, 98 %) as viscous oil; ^{1}H NMR (500 MHz, MeOD) δ 7.36 – 7.17 (m, 10H), 6.17 (d, *J* = 5.4 Hz, 1H), 4.59 – 4.53 (m, 1H), 4.49 – 4.42 (m, 1H), 3.84 – 3.74 (m, 4.1 Hz, 1H), 3.73 – 3.64 (m, 1H), 3.64 – 3.38 (m, 2H), 2.36 – 2.08 (m, 2H), 2.08 – 1.88 (m, 3H), 1.88 – 1.70 (m, 3H), 1.70 – 1.59 (m, 1H), 1.59 – 1.25 (m, 3H), 1.18 – 1.03 (m, 1H); ^{13}C NMR (125 MHz, MeOD) δ 175.5, (174.7), 163.4, 143.1, 143.0, 129.54, 129.48, 128.8, 128.7, 128.6, 128.4, 64.0, (61.8), 58.7, (58.2), 57.9, 51.6, 47.1, 31.9,

31.1, (29.9), 29.8, 26.8, (26.7), 26.6, 25.6; HRMS *m/z* calculated for $C_{25}H_{32}N_4NaO_2$ $[M+Na]^+$ 443.2418, found 443.2406.

_N_-Fmoc-Alaninyl-aza-cyclohexaneglycinyl-L-proline Benzhydrylamide (3.26)

Employing the protocol described for the synthesis of *N*-Fmoc-azapeptide **3.23**, *N*-Fmoc-L-alanine acid chloride (1.5 eq., 0.08 g, 0.245 mmol) was reacted with azapeptide **3.25** (1 eq., 0.068 g, 0.163 mmol) and DIEA (2 eq., 0.0422 g, 0.054 mL, 0.327 mmol). The residue was purified by column chromatography using 1:1 hexane:EtOAc as eluant to give *N*-Fmoc-azapeptide **3.26** (0.038 g, 0.0691 mmol, 44 %) as pale yellow solid: Rf 0.54 (1:4 hexane:EtOAc); ^{1}H NMR (500 MHz, $CDCl_3$) δ 8.49 (s, 1H), 8.10 – 7.97 (m, 1H), 7.77 (d, *J* = 7.6 Hz, 2H), 7.55 (t, *J* = 6.4 Hz, 2H), 7.45 – 7.37 (m, 2H), 7.37 – 7.27 (m, 7H), 7.25 – 7.14 (m, 5H), 6.32 (d, *J* = 9.1 Hz, 1H), 5.11 (d, *J* = 6.1 Hz, 1H), 4.62 (t, *J* = 7.7 Hz, 1H), 4.43 (d, *J* = 6.7 Hz, 2H), 4.26 – 4.16 (m, 2H), 4.10 – 4.00 (m, 1H), 3.39 – 3.29 (m, 1H), 3.18 – 3.06 (m, 1H), 2.40 – 2.25 (m, 1H), 2.03 – 1.95 (m, 1H), 1.85 – 1.72 (m, 7.0 Hz, 3H), 1.71 – 1.58 (m, 3H), 1.39 – 1.19 (m, 6H), 1.13 (d, *J* = 6.6 Hz, 3H); ^{13}C NMR (125 MHz, $CDCl_3$) δ 171.6, 171.0, 159.5, 156.6, 143.6, 142.7, 141.54, 141.47, 128.7, 128.34, 128.28, 128.1, 127.7, 127.5, 127.3, 127.2, 126.9, 124.9, 120.3, 67.6, 62.6, 58.6, 56.3, 50.6, 48.6, 47.2, 30.3, 30.0, 29.8, 29.0, 25.9, 25.8, 25.7, 25.4; LCMS *m/z* detected molecular ions for $C_{43}H_{47}N_5NaO_5$ $[M+Na]^+$ 736, R.T. = 9.5 min [20%-90% MeOH (0.1% FA) in water (0.1% FA) for 8 min, followed by 90% MeOH (0.1% FA) in water (0.1% FA) for 2.0 min].

Alaninyl-aza-cyclohexaneglycinyl-L-proline Benzhydrylamide (3.11)

Employing the protocol described for the synthesis of azapeptide **3.9**, *N*-Fmoc-azapeptide **3.22** (1 eq., 0.018 g, 0.0252 mmol) was treated with DEA (5 eq., 0.00922 g, 0.013 mL, 0.126 mmol) and stirred for 4h, at which point complete disappearance of starting material **3.26** was observed by TLC (Rf 0.54, 1:4 hexane:EtOAc). The volatiles were removed under vacuum. The residue was dissolved in CH_2Cl_2, evaporated and freeze-dried to give a pale yellow solid, which was purified using preparative HPLC on a Waters™ PrepLC instrument with a reverse-phase Gemini™ C18 column (250 × 21.2 mm, 5 μm), UV detection at 214 nm and a binary solvent system consisting of MeOH (0.1% FA) in H_2O (0.1% FA) at a flow rate of 10.0 mL/min. Fractions containing pure peptide were combined

and freeze-dried to afford azapeptide **3.11** (0.0052 g, 0.0106 mmol, 42 %) as white solid: mp 155−156 °C; $[\alpha]_D^{20}$ −5.6° (*c* 0.16, MeOH); ^{1}H NMR (700 MHz, DMSO) δ 8.57 – 7.91 (br, 3H), 7.42 – 7.16 (m, 10H), 6.45 (s, 1H), 6.13 (d, *J* = 9.3 Hz, 1H), 4.35 (t, *J* = 7.7 Hz, 1H), 3.95 (dd, *J* = 13.2, 6.5 Hz, 1H), 3.88 – 3.78 (m, 1H), 3.42 – 3.29 (br, 1H), 2.21 – 2.04 (br, 1H), 1.90 – 1.77 (m, 2H), 1.77 – 1.63 (m, 4H), 1.56 (d, *J* = 12.5 Hz, 2H), 1.42 – 1.30 (m, 3H), 1.30 – 1.19 (m, 4H), 1.13 – 0.98 (m, 1H); ^{13}C NMR (175 MHz, DMSO) δ 171.0, 169.6, 162.9, 142.5, 142.4, 128.2, 128.0, 127.6, 127.1, 126.8, 126.6, 61.8, 58.0, 55.4, 47.1, 29.6, 29.5, 28.9, 25.2, 25.1, 25.0, 17.2. IR (neat) ν_{max}/cm^{-1} 2923 (br), 1635, 1526, 1495, 1411, 1325, 1210, 1096; HRMS *m/z* calculated for $C_{28}H_{37}N_5NaO_3$ $[M+Na]^+$ 514.2430; found 514.2429.

Cell viability

MCF7 cells were grown in Eagle's Minimum Essential medium (MEM) supplemented with 10% fetal bovine serum, penicillin/streptomycin and MEM Non-Essential Amino Acids (100x). Cells were maintained at 37ºC in 5% CO_2. Cells were serum starved for 6 h before the experiments, treated with either DMSO, Etoposide, AVPI-NH_2 or the indicated Smac mimic for 72 h. Cells were harvested by trypsinization, stained for trypan blue and counted for each condition.

Acknowledgments

This research was supported by the Natural Sciences and Engineering Research Council of Canada (NSERC). We thank M. C. Tang, Sylvie Bilodeau, and Cédric Malveau of the Université de Montréal centers for HR-MS analysis, and NMR spectroscopy, respectively.

Article 3

Chingle, R.; Lubell, W. D. “Peptide Coupling Challenges on Route to Aza-Pipecolyl Smac Mimetic” In *Proceedings of the 24th American Peptide Symposium*, Ved Srivastava, Andrei Yudin, and Michal Lebl (Editors) American Peptide Society, **2015**, 172-173.

All synthetic work for this article has been done by myself.

The article is written by myself and edited by Professor William D. Lubell.

Peptide Coupling Challenges on Route to Aza-Pipecolyl Smac Mimetic

Ramesh Chingle and William D. Lubell*

Département of Chemistry, Universite of Montréal, C.P. 6128, Succursale Centre-Ville, Montréal, Québec, H3C 3J7, Canada

E-mail: william.lubell@umontreal.ca

Introduction

Azopeptides are reactive peptide analogs bearing a diazo dicarbonyl moiety as a dehydro N-(acyl)amino acid surrogate.[28] Azopeptides have been employed in the synthesis of peptide analogs bearing semicarbazides as amino amide surrogates, so called azapeptides.[13b] For example, the Diels-Alder reaction of a diazine residue with cyclopentadiene provided aza-methano-pipecolyl peptide **3.15** (Scheme 3.6).[28] In the context of research towards anticancer drugs, we perceive the aza-methanopipecolyl structure as a constrained valine analog for insertion into a mimic of the *N*-terminal AVPI binding motif of the second mitochondria-derived activator of caspases (Smac). Coupling to the azamethano-pipecolyl residue proved however challenging during efforts to prepare Smac mimetic **3.7**.

Results and Discussion

The AVPI peptide amide **3.3** has served as a lead for the development of Smac mimetics that bind the inhibitor of apoptosis protein-3 and induce apoptosis (Figure 3.6).[9,18,23b,43] Considering the turn conformation adopted by this peptide on receptor binding, constrained analogs such as indolizidinone amino acids have been used to rigidify the Val-Pro dipeptide to enhance potency (e.g., **3.5**).[25] Although such bicyclic amino acid analogs represent an important class of Smac mimetics, their multiple step synthesis has restricted analog development. Employing aza-amino acyl proline analogs as indolizidinone amino acid surrogates, azapeptide smac mimetics (e.g., **3.6**) have been developed that induce cell death by a caspase-9 mediated apoptotic pathway.[9] In the interest to further restrict the conformation of the aza-amino acid residue, aza-methano-pipecolate was pursued as a rigid valine analog in smac mimetic **3.7**.

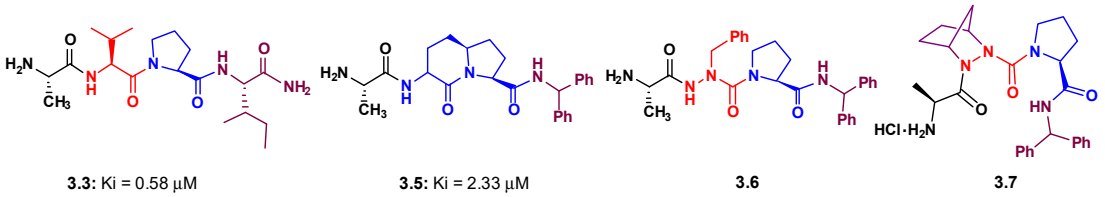

Figure 3.6. AVPI-NH_2 and peptide mimetic activators of caspase-9.

Hydrogenation aza-Diels-Alder adduct **3.15** removed the Cbz group and reduced the olefin to provide bicyclic semicarbazide **3.18** (Scheme 3.6). The acylation of semicarbazide **3.18** with Boc-Ala proved particularly challenging presumably because of the combination of steric hindrance and electronic deactivation. A variety of coupling conditions were examined to achieve acylation, albeit with minimal success. For example, various coupling conditions failed to afford the Boc protected aza-tripeptide amide **3.20**: TBTU/HOBT,[34] EDCl/HOBT,[35] and DIC/AtOH[36]. Moreover, attempts were unsuccessful using the mixed anhydride generated from Boc-Ala, *iso*-butyl chloroformate and *N*-methylmorpholine.[37] On the other hand, PyBOP and diisopropyl ethyl amine (DIEA) proved effective in the reaction of semicarbazide **3.18** with Boc-Ala, and gave tripeptide amide **3.20** in 58% yield.[38] Removal of the Boc group with 25% TFA in dichloromethane, salt exchange using 1N HCl for 30 min and freeze-drying afforded hydrochloride salt **3.7** (HRMS m/z calculated for $C_{27}H_{34}N_5O_3$ $[M+H]^+$ 476.2656; found 476.2663).

Scheme 3.6. Synthesis of aza-methano-pipecolyl Smac mimetic **3.7**.

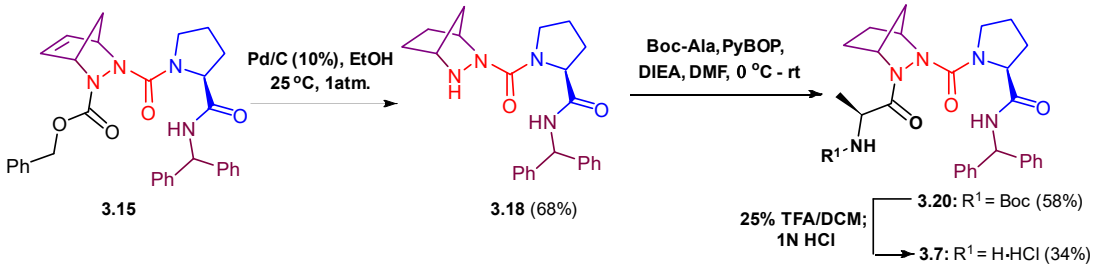

Conclusion

In conclusion, we have disclosed the incorporation of a novel constrained valine into an azapeptide Smac mimetic analog. Application of PyBOP surmounted difficulties in

coupling to the bulky and electron deficient aza-methano-pipecolyl residue. Smac mimetic analog **3.7** will be examined for bioactivity to probe further structure-activity relationships at the AVPI binding site towards the development of improved therapy for treating cancer.

Acknowledgments

This research was supported by the Natural Sciences and Engineering Research Council of Canada (NSERC).

References

(1) (a) Freidinger, R. M.; Veber, D. F.; Perlow, D. S.; Saperstein, R., Bioactive conformation of luteinizing hormone-releasing hormone: evidence from a conformationally constrained analog. *Science* **1980**, *210*, 656-658. (b) Freidinger, R. M.; Perlow, D. S.; Randall, W. C.; Saperstein, R.; Arison, B. H.; Veber, D. F., Conformational modifications of cyclic hexapeptide somatostatin analogs. *Chem. Biol. Drug Des.* **1984**, *23*, 142-150.

(2) Levitt, M., Conformational preferences of amino acids in globular proteins. *Biochemistry* **1978**, *17*, 4277-4285.

(3) Hutchinson, E. G.; Thornton, J. M., A revised set of potentials for β-turn formation in proteins. *Protein Sci.* **1994**, *3*, 2207-2216.

(4) Wolf, J. P.; Rapoport, H., Conformationally constrained peptides. Chirospecific synthesis of 4-alkyl-substituted. gamma.-lactam-bridged dipeptides from L-aspartic acid. *J. Org. Chem.* **1989**, *54*, 3164-3173.

(5) Sharma, R.; Lubell, W. D., Regioselective enolization and alkylation of 4-oxo-N-(9-phenylfluoren-9-yl) proline: Synthesis of enantiopure proline− valine and hydroxyproline− valine chimeras. *J. Org. Chem.* **1996**, *61*, 202-209.

(6) Chingle, R.; Ratni, S.; Claing, A.; Lubell, W. D., Application of constrained aza-valine analogs for Smac mimicry. *Biopolymers* **2016**, *106*, 235-244.

(7) Sun, H.; Nikolovska-Coleska, Z.; Yang, C.-Y.; Qian, D.; Lu, J.; Qiu, S.; Bai, L.; Peng, Y.; Cai, Q.; Wang, S., Design of small-molecule peptidic and nonpeptidic Smac mimetics. *Acc. Chem. Res.* **2008**, *41*, 1264-1277.

(8) Wu, G.; Chai, J.; Suber, T. L.; Wu, J. W.; Du, C.; Wang, X.; Shi, Y., Structural basis of IAP recognition by Smac/DIABLO. *Nature* **2000**, *408*, 1008-1012.

(9) Bourguet, C. B.; Boulay, P.-L.; Claing, A.; Lubell, W. D., Design and synthesis of novel azapeptide activators of apoptosis mediated by caspase-9 in cancer cells. *Bioorg. Med. Chem. Lett.* **2014**, *24*, 3361-3365.

(10) Chingle, R.; Lubell, W. D., Peptide coupling challenges in azopeptide route to aza-pipecolyl Smac mimetic. *Proceeding of the 24th Am. Pept. Symp., Ved Srivastava, Andrei Yudin, and Michal Lebl (Editors) Am. Pept. Soc.* **2015**, 172-173.

(11) Petrucci, E.; Pasquini, L.; Bernabei, M.; Saulle, E.; Biffoni, M.; Accarpio, F.; Sibio, S.; Di Giorgio, A.; Di Donato, V.; Casorelli, A., A small molecule SMAC mimic LBW242 potentiates TRAIL-and anticancer drug-mediated cell death of ovarian cancer cells. *PloS one* **2012**, *7*, e35073.

(12) West, A.; Martin, B.; Andrews, D.; Hogg, S.; Banerjee, A.; Grigoriadis, G.; Johnstone, R.; Shortt, J., The SMAC mimetic, LCL-161, reduces survival in aggressive MYC-driven lymphoma while promoting susceptibility to endotoxic shock. *Oncogenesis* **2016**, *5*, e216.

(13) (a) Gante, J., Azapeptides. *Synthesis* **1989**, *1989*, 405-413. (b) Proulx, C.; Sabatino, D.; Hopewell, R.; Spiegel, J.; Garcia, R. Y.; Lubell, W. D., Azapeptides and their therapeutic potential. *Future Med. Chem.* **2011**, *3*, 1139-1164.

(14) Proulx, C.; Sabatino, D.; Hopewell, R.; Spiegel, J.; García Ramos, Y.; Lubell, W. D., Azapeptides and their therapeutic potential. *Future Med Chem* **2011**, *3*, 1139-1164.

(15) Thormann, M.; Hofmann, H.-J., Conformational properties of azapeptides. *J. Mol. Str.: THEOCHEM* **1999**, *469*, 63-76.

(16) (a) Andre, F.; Vicherat, A.; Boussard, G.; Aubry, A.; Marraud, M., Aza-peptides. III. Experimental structural analysis of aza-alanme and aza-asparagine-containing peptides. *The Journal of peptide research* **1997**, *50*, 372-381. (b) Zouikri, M.; Vicherat, A.; Aubry, A.; Marraud, M.; Boussard, G., Azaproline as a β-turn-inducer residue opposed to proline. *J. Peptide Res.* **1998**, *52*, 19-26.

(17) (a) Andre, F.; Boussard, G.; Bayeul, D.; Didierjean, C.; Aubrey, A.; Marraud, M., Aza-peptides II. X-Ray structures of aza-alanine and aza-asparagine-containing peptides. *J. Peptide Res.* **1997**, *49*, 556-562. (b) Lecoq, A.; Boussard, G.; Marraud, M.; Aubry, A., Crystal state conformation of three azapeptides containing the Azaproline residue, a β-turn regulator. *Biopolymers* **1993**, *33*, 1051-1059.

(18) Kerr, J. F.; Wyllie, A. H.; Currie, A. R., Apoptosis: a basic biological phenomenon with wide-ranging implications in tissue kinetics. *Br. J. Cancer* **1972**, *26*, 239.

(19) Thompson, C. B., Apoptosis in the pathogenesis and treatment of disease. *Science* **1995**, *267*, 1456.

(20) Deveraux, Q. L.; Reed, J. C., IAP family proteins-suppressors of apoptosis. *Genes Dev.* **1999**, *13*, 239-252.

(21) (a) Du, C.; Fang, M.; Li, Y.; Li, L.; Wang, X., Smac, a mitochondrial protein that promotes cytochrome c–dependent caspase activation by eliminating IAP inhibition. *Cell* **2000**, *102*, 33-42. (b) Verhagen, A. M.; Ekert, P. G.; Pakusch, M.; Silke, J.; Connolly, L. M.; Reid, G. E.; Moritz, R. L.; Simpson, R. J.; Vaux, D. L., Identification of DIABLO, a mammalian protein that promotes apoptosis by binding to and antagonizing IAP proteins. *Cell* **2000**, *102*, 43-53.

(22) (a) Wu, G.; Chai, J.; Suber, T. L.; Wu, J.-W.; Du, C.; Wang, X.; Shi, Y., Structural basis of IAP recognition by Smac/DIABLO. *Nature* **2000**, *408*, 1008. (b) Liu, Z.; Sun, C.; Olejniczak, E. T.; Meadows, R. P.; Betz, S. F.; Oost, T.; Herrmann, J.; Wu, J. C.; Fesik, S. W., Structural basis for binding of Smac/DIABLO to the XIAP BIR3 domain. *Nature* **2000**, *408*, 1004.

(23) (a) Fadeel, B.; Orrenius, S., Apoptosis: a basic biological phenomenon with wide-ranging implications in human disease. *J. Intern. Med.* **2005**, *258*, 479-517. (b) Deveraux, Q. L.; Reed, J. C., IAP family proteins—suppressors of apoptosis. *Genes Dev.* **1999**, *13*, 239-252.

(24) Chen, K.-F.; Lin, J.-P.; Shiau, C.-W.; Tai, W.-T.; Liu, C.-Y.; Yu, H.-C.; Chen, P.-J.; Cheng, A.-L., Inhibition of Bcl-2 improves effect of LCL161, a SMAC mimetic, in hepatocellular carcinoma cells. *Biochem. Pharmacol.* **2012**, *84*, 268-277.

(25) (a) Sun, H.; Nikolovska-Coleska, Z.; Yang, C.-Y.; Xu, L.; Tomita, Y.; Krajewski, K.; Roller, P. P.; Wang, S., Structure-based design, synthesis, and evaluation of conformationally constrained mimetics of the second mitochondria-derived activator of caspase that target the X-linked inhibitor of apoptosis protein/caspase-9 interaction site. *J. Med. Chem.* **2004**, *47*, 4147-4150. (b) Sun, H.; Nikolovska-Coleska, Z.; Yang, C.-Y.; Xu, L.; Liu, M.; Tomita, Y.; Pan, H.; Yoshioka, Y.; Krajewski, K.; Roller, P. P., Structure-based design of potent, conformationally constrained Smac mimetics. *J. Am. Chem. Soc.* **2004**, *126*, 16686-16687. (c) Khashper, A.; Lubell, W. D., Design, synthesis, conformational analysis and application of indolizidin-2-one dipeptide mimics. *Org. Biomol. Chem.* **2014**, *12*, 5052-5070.

(26) (a) Bourguet, C. B.; Proulx, C.; Klocek, S.; Sabatino, D.; Lubell, W. D., Solution-phase submonomer diversification of aza-dipeptide building blocks and their application in aza-peptide and aza-DKP synthesis. *J. Pept. Sci.* **2010**, *16*, 284-296. (b) Bourguet, C. B.; Dorr,

A.; Godina, T.; Proulx, C.; Fridkin, G.; Jamieson, A.; Sabatino, D.; Kassem, T.; Boutard, N.; Arsenault, J.; Ronga, L.; Brouillette, Y.; Bednarek, M.; Tolles, J. C.; Lubell, W. D., Portraits of the pioneers of the American Peptide Society. *Adv Exp Med Biol* **2009**, *611*, xlix-lxix.

(27) Bourguet, C. B.; Boulay, P. L.; Claing, A.; Lubell, W. D., Design and synthesis of novel azapeptide activators of apoptosis mediated by caspase-9 in cancer cells. *Bioorg. Med. Chem. Lett.* **2014**, *24*, 3361-3365.

(28) Chingle, R.; Lubell, W. D., Azopeptides: Synthesis and Pericyclic Chemistry. *Org. Lett.* **2015**, *17*, 5400-5403.

(29) (a) Sabatino, D.; Proulx, C.; Klocek, S.; Bourguet, C. B.; Boeglin, D.; Ong, H.; Lubell, W. D., Exploring side-chain diversity by submonomer solid-phase aza-peptide synthesis. *Org. Lett.* **2009**, *11*, 3650-3653. (b) Boeglin, D.; Lubell, W. D., Aza-amino acid scanning of secondary structure suited for solid-phase peptide synthesis with Fmoc chemistry and aza-amino acids with heteroatomic side chains. *J. Comb. Chem.* **2005**, *7*, 864-878. (c) Melendez, R. E.; Lubell, W. D., Aza-amino acid scan for rapid identification of secondary structure based on the application of N-Boc-aza1-dipeptides in peptide synthesis. *J. Am. Chem. Soc.* **2004**, *126*, 6759-6764. (d) Freeman, N. S.; Tal-Gan, Y.; Klein, S.; Levitzki, A.; Gilon, C., Microwave-assisted solid-phase aza-peptide synthesis: aza scan of a PKB/Akt inhibitor using aza-arginine and aza-proline precursors. *The Journal of organic chemistry* **2011**, *76*, 3078-3085. (e) Falb, E.; Yechezkel, T.; Salitra, Y.; Gi1on, C., In situ generation of Fmoc-amino acid chlorides using bis-(trichloromethyl) carbonate and its utilization for difficult couplings in solid-phase peptide synthesis. *J. Peptide Res.* **1999**, *53*, 507-517.

(30) Gray, C.; Quibell, M.; Baggett, N.; Hammerle, T., Incorporation of azaglutamine residues into peptides synthesised by the ultra-high load solid (gel)-phase technique. *Int. J. Pept. Protein Res.* **1992**, *40*, 351-362.

(31) Hess, H.-J.; Moreland, W. T.; Laubach, G. D., N-[2-Isopropyl-3-(L-aspartyl-L-arginyl)-carbazoyl]-L-tyrosyl-L-valyl-L-histidyl-L-prolyl-L-phenylalanine, 1 an Isostere of Bovine Angiotensin II. *J. Am. Chem. Soc.* **1963**, *85*, 4040-4041.

(32) Gibson, C.; Goodman, S. L.; Hahn, D.; Hölzemann, G.; Kessler, H., Novel solid-phase synthesis of azapeptides and azapeptoides via Fmoc-strategy and its application in the synthesis of RGD-mimetics. *J. Org. Chem.* **1999**, *64*, 7388-7394.

(33) (a) Freeman, N. S.; Hurevich, M.; Gilon, C., Synthesis of N′-substituted Ddz-protected hydrazines and their application in solid phase synthesis of aza-peptides. *Tetrahedron* **2009**, *65*, 1737-1745. (b) Zhang, J.; Proulx, C.; Tomberg, A.; Lubell, W. D., Multicomponent diversity-oriented synthesis of aza-lysine-peptide mimics. *Org. Lett.* **2013**, *16*, 298-301.

(34) Bourguet, C. B.; Sabatino, D.; Lubell, W. D., Benzophenone semicarbazone protection strategy for synthesis of aza-glycine containing aza-peptides. *Peptide Science* **2008**, *90*, 824-831.

(35) Chakraborty, T. K.; Ghosh, A.; Sankar, A. R.; Kunwar, A. C., Development of 2, 3-diazabicyclo [2.2. 1] heptane as a constrained azapeptide template and its uses in peptidomimetic studies. *Tetrahedron Lett.* **2002**, *43*, 5551-5554.

(36) Hemmerlin, C.; Cung, M. T.; Boussard, G., Synthesis and conformational preferences in solution and crystalline states of an aza-tripeptide. *Tetrahedron Lett.* **2001**, *42*, 5009-5012.

(37) (a) Anderson, G. W.; Zimmerman, J. E.; Callahan, F. M., Reinvestigation of the mixed carbonic anhydride method of peptide synthesis. *J. Am. Chem. Soc.* **1967**, *89*, 5012-5017. (b) Zaitsev, A. B.; Adolfsson, H., Enantioswitchable catalysts for the asymmetric transfer hydrogenation of aryl alkyl ketones. *Org. Lett.* **2006**, *8*, 5129-5132.

(38) Coste, J.; Le-Nguyen, D.; Castro, B., PyBOP®: A new peptide coupling reagent devoid of toxic by-product. *Tetrahedron Lett.* **1990**, *31*, 205-208.

(39) (a) Wiberg, K. B., The concept of strain in organic chemistry. *Angew. Chem. Int. Ed. Engl.* **1986**, *25*, 312-322. (b) Pilet, O.; Vogel, P., Synthesis and Diels-Alder Reactivity of 2, 3, 5, 6-Tetramethylidenenorbornane. *Helv. Chim. Acta* **1981**, *64*, 2563-2570.

(40) Laungani, A. C.; Slattery, J. M.; Krossing, I.; Breit, B., Supramolecular Bidentate Ligands by Metal-Directed in situ Formation of Antiparallel β-Sheet Structures and Application in Asymmetric Catalysis. *Chem. Eur. J.* **2008**, *14*, 4488-4502.

(41) Still, W. C.; Kahn, M.; Mitra, A., Rapid chromatographic technique for preparative separations with moderate resolution. *J. Org. Chem.* **1978**, *43*, 2923-2925.

(42) Stebbins, J. F., Nuclear magnetic resonance at high temperature. *Chem. Rev.* **1991**, *91*, 1353-1373.

(43) Fadeel, B.; Orrenius, S., Apoptosis: a basic biological phenomenon with wide-ranging implications in human disease. *J. Intern. Med.* **2005**, *258*, 479-517.

Chapter 4: Identification of Active Peptide Conformations by Application of aza-Pipecolyl Residue Insertion Using Solid-Phase Azopeptide Diels-Alder Chemistry

4.1 Context

The β-turn is a well-studied motif in both proteins and cyclic peptides, and plays important roles in protein folding.[1] Proline is a common component of the central residues in β-turns. The amide *N*-terminal to proline, the so-called prolyl amide, can exist in *cis* and *trans* isomers of similar stability (*cis*- **4.1** and *trans*- **4.2**, Figure 4.1). The difference in free energy between the *cis* and *trans* isomers about the tertiary amide is estimated at 2 kcal/mol, compared to the >10 kcal/mol difference between the *cis* and *trans* isomers of a secondary peptide bond. Prolyl amide isomerization has profound effects on structure,[2] with potential implications upon activity. Mixtures of prolyl amide isomers have been observed in various peptides and proteins, including ribonuclease,[3] and bradykinin.[4] Although the prolyl amide *trans* isomer is typically more stable in solution, the *cis* isomer has been suggested to be preferred for receptor recognition of various peptides,[5 8] including angiotensin and thyroliberin.[6] Prolyl *cis* amides are central in type-VI β-turns,[1c] and may influence the transport, metabolism, and reactivity of biologically active peptides.[7] Constrained prolyl amide isomers have thus been synthesized to study their respective importance for receptor binding affinity and activity.[8] Sterically bulky 5-position substituents have been employed to favor prolyl *cis* isomer conformation.[8c,8f] For example, (2*S*,5*R*)-5-*tert*-butylproline[9] favored prolyl *cis* amides and VIa *β*-turns in *N*-(acetyl)dipeptide *N*′-methylamides.[8f,11] Double bond isosteres of the prolyl *cis* amides have stabilized the bioactive conformations,[10] as demonstrated using substrate analogues of peptidyl prolyl isomerase enzymes.[11] Such constraints are typically challenging to introduce into peptide structures due to issues of acylating a sterically hindered prolyl residue and controlling olefin geometry during synthesis.[12] Aza-pipecolyl can favor amide *cis* isomer geometry and type VI β-turn conformation due to the electronic and structural constraints of the cyclic semicarbazide.[13] An effective means to install aza-Pip residues into peptides was thus pursued to enable production of constrained amide *cis* isomer libraries to explore the importance of this structure in various biologically active peptides.

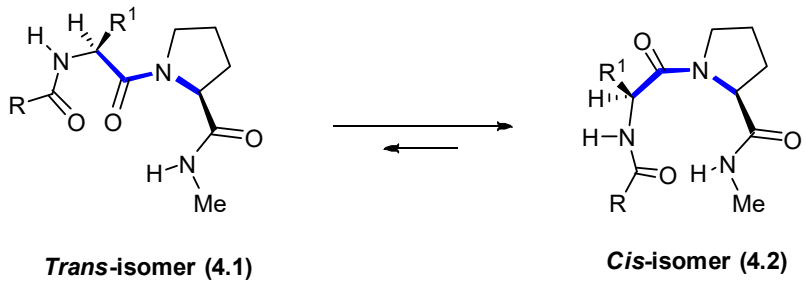

***Trans*-isomer (4.1)** ***Cis*-isomer (4.2)**

Figure 4.1. Amide isomer equilibrium in proline **4.1** and **4.2.**

In the Chapter, solid-phase azopeptide chemistry was developed featuring Diels-Alder reactions to insert aza-pipecolyl residues into peptides. Although aza-pipecolic acid has previously shown to favor *N*-terminal amide *cis* isomer geometry, the chapter describes the first uses of the aza-amino acid to study biologically active peptides: e.g., the mu selective opioid ligands morphiceptin and the endomorphins,[14] and the cluster of differentiation 36 receptor (CD36) ligand growth hormone releasing peptide-6 (GHRP-6).[15] Conformational analysis of constrained morphiceptin and endomorphin analogs exhibiting potent agonist activity and high selectivity for the mu opioid receptor subtype revealed NMR spectra characteristic of a biologically active *cis* conformer.[14] The proline residue in morphiceptin and the endomorphins was thus replaced by aza-pipecolyl residues to further study the relevance of the prolyl amide *cis* isomer for potency and receptor selectivity in the context of developing antinociceptive agents. Selective CD36 binding affinity was exhibited by [azaPro^3]GHRP-6, which displayed antiangiogenic properties.[15a] Aza-pipecolyl residues were thus respectively incorporated in place of Ala^3 and Trp^4 in GHRP-6 peptide to study influences of turn induction on CD36 modulation in an inflammation assay.

The proven effectiveness of the solid-phase method for making aza-Pip peptides bears well for application to other biologically relevant examples. Considering the numbers of active peptides bearing proline and pipecolate residues, [16] the employment of aza-Pip to understand the relevance of prolyl amide *cis* isomer geometry and type VI β-turns on folding and function offers significant potential to achieve more potent and selective compounds for the drug discovery.

Article 4

Chingle, R.; Mulumba, M.; Chung, N. N.; Nguyen, T. M.-D.; Ong, H.; Ballet, S.; Schiller, P. W.; Lubell, W. D. "Active Peptide Conformers by aza-Pipecolyl Residue Insertion with Solid-Phase Azopeptide Diels-Alder Chemistry" *In Preperation*, **2018**.

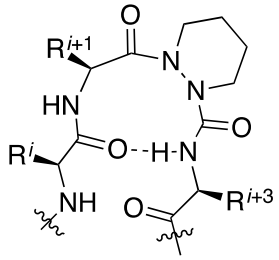

All synthetic work for this article has been done by myself.

The article is written by myself and edited by Professor William D. Lubell.

The idea of introducing aza-pipecolyl residues into opioid ligands was conceived in collaboration with Professor Steven Ballet at the Research Group of Organic Chemistry, Vrije Universiteit Brussel, Brussels, Belgium.

The aza-pipecolyl opioid analogs were tested for biological activity in the lab of Professor Peter W. Schiller by his students Nga N. Chung and Thi M.-D Nguyen at the laboratory of Chemical Biology and Peptide Research, Clinical Research Institute of Montreal, Canada and description of the biological experiments written.

The aza-pipecolyl GHRP-6 analogs were examined by Dr. Mukandila Mulumba under the supervision of Professor Huy Ong at the Faculté de Pharmacie Université de Montréal, Canada and description of the biological experiments written.

In its present form, the manuscript and chapter were written by myself employing texts from earlier publications in which the biological studies were previously described, and the documents were subsequently edited by Professor Lubell.

Identification of Active Peptide Conformations by Application of aza-Pipecolyl Residue Insertion Using Solid-Phase Azopeptide Diels-Alder Chemistry

Ramesh Chingle,[†] Mukandila Mulumba,[‡] Nga N. Chung,[‖] Thi M.-D Nguyen,[‖] Huy Ong,[*,‡] Steven Ballet,[*,§] Peter W. Schiller,[*,‖] and William D. Lubell[*,†]

[†]*Département de Chimie, and* [‡]*Faculté de Pharmacie Université de Montréal, C.P. 6128, Succursale, Centre-Ville, Montréal, Québec H3C 3J7, Canada*

[§]*Research Group of Organic Chemistry, Vrije Universiteit Brussel, Pleinlaan 2, B-1050 Brussels, Belgium*

[‖]*Laboratory of Chemical Biology and Peptide Research, Clinical Research Institute of Montreal, 110 Pine Avenue West, Montréal, Québec H2W 1R7, Canada*

E-mail : william.lubell@umontreal.ca

Abstract

Aza-pipecolyl residues introduce a combination of electronic and structural constraints in model peptides that favor *cis*-amide isomer geometry and type VI β-turn conformation; however, their synthesis has inhibited application in studies of biologically relevant targets. Targeting understanding of the conformational requirements of opioid and cluster of differentiation 36 receptor (CD36) ligands, an efficient method for introducing aza-pipecolyl residues into peptides has been developed featuring azopeptide construction and Diels-Alder chemistry using a solid-phase synthesis strategy, which employs a modified Fmoc-protection protocol. The relevance of specific turn structures for receptor affinity, selectivity and activity was ascertained using this protocol, which offers an effective means for exploring peptide conformation by the construction of targeted aza-pipecolate libraries.

Keywords

GHRP-6, Growth hormone releasing peptide 6, CD36 receptor, cluster of differentiation 36, *N*,*N*'-disuccinimidyl carbonate, opioid agonist peptide, agonist, antagonist, structure-activity relationships, receptor binding.

Introduction

The therapeutic potential of peptides can be enhanced through synthetic modifications that preserve biological activity while improving bioavailability, metabolic stability and receptor selectivity.[17] Structures that favor specific geometry, such as *β*-turn conformations, are particularly desirable because of their privileged roles in peptide recognition.[18] For example, aza-proline (azaPro) **4.3** and its homologue aza-pipecolic acid (azaPip) **4.4**, which contain a nitrogen atom in place of the C*α*H group, both have been shown to favor *N*-terminal amide bond (often called the prolyl amide bond) *cis*-isomer geometry and to accommodate the *i* + 2 position of type VI *β*-turns in peptides, as predicted by computational analysis,[19] and demonstrated in the solid state by X-ray diffraction,[13,20] and in solution by IR and NMR spectroscopy of model peptides (Figure 4.2).[21]

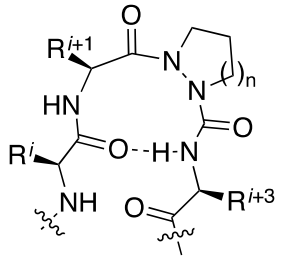

Figure 4.2. Amide *cis*-isomer *N*-terminal to an aza-proline (n = 1) **4.3** or aza-pipecolic acid (n = 2) **4.4** residue in a type VI β-turn.

Aza-proline has been employed to study the active conformation of a variety of biologically relevant peptides, including the *C*-terminal peptide fragment of human calcitonin gene-related peptide,[22] thyrotropin-releasing hormone,[19b] collagen,[23] a mucin tandem repeat motif,[24] as well as inhibitors of activated protein kinase B (PKB/Akt),[25] dipeptidyl peptidase IV and prolyl oligopeptidase enzymes.[16d] In contrast, aza-pipecolate has been much less frequently employed in the study of peptides.[26] Notably, small molecule azaPip peptidyl-prolyl isomerase ligands have exhibited promising neuroprotective and neuro-regenerative effects *in vitro* and *in vivo*.[16e] In contrast, pipecolic acid is present in numerous natural products and peptides exhibiting activity as antimicrobials, immunosuppressants, and peptidyl-prolyl isomerase, histone deacetylase and ATPase enzyme inhibitors.[23 -16f]

Considering the parent piperidine carboxylic acid has been often used as a proline surrogate,[16a-c,21b,27] the absence of aza-Pip application to study biologically active peptides is regrettable and likely due to difficulties in the synthesis and coupling of this aza-amino acid.[13]

Application of cyclic aza-residues in peptide-oriented medicinal chemistry is handicapped by the multiple step syntheses need to install and differentiate their hydrazine nitrogen in the respective heterocycles prior to peptide coupling.[13,21] Applying Boc and Cbz protected azopeptides in Diels-Alder chemistry, we have recently developed solution-phase chemistry for making azaPip peptide building blocks which were later introduced into longer structures.[26] A novel Fmoc-based approach to generate azo-glycine on resin is now reported in a versatile method for making azaPip peptides using solid-phase synthesis. The utility of the solid-phase azopeptide approach was further demonstrated by the synthesis of azaPip analogs of biologically relevant opioid and cluster of differentiation-36 receptor (CD36) ligands.

The opioid peptides and their respective receptor subtypes have been intensively studied with the principal interest of creating agents to control pain, while suppressing the common detrimental effects of clinically applied analgesics. Among various natural ligands, morphiceptin (H-Tyr-Pro-Phe-Pro-NH_2),[28] the amide from a fragment of the milk protein β-casein, and the endomorphins [endomorphin-1 (H-Tyr-Pro-Trp-Phe-NH_2) and endomorphin-2 (H-Tyr-Pro-Phe-Phe-NH_2)] have attracted considerable attention due to their agonist activity and high selectivity for the mu opioid (MOP) receptors.[29] Dynamic equilibria about the prolyl amide bonds in these opioid peptides has evoked significant effort to investigate the isomer configuration responsible for biological activity. In particular, evidence indicating that morphiceptin and endomorphin-2 adopt *cis*-amide bond geometry about the Tyr-Pro peptide bond in their bioactive conformations was obtained by employing 2,2-dimethyl thiazolidine- and oxazolidine-carboxylates, which were observed by nuclear magnetic resonance (NMR) spectroscopy to have predominant (>98%) prolyl *cis*-amide populations in [D-Phe^3]morphiceptin- and endomorphin-2 analogs retaining full mu agonist potency in the guinea pig ileum (GPI) assay, and displaying nanomolar mu receptor binding affinities and high MOP selectivity.[14] Subsequently, the *cis*-isomer conformer was supported by

employment of a series of proline surrogates [e.g., *cis*-2-aminocyclopentane and pentene-1-carboxylic acids,[30] and 1- and *cis*-2-aminocyclohexane-1-carboxlylic acid],[31] which combined with data from applications of ring substituted tyrosine and phenylalanine residues,[32] all illustrated the importance of side chain orientations in a bent backbone structure for receptor affinity and selectivity. Additionally, the *cis*-amide was also observed for the bifunctional MOP agonist/delta opioid (DOP) receptor antagonist Dmt-Tic-Phe-Phe-NH_2 (DIPP-NH_2), when co-crystallized with the inactive state of DOP.[33] It could be hypothesized that the Dmt-Tic peptide also adopts this amide bond geometry upon binding to the active state of MOP.

Expressed on macrophage plasma membranes, CD36 serves key roles in recognition and phagocytosis as a scavenger of multiple-ligands, such as oxidized lipoproteins and thrombospondin, and has been implicated in various pathologies including atherosclerosis and angiogenesis.[34] Aza-analogs of growth hormone releasing peptide-6 (GHRP-6, H-His-D-Trp-Ala-Trp-D-Phe-Lys-NH_2) have previously been shown to exhibit selective binding affinity and potential to modulate CD36 activity.[15a,35] For example, the selective ligands [azaY^4]- and [aza(4-F)F^4]-GHRP-6 reduced significantly CD36-mediated overproduction of nitric oxide (NO) in macrophage cells after treatment with the Toll-like receptor (TLR)-2-agonist fibroblast-stimulating lipopeptide (R-FSL-1), and attenuated induced neovascularization relative to control in a microvascular sprouting assay on mouse choroidal explants.[35] Moreover, enhanced myocardial performance with increased circulating adiponectin, reduced myocardial oxidative stress and diminished apoptosis was achieved on treating isolated hearts with [A^1,azaF^4]-GHRP-6 by way of a CD36 dependent mechanism.[36] In contrast to the parent peptide, which lacked receptor selectivity and exhibited a random coil conformation, GHRP-6 analogs possessing an aza-phenylalanine at the 4-position displayed circular dichroism (CD) and NMR spectra indicative of a β-turn conformation.[15b] In addition, [azaP^3]-GHRP-6 exhibited selective affinity for CD36, likely by inducing a turn conformation.[15a]

To explore the relationship between conformation and activity in the opioid peptides, aza-pipecolate residues were installed respectively in place of Pro^2 in [D-Phe^3]morphiceptin,

and endomorphin-1 and -2, as well as their 2,6-dimethyltyrosine (Dmt^1) analogs.[37] Moreover, to study CD36 activity, azapipecolate was introduced at the 3- and 4-positions of GHRP-6. By employing butadiene and 2,3-dimethylbutadiene as dienophiles in Diels-Alder reactions with the corresponding azo-glycinyl peptide resins, (Δ^4)- and (4,5-dimethyl-Δ^4)-aza-dehydropipecolate residues were obtained, and the former were reduced after azapeptide cleavage from the resin to give the corresponding aza-pipecolate analogs. The [$azaPip^2$]opioid peptides were examined for agonist potency based on inhibition of electrically induced contractions of the GPI,[38] and mouse vas deferens (MVD),[39] in which opioid activity are respectively mediated predominantly by the MOP and DOP receptor subtypes. The [azaPip]GHRP-6 analogs were examined in macrophage cells treated with the Toll-like receptor-2 (TLR2) agonist R-FSL-1 to ascertain capacity to modulate CD36-mediated overproduction of NO, because this marker of inflammation can be effectively measured as nitrite.[40] The power of the solid-phase approach to synthesize strategic libraries of biologically active aza-pipecolate peptides has thus been validated by the preparation of the first examples of [$azaPip^2$]opioid and [azaPip]GHRP-6 analogs, which exhibit pertinent activity and selectivity due to the conformational preferences of the cyclic aza-residue.

Results and Discussion

Aza-pipecolyl residues were inserted into the peptide chain linked to the resin by introducing a three-step process into a conventional Fmoc-based Solid-Phase Peptide Synthesis (SPPS) protocol:[15b] (1) amino acylation with an activated fluorenylmethyl carbazate, (2) oxidation of the resulting azaglycinyl residue to its azo-counterpart, and (3) [4+2]-cycloaddition (Scheme 4.1). Subsequent Fmoc removal, semicarbazide acylation, peptide elongation, deprotection and cleavage gave the (Δ^4)-aza-dehydropipecolate peptides, which were finally hydrogenated in solution to obtain the aza-pipecolyl opioid and GHRP-6 analogs (Schemes 4.2 and 4.3).

Scheme 4.1. Installation of (Δ^4)-aza-pipecolyl residue.

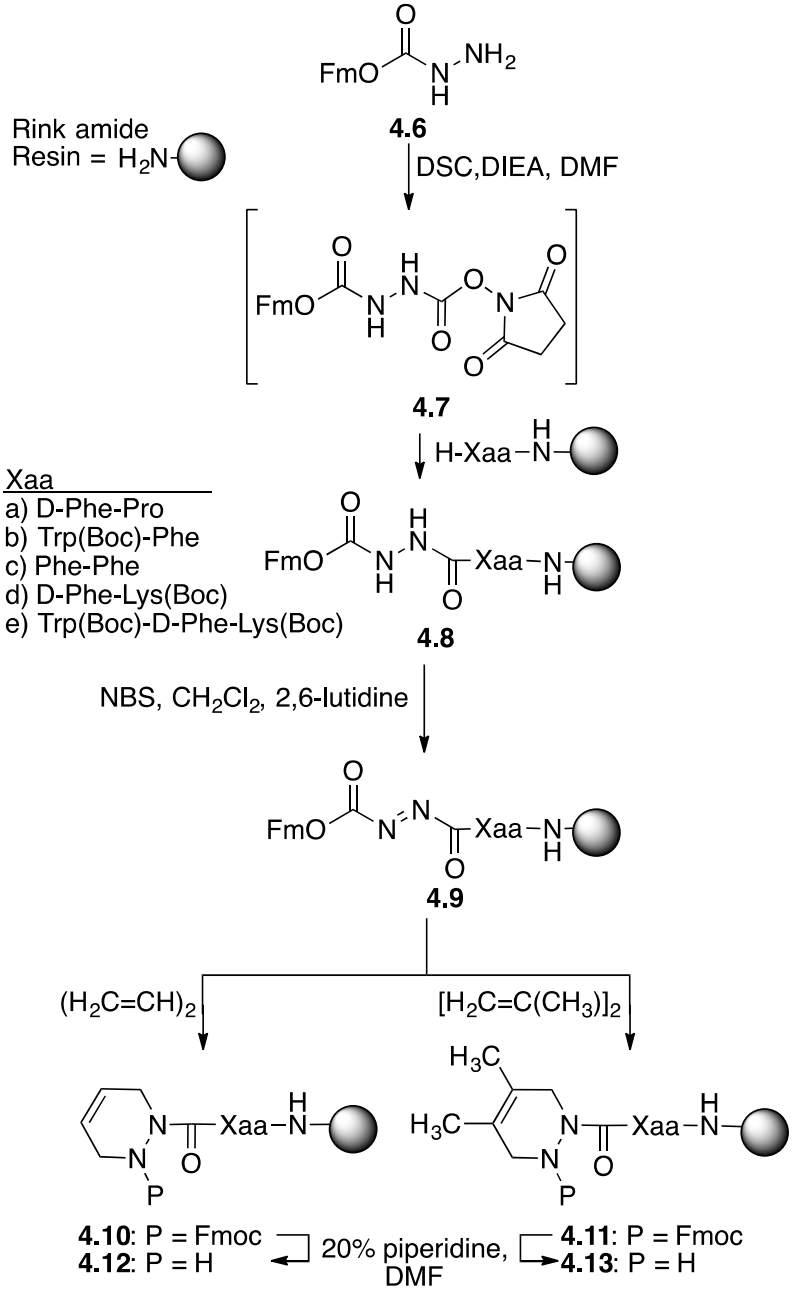

The precursor for aza-Gly, fluoren-9-ylmethyl carbazate **4.6** was prepared by acylation of excess hydrazine **4.5** with fluoren-9-ylmethyl chloroformate.[41] *N*-(Fmoc)-Hydrazine **4.6** was treated with *N*,*N*′-disuccinimidyl carbonate (DSC) and the activated carbazate **4.7** was coupled respectively to a) D-phenylalanyl-prolinamide, b) *N*'-

(Boc)tryptophyl-phenylalaninamide, c) phenylalanyl-phenylalaninamide, d) D-phenylalanyl-N^{ε}-(Boc)lysinamide and e) *N*'-(Boc)tryptophyl-D-phenylalanyl-N^{ε}-(Boc)lysinamide, all linked to Rink amide resin to provide aza-glycyl peptides **4.8a-e** (Scheme 4.1). In contrast to carbazate activation with other reagents such as phosgene and carbonyldiimidazole which are plagued by oxadiazalone formation,[42] DSC provided the right balance of stability and reactivity to provide azapeptide. Although *N*-(Boc)- and *N*-(Cbz)-azaglycine residues could be oxidized to the corresponding azoglycines using *N*-bromosuccinimide (NBS) and pyridine in dichloromethane, oxidation of the corresponding *N*-(Fmoc)aza-glycines under similar conditions was prevented due to loss of Fmoc protection.[43] Fortunately, the weaker base 2,6-lutidine circumvented loss of the Fmoc group and enabled NBS oxidation of *N*-(Fmoc)-aza-glycine peptides **4.8a-e** in dichloromethane at −40 °C to room temperature to afford azo-glycine resins **4.9a-e**, respectively. The IR spectra of the azopeptide resins exhibited a characteristic band between 1700 to 1760 cm^{-1} indicative of the N=N stretching vibration.[44] Azopeptides **4.9a-e** underwent Diels–Alder reactions respectively with butadiene and 2,3-dimethyl butadiene to give (Δ^4)- and (4,5-dimethyl-Δ^4)-aza-dehydropipecolate resins **4.10a-e** and **4.11a-e** from which the Fmoc group was removed using a 20% piperidine solution in DMF to provide the corresponding semicarbazides **4.12a-e** and **4.13a-e**.[43]

Semicarbazides are much less nucleophilic than their amino acid equivalents.[45] Furthermore, *N*-acylations of cyclic amino acids (e.g., Pro and Pip) are generally more difficult than their primary amino acid counterparts. The acylations of (Δ^4)-aza-dehydropipecolates **4.12a-e** and **4.13a-e** were challenging as anticipated and LC/MS analyses after resin cleavage with TFA showed little success after initial attempts with a variety of common coupling agents and conditions: e.g., DIC/HOBt,[46] DIC/oxyma,[47] HATU,[48] PyBop,[26] T3P,[49] and COMU.[50] Acylation was however achieved using *N*-Fmoc-amino acid chlorides [300 mol%, generated *in situ* with bis-(trichloromethyl)carbonate, BTC],[51] and 2,4,6-collidine in THF with microwave irradiation to afford azapeptides (Schemes 4.2 and 4.3).[25,51] For example, Fmoc-Tyr(*t*-Bu)-Cl reacted with (Δ^4)-aza-dehydropipecoyl tripeptides **4.12a-c** and **4.13a-c** to provide respectively azapeptides **4.14a-c** and **4.15a-c** in good conversion (see supporting information). Similarly, the acid chlorides from Fmoc-Ala-

OH and Fmoc-D-Trp(Boc)-OH reacted with (Δ^4)-aza-dehydropipecolates **4.12d,e** and **4.13e** to give the corresponding azapeptides **4.24-4.26**. On the other hand, the acid chloride derived from the more sterically demanding Fmoc-Dmt-OH reacted respectively with (Δ^4)-aza-dehydropipecoyl tripeptides **4.12a** and **4.13a** to provide azapeptides **4.16a** and **4.17a** in lower conversion, as further indicated by the relatively poorer final [Dmt^1]morphiceptin yields, as compared to those of their Tyr^1 counterparts (Table 4.1). Considering the challenging coupling with the Dmt residue and the high affinity and selectivity of [Dmt^1]morphiceptin analogs, the initial aza-pipecolate study targeted only at [Dmt^1,D-Phe^3]morphiceptin analogs to provide three azaPip^2 derivatives.[14,52]

Scheme 4.2. Conversion of (Δ^4)-aza-dehydropipecolates **4.12a-c** and **4.13a-c** to [azaPip^2]-morphiceptin and endomorphin analogs **4.18**-**4.23**.

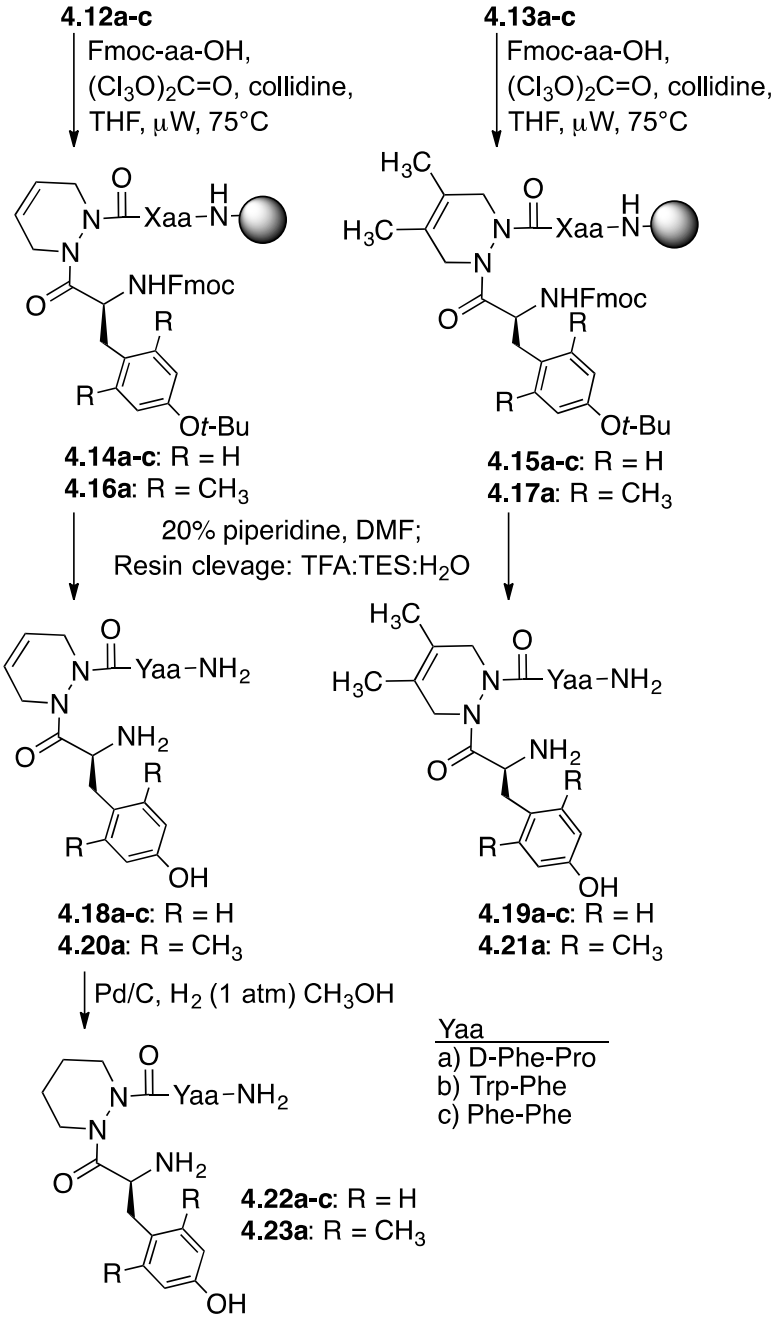

Scheme 4.3. Conversion of (Δ^4)-aza-pipecolates **4.12d,e** and **4.13e** to [azaPip]-GHRP-6 analogues **4.27**-**4.31**.

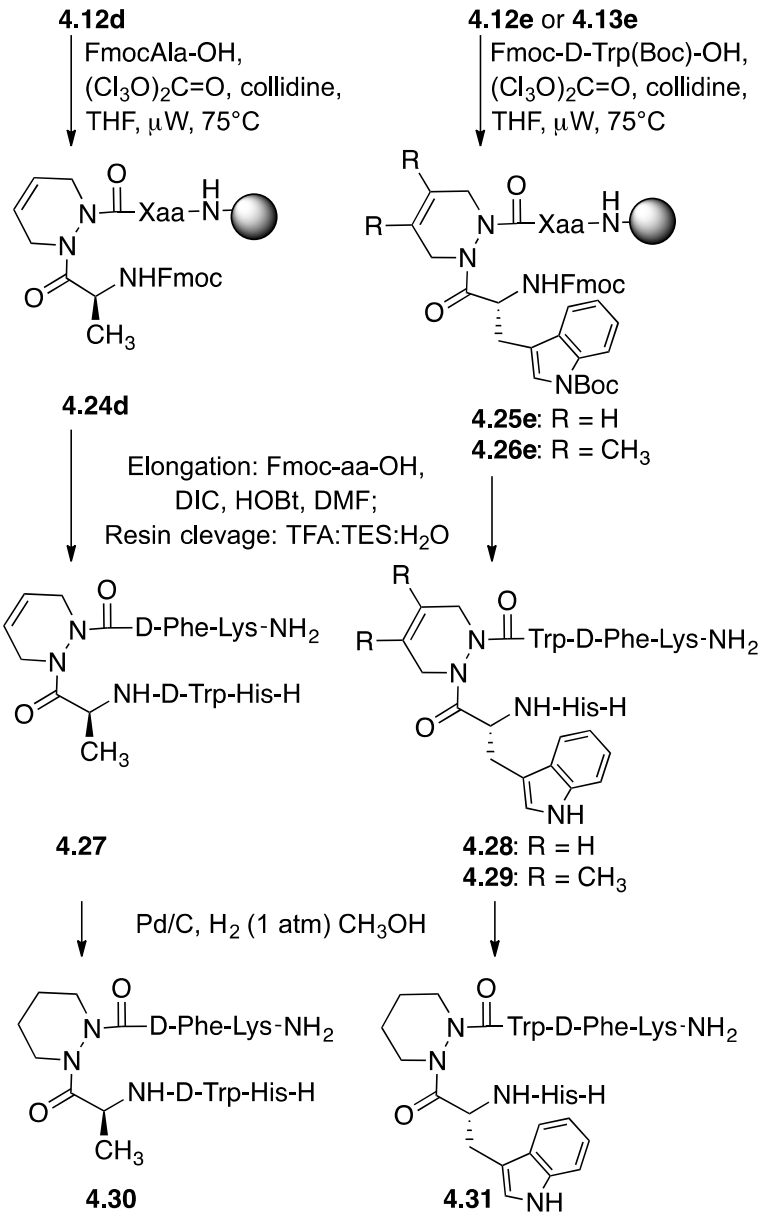

After removal of the Fmoc group from azapeptides **4.14**-**4.17**, resin cleavage with side chain deprotection was performed using a freshly made TFA/TES/H_2O (95:2.5:2.5, v/v/v) cocktail to provide (Δ^4)-aza-dehydropipecoyl morphiceptins and endomorphins **4.18**-**4.21** (Scheme 4.2). Elongation of (Δ^4)-aza-dehydropipecolates **4.24**-**4.26** was performed using standard Fmoc-based SPPS methods employing DIC with HOBt for amino acid

couplings in DMF.[26b] Resin cleavage with side chain deprotection was performed as described above to provide [(Δ^4)-azaPip]GHRP-6 analogues **4.27**-**4.29**.

After resin cleavage the respective (Δ^4)-aza-dehydropipecoyl azapeptides were precipitated with Et_2O, dissolved in 1:1 acetonitrile/H_2O, and freeze-dried to white foams that were analyzed by RP-HPLC to assess purity. The [(Δ^4)-azaPip]opioid and [(Δ^4)-azaPip]GHRP-6 peptides were purified by preparative RP-HPLC using a Gemini® 5-micron C18 110A column (Phenomenex® Inc., 250×21.2 mm, 5 μm). The desired pure fractions were combined, and freeze-dried to white fluffy powders. In cases of [Dmt^1,D-Phe^3]morphiceptin analogs **4.16a** and **4.17a**, purification was performed twice using preparative RP-HPLC to obtain suitable purity. The purities of azapeptides **4.18**-**4.21** and **4.27**-**4.29** were analyzed by analytical RP-HPLC on a Sunfire™, Gemini®, BEH and CSH C18 column (Table 4.1).

After their purification as described above, hydrogenations of [(Δ^4)-azaPip]opioids **4.18a-c** and **4.20a**, as well as [(Δ^4)-azaPip]GHRP-6 analogues **4.27** and **4.28** were respectively performed using palladium-on-carbon (10 wt%) in methanol under a balloon of hydrogen (1 atm). Saturated [azaPip]morphiceptins **4.22a** and **4.23a**, endomorphins **4.22b,c** and [azaPip^4]- and [azaPip^3]GHRP-6 analogues **4.30** and **4.31** were isolated by removal of the catalyst on filtration over Celite™. After washing with methanol, and evaporation of the combined filtrate and washings, the residue was freeze-dried to furnish the azapeptides as off-white solids, that were analyzed by RP-HPLC to assess purity (Schemes 4.2 and 4.3, Table 4.1).

Table 4.1. Purity, retention times, and mass analyses of [azaPip]opioid and GHRP-6 analogues **4.18-4.23** and **4.27-4.31**.

Compound	RT (min)			MS [M + 1]	
	CH_3OH	CH_3CN	purity at 214 nm	*m/z* (calcd)	*m/z* (obsd)
4.18a H-Tyr-(Δ^4)azaPip-D-Phe-Pro-NH_2	7.55	6.42	>99	535.2663	535.2679
4.18b H-Tyr-(Δ^4)azaPip-Trp-Phe-NH_2	8.37	6.61	>99	624.2929	624.2944
4.18c H-Tyr-(Δ^4)azaPip-Phe-Phe-NH_2	8.25	5.60	>99	585.2820	585.2835
4.19a H-Tyr-(4,5-dimethyl-Δ^4)azaPip-D-Phe-Pro-NH_2	6.70	4.76	>99	563.2976	563.2964
4.19b H-Tyr-(4,5-dimethyl-Δ^4)azaPip-Trp-Phe-NH_2	7.38	5.12	>98	652.3242	652.3234
4.19c H-Tyr-(4,5-dimethyl-Δ^4)azaPip-Phe-Phe-NH_2	7.32	5.18	>98	613.3133	613.3112
4.20a H-Dmt-(Δ^4)azaPip-D-Phe-Pro-NH_2	6.14	4.34	>99	563.2976	563.2962
4.21a H-Dmt-(4,5-dimethyl-Δ^4)azaPip-D-Phe-Pro-NH_2	7.01	4.96	>96	591.3289	591.3284
4.22a H-Tyr-azaPip-D-Phe-Pro-NH_2	5.73	4.07	>98	537.2820	537.2826
4.22b H-Tyr-azaPip-Trp-Phe-NH_2	6.61	4.68	>99	626.3085	626.3099
4.22c H-Tyr-azaPip-Phe-Phe-NH_2	6.47	4.58	>99	587.2976	587.2991
4.23a H-Dmt-azaPip-D-Phe-Pro-NH_2	6.09	4.29	>98	565.3133	565.3138
4.27 His-D-Trp-Ala-(Δ^4)azaPip-D-Phe-Lys-NH_2	4.87	3.92	>99	797.4206	797.4189
4.28 His-D-Trp-(Δ^4)azaPip-Trp-D-Phe-Lys-NH_2	5.98	5.82	>98	912.4628	912.4628
4.29 His-D-Trp-(4,5-dimethyl-Δ^4)azaPip-Trp-D-Phe-Lys-NH_2	4.91	5.26	>95	962.4760	962.4764
4.30 His-D-Trp-Ala-azaPip-D-Phe-Lys-NH_2	5.15	3.97	>99	799.4362	799.4381

4.31 His-D-Trp-azaPip-Trp-D-Phe-Lys-NH_2	6.07	4.70	>96	914.4784	914.4780

Biology

The influence of replacing proline by the aza-pipecolyl residues at the 2-position of [D-Phe^3]morphiceptin and endomorphin was ascertained by examining their potency and mu and delta receptor subtype selectivity in the GPI and MVD assays.[38 ,39] The influence of azaPip relative to unsaturated variants (Δ^4)-azaPip and 3,4-dimethyl-(Δ^4)-azaPip was similarly compared. Moreover, Dmt was replaced for Tyr^1 in the [azaPip^2, D-Phe^3]morphiceptin analogs because the extra hydrophobicity and influences of the 2',6'-dimethyl substituents on χ-dihedral angle geometry have been previously shown to enhance MOP selectivity and affinity (Table 4.2).[32a,53 ,52]

In the case of [D-Phe^3]morphiceptin, replacement of Pro^2 by azaPip^2 in **4.22a** caused nearly 20- and 6-fold improvements in potency in the GPI and MVD assays with a slight enhancement of MOP selectivity. Relative to the azaPip^2 analog **4.22a**, unsaturated [(Δ^4)-azaPip^2, D-Phe^3]morphiceptins were less potent and less selective: (Δ^4)-azaPip^2 analog **4.18a** and 4,5-dimethyl-(Δ^4)-dehydropipecolate **4.19a** were respectively equipotent and about 7-fold less in potent in the GPI assay, and both were about 2-fold more potent in the MVD assay, relative to [D-Phe^3]morphiceptin.

On the other hand, replacement of Pro^2 by azaPip^2 in endomorphin-1 analog **4.22b** resulted respectively in 5- and 17-fold decreases in potency in the GPI and MVD assays with a net reduction of mu selectivity. Similar substitutions caused >100 fold reductions in potency of endomorphin-2 analog **4.22c**, without significant influence on mu/delta selectivity. Although the endomorphin analogs **4.19b** and **c** containing the dimethyl-(Δ^4)-dehydropipecolate residue were nearly inactive, the (Δ^4)-azaPip^2 counterparts **4.18b** and **c** were strikingly more potent that their saturated counterpart, yet not as active as the natural Pro^2 endomorphins.

Replacement of tyrosine for 2,6-dimethyltyrosine (Dmt) in [azaPip^2, D-Phe^3]morphiceptin analogs **4.20a**, **4.21a** and **4.23a** caused significant gains in potency in both

the GPI (20 to 150-fold increase) and MVD (>250-fold increase) assays with about a 2 to 15-fold reduction in MOP/DOP selectivity. For comparison, [Pip^2]morphiceptin (H-Dmt-Pip-Phe-Pro-NH_2) was synthesized and shown to exhibit significant mu/delta selectivity due to low potency on the DOP receptor subtype. Moreover, [Dmt^1, azaPip^2, D-Phe^3]morphiceptins **4.20a**, **4.21a** and **4.23a** compared favourably with [Dmt^1, D-1-Nal^3]morphiceptin (H-Dmt-Pro-D-1-Nal-Pro-NH_2, Nal = naphthylalanine), which has been characterized to be a potent and long acting mu receptor subtype agonist (IC_{50} = 0.45 nM) exhibiting relatively low mu/delta selectivity (Table 4.2).[52] The improved potency of the [azaPip^2, D-Phe^3]morphiceptin analogues relative to their Pro^2 counterparts may be explained by the preference for the aza-residue to stabilize an *N*-terminal amide *cis* isomer geometry, providing further support for the Tyr-Pro peptide bond of morphiceptin assuming the *cis* conformation in the receptor-bound conformation.

Table 4.2. GPI and MVD Assay of Opioid Peptide Analogues **4.18**-**4.23**.

No.	Compound	GPI IC_{50} [nM][a]	MVD IC_{50} [nM][a]	MVD/GPI IC_{50} ratio
	H-Tyr-Pro-D-Phe-Pro-NH_2[c] [**(D-Phe^3)Morphiceptin**]	109 ± 16	594 ± 77	5.45
4.18a	[(Δ^4)azaPip^2]	113 ± 29	321 ± 45	2.84
4.19a	[(4,5-dimethyl-Δ^4)azaPip^2]	737 ± 108	373 ± 44	0.51
4.20a	[Dmt^1,(Δ^4)azaPip^2]	0.723 ± 0.073	1.77 ± 0.155	2.45
4.21a	[Dmt^1, (4,5-dimethyl-Δ^4)azaPip^2]	5.52 ± 0.19	1.96 ± 0.33	0.36
4.22a	[azaPip^2]	17.4 ± 4.1	101 ± 9	5.81
4.23a	[Dmt^1, azaPip^2]	0.845 ± 0.058	2.19 ± 0.12	2.59
	H-Tyr-Pro-Trp-Phe-NH_2[d] [**Endomorphin 1**]	17.2 ± 2.4	26.3 ± 3.9	1.53
4.18b	[(Δ^4)azaPip^2]	85.7 ± 13.7	263 ± 38	3.07
4.19b	[(4,5-dimethyl-Δ^4)azaPip^2]	Inactive	K_e = 1210± 79[b]	-
4.22b	[azaPip^2]	93.8 ± 10.0	460 ± 122	4.90
	H-Tyr-Pro-Phe-Phe-NH_2[d] [**Endomorphin 2**]	7.71 ± 1.47	15.3 ± 1.8	1.98

4.18c [(Δ^4)azaPip^2]	116 ± 31	393 ± 16	3.39
4.19c [(4,5-dimethyl-Δ^4)azaPip^2]	3980 ± 30	Inactive	-
4.22c [azaPip^2]	961 ± 28	2160 ± 340	2.25
H-Dmt-Pip-Phe-Pro-NH_2	6.46 ± 0.51	610 ± 16	94.43
H-Dmt-Pro-D-1-Nal-Pro-NH_2[e]	0.45 ± 0.06	0.64 ± 0.06	1.42

[a] Mean ± SEM. [b] Antagonist, K_e determined against DPDPE. [c] Data taken from Keller *et al*., J. Med. Chem. 44, 3896-3903 (2001), [d] Data taken from J. Fichna *et al*., J. Med. Chem. 50, 512-520 (2007), [e] Data taken from J. Fichna et al., Peptides 29, 633-638 (2008),

The conformation responsible for aza-GHRP-6 analog activity was explored by the synthesis of five aza-pipecolyl-GHRP-6 analogues in which azaPip analogs were respectively incorporated at the Ala^3 and Trp^4 positions.[15a,35] The five azapeptides were examined for ability to modulate NO overproduction in RAW macrophage cell lines after stimulation with the TLR-2 agonist R-FSL-1 (Figure 4.3).[15a,35] In this assay, [azaY^4]GHRP-6 (MPE-001) causes a significant reduction (30%) of nitrite production at [10^{-6} M]. Notably, [(Δ^4)-azaPip^3]- and [(Δ^4)-azaPip^4]GHRP-6 (**4.21** and **4.19**) caused similarly significant reductions of NO production. Their saturated azaPip counterparts **4.22** and **4.23** also inhibited R-FSL-1-induced NO production relative to control, but [4,5-dimethyl-(Δ^4)-azaPip^3]GHRP-6 was inactive. Considering the effects of the azaPip analogs on NO production add further support to the importance of turn geometry as indicated by [azaP^3]GHRP-6[15a] further analysis of their binding affinity is currently under investigation and will be reported in due time.

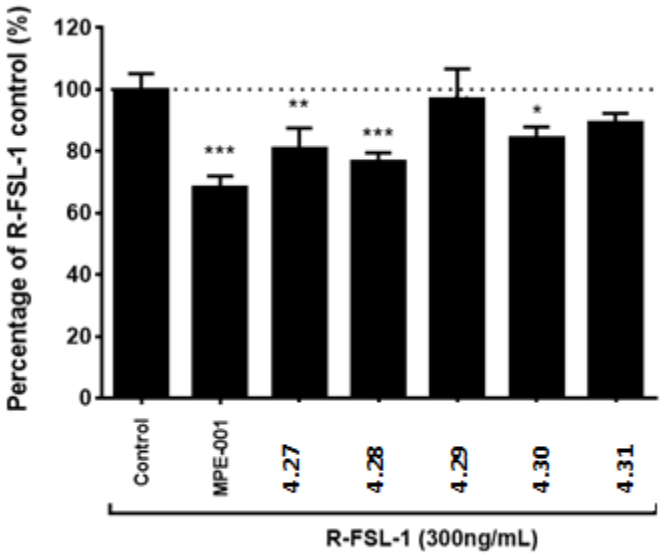

Figure 4.3. Effects of [azapipecolyl]-GHRP-6 analogues **4.27**-**4.31** [10^{-6} M] on the overproduction of NO induced by the TLR-2 agonist R-FSL-1 in RAW macrophage cell line.

Conclusion

A relatively high barrier for interconversion and low difference in the energy of the amide isomers *N*-terminal to proline residues accounts for the observance of 25-40% *cis* conformer in prolyl peptides in various solvents.[8c,8e,14] Although the prolyl amide *trans* isomer may predominate in solution due to steric and electronic reasons,[8e,54] the *cis*-isomer may favor binding and activity at the receptor in spite the energy costs for ligand-receptor interaction. Steric interactions have been primarily used to favor prolyl amide *cis*-isomer,[8c] and have provided potent, MOP selective ligands in the cases of the morphiceptin and endomorphins.[14] Steric bulk may however interfere with receptor binding giving a less clear biological outcome.[8d,55] The electronic effects that stabilize *cis*-isomer geometry *N*-terminal to aza-pipecolate residues may thus offer an effective means to study peptide geometry without complications due to competing steric effects on interaction with the receptor.

Employing an effective solid-phase method twelve aza-pipecolyl opioid analogs and five aza-pipecolyl GHRP-6 derivatives were synthesized in yields and purities suitable for biological evaluation. Activation of fluorenylmethyl-carbazate using DSC provided aza-glycine peptide resins without significant formation of oxadiazole side product. Oxidation of the *N*-(Fmoc)aza-glycine residues on solid phase was achieved without loss of the Fmoc group using NBS and 2,6-lutidine to afford the corresponding azo-glycine residues, which reacted effectively in Diels−Alder reactions with different dienes. Elongation of the resulting aza-pipecolates was achieved by employing *N*-(Fmoc)amino acid chlorides to acylate the relatively non-nucleophilic semicarbazide and deliver peptides suitable for elongation under standard SPPS conditions. Employing this method to study the opioids and GHRP-6, the first examples of biologically active azaPip peptides have been obtained and used to provide insight about conformational requirements for activity and receptor selectivity. Considering the plethora of biologically active peptides that possess proline and pipecolate residues exhibiting *N*-terminal amide equilibria, the effectiveness of this approach for introducing aza-pipecolate to favor amide *cis* isomer geometry and type VI β-turns constitutes an important means to study backbone geometry towards the conception of more potent and selective prototypes for drug discovery.

Experimental section

In Vitro Bioassays and Receptor Binding Assays. The GPI and MVD bioassays were performed by measuring inhibitory on electrically induced contractions as reported in detail elsewhere.[56]

The MVD assay was performed essentially as described in the literature.[39,56b] Briefly, adult, male albino mice (Swiss Webster, 30-50 g: Canadian Breeding Laboratories, Montreal) were killed by cervical dislocation, and the vasa deferentia were dissected out. After removal of extraneous fat and connective tissue, the vas was stripped of its associated blood vessel, and the semen was gently expressed from the lumen. The vas was then mounted under 0.5-g tension in a 5 mL organ bath containing warmed (37 °C), oxygenated (95% 02, 5% CO_2), Mg^{2+}-free Krebs solution of the following composition [mM]: NaC1, 118; $CaCl_2$, 2.54; KCl,

4.75; KHzP04, 1.19; $NaHCO_3$, 25; glucose, 11; L-tyrosine, 0.2. A modified Harvard apparatus stimulator delivered repetitive field stimulation through platinum wire ring electrodes at the top and bottom of the bath, consisting of twin, rectangular pulses (80 V, 0.15 Hz, 10-ms delay, 1.0-ms duration). Contractions of the muscle were recorded via a Hewlett-Packard Model FTA-1-1 force transducer connected to a Hewlett-Packard 7702B recorder. Determination of the reduction in the twitch height at various doses permitted the construction of log dose-response curves. A log dose-response curve was determined with [Leu5]enkephalin as standard for each ileum or vas preparation, and IC_{50} values of the enkephalin analogues being tested were normalized according to a published procedure.[57]

Influence of aza-Pipecolyl Peptide on the Overproduction of NO Induced by the TLR-2 Agonist R-FSL-1 in Macrophage Cell Line: murine RAW264.7 macrophage cell lines (American Type Cell Collection catalogue no. TIB-71) were seeded at 1.5 × 105 cells/well in DMEM medium supplemented with penicillin and streptomycin in a 48-well plate format and incubated at 37 °C with 5% CO_2. After 2 h, the medium of adhered cells was changed to DMEM-Pen/ Strep with 0.2% of bovine serum albumin (BSA), and the cells were treated with aza-pipecolyl-GHRP-6 analogs (**4.27**-**4.31**), or with MPE-001 as positive control at a final concentration of 10^{-6} M. After a 1 h pre-incubation period, the cells were stimulated overnight with the TLR-2 ligand fibroblast-stimulating lipopeptide (R-FSL-1, 300 ng/mL, Invivogen catalogue no. L7022). Supernatants were collected for nitrite determination by reaction with 2,3-diaminonaphthalene (DAN) and measurement of fluorescence. Briefly, 25 μL of sample were incubated with 0.5 μg of DAN in a 100 μL final volume of phosphate buffer (50 mM, pH 7.5) at room temperature in the dark. After 15 min, the reaction was stopped with 20 μL of NaOH (2.8N) and fluorescence was read using a fluorescence plate reader (TECAN Safire, λ_{exc} 365 nm and λ_{em} 430 nm).

Acknowledgments

We thank the NSERC of Canada, the CIHR, the Ministère du développement économique de l'innovation et de l'exportation du Quebec (No. 878-2012), Amorchem and Mperia Therapeutics Inc. for support. SB thanks the Strategic Research Program – Growth

Funding of the Vrije Universiteit Brussel for financial support. We thank Marie-Christine Tang, Karine Venne, Simon Comtoi-Marotte, Pedro Aguiar, and Sylvie Bilodeau for the HRMS, LCMS and NMR spectroscopy of the Université de Montréal.

References

(1) (a) Wilmot, C.; Thornton, J., Analysis and prediction of the different types of β-turn in proteins. *J. Mol. Bio.* **1988**, *203*, 221-232. (b) Rose, G. D.; Glerasch, L. M.; Smith, J. A.: Turns in peptides and proteins. In *Adv. Protein Chem.*; Elsevier, 1985; Vol. 37; pp 1-109. (c) Richardson, J. S.: The anatomy and taxonomy of protein structure. In *Adv. Protein Chem.*; Elsevier, 1981; Vol. 34; pp 167-339.

(2) Ramachandran, G.; Mitra, A. K., An explanation for the rare occurrence of cis peptide units in proteins and polypeptides. *J. Mol. Bio.* **1976**, *107*, 85-92.

(3) Lewis, P. N.; Momany, F. A.; Scheraga, H. A., Chain reversals in proteins. *Biochim. Biophys. Acta* **1973**, *303*, 211-229.

(4) London, R. E.; Stewart, J. M.; Williams, R.; Cann, J. R.; Matwiyoff, N., Carbon-13 NMR spectroscopy of [20%-1, 2-13C2-Gly6]-bradykinin. Role of serine in reducing structural heterogeneity. *J. Am. Chem. Soc.* **1979**, *101*, 2455-2462.

(5) MacArthur, M. W.; Thornton, J. M., Influence of proline residues on protein conformation. *J. Mol. Bio.* **1991**, *218*, 397-412.

(6) Liakopoulou-Kyriakides, M.; Galardy, R. E., s-Cis and s-trans isomerism of the His-Pro peptide bond in angiotensin and Thyroliberin analogs. *Biochemistry* **1979**, *18*, 1952-1957.

(7) (a) Yaron, A.; Naider, F.; Scharpe, S., Proline-dependent structural and biological properties of peptides and proteins. *Crit. Rev. Biochem. Mol. Biol.* **1993**, *28*, 31-81. (b) Williams, K. A.; Deber, C. M., Proline residues in transmembrane helixes: structural or dynamic role? *Biochemistry* **1991**, *30*, 8919-8923. (c) Richard, N. G.; Hinds, M. G.; Brennand, D. M.; Glennie, M. J.; Welsh, J. M.; Robinson, J. A., Probing the role of proline as a recognition element in peptide antigens. *Biochem. Pharmacol.* **1990**, *40*, 119-123. (d) Lin, L.-N.; Brandts, J. F., Evidence suggesting that some proteolytic enzymes may cleave only the trans form of the peptide bond. *Biochemistry* **1979**, *18*, 43-47.

(8) (a) Juvvadi, P.; Dooley, D. J.; Humblet, C. C.; Lu, G. H.; Lunney, E. A.; Panek, R. L.; Skeean, R.; Marshall, G. R., Bradykinin and angiotensin II analogs containing a conformationally constrained proline analog. *Int. J. Pept. Protein Res.* **1992**, *40*, 163-170. (b) Lenman, M. M.; Ingham, S. L.; Gani, D., Syntheis and structure of cis-peptidyl prolinamide mimetics based upon 1, 2, 5-triazepine-3, 6-diones. *Chem. Comm.* **1996**, 85-

87. (c) Beausoleil, E.; Lubell, W. D., Steric Effects on the Amide Isomer Equilibrium of Prolyl Peptides. Synthesis and Conformational Analysis of N-Acetyl-5-tert-butylproline N'-Methylamides. *J. Am. Chem. Soc.* **1996**, *118*, 12902-12908. (d) Bélec, L.; Slaninova, J.; Lubell, W. D., A study of the relationship between biological activity and prolyl amide isomer geometry in oxytocin using 5-tert-butylproline to augment the Cys6-Pro7 amide cis-isomer population. *J. Med. Chem.* **2000**, *43*, 1448-1455. (e) Halab, L.; Lubell, W. D., Effect of Sequence on Peptide Geometry in 5-tert-Butylprolyl Type VI β-Turn Mimics. *J. Am. Chem. Soc.* **2002**, *124*, 2474-2484. (f) Halab, L.; Lubell, W. D., Use of Steric Interactions To Control Peptide Turn Geometry. Synthesis of Type VI β-Turn Mimics with 5-tert-Butylproline. *J. Org. Chem.* **1999**, *64*, 3312-3321. (g) Halab, L.; Lubell, W. D., Influence of N-terminal residue stereochemistry on the prolyl amide geometry and the conformation of 5-tert-butylproline type VI β-turn mimics. *J. Pept. Sci.* **2001**, *7*, 92-104.

(9) Halab, L.; Bélec, L.; Lubell, W. D., Improved synthesis of (2S, 5S)-5-tert-butylproline. *Tetrahedron* **2001**, *57*, 6439-6446.

(10) (a) Hart, S. A.; Sabat, M.; Etzkorn, F. A., Enantio-and regioselective synthesis of a (Z)-alkene cis-proline mimic. *J. Org. Chem.* **1998**, *63*, 7580-7581. (b) Andres, C. J.; Macdonald, T. L.; Ocain, T. D.; Longhi, D., Conformationally defined analogs of prolylamides. trans-Prolyl peptidomimetics. *J. Org. Chem.* **1993**, *58*, 6609-6613.

(11) Hart, S. A.; Etzkorn, F. A., Cyclophilin inhibition by a (Z)-alkene cis-proline mimic. *J. Org. Chem.* **1999**, *64*, 2998-2999.

(12) Halab, L.; Gosselin, F.; Lubell, W., Type VI beta-turn mimetic design; Synthesis of 5-tert-butylproline analogues of the FKBP substrate Ala-Leu-Pro-Phe. *Abstracts of papers of the American Chemical Society* **1997**, *213*, 326.

(13) Hemmerlin, C.; Cung, M. T.; Boussard, G., Synthesis and conformational preferences in solution and crystalline states of an aza-tripeptide. *Tetrahedron Lett.* **2001**, *42*, 5009-5012.

(14) Keller, M.; Boissard, C.; Patiny, L.; Chung, N. N.; Lemieux, C.; Mutter, M.; Schiller, P. W., Pseudoproline-Containing Analogues of Morphiceptin and Endomorphin-2: Evidence for a Cis Tyr− Pro Amide Bond in the Bioactive Conformation. *J. Med. Chem.* **2001**, *44*, 3896-3903.

(15) (a) Proulx, C.; Picard, E.; Boeglin, D.; Pohankova, P.; Chemtob, S.; Ong, H.; Lubell, W. D., Azapeptide Analogues of the Growth Hormone Releasing Peptide 6 as Cluster of Differentiation 36 Receptor Ligands with Reduced Affinity for the Growth Hormone Secretagogue Receptor 1a. *J. Med. Chem.* **2012**, *55*, 6502-6511. (b) Sabatino, D.; Proulx, C.; Pohankova, P.; Ong, H.; Lubell, W. D., Structure-Activity Relationships of GHRP-6 Azapeptide Ligands of the CD36 Scavenger Receptor by Solid-Phase Submonomer Azapeptide Synthesis. *J. Am. Chem. Soc.* **2011**, *133*, 12493-12506. (c) Demers, A.; McNICOLL, N.; Febbraio, M.; Servant, M.; Marleau, S.; Silverstein, R.; Huy, O., Identification of the growth hormone-releasing peptide binding site in CD36: a photoaffinity cross-linking study. *Biochemical Journal* **2004**, *382*, 417-424.

(16) (a) Kovács, G. L.; Szabó, G.; Telegdy, G.; Baláspiri, L.; Pálos, É.; Szpornyi, L., Antiamnesic effects of D-pipecolic acid and analogues of Pro-Leu-Gly-NH 2 in rats. *Pharmacol. Biochem. Behav.* **1988**, *31*, 833-837. (b) Fragiadaki, M.; Magafa, V.; Borovicková, L.; Slaninová, J.; Cordopatis, P., Synthesis and biological activity of oxytocin analogues containing conformationally-restricted residues in position 7. *Eur. J. Med. Chem.* **2007**, *42*, 799-806. (c) Formica, J. V.; Shatkin, A. J.; Katz, E., Actinomycin analogues containing pipecolic acid: relationship of structure to biological activity. *J. Bacteriol.* **1968**, *95*, 2139-2150. (d) Borloo, M.; Augustyns, K.; Belyaev, A.; de Meester, I.; Lambeir, A.-M.; Goossens, F.; Bollaert, W.; Rajan, P.; Scharpé, S.; Haemers, A., Synthesis and evaluation of azaproline peptides as potential inhibitors of dipeptidyl peptidase IV and prolyl oligopeptidase. *Lett. Pep. Sci.* **1995**, *2*, 198-202. (e) Wilkinson, D. E.; Thomas, B. E.; Limburg, D. C.; Holmes, A.; Sauer, H.; Ross, D. T.; Soni, R.; Chen, Y.; Guo, H.; Howorth, P., Synthesis, molecular modeling and biological evaluation of aza-proline and aza-pipecolic derivatives as FKBP12 ligands and their in vivo neuroprotective effects. *Bioorg. Med. Chem.* **2003**, *11*, 4815-4825. (f) Sadiq, A.; Sewald, N., 6-Alkynyl- and 6-aryl-substituted (R)-pipecolic acid derivatives. *Org. lett.* **2013**, *15*, 2720-2722.

(17) (a) Chingle, R.; Proulx, C.; Lubell, W. D., Azapeptide Synthesis Methods for Expanding Side-Chain Diversity for Biomedical Applications. *Acc. Chem. Res.* **2017**. (b) Proulx, C.; Sabatino, D.; Hopewell, R.; Spiegel, J.; Garcia, R. Y.; Lubell, W. D., Azapeptides and

their therapeutic potential. *Future Med. Chem.* **2011**, *3*, 1139-1164. (c) Gante, J., Azapeptides. *Synthesis* **1989**, 405-413.

(18) (a) Loughlin, W. A.; Tyndall, J. D.; Glenn, M. P.; Fairlie, D. P., Beta-strand mimetics. *Chem. Rev.* **2004**, *104*, 6085-6118. (b) Tyndall, J. D.; Nall, T.; Fairlie, D. P., Proteases universally recognize beta strands in their active sites. *Chem. Rev.* **2005**, *105*, 973-1000. (c) Tyndall, J. D.; Pfeiffer, B.; Abbenante, G.; Fairlie, D. P., Over one hundred peptide-activated G protein-coupled receptors recognize ligands with turn structure. *Chem. Rev.* **2005**, *105*, 793-826.

(19) (a) Che, Y.; Marshall, G. R., Impact of azaproline on peptide conformation. *J. Org. Chem.* **2004**, *69*, 9030-9042. (b) Zhang, W.-J.; Berglund, A.; Kao, J. L.-F.; Couty, J.-P.; Gershengorn, M. C.; Marshall, G. R., Impact of azaproline on amide cis− trans isomerism: conformational analyses and NMR studies of model peptides including TRH analogues. *J. Am. Chem. Soc.* **2003**, *125*, 1221-1235. (c) Che, Y.; Marshall, G. R., Engineering cyclic tetrapeptides containing chimeric amino acids as preferred reverse-turn scaffolds. *J. Med. Chem.* **2006**, *49*, 111-124.

(20) (a) Lecoq, A.; Boussard, G.; Marraud, M.; Aubry, A., Crystal state conformation of three azapeptides containing the azaproline residue, a β-turn regulator. *Biopolymers* **1993**, *33*, 1051-1059. (b) Didierjean, C.; Aubry, A.; Wyckaert, F.; Boussard, G., Structural features of the Pip/AzPip couple in the crystalline state: influence of the relative AzPip location in an aza dipeptide sequence upon the induced chirality and conformational characteristics. *J. Pept. Res.* **2000**, *55*, 308-317.

(21) (a) Lecoq, A.; Boussard, G.; Marraud, M.; Aubry, A., The couple Pro/AzaPro: a means of β-turn formation control synthesis and conformation of two azapro-containing dipeptides. *Tetrahedron Lett.* **1992**, *33*, 5209-5212. (b) Zouikri, M.; Vicherat, A.; Aubry, A.; Marraud, M.; Boussard, G., Azaproline as a β-turn-inducer residue opposed to proline. *J. Pept. Res.* **1998**, *52*, 19-26.

(22) Melendez, R. E.; Lubell, W. D., Aza-Amino Acid Scan for Rapid Identification of Secondary Structure Based on the Application of N-Boc-Aza1-Dipeptides in Peptide Synthesis. *J. Am. Chem. Soc.* **2004**, *126*, 6759-6764.

(23) Zhang, Y.; Malamakal, R. M.; Chenoweth, D. M., A Single Stereodynamic Center Modulates the Rate of Self-Assembly in a Biomolecular System. *Angew. Chem., Int. Ed.* **2015**, *54*, 10826-10832.

(24) Bac, A.; Rivoal, K.; Cung, M. T.; Boussard, G.; Marraud, M.; Soudan, B.; Tetaert, D.; Degand, P., Conformational disturbance induced by AzPro/Pro substitution in peptides. *Lett. Pep. Sci.* **1997**, *4*, 251-258.

(25) Freeman, N. S.; Tal-Gan, Y.; Klein, S.; Levitzki, A.; Gilon, C., Microwave-assisted solid-phase aza-peptide synthesis: Aza scan of a PKB/Akt inhibitor using aza-arginine and aza-proline precursors. *J. Org. Chem.* **2011**, *76*, 3078-3085.

(26) Chingle, R.; Ratni, S.; Claing, A.; Lubell, W. D., Application of constrained aza-valine analogs for Smac mimicry. *Biopolymers* **2016**, *106*, 235-244.

(27) (a) Schmidt, R.; Kalman, A.; Chung, N. N.; Lemieux, C.; Horvath, C.; Schiller, P. W., Structure-activity relationships of dermorphin analogues containing N-substituted amino acids in the 2-position of the peptide sequence. *Chem. Bio. Drug Design* **1995**, *46*, 47-55. (b) Liebmann, C.; Szücs, M.; Neubert, K.; Hartrodt, B.; Arold, H.; Barth, A., Opiate receptor binding affinities of some D-amino acid substituted β-casomorphin analogs. *Peptides* **1986**, *7*, 195-199. (c) Zhao, Z.; Liu, X.; Shi, Z.; Danley, L.; Huang, B.; Jiang, R.-T.; Tsai, M.-D., Mechanism of adenylate kinase. 20. Probing the importance of the aromaticity in tyrosine-95 and the ring size in proline-17 with unnatural amino acids. *J. Am. Chem. Soc.* **1996**, *118*, 3535-3536.

(28) Chang, K.-J.; Lillian, A.; Hazum, E.; Cuatrecasas, P.; Chang, J.-K., Morphiceptin (NH4-tyr-pro-phe-pro-COHN2): a potent and specific agonist for morphine (mu) receptors. *Science* **1981**, *212*, 75-77.

(29) Zadina, J. E.; Hackler, L.; Ge, L.-J.; Kastin, A. J., A potent and selective endogenous agonist for the μ-opiate receptor. *Nature* **1997**, *386*, 499.

(30) (a) Yamazaki, T.; Probstl, A.; Sschiller, P. W.; Goodman, M., Biological and conformational studies of [Val4] morphiceptin and [D-Val4] morphiceptin analogs incorporating cis-2-aminocyclopentane carboxylic acid as a peptidomimetic for proline. *J. Bacteriol.* **1991**, *37*, 364-381. (b) Borics, A.; Mallareddy, J. R.; Timári, I. n.; Kövér, K.

E.; Keresztes, A.; Tóth, G. z., The effect of Pro2 modifications on the structural and pharmacological properties of endomorphin-2. *J. Med. Chem.* **2012**, *55*, 8418-8428.

(31) (a) Doi, M.; Asano, A.; Komura, E.; Ueda, Y., The structure of an endomorphin analogue incorporating 1-aminocyclohexane-1-carboxlylic acid for proline is similar to the β-turn of Leu-enkephalin. *Biochem. Biophys. Res. Commun.* **2002**, *297*, 138-142. (b) Mallareddy, J. R.; Borics, A.; Keresztes, A.; Kövér, K. E.; Tourwé, D.; Tóth, G. z., Design, synthesis, pharmacological evaluation, and structure− activity study of novel endomorphin analogues with multiple structural modifications. *J. Med. Chem.* **2011**, *54*, 1462-1472.

(32) (a) Bryant, S. D.; Jinsmaa, Y.; Salvadori, S.; Okada, Y.; Lazarus, L. H., Dmt and opioid peptides: a potent alliance. *Pept. Sci.* **2003**, *71*, 86-102. (b) Li, T.; Shiotani, K.; Miyazaki, A.; Tsuda, Y.; Ambo, A.; Sasaki, Y.; Jinsmaa, Y.; Marczak, E.; Bryant, S. D.; Lazarus, L. H., Bifunctional [2 ‘, 6 ‘-Dimethyl-l-tyrosine] endomorphin-2 Analogues Substituted at Position 3 with Alkylated Phenylalanine Derivatives Yield Potent Mixed μ-Agonist/δ-Antagonist and Dual μ-Agonist/δ-Agonist Opioid Ligands. *J. Med. Chem.* **2007**, *50*, 2753-2766.

(33) Fenalti, G.; Zatsepin, N. A.; Betti, C.; Giguere, P.; Han, G. W.; Ishchenko, A.; Liu, W.; Guillemyn, K.; Zhang, H.; James, D., Structural basis for bifunctional peptide recognition at human δ-opioid receptor. *Nature Str. Mo. Bio.* **2015**, *22*, 265.

(34) Park, Y. M., CD36, a scavenger receptor implicated in atherosclerosis. *Exp. Mol. Med.* **2014**, *46*, e99.

(35) Chignen Possi, K.; Mulumba, M.; Omri, S.; Garcia-Ramos, Y.; Tahiri, H.; Chemtob, S.; Ong, H.; Lubell, W. D., Influences of Histidine-1 and Azaphenylalanine-4 on the Affinity, Anti-inflammatory, and Antiangiogenic Activities of Azapeptide Cluster of Differentiation 36 Receptor Modulators. *J. Med. Chem.* **2017**, *60*, 9263-9274.

(36) Huynh, D. N.; Bessi, V. L.; Ménard, L.; Piquereau, J.; Proulx, C.; Febbraio, M.; Lubell, W. D.; Carpentier, A. C.; Burelle, Y.; Ong, H., Adiponectin has a pivotal role in the cardioprotective effect of CP-3 (iv), a selective CD36 azapeptide ligand, after transient coronary artery occlusion in mice. *FASEB J.* **2017**, *32*, 807-818.

(37) (a) Fichna, J.; do-Rego, J.-C.; Chung, N. N.; Lemieux, C.; Schiller, P. W.; Poels, J.; Vanden Broeck, J.; Costentin, J.; Janecka, A., Synthesis and Characterization of Potent

and Selective μ-Opioid Receptor Antagonists,[Dmt, d-2-Nal4] endomorphin-1 (Antanal-1) and [Dmt1, d-2-Nal4] endomorphin-2 (Antanal-2). *J. Med. Chem.* **2007**, *50*, 512-520. (b) Fenalti, G.; Zatsepin, N. A.; Betti, C.; Giguere, P.; Han, G. W.; Ishchenko, A.; Liu, W.; Guillemyn, K.; Zhang, H.; James, D., Structural basis for bifunctional peptide recognition at human δ-opioid receptor. *Nat. Struct. Mol. Biol.* **2015**, *22*, 265.

(38) Paton, W. D., The action of morphine and related substances on contraction and on acetylcholine output of coaxially stimulated guinea-pig ileum. *Br. J. Pharmacol.* **1957**, *12*, 119-127.

(39) Henderson, G.; Hughes, J.; Kosterlitz, H., A new example of a morphine-sensitive neuro-effector junction: adrenergic transmission in the mouse vas deferens. *Br. J. Pharmacol.* **1972**, *46*, 764-766.

(40) Korhonen, R.; Lahti, A.; Kankaanranta, H.; Moilanen, E., Nitric oxide production and signaling in inflammation. *Curr. Drug Targets Inflamm. Allergy* **2005**, *4*, 471-479.

(41) (a) Carpino, L. A.; Han, G. Y., 9-Fluorenylmethoxycarbonyl amino-protecting group. *J. Org. Chem.* **1972**, *37*, 3404-3409. (b) Boeglin, D.; Lubell, W. D., Aza-Amino Acid Scanning of Secondary Structure Suited for Solid-Phase Peptide Synthesis with Fmoc Chemistry and Aza-Amino Acids with Heteroatomic Side Chains. *J. Comb. Chem.* **2005**, *7*, 864-878.

(42) (a) Bourguet, C. B.; Proulx, C.; Klocek, S.; Sabatino, D.; Lubell, W. D., Solution-phase submonomer diversification of aza-dipeptide building blocks and their application in aza-peptide and aza-DKP synthesis. *J. Pept. Sci.* **2010**, *16*, 284-296. (b) Bourguet, C. B.; Sabatino, D.; Lubell, W. D., Benzophenone semicarbazone protection strategy for synthesis of aza-glycine containing aza-peptides. *Biopolymers* **2008**, *90*, 824-831.

(43) Chingle, R.; Lubell, W. D., Azopeptides: Synthesis and Pericyclic Chemistry. *Org. Lett.* **2015**, *17*, 5400-5403.

(44) Fahr, E.; Lind, H., The chemistry of α-carbonyl azo compounds. *Angew. Chem., Int. Ed. Engl.* **1966**, *5*, 372-384.

(45) Gray, C.; Quibell, M.; Baggett, N.; Hammerle, T., Incorporation of azaglutamine residues into peptides synthesised by the ultra-high load solid (gel)-phase technique. *Int. J. Pept. Protein Res.* **1992**, *40*, 351-362.

(46) (a) Meienhofer, J.; Waki, M.; Heimre, E. P.; Lambros, T. J.; Makofske, R. C.; Chang, C., Solid phase synthesis without repetitive acidolysis. *Int. J. Peptide Protein. Res.* **1979**, *13*, 35-42. (b) Lubell, W.; Blankenship, J.; Fridkin, G.; Kaul, R., Science of Synthesis 21.11. *Peptides* **2005**, 713-809.

(47) (a) Subirós-Funosas, R.; Khattab, S. N.; Nieto-Rodriguez, L.; El-Faham, A.; Albericio, F., Advances in acylation methodologies enabled by oxyma-based reagents. *Aldrichim Acta* **2013**, *46*, 21-40. (b) Subirós-Funosas, R.; Prohens, R.; Barbas, R.; El-Faham, A.; Albericio, F., Oxyma: An Efficient Additive for Peptide Synthesis to Replace the Benzotriazole-Based HOBt and HOAt with a Lower Risk of Explosion [1]. *Chem. Eur. J.* **2009**, *15*, 9394-9403.

(48) Carpino, L. A., 1-Hydroxy-7-azabenzotriazole. An efficient peptide coupling additive. *J. Am. Chem. Soc.* **1993**, *115*, 4397-4398.

(49) Wissmann, H.; Kleiner, H. J., New peptide synthesis. *Angew. Chem., Int. Ed.* **1980**, *19*, 133-134.

(50) (a) El-Faham, A.; Albericio, F., COMU: A third generation of uronium-type coupling reagents. *J. Pep. Sci.* **2010**, *16*, 6-9. (b) El-Faham, A.; Funosas, R. S.; Prohens, R.; Albericio, F., COMU: A Safer and More Effective Replacement for Benzotriazole-Based Uronium Coupling Reagents. *Chem. Eur. J.* **2009**, *15*, 9404-9416.

(51) Falb, E.; Yechezkel, T.; Salitra, Y.; Gi1on, C., In situ generation of Fmoc-amino acid chlorides using bis-(trichloromethyl) carbonate and its utilization for difficult couplings in solid-phase peptide synthesis. *J. Pept. Res.* **1999**, *53*, 507-517.

(52) Fichna, J.; do-Rego, J.-C.; Chung, N. N.; Costentin, J.; Schiller, P. W.; Janecka, A., [Dmt1, d-1-Nal3] morphiceptin, a novel opioid peptide analog with high analgesic activity. *Peptides* **2008**, *29*, 633-638.

(53) Hansen Jr, D. W.; Stapelfeld, A.; Savage, M. A.; Reichman, M.; Hammond, D. L.; Haaseth, R. C.; Mosberg, H. I., Systemic analgesic activity and. delta.-opioid selectivity in [2, 6-dimethyl-Tyr1, D-Pen2, D-Pen5] enkephalin. *J. Med. Chem.* **1992**, *35*, 684-687.

(54) Newberry, R. W.; Raines, R. T.: 4-Fluoroprolines: Conformational analysis and effects on the stability and folding of peptides and proteins. In *Peptidomimetics I*; Springer, 2016; pp 1-25.

(55) Bélec, L.; Lubell, W.; Maletinska, L.; Slaninová, J., The influence of steric interactions on the conformation and biology of oxytocin. Synthesis and analysis of penicillamine6-oxytocin and penicillamine6-5-tert-butylproline7-oxytocin analogs. *Pept. Res.* **2001**, *58*, 263-273.

(56) (a) Schiller, P. W.; Lipton, A.; Horrobin, D. F.; Bodanszky, M., Unsulfated C-terminal 7-peptide of cholecystokinin: a new ligand of the opiate receptor. *Biochem. Biophys. Res. Commun.* **1978**, *85*, 1332-1338. (b) DiMaio, J.; Nguyen, T. M.; Lemieux, C.; Schiller, P. W., Synthesis and pharmacological characterization in vitro of cyclic enkephalin analogs: effect of conformational constraints on opiate receptor selectivity. *J. Med. Chem.* **1982**, *25*, 1432-1438. (c) Weltrowska, G.; Chung, N. N.; Lemieux, C.; Guo, J.; Lu, Y.; Wilkes, B. C.; Schiller, P. W., "Carba"-analogues of fentanyl are opioid receptor agonists. *J. Med. Chem.* **2010**, *53*, 2875-2881.

(57) Waterfield, A. A.; Leslie, F. M.; Lord, J. A.; Ling, N.; Kosterlitz, H. W., Opioid activities of fragments of β-endorphin and of ites leucine65-analogue. Comparison of the binding properties of methionine-and leucine-enkephalin. *Eur. J. Pharmacol.* **1979**, *58*, 11-18.

Chapter 5: Conclusion and perspectives

5.1 Conclusion and perspectives

The successful employment of semicarbazides as amino amide surrogates to restrict the conformation and enhance the physical properties of peptides has provided peptidomimetics with enhanced utility as receptor ligands and enzyme inhibitors in medicinal chemistry efforts towards drug discovery. The synthesis of such azapeptides has however been challenging due to difficulties in combining hydrazine and peptide chemistry. Through study of the insertion of an azodicarbonyl unit into the polyamide backbone, the thesis has forged new pathways for making challenging aza-amino acid residues by harnessing the power of pericyclic chemistry using azopeptides.[1]

Solution- and solid-phase methods for introducing and oxidizing carbamate protected aza-glycine residues at the *N*-terminal of a peptide chain have delivered the imino urea unit, which reacted in Diels-Alder and Alder-ene chemistry to provide respectively aza-pipecolyl and aza-allylglycyl residues.[1b] Acylation of the *N*-terminal of the electron deficient aza-pipecolyl semicarbazide proved challenging but was surmounted using coupling agents such as PyBOP and *N*-(Fmoc)amino acid chlorides to deliver good yields of final azapeptide. The success of the pericyclic reactions of azopeptides bears well for further exploration of the rich diversity of azodicarbonyl chemistry to prepare a variety of constrained azapeptides without employing ionic chemistry to add side chains to hydrazine residues.[2]

Atom economical, pericyclic chemistry gave effective access to cyclic and unsaturated systems. Likewise, azopeptides may be used to explore other types of azodicarboxylate reactions such as electrophilic amination.[3] For example, aza-Baylis–Hillman reactions at the α-nitrogen may give ene-hydrazines, because azodicarboxylates **5.1** have been reacted with α,β-unsaturated ketones, acrylates and acrylonitrile in the presence of DABCO to provide ene-hydrazine adducts **5.2**.[4] Subsequent cyclization by 1,2-attack or 1,4-attack of the urea nitrogen onto the resulting unsaturated system may provide substituted *N*-aminoimidazolidin-2-one (Aid) peptidomimetics **5.4** or **5.3** (Scheme 5.1). Cyclization on ene adduct **5.2** could be take place in two ways. The 5-*endo trig* cyclization would give you aspartate derivative **5.3**. Although a violation of Baldwin rules,[5] several literature examples

support the type of cyclization.[6] Alternatively, the 5-*exo trig* cyclization is favoured and in the case of acrylate may provide **5.4**. Notably, unsubstituted Aid residues have been introduced into peptide sequences by alkylation of semicarbazones with 1,2-dibromoethane.[7] The electronic and structural constraints induced by Aid residues to restrict rotation about the backbone ϕ-, ψ-, and ω-dihedral angles can stabilize β-turn conformations offering potential for exploring structure–activity relationships to elucidate active conformers of biologically relevant peptides.[8] 5-Carboxylate *N*-aminoimidazolidin-2-ones **5.3** from the proposed sequence could serve as a constrained aspartate residues (Scheme 5.1).[8]

Scheme 5.1. Proposed aza-Baylis–Hillman reaction of an azopeptide with α,β-unsaturated ketones catalyzed by DABCO and reactivity of resulting dehydroalanines.

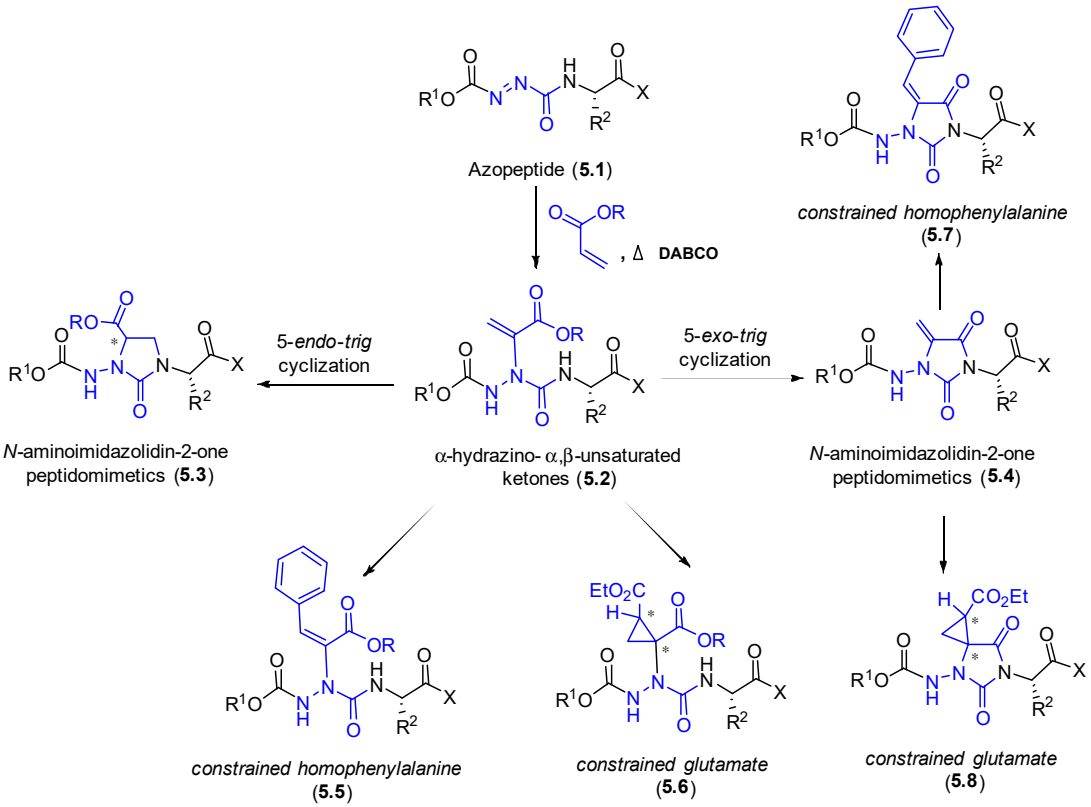

Furthermore, olefins **5.2** and **5.4** may react in palladium-catalyzed Heck chemistry using aryl iodides and bromides to make constrained homophenylalanine derivatives (e.g. **5.5** and **5.7**).[9] Similarly, olefins **5.2** and **5.4** may undergo cyclopropanations catalyzed by rhodium acetate via decomposition of diazo reagents, such as ethyl diazoacetate to access

constrained glutamates (Scheme 5.1, e.g. **5.6** and **5.8**).[10] Moreover, polymer-supported dehydroalanines have been found to be reactive in Diels-Alder cycloadditions to access cycloaliphatic peptides.[11]

X-ray crystallographic analyses of aza-products have demonstrated potential for stabilizing type I and VI *β*-turn conformations to favour receptor recognition (Chapter 2). Moreover, IR spectroscopy, NMR spectroscopy and X-ray crystallographic analyses were performed on the azopeptide to give insight into the imino urea configuration. Azopeptide formed in the reaction was observed as a new relatively nonpolar bright yellow spot on the TLC plate and the formation of the N=N bond was detected using IR spectroscopy on compounds synthesized in solution and directly on resin. Azopeptides exhibited bands between 1700 to 1765 cm^{-1} indicative of the N=N stretching vibration. Crystal structures of azopeptide **2.16a** showed a bent conformation with a dihedral angle value of −173° with an N=N bond length of ∼1.24 Å and *E*-diazine configuration.

The effective methods for synthesizing and employing azopeptides to prepare diverse aza-pipecolate and aza-allylglycine analogues has empowered their application to explore structure-activity relationships of a series of biologically relevant peptides. For example, two aza-pipecolate analogs of melanocyte-stimulating hormone release inhibiting factor-1 (MIF-1, H-Pro-Leu-Gly-NH_2) **2.40** and **2.41** were effectively prepared in solution. Their biological assessment was however not promising and indicated that replacement of *N*-terminal amino acids in a peptide by semicarbazides may have limitations due to different states of physiological protonation.

In contrast, employment of aza-pipecolate and aza-allylglycine analogues in the interior of the peptide chain introduced conformational control and provided azapeptides with promising activity. Such azapeptides provided insight for developing anti-cancer, antinociceptive and anti-inflammatory agents. For example, application of aza-pipecolate and aza-allylglycine as constrained valine analogs in the H-Ala-Val-Pro-Ile-NH_2 **3.3** sequence provided Smac mimics **3.11** which induced cell death relative to vehicle in a breast cancer cell assay.

To employ azopeptides in a combinatorial manner, a solid-phase approach was devised featuring Diels-Alder chemistry to install aza-pipecolate residues into libraries of biologically active peptide targets.[12] Specifically, opioid and CD36 receptor ligands were synthesized exhibiting promising activity and selectivity. Among seventeen aza-pipecolyl analogs from Diels-Alder chemistry on azo-residues, [Dmt[1], azaPip[2], D-Phe[3]]morphiceptin analogs were more potent than [Pip[2]]morphiceptin (H-Dmt-Pip-Phe-Pro-NH_2) and compared in activity the potent and long acting mu receptor subtype agonist [Dmt[1], D-1-Nal[3]]morphiceptin.[13] Significant reductions of NO production after stimulation with a Toll-like receptor agonist were exhibited by [(Δ^4)-azaPip[3]]- and [(Δ^4)-azaPip[4]]GHRP-6 and their saturated azaPip counterparts.[12] Providing critical information about conformational requirements for activity and receptor selectivity, the aza-pipecolyl peptides offered respectively interesting utility for the conception of prototypical molecules to treat pain and inflammation. Considering the diverse spectrum of biologically active sequences containing proline[14] and pipecolate residues,[15] which exhibit *N*-terminal amide equilibria, the effectiveness of the approach for introducing aza-pipecolate to favor amide *cis*-isomer geometry and type VI β-turn conformers constitutes an important means to probe active backbone geometry to study peptide chemical biology and medicinal chemistry.[12]

To further demonstrate the power of the solid-phase approach for making aza-pipecolic acid containing peptides several targets may be considered to explore their biologically relevant conformations towards drug discovery. The laboratory of Professor Etzkorn has designed and synthesized olefin isosteres of the prolyl amide *cis* and *trans* isomers of Pin1 [Protein interacting with Never in Mitosis A (NIMA) Kinase] substrates.[16] Replacement of the central phosphoSer-Pro core of the Pin1 substrate *cis* and *trans*-**5.5** with amide isosteres in AcPhe-Phe-pSer-Ψ[(*Z* and *E*)CH=C]-Pro-Arg-NH_2 peptidomimetics has demonstrated that the olefin *cis*-isomer was a better inhibitor.[17] Considering the potential for aza-pipecolic acid to stabilize of the amide *cis*-isomer,[18] Pin1 substrate analog **5.6** merits investigation to develop a novel peptidyl-prolyl isomerase inhibitor (Figure 5.1) Note, the serine residue of the peptide precursor may be phosphorylated using (*N*,*N*-diisopropyl)dibenzylphosphoramidite, followed by hydrogen peroxide oxidation.[19]

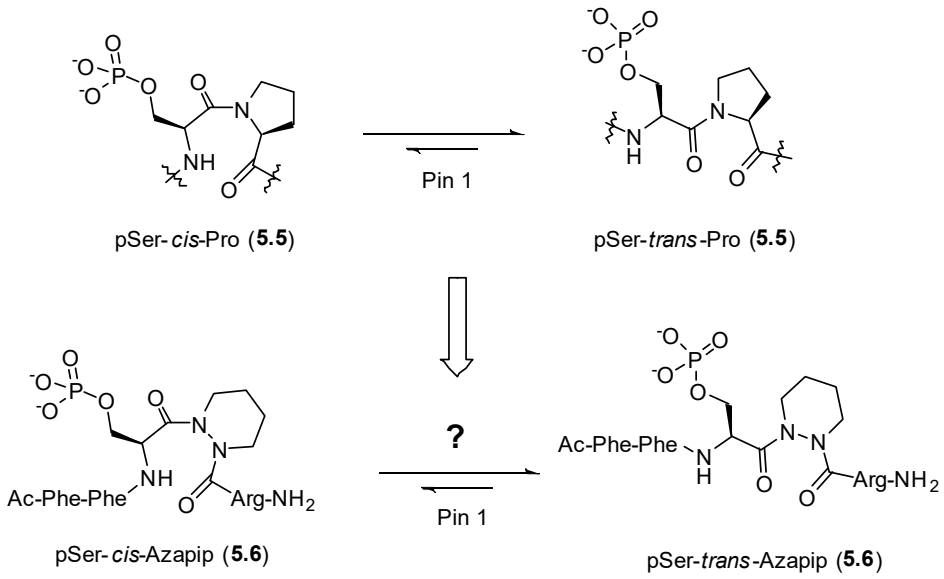

Figure 5.1. Isomerization of phosphoSer-Pro Pin1 substrate **5.5**. Bottom: proposed azapipecolyl inhibitor **5.6**.

Considering the plethora of biologically active peptides that possess proline and pipecolate residues exhibiting *N*-terminal amide equilibria, the effectiveness of the approach for introducing aza-pipecolate to favor amide *cis* isomer geometry and type VI β-turns constitutes an important means to study backbone geometry towards the conception of more potent and selective prototypes for drug discovery.

References

(1) (a) Chingle, R.; Proulx, C.; Lubell, W. D., Azapeptide Synthesis Methods for Expanding Side-Chain Diversity for Biomedical Applications. *Acc. Chem. Res.* **2017**. (b) Chingle, R.; Lubell, W. D., Azopeptides: Synthesis and Pericyclic Chemistry. *Org. Lett.* **2015**, *17*, 5400-5403.

(2) Chingle, R.; Ratni, S.; Claing, A.; Lubell, W. D., Application of constrained aza-valine analogs for Smac mimicry. *Biopolymers* **2016**, *106*, 235-244.

(3) (a) Trimble, L. A.; Vederas, J. C., Amination of chiral enolates by dialkyl azodiformates. Synthesis of. alpha.-hydrazino acids and. alpha.-amino acids. *J. Am. Chem. Soc.* **1986**, *108*, 6397-6399. (b) Harris, J. M.; McDonald, R.; Vederas, J. C., Synthesis of a chiral azodicarboxamide containing a bridging binaphthyl moiety: electrophilic amination reactions of achiral ester enolates. *J. Chem. Soc., Perkin Trans. 1* **1996**, 2669-2674.

(4) (a) Shi, M.; Zhao, G.-L., Aza-Baylis–Hillman reactions of diisopropyl azodicarboxylate or diethyl azodicarboxylate with acrylates and acrylonitrile. *Tetrahedron* **2004**, *60*, 2083-2089. (b) Kamimura, A.; Gunjigake, Y.; Mitsudera, H.; Yokoyama, S., A facile preparation of α-hydrazino-α, β-unsaturated ketones via aza-Baylis-Hillman reaction. *Tetrahedron Lett.* **1998**, *39*, 7323-7324.

(5) (a) Baldwin, J. E.; Cutting, J.; Dupont, W.; Kruse, L.; Silberman, L.; Thomas, R. C., 5-Endo-trigonal reactions: a disfavoured ring closure. *J. Chem. Soc., Chem. Commun.* **1976**, 736-738. (b) Baldwin, J. E., Rules for ring closure. *J. Chem. Soc., Chem. Commun.* **1976**, 734-736.

(6) (a) Gilmore, K.; Manoharan, M.; Wu, J. I.-C.; Schleyer, P. v. R.; Alabugin, I. V., Aromatic transition states in nonpericyclic reactions: anionic 5-endo cyclizations are aborted sigmatropic shifts. *J. Am. Chem. Soc.* **2012**, *134*, 10584-10594. (b) Perkins, M. J.; Wong, P. C.; Barrett, J.; Dhaliwal, G., Formation of dioxolanes from carbonyl compounds: favored 5-trigonal cyclizations. *J. Org. Chem.* **1981**, *46*, 2196-2199.

(7) (a) Doan, N.-D.; Hopewell, R.; Lubell, W. D., N-aminoimidazolidin-2-one peptidomimetics. *Org Lett* **2014**, *16*, 2232-2235. (b) Doan, N.-D.; Lubell, W. D., X-ray structure analysis reveals β-turn mimicry by N-amino-imidazolidin-2-ones. *Biopolymers* **2015**, *104*, 629-635.

(8) St-Cyr, D. J.; García-Ramos, Y.; Doan, N.-D.; Lubell, W. D.: Aminolactam, N-Aminoimidazolone, and N-Aminoimdazolidinone Peptide Mimics. In *Peptidomimetics I*; Springer, 2017; pp 125-175.

(9) (a) Heck, R.; Nolley Jr, J., Palladium-catalyzed vinylic hydrogen substitution reactions with aryl, benzyl, and styryl halides. *J. Org. Chem.* **1972**, *37*, 2320-2322. (b) Doi, T.; Fujimoto, N.; Watanabe, J.; Takahashi, T., Palladium (0)-catalyzed Mizoroki–Heck reaction and Rh (I)-catalyzed asymmetric hydrogenation of polymer-supported dehydroalanine system. *Tetrahedron Lett.* **2003**, *44*, 2161-2165. (c) Byk, G.; Cohen-Ohana, M.; Raichman, D., Fast and versatile microwave-assisted intramolecular Heck reaction in peptide macrocyclization using microwave energy. *Biopolymers* **2006**, *84*, 274-282.

(10) Gober, J. G.; Ghodge, S. V.; Bogart, J. W.; Wever, W. J.; Watkins, R. R.; Brustad, E. M.; Bowers, A. A., P450-mediated non-natural cyclopropanation of dehydroalanine-containing thiopeptides. *ACS Chem. Biol.* **2017**, *12*, 1726-1731.

(11) Burkett, B. A.; Chai, C. L., The Diels-Alder reactions of polymer bound dehydroalanine derivatives. *Tetrahedron Lett.* **1999**, *40*, 7035-7038.

(12) Chingle, R.; Mulumba, M.; Chung, N. N.; Ong, H.; Ballet, S.; Schiller, P. W.; Lubell, W. D., Identification of Active Peptide Conformations by Application of aza-Pipecolyl Residue Insertion Using Solid-Phase Azopeptide Diels-Alder Chemistry. *In Preparation* **2018**.

(13) (a) Fichna, J.; do-Rego, J.-C.; Chung, N. N.; Costentin, J.; Schiller, P. W.; Janecka, A., [Dmt1, d-1-Nal3] morphiceptin, a novel opioid peptide analog with high analgesic activity. *Peptides* **2008**, *29*, 633-638. (b) Keller, M.; Boissard, C.; Patiny, L.; Chung, N. N.; Lemieux, C.; Mutter, M.; Schiller, P. W., Pseudoproline-Containing Analogues of Morphiceptin and Endomorphin-2: Evidence for a Cis Tyr− Pro Amide Bond in the Bioactive Conformation. *J. Med. Chem.* **2001**, *44*, 3896-3903.

(14) (a) Beausoleil, E.; Lubell, W. D., Steric Effects on the Amide Isomer Equilibrium of Prolyl Peptides. Synthesis and Conformational Analysis of N-Acetyl-5-tert-butylproline N'-Methylamides. *J. Am. Chem. Soc.* **1996**, *118*, 12902-12908. (b) Bélec, L.; Slaninova, J.; Lubell, W. D., A study of the relationship between biological activity and prolyl amide

isomer geometry in oxytocin using 5-tert-butylproline to augment the Cys6-Pro7 amide cis-isomer population. *J. Med. Chem.* **2000**, *43*, 1448-1455. (c) Halab, L.; Lubell, W. D., Effect of Sequence on Peptide Geometry in 5-tert-Butylprolyl Type VI β-Turn Mimics. *J. Am. Chem. Soc.* **2002**, *124*, 2474-2484. (d) Halab, L.; Lubell, W. D., Use of Steric Interactions To Control Peptide Turn Geometry. Synthesis of Type VI β-Turn Mimics with 5-tert-Butylproline. *J. Org. Chem.* **1999**, *64*, 3312-3321. (e) Halab, L.; Lubell, W. D., Influence of N-terminal residue stereochemistry on the prolyl amide geometry and the conformation of 5-tert-butylproline type VI β-turn mimics. *J. Pept. Sci.* **2001**, *7*, 92-104.

(15) Hemmerlin, C.; Cung, M. T.; Boussard, G., Synthesis and conformational preferences in solution and crystalline states of an aza-tripeptide. *Tetrahedron Lett.* **2001**, *42*, 5009-5012.

(16) Lu, K. P.; Hanes, S. D.; Hunter, T., A human peptidyl–prolyl isomerase essential for regulation of mitosis. *Nature* **1996**, *380*, 544.

(17) (a) Wang, X. J.; Xu, B.; Mullins, A. B.; Neiler, F. K.; Etzkorn, F. A., Conformationally locked isostere of phosphoSer− cis-Pro inhibits Pin1 23-fold better than phosphoSer− trans-Pro isostere. *J. Am. Chem. Soc.* **2004**, *126*, 15533-15542. (b) Wang, X. J.; Etzkorn, F. A., Peptidyl-prolyl isomerase inhibitors. *Biolpolymers* **2006**, *84*, 125-146.

(18) Che, Y.; Marshall, G. R., Impact of azaproline on peptide conformation. *J. Org. Chem.* **2004**, *69*, 9030-9042.

(19) McMurray, J. S.; Coleman, D. R.; Wang, W.; Campbell, M. L., The synthesis of phosphopeptides. *Biolpolymers* **2001**, *60*, 3-31.

Annex 1: Experimental part of Chapter 2

General Methods

Unless specified, all non-aqueous reactions were run under an inert argon atmosphere. All glassware was stored in the oven or flame-dried, and let cool under an inert atmosphere prior to use. Anhydrous solvents (THF, DCM, and DMF) were obtained by passage through solvent filtration systems (GlassContour, Irvine, CA). Visualization of the developed chromatogram was performed by UV absorbance or staining with ceric ammonium molybdate or potassium permanganate solutions. Silica gel chromatography[1] was performed using 230-400 mesh silica gel (Silicycle), and TLC was on glass-backed silica plates. Melting points were obtained on a Buchi melting point B-540 apparatus and are uncorrected. Specific rotations, $[\alpha]_D$ values, were calculated from optical rotations measured at 20 °C in $CHCl_3$ or MeOH at the specified concentrations (*c* in g/100 ml) using a 1-dm cell length (*l*) on a Perkin-Elmer Polarimeter 241 at 589 nm, using the general formula: $[\alpha]_D^{20} = (100 \times \alpha)/(l \times c)$. Nuclear magnetic resonance spectra (^1H, ^{13}C, HMBC) were recorded on Bruker AV 400, AV III 400 and AV 500 spectrometers. ^1H NMR spectra were referenced to $CDCl_3$ (7.26 ppm), CD_3OD (3.31 ppm), DMSO-d_6 (2.50 ppm) or $(CD_3)_2CO$ (2.05 ppm) and ^{13}C NMR spectra were measured in $CDCl_3$ (77.16 ppm), CD_3OD (49.0 ppm), or DMSO-d_6 (39.52 ppm), or $(CD_3)_2CO$ (29.84 ppm) as specified below. Coupling constants, *J* values were measured in hertz (Hz) and chemical shift values in parts per million (ppm). Non-uniform sampling (NUS) NMR experiments[2] at 120 °C were used to assign the regiochemistry of **2.33a** and **2.34a**. In cases of isomers of conformation, the minor isomer ^1H and ^{13}C NMR data are reported in brackets and parentheses respectively. Infrared spectra were recorded in the neat on a Perkin Elmer Spectrum One FTIR instrument, and are reported in reciprocal centimetres (cm^{-1}). Accurate mass measurements were performed on a LC-MSD instrument from Agilent technologies in positive electrospray ionisation (ESI) mode at the Université de Montréal Mass Spectrometry facility. Sodium adducts $[M+Na]^+$ were used for empirical formula confirmation. Analytical supercritical fluid chromatography (SFC) was performed in the Laboratory for chiral separation at the Université de Montréal and data are reported as

follows: column type, eluent, flow rate, temperature, backpressure, wavelength and retention times (R*t*). Crystallogarphic data studies for **2.16a**, **2.30a** and **2.35a** were performed on a Bruker venture metaljet diffractometer at the Université de Montréal X-ray Regional Facility.

Reagents used: Aza-glycinyl proline/phenyl alanine/sarcosine benzhydrylamide hydrochloride analogues, all were synthesized according to literature methods.[3] The hydrochloride salt of leucinyl-glycine benzyl ester was synthesized from the corresponding amino acids by coupling Boc-Leu-OH and HCl•Gly-OBn using 1-(3-dimethylaminopropyl)-3-ethylcarbodiimide hydrochloride (EDCI) and 1-hydroxybenzotriazole (HOBt) in DMF followed by Boc group removal.[4] *N*-Bromo succinimide (NBS), pyridine, disuccinimidyl carbonate (DSC), benzyl carbazate, *tert*-butyl carbazate, diisopropyl ethyl amine (DIEA), 1,3-butadiene, 2,3-dimethylbutadiene, isobutylene, cyclohexadiene, cycloheptatriene, and magnessium nitride (Mg_3N_2), all were purchased from Aldrich and used as received. Benzophenone hydrazone, *p*-nitrophenyl chloroformate, diphenylmethylamine, benzyl chloroformate, all were purchased from Aldrich or Alfa Aesar and used without further purification. Dicyclopentadiene was cracked at 180 °C into cyclopentadiene prior to use in the Diels-Alder reaction. Proline, phenylalanine, sarcosine, and coupling reagents, such as HOBT, TBTU, all were purchased from GL Biochem™ and used as received.

Synthetic experimental conditions and characterization data of compounds:

Synthesis of Aza-peptides

N-Cbz-L-Alaninyl-aza-glycinyl-L-proline Benzhydrylamide (2.6a)

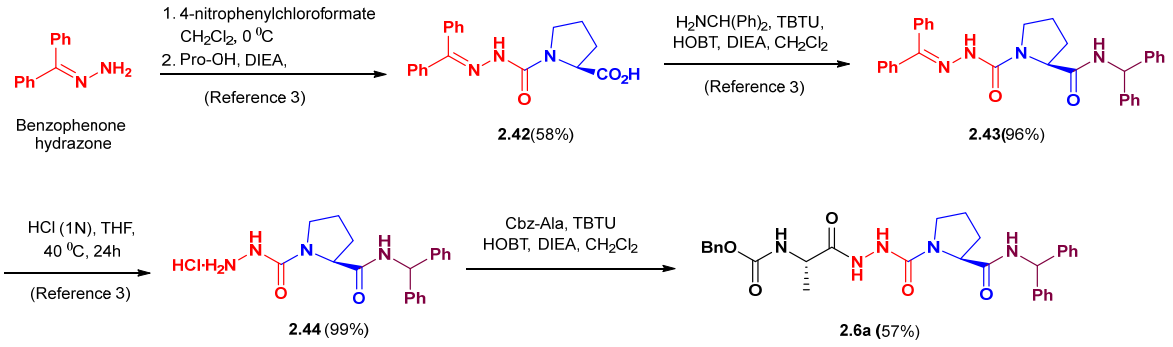

A solution of aza-glycinyl-proline benzhydrylamide hydrochloride **2.44** (0.3 g, 0.887 mmol, prepared according to reference 3) and DIPEA (0.293 mL, 1.77 mmol) in dry DCM (5 mL) was added to a solution of *N*-Cbz-L-alanine (0.198 g, 0.887 mmol), HOBt (0.12 g, 0.887 mmol), and TBTU (0.285 g, 0.887 mmol) in DCM (10 mL), and stirred overnight. The volatiles were removed under vacuum. The residue was dissolved in EtOAc (20 mL), washed with 5 mL of saturated aqueous $NaHCO_3$ and HCl (1N), dried over Na_2SO_4, and concentrated under vacuum. The residue was purified by column chromatography using 100% EtOAc as eluant to give aza-tripeptide **2.6a** (0.275 g, 57%) as white solid: R_f 0.41 (100% EtOAc); mp 118−119 °C; $[\alpha]_D^{20}$ −72.5° (*c* 0.64, CH_3OH); ^1H NMR (500 MHz, CD_3OD) δ 7.42 – 7.16 (m, 15H), 6.17 (s, 1H), 5.09 (s, 2H), 4.46 (dd, *J* = 8.4, 3.0 Hz, 1H), 4.27 (q, *J* = 7.1 Hz, 1H), 3.55 (dt, *J* = 8.9, 6.1 Hz, 1H), 3.46 – 3.38 (m, 1H), 2.22 – 2.09 (m, 1H), 2.04 – 1.90 (m, 3H), 1.41 (d, *J* = 7.2 Hz, 3H); ^{13}C NMR (125 MHz, MeOD) δ 175.5, 174.4, 158.3, 158.1, 143.0, 142.9, 138.2, 129.5, 129.0, 128.9, 128.8, 128.7, 128.3, 128.2, 67.7, 62.1, 58.1, 50.6, 47.3, 31.0, 25.7, 18.5. IR (neat) ν_{max}/cm^{-1} 3281, 1681, 1655, 1541, 1494, 1381, 1303, 1070; HRMS *m/z* calculated for $C_{30}H_{33}N_5NaO_5$ $[M+Na]^+$ 566.2374; found 566.2394.

_N_-Boc-L-Alaninyl-aza-glycinyl-L-proline Benzhydrylamide (2.6b)

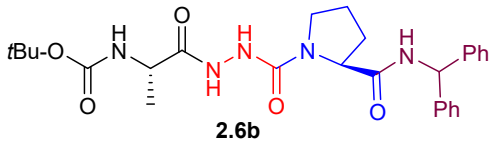

2.6b

Employing the procedure described for aza-glycinyl tripeptide **2.6a**, aza-glycinyl-proline benzhydrylamide hydrochloride **2.43** (1g, 2.96 mmol, prepared according to reference 3) was reacted with *N*-Boc-L-alanine (0.559 g, 2.96 mmol), HOBt (1 eq., 0.399 g, 2.96 mmol) and TBTU (1 eq., 0.299 g, 0.411 mL, 2.96 mmol). The residue was purified by column chromatography eluting with 100% EtOAc to afford aza-tripeptide **2.6b** (1.02 g, 68%) as white solid: R_f 0.39 (100% EtOAc); mp 116−118 °C; $[\alpha]_D^{20}$ −55.7° (*c* 1, $CHCl_3$); ^{1}H NMR (500 MHz, $CDCl_3$) δ 8.88 – 8.74 (br s, 1H), 7.86 (d, *J* = 8.2 Hz, 1H), 7.34 – 7.13 (m, 10H), 7.13 – 6.87 (br s, 1H), 6.19 (d, *J* = 8.4 Hz, 1H), 5.51 (d, *J* = 7.5 Hz, 1H), 4.43 – 4.22 (br s, 2H), 3.45 – 3.35 (m, 1H), 3.25 – 3.12 (m, 1H), 2.28 – 2.07 (br s, 1H), 1.96 – 1.64 (m, 3H), 1.43 (s, 9H), 1.35 (d, *J* = 7.1 Hz, 3H); ^{13}C NMR (125 MHz, $CDCl_3$) δ 173.3, 171.4, 157.2, 155.8, 141.9, 141.7, 128.7, 128.6, 127.7, 127.6, 127.3, 127.2, 80.3, 60.8, 57.0, 49.1, 46.4, 28.9, 28.5, 22.8, 18.4; IR (neat) ν_{max}/cm^{-1} 3250, 1678, 1655, 1524, 1493, 1365, 1246, 1160, 1025; HRMS *m/z* calculated for $C_{27}H_{35}N_5NaO_5$ $[M+Na]^+$ 532.2530; found 532.2549.

_N_-Phenylacetyl-aza-glycinyl-L-proline Benzhydrylamide (2.7)

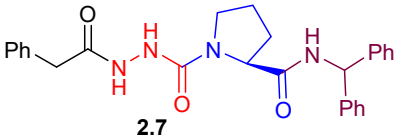

2.7

A solution of aza-glycinyl-proline benzhydrylamide hydrochloride **2.43** (0.115 g, 0.34 mmol, prepared according to reference 3) in 20 mL of EtOAc was treated with phenyl acetyl chloride (1.2 eq., 0.063 g, 0.0543 mL, 0.408 mmol) and DIEA (2 eq., 0.0878 g, 0.112 mL, 0.68 mmol), stirred for 12 h, and quenched with 10 mL of 1 N HCl. The organic phase was separated and washed with 10 mL of brine, dried over Na_2SO_4, filtered and evaporated. After evaporation of the volatiles, the residue was purified by chromatography on silica gel

using a mixture of 4% MeOH in DCM as eluant to afford phenyl acetyl aza-proline tripeptide **7** (0.145 g, 93%) as white solid: R_f 0.36 (9:1 $CHCl_3$:MeOH); mp 74−76 °C; $[\alpha]_D^{20}$ −50.4° (*c* 1, $CHCl_3$); ^{1}H NMR (500 MHz, $CDCl_3$) δ 8.43 (s, 1H), 7.74 (d, *J* = 8.4 Hz, 1H), 7.35 – 7.15 (m, 15H), 7.14 – 7.08 (br, 1H), 6.16 (d, *J* = 8.4 Hz, 1H), 4.44 (dd, *J* = 7.9, 1.9 Hz, 1H), 3.47 (s, 2H), 3.40 – 3.32 (m, 1H), 3.19 (dd, *J* = 15.7, 8.4 Hz, 1H), 2.28 – 2.19 (m, 1H), 1.97 – 1.71 (m, 3H); ^{13}C NMR (125 MHz, $CDCl_3$) δ 171.1, 170.8, 157.4, 141.8, 141.6, 134.2, 129.5, 129.4, 128.9, 128.71, 128.67, 127.5, 127.41, 127.37, 127.31, , 60.9, 57.1, 46.4, 41.1, , 28.5, 24.9; IR (neat) ν_{max}/cm^{-1} 3246, 1642, 1518, 1493, 1453, 1383, 1354, , 1031; HRMS *m/z* calculated for $C_{27}H_{28}N_4NaO_3$ $[M+Na]^+$ 479.2054; found 479.2072.

_N_-Cbz-Aza-glycinyl-L-proline Benzhydrylamide (2.8a)

2.8a

A stirred suspension of aza-glycinyl-proline benzhydrylamide hydrochloride **2.43** (0.4 g, 1.18 mmol, prepared according to reference 3) and anhydrous sodium carbonate (0.251 g, 2.36 mmol) in a mixture of THF (20 mL) and water (20 mL) was treated with a solution of the benzyl chloroformate (0.242 g, 0.202 mL, 1.42 mmol) in 10 mL of THF at 0 °C. The mixture was stirred at 0 °C for 1 h, and at room temperature for 12 h, when a precipitate was observed. The volatiles were evaporated to give a residue that was dissolved in EtOAc (100 mL), washed with sat. $NaHCO_3$ (20 mL), followed by brine (20 mL), dried over Na_2SO_4, filtered and evaporated. The residue was purified by column chromatography using 1:4 hexane:EtOAc as eluant to give Cbz proline dipeptide **2.8a** (0.46 g, 82%) as white solid: R_f 0.30 (1:4 hexane:EtOAc); mp 77−78 °C; $[\alpha]_D^{20}$ −62.4° (*c* 1, $CHCl_3$); ^{1}H NMR (400 MHz, $CDCl_3$) δ 7.72 (d, *J* = 8.2 Hz, 1H), 7.40 – 7.18 (m, 15H), 6.70 – 6.59 (br s, 1H), 6.45 – 6.34 (br s, 1H), 6.18 (d, *J* = 8.5 Hz, 1H), 5.15 (d, *J* = 11.6 Hz, 2H), 4.54 (d, *J* = 7.4 Hz, 1H), 3.43 (dd, *J* = 9.2, 7.5 Hz, 1H), 3.30 (dd, *J* = 16.1, 8.7 Hz, 1H), 2.48 – 2.31 (m, 1H), 2.10 – 1.81 (m, 3H); ^{13}C NMR ($CDCl_3$, 100 MHz) δ 171.0, 157.7, 157.5, 141.9, 141.7, 136.0,

128.71, 128.7, 128.6, 128.4, 128.3, 127.5, 127.45, 127.36, 127.3, 67.7, 60.9, 57.1, 46.2, 28.3, 25.0; IR (neat) ν_{max}/cm^{-1} 3253, 1729, 1652, 1517, 1494, 1453, 1378, 1212; HRMS *m/z* calculated for $C_{27}H_{28}N_4NaO_4$ $[M+Na]^+$ 495.2003; found 495.2002.

_N_-Boc-Aza-glycinyl-L-proline Benzhydrylamide (2.8b)

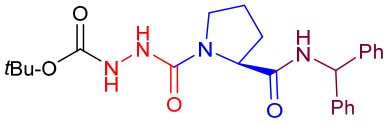

2.8b

A 0 °C solution of aza-glycinyl-proline benzhydrylamide hydrochloride **2.43** (0.3 g, 0.887 mmol, synthesized as previously reported 3) and TEA (0.246 mL, 1.77 mmol) in 10 mL of DCM was treated with di-*tert*-butyl dicarbonate (0.232 g, 0.228 mL, 1.06 mmol). The bath was removed and the reaction mixture was stirred at room temperature overnight. The volatiles were evaporated, and the residue was partitioned between EtOAc and brine. The aqueous layer was separated and extracted with EtOAc. The combined organic layer was dried over Na_2SO_4, filtered, and evaporated. The residue was purified by silica gel chromatography eluting with 70% EtOAc in hexane as solvent system to obtain *N*-Boc-aza-glycinyl proline dipeptide **2.8b** (0.29 g, 0.661 mmol, 75%) as white solid: R_f 0.38 (1:4 hexane:EtOAc); mp 151−152 °C; $[\alpha]_D^{20}$ −65.8° (*c* 1, $CHCl_3$); ^1H NMR (500 MHz, $CDCl_3$) δ 7.84 (d, *J* = 6.8 Hz, 1H), 7.37 – 7.16 (m, 10H), 6.55 – 6.47 (br s, 1H), 6.47 – 6.39 (br s, 1H), 6.18 (d, *J* = 8.5 Hz, 1H), 4.54 (d, *J* = 6.6 Hz, 1H), 3.40 (dd, *J* = 11.6, 5.3 Hz, 1H), 3.26 (dd, *J* = 16.0, 8.9 Hz, 1H), 2.45 – 2.35 (m, 1H), 2.00 – 1.80 (m, 3H), 1.45 (s, 9H); ^{13}C NMR (125 MHz, $CDCl_3$) δ 170.6, 157.9, 156.6, 141.9 (2C), 128.74, 128.71, 127.45, 127.42, 127.32, 127.30, 81.8, 60.9, 57.2, 46.3, 28.3, 28.0, 25.1; IR (neat) ν_{max}/cm^{-1} 3266, 1719, 1655, 1522, 1493, 1366, 1233, 1156; HRMS *m/z* calculated for $C_{24}H_{30}N_4NaO_4$ $[M+Na]^+$ 461.2159; found 461.2177.

_N_-Cbz-Aza-glycinyl-L-proline _tert_-Butyl Ester (2.9a)

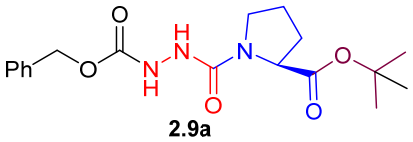

2.9a

A stirred 0 °C solution of disuccinimidyl carbonate (0.848 g, 3.31 mmol) in a mixture of DCM (20 mL) and DMF (5 mL) was treated dropwise by cannula with a 0 °C solution of benzyl carbazate (0.5 g, 3.01 mmol) in dry DCM (10ml). The ice bath was removed, and the reaction mixture was allowed to warm to room temperature. After stirring for 1 h, the mixture was cooled to 0 °C and treated dropwise by cannula with a premixed solution of proline *tert*-butyl ester hydrochloride (0.515 g, 3.01 mmol) and DIEA (0.995 mL, 6.02 mmol) in 5 mL of dry DCM. The ice bath was removed, the reaction was allowed to warm to room temperature and stirred overnight. The volatiles were evaporated and the residue was partitioned between EtOAc and brine. The aqueous layer was separated and extracted with EtOAc. The combined organic layer was dried over Na_2SO_4, filtered, and evaporated. The residue was purified by silica gel chromatography eluting with 80% EtOAc in hexane as solvent system to obtain *N*-Cbz-aza-glycinyl proline ester **2.9a** (0.98 g, 90%) as colourless oily liquid: R_f 0.46 (1:4 hexane:EtOAc); $[\alpha]_D^{20}$ −55.2° (*c* 1.07, $CHCl_3$); ^{1}H NMR (500 MHz, $CDCl_3$) δ 7.36 – 7.27 (m, 5H), 7.12 – 6.96 (br s, 1H), 6.96 – 6.80 (br s, 1H), 5.12 (dd, *J* = 36.3, 12.3 Hz, 2H), 4.33 (d, *J* = 7.1 Hz, 1H), 3.59 – 3.40 (m, 2H), 2.19 – 2.07 (m, 1H), 2.02 – 1.89 (m, 3H), 1.43 (s, 9H); ^{13}C NMR (125 MHz, $CDCl_3$) δ 172.5, 157.3, 156.7, 136.2, 128.5, 128.2, 82.1, 67.4, 60.2, 45.9, 29.8, 29.6, 28.0, 24.5; IR (neat) ν_{max}/cm^{-1} 3304, 1725, 1656, 1527, 1367, 1213, 1149, 1040; HRMS *m/z* calculated for $C_{18}H_{25}N_3NaO_5$ $[M+Na]^+$ 386.1686; found 386.1703.

_N_-Boc-Aza-glycinyl-L-proline _tert_-Butyl Ester (2.9b)

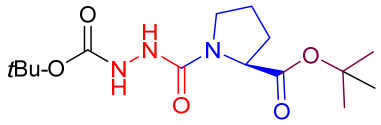

2.9b

Using the procedure described for the synthesis of Boc-aza-dipeptide **2.9a**, *tert*-butyl carbazate (0.5 g, 3.78 mmol), was reacted with disuccinimidyl carbonate (1.07 g, 4.16 mmol), DIEA (1.25 mL, 7.57 mmol) and proline *tert*-butyl ester hydrochloride (0.648 g, 3.78 mmol). The residue was purified by silica gel chromatography using 20-30% EtOAc in hexane to give Boc-aza-glycinyl proline ester **2.9b** (0.85 g, 2.58 mmol, 68%) as white solid: R_f 0.56 (1:4 hexane:EtOAc); mp 110−111 °C; $[\alpha]_D^{20}$ −66.4° (*c* 0.5, $CHCl_3$); ^1H NMR (500 MHz, $CDCl_3$) δ 6.71 – 6.58 (br s, 1H), 6.58 – 6.45 (br s, 1H), 4.34 (d, *J* = 7.4 Hz, 1H), 3.54 – 3.40 (m, 2H), 2.19 – 2.06 (m, 1H), 2.06 – 1.89 (m, 3H), 1.45 (s, 18H); ^{13}C NMR (125 MHz, $CDCl_3$) δ 172.2, 156.64, 156.59, 81.9, 81.2, 60.1, 46.0, 29.7, 28.3, 28.1, 24.5; IR (neat) ν_{max}/cm^{-1} 3246, 1739, 1714, 1656, 1547, 1392, 1367, 1144; HRMS *m/z* calculated for $C_{15}H_{27}N_3NaO_5$ $[M+Na]^+$ 352.1843; found 352.1855.

_N_-Cbz-Aza-glycinyl-L-phenylalanine Benzhydrylamide (2.10a)

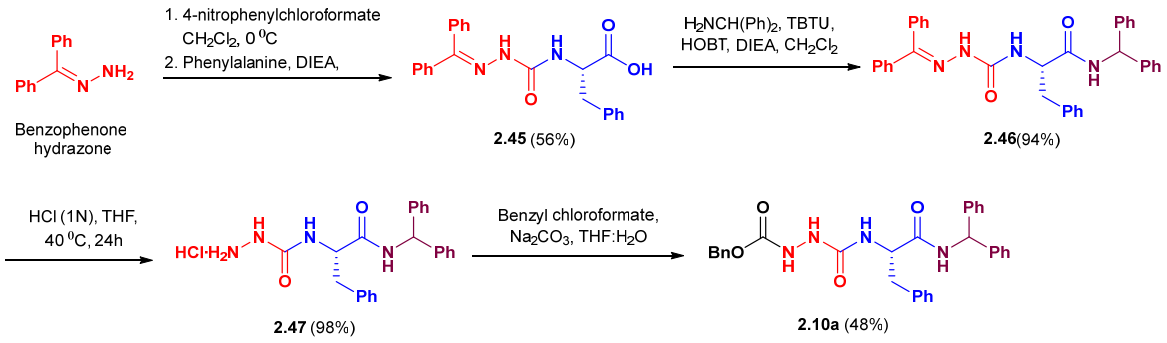

Employing the procedure described for aza-glycinyl tripeptide **2.8a**, aza-glycinyl-phenylalanine benzhydrylamide hydrochloride **2.47** (1.15 g, 2.96 mmol, prepared from phenylalanine according to the procedure described for the synthesis of **2.44** in reference 3)

was reacted with sodium carbonate (0.376 g, 3.55 mmol) and benzyl chloroformate (0.605 g, 0.504 mL, 3.55 mmol). The residue was purified by column chromatography using 60% EtOAc in hexane as eluant to afford white solid, **2.10a** (0.741 g, 48%): R_f 0.52 (1:4 hexane:EtOAc); mp 89−91 °C; $[\alpha]_D^{20}$ −3.5° (*c* 0.59, $CHCl_3$); ^{1}H NMR (500 MHz, $CDCl_3$) δ 7.71 – 7.47 (m, 1H), 7.33 – 6.98 (m, 20H), 6.87 – 6.79 (m, 2H), 6.79 – 6.66 (br, 1H), 5.99 (d, *J* = 8.0 Hz, 1H), 4.87 (s, 2H), 4.71 (dd, *J* = 13.3, 7.8 Hz, 1H), 2.94 (ddd, *J* = 22.1, 13.3, 7.0 Hz, 2H); ^{13}C NMR (125 MHz, $CDCl_3$) δ 171.1, 158.1, 157.2, 141.3, 141.1, 136.6, 135.9, 129.6, 128.6, 128.5, 128.3, 128.1, 127.7, 127.6, 127.3, 127.3, 126.8, 67.6, 56.9, 55.6, 39.6; IR (neat) ν_{max}/cm^{-1} 3269, 1729, 1637, 1534, 1493, 1453, 1213, 1028; HRMS *m/z* calculated for $C_{31}H_{30}N_4NaO_4$ $[M+Na]^+$ 545.2159; found 545.2157.

N-Cbz-Aza-glycinyl-sarcosine Benzhydrylamide (2.11a)

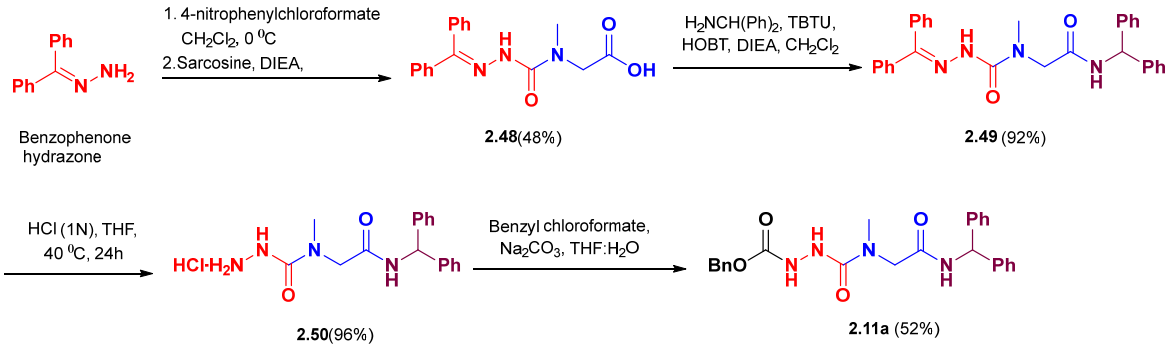

Employing the procedure described for aza-glycinyl tripeptide **2.8a**, aza-glycinyl-sarcosine benzhydrylamide hydrochloride **2.50** (0.5 g, 1.6 mmol, prepared from sarcosine according to the procedure described for the synthesis of **2.44** in reference 3) was reacted with benzyl chloroformate (0.273 mL, 1.92 mmol) and sodium carbonate (0.339 g, 3.2 mmol). The residue was purified by column chromatography using 80% EtOAc in hexane as eluant to afford white solid, **2.11a** (0.37 g, 0.829 mmol, 52%): R_f 0.2 (1:4 hexane:EtOAc); mp 71−73 °C; ^{1}H NMR (400 MHz, CD_3OD) δ 7.42 – 7.19 (m, 15H), 6.22 (s, 1H), 5.12 (s, 2H), 4.07 (s, 2H), 2.96 (s, 3H); ^{13}C NMR (100 MHz, CD_3OD) δ 170.9, 160.5, 159.6, 142.9, 137.8, 137.1, 129.5, 129.4, 129.1, 129.0, 128.7, 128.3, 68.2, 58.1, 53.1, 35.8; IR (neat)

ν_{max}/cm^{-1} 3286, 1796, 1651, 1493, 1153, 1062, 1010; HRMS *m/z* calculated for $C_{25}H_{26}N_4NaO_4$ $[M+Na]^+$ 469.1846; found 469.1868.

_N_-Cbz-Aza-glycinyl-L-leucinyl-glycine Benzyl Ester (2.12a)

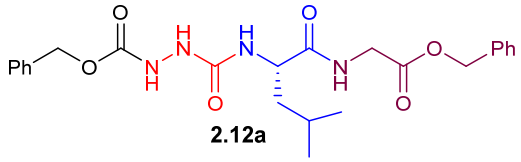

2.12a

Using the representative procedure for the synthesis of Boc-aza-dipeptide **2.9a**, benzyl carbazate (0.396 g, 2.38 mmol), was reacted with disuccinimidyl carbonate (0.671 g, 2.62 mmol), DIEA (0.787 mL, 4.76 mmol) and leucinyl-glycine benzyl ester hydrochloride (0.75 g, 2.38 mmol, prepared according to reference 4). The residue was purified by silica gel chromatography using 80% EtOAc in hexane to give ester **2.12a** (0.92 g, 82%) as a white solid; R_f 0.46 (1:4 hexane:EtOAc); mp 45−46 °C; $[\alpha]_D^{20}$ −18.9° (*c* 0.23, MeOH); ^{1}H NMR (500 MHz, $CDCl_3$) δ 7.72 – 7.48 (br s, 1H), 7.38 – 7.16 (m, 10H), 6.53 – 6.32 (br s, 1H), 5.08 (s, 2H), 5.07 – 5.01 (m, 2H), 4.41 (td, *J* = 8.9, 5.4 Hz, 1H), 4.02 – 3.87 (m, 2H), 1.69 – 1.56 (m, 2H), 1.56 – 1.45 (m, 1H), 0.86 (dd, *J* = 10.2, 6.1 Hz, 6H); ^{13}C NMR (125 MHz, $CDCl_3$) δ 174.2, 170.1, 158.6, 157.3, 135.8, 135.3, 128.7, 128.63, 128.56, 128.44, 128.41, 128.2, 67.8, 67.2, 52.5, 41.5, 24.7, 23.0, 22.1; IR (neat) ν_{max}/cm^{-1} 3293, 1735, 1647, 1542, 1498, 1455, 1201, 1190; HRMS *m/z* calculated for $C_{24}H_{30}N_4NaO_6$ $[M+Na]^+$ 493.2058; found 493.2073.

_N_-Boc-Aza-glycinyl-L-leucine glycine Benzyl Ester (2.12b)

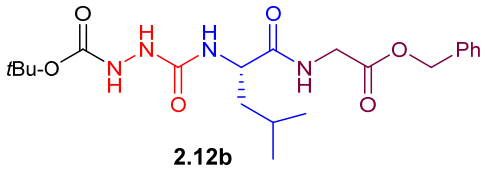

2.12b

Using the representative procedure for the synthesis of Boc-aza-dipeptide **2.9a**, *tert*-butyl carbazate (1 eq., 0.315 g, 0.309 mL, 2.38 mmol), was reacted with disuccinimidyl

carbonate (0.671 g, 2.62 mmol), DIEA (0.616 g, 0.787 mL, 4.76 mmol) and leucinyl-glycine benzyl ester hydrochloride (0.75 g, 2.38 mmol, prepared according to reference 4). The residue was purified by silica gel chromatography using 60% EtOAc in hexane to give ester **2.12b** (0.79 g, 76%) as white solid: R_f 0.48 (1:4 hexane:EtOAc); mp 51−54 °C; $[\alpha]_D^{20}$ −13.2° (*c* 0.28, MeOH); ^{1}H NMR (500 MHz, $CDCl_3$) δ 7.64 – 7.55 (br s, 1H), 7.38 – 7.28 (m, 5H), 7.23 – 6.99 (br s, 1H), 6.86 (s, 1H), 6.33 – 6.04 (br s, 1H), 5.12 (s, 2H), 4.41 (td, *J* = 9.2, 5.0 Hz, 1H), 4.01 (d, *J* = 5.7 Hz, 2H), 1.73 – 1.59 (m, 2H), 1.53 (dd, *J* = 15.5, 6.8 Hz, 1H), 1.43 (s, 9H), 0.89 (t, *J* = 6.2 Hz, 6H); ^{13}C NMR (125 MHz, $CDCl_3$) δ 173.9, 170.1, 158.8, 156.4, 135.4, 128.7, 128.6, 128.4, 81.9, 67.2, 52.4, 41.5, 29.8, 28.2, 24.7, 23.0, 22.0; IR (neat) ν_{max}/cm^{-1} 3296, 1735, 1648, 1543, 1236, 1156; HRMS *m/z* calculated for $C_{21}H_{32}N_4NaO_6$ $[M+Na]^+$ 459.2214; found 459.2228.

N-Cbz-Azo-glycinyl-L-proline Benzhydrylamide (2.13a)

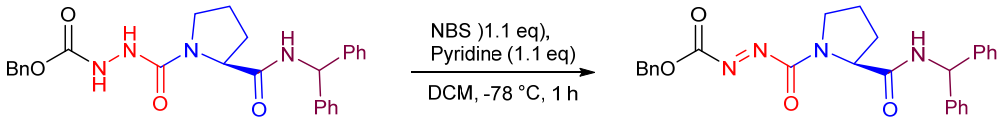

2.8a **2.13a**

A stirred solution of *N*-Cbz-aza-glycinyl-proline benzhydrylamide (**2.8a**, 0.4 g, 0.846 mmol) and pyridine (0.0753 mL, 0.931 mmol), in DCM (20 mL) at –78 °C was treated with NBS (0.166 g, 0.931 mmol) in a single portion. The bath was removed. The reaction mixture was allowed to warm to room temperature and stirred for 1h, when the reaction mixture color had changed to a pale yellow, and a new less polar bright yellow spot appeared on the TLC plate. The reaction mixture was concentrated to a reduced volume that was partitioned between aqueous sodium bicarbonate and ethyl acetate. The organic phase was dried over anhydrous Na_2SO_4 and the volatiles were evaporated to afford azopeptide 2.**13a** (0.39 g, 98%) as orange lustrous solid that were used in the next step without further purification: R_f 0.76 (1:4 hexane:EtOAc); ^{1}H NMR (400 MHz, $CDCl_3$) showed a 1:3 mixture of isomers: δ 7.56 – 7.17 (m, 15H), 7.11 (d, *J* = 6.5 Hz, 1H), 6.19 (d, *J* = 8.1 Hz, 1H), [6.16 (d, *J* = 8.3 Hz, 1H)], 5.46 (s, 2H), [5.35 (s, 2H)], 4.71 (dd, *J* = 7.1, 2.3 Hz, 1H), [4.65 (dd, *J* = 8.5, 1.8 Hz,

1H)], [3.85 – 3.77 (m, 2H)], 3.68 – 3.56 (m, 2H), 2.58 – 2.48 (m, 1H), 2.38 – 2.22 (m, 1H), 2.10 – 1.93 (m, 2H); IR (neat) ν_{max}/cm^{-1} 3294, 1763, 1707, 1658, 1532, 1495, 1454, 1407, 1377, 1202.

_N_-Boc-Azo-glycinyl-L-proline Benzhydrylamide (2.13b)

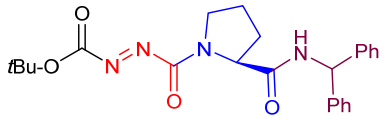

2.13b

Azopeptide **2.13b** (0.22 g, 97%) was prepared from Cbz-aza-glycinyl proline dipeptide **2.8b** (0.23 g, 0.524 mmol) by the protocol described for the synthesis of azopeptide **2.13a**, isolated as orange lustrous solid after aqueous work-up and used without further purification: R_f 0.8 (1:4 hexane:EtOAc); ^{1}H NMR (500 MHz, $CDCl_3$) showed a 1:3 mixture of isomers: δ 7.55 (d, J = 8.2 Hz, 1H), 7.35 – 7.13 (m, 10H), 6.19 (d, J = 8.3 Hz, 1H), [6.18 – 6.16 (br s, 1H)], 4.71 (dd, J = 8.1, 2.7 Hz, 1H), [4.66 (dd, J = 8.3, 2.4 Hz, 1H)], [3.83 – 3.76 (m, 2H)], 3.69 – 3.59 (m, 2H), 2.57 – 2.48 (m, 1H), 2.27 – 2.11 (m, 1H), 2.08 – 1.95 (m, 2H), 1.64 (s, 9H), [1.57 (s, 9H)]; IR (neat) ν_{max}/cm^{-1} 3293, 1758, 1707, 1656, 1535, 1371, 1254, 1145.

_N_-Cbz-Azo-glycinyl-L-proline *tert*-Butyl Ester (2.14a)

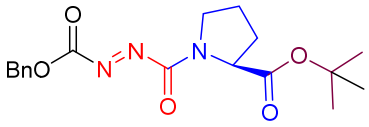

2.14a

Azopeptide **2.14a** (0.058 g, 97%) was prepared from Cbz-aza-glycinyl proline ester **2.9a** (0.06 g, 0.165 mmol) by the protocol described for the synthesis of azopeptide **2.13a**, isolated as orange liquid by aqueous work-up and used without further purification: R_f 0.8 (1:4 hexane:EtOAc); $[\alpha]_D^{20}$ −12.4° (*c* 0.21, $CHCl_3$); ^{1}H NMR (500 MHz, $CDCl_3$) showed a 1:1 mixture of isomers: δ 7.47 – 7.33 (m, 5H), [5.43 (s, 2H)], 5.41 (s, 2H), 4.66 (dd, J = 8.6, 3.2 Hz, 1H), [4.52 (dd, J = 8.5, 3.8 Hz, 1H)], 3.88 – 3.60 (m, 2H), 2.38 – 2.18 (m, 2H), 2.12

– 1.93 (m, 2H), [1.47 (s, 9H)], 1.33 (s, 9H); ^{13}C NMR (125 MHz, $CDCl_3$) δ 170.4, (170.1), 162.0, (161.7), (158.4), 157.1, 133.9, (129.22), 129.20, (128.91), 128.88, 128.85, (128.79), 82.6, (82.3), (70.6), 70.5, (60.8), 60.4, 47.8, (47.4), 31.1, (29.4), (28.1), 27.9, (24.8), 22.8; IR (neat) ν_{max}/cm^{-1} 1766, 1708, 1406, 1368, 1343, 1221, 1149, 1091; HRMS *m/z* calculated for $C_{18}H_{23}N_3NaO_5$ $[M+Na]^+$ 384.1530; found 384.1535.

_N_-Boc-Azo-glycinyl-L-proline _tert_-Butyl Ester (2.14b)

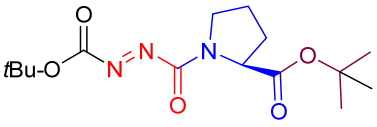

2.14b

Azopeptide **2.14b** (0.048 g, 97%) was prepared from Boc-aza-glycinyl proline ester **2.9b** (0.050 g, 0.152 mmol) following the protocol for the synthesis of azopeptide **2.13a**, isolated as orange liquid by aqueous work-up and employed without further purification: R_f 0.82 (1:4 hexane:EtOAc); $[\alpha]_D^{20}$ −13° (*c* 0.1, $CHCl_3$); ^{1}H NMR (500 MHz, $CDCl_3$) showed a 1:1 mixture of isomers: δ 4.68 (dd, *J* = 8.6, 3.3 Hz, 1H), [4.52 (dd, *J* = 8.6, 3.7 Hz, 1H)], 3.89 – 3.62 (m, 2H), 2.39 – 2.18 (m, 2H), 2.12 – 1.93 (m, 2H), [1.61 (s, 9H)], 1.59 (s, 9H), [1.48 (s, 9H)], 1.41 (s, 9H). ^{13}C NMR (125 MHz, $CDCl_3$) δ 170.6, (170.2), 160.8, (160.6), (158.8), 157.4, (86.7), 86.6, 82.5, (82.3), (60.7), 60.4, 47.8, (47.4), 31.1, (29.4), (28.1), 28.0 (2C), (24.8), 22.9; IR (neat) ν_{max}/cm^{-1} 1761, 1738, 1711, 1397, 1370, 1255, 1146; HRMS *m/z* calculated for $C_{15}H_{25}N_3NaO_5$ $[M+Na]^+$ 350.1686; found 350.1685.

_N_-Cbz-Azo-glycinyl-L-phenyl alanine Benzhydrylamide (2.15a)

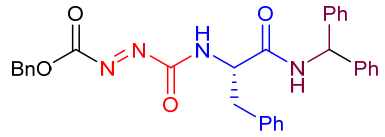

2.15a

Azopeptide **2.15a** (0.097 g, 97%) was prepared from Cbz-aza-glycinyl phenylalanine dipeptide **2.10a** (0.1 g, 0.191 mmol) following the protocol for the synthesis of azopeptide **2.13a**, isolated as orange lustrous solid by aqueous work-up and employed without further

purification: R_f 0.84 (1:4 hexane:EtOAc); ^{1}H NMR (500 MHz, $CDCl_3$) showed a 1:3 mixture of isomers: δ 7.46 – 7.07 (m, 20H), 6.94 – 6.87 (m, 1H), 6.24 – 6.16 (m, 1H), 6.11 (d, J = 8.0 Hz, 1H), 5.43 (s, 2H), 4.78 – 4.69 (m, 1H), [4.48 – 4.41 (m, 1H)], [3.36 (dd, J = 13.9, 4.5 Hz, 1H)], 3.27 (dd, J = 13.6, 5.3 Hz, 1H), [3.23 – 3.18 (m, 1H)], 3.13 – 3.03 (m, 1H); IR (neat) ν_{max}/cm^{-1} 3260, 1765, 1709, 1649, 1528, 1494, 1454, 1263, 1233.

_N_-Cbz-Azo-glycinyl sarcosine Benzhydrylamide (2.16a)

2.16a

Azopeptide **2.16a** (0.29 g, 97%) was prepared from Cbz-aza-glycinyl sarcosine dipeptide **2.11a** (0.3 g, 0.672 mmol) following the protocol for the synthesis of azopeptide **2.13a**, isolated as orange lustrous solid by aqueous work-up and employed without further purification: R_f 0.74 (1:4 hexane:EtOAc); ^{1}H NMR (500 MHz, MeOD) showed a 1:1 mixture of isomers: δ 7.49 – 7.17 (m, 15H), [6.22 (s, 1H)], 6.13 (s, 1H), [5.47 (s, 2H)], 5.42 (s, 2H), 4.33 (s, 2H), [4.29 (s, 2H)], 3.16 (s, 3H), [3.13 (s, 3H)]; ^{13}C NMR (125 MHz, $CDCl_3$) δ 166.3, 165.9, (161.21), 161.17, 141.1, (140.8), 133.8, 129.4, (128.97), 128.91, 127.9, 127.8, 127.5, 127.4, 70.8, 57.3, 53.5, (52.7), 36.6, (36.5); IR (neat) ν_{max}/cm^{-1} 3242, 1756, 1704, 1645, 1552, 1259, 1232, 1205; HRMS *m/z* calculated for $C_{25}H_{24}N_4NaO_4$ $[M+Na]^+$ 467.1690; found 467.1694.

_N_-Cbz-Azo-glycinyl-L-leucine glycine Benzyl Ester (2.17a)

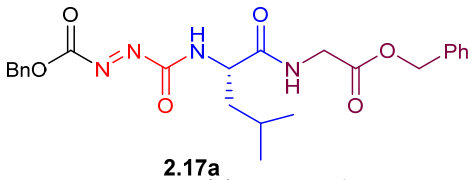

2.17a

Azopeptide **2.17a** (0.108 g, 0.231 mmol, 99%) was prepared from Cbz-aza-glycinyl leucine glycine benzyl ester **2.12a** (0.11 g, 0.234 mmol) following the protocol for the synthesis of azopeptide **2.13a**, isolated as orange lustrous solid by aqueous work-up and employed without further purification: R_f 0.78 (1:4 hexane:EtOAc); ^{1}H NMR (500 MHz,

$CDCl_3$) δ 7.44 – 7.32 (m, 10H), 6.97 (d, *J* = 8.6 Hz, 1H), 6.49 (t, *J* = 5.3 Hz, 1H), 5.43 (s, 2H), 5.18 (s, 2H), 4.60 – 4.52 (m, 1H), δ 4.13 (dd, *J* = 18.4, 5.6 Hz, 1H), 4.03 (dd, *J* = 18.3, 5.1 Hz, 1H), 1.80 – 1.63 (m, 3H), 0.98 – 0.94 (m, 6H); IR (neat) ν_{max}/cm^{-1} 3282, 1711, 1664, 1529, 1498, 1455, 1218, 1188.

N-Boc-Azo-glycinyl-L-leucine glycine Benzyl Ester (2.17b)

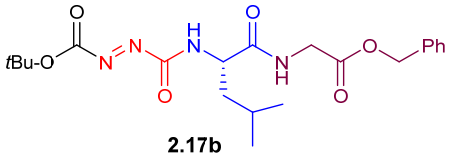

2.17b

Azopeptide **2.17b** (0.198 g, 0.456 mmol, 99%) was prepared from Boc-aza-glycinyl leucine glycine benzyl ester **2.12b** (0.2 g, 0.458 mmol) following the protocol for the synthesis of azopeptide **2.13a**, isolated as orange lustrous solid by aqueous work-up and employed without further purification: R_f 0.8 (1:4 hexane:EtOAc); ^{1}H NMR (500 MHz, $CDCl_3$) δ 7.41 – 7.31 (m, 5H), 6.87 (d, *J* = 8.7 Hz, 1H), 6.46 (t, *J* = 5.1 Hz, 1H), 5.19 (s, 2H), 4.61 – 4.52 (m, 1H), 4.16 (dd, *J* = 18.3, 5.6 Hz, 1H), 4.05 (dd, *J* = 18.3, 5.0 Hz, 1H), 1.82 – 1.65 (m, 3H), 1.62 (s, 9H), 0.97 (t, *J* = 6.5 Hz, 6H); IR (neat) ν_{max}/cm^{-1} 3290, 1755, 1663, 1529, 1371, 1235, 1176, 1146.

N-Cbz-Aza-Δ^4-dehydropipecolyl-L-proline Benzhydrylamide (2.19a)

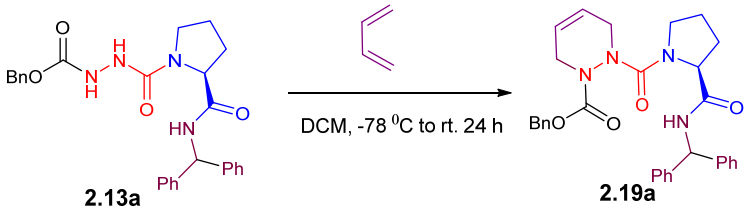

2.13a **2.19a**

A –78 °C stirred solution of Cbz-azo-glycinyl-proline dipeptide **2.13a** (0.2 g, 0.425 mmol) in dry DCM in pressure sealed tube vessel was treated dropwise via a cannula with a solution of 1,3-butadiene in dry DCM (1M, 4.25 mL, 4.25 mmol). After complete addition, the reaction mixture was allowed to warm to room temperature. After stirring overnight, the color of the reaction mixture changed from pale yellow to colourless and a new lower R_f spot

appeared on the TLC plate. The solution was concentrated to a residue, that was purified by column chromatography on silica gel using 80% EtOAc in hexane as eluant to afford azapeptide **2.19a** (0.22 g, 99%) as gummy liquid: R_f 0.3 (1:4 hexane:EtOAc); $[\alpha]_D^{20}$ 50° (*c* 0.1, $CHCl_3$. ^1H NMR (400 MHz, DMSO-d_6, 120 °C) δ 8.08 (d, *J* = 8.4 Hz, 1H), 7.41 – 7.19 (m, 15H), 6.10 (d, *J* = 8.4 Hz, 1H), 5.86 – 5.76 (m, 2H), 5.08 (s, 2H), 4.48 (dd, *J* = 7.8, 5.4 Hz, 1H), 4.09 (dd, *J* = 34.1, 18.0 Hz, 2H), 3.8-4.0 (br, 2H), 3.47 – 3.31 (m, 2H), 2.16 – 2.00 (m, 1H), 1.89 – 1.64 (m, 3H); ^{13}C NMR (100 MHz, DMSO-d_6, 120 °C) δ 170.5, 157.5, 155.1, 141.8, 141.7, 135.6, 128.7, 127.7, 127.5, 127.3, 127.0, 126.8, 126.6, 126.2, 126.1, 123.4, 122.9, 67.0, 60.8, 55.7, 47.6, 44.5, 43.3, 28.9, 23.8; IR (neat) ν_{max}/cm^{-1} 3326, 2921, 1702, 1640, 1399, 1218, 1064; HRMS *m/z* calculated for $C_{31}H_{32}N_4NaO_4$ $[M+Na]^+$ 547.2316; found 547.2329.

_N_-Boc-Aza-Δ^4-dehydropipecolyl-L-proline Benzhydrylamide (2.19b)

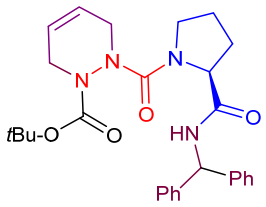

2.19b

Employing the protocol described for the synthesis of aza-pipecolinamide **2.19a**, azopeptide **2.13b** (0.29 g, 0.664 mmol) was treated with 1,3-butadiene in dry DCM (1 M, 6.64 mL, 6.64 mmol), and the product was purified by silica gel chromatography using 60% ethyl acetate in hexane to give azapeptide **2.19b** (0.32 g, 0.652 mmol, 98%) as white solid: R_f 0.34 (1:4 hexane:EtOAc); mp 65−67 °C; $[\alpha]_D^{20}$ 31.9° (*c* 0.53, $CHCl_3$); ^1H NMR (500 MHz, $CDCl_3$) δ 7.98 (br, 1H), 7.46 – 7.14 (m, 10H), 6.44 – 6.10 (br s, 1H), 5.93 – 5.56 (m, 2H), 4.70 – 4.55 (br, 1H), δ 4.32 (d, *J* = 15.2 Hz, 1H), 4.17 (d, *J* = 15.7 Hz, 1H), 3.85 (d, *J* = 16.4 Hz, 1H), 3.77 (d, *J* = 15.3 Hz, 1H) , 3.60 – 3.24 (br, 2H), 2.44 – 2.19 (br, 1H), 2.04 – 1.75 (br, 3H), 1.55 – 1.07 (br, 9H); ^{13}C NMR (125 MHz, $CDCl_3$) δ 171.6, 158.9, 154.8, 142.5, 141.4, 128.5, 128.2, 127.9, 127.4, 127.1, 126.8, 124.4, 123.3, 82.7, 62.7, 56.4, 49.4, 46.8,

43.7, 30.0, 28.0, 25.9; IR (neat) ν_{max}/cm^{-1} 3324, 2973, 1697, 1643, 1365, 1149, 1066; HRMS *m/z* calculated for $C_{28}H_{34}N_4NaO_4$ $[M+Na]^+$ 513.2472; found 513.2485.

_N_-Cbz-Aza-4,5-dimethyl-Δ^4-dehydropipecolyl-L-proline Benzhydrylamide (2.20a)

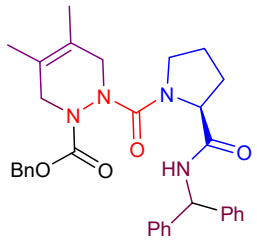

2.20a

To a stirred solution of azopeptide **2.13a** (0.15 g, 0.319 mmol) in DCM (20 mL) at –78 °C, was treated with 2,3-dimethyl-1,3-butadiene (0.262 g, 0.361 mL, 3.19 mmol). The bath was removed. The reaction mixture was allowed to warm to room temperature and stirred for overnight. The volatiles were removed under vacuum and the obtained residue was purified by silica gel chromatography using 70% Ethyl acetate in hexane to give **2.20a** (0.17 g, 0.308 mmol, 96%) as white solid: R_f 0.44 (1:4 hexane:EtOAc); mp 63−66 °C; $[\alpha]_D^{20}$ 45.4° (*c* 1, $CHCl_3$); ^{1}H NMR (500 MHz, DMSO-*d*$_6$, 100 °C) δ 8.14 (d, *J* = 7.7 Hz, 1H), 7.41 – 7.19 (m, 15H), 6.10 (d, *J* = 8.4 Hz, 1H), 5.08 (s, 2H), 4.46 (dd, *J* = 7.9, 5.4 Hz, 1H), 3.95 – 3.81 (m, 2H), 3.80 – 3.64 (br s, 2H), 3.46 – 3.31 (m, 2H), 2.15 – 2.05 (m, 1H), 1.86 – 1.67 (m, 3H), 1.58 (d, *J* = 15.0 Hz, 6H); ^{13}C NMR (125 MHz, DMSO-*d*$_6$, 100 °C) δ 171.6, 158.4, 156.2, 142.9, 142.8, 136.7, 128.8, 128.62, 128.61, 128.4, 128.0, 127.9, 127.7, 127.3, 127.2, 123.3, 122.9, 68.0, 61.9, 56.7, 49.0, 48.7, 47.9, 30.2, 24.8, 15.7, 15.5; IR (neat) ν_{max}/cm^{-1} 3325, 2919, 1705, 1643, 1398, 1221, 1123; HRMS *m/z* calculated for $C_{33}H_{36}N_4NaO_4$ $[M+Na]^+$ 575.2628; found 575.2648.

_N_-Cbz-Aza-4- and 5-methyl-Δ^4-dehydropipecolyl-L-proline benzhydrylamide (2.21a)

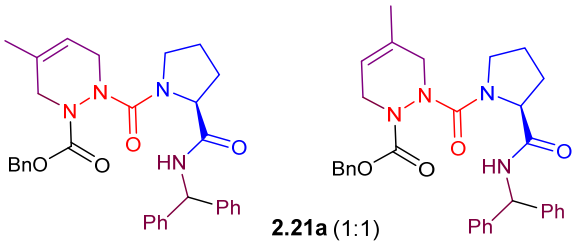

2.21a (1:1)

Employing the protocol described for the synthesis of aza-pipecolinamide **2.20a**, azopeptide **2.13a** (0.2 g, 0.425 mmol) dissolved in DCM (20 mL) was reacted with 2-methyl-1,3-butadiene (0.29 g, 0.426 mL, 4.25 mmol). The residue was purified by silica gel chromatography using 70% ethyl acetate in hexane to give a 1:1 mixture of *N*-Cbz-aza-4- and 5-methyl-Δ^4-dehydropipecolyl-L-proline benzhydrylamide **2.21a** (0.21 g, 0.39 mmol, 92 %) as white solid: R$_f$ 0.42 (1:4 hexane:EtOAc); ^{1}H NMR (500 MHz, DMSO-d_6, 120 °C) δ 8.03 – 7.92 (m, 1H), 7.32 – 7.08 (m, 15H), 6.01 (d, J = 8.4 Hz, 1H), 5.43 – 5.35 (m, 1H), 4.98 (overlapping singlet, 2H), 4.38 (dd, J = 7.9, 5.1 Hz,, 1H), 4.03 – 3.60 (m, 4H), 3.37 – 3.23 (m, 2H), 2.06 – 1.92 (m, 1H), 1.79 – 1.58 (m, 3H), 1.58 – 1.48 (2 × d, J = 1.4 Hz, J = 1.4 Hz,, 3H); ^{13}C NMR (125 MHz, DMSO-d_6, 120 °C) δ 170.54, (170.52), 157.48, (157.44), (155.18), 155.14, 141.8, (141.74), 135.61, (135.59), (130.57), 130.04, 127.7, 127.5, 127.3, 127.0, 126.92, (126.85), 126.83. 126.6, 126.2, 126.1, 117.2, (116.7), (66.95), 66.93, (60.89), 60.83, 55.67, 47.88, 47.69, (47.64), (46.80), (44.07), 43.05, 28.99, (28.92), (28.87), (23.85), 23.76, (18.82), 18.60. The isomeric ratio (1:1) for azapeptide was determined by SFC analysis on chiral stationary phase [Chiralcel OJ-H 25cm, 6% EtOH, 3 mL/min, 30°C, 150 bar, Rt (minor) 10.1min, Rt (major) 11.7 min].

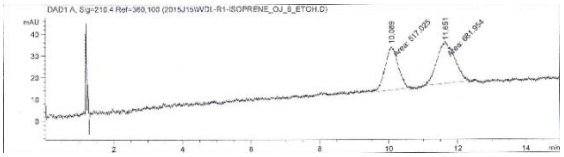

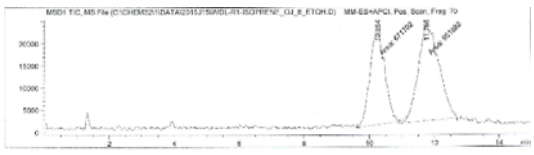

Signal 1: DAD1 A, Sig=210,4 Ref=360,100

Peak #	RetTime [min]	Type	Width [min]	Area [mAU*s]	Height [mAU]	Area %
1	10.089	MM	0.4262	517.02484	20.21652	43.1221
2	11.651	MM	0.5815	681.95367	19.54666	56.8779

Peak #	RetTime [min]	Type	Width [min]	Area	Height	Area %
1	10.264	MM	0.5231	6.71702e5	2.14008e4	41.3767
2	11.756	MM	0.7328	9.51681e5	2.16445e4	58.6233

N-Cbz-Aza-3,6-methano-Δ^4-dehydropipecolyl-L-proline Benzhydrylamide (2.22a)

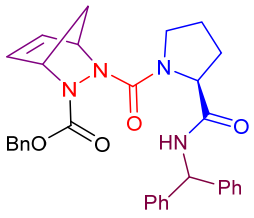

2.22a

To a stirred solution of azopeptide **2.13a** (0.38 g, 0.808 mmol) in DCM (20 mL) at –78 °C, was reacted with freshly cracked cyclopentadiene (0.534 g, 8.08 mmol) (cyclopentadiene is prepared by neat refluxing of dicyclopentadiene in a flask fitted with a fractionating column and condenser set for distillation at 170-180 °C. The collected cyclopentadiene is highly flammable and dimerizes slowly at room temperature and should be used without delay). The bath was removed. The reaction mixture was allowed to warm to room temperature and stirred for overnight. The volatiles were removed under vacuum and the residue was purified by silica gel chromatography using 80% Ethyl acetate in hexane to give azapeptide **2.22a** (0.42 g, 97%) as gummy liquid: R_f 0.22 (1:4 hexane:EtOAc); $[\alpha]_D^{20}$ −50.7° (*c* 1, MeOH); ^{1}H NMR (400 MHz, $CDCl_3$) δ 7.75 – 7.53 (br, 1H), 7.41 – 7.16 (m, 15H), 6.67 – 6.34 (m, 2H), 6.24 (d, *J* = 8.6 Hz, 1H), 5.19 – 4.97 (m, 3H), 4.83 – 4.62 (m, 2H), 3.91 – 3.70 (m, 1H), 3.56 – 3.34 (m, 1H), 2.45 – 2.28 (m, 1H), 2.13 – 1.93 (m, 2H), 1.89 – 1.56 (m, 3H); ^{13}C NMR (100 MHz, $CDCl_3$) δ 171.1, 170.4, 162.3, (141.8), (141.7), (141.6), 141.5, 136.0, (135.4), (134.7), 134.5, 128.6, 128.55, 128.50, 128.45, 128.1, 127.6, 127.4, 127.3, 127.28, 127.25, 127.2, (68.5), 67.7, (66.7), (64.2), (63.6), (60.9), 60.7, (60.4), (57.0), 56.9, 49.3, (49.2), 47.5, 46.4, 25.4, (25.3), 21.0, 14.2; IR (neat) ν_{max}/cm^{-1} 3305, 2952, 1657, 1388, 1111, 1025; HRMS *m/z* calculated for $C_{32}H_{32}N_4NaO_4$ $[M+Na]^+$ 559.2316; found 559.2312. The diastereomeric ratio (1:3) for azapeptide 2.**22a** was determined by SFC analysis on chiral stationary phase [Chiralcel OJ-H 25cm, 8% MeOH, 3 mL/min, 30°C, 150 bar, R*t* (minor) 8.6min, R*t* (major) 9.9 min].

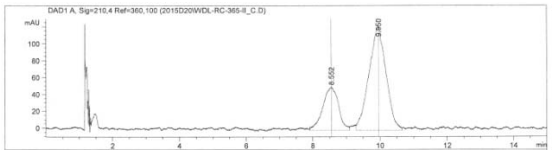

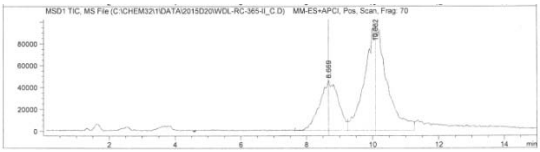

Signal 1: DAD1 A, Sig=210,4 Ref=360,100

Peak #	RetTime [min]	Type	Width [min]	Area [mAU*s]	Height [mAU]	Area %
1	8.552	VV	0.3903	1688.64392	51.53117	28.0692
2	9.950	VV	0.4326	4327.34863	123.56705	71.9308

Peak #	RetTime [min]	Type	Width [min]	Area	Height	Area %
1	8.669	VV	0.4909	1.81554e6	4.56938e4	29.0392
2	10.082	VV	0.5649	4.43649e6	9.53173e4	70.9608

_N_-Boc-Aza-3,6-methano-Δ^4-dehydropipecolyl-L-proline Benzhydrylamide (2.22b)

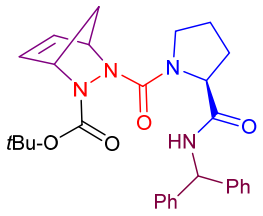

2.22b

Employing the protocol described for the synthesis of aza-pipecolinamide **2.22a**, azopeptide **2.13b** (0.2 g, 0.458 mmol) dissolved in DCM (10 mL), was reacted with freshly cracked cyclopentadiene (0.303 g, 4.58 mmol). The residue was purified by silica gel chromatography using 60-70% Ethyl acetate in hexane to give azapeptide **2.22b** (0.22 g, 0.438 mmol, 96%) as a white solid: R_f 0.24 (1:4 hexane:EtOAc); mp 72−74 °C; $[\alpha]_D^{20}$ −63.2° (*c* 0.11, $CHCl_3$); ^{1}H NMR (500 MHz, $CDCl_3$) δ 7.79 – 7.59 (br, 1H), 7.37 – 7.16 (m, 10H), 6.61 – 6.32 (br, 2H), 6.23 (d, *J* = 8.6 Hz, 1H), 5.02 – 4.91 (br s, 1H), 4.84 – 4.64 (m, 2H), 3.88 – 3.73 (m, 1H), 3.56 – 3.39 (m, 1H), 2.40 – 2.26 (m, 1H), 2.12 – 1.95 (m, 2H), 1.91 – 1.80 (m, 1H), 1.80 – 1.56 (m, 2H), 1.44 (d, *J* = 9.3 Hz, 9H); ^{13}C NMR (125 MHz, $CDCl_3$) δ 170.8 (170.7), 162.5, (162.2), 157.4, (156.9), (142.0), (141.8), (141.7), 141.5, (135.7), 134.4, 128.6, 128.5, 127.7, 127.5, 127.45, 127.4, 127.3, 127.18, 81.5, (68.1), (66.5), (64.5), (64.1), (61.1), 60.8, (57.0), 56.9, 49.3, (49.1), 47.4, 46.6, 29.7, 28.2, (27.9), 27.5, 25.6, (25.4); IR (neat) ν_{max}/cm^{-1} 3306, 2973, 1653, 1366, 1156, 1113; HRMS *m/z* calculated for $C_{29}H_{34}N_4NaO_4$ $[M+Na]^+$ 525.2472; found 525.2486. The diastereomeric ratio (4:1) for 2.**22b** was determined by SFC analysis on chiral stationary phase [Chiralcel OJ-H 25cm, 5% *i*-PrOH, 3 mL/min, 30°C, 150 bar, R*t* (major) 7.8 min, R*t* (minor) 12.8 min].

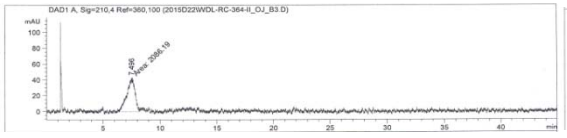

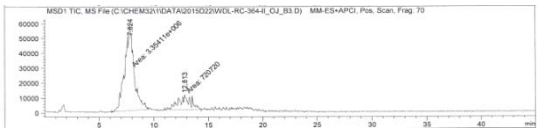

Signal 1: DAD1 A, Sig=210,4 Ref=360,100

Peak #	RetTime [min]	Type	Width [min]	Area [mAU*s]	Height [mAU]	Area %
1	7.496	MM	0.7940	2086.19336	43.79315	100.0000

Signal 2: MSD1 TIC, MS File

Peak #	RetTime [min]	Type	Width [min]	Area	Height	Area %
1	7.824	MM	0.9488	3.35411e6	5.89161e4	82.3129
2	12.813	MM	1.2094	7.20720e5	9932.05176	17.6871

_N_-Cbz-Aza-Δ[4]-dehydropipecolyl-L-proline _tert_-Butyl Ester (2.23a)

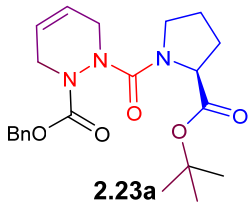

2.23a

Employing the protocol described for the synthesis of aza-pipecolinamide **2.19a**, azopeptide **2.14a** (0.04 g, 0.111 mmol) was treated with 1,3-butadiene in dry DCM (1 M, 1.11 mL, 1.11 mmol), and the product was purified by silica gel chromatography using 50% ethyl acetate in hexane to give azapeptide **2.23a** (0.045 g, 98 %) as oily liquid: R_f 0.56 (1:4 hexane:EtOAc); $[\alpha]_D^{20}$ −27.2° (*c* 1, $CHCl_3$); ^{1}H NMR (400 MHz, DMSO-*d*$_6$, 115 °C) δ 7.39 – 7.29 (m, 5H), 5.87 – 5.78 (m, 2H), 5.20 (d, *J* = 12.5 Hz, 1H), 5.16 (d, *J* = 12.5 Hz, 1H), 4.21 (dd, *J* = 8.3, 4.1 Hz, 1H), 4.16 – 4.01 (br, 2H), 4.01 – 3.81 (br, 2H), 3.48 – 3.40 (m, 1H), 3.38 – 3.30 (m, 1H), 2.13 – 2.00 (m, 1H), 1.89 – 1.71 (m, 3H), 1.40 (s, 9H); ^{13}C NMR (100 MHz, DMSO-*d*$_6$, 115 °C) δ 170.8, 157.0, 155.2, 135.6, 127.7, 127.3, 127.0, 123.6, 122.8, 79.7, 67.0, 60.4, 47.0, 44.3, 43.1, 28.6, 27.2, 23.2; IR (neat) ν_{max}/cm^{-1} 2975, 1717, 1662, 1409, 1366, 1236, 1147; HRMS *m/z* calculated for $C_{22}H_{29}N_3NaO_5$ $[M+Na]^+$ 438.1999; found 438.2015.

_N_-Boc-Aza-Δ[4]-dehydropipecolyl-L-proline _tert_-Butyl Ester (2.23b)

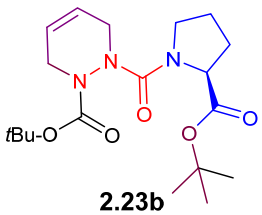

2.23b

Employing the protocol described for the synthesis of aza-pipecolinamide 2.**19a**, azopeptide 2.**14b** (0.025 g, 0.0764 mmol) was treated with 1,3-butadiene in dry DCM (1 M, 0.764 mL, 0.764 mmol), and the product was purified by silica gel chromatography using 35% ethyl acetate in hexane to give azapeptide **2.23b** (0.028 g, 97 %) as oily liquid: R_f 0.62 (1:4 hexane:EtOAc); $[\alpha]_D^{20}$ −34.2° (*c* 0.48, $CHCl_3$); ^{1}H NMR (400 MHz, DMSO-*d*$_6$, 110 °C)

δ 5.85 – 5.78 (m, 2H), 4.22 (dd, J = 8.1, 3.6 Hz, 1H), 4.10 – 3.93 (br s, 2H), 3.94 – 3.74 (br s, 2H), 3.56 – 3.44 (m, 1H), 3.44 – 3.34 (m, 1H), 2.17 – 2.03 (m, 1H), 1.96 – 1.75 (m, 3H), 1.43 (s, 9H), 1.42 (s, 9H); ^{13}C NMR (100 MHz, DMSO-d_6, 110 °C) δ 170.9, 157.1, 151.1, 123.5, 123.2, 80.6, 79.6, 60.3, 46.9, 44.3, 42.7, 28.8, 27.3, 27.2, 23.1; IR (neat) ν_{max}/cm^{-1} 2973, 1718, 1661, 1404, 1367, 1217, 1149; HRMS *m/z* calculated for $C_{19}H_{31}N_3NaO_5$ $[M+Na]^+$ 404.2156; found 404.2174.

_N_-Cbz-Aza-Δ^4-dehydropipecolyl-L-phenylalanine Benzhydrylamide (2.24a)

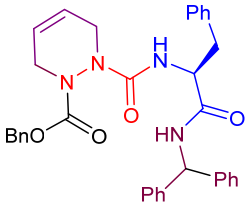

2.24a

Employing the protocol described for the synthesis of aza-pipecolinamide **2.19a**, azopeptide **2.15a** (0.15 g, 0.288 mmol) was treated with a solution of 1,3-butadiene in dry DCM (1 M, 2.88 mL, 2.88 mmol). The residue was purified by silica gel chromatography using 40% Ethyl acetate in hexane to give azapeptide **2.24a** (0.164 g, 0.285 mmol, 99%) as a white solid; R_f 0.58 (2:3 hexane:EtOAc); mp 71−73 °C; $[\alpha]_D^{20}$ 4.3° (*c* 0.306, $CHCl_3$); ^{1}H NMR (500 MHz, $(CD_3)_2CO$) δ 8.06 – 7.94 (m, 1H), 7.41 – 7.10 (m, 20H), 6.73 (d, J = 8.0 Hz, 1H), [6.69 (d, J = 7.8 Hz, 1H)], 6.24 (d, J = 8.5 Hz, 1H), [6.17 (d, J = 8.5 Hz, 1H)], 5.83 – 5.80 (br, 1H), 5.79 – 5.74 (br, 1H), 5.26 – 4.82 (m, 2H), 4.67 (td, J = 8.6, 5.0 Hz, 1H), [4.61 (td, J = 8.1, 6.1 Hz, 1H)], 4.54 – 4.28 (m, 2H), 3.71 (d, J = 17.1 Hz, 1H), [3.58 (d, J = 17.2 Hz, 2H)], 3.29 – 2.90 (m, 2H); ^{13}C NMR (125 MHz, $CDCl_3$) δ 170.6, (156.9), 156.8, 156.3, (156.0), 141.8, 141.4, (141.3), 136.9, (136.8), 135.5, (135.4), (129.43), 129.4, 128.82, 128.75, 128.67, 128.6, 128.1, 128.0, 127.8, 127.53, (127.46), 127.4, (127.37), (127.32), 127.27, 127.02, (126.9), 124.3, (124.2), 123.4, (123.1), (68.81), 68.75, 57.1, (56.9), 55.7, (54.9), 45.3, 41.13, (41.05), 38.3 (37.8); IR (neat) ν_{max}/cm^{-1} 3291, 2921, 1717, 1637, 1521, 1219, 1068; HRMS *m/z* calculated for $C_{35}H_{34}N_4NaO_4$ $[M+Na]^+$ 597.2472; found 597.2483.

_N_-Cbz-Aza-3,6-methano-Δ[4]-dehydropipecolyl-L-phenyl alanine Benzhydrylamide (2.25a)

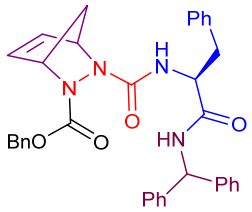

2.25a

Employing the protocol described for the synthesis of aza-pipecolinamide **2.22a**, azopeptide **2.15a** (0.26 g, 0.499 mmol) dissolved in DCM (12 mL), was reacted with freshly cracked cyclopentadiene (0.33 g, 4.99 mmol). The residue was purified by silica gel chromatography using 40-50% Ethyl acetate in hexane to give azapeptide **2.25a** (0.28 g, 0.477 mmol, 96%) as white solid: R*f* 0.5 (2:3 Hexane:EtOAc); mp 58−60 °C; $[\alpha]_D^{20}$ −15.1° (*c* 0.8, $CHCl_3$); ^{1}H NMR (500 MHz, $(CD_3)_2CO$) δ 8.04 – 7.78 (m, 1H), 7.43 – 7.09 (m, 20H), 6.78 (d, *J* = 7.2 Hz, 1H), [6.66 (d, *J* = 5.2 Hz, 1H)], 6.46 – 6.26 (m, 2H), 6.23 (dd, *J* = 8.5, 2.4 Hz, 1H), 5.18 – 4.95 (m, 4H), 4.75 – 4.60 (m, 1H), 3.19 (dd, *J* = 13.9, 5.2 Hz, 1H), [3.13 (dd, *J* = 14.0, 5.5 Hz, 1H)], 2.98 – 2.77 (m, 1H), 1.65 – 1.33 (m, 2H); ^{13}C NMR (125 MHz, $(CD_3)_2CO$) δ 171.04, (170.99), 161.7, (161.4), 160.3, (160.1), 143.31, (143.28), 143.23, (143.20), 138.7, (138.5), 137.14, (137.07), (130.3), 130.2, 129.4, (129.27), 129.26, 129.2, 129.1, 129.0, (128.98), (128. 94), 128.73, 128.67, 128.5, 128.4, 128.33, 128.28, (127.9), 127.88, 127.23, (127.18), 68.64, (68.6), 66.2, 66.0, (65.8), 57.5, 56.2, 48.2, (48.16), 38.54, (38.45); IR (neat) ν_{max}/cm^{-1} 3293, 2949, 1716, 1648, 1493, 1298, 1032; HRMS *m/z* calculated for $C_{36}H_{34}N_4NaO_4$ $[M+Na]^+$ 609.2472; found 609.2486. The diastereomeric ratio (1:1) for azapeptide **2.25a** was determined by SFC analysis on chiral stationary phase [Chiralcel OJ-H 25cm, 5% MeOH, 3 mL/min, 30°C, 150 bar, R*t* (minor) 26.1 min, R*t* (major) 32.0 min].

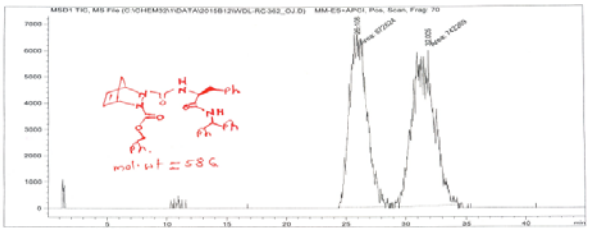

Signal 1: MSD1 TIC, MS File

Peak #	RetTime [min]	Type	Width [min]	Area	Height	Area %
1	26.108	MM	1.6230	6.72624e5	6907.19727	47.5388
2	32.005	MM	2.0525	7.42269e5	6027.24512	52.4612

_N_-Cbz-Aza-Δ^4-dehydropipecolyl-sarcosine Benzhydrylamide (2.26a)

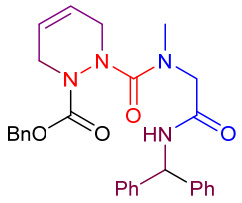

2.26a

Employing the protocol described for the synthesis of aza-pipecolinamide **2.19a**, azopeptide **2.16a** (0.4 g, 0.9 mmol) was treated with a solution of 1,3-butadiene in dry DCM (1 M, 9 mL, 9 mmol). The residue was purified by silica gel chromatography using 60% Ethyl acetate in hexane to give azapeptide **2.25a** (0.43 g, 0.862 mmol, 97%) as white solid; R_f 0.4 (1:4 hexane:EtOAc); mp 136−137 °C; ^{1}H NMR (400 MHz, DMSO-d_6, 120 °C) δ 8.28 (d, J = 7.7 Hz, 1H), 7.42 – 7.20 (m, 15H), 6.15 (d, J = 8.4 Hz, 1H), 5.87 – 5.75 (m, 2H), 5.10 (s, 2H), 4.15 – 4.08 (br s, 2H), 3.94 (s, 2H), 3.89 – 3.84 (br s, 2H), 2.86 (s, 3H); ^{13}C NMR (100 MHz, DMSO-d_6, 120 °C) δ 167.3, 159.8, 155.0, 141.7, 135.7, 127.7, 127.6, 127.2, 126.8, 126.7, 126.2, 123.2, 122.8, 66.8, 55.7, 52.3, 44.4, 44.0, 36.2.; IR (neat) ν_{max}/cm^{-1} 3294, 2922, 1630, 1492, 1396, 1223, 1057; HRMS *m/z* calculated for $C_{29}H_{30}N_4NaO_4$ $[M+Na]^+$ 521.2159; found 521.2180.

_N_-Cbz-Aza-3,6-methano-Δ^4-dehydropipecolyl-sarcosine Benzhydrylamide (2.27a)

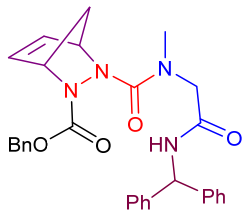

2.27a

Employing the protocol described for the synthesis of aza-pipecolinamide **2.21a**, azopeptide **2.16a** (0.25 g, 0.562 mmol) dissolved in DCM (12 mL), was reacted with freshly cracked cyclopentadiene (0.372 g, 5.62 mmol). The residue was purified by silica gel chromatography using 80% Ethyl acetate in hexane to give azapeptide **2.27a (**0.275 g,, 96%)

as a white solid; R_f 0.24 (1:4 hexane:EtOAc); mp 69−72 °C; ^{1}H NMR (500 MHz, $CDCl_3$) δ 7.72 – 7.46 (br s, 1H), 7.38 – 7.12 (m, 15H), 6.57 – 6.44 (br s, 1H), 6.40 – 6.30 (br s, 1H), 6.25 (d, J = 8.5 Hz, 1H), 5.08 (s, 1H), 5.05 – 4.92 (m, 2H), 4.72-4.70 (m, 1H), 4.18 – 4.00 (m, 2H), 3.11 (s, 3H), 1.99 (d, J = 8.5 Hz, 1H), 1.68 (d, J = 8.7 Hz, 1H); ^{13}C NMR (125 MHz, $CDCl_3$) δ 168.2, 163.2, 157.3, 141.7, 137.8, 136.2, 134.4, 128.72, 128.70, 128.6, 128.1, 127.94, 127.91, 127.54, 127.48, 127.4, 68.6, 67.7, 63.7, 57.0, 54.1, 46.8, 36.9; IR (neat) ν_{max}/cm^{-1} 3306, 2948, 1654, 1493, 1390, 1112, 1032; HRMS *m/z* calculated for $C_{30}H_{30}N_4NaO_4$ $[M+Na]^+$ 533.2159; found 533.2171. The diastereomeric ratio (1:1) for azapeptide 2.**27a** was determined by SFC analysis on chiral stationary phase [Chiralcel OJ-H 25 cm, 10% MeOH, 3 mL/min, 30°C, 150 bar, R*t* (major) 8.9 min, R*t* (minor) 14.4 min].

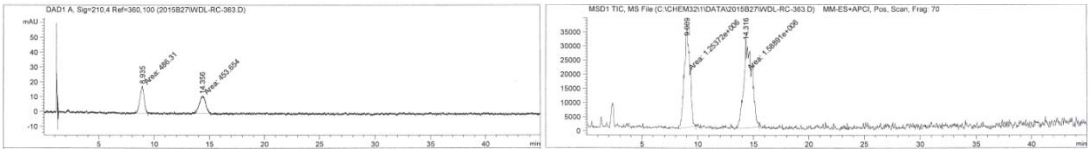

Signal 1: DAD1 A, Sig=210,4 Ref=360,100

Peak #	RetTime [min]	Type	Width [min]	Area [mAU*s]	Height [mAU]	Area %
1	8.935	MM	0.4370	486.31039	18.54895	51.7371
2	14.356	MM	0.6414	453.65350	11.78891	48.2629

Peak #	RetTime [min]	Type	Width [min]	Area	Height	Area %
1	9.009	MM	0.5622	1.25372e6	3.71655e4	44.1042
2	14.316	MM	0.7962	1.58891e6	3.32612e4	55.8958

N-Cbz-Aza-Δ^4-dehydropipecolyl-L-leucine glycine Benzyl Ester (2.28a)

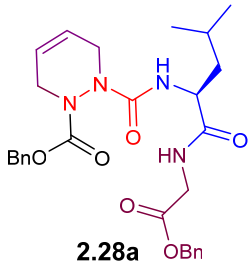

2.28a

Employing the protocol described for the synthesis of aza-pipecolinamide **2.19a**, azopeptide **2.17a** (0.1 g, 0.213 mmol) was treated dropwise via a cannula with a solution of 1,3-butadiene in DCM (1 M, 2.13 mL, 2.13 mmol). The residue was purified by silica gel chromatography using 60% Ethyl acetate in hexane to give azapeptide **2.28a** (0.11 g, 99%)

as gummy liquid; R_f 0.6 (1:4 Hexane:EtOAc); $[\alpha]_D^{20}$ −10.7° (*c* 0.15, MeOH); ^{1}H NMR (500 MHz, $CDCl_3$) δ 7.39 – 7.28 (m, 10H), 6.76 (t, *J* = 5.1 Hz, 1H), 5.86 – 5.73 (m, 2H), 5.68 (d, *J* = 8.4 Hz, 1H), [5.63 (d, *J* = 6.2 Hz, 1H)], 5.24 – 5.09 (m, 4H), 4.63 – 4.44 (m, 2H), 4.43 – 4.34 (m, 1H), 4.07 (dd, *J* = 18.3, 5.5 Hz, 1H), 3.99 (dd, *J* = 18.3, 5.3 Hz, 1H), 3.90 – 3.63 (m, 2H), 1.75-1.90 (br, 1H), 1.69 – 1.41 (m, 2H), 0.92 (dd, *J* = 8.2, 6.6 Hz, 3H), 0.85 (dd, *J* = 6.2, 4.6 Hz, 3H); ^{13}C NMR (125 MHz, $CDCl_3$) δ 173.1, (173.0), (169.73), 169.66, 157.3, (157.1), (156.4), 156.1, 135.5, (135.4), 135.3, 128.8, 128.74 ,128.71, 128.61, 128.63, 128.6, 128.5, 128.4, 128.1, 128.0, (124.5), 124.2, 123.4 (123.2), (69.1), 68.8, 67.3 (67.1), (52.6), 52.4, (45.7), 45.3, (41.4), 41.2, 41.1, 40.8, (25.0), 24.7, (23.2), 23.1, 21.9, (21.8); IR (neat) ν_{max}/cm^{-1} 3289, 2954, 1714, 1644, 1524, 1219, 1174; HRMS *m/z* calculated for $C_{28}H_{34}N_4NaO_6$ $[M+Na]^+$ 545.2371; found 545.2390.

_N_-Boc-Aza-Δ^4-dehydropipecolyl-L-leucine glycine Benzyl Ester (2.28b)

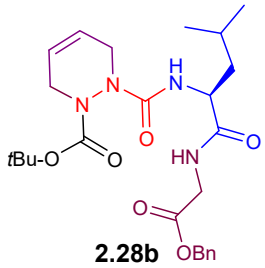

2.28b OBn

Employing the protocol described for the synthesis of aza-pipecolinamide **2.19a**, azopeptide **2.17b** (0.19 g, 0.435 mmol) was treated with a solution of 1,3-butadiene in dry DCM (1 M, 4.35 mL, 4.35 mmol). The residue was purified by silica gel chromatography using 60% Ethyl acetate in hexane to give azapeptide **2.28b** (0.21 g, 99%) as a white solid; R_f 0.62 (1:4 hexane:EtOAc); mp 124−125 °C; $[\alpha]_D^{20}$ −5.6° (*c* 0.5, MeOH); ^{1}H NMR (500 MHz, $CDCl_3$) δ 7.37 – 7.28 (m, 5H), 6.95 (t, *J* = 5.0 Hz, 1H), 5.84 – 5.72 (m, 2H), 5.69 (d, *J* = 8.4 Hz, 1H), [5.61 (d, *J* = 5.7 Hz, 1H)], 5.20 – 5.09 (m, 2H), 4.55 – 4.31 (m, 3H), 4.07 (dd, *J* = 18.3, 5.5 Hz, 1H), 3.98 (dd, *J* = 18.3, 5.3 Hz, 1H), 3.80 – 3.56 (m, 2H), 1.81 – 1.60 (m, 2H), 1.60 – 1.46 (m, 1H), 1.43 (d, *J* = 10.8 Hz, 9H), 0.98 – 0.84 (m, 6H); ^{13}C NMR (125 MHz, $CDCl_3$) δ 173.3 (173.2), 169.7 (169.6), (156.4), 156.36, 156.0, (135.4), 135.3, 128.69,

128.65, 128.6, 128.5, 128.4, (124.3), 124.0, 123.7, (123.5), 82.7, 67.2, (67.0), (52.5), 52.3, 45.2, 41.4, (41.3), (41.2), (40.9), 40.8, 40.7, 28.1, (28.0), (24.9), 24.6, 23.21 (23.15), (21.83), 21.76; IR (neat) ν_{max}/cm^{-1} 3273, 2923, 1724, 1638, 1534, 1226, 1166; HRMS *m/z* calculated for $C_{25}H_{36}N_4NaO_6$ $[M+Na]^+$ 511.2527; found 511.2545.

_N_-Cbz-Aza-3,6-methano-Δ^4-dehydropipecolyl-L-leucinyl-glycine Benzyl Ester (2.29a)

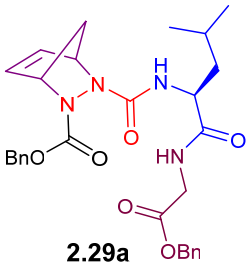

2.29a

Employing the protocol described for the synthesis of aza-pipecolinamide **2.22a**, azopeptide **2.17a** (0.1 g, 0.213 mmol) dissolved in DCM (10 mL), was reacted with freshly cracked cyclopentadiene (0.141 g, 2.13 mmol). The residue was purified by silica gel chromatography using 60% Ethyl acetate in hexane to give azapeptide **2.29a** (0.112 g, 98%) as a gummy liquid: R$_f$ 0.56 (1:4 hexane:EtOAc); $[\alpha]_D^{20}$ 1.4° (*c* 0.56, MeOH); ^{1}H NMR (500 MHz, $CDCl_3$) δ 7.39 – 7.29 (m, 10H), 6.98 – 6.82 (br, 1H), 6.58 – 6.50 (br s, 1H), 6.50 – 6.38 (br s, 1H), 5.88 (d, *J* = 8.2 Hz, 1H), 5.33 – 5.24 (br s, 1H), 5.24 – 5.11 (m, 4H), 5.11 – 5.02 (br s, 1H), 4.42 – 4.30 (m, 1H), 4.11 – 3.79 (m, 2H), 1.78 – 1.64 (m, 3H), 1.62 – 1.49 (m, 1H), 1.47 – 1.36 (m, 1H), 0.92 – 0.78 (m, 6H); ^{13}C NMR (125 MHz, $CDCl_3$) δ 172.7, (172.6), 169.7, (169.6), 161.7, (161.3), (160.1), 160.0, 135.4, (135.3), 128.8, 128.72, 128.68, 128.6, 128.57, 128.47, 128.45, 128.31, 128.26, (68.9), 68.8, 67.2, (67.1), 65.74, (65.69), 65.3, (52.9), 52.8, 48.0, (41.4), 41.3, (40.5), 40.4, (24.9), 24.7, 23.2, (21.6), 21.5; IR (neat) ν_{max}/cm^{-1} 3338, 2954, 1714, 1655, 1499, 1300, 1176; HRMS *m/z* calculated for $C_{29}H_{34}N_4NaO_6$ $[M+Na]^+$ 557.2371; found 557.2391. The diastereomeric ratio (2:1) for azapeptide **2.29a** was determined by SFC analysis on chiral stationary phase [Chiralcel OJ-H 25cm, 10% MeOH:H_2O (19:1), 3 mL/min, 30°C, 150 bar, R*t* (major) 4.4min, R*t* (minor) 6.3 min].

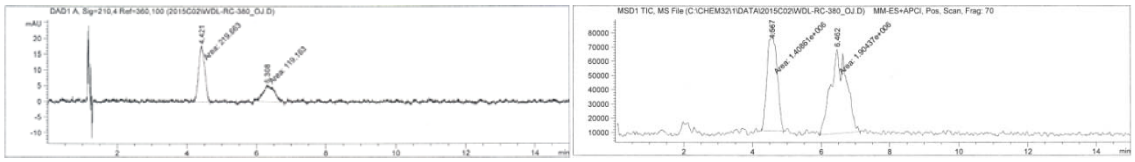

Signal 1: DAD1 A, Sig=210,4 Ref=360,100

Peak #	RetTime [min]	Type	Width [min]	Area [mAU*s]	Height [mAU]	Area %
1	4.421	MM	0.2061	219.66335	17.76638	64.8306
2	6.308	MM	0.3795	119.16331	5.23271	35.1694

Peak #	RetTime [min]	Type	Width [min]	Area	Height	Area %
1	4.567	MM	0.3138	1.40861e6	7.48218e4	42.5178
2	6.462	MM	0.5342	1.90437e6	5.94191e4	57.4822

_N_-Cbz-Aza-1,4-cyclohexadienylglycinyl-L-proline Benzhydrylamide (2.30a)

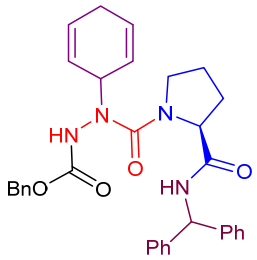

2.30a

Employing the protocol described for the synthesis of aza-pipecolinamide **2.20a**, azopeptide **2.13a** (0.52 g, 1.11 mmol) dissolved in DCM (50 mL), was reacted with cyclohexadiene (0.886 g, 1.03 mL, 11.1 mmol). The residue was purified by silica gel chromatography using 80% Ethyl acetate in hexane to give azapeptide **2.30a** (0.56 g, 92%) as white solid: R_f 0.2 (1:4 hexane:EtOAc); mp 83−85 °C; $[\alpha]_D^{20}$ 110.7° (*c* 0.62, $CHCl_3$); ^{1}H NMR (500 MHz, $(CD_3)_2CO$) δ 8.75 (s, 1H), 8.26 (d, *J* = 8.9 Hz, 1H), 7.55 – 7.04 (m, 15H), 6.35 (d, *J* = 9.2 Hz, 1H), 6.01 (d, *J* = 10.0 Hz, 1H), 5.94 (d, *J* = 9.9 Hz, 1H), 5.84 (d, *J* = 10.3 Hz, 1H), 5.58 (d, *J* = 9.6 Hz, 1H), 5.34 (s, 1H), 4.87 (q, *J* = 12.2 Hz, 2H), 4.43 (dd, *J* = 9.7, 7.3 Hz, 1H), 3.55 – 3.45 (m, 1H), 3.04 (dd, *J* = 16.6, 9.7 Hz, 1H), 2.57 (ddd, *J* = 5.9, 4.5, 2.6 Hz, 2H), 2.31 – 2.19 (m, 1H), 1.82 – 1.66 (m, 2H), 1.65 – 1.54 (m, 1H); ^{13}C NMR (125 MHz, $(CD_3)_2CO$) δ 171.7, 159.9, 157.3, 144.1, 143.5, 137.2, 130.5, 129.4, 129.22, 129.16, 129.1, 129.0, 128.9, 128.7, 128.6, 127.9, 127.4, 125.2, 125.0, 67.8, 63.8, 56.8, 53.3, 50.8, 31.0, 26.6, 26.3; IR (neat) ν_{max}/cm^{-1} 3306, 3028, 1718, 1639, 1524, 1400, 1262, 1210; HRMS *m/z* calculated for $C_{33}H_{34}N_4NaO_4$ $[M+Na]^+$ 573.2472; found 573.2486.

_N_-Cbz-Aza-1,4-cyclohexadienylglycinyl-L-phenylalanine Benzhydrylamide (2.31a)

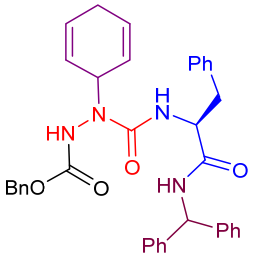

2.31a

Employing the protocol described for the synthesis of aza-pipecolinamide **2.20a**, azopeptide **2.15a** (0.1 g, 0.192 mmol) dissolved in DCM (10 mL), was reacted with cyclohexadiene (0.154 g, 0.179 mL, 1.92 mmol). The residue was purified with silica gel chromatography using 1% MeOH in chloroform to give azapeptide **2.31a** (0.11 g, 95%) as a white solid; R_f 0.68 (1:4 Hexane:EtOAc); mp 207−208 °C; $[\alpha]_D^{20}$ 128.7° (*c* 0.23, 1:1 $CHCl_3$:MeOH); ^{1}H NMR (400 MHz, DMSO-*d*$_6$, 120 °C) δ 8.29 (d, *J* = 8.9 Hz, 1H), 7.77 (s, 1H), 7.38 – 7.09 (m, 20H), 6.24 (d, *J* = 7.9 Hz, 1H), 6.11 (d, *J* = 8.3 Hz, 1H), 5.90 – 5.80 (m, 2H), 5.70 – 5.58 (m, 2H), 5.18 – 5.02 (m, 3H), 4.60 (dd, *J* = 14.2, 7.3 Hz, 1H), 3.06 – 2.92 (m, 2H), 2.63 – 2.46 (m, 2H); ^{13}C NMR (100 MHz, DMSO-*d*$_6$, 120 °C) δ 169.9, 156.5, 155.3, 141.6, 141.5, 137.0, 136.0, 128.6, 127.7, 127.57, 127.56, 127.54, 127.3, 127.0, 126.8, 126.6, 126.2, 126.1, 125.4, 123.2, 123.1, 66.3, 55.8, 53.9, 52.1, 37.7, 25.0; IR (neat) ν_{max}/cm^{-1} 3297, 2921, 1680, 1650, 1535, 1390, 1295, 1112; HRMS *m/z* calculated for $C_{37}H_{36}N_4NaO_4$ $[M+Na]^+$ 623.2629; found 623.2647.

_N_-Cbz-Aza-1,4-cyclohexadienylglycinyl-sarcosine Benzhydrylamide (2.32a)

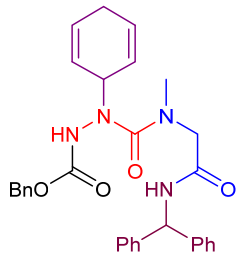

2.32a

Employing the protocol described for the synthesis of aza-pipecolinamide **2.20a**, azopeptide **2.16a** (0.2 g, 0.45 mmol) dissolved in DCM (20 mL), was reacted with cyclohexadiene (0.361 g, 0.419 mL, 4.5 mmol). The residue was purified by silica gel chromatography using 80% Ethyl acetate in hexane to give azapeptide **2.32a** (0.21 g, 89%) as white solid: R_f 0.24 (1:4 hexane:EtOAc); mp 78−82 °C; ^{1}H NMR (400 MHz, DMSO-d_6, 120 °C) δ 8.53 (s, 1H), 8.20 (d, J = 8.2 Hz, 1H), 7.41 – 7.20 (m, 15H), 6.17 (d, J = 8.5 Hz, 1H), 5.91 (dtd, J = 10.3, 3.3, 1.8 Hz, 2H), 5.72 – 5.66 (m, 2H), 5.04 – 4.97 (m, 1H), 4.96 (s, 2H), 3.93 (s, 2H), 2.88 (s, 3H), 2.60 – 2.53 (m, 2H); ^{13}C NMR (100 MHz, DMSO-d_6, 120 °C) δ 167.4, 160.5, 155.4, 141.7, 136.0, 127.8, 127.6, 127.1, 126.9, 126.7, 126.2, 123.8, 65.5, 55.6, 53.1, 52.9, 36.7, 25.1; IR (neat) ν_{max}/cm^{-1} 3294, 3030, 1718, 1637, 1527, 1390, 1264, 1206; HRMS *m/z* calculated for $C_{31}H_{32}N_4NaO_4$ $[M+Na]^+$ 547.2316; found 547.2331.

***N*-Cbz-*N*-isobutylenyl-aza-glycinyl-L-proline Benzhydrylamide (2.33a)**

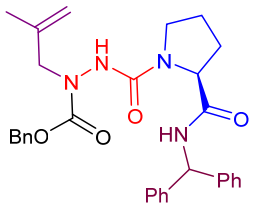

2.33a

A stirred solution of *N*-(Cbz)-aza-glycinyl proline benzhydrylamide (**2.8a**, 0.15 g, 0.317 mmol) and pyridine (0.038 g, 0.0385 mL, 0.476 mmol), in DCM (20 mL) at –78 °C, was treated with NBS (0.085 g, 0.476 mmol) in a single portion. The bath was removed. The reaction mixture was allowed to warm to room temperature and stirred for 1h, when the color of the reaction mixture changed to a pale yellow, and a new less polar bright yellow spot was observed on the TLC plate. The reaction mixture was transferred to a pressure tube vessel, which is later sealed and cooled to –78°C under a stream of argon, treated drop-wise via a cannula with a solution of 2-methylprop-1-ene in dry DCM (1 M, 3.17 mL, 3.17 mmol) and stirred at rt for overnight. The volatiles were removed under vacuum. The residue was purified by silica gel chromatography using 55-60% Ethyl acetate in hexane to give **2.33a**

(0.087 g, 52%) as a white solid; R_f 0.38 (2:3 Hexane:EtOAc); mp 56−58 °C; $[\alpha]_D^{20}$ −54° (*c* 0.1, $CHCl_3$); ^1H NMR (400 MHz, DMSO-d_6, 120 °C, NUS) δ 8.31 (s, 1H), 8.14 (d, *J* = 8.1 Hz, 1H), 7.38 – 7.18 (m, 15H), 6.08 (d, *J* = 8.3 Hz, 1H), 5.08 (q, *J* = 12.8 Hz, 2H), 4.84 (ddd, *J* = 24.9, 1.9, 1.2 Hz, 2H), 4.46 (dd, *J* = 6.2, 5.2 Hz, 1H), 3.99 (q, *J* = 15.4 Hz, 2H), 3.47 – 3.29 (m, 2H), 1.98 (dt, *J* = 7.0, 5.0 Hz, 2H), 1.95 – 1.79 (m, 2H), 1.72 (s, 3H); ^{13}C NMR (100 MHz, DMSO-d_6, 120 °C, NUS) δ 170.4, 155.7, 155.5, 141.8, 141.7, 140.2, 136.1, 127.6, 127.5, 127.5, 127.0, 126.6, 126.5, 126.2, 126.1, 111.9, 66.2, 59.4, 55.83, 55.76, 45.6, 28.2, 23.5, 19.3; IR (neat) ν_{max}/cm^{-1} 3294, 2928, 1709, 1656, 1517, 1495, 1365, 1223, 1131; HRMS *m/z* calculated for $C_{31}H_{34}N_4NaO_4$ $[M+Na]^+$ 549.2472; found 549.2493.

_N_-Cbz-Aza-isobutylenylglycinyl-L-phenylalanine Benzhydrylamide (2.34a)

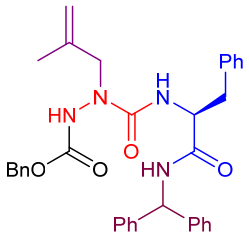

2.34a

A –78 °C stirred solution of Cbz-azo-glycinyl-phenyl alanine dipeptide azopeptide **2.15a** (0.2 g, 0.384 mmol) in dry DCM in pressure sealed tube vessel was treated dropwise via a cannula with a solution of 2-methylprop-1-ene in dry DCM (1 M, 3.84 mL, 3.84 mmol). After complete addition, the reaction mixture was allowed to warm to room temperature. After stirring overnight, the color of the reaction mixture changed from pale yellow to colourless and a new spot lower to the starting material appeared on the TLC plate. The solution was concentrated and the obtained crude residue was purified by silica gel chromatography using 30% Ethyl acetate in hexane to give azapeptide **2.34a** (0.19 g, 86%) as white solid; R_f 0.63 (2:3 hexane:EtOAc); mp 151−152 °C; $[\alpha]_D^{20}$ 25° (*c* 0.12, $CHCl_3$); ^1H NMR (400 MHz, DMSO-d_6, 120 °C, NUS) δ 8.95 (s, 1H), 8.28 (d, *J* = 8.1 Hz, 1H), 7.40 – 7.10 (m, 20H), 6.30 (d, *J* = 8.0 Hz, 1H), 6.12 (d, *J* = 8.3 Hz, 1H), 5.14 – 5.01 (m, 2H), 4.78 (ddd, *J* = 2.7, 1.5, 0.7 Hz, 2H), 4.59 (td, *J* = 7.5, 5.9 Hz, 1H), 3.96 (q, *J* = 15.1 Hz, 2H), 3.01

(qd, J = 13.9, 6.6 Hz, 2H), 1.65 (s, 3H); ^{13}C NMR (100 MHz, DMSO-d_6, 120 °C, NUS) δ 169.9, 156.4, 154.8, 141.6, 141.5, 140.4, 136.9, 135.8, 129.2, 128.5, 127.6, 127.5, 127.3, 127.2, 126.9, 126.7, 126.6, 126.2, 126.2, 125.4, 112.4, 65.8, 55.8, 54.6, 53.1, 37.5, 19.1; IR (neat) ν_{max}/cm^{-1} 3291, 2923, 1737, 1635, 1515, 1494, 1195, 1050; HRMS *m/z* calculated for $C_{35}H_{36}N_4NaO_4$ $[M+Na]^+$ 559.2629; found 559.2640.

N-Cbz-N-Cycloheptatrienyl-aza-glycinyl-L-proline Benzhydrylamide (2.35a)

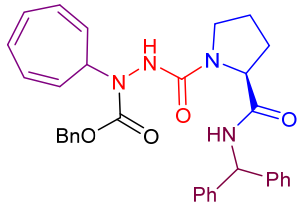

2.35a

A stirred –78 °C solution of *N*-(Cbz)-aza-glycinyl-proline benzhydrylamide **2.8a** (0.09 g, 0.19 mmol), and pyridine (0.023 g, 0.0231 mL, 0.286 mmol) in DCM (20mL) was treated with NBS (0.051 g, 0.286 mmol) in a single portion. The bath was removed. The reaction mixture was allowed to warm to room temperature and stirred for 1h, when the color of the reaction mixture changed to a pale yellow, and a new less polar bright yellow spot was observed on the TLC plate. This reaction mixture was cooled to –78°C. Cycloheptatriene (0.175 g, 1.9 mmol) was added drop wise to the mixture, which was stirred at rt overnight. The volatiles were removed under vacuum. The residue was purified by silica gel chromatography using 45-50% Ethyl acetate in hexane to give **2.35a** (0.03 g, 28%) as white solid: R_f 0.56 (1:4 hexane:EtOAc); mp 64−67 °C; $[\alpha]_D^{20}$ −23.1° (*c* 0.13, $CHCl_3$); ^{1}H NMR (400 MHz, DMSO-d_6, 120 °C) δ 8.56 (s, 1H), 8.18 (d, J = 7.7 Hz, 1H), 7.40 – 7.19 (m, 15H), 6.64 (dd, J = 3.4, 2.9 Hz, 2H), 6.18 – 6.02 (m, 3H), 5.65 (td, J = 9.6, 4.9 Hz, 2H), 5.08 (q, J = 12.8 Hz, 2H), 4.51 (t, J = 5.7 Hz, 1H), 4.01 (tt, J = 4.8, 1.7 Hz, 1H), 3.54 – 3.39 (m, 2H), 2.01 (dt, J = 11.6, 4.1 Hz, 2H), 1.96 – 1.80 (m, 2H); ^{13}C NMR (100 MHz, DMSO-d_6, 120 °C) δ 170.4, 156.3, 154.9, 141.8, 141.7, 136.0, 130.2, 130.1, 127.6, 127.5, 127.0, 126.6, 126.5, 126.2, 126.1, 126.5, 123.4, 121.9, 121.8, 66.3, 59.5, 57.8, 55.9, 45.7, 28.4, 23.5; IR

(neat) ν_{max}/cm^{-1} 3270, 2920, 1708, 1656, 1517, 1495, 1376, 1291; HRMS *m/z* calculated for $C_{34}H_{34}N_4NaO_6$ $[M+Na]^+$ 585.2472; found 585.2483.

Hydrolytic cleavage of azapeptides 2.30a and 2.31a and detection of molecular ions for 2.36 and 2.37

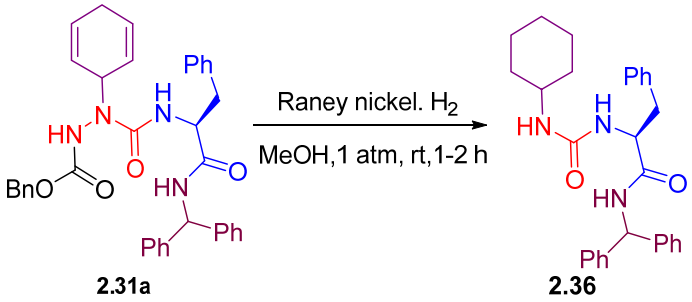

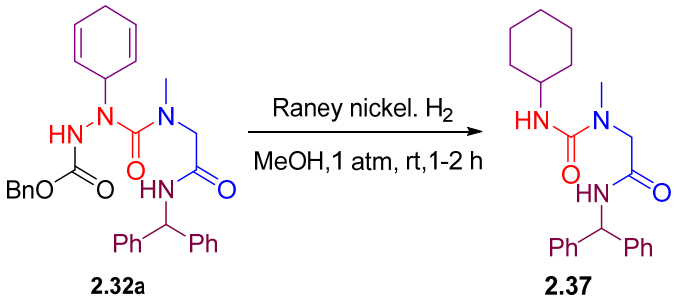

To solutions of azapeptide **2.31a** and **2.32a** in methanol, Raney nickel was respectively added at room temperature. The reaction mixtures were placed under hydrogenation atmosphere using balloons filled with hydrogen gas and stirred for the 1-2 h. After filtration of the Raney nickel over Celite™, the crude filtrates were examined by LCMS, which detected respectively molecular ions corresponding to the di- and tri-substituted ureas: **2.36** [*m/z* $[M+H]^+$ 456, 20-90% MeOH, 14 min, R.T. = 7.6 min] and **37** [*m/z* $[M+H]^+$ 380, 20-90% MeOH, 14 min, R.T. = 8.6 min].

Aza-Δ^4-dehydropipecolyl-L-leucine glycine Benzyl Amide (2.40)

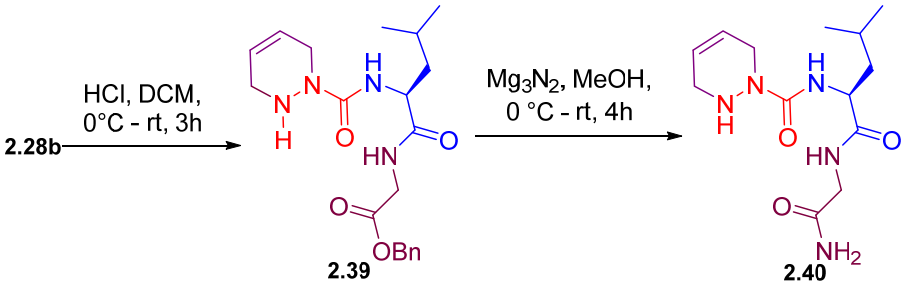

Carbamate **2.28b** (0.06 g, 0.123 mmol) was dissolved in DCM (6 mL), stirred and treated with bubbles of dry HCl gas at rt for 3h. The volatiles were removed under vacuum to give hydrochloride **2.39** (0.052g, 99%) as white solid: mp 53−56 °C; $[\alpha]_D^{20}$ −12.1° (*c* 0.14, MeOH); ^{1}H NMR (500 MHz, $CDCl_3$) δ 8.08 – 7.77 (br s, 1H), 7.76 – 7.48 (br s, 1H), 7.40 – 7.28 (m, 5H), 5.94 – 5.66 (br s, 2H), 5.12 (s, 2H), 4.52 – 4.18 (br, 3H), 4.18 – 3.97 (br s, 2H), 3.85 (d, *J* = 36.0 Hz, 2H), 1.79 – 1.48 (br s, 3H), 0.94 – 0.88 (m, 3H), 0.88 – 0.79 (m, 3H); ^{13}C NMR (125 MHz, $CDCl_3$) δ 174.3, 170.1, 156.9, 135.3, 128.7, 128.6, 128.3, 123.6, 119.9, 67.2, 53.9, 45.5, 43.6, 41.6, 41.0, 25.0, 23.1, 21.9; IR (neat) ν_{max}/cm^{-1} 3255, 2956, 1745, 1656, 1520, 1386, 1175; HRMS *m/z* calculated for $C_{20}H_{28}N_4NaO_4$ $[M+Na]^+$ 411.2003; found 411.2018.

To a microwave vial containing a stirred solution of benzyl ester **2.39** (0.02 g, 0.0515 mmol) in 2 mL of methanol at 0 °C, magnessium nitride (0.026 g, 0.257 mmol) was added in a single portion. The vial was immediately sealed, the ice bath was removed, and the reaction mixture was allowed to warm to room temperature. After 4h, the reaction mixture was diluted with 3N HCl and stirred for 30 min. The clear reaction mixture was passed through a pad of Celite™ that was washed with methanol. The combined filtrate and washings were concentrated to a reduced volume that was freeze-dried. The residue was further purified using preparative HPLC conducted on a Waters™ PrepLC instrument equipped with a reverse-phase Gemini™ C18 column (250 × 21.2 mm, 5 µm), using a binary solvent system consisting of MeOH (0.1% FA) in H_2O (0.1% FA) at a flow rate of 10.0

mL/min and UV detection at 214 nm. Fractions containing pure peptide were combined, freeze-dried and lyophilized to afford **2.40** (1.9 mg, 12 %) as a white solid: ^{1}H NMR (700 MHz, DMSO) δ 8.42 (s, 1H), 8.15 (t, *J* = 5.5 Hz, 1H), 7.25 (s, 1H), 7.02 (s, 1H), 6.84 (d, *J* = 8.2 Hz, 1H), 5.89 – 5.84 (m, 1H), 5.83 – 5.78 (m, 1H), 4.91 (t, *J* = 7.1 Hz, 1H), 4.13 (dd, *J* = 15.2, 7.7 Hz, 1H), 3.91 – 3.77 (br s, 2H), 3.64 (dd, *J* = 16.7, 6.1 Hz, 1H), 3.55 (dd, *J* = 16.7, 5.6 Hz, 1H), 3.23 (br, 2H), 1.62 – 1.54 (m, *J* = 13.4, 6.7 Hz, 1H), 1.47 (t, *J* = 7.2 Hz, 2H), 0.87 (dd, *J* = 15.9, 6.6 Hz, 6H); ^{13}C NMR (175 MHz, DMSO) δ 173.1, 171.0, 157.4, 125.9, 124.0, 51.9, 44.8, 41.9, 41.6, 40.6, 24.3, 23.1, 21.8. IR (neat) ν_{max}/cm^{-1} 3552, 3074 (br), 1618, 1528, 1459, 1389, 1353, 1248, 1182; HRMS *m/z* calculated for $C_{13}H_{23}N_5NaO_3$ $[M+Na]^+$ 320.1693; found 320.1707.

Additional supporting information for chapter 2

Aza-pipecolyl-L-leucine glycine Benzyl Amide (2.41)

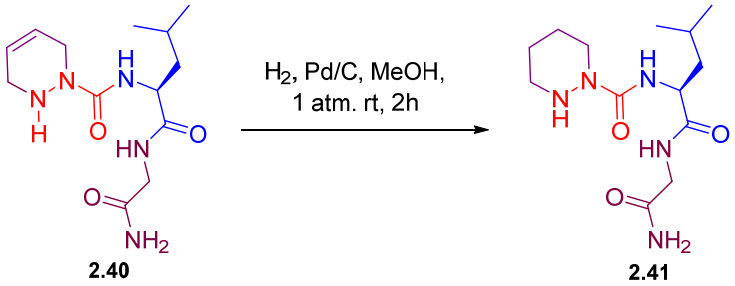

A solution of Aza-Δ^4-dehydropipecolyl-L-leucine glycine Benzyl Amide **2.40** (1 eq., 2 mg, 0.00673 mmol) in methanol (0.2 mL) was treated carefully with 10 wt% palladium-on-carbon (1 eq., ~ 1 mg) under a stream of argon. The resulting suspension was placed under hydrogen atmosphere (1 atm), stirred under a balloon of hydrogen at room temperature for 1–2 h, and filtered on Celite^{TM}, which was washed with methanol. The filtrate and washings were combined and concentrated under vacuum. The residue was freeze-dried to furnish Aza-pipecolyl-L-leucine glycine Benzyl Amide **2.41** (2 mg, 99 %) as a white solid: ^{1}H NMR (700 MHz, DMSO) δ 8.10 (t, *J* = 5.8 Hz, 1H), 7.24 (s, 1H), 7.03 (s, 1H), 6.77 (d, *J* = 8.1 Hz, 1H), 4.65 (t, *J* = 7.1 Hz, 1H), 4.12 – 4.07 (m, 1H), 3.64 (dd, *J* = 16.7, 6.1 Hz, 1H), 3.55 (dd, *J* = 16.8, 5.5 Hz, 1H), 3.33 (br, 2H), 2.81 – 2.63 (m, 2H), 1.61 – 1.54 (m, 1H), 1.54 – 1.48 (m, 4H), 1.48 – 1.42 (m, 2H), 0.88 (d, *J* = 6.6 Hz, 3H), 0.86 (d, *J* = 6.5 Hz, 3H). ; ^{13}C NMR (175 MHz, DMSO) δ 173.1, 170.9, 157.2, 52.0, 46.4, 42.3, 41.9, 41.5, 24.5, 24.3, 23.7, 23.1, 21.8. IR (neat) ν_{max}/cm^{-1} 3306 (br), 2953 (br), 1648, 1621, 1509, 1253, 1240, 1030; HRMS m/z calculated for $C_{13}H_{26}N_5O_3$ $[M+H]^+$ 300.203; found 300.2042.

Université de Montréal

CRYSTAL AND MOLECULAR STRUCTURE OF

$C_{25}H_{24}N_4O_4$ (COMPOUND 2.16a)

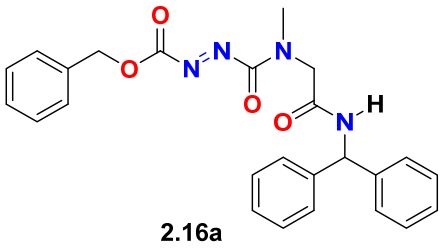

2.16a

Lubell group

Département de chimie, Université de Montréal,

C.P. 6128, Succ. Centre-Ville, Montréal, Québec, H3C 3J7 (Canada)

Structure solved and refined in the laboratory of X-ray diffraction Université de Montréal by Francine Bélanger.

Crystallography data and Molecular structure for compounds 2.16a, 2.30a and 2.35a

Compound 2.16a (lube96)

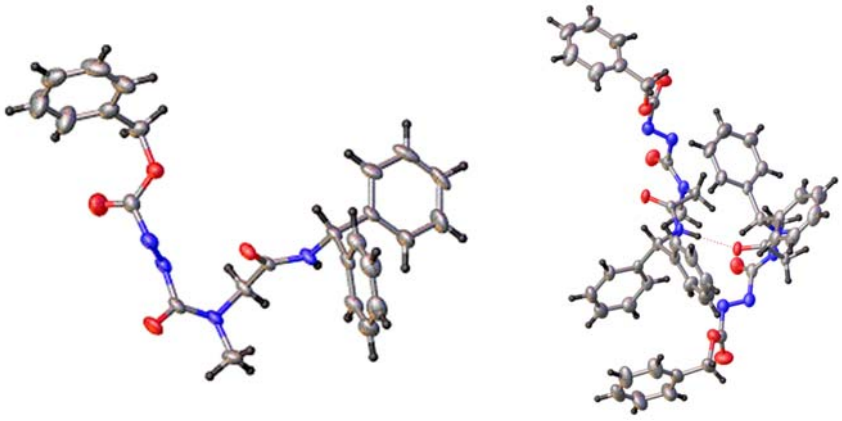

Table 1 Crystal data and structure refinement for lube96.

Identification code	lube96
Empirical formula	$C_{25}H_{24}N_4O_4$
Formula weight	444.48
Temperature/K	105
Crystal system	orthorhombic
Space group	$Pna2_1$
a/Å	8.7914(4)
b/Å	22.2498(11)
c/Å	11.9566(5)
α/°	90
β/°	90
γ/°	90
Volume/Å^3	2338.79(19)
Z	4
ρ_{calc}g/cm^3	1.262

μ/mm^{-1}	0.458
F(000)	936.0
Crystal size/mm^3	0.24 × 0.2 × 0.04
Radiation	GaKα (λ = 1.34139)
2Θ range for data collection/°	6.912 to 121.348
Index ranges	$-10 \leq h \leq 11$, $-28 \leq k \leq 26$, $-15 \leq l \leq 15$
Reflections collected	36324
Independent reflections	5333 [R_{int} = 0.0540, R_{sigma} = 0.0384]
Data/restraints/parameters	5333/1/300
Goodness-of-fit on F^2	1.050
Final R indexes [I>=2σ (I)]	R_1 = 0.0388, wR_2 = 0.0922
Final R indexes [all data]	R_1 = 0.0490, wR_2 = 0.0979
Largest diff. peak/hole / e $Å^{-3}$	0.24/-0.18
Flack parameter	0.08(9)

Table 2 Fractional Atomic Coordinates (×10^4) and Equivalent Isotropic Displacement Parameters ($Å^2$×10^3) for lube96. U_{eq} is defined as 1/3 of of the trace of the orthogonalised U_{IJ} tensor.

Atom	*x*	*y*	*z*	U(eq)
O1	4368.5(16)	2882.1(7)	4303.3(12)	28.8(3)
O2	4059(2)	3449.4(9)	1291.9(13)	42.9(4)
O3	4268(3)	5185.3(9)	3193.7(18)	57.3(6)
O4	3827.0(19)	4662.6(7)	4777.6(14)	36.6(4)
N1	6382.4(19)	2377.1(8)	5013.3(14)	26.7(4)
N2	5953(2)	3018.2(9)	2316.0(15)	29.5(4)
N3	5105(2)	3984.3(9)	2771.3(15)	32.3(4)

N4	3867(2)	4162.3(9)	3130.3(17)	34.3(5)
C1	5522(2)	2096.4(11)	5928.5(18)	27.7(5)
C2	5725(2)	2744.5(10)	4288.2(17)	24.5(4)
C3	6750(2)	3007.8(11)	3380.2(17)	27.9(5)
C4	5868(3)	2452.2(13)	1708(2)	41.1(6)
C5	4941(3)	3448.5(11)	2070.2(19)	30.9(5)
C6	4043(3)	4731.5(11)	3701(2)	35.2(5)
C7	3871(3)	5216.4(12)	5458(2)	44.1(6)
C8	2347(3)	5516.6(12)	5474(2)	43.3(6)
C9	1946(4)	5930.7(15)	4656(4)	69.4(10)
C10	506(4)	6184.5(17)	4653(4)	76.0(11)
C11	-519(4)	6040.4(15)	5472(3)	59.7(9)
C12	-130(4)	5640.8(19)	6293(3)	67.7(10)
C13	1312(4)	5374.9(17)	6285(2)	59.8(8)
C14	6616(3)	1943.4(11)	6870.5(17)	29.5(5)
C15	6674(3)	2298.8(13)	7823.2(19)	39.1(6)
C16	7682(3)	2156.1(16)	8688(2)	51.6(8)
C17	8615(3)	1668.8(16)	8603(2)	51.1(8)
C18	8587(4)	1319.7(15)	7646(3)	53.2(7)
C19	7590(3)	1456.3(13)	6783(2)	42.7(6)
C20	4628(2)	1549.9(10)	5530.6(18)	29.7(5)
C21	3313(3)	1386.0(12)	6111(2)	38.9(6)
C22	2503(3)	877.6(14)	5803(2)	48.9(7)
C23	2991(3)	523.9(14)	4928(3)	50.5(7)
C24	4294(3)	677.9(13)	4356(2)	45.3(6)
C25	5101(3)	1190.4(12)	4648.0(19)	36.2(5)

Table 3 Anisotropic Displacement Parameters ($Å^2 \times 10^3$) for lube96. The Anisotropic displacement factor exponent takes the form: $-2\pi^2[h^2a^{*2}U_{11}+2hka^*b^*U_{12}+\ldots]$.

Atom	U_{11}	U_{22}	U_{33}	U_{23}	U_{13}	U_{12}
O1	18.2(7)	46.0(9)	22.2(7)	5.2(7)	0.4(6)	0.8(6)
O2	42.2(10)	65.0(12)	21.4(8)	0.3(8)	-11.2(7)	6.8(8)
O3	80.5(16)	42.0(11)	49.4(11)	10.2(9)	4.8(11)	-4.9(10)
O4	40.2(9)	39.8(9)	29.9(9)	-1.3(7)	-0.2(7)	6.2(7)
N1	16.3(8)	45.9(11)	17.9(8)	6.0(8)	1.2(7)	0.6(7)
N2	25.7(9)	46.9(11)	15.9(8)	2.4(8)	0.4(7)	2.1(8)
N3	30.3(10)	44.2(11)	22.3(9)	7.6(8)	-1.3(8)	1.1(9)
N4	33.5(11)	44.0(12)	25.4(10)	2.4(9)	0.8(8)	0.4(9)
C1	22.5(10)	43.1(12)	17.4(9)	5.7(9)	4.0(8)	2.8(9)
C2	20.4(10)	36.7(11)	16.4(9)	0.7(9)	-1.3(8)	-2.3(8)
C3	19.3(10)	45.1(12)	19.4(10)	6.1(9)	-2.0(8)	-0.2(9)
C4	39.3(14)	57.0(15)	27.1(11)	-9.5(12)	2.6(10)	7.2(12)
C5	27.3(11)	48.9(13)	16.5(9)	5.8(9)	0.8(8)	0.5(10)
C6	32.5(12)	40.2(13)	33.0(12)	4.3(10)	-1.9(10)	0.5(10)
C7	43.1(15)	46.7(14)	42.4(14)	-14.2(12)	-8.1(12)	7.5(11)
C8	41.5(14)	44.0(14)	44.4(15)	-13.8(12)	-6.4(12)	6.3(11)
C9	60(2)	59.2(19)	89(3)	19.4(18)	16.1(19)	20.1(15)
C10	67(2)	71(2)	91(3)	18(2)	4(2)	31.7(18)
C11	50.1(18)	66.8(19)	62.4(19)	-25.4(17)	-13.7(16)	21.6(15)
C12	50.1(18)	110(3)	43.2(16)	-21.4(18)	5.3(15)	15.9(18)
C13	56.6(18)	91(2)	31.7(14)	-8.3(15)	-3.1(14)	20.5(17)
C14	26.2(11)	46.5(12)	15.7(10)	5.9(9)	2.5(8)	-2.7(9)

C15	32.9(13)	62.1(16)	22.3(11)	-1.6(11)	7.1(10)	-3.9(11)
C16	42.4(15)	94(2)	17.9(11)	-4.0(13)	2.8(11)	-18.8(15)
C17	37.8(14)	93(2)	22.6(12)	17.9(13)	-9.2(11)	-7.0(15)
C18	48.3(17)	69.8(19)	41.4(15)	14.9(14)	-15.4(13)	8.7(14)
C19	42.6(15)	57.7(15)	27.8(12)	1.4(12)	-9.7(11)	10.3(12)
C20	23.3(10)	44.3(12)	21.4(10)	8.8(10)	-2.7(8)	3.0(9)
C21	29.4(12)	55.3(15)	32.0(12)	7.2(11)	5(1)	-1.3(11)
C22	33.4(13)	63.2(17)	50.0(17)	13.9(14)	1.4(12)	-11.6(12)
C23	42.5(15)	55.2(16)	53.7(17)	6.5(14)	-15.1(13)	-9.2(13)
C24	47.2(15)	54.5(15)	34.3(13)	-5.4(12)	-10.2(12)	-0.6(12)
C25	30.5(12)	54.8(15)	23.3(11)	3.5(10)	-0.7(9)	-0.7(10)

Table 4 Bond Lengths for lube96.

Atom	Atom	Length/Å	Atom	Atom	Length/Å
O1	C2	1.232(2)	C8	C13	1.367(4)
O2	C5	1.212(3)	C9	C10	1.386(5)
O3	C6	1.194(3)	C10	C11	1.369(5)
O4	C6	1.310(3)	C11	C12	1.368(5)
O4	C7	1.477(3)	C12	C13	1.399(5)
N1	C1	1.469(3)	C14	C15	1.388(3)
N1	C2	1.324(3)	C14	C19	1.386(4)
N2	C3	1.453(3)	C15	C16	1.398(4)
N2	C4	1.456(3)	C16	C17	1.363(5)
N2	C5	1.340(3)	C17	C18	1.383(5)
N3	N4	1.236(3)	C18	C19	1.387(4)
N3	C5	1.464(3)	C20	C21	1.397(3)

N4	C6	1.447(3)	C20	C25	1.388(3)
C1	C14	1.519(3)	C21	C22	1.387(4)
C1	C20	1.524(3)	C22	C23	1.377(4)
C2	C3	1.528(3)	C23	C24	1.378(4)
C7	C8	1.497(4)	C24	C25	1.388(4)
C8	C9	1.390(5)			

Table 5 Bond Angles for lube96.

Atom	Atom	Atom	Angle/°	Atom	Atom	Atom	Angle/°
C6	O4	C7	116.1(2)	C13	C8	C9	118.9(3)
C2	N1	C1	121.70(17)	C10	C9	C8	120.3(3)
C3	N2	C4	116.63(19)	C11	C10	C9	120.3(3)
C5	N2	C3	121.60(19)	C12	C11	C10	120.0(3)
C5	N2	C4	118.3(2)	C11	C12	C13	119.8(3)
N4	N3	C5	111.90(19)	C8	C13	C12	120.7(3)
N3	N4	C6	110.5(2)	C15	C14	C1	120.3(2)
N1	C1	C14	108.77(17)	C19	C14	C1	120.7(2)
N1	C1	C20	111.84(18)	C19	C14	C15	119.0(2)
C14	C1	C20	112.28(19)	C14	C15	C16	120.1(3)
O1	C2	N1	124.50(19)	C17	C16	C15	120.4(3)
O1	C2	C3	119.10(18)	C16	C17	C18	119.8(2)
N1	C2	C3	116.40(18)	C17	C18	C19	120.2(3)
N2	C3	C2	110.13(17)	C14	C19	C18	120.4(3)
O2	C5	N2	126.5(2)	C21	C20	C1	118.7(2)
O2	C5	N3	120.1(2)	C25	C20	C1	122.8(2)
N2	C5	N3	112.99(19)	C25	C20	C21	118.4(2)

O3	C6	O4	128.5(3)	C22	C21	C20	120.4(3)
O3	C6	N4	121.2(2)	C23	C22	C21	120.6(3)
O4	C6	N4	110.2(2)	C22	C23	C24	119.6(3)
O4	C7	C8	110.8(2)	C23	C24	C25	120.3(3)
C9	C8	C7	120.9(3)	C24	C25	C20	120.8(2)
C13	C8	C7	120.2(3)				

Table 6 Hydrogen Bonds for lube96.

D	H	A	d(D-H)/Å	d(H-A)/Å	d(D-A)/Å	D-H-A/°
N1	H1	O1[1]	0.88	1.97	2.819(2)	162.3

[1]1/2+X,1/2-Y,+Z

Table 7 Torsion Angles for lube96.

A	B	C	D	Angle/°	A	B	C	D	Angle/°
O1	C2	C3	N2	-40.3(3)	C6	O4	C7	C8	85.5(3)
O4	C7	C8	C9	-88.3(3)	C7	O4	C6	O3	-0.3(4)
O4	C7	C8	C13	90.2(3)	C7	O4	C6	N4	-176.07(18)
N1	C1	C14	C15	103.3(2)	C7	C8	C9	C10	177.1(3)
N1	C1	C14	C19	-75.3(3)	C7	C8	C13	C12	-178.3(3)
N1	C1	C20	C21	-153.4(2)	C8	C9	C10	C11	1.6(6)
N1	C1	C20	C25	29.7(3)	C9	C8	C13	C12	0.1(5)
N1	C2	C3	N2	139.6(2)	C9	C10	C11	C12	-0.5(6)
N3	N4	C6	O3	73.1(3)	C10	C11	C12	C13	-0.7(5)
N3	N4	C6	O4	-110.7(2)	C11	C12	C13	C8	0.9(5)

N4	N3	C5	O2	52.8(3)	C13	C8	C9	C10	-1.4(6)
N4	N3	C5	N2	-133.9(2)	C14	C1	C20	C21	84.0(2)
C1	N1	C2	O1	-0.3(3)	C14	C1	C20	C25	-92.9(2)
C1	N1	C2	C3	179.75(19)	C14	C15	C16	C17	0.1(4)
C1	C14	C15	C16	180.0(2)	C15	C14	C19	C18	1.3(4)
C1	C14	C19	C18	179.9(2)	C15	C16	C17	C18	1.3(4)
C1	C20	C21	C22	-177.4(2)	C16	C17	C18	C19	-1.4(5)
C1	C20	C25	C24	176.3(2)	C17	C18	C19	C14	0.1(5)
C2	N1	C1	C14	-155.08(19)	C19	C14	C15	C16	-1.4(4)
C2	N1	C1	C20	80.3(3)	C20	C1	C14	C15	-132.4(2)
C3	N2	C5	O2	-168.1(2)	C20	C1	C14	C19	49.0(3)
C3	N2	C5	N3	19.2(3)	C20	C21	C22	C23	0.7(4)
C4	N2	C3	C2	-78.9(2)	C21	C20	C25	C24	-0.5(3)
C4	N2	C5	O2	-9.8(3)	C21	C22	C23	C24	-0.1(4)
C4	N2	C5	N3	177.50(19)	C22	C23	C24	C25	-0.9(4)
C5	N2	C3	C2	79.8(3)	C23	C24	C25	C20	1.1(4)
C5	N3	N4	C6	-172.90(18)	C25	C20	C21	C22	-0.4(3)

Table 8 Hydrogen Atom Coordinates (Å×10^4) and Isotropic Displacement Parameters (Å^2×10^3) for lube96.

Atom	***x***	***y***	***z***	**U(eq)**
H1	7359	2299	4945	46(8)
H1A	4779	2399	6218	33
H3A	7053	3421	3589	34

H3B	7684	2762	3311	34
H4A	6889	2279	1642	62
H4B	5451	2524	960	62
H4C	5206	2172	2113	62
H7A	4637	5496	5145	53
H7B	4179	5116	6232	53
H9	2661	6040	4097	83
H10	230	6460	4080	91
H11	-1502	6218	5470	72
H12	-837	5544	6866	81
H13	1574	5093	6850	72
H15	6029	2639	7888	47
H16	7717	2400	9339	62
H17	9282	1569	9200	61
H18	9252	985	7579	64
H19	7576	1214	6129	51
H21	2972	1624	6721	47
H22	1604	772	6198	59
H23	2432	176	4720	61
H24	4642	432	3758	54
H25	5988	1296	4239	43

Experimental

Single crystals of $C_{25}H_{24}N_4O_4$ lube 96 (2.**16a**) were grown in acetone-hexane mixture. A suitable crystal was selected and mounted on the diffractometer. The crystal was kept at 105 K during data collection. Using Olex2[5], the structure was solved with the XT[6] structure solution program using Direct Methods and refined with the XL[7] refinement package using Least Squares minimisation.

Crystal structure determination of [lube96]

Crystal Data for $C_{25}H_{24}N_4O_4$ (M =444.48 g/mol): orthorhombic, space group $Pna2_1$ (no. 33), a = 8.7914(4) Å, b = 22.2498(11) Å, c = 11.9566(5) Å, V = 2338.79(19) Å^3, Z = 4, T = 105 K, μ(GaKα) = 0.458 mm^{-1}, *Dcalc* = 1.262 g/cm^3, 36324 reflections measured (6.912° ≤ 2Θ ≤ 121.348°), 5333 unique (R_{int} = 0.0540,

R_{sigma} = 0.0384) which were used in all calculations. The final R_1 was 0.0388 (I > 2σ(I)) and wR_2 was 0.0979 (all data).

Refinement model description

Number of restraints - 1, number of constraints - unknown.

Details:

```
1. Fixed Uiso
 At 1.2 times of:
  All C(H) groups, All C(H,H) groups
 At 1.5 times of:
  All C(H,H,H) groups
2.a Riding coordinates:
 N1(H1)
2.b Ternary CH refined with riding coordinates:
 C1(H1A)
2.c Secondary CH2 refined with riding coordinates:
 C3(H3A,H3B), C7(H7A,H7B)
2.d Aromatic/amide H refined with riding coordinates:
 C9(H9), C10(H10), C11(H11), C12(H12), C13(H13), C15(H15), C16(H16), C17(H17),
 C18(H18), C19(H19), C21(H21), C22(H22), C23(H23), C24(H24), C25(H25)
2.e Idealised Me refined as rotating group:
 C4(H4A,H4B,H4C)
```

Université de Montréal

CRYSTAL AND MOLECULAR STRUCTURE OF

$C_{33}H_{34}N_4O_4$ (COMPOUND 2.30a)

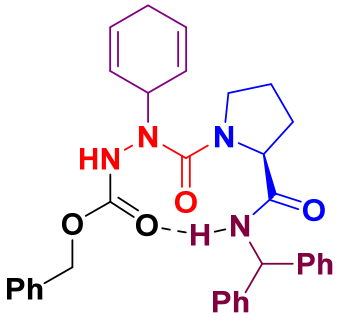

2.30a

Lubell group

Département de chimie, Université de Montréal,

C.P. 6128, Succ. Centre-Ville, Montréal, Québec, H3C 3J7 (Canada)

Structure solved and refined in the laboratory of X-ray diffraction Université de Montréal by Francine Bélanger.

Compound 2.30a (lube78)

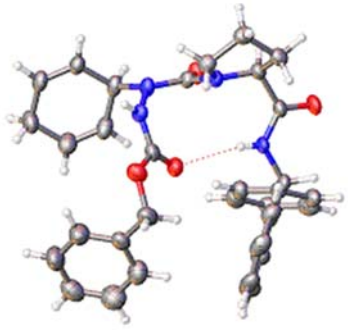

Table 9 Crystal data and structure refinement for lube78.

Identification code	lube78
Empirical formula	$C_{37}H_{42}N_4O_6$
Formula weight	638.74
Temperature/K	100
Crystal system	orthorhombic
Space group	$P2_12_12_1$
a/Å	7.8202(5)
b/Å	15.4330(9)
c/Å	28.4386(17)
α/°	90
β/°	90
γ/°	90
Volume/Å^3	3432.2(4)
Z	4
ρ_{calc}g/cm^3	1.236
μ/mm^{-1}	0.439
F(000)	1360.0

Crystal size/mm^3	0.25 × 0.09 × 0.03
Radiation	GaKα (λ = 1.34139)
2Θ range for data collection/°	5.408 to 121.586
Index ranges	-10 ≤ h ≤ 9, -20 ≤ k ≤ 20, -36 ≤ l ≤ 36
Reflections collected	49840
Independent reflections	7899 [R_{int} = 0.0541, R_{sigma} = 0.0347]
Data/restraints/parameters	7899/4/445
Goodness-of-fit on F^2	1.022
Final R indexes [I>=2σ (I)]	R_1 = 0.0437, wR_2 = 0.1225
Final R indexes [all data]	R_1 = 0.0460, wR_2 = 0.1248
Largest diff. peak/hole / e Å^{-3}	0.45/-0.23
Flack parameter	0.11(5)

Table 10 Fractional Atomic Coordinates (×10^4) and Equivalent Isotropic Displacement Parameters (Å^2×10^3) for lube78. U_{eq} is defined as 1/3 of the trace of the orthogonalised U_{IJ} tensor.

Atom	*x*	*Y*	*z*	U(eq)
O1	10872(2)	9026.6(9)	7186.3(6)	41.9(4)
O2	7090.4(19)	7398.3(9)	7567.9(6)	38.6(3)
O3	8536(2)	6186(1)	6566.6(6)	40.7(4)
O4	9474(2)	4793.3(11)	6581.5(6)	44.7(4)
N1	10373(2)	7816.1(11)	6770.8(6)	32.1(4)
N2	9787(2)	6850.3(10)	7574.2(6)	29.7(3)
N3	7430(2)	5941.4(10)	7479.0(6)	32.3(4)
N4	8389(2)	5347.3(11)	7224.2(7)	32.7(4)

C1	10578(3)	8269.7(13)	6323.4(7)	33.8(4)
C2	10551(3)	8242.5(12)	7176.4(7)	31.6(4)
C3	10469(3)	7729.0(12)	7629.9(7)	30.9(4)
C4	12273(3)	7582.3(15)	7831.8(8)	38.1(4)
C5	12047(3)	6751.4(16)	8117.5(8)	39.8(5)
C6	10909(3)	6197.1(13)	7799.3(8)	35.1(4)
C7	8047(3)	6773.5(12)	7540.2(7)	30.1(4)
C8	8753(3)	5509.1(13)	6771.9(8)	35.4(4)
C9	9887(3)	4876(2)	6085.0(9)	51.0(6)
C10	8326(3)	4752.2(16)	5779.4(8)	45.3(5)
C11	8095(4)	5268.5(19)	5387.4(12)	59.1(7)
C12	6722(5)	5137(2)	5082.5(13)	69.3(9)
C13	5544(5)	4515(2)	5177.2(12)	62.6(8)
C14	5743(5)	4008(2)	5568.9(13)	72.5(9)
C15	7141(5)	4115(2)	5868.6(11)	66.5(8)
C16	11238(3)	7635.2(13)	5954.1(8)	35.8(4)
C17	10560(4)	7591.7(16)	5504.1(8)	43.5(5)
C18	11227(4)	7019.5(18)	5172.8(9)	54.0(6)
C19	12571(4)	6488.5(17)	5283.3(10)	52.8(7)
C20	13291(4)	6532.0(18)	5727.8(10)	53.5(7)
C21	12625(3)	7100.1(16)	6062.3(9)	46.6(5)
C22	8966(3)	8754.9(13)	6184.8(7)	35.0(4)
C23	9066(3)	9624.6(14)	6056.3(8)	41.7(5)
C24	7612(4)	10077.5(16)	5918.6(9)	49.4(6)
C25	6053(4)	9671.1(18)	5907.0(9)	50.1(6)
C26	5928(3)	8802.5(18)	6043.2(9)	47.8(5)

C27	7380(3)	8351.8(14)	6178.9(8)	40.6(5)
C28	5555(3)	5803.5(13)	7469.0(9)	36.3(4)
C29	4871(3)	5780.5(16)	6976.5(10)	45.1(5)
C30	3961(4)	5129.9(18)	6808.8(10)	50.2(6)
C31	3478(4)	4348.1(16)	7089(1)	50.3(6)
C32	4200(3)	4353.6(14)	7571.5(9)	40.7(5)
C33	5134(3)	4995.3(14)	7743.1(8)	37.2(4)
O41	-589(4)	2156.8(18)	5631(1)	79.6(7)
C41	566(5)	3160(3)	5059.8(12)	71.7(9)
C42	547(4)	2618.0(19)	5490.5(10)	54.1(6)
O42A	1978(17)	2822(6)	5750(4)	57(2)
C43A	2200(9)	2391(5)	6202(2)	64.4(13)
C44A	3089(10)	1556(4)	6161(2)	63.4(12)
O42B	2070(20)	2571(7)	5702(5)	57(2)
C43B	2175(10)	1911(6)	6060(3)	64.4(13)
C44B	3915(10)	1950(5)	6269(2)	63.4(12)

Table 11 Anisotropic Displacement Parameters ($Å^2 \times 10^3$) for lube78. The Anisotropic displacement factor exponent takes the form: $-2\pi^2[h^2a^{*2}U_{11}+2hka^*b^*U_{12}+\ldots]$.

Atom	U_{11}	U_{22}	U_{33}	U_{23}	U_{13}	U_{12}
O1	58.7(10)	20.1(6)	46.8(8)	-3.0(6)	-7.2(7)	-8.2(6)
O2	35.5(7)	21.0(6)	59.3(9)	-1.1(6)	-1.8(7)	4.1(5)
O3	53.2(9)	29.8(7)	39.0(7)	2.9(6)	-1.3(7)	-7.9(7)
O4	51.0(9)	40.6(8)	42.4(8)	-8.4(7)	1.2(7)	4.2(7)
N1	46.7(9)	17.6(7)	32.0(8)	1.4(6)	-2.1(7)	-7.1(7)
N2	33.9(8)	20.1(7)	35.0(8)	1.7(6)	-1.6(7)	2.0(6)

N3	33.8(8)	18.4(7)	44.8(9)	1.6(6)	3.5(7)	2.3(6)
N4	40.4(9)	18.3(7)	39.3(9)	2.0(7)	2.6(7)	4.2(6)
C1	42.6(10)	23.6(9)	35.1(9)	3.9(7)	-0.6(8)	-7.8(8)
C2	34.2(9)	22.1(8)	38.4(10)	-1.1(7)	-4.8(8)	-3.4(7)
C3	35.4(9)	24.4(8)	33.0(9)	-2.2(7)	-1.5(8)	0.0(7)
C4	37.1(10)	38.3(11)	39(1)	-3.3(9)	-6.0(9)	-0.4(9)
C5	38.5(10)	43.7(12)	37.3(10)	5.2(9)	-2.1(9)	8.6(9)
C6	37.2(10)	29.0(9)	39.1(10)	5.9(8)	-1.2(8)	7.7(8)
C7	36.4(9)	20.2(8)	33.6(9)	2.7(7)	0.4(8)	1.0(7)
C8	37.8(10)	28.4(9)	40(1)	-3.9(8)	-3.8(8)	-4.4(8)
C9	51.0(14)	57.6(15)	44.4(12)	-12.0(11)	4.4(10)	-3.1(12)
C10	53.0(13)	40.8(12)	42.0(11)	-11.6(9)	3.3(10)	-2.2(10)
C11	63.5(16)	42.7(14)	71.1(17)	6.1(13)	-2.1(14)	-2.5(12)
C12	79(2)	58.2(17)	70.4(19)	8.6(15)	-11.0(17)	10.8(16)
C13	67.3(18)	57.1(17)	63.3(17)	-13.7(14)	-15.8(15)	5.6(15)
C14	77(2)	70(2)	71.1(19)	-0.2(16)	-10.2(17)	-31.5(18)
C15	79(2)	66.5(19)	53.9(15)	6.1(14)	-8.8(15)	-21.6(17)
C16	43.6(11)	24.4(9)	39.3(10)	5.6(8)	6.2(9)	-4.8(8)
C17	54.0(13)	37.2(11)	39.1(11)	1.1(9)	3.3(10)	2.3(10)
C18	72.1(17)	49.0(14)	40.8(12)	-5.3(10)	8.0(12)	-2.1(13)
C19	70.6(17)	36.1(12)	51.7(13)	1.4(10)	25.5(13)	0.1(12)
C20	58.7(15)	41.7(13)	60.0(15)	13.1(11)	18.9(12)	10.7(11)
C21	50.9(13)	42.0(12)	46.9(12)	11(1)	6(1)	4.5(10)
C22	48.9(11)	25.7(9)	30.4(9)	0.0(7)	-0.2(8)	-0.4(8)
C23	60.0(14)	26.0(9)	39.2(10)	1.5(8)	-1.4(10)	-3.0(9)
C24	73.2(17)	31(1)	44.1(12)	-1.1(9)	-2.0(11)	11.8(11)

C25	60.6(15)	44.5(13)	45.1(13)	-6.3(10)	-5.2(11)	17.4(12)
C26	47.8(13)	46.1(13)	49.5(13)	-5.6(11)	1.9(11)	0.9(11)
C27	48.3(12)	30.4(10)	43.2(11)	0.0(8)	0.1(10)	-2.6(9)
C28	33.1(9)	22.4(8)	53.6(12)	3.3(8)	4.3(9)	0.4(7)
C29	37.4(11)	35.4(11)	62.4(15)	17.4(10)	-5.5(10)	-1.9(9)
C30	49.5(13)	47.2(13)	53.9(14)	12.2(11)	-12.1(11)	-4.8(11)
C31	56.4(14)	32.7(11)	61.8(15)	3.9(10)	-12.7(12)	-9.5(10)
C32	42.3(11)	26.1(9)	53.7(13)	7.7(9)	1.6(10)	-3.6(8)
C33	40.3(10)	29.3(10)	42.1(11)	3.5(8)	4.4(9)	-2.9(8)
O41	74.0(15)	75.4(16)	89.4(17)	5.7(14)	-1.9(14)	-15.5(13)
C41	77(2)	81(2)	56.5(16)	4.8(16)	-0.4(15)	23.6(19)
C42	52.9(14)	50.7(14)	58.7(15)	-5.2(12)	0.6(12)	1.4(13)
O42A	56.4(17)	60(5)	56(2)	10(4)	-2.0(18)	-3(4)
C43A	58(2)	80(4)	55(3)	6(2)	0(2)	-9(3)
C44A	71(3)	67(3)	51(2)	9(2)	-9(2)	10(2)
O42B	56.4(17)	60(5)	56(2)	10(4)	-2.0(18)	-3(4)
C43B	58(2)	80(4)	55(3)	6(2)	0(2)	-9(3)
C44B	71(3)	67(3)	51(2)	9(2)	-9(2)	10(2)

Table 12 Bond Lengths for lube78.

Atom	Atom	Length/Å	Atom	Atom	Length/Å
O1	C2	1.236(2)	C16	C17	1.387(3)
O2	C7	1.223(2)	C16	C21	1.398(3)
O3	C8	1.209(3)	C17	C18	1.393(4)
O4	C8	1.354(3)	C18	C19	1.369(5)
O4	C9	1.454(3)	C19	C20	1.386(5)

N1	C1	1.461(2)	C20	C21	1.395(4)
N1	C2	1.335(3)	C22	C23	1.393(3)
N2	C3	1.466(2)	C22	C27	1.388(3)
N2	C6	1.482(2)	C23	C24	1.391(4)
N2	C7	1.370(3)	C24	C25	1.372(4)
N3	N4	1.389(2)	C25	C26	1.399(4)
N3	C7	1.383(2)	C26	C27	1.387(4)
N3	C28	1.482(3)	C28	C29	1.500(4)
N4	C8	1.341(3)	C28	C33	1.507(3)
C1	C16	1.526(3)	C29	C30	1.320(4)
C1	C22	1.518(3)	C30	C31	1.494(4)
C2	C3	1.515(3)	C31	C32	1.484(4)
C3	C4	1.540(3)	C32	C33	1.324(3)
C4	C5	1.528(3)	O41	C42	1.207(4)
C5	C6	1.530(3)	C41	C42	1.483(5)
C9	C10	1.510(4)	C42	O42A	1.377(12)
C10	C11	1.382(4)	C42	O42B	1.335(13)
C10	C15	1.375(4)	O42A	C43A	1.458(12)
C11	C12	1.395(5)	C43A	C44A	1.469(10)
C12	C13	1.358(5)	O42B	C43B	1.443(13)
C13	C14	1.371(5)	C43B	C44B	1.486(10)
C14	C15	1.396(5)			

Table 13 Bond Angles for lube78.

Atom	Atom	Atom	Angle/°	Atom	Atom	Atom	Angle/°
C8	O4	C9	114.2(2)	C10	C15	C14	120.0(3)

C2	N1	C1	120.32(16)	C17	C16	C1	122.5(2)
C3	N2	C6	111.53(16)	C17	C16	C21	118.1(2)
C7	N2	C3	116.70(16)	C21	C16	C1	119.3(2)
C7	N2	C6	124.07(16)	C16	C17	C18	120.8(3)
N4	N3	C28	115.46(17)	C19	C18	C17	120.8(3)
C7	N3	N4	119.36(17)	C18	C19	C20	119.5(2)
C7	N3	C28	118.75(16)	C19	C20	C21	120.1(3)
C8	N4	N3	119.48(17)	C20	C21	C16	120.7(3)
N1	C1	C16	109.22(16)	C23	C22	C1	119.8(2)
N1	C1	C22	111.79(18)	C27	C22	C1	121.61(18)
C22	C1	C16	114.75(18)	C27	C22	C23	118.6(2)
O1	C2	N1	121.56(19)	C24	C23	C22	120.8(2)
O1	C2	C3	120.06(18)	C25	C24	C23	120.2(2)
N1	C2	C3	118.24(16)	C24	C25	C26	119.6(2)
N2	C3	C2	114.03(16)	C27	C26	C25	120.0(3)
N2	C3	C4	103.74(16)	C26	C27	C22	120.7(2)
C2	C3	C4	110.86(17)	N3	C28	C29	111.99(19)
C5	C4	C3	102.45(17)	N3	C28	C33	108.97(17)
C4	C5	C6	102.82(17)	C29	C28	C33	112.67(18)
N2	C6	C5	102.68(16)	C30	C29	C28	123.2(2)
O2	C7	N2	122.34(18)	C29	C30	C31	123.9(2)
O2	C7	N3	121.81(19)	C32	C31	C30	113.1(2)
N2	C7	N3	115.84(17)	C33	C32	C31	123.7(2)
O3	C8	O4	124.8(2)	C32	C33	C28	123.3(2)
O3	C8	N4	126.5(2)	O41	C42	C41	127.8(3)
N4	C8	O4	108.68(18)	O41	C42	O42A	123.8(6)

O4	C9	C10	111.6(2)	O41	C42	O42B	118.4(7)
C11	C10	C9	119.8(3)	O42A	C42	C41	107.8(6)
C15	C10	C9	121.9(3)	O42B	C42	C41	113.2(7)
C15	C10	C11	118.2(3)	C42	O42A	C43A	117.7(10)
C10	C11	C12	121.2(3)	O42A	C43A	C44A	112.8(7)
C13	C12	C11	120.1(3)	C42	O42B	C43B	114.0(11)
C12	C13	C14	119.2(3)	O42B	C43B	C44B	107.8(8)
C13	C14	C15	121.1(3)				

Table 14 Hydrogen Bonds for lube78.

D	H	A	d(D-H)/Å	d(H-A)/Å	d(D-A)/Å	D-H-A/°
N1	H1	O3	0.75(4)	2.24(4)	2.955(2)	160(3)
N4	H4	O1[1]	0.82(3)	1.91(3)	2.701(2)	160(3)

[1]2-X,-1/2+Y,3/2-Z

Table 15 Torsion Angles for lube78.

A	B	C	D	Angle/°	A	B	C	D	Angle/°
O1	C2	C3	N2	169.83(19)	C9	O4	C8	O3	-4.0(3)
O1	C2	C3	C4	-73.5(3)	C9	O4	C8	N4	178.33(19)
O4	C9	C10	C11	140.4(3)	C9	C10	C11	C12	176.2(3)
O4	C9	C10	C15	-42.0(4)	C9	C10	C15	C14	-178.1(3)
N1	C1	C16	C17	134.8(2)	C10	C11	C12	C13	2.6(5)
N1	C1	C16	C21	-48.0(3)	C11	C10	C15	C14	-0.5(5)
N1	C1	C22	C23	129.4(2)	C11	C12	C13	C14	-1.5(5)
N1	C1	C22	C27	-51.1(3)	C12	C13	C14	C15	-0.5(6)

N1	C2	C3	N2	-14.3(3)	C13	C14	C15	C10	1.5(6)
N1	C2	C3	C4	102.4(2)	C15	C10	C11	C12	-1.5(5)
N2	C3	C4	C5	-31.1(2)	C16	C1	C22	C23	-105.5(2)
N3	N4	C8	O3	11.0(3)	C16	C1	C22	C27	74.0(3)
N3	N4	C8	O4	-171.31(17)	C16	C17	C18	C19	-0.2(4)
N3	C28	C29	C30	125.0(3)	C17	C16	C21	C20	-0.7(4)
N3	C28	C33	C32	-127.6(2)	C17	C18	C19	C20	-1.0(4)
N4	N3	C7	O2	147.7(2)	C18	C19	C20	C21	1.3(4)
N4	N3	C7	N2	-33.2(3)	C19	C20	C21	C16	-0.4(4)
N4	N3	C28	C29	-55.8(2)	C21	C16	C17	C18	1.1(4)
N4	N3	C28	C33	69.6(2)	C22	C1	C16	C17	8.4(3)
C1	N1	C2	O1	0.8(3)	C22	C1	C16	C21	-174.38(19)
C1	N1	C2	C3	-175.08(19)	C22	C23	C24	C25	-0.1(4)
C1	C16	C17	C18	178.3(2)	C23	C22	C27	C26	0.7(3)
C1	C16	C21	C20	-178.1(2)	C23	C24	C25	C26	1.2(4)
C1	C22	C23	C24	178.6(2)	C24	C25	C26	C27	-1.4(4)
C1	C22	C27	C26	-178.8(2)	C25	C26	C27	C22	0.5(4)
C2	N1	C1	C16	150.5(2)	C27	C22	C23	C24	-0.9(3)
C2	N1	C1	C22	-81.4(2)	C28	N3	N4	C8	90.5(2)
C2	C3	C4	C5	-153.92(17)	C28	N3	C7	O2	-2.8(3)
C3	N2	C6	C5	15.8(2)	C28	N3	C7	N2	176.25(19)
C3	N2	C7	O2	-2.1(3)	C28	C29	C30	C31	1.1(4)

C3	N2	C7	N3	178.83(17)	C29	C28	C33	C32	-2.6(3)
C3	C4	C5	C6	41.0(2)	C29	C30	C31	C32	-2.9(4)
C4	C5	C6	N2	-34.9(2)	C30	C31	C32	C33	1.9(4)
C6	N2	C3	C2	130.28(18)	C31	C32	C33	C28	0.8(4)
C6	N2	C3	C4	9.6(2)	C33	C28	C29	C30	1.7(3)
C6	N2	C7	O2	144.7(2)	O41	C42	O42A	C43A	5.9(12)
C6	N2	C7	N3	-34.4(3)	O41	C42	O42B	C43B	4.2(13)
C7	N2	C3	C2	-79.0(2)	C41	C42	O42A	C43A	177.7(7)
C7	N2	C3	C4	160.35(17)	C41	C42	O42B	C43B	-167.6(8)
C7	N2	C6	C5	-132.4(2)	C42	O42A	C43A	C44A	87.3(11)
C7	N3	N4	C8	-61.0(3)	C42	O42B	C43B	C44B	-178.8(9)
C7	N3	C28	C29	95.9(2)	O42A	C42	O42B	C43B	117(5)
C7	N3	C28	C33	-138.74(19)	O42B	C42	O42A	C43A	-72(4)
C8	O4	C9	C10	-79.5(3)					

Table 16 Hydrogen Atom Coordinates (Å×10^4) and Isotropic Displacement Parameters (Å^2×10^3) for lube78.

Atom	*x*	*Y*	*z*	U(eq)
H1	10060(40)	7360(20)	6767(11)	49(8)
H4	8580(40)	4870(20)	7347(10)	46(8)
H1A	11493	8714	6370	41
H3	9762	8052	7865	37
H4A	13125	7504	7578	46
H4B	12629	8072	8034	46
H5A	11481	6870	8422	48

H5B	13160	6466	8176	48
H6A	11597	5881	7562	42
H6B	10235	5775	7985	42
H9A	10760	4439	6000	61
H9B	10378	5457	6026	61
H11	8886	5721	5324	71
H12	6612	5484	4808	83
H13	4592	4433	4974	75
H14	4915	3575	5638	87
H15	7273	3748	6134	80
H17	9630	7956	5421	52
H18	10744	6997	4867	65
H19	13007	6093	5057	63
H20	14239	6174	5805	64
H21	13120	7124	6367	56
H23	10140	9912	6063	50
H24	7699	10671	5832	59
H25	5064	9978	5807	60
H26	4847	8521	6043	57
H27	7288	7761	6269	49
H28	5008	6304	7634	44
H29	5103	6258	6775	54
H30	3590	5161	6491	60
H31A	2216	4315	7110	60
H31B	3883	3823	6923	60
H32	3980	3869	7768	49

H33	5561	4944	8055	45
H41A	1341	2902	4828	108
H41B	960	3745	5139	108
H41C	-591	3190	4928	108
H43A	1063	2294	6346	77
H43B	2859	2774	6414	77
H44A	2488	1188	5934	95
H44B	3106	1268	6468	95
H44C	4264	1653	6054	95
H43C	1971	1333	5920	77
H43D	1300	2014	6305	77
H44D	4756	1751	6038	95
H44E	3961	1576	6548	95
H44F	4174	2548	6360	95

Table 17 Atomic Occupancy for lube78.

Atom	***Occupancy***	**Atom**	***Occupancy***	**Atom**	***Occupancy***
O42A	0.527(5)	C43A	0.527(5)	H43A	0.527(5)
H43B	0.527(5)	C44A	0.527(5)	H44A	0.527(5)
H44B	0.527(5)	H44C	0.527(5)	O42B	0.473(5)
C43B	0.473(5)	H43C	0.473(5)	H43D	0.473(5)
C44B	0.473(5)	H44D	0.473(5)	H44E	0.473(5)
H44F	0.473(5)				

Experimental

Single crystals of $C_{37}H_{42}N_4O_6$ lube78 (2.**29a**) were grown in ethyl acetate-hexane mixture. A suitable crystal was selected and mounted on the diffractometer. The crystal was kept at 100 K during data collection. Using Olex2,[5] the structure was solved with the XT[7] structure solution program using Direct Methods and refined with the XL[7] refinement package using Least Squares minimisation.

Crystal structure determination of [lube78]

Crystal Data for $C_{37}H_{42}N_4O_6$ (M =638.74 g/mol): orthorhombic, space group $P2_12_12_1$ (no. 19), a = 7.8202(5) Å, b = 15.4330(9) Å, c = 28.4386(17) Å, V = 3432.2(4) Å^3, Z = 4, T = 100 K, μ(GaKα) = 0.439 mm^{-1}, *Dcalc* = 1.236 g/cm^3, 49840 reflections measured (5.408° ≤ 2Θ ≤ 121.586°), 7899 unique (R_{int} = 0.0541, R_{sigma} = 0.0347) which were used in all calculations. The final R_1 was 0.0437 (I > 2σ(I)) and wR_2 was 0.1248 (all data).

Refinement model description

Number of restraints - 4, number of constraints - unknown.
Details:

```
1. Fixed Uiso

 At 1.2 times of:

  All C(H) groups, All C(H,H) groups

 At 1.5 times of:

  All C(H,H,H) groups

2. Restrained distances

 C42-O42A ≈ C42-O42B

 with sigma of 0.02

 O42A-C43A ≈ O42B-C43B

 with sigma of 0.02

 C43A-C44A ≈ C43B-C44B

 with sigma of 0.02

3. Uiso/Uaniso restraints and constraints

Uanis(O42A) = Uanis(O42B)

Uanis(C43A) = Uanis(C43B)

Uanis(C44A) = Uanis(C44B)

4. Same fragment restrains

{O42A, C43A, C44A}

as

{O42B, C43B, C44B}

5. Others

 Sof(O42B)=Sof(C43B)=Sof(H43C)=Sof(H43D)=Sof(C44B)=Sof(H44D)=Sof(H44E)=

 Sof(H44F)=1-FVAR(1)
```

```
 Sof(O42A)=Sof(C43A)=Sof(H43A)=Sof(H43B)=Sof(C44A)=Sof(H44A)=Sof(H44B)=

 Sof(H44C)=FVAR(1)

6.a Ternary CH refined with riding coordinates:

 C1(H1A), C3(H3), C28(H28)

6.b Secondary CH2 refined with riding coordinates:

 C4(H4A,H4B), C5(H5A,H5B), C6(H6A,H6B), C9(H9A,H9B), C31(H31A,H31B), C43A(H43A,

 H43B), C43B(H43C,H43D)
+
6.c Aromatic/amide H refined with riding coordinates:

 C11(H11), C12(H12), C13(H13), C14(H14), C15(H15), C17(H17), C18(H18),

 C19(H19), C20(H20), C21(H21), C23(H23), C24(H24), C25(H25), C26(H26), C27(H27),

  C29(H29), C30(H30), C32(H32), C33(H33)

6.d Idealised Me refined as rotating group:

 C41(H41A,H41B,H41C), C44A(H44A,H44B,H44C), C44B(H44D,H44E,H44F)
```

This report has been created with Olex2, compiled on 2014.08.28 svn.r2986 for OlexSys. Please let us know if there are any errors or if you would like to have additional features.

Université de Montréal

CRYSTAL AND MOLECULAR STRUCTURE OF

$C_{34}H_{34}N_4O_4$ (COMPOUND 2.35a)

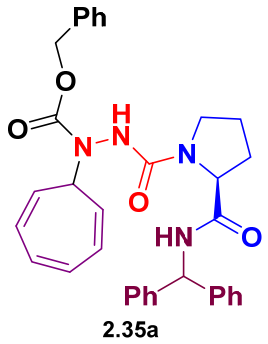

2.35a

Lubell group

Département de chimie, Université de Montréal,

C.P. 6128, Succ. Centre-Ville, Montréal, Québec, H3C 3J7 (Canada)

Structure solved and refined in the laboratory of X-ray diffraction Université de Montréal by Francine Bélanger.

Compound 2.35a (lube89)

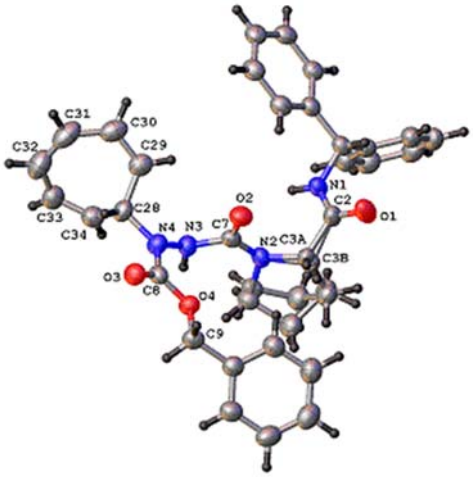

Table 18 Crystal data and structure refinement for lube89.

Identification code	lube89
Empirical formula	$C_{34}H_{34}N_4O_4$
Formula weight	562.65
Temperature/K	110
Crystal system	monoclinic
Space group	$P2_1$
a/Å	10.2983(4)
b/Å	10.6899(5)
c/Å	13.1072(6)
α/°	90
β/°	94.794(3)
γ/°	90
Volume/Å^3	1437.90(11)
Z	2
ρ_{calc}g/cm^3	1.300

μ/mm^{-1}	0.446
F(000)	596.0
Crystal size/mm^3	0.08 × 0.06 × 0.02
Radiation	GaKα (λ = 1.34139)
2Θ range for data collection/°	5.886 to 109.898
Index ranges	$-12 \leq h \leq 12$, $-13 \leq k \leq 13$, $-15 \leq l \leq 15$
Reflections collected	61549
Independent reflections	5472 [R_{int} = 0.0637, R_{sigma} = 0.0351]
Data/restraints/parameters	5472/7/400
Goodness-of-fit on F^2	1.030
Final R indexes [I>=2σ (I)]	R_1 = 0.0371, wR_2 = 0.0778
Final R indexes [all data]	R_1 = 0.0576, wR_2 = 0.0846
Largest diff. peak/hole / e $Å^{-3}$	0.13/-0.12
Flack parameter	0.06(10)

Table 19 Fractional Atomic Coordinates (×10^4) and Equivalent Isotropic Displacement Parameters (Å^2×10^3) for lube89. U_{eq} is defined as 1/3 of the trace of the orthogonalised U_{IJ} tensor.

Atom	*x*	*Y*	*z*	U(eq)
O1	1714.0(19)	6808(2)	1676.3(17)	66.3(6)
O2	3909.1(18)	7037(2)	4224.1(15)	52.3(5)
O3	7173.4(17)	8140(2)	5906.9(14)	49.9(5)
O4	6978.5(16)	7287.4(17)	4325.2(13)	44.0(5)
N1	1778(2)	5127(2)	2726.7(18)	44.3(6)
N2	4487.7(19)	5501(2)	3164.3(16)	42.4(5)

N3	5419(2)	5583(2)	4823.5(17)	43.1(5)
N4	5939(2)	6410(2)	5569.7(16)	44.6(6)
C1	356(2)	4952(3)	2674(2)	44.2(7)
C2	2325(3)	6037(3)	2215(2)	47.1(7)
C3A	3786(13)	6137(13)	2310(8)	43.8(15)
C4A	4339(5)	5503(5)	1376(4)	51.2(13)
C5A	4792(5)	4244(5)	1791(3)	59.2(12)
C6A	5329(6)	4517(9)	2880(5)	45.8(15)
C3B	3840(40)	5950(40)	2120(30)	43.8(15)
C4B	4193(15)	4928(16)	1372(14)	51.2(13)
C5B	5632(12)	4715(14)	1691(8)	59.2(12)
C6B	5690(20)	4670(30)	2843(15)	45.8(15)
C7	4558(2)	6112(3)	4060(2)	41.0(6)
C8	6740(2)	7354(3)	5313(2)	41.1(6)
C9	7823(3)	8256(3)	3979(2)	47.6(7)
C10	7828(3)	8152(3)	2838(2)	45.4(6)
C11	8972(3)	8122(3)	2372(2)	53.7(7)
C12	8966(3)	8084(4)	1314(3)	64.3(9)
C13	7817(3)	8082(3)	710(2)	62.9(8)
C14	6651(3)	8124(4)	1173(2)	62.8(8)
C15	6659(3)	8160(3)	2221(2)	56.1(7)
C16	-67(2)	3842(3)	2006(2)	46.4(7)
C17	-1060(3)	3989(3)	1222(2)	54.0(8)
C18	-1456(3)	2970(4)	614(2)	59.6(8)
C19	-894(3)	1827(4)	770(2)	61.0(9)
C20	90(3)	1668(3)	1542(2)	59.8(8)

C21	497(3)	2682(3)	2153(2)	52.5(8)
C22	-104(2)	4925(3)	3748(2)	42.5(6)
C23	-1088(2)	4123(3)	4010(2)	44.4(7)
C24	-1517(3)	4146(3)	4985(2)	48.2(7)
C25	-979(3)	4981(3)	5705(2)	51.0(7)
C26	-7(3)	5791(3)	5453(2)	51.7(7)
C27	423(3)	5754(3)	4481(2)	49.1(7)
C28	5658(3)	6181(3)	6623(2)	48.3(7)
C29	4236(3)	6203(3)	6776(2)	55.1(8)
C30	3836(3)	6258(3)	7720(3)	63.3(9)
C31	4709(4)	6213(4)	8645(3)	74.2(10)
C32	5841(4)	5581(4)	8793(3)	74.2(10)
C33	6377(3)	4790(3)	8047(2)	61.4(9)
C34	6216(3)	4979(3)	7033(2)	54.8(8)

Table 20 Anisotropic Displacement Parameters ($Å^2×10^3$) for lube89. The Anisotropic displacement factor exponent takes the form: $-2\pi^2[h^2a^{*2}U_{11}+2hka^*b^*U_{12}+\ldots]$.

Atom	U_{11}	U_{22}	U_{33}	U_{23}	U_{13}	U_{12}
O1	45.6(11)	82.8(16)	69.1(14)	32.6(13)	-4(1)	-5.7(11)
O2	45.6(11)	57.1(13)	55.2(12)	3.8(10)	10.2(9)	7.2(10)
O3	49.5(11)	54.8(12)	45.2(11)	-8.1(10)	2.9(9)	-4.6(10)
O4	42.4(10)	49.0(11)	41.2(11)	-1.3(9)	7.1(8)	-4.1(9)
N1	33.5(11)	54.1(15)	44.7(13)	8.5(12)	-0.5(10)	-2.2(11)
N2	35.0(11)	49.9(14)	41.3(13)	0.4(11)	-2.8(9)	-3.4(11)
N3	43.0(13)	46.4(13)	39.2(13)	-1.7(11)	-0.1(10)	0.2(12)
N4	47.2(12)	49.0(15)	37.5(13)	-3.9(11)	3.9(10)	-3.8(11)

C1	32.7(13)	50.6(17)	48.7(16)	5.4(14)	-0.8(11)	0.0(13)
C2	42.6(15)	59(2)	39.1(15)	11.3(15)	-2.4(12)	-3.0(15)
C3A	37.3(19)	62(4)	32(5)	6(3)	3(3)	-4(2)
C4A	52(2)	63(4)	39.2(18)	0(3)	4.7(16)	-7(3)
C5A	58(3)	71(3)	48(2)	-8(2)	2(2)	1(2)
C6A	37(4)	50(3)	51.4(18)	-3.0(17)	4(2)	-1(3)
C3B	37.3(19)	62(4)	32(5)	6(3)	3(3)	-4(2)
C4B	52(2)	63(4)	39.2(18)	0(3)	4.7(16)	-7(3)
C5B	58(3)	71(3)	48(2)	-8(2)	2(2)	1(2)
C6B	37(4)	50(3)	51.4(18)	-3.0(17)	4(2)	-1(3)
C7	31.2(13)	48.4(17)	43.6(16)	4.6(14)	4.8(11)	-4.5(13)
C8	33.7(13)	48.9(17)	40.3(16)	-6.6(14)	0.6(12)	1.3(13)
C9	42.3(15)	50.5(17)	50.5(17)	3.4(14)	7.3(12)	-8.4(14)
C10	44.8(15)	43.7(15)	48.1(16)	2.8(14)	5.6(12)	-0.4(13)
C11	45.7(16)	61.0(19)	55.0(19)	4.4(16)	8.0(13)	4.8(15)
C12	62(2)	73(2)	60(2)	9.1(19)	22.1(16)	12.6(18)
C13	81(2)	60(2)	48.4(18)	6.5(17)	8.2(17)	10(2)
C14	63.4(19)	70(2)	53(2)	3.1(18)	-2.8(15)	1.4(18)
C15	45.4(16)	66(2)	56.5(19)	1.2(17)	2.4(13)	-2.1(16)
C16	36.8(14)	61(2)	41.9(16)	4.4(14)	5.2(12)	-8.8(14)
C17	42.8(16)	74(2)	45.1(17)	3.8(16)	1.0(14)	-1.6(16)
C18	49.4(17)	85(3)	43.4(18)	0.1(18)	-2.4(14)	-11.3(19)
C19	60.8(19)	78(3)	44.7(18)	-7.6(17)	7.0(15)	-18.4(19)
C20	63.1(19)	63(2)	54.1(19)	-1.3(17)	8.2(16)	-7.7(17)
C21	47.4(17)	63(2)	45.9(17)	1.5(15)	0.1(13)	-5.9(15)
C22	33.7(13)	47.2(17)	46.1(16)	4.6(14)	-0.3(11)	3.5(13)

C23	36.0(13)	48.7(17)	48.3(17)	1.0(14)	2.1(12)	4.0(13)
C24	37.6(14)	48.8(18)	59.0(19)	4.2(15)	9.0(13)	6.0(14)
C25	42.4(15)	61.3(19)	49.8(17)	-1.8(16)	6.6(13)	11.1(15)
C26	43.7(15)	56.4(19)	54.8(18)	-8.7(15)	3.2(13)	1.1(14)
C27	41.1(14)	51.3(18)	54.9(18)	1.8(15)	3.7(13)	-1.0(14)
C28	53.4(16)	56.0(18)	35.6(15)	-1.6(14)	3.3(12)	-4.4(15)
C29	58.8(17)	53.8(19)	53.5(19)	1.0(15)	9.9(14)	-1.5(16)
C30	72(2)	59(2)	62(2)	2.6(17)	24.9(18)	2.0(18)
C31	109(3)	66(2)	51(2)	-1.2(18)	26(2)	6(2)
C32	99(3)	76(2)	47(2)	1.0(19)	3.2(18)	-5(2)
C33	60.4(19)	72(2)	52(2)	10.5(17)	2.1(15)	-2.9(17)
C34	47.8(16)	64(2)	53.4(19)	2.7(17)	7.9(13)	2.0(15)

Table 21 Bond Lengths for lube89.

Atom	Atom	Length/Å	Atom	Atom	Length/Å
O1	C2	1.225(3)	C9	C10	1.500(4)
O2	C7	1.222(3)	C10	C11	1.372(4)
O3	C8	1.206(3)	C10	C15	1.393(4)
O4	C8	1.339(3)	C11	C12	1.386(4)
O4	C9	1.449(3)	C12	C13	1.368(5)
N1	C1	1.472(3)	C13	C14	1.390(4)
N1	C2	1.332(4)	C14	C15	1.373(4)
N2	C3A	1.450(12)	C16	C17	1.396(4)
N2	C6A	1.432(10)	C16	C21	1.376(4)
N2	C3B	1.55(4)	C17	C18	1.391(5)
N2	C6B	1.61(3)	C18	C19	1.360(5)

N2	C7	1.340(3)	C19	C20	1.382(4)
N3	N4	1.392(3)	C20	C21	1.391(4)
N3	C7	1.400(3)	C22	C23	1.392(4)
N4	C8	1.363(4)	C22	C27	1.383(4)
N4	C28	1.454(3)	C23	C24	1.387(4)
C1	C16	1.517(4)	C24	C25	1.382(4)
C1	C22	1.523(4)	C25	C26	1.384(4)
C2	C3A	1.503(14)	C26	C27	1.384(4)
C2	C3B	1.58(4)	C28	C29	1.495(4)
C3A	C4A	1.550(8)	C28	C34	1.490(4)
C4A	C5A	1.511(7)	C29	C30	1.338(4)
C5A	C6A	1.516(7)	C30	C31	1.447(5)
C3B	C4B	1.53(2)	C31	C32	1.348(5)
C4B	C5B	1.522(17)	C32	C33	1.438(5)
C5B	C6B	1.507(19)	C33	C34	1.341(4)

Table 22 Bond Angles for lube89.

Atom	Atom	Atom	Angle/°	Atom	Atom	Atom	Angle/°
C8	O4	C9	115.3(2)	O3	C8	N4	123.7(2)
C2	N1	C1	122.0(2)	O4	C8	N4	111.3(2)
C6A	N2	C3A	114.6(4)	O4	C9	C10	108.1(2)
C3B	N2	C6B	102.8(11)	C11	C10	C9	121.4(2)
C7	N2	C3A	115.8(4)	C11	C10	C15	118.2(3)
C7	N2	C6A	126.6(3)	C15	C10	C9	120.3(2)
C7	N2	C3B	127.7(9)	C10	C11	C12	121.0(3)
C7	N2	C6B	120.8(8)	C13	C12	C11	120.6(3)

N4	N3	C7	115.4(2)	C12	C13	C14	119.0(3)
N3	N4	C28	117.7(2)	C15	C14	C13	120.2(3)
C8	N4	N3	120.1(2)	C14	C15	C10	120.9(3)
C8	N4	C28	122.1(2)	C17	C16	C1	119.6(3)
N1	C1	C16	111.3(2)	C21	C16	C1	121.7(2)
N1	C1	C22	110.1(2)	C21	C16	C17	118.6(3)
C16	C1	C22	115.0(2)	C18	C17	C16	119.7(3)
O1	C2	N1	124.3(2)	C19	C18	C17	121.1(3)
O1	C2	C3A	117.5(6)	C18	C19	C20	119.8(3)
O1	C2	C3B	117.0(16)	C19	C20	C21	119.5(3)
N1	C2	C3A	118.2(6)	C16	C21	C20	121.2(3)
N1	C2	C3B	117.6(16)	C23	C22	C1	121.9(2)
N2	C3A	C2	117.5(10)	C27	C22	C1	119.7(2)
N2	C3A	C4A	102.3(6)	C27	C22	C23	118.4(2)
C2	C3A	C4A	109.5(8)	C24	C23	C22	120.7(3)
C5A	C4A	C3A	103.2(6)	C25	C24	C23	120.0(3)
C4A	C5A	C6A	104.2(5)	C24	C25	C26	119.8(3)
N2	C6A	C5A	101.9(5)	C25	C26	C27	119.7(3)
N2	C3B	C2	107(2)	C22	C27	C26	121.3(3)
C4B	C3B	N2	104(2)	N4	C28	C29	113.5(2)
C4B	C3B	C2	112(3)	N4	C28	C34	112.7(2)
C5B	C4B	C3B	102.0(17)	C34	C28	C29	108.5(2)
C6B	C5B	C4B	103.6(13)	C30	C29	C28	120.3(3)
C5B	C6B	N2	106.3(15)	C29	C30	C31	123.8(3)
O2	C7	N2	123.9(2)	C32	C31	C30	127.4(3)
O2	C7	N3	121.6(3)	C31	C32	C33	124.9(3)

N2	C7	N3	114.4(2)	C34	C33	C32	124.3(3)
O3	C8	O4	125.0(3)	C33	C34	C28	119.9(3)

Table 23 Hydrogen Bonds for lube89.

D	H	A	d(D-H)/Å	d(H-A)/Å	d(D-A)/Å	D-H-A/°
N1	H1	O3[1]	0.88(3)	2.08(3)	2.926(3)	161(2)

[1]1-X,-1/2+Y,1-Z

Table 24 Torsion Angles for lube89.

A	B	C	D	Angle/°	A	B	C	D	Angle/°
O1	C2	C3A	N2	161.5(5)	C6B	N2	C3B	C4B	27(3)
O1	C2	C3A	C4A	-82.4(9)	C6B	N2	C7	O2	155.9(11)
O1	C2	C3B	N2	151.3(14)	C6B	N2	C7	N3	-25.9(11)
O1	C2	C3B	C4B	-96(3)	C7	N2	C3A	C2	-81.9(8)
O4	C9	C10	C11	-129.9(3)	C7	N2	C3A	C4A	158.2(5)
O4	C9	C10	C15	54.0(4)	C7	N2	C6A	C5A	-178.4(3)
N1	C1	C16	C17	-128.6(3)	C7	N2	C3B	C2	-67(3)
N1	C1	C16	C21	51.8(3)	C7	N2	C3B	C4B	174.4(12)
N1	C1	C22	C23	-141.9(3)	C7	N2	C6B	C5B	-150.1(11)
N1	C1	C22	C27	41.1(3)	C7	N3	N4	C8	-65.0(3)
N1	C2	C3A	N2	-17.8(8)	C7	N3	N4	C28	118.6(2)
N1	C2	C3A	C4A	98.3(8)	C8	O4	C9	C10	-171.9(2)
N1	C2	C3B	N2	-41(2)	C8	N4	C28	C29	123.6(3)
N1	C2	C3B	C4B	73(3)	C8	N4	C28	C34	-112.5(3)

N2	C3A	C4A	C5A	24.9(10)	C9	O4	C8	O3	-0.2(4)
N2	C3B	C4B	C5B	-45(3)	C9	O4	C8	N4	179.9(2)
N3	N4	C8	O3	176.2(2)	C9	C10	C11	C12	-177.0(3)
N3	N4	C8	O4	-3.9(3)	C9	C10	C15	C14	176.9(3)
N3	N4	C28	C29	-60.1(3)	C10	C11	C12	C13	0.3(6)
N3	N4	C28	C34	63.8(3)	C11	C10	C15	C14	0.7(5)
N4	N3	C7	O2	-28.1(3)	C11	C12	C13	C14	0.3(5)
N4	N3	C7	N2	153.7(2)	C12	C13	C14	C15	-0.4(6)
N4	C28	C29	C30	-166.6(3)	C13	C14	C15	C10	-0.1(6)
N4	C28	C34	C33	160.9(3)	C15	C10	C11	C12	-0.8(5)
C1	N1	C2	O1	1.1(4)	C16	C1	C22	C23	-15.2(4)
C1	N1	C2	C3A	-179.6(4)	C16	C1	C22	C27	167.8(2)
C1	N1	C2	C3B	-166.1(12)	C16	C17	C18	C19	0.2(4)
C1	C16	C17	C18	-179.5(2)	C17	C16	C21	C20	-0.3(4)
C1	C16	C21	C20	179.3(3)	C17	C18	C19	C20	-0.2(4)
C1	C22	C23	C24	-177.9(2)	C18	C19	C20	C21	0.0(4)
C1	C22	C27	C26	177.4(2)	C19	C20	C21	C16	0.3(4)
C2	N1	C1	C16	104.7(3)	C21	C16	C17	C18	0.1(4)
C2	N1	C1	C22	-126.6(3)	C22	C1	C16	C17	105.3(3)
C2	C3A	C4A	C5A	-100.5(8)	C22	C1	C16	C21	-74.2(3)
C2	C3B	C4B	C5B	-160(2)	C22	C23	C24	C25	0.9(4)
C3A	N2	C6A	C5A	-18.9(9)	C23	C22	C27	C26	0.2(4)
C3A	N2	C7	O2	12.1(8)	C23	C24	C25	C26	-0.3(4)
C3A	N2	C7	N3	-169.7(7)	C24	C25	C26	C27	-0.2(4)
C3A	C4A	C5A	C6A	-36.8(7)	C25	C26	C27	C22	0.3(4)

C4A	C5A	C6A	N2	34.0(5)	C27	C22	C23	C24	-0.8(4)
C6A	N2	C3A	C2	116.2(5)	C28	N4	C8	O3	-7.6(4)
C6A	N2	C3A	C4A	-3.7(12)	C28	N4	C8	O4	172.4(2)
C6A	N2	C7	O2	171.5(4)	C28	C29	C30	C31	-4.4(5)
C6A	N2	C7	N3	-10.3(5)	C29	C28	C34	C33	-72.4(3)
C3B	N2	C6B	C5B	0(3)	C29	C30	C31	C32	-32.9(6)
C3B	N2	C7	O2	14(2)	C30	C31	C32	C33	-2.0(6)
C3B	N2	C7	N3	-168(2)	C31	C32	C33	C34	31.8(6)
C3B	C4B	C5B	C6B	45(2)	C32	C33	C34	C28	11.4(5)
C4B	C5B	C6B	N2	-27(2)	C34	C28	C29	C30	67.2(4)
C6B	N2	C3B	C2	146.3(17)					

Table 25 Hydrogen Atom Coordinates (Å×10^4) and Isotropic Displacement Parameters (Å^2×10^3) for lube89.

Atom	*x*	*Y*	*z*	U(eq)
H1	2250(30)	4650(30)	3160(20)	45(8)
H3	5970(30)	5000(30)	4600(20)	53(9)
H1A	-42	5711	2329	53
H3A	4037	7041	2325	53
H4AA	3656	5408	802	61
H4AB	5073	5990	1137	61
H5AA	5476	3893	1386	71
H5AB	4057	3646	1779	71
H6AA	5267	3775	3326	55
H6AB	6247	4798	2908	55
H3B	4203	6782	1922	53

H4BA	3677	4160	1459	61
H4BB	4058	5213	653	61
H5BA	5936	3916	1411	71
H5BB	6170	5407	1455	71
H6BA	6524	5023	3145	55
H6BB	5609	3801	3084	55
H9A	8718	8149	4307	57
H9B	7500	9091	4167	57
H11	9779	8128	2779	64
H12	9769	8059	1006	77
H13	7816	8052	-14	75
H14	5846	8129	762	75
H15	5857	8191	2529	67
H17	-1463	4781	1106	65
H18	-2131	3075	80	72
H19	-1178	1140	349	73
H20	487	872	1655	72
H21	1177	2571	2682	63
H23	-1470	3554	3515	53
H24	-2181	3586	5158	58
H25	-1275	5000	6372	61
H26	363	6369	5945	62
H27	1093	6309	4313	59
H28	6078	6869	7050	58
H29	3612	6178	6200	66
H30	2928	6331	7788	76

H31	4454	6681	9211	89
H32	6322	5665	9441	89
H33	6878	4088	8288	74
H34	6458	4346	6576	66

Table 26 Atomic Occupancy for lube89.

Atom	*Occupancy*	Atom	*Occupancy*	Atom	*Occupancy*
C3A	0.729(5)	H3A	0.729(5)	C4A	0.729(5)
H4AA	0.729(5)	H4AB	0.729(5)	C5A	0.729(5)
H5AA	0.729(5)	H5AB	0.729(5)	C6A	0.729(5)
H6AA	0.729(5)	H6AB	0.729(5)	C3B	0.271(5)
H3B	0.271(5)	C4B	0.271(5)	H4BA	0.271(5)
H4BB	0.271(5)	C5B	0.271(5)	H5BA	0.271(5)
H5BB	0.271(5)	C6B	0.271(5)	H6BA	0.271(5)
H6BB	0.271(5)				

Experimental

Single crystals of $C_{34}H_{34}N_4O_4$ lube89 (2.**34a**) were grown in ethyl acetate-hexane mixture. A suitable crystal was selected and mounted on the diffractometer. The crystal was kept at 110 K during data collection. Using Olex2,[5] the structure was solved with the ShelXT[7] structure solution program using Direct Methods and refined with the XL[7] refinement package using Least Squares minimisation.

Crystal structure determination of [lube89]

Crystal Data for $C_{34}H_{34}N_4O_4$ (M =562.65 g/mol): monoclinic, space group $P2_1$ (no. 4), a = 10.2983(4) Å, b = 10.6899(5) Å, c = 13.1072(6) Å, β = 94.794(3)°, V = 1437.90(11) Å^3, Z = 2, T = 110 K, μ(GaKα) = 0.446 mm^{-1}, *Dcalc* = 1.300 g/cm^3, 61549 reflections measured (5.886° ≤ 2Θ ≤ 109.898°), 5472 unique (R_{int} = 0.0637, R_{sigma} = 0.0351) which were used in all calculations. The final R_1 was 0.0371 (I > 2σ(I)) and wR_2 was 0.0846 (all data).

Refinement model description

Number of restraints - 7, number of constraints - unknown.

Details:

```
1. Fixed Uiso

 At 1.2 times of:

  All C(H) groups, All C(H,H) groups
```

```
2. Uiso/Uaniso restraints and constraints

Uanis(C3A) = Uanis(C3B)

Uanis(C4A) = Uanis(C4B)

Uanis(C5A) = Uanis(C5B)

Uanis(C6A) = Uanis(C6B)

3. Same fragment restrains

{C3A, C4A, C5A, C6A} sigma for 1-2: 0.02, 1-3: 0.04

as

{C3B, C4B, C5B, C6B}

4. Others

 Sof(C3B)=Sof(H3B)=Sof(C4B)=Sof(H4BA)=Sof(H4BB)=Sof(C5B)=Sof(H5BA)=Sof(H5BB)=

 Sof(C6B)=Sof(H6BA)=Sof(H6BB)=1-FVAR(1)

 Sof(C3A)=Sof(H3A)=Sof(C4A)=Sof(H4AA)=Sof(H4AB)=Sof(C5A)=Sof(H5AA)=Sof(H5AB)=

 Sof(C6A)=Sof(H6AA)=Sof(H6AB)=FVAR(1)

5.a Ternary CH refined with riding coordinates:

 C1(H1A), C3A(H3A), C3B(H3B), C28(H28)

5.b Secondary CH2 refined with riding coordinates:

 C4A(H4AA,H4AB), C5A(H5AA,H5AB), C6A(H6AA,H6AB), C4B(H4BA,H4BB), C5B(H5BA,

 H5BB), C6B(H6BA,H6BB), C9(H9A,H9B)

5.c Aromatic/amide H refined with riding coordinates:

 C11(H11), C12(H12), C13(H13), C14(H14), C15(H15), C17(H17), C18(H18),

 C19(H19), C20(H20), C21(H21), C23(H23), C24(H24), C25(H25), C26(H26), C27(H27),

  C29(H29), C30(H30), C31(H31), C32(H32), C33(H33), C34(H34)
```

References

(1) Still, W. C.; Kahn, M.; Mitra, A., Rapid chromatographic technique for preparative separations with moderate resolution. *J. Org. Chem.* **1978**, *43*, 2923-2925.

(2) Stebbins, J. F., Nuclear magnetic resonance at high temperature. *Chem. Rev.* **1991**, *91*, 1353-1373.

(3) Bourguet, C. B.; Sabatino, D.; Lubell, W. D., Benzophenone semicarbazone protection strategy for synthesis of aza-glycine containing aza-peptides. *Peptide Science* **2008**, *90*, 824-831.

(4) Jlalia, I.; Lensen, N.; Chaume, G.; Dzhambazova, E.; Astasidi, L.; Hadjiolova, R.; Bocheva, A.; Brigaud, T., Synthesis of an MIF-1 analogue containing enantiopure (S)-α-trifluoromethyl-proline and biological evaluation on nociception. *Eur. J. Med. Chem.* **2013**, *62*, 122-129.

(5) Dolomanov, O. V.; Bourhis, L. J.; Gildea, R. J.; Howard, J. A.; Puschmann, H., OLEX2: a complete structure solution, refinement and analysis program. *J. Appl. Cryst.* **2009**, *42*, 339-341.

(6) Sheldrick, G. M., SHELXT-Integrated space-group and crystal-structure determination. *Acta Cryst.* **2015**, *A71*, 3-8.

(7) Sheldrick, G. M., A short history of SHELX. *Acta Cryst.* **2007**, *64*, 112-122.

Annex 2: Experimental part of Chapter 3

The experimental procedures for Chapter 3 is reported in the **Article 2** section of **Chapter 3**, and characterization data of compounds related to articles were included in the **Annex 4:** NMR spectra section. (Chingle, R.; Ratni, S.; Claing, A.; Lubell, W. D. "Application of Constrained aza-Valine Analogs for Smac Mimicry" *Biopolymers (Pept. Sci.)* 2016, *106*, 235-244. DOI: 10.1002/bip.22851)

Annex 3: Experimental part of Chapter 4

1. Experimental Section

1.1 General experimental procedures.

Chemicals were used as received from commercial sources without further purification unless stated otherwise. Polystyrene Rink amide resin (0.5 mmol/g 75−100 mesh) was purchased from Advanced Chemtech™ (Louisville, Kentucky, USA), and the manufacturer's reported resin loading was used in the calculation of final product yields. Solvents were obtained from Fisher Scientific. Anhydrous dichloromethane (DCM), tetrahydrofuran (THF) and *N*,*N*-dimethyl formamide (DMF) were obtained by passage through a solvent filtration system (Glass-Contour, Irvine, CA). 9-*H*-Fluoren-9-ylmethyl carbazate was synthesized according to the literature method.[1] Triphosgene, 2,4,6-collidine, *N*-bromosuccinimide (NBS), 2,6-lutidine, *N*,*N*-diisopropylethylamine (DIEA), 1,3-butadiene, and 2,3-dimethylbutadiene, all were purchased from Aldrich® and used as received. Amino acids [e.g., Fmoc-Pro-OH, Fmoc-Phe-OH, Fmoc-Lys(Boc)-OH, Fmoc-D-Phe-OH, Fmoc-Trp(Boc)-OH, Fmoc-Ala-OH, Fmoc-D-Trp(Boc)-OH, Boc-His(Trt)-OH], and coupling reagents including diisopropylcarbodiimide (DIC), *N,N′*-disuccinimidyl carbonate (DSC), hydroxybenzotriazole (HOBt), 9-fluorenylmethyl *N*-succinimidyl carbonate (Fmoc-OSu) all were purchased from Chem Impex and CS Bio™. *N*-Fmoc-2′,6′-dimethyl-L-tyrosine (Dmt) was synthesized in house as described below from *N*-Boc-2′,6′-dimethyl-L-tyrosine, which was received from Santa Cruise Biotechnology. Nuclear magnetic resonance spectra (^{1}H, ^{13}C) were recorded on Bruker AV 500 spectrometer. ^{1}H NMR spectra were referenced to DMSO-d_6 (2.50 ppm) and ^{13}C NMR spectra were measured in DMSO-d_6 (39.52 ppm), as specified below. Coupling constants, *J* values were measured in Hertz (Hz) and chemical shift values in parts per million (ppm). Accurate mass measurements were performed on a LC-MSD instrument from Agilent technologies in positive electrospray ionisation (ESI) mode at the Université de Montréal Mass Spectrometry Facility. Sodium and proton adducts ($[M+Na]^+$ and $[M+H]^+$) were used for empirical formula confirmation. Unless stated otherwise, all coupling reactions were monitored by reverse

phase high performance liquid chromatography-mass spectrometry (RP-HPLC-MS) on a Sunfire™ C18 column (particle size: 3.5 micron, 2.1 x 50 mm).

RP-HPLC analyses of crude and purified peptides were performed either on a CSH C18 column (particle size: 5 micron, 4.6 x 100 mm) for the compounds **4.18**, or a Sunfire™ C18 column (particle size: 3.5 micron, 2.1 x 50 mm) for the compounds **419**-**423**, **4.27**-**4.28**, and **4.30**-**4.31**; or a or BEH C18 column (particle size: 1.7 micron for , 2.1 x 100mm) for the compound **4.29**, using UV detection at λ = 214 nm, a flow rate of 0.4 mL / min for the Sunfire™ column or 0.5 mL / min for the BEH and CSH C18 columns with an eluent containing solvent A [H_2O containing 0.1% formic acid (FA)] and solvent B (MeOH or ACN containing 0.1% FA). Final peptide analogs were purified using a Waters™ PrepLC instrument with either a reverse-phase Gemini® C18 column (Phenomenex® Inc., pore size: 110 Å, particle size: 5 µm, 250×21.2 mm) or a reverse-phase Sunfire™ C18 column (pore size: 110 Å, particle size: 5 µm; 150 × 19 mm) employing a specified linear gradient of 5-60% of MeOH containing 0.1% FA in water containing 0.1% FA, with a flow rate of 10.0 mL / min and monitored with a UV detector at 214 nm and 254 nm. Infrared spectra were recorded in the neat on a Perkin Elmer Spectrum One FTIR instrument and are reported in reciprocal centimetres (cm^{-1}).

Fmoc-based peptide synthesis. On an automated shaker using polystyrene Rink amide resin (0.50 mmol/g, 75-100 mesh), Fmoc-based peptide synthesis was performed under standard conditions.[2] Couplings of amino acids (3 equiv) were performed in DMF using DIC (3 equiv) and HOBt (3 equiv). Fmoc removal was performed by treating the resin twice with 20% piperidine in DMF for 30 min. After each coupling and deprotection step, the resin was washed using 15 sec agitations with DMF (3 times), MeOH (3 times) and DCM (3 times), sequentially.

General protocol for cleavage of aliquots of resin-bound peptide for analysis by LC-MS. An aliquot of peptide bound resin (3-5 mg) was treated with a freshly made solution of TFA/H_2O/TES (95:2.5:2.5, v/v/v, 0.5 mL) for 30 min at room temperature. The resin was

removed by filtration. The filtrate was collected in a 1.5 mL Eppendorf® tube. The filtrate volume was concentrated, and the crude peptide was precipitated with cold ether (1.5 mL). After agitation on a vortex shaker, the mixture was spun in a centrifuge. The supernatant was decanted leaving a pellet, which was dissolved in methanol (or H_2O, 1 mg/mL) and subjected to LC/MS analysis.

1.2. Representative synthesis of [azapipecolyl]-GHRP-6 analogs

Fmoc-azaGly-D-Phe-Lys(Boc)-NH-Rink resin 4.8d:

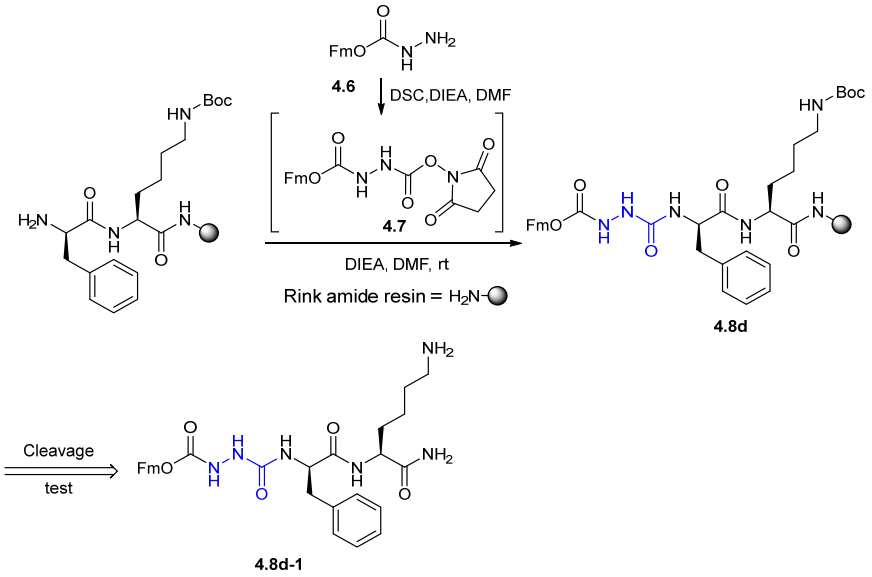

A solution of DSC (3 eq., 0.769 g, 3 mmol) in DMF (15 mL) was treated dropwise with a solution of 9-*H*-fluoren-9-ylmethyl carbazate **4.6** (3 eq., 0.763 g, 3 mmol) in 15 mL of DMF over 15 min at 0 °C, stirred for 1 h at rt, and transferred to a syringe tube, equipped with a Teflon™ filter, stopper and stopcock, containing Phe-Lys(Boc)-NH-Rink resin (1 eq., 2.15 g, 1 mmol) swollen in 12 mL of DMF. The resin mixture was treated with DIEA (6 eq., 0.775 g, 0.992 mL, 6 mmol), shaken on an automated shaker for 12 h and filtered. After filtration, the resin was washed sequentially with DMF (3 times), MeOH (3 times), and DCM (3 times), to afford aza-glycine resin **4.8d**; IR (neat) ν_{max}/cm^{-1} 2921, 1671, 1603, 1506, 1492,

1451, 1243, 1207, 1171. LC-MS analysis of a cleaved resin aliquot as described above indicated complete conversion and a peak with molecular ion coherent with Fmoc-azaGly-D-Phe-Lys-NH_2 (**4.8d-1)**: LCMS [10–90% MeOH (0.1% FA) in water (0.1% FA) over 10 min, followed by 10% MeOH (0.1% FA) in water (0.1% FA) for 4 min] R. T. = 6.44 min. ESI-MS m/z: calculated for $C_{31}H_{37}N_6O_5$ $[M+H]^+$ 573.27; found 573.5.

Fmoc-(Δ^4)azaPip-D-Phe-Lys(Boc)-NH-Rink resin 4.10d:

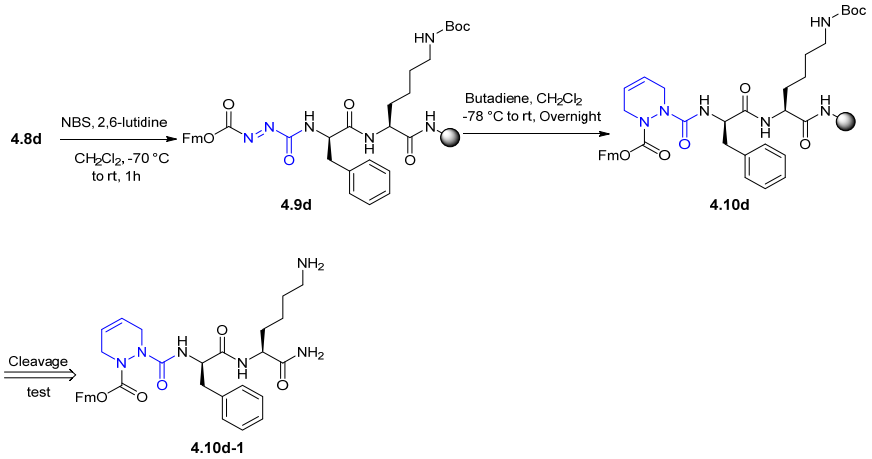

A sealed flask containing swollen Fmoc-azaGly-D-Phe-Lys-NH-Rink resin **4.8d** (1 eq., 2.43 g, 1 mmol) in dry DCM (24 ml) under argon was cooled to –78 °C, treated with 2,6-lutidine (0.321 g, 0.349 mL, 3 mmol), stirred for 1 min, and treated with a single portion of NBS (3 eq., 0.534 g, 3 mmol). The bath was removed. The reaction mixture was allowed to warm to room temperature with shaking on an automated shaker for 1 h and filtered. The filtered resin was washed successively using 15 sec agitations with DCM (3 times) and dried under vacuum to provide azopeptide resin **4.9d**: IR (neat) ν_{max}/cm^{-1} 2922, 1710, 1678, 1601, 1492, 1451, 1243, 1207, 1172. Fmoc-azoGly-Trp-D-Phe-Lys(Boc)-NH-Rink amide resin **4.9e** was synthesized using the above protocol: IR (neat) ν_{max}/cm^{-1} 2920, 1699, 1602, 1493, 1450, 1368, 1256, 1156, 1020.

Vacuum dried azopeptide resin **4.9d** (~2.5 g, 1 mmol) was suspended in anhydrous DCM (5 mL), placed in a sealed flask under argon, cooled to –78 °C and treated

dropwise via a cannula with a solution of 1,3-butadiene (1 M, 10 mL, 10 mmol) in dry DCM (5 mL). The reaction mixture was warmed to room temperature, shaken on an automated shaker overnight, and filtered. The resin was washed and filtered successively using 15 sec agitations with DCM (3 times) to afford resin **4.10d**. A cleaved resin aliquot was analyzed as described above by LC-MS, which indicated complete conversion. A peak was observed with molecular ion consistent with Fmoc-(Δ^4)azaPip-D-Phe-Lys-NH_2 (**4.10d-1**): LCMS [10–90% MeOH (0.1% FA) in water (0.1% FA) over 10 min, followed by 10% MeOH (0.1% FA) in water (0.1% FA) for 4 min] R. T. = 7.99 min. ESI-MS m/z: calculated for $C_{35}H_{41}N_6O_5$ $[M+H]^+$ 625.31; found 625.3.

Fmoc-(Δ^4)azaPip-D-Phe-Lys-NH_2 (**4.10d-1**) was cleaved from resin **4.10d**, (~0.5 g) using a freshly made solution of TFA/H_2O/TES (95:2.5:2.5, v/v/v, 20 mL/g of peptide resin) at room temperature for 2 h. The resin was filtered and rinsed with TFA. The filtrate and rinses were concentrated to an oil, from which a precipitate was obtained upon addition of cold ether (10-15 mL). After centrifugation, the supernatant was decanted, and the precipitated peptide was taken up in aqueous acetonitrile (10% v/v) and freeze-dried prior to analysis and purification. The crude sample was purified by preparative RP-HPLC on a reverse-phase Gemini® C18 column (Phenomenex® Inc., pore size: 110 Å, particle size: 5 μm, 250×21.2 mm) using a binary solvent system consisting of a gradient of 5%-60% MeOH (0.1% FA) in water (0.1% FA), with a flow rate of 10.0 mL/min, and UV detection at 214 nm. The desired fractions were combined and freeze-dried to white fluffy powder: azapeptide **4.10d-1** (15 mg, 12%). ^{1}H NMR (500 MHz, DMSO-d_6) δ 8.35 (s, 1H), 7.98 – 7.92 (m, 1H), 7.90 – 7.85 (m, 2H), 7.85 – 7.81 (m, 2H), 7.44 – 7.37 (m, 2H), 7.37 – 7.32 (m, 2H), 7.29 – 7.23 (m, 2H), 7.23 – 7.15 (m, 3H), 6.92 – 6.80 (m, 2H), 5.87 – 5.81 (m, 1H), 5.81 – 5.74 (m, 1H), 4.82 (s, 1H), 4.46 – 4.36 (m, 1H), 4.15 – 4.05 (m, 2H), 3.96 – 3.66 (m, 4H), 3.29 – 3.17 (m, 1H), 3.17 – 3.08 (m, 1H), 3.03 – 2.92 (m, 1H), 2.92 – 2.84 (m, 1H), 2.74 – 2.59 (m, 2H), 1.70 – 1.55 (m, 1H), 1.51 – 1.36 (m, 3H), 1.36 – 1.22 (m, 1H), 1.22 – 1.07 (m, 2H); ^{13}C NMR (125 MHz, DMSO-d_6) δ 172.9, 171.1, 161.3, 156.7, 139.1, 137.3, 137.1, 128.7, 128.3, 127.5,

126.7, 125.7, 125.2, 123.5, 120.7, 119.3, 61.9, 54.4, 52.0, 44.3, 40.1, 37.8, 37.0, 31.0, 30.3, 21.9, 21.3. HRMS m/z calcd for $C_{35}H_{41}N_6O_5$ $[M+H]^+$ 625.3133; found 625.3126.

Fmoc-Ala-(Δ^4)azaPip-D-Phe-Lys(Boc)-NH-Rink resin 4.24d:

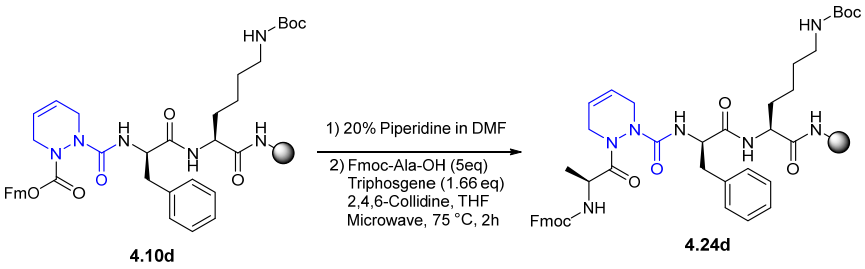

4.10d 4.24d

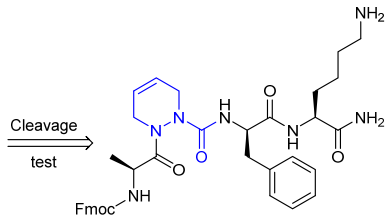

4.24d-1

Resin **4.10d** was treated with 20% piperidine in DMF to remove the Fmoc group using the protocol above. The resulting H-(Δ^4)azaPip-D-Phe-Lys(Boc)-NH-Rink resin (**4.12d**, ~387 mg, 0.171 mmol) was transferred into a microwave vial, and swollen in THF. A premixed 0 °C solution of Fmoc-Ala-OH (5 eq., 266 mg, 0.857 mmol) and triphosgene (1.66 eq., 84.4 mg, 0.284 mmol) in THF (8 mL) was treated dropwise with 2,4,6-collidine (23 eq., 477 mg, 0.525 mL, 3.94 mmol) over 1 min, and transferred into the microwave vial containing the swollen resin. The vial was sealed and irradiated (25W) at 75 °C for 2 h. After cooling, the resin was filtered and washed sequentially with DMF (3 times), MeOH (3 times), and DCM (3 times) to afford resin **4.24d**. A resin aliquot was cleaved as described above and analyzed by LC-MS which indicated complete conversion. A peak was observed with molecular ion consistent with Fmoc-Ala-(Δ^4)azaPip-D-Phe-Lys-NH_2 (**4.24d-1**): LCMS [10–90% MeOH (0.1% FA) in water (0.1% FA) over 10 min, followed by 10% MeOH (0.1% FA)

in water (0.1% FA) for 4 min] R. T. = 8.04 min. ESI-MS m/z: calculated for $C_{38}H_{46}N_7O_6$ $[M+H]^+$ 696.34; found 696.3.

His-D-Trp-Ala-(Δ^4)azaPip-D-Phe-Lys-NH_2 (4.27):

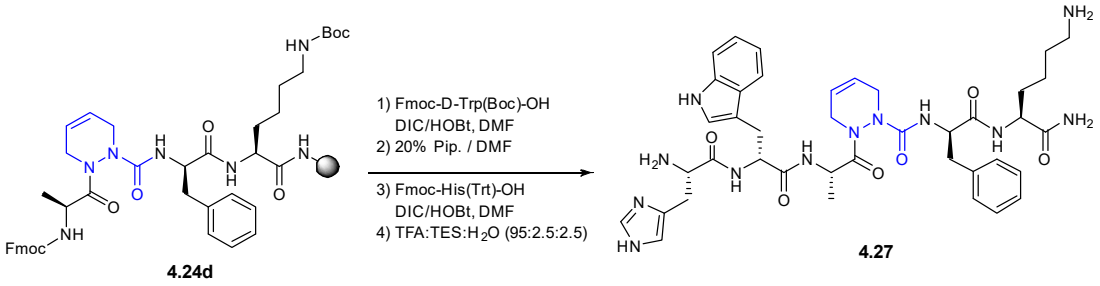

Aza-4,5-dehydropipecolate peptide **4.27** was synthesized from resin **4.24d** (~400 mg) by sequential Fmoc group removals, DIC/HOBt couplings of Fmoc-D-Trp(Boc), followed by Boc-His(Trt), and resin cleavage using the respective general protocols described above. A resin aliquot was cleaved as described above and analyzed by LC-MS which indicated complete conversion, and a peak with molecular ion consistent with His-D-Trp-Ala-(Δ^4)azaPip-D-Phe-Lys-NH_2 (**4.27**) of 44% purity: R. T. 4.58 min on a Sunfire™ column with a gradient of 5-50% MeOH (0.1% FA) in water (0.1% FA) over 9 min, followed by 5% MeOH (0.1% FA) in water (0.1% FA) for 5 min. ESI-MS m/z: calcd for $C_{40}H_{53}N_{12}O_6$ $[M+H]^+$ 797.41, found 797.4.

His-D-Trp-Ala-(Δ^4)azaPip-D-Phe-Lys-NH_2 (**4.27**) was cleaved from the resin using a freshly made solution of TFA/H_2O/TES (95:2.5:2.5, v/v/v, 20 mL/g of peptide resin) at room temperature for 2 h. The resin was filtered and rinsed with TFA. The filtrate and rinses were concentrated to an oil, from which a precipitate was obtained by addition of cold ether (10-15 mL). After centrifugation, the supernatant was decanted, and the precipitated peptide was taken up in aqueous acetonitrile (10% v/v) and freeze-dried prior to analysis and purification. The crude sample was purified by RP-HPLC on a reverse-phase Gemini® C18 column (Phenomenex® Inc., pore size: 110 Å, particle size: 5 µm, 250×21.2 mm) using a

binary solvent system consisting of a gradient of 5%-60% MeOH (0.1% FA) in water (0.1% FA), with a flow rate of 10.0 mL/min, and UV detection at 214 nm. The desired fractions were combined and freeze-dried to white fluffy powder: azapeptide **4.27** (5.8 mg, 4.2%). The purified product was analyzed to be of >99% purity by analytical RP-HPLC on a Sunfire™ column using gradient 1: 5-50% of MeOH (0.1% FA) in H_2O (0.1% FA) over 9 min, followed by 5% MeOH for 5 min, R.T. = 4.87 min; gradient 2: 5-50% of MeCN (0.1% FA) in H_2O (0.1% FA) over 9 min, followed by 5% MeCN for 5 min, R.T. = 3.92 min; HRMS m/z calcd for $C_{40}H_{53}N_{12}O_6$ $[M+H]^+$ 797.4206, found 797.4189.

His-D-Trp-Ala-azaPip-D-Phe-Lys-NH_2 (4.30):

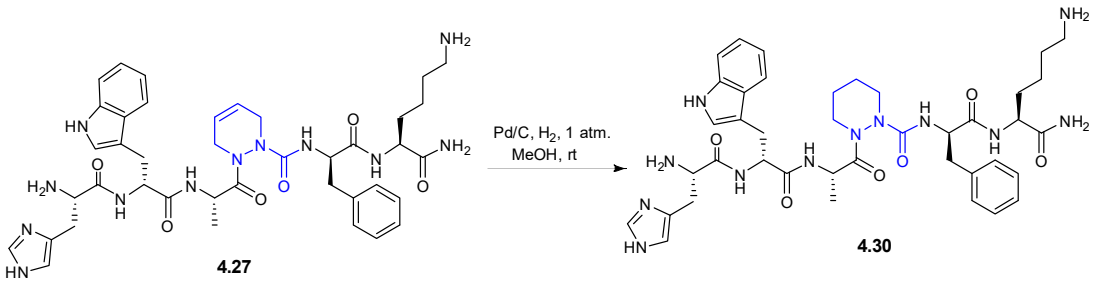

A solution of [aza-4,5-dehydropipecolyl[4]]-GHRP-6 (**4.27**, 1 eq., 2 mg, 0.00251 mmol) in methanol (0.2 mL) was treated carefully with 10 wt% palladium-on-carbon (1 eq., ~ 1 mg) under a stream of argon. The resulting suspension was placed under hydrogen atmosphere (1 atm), stirred under a balloon of hydrogen at room temperature for 1–2 h, and filtered on Celite™, which was washed with methanol. The filtrate and washings were combined and concentrated under vacuum. The residue was freeze-dried to furnish [azapipecolyl[4]]-GHRP-6 (**4.30**, 2 mg, 99 %) as off white solid: RP-HPLC on a Sunfire™ column revealed >99% purity using gradient 1: 5-50% of MeOH (0.1% FA) in H_2O (0.1% FA) over 9 min, followed by 5% MeOH over 5 min, R.T. = 5.15 min; gradient 2: 5-50% MeCN (0.1% FA) in H_2O (0.1% FA) over 9 min, followed by 5% MeCN over 5 min, R.T. = 3.97 min; HRMS m/z calcd for $C_{40}H_{55}N_{12}O_6$ $[M+H]^+$ 799.4362, found 799.4381.

_N_-Fmoc-2′,6′-dimethyl-L-tyrosine (Fmoc-Dmt-OH):

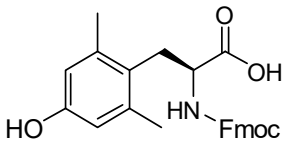

N-Boc-2′,6′-Dimethyl-L-tyrosine acid (0.22 g, 0.711 mmol) was dissolved in DCM (10 mL), stirred and treated with bubbles of dry HCl gas at rt for 3h. The volatiles were removed under vacuum to give hydrochloride salt (~0.15 g, 99%) as white solid. The hydrochloride salt (1 eq., ~0.15 g, 0.711 mmol) was dissolved in 10 mL of acetone/water (1:1 v/v), treated with sodium carbonate (1.1 eq., 0.0829 g, 0.783 mmol) and Fmoc-OSu (1 eq., 0.24 g, 0.711 mmol), and stirred for 12h. The volatiles were evaporated. Ethyl acetate was added to the mixture, which was acidified using 6 M aqueous HCl. The organic phase was separated and washed with 1N HCl and brine, dried over Na_2SO_4, filtered and evaporated to a residue, that was purified by chromatography on silica gel using a mixture of CH_2Cl_2/MeOH/AcOH 95.5:2.5:2 v/v to afford N-Fmoc-2′,6′-dimethyl-L-tyrosine acid (0.24 g, 78 %). ^{1}H NMR (500 MHz, DMSO) δ 12.67 (br s 12.67), 8.95 (s, 1H), 7.92 – 7.86 (m, 2H), 7.74 (d, *J* = 8.7 Hz, 1H), 7.71 – 7.65 (m, 2H), 7.47 – 7.38 (m, 2H), 7.36 – 7.27 (m, 2H), 6. 42 – 6.37 (m, 2H), 4.23 – 4.17 (m, 3H), 4.13 – 4.01 (m, 1H), 3.00 (dd, *J* = 14.3, 6.0 Hz, 1H), 2.82 (dd, *J* = 14.3, 8.8 Hz, 1H), 2.20 (s, 6H); ^{13}C NMR (125 MHz, DMSO-d_6) δ 173.7, 155.9, 155.1, 143.9, 140.7, 137.8, 127.6, 127.1, 125.3, 120.1, 114.8, 65.7, 59.9, 46.6, 29.7, 20.1; IR (neat) ν_{max}/cm^{-1} 3321, 1702, 1596, 1536, 1449, 1261, 1140, 1025; HRMS m/z calculated for $C_{26}H_{26}NO_5$ $[M+H]^+$ 432.1805; found 432.1815.

2. Yields and purities of [aza-pipecolate]GHRP-6 and Opioid analogues

[aza-Pip] in Opioid and GHRP-6	Isolated Yield (%)	Purity[a]	HRMS	
			$[M + H]^+$ m/z (calcd)	or $[M + Na]^+$ m/z (obsd)
4.18a	12	95%	535.2663	535.2679
4.18b	8.2	99%	624.2929	624.2944
4.18c	9	99%	585.2820	585.2835
4.19a	8.6	99%	563.2976	563.2964
4.19b	6.5	98%	652.3242	652.3234
4.19c	7.2	98%	613.3133	613.3112
4.20a	4.6	99%	563.2976	563.2962
4.21a	2	96%	591.3289	591.3284
4.22a	12	98%	537.2820	537.2826
4.22b	8.2	99%	626.3085	626.3099
4.22c	9	99%	587.2976	587.2991
4.23a	4.6	98%	565.3133	565.3138
4.27	4.2	99%	797.4206	797.4189
4.28	3.9	98%	912.4628	912.4628
4.29	4.6	95%	962.4760	962.4764
4.30	4.2	99%	799.4362	799.4381
4.31	3.9	96%	914.4784	914.4780

[a] Ascertained by LC-MS using both acetonitrile (1% FA)/H_2O (1% FA) and methanol (1% FA)/H_2O (1% FA) as solvent systems.

3. Analytical LC-MS characterization of purified azapipecolyl opioids analogues (4.18-4.23).

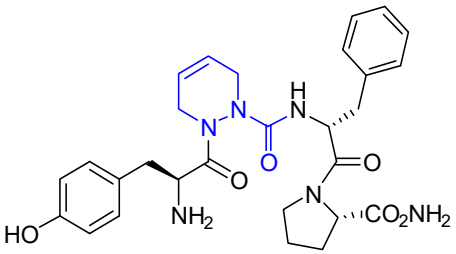

4.18a

Tyr-(Δ^4)azaPip-D-Phe-Pro-NH_2 (4.18a): LC-MS analysis (a) 20-95% of MeOH (0.1% FA) in H_2O (0.1% FA) over 11 min, then 20% MeOH for 4 min, R.T. = 7.55 min; (b) 10-95% MeCN (0.1% FA) in H_2O (0.1% FA) over 11 min, then 10% MeCN for 4 min, R.T. = 6.42 min; HRMS m/z calcd for $C_{28}H_{35}N_6O_5$ $[M+H]^+$ 535.2663, found 535.2679.

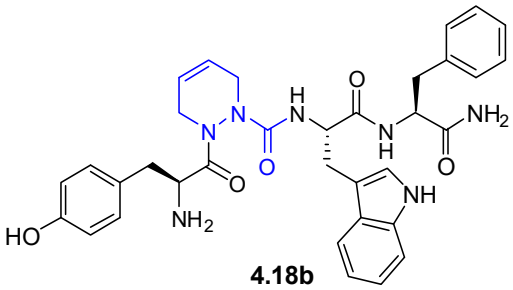

4.18b

Tyr-(Δ^4)azaPip-Trp-Phe-NH_2 (4.18b): LC-MS analysis (a) 20-95% of MeOH (0.1% FA) in H_2O (0.1% FA) over 11 min, then 20% MeOH for 4 min, R.T. = 8.37 min; (b) 20-95% MeCN (0.1% FA) in H_2O (0.1% FA) over 15 min, then 20% MeCN for 3 min, R.T. = 6.61 min; HRMS m/z calcd for $C_{34}H_{38}N_7O_5$ $[M+H]^+$ 624.2929, found 624.2944.

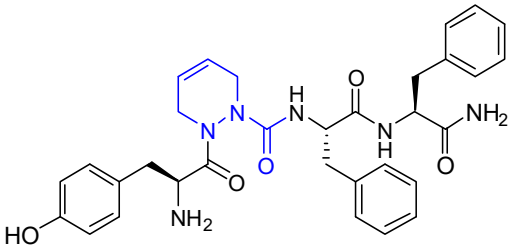

4.18c

Tyr-(Δ[4])azaPip-Phe-Phe-NH$_2$ (4.18c): (a) LC-MS analysis (a) 20-95% of MeOH (0.1% FA) in H_2O (0.1% FA) over 11 min, then 20% MeOH for 4 min, R.T. = 8.25 min; (b) 20-95% MeCN (0.1% FA) in H_2O (0.1% FA) over 11 min, then 20% MeCN for 4 min, R.T. = 5.60 min; HRMS m/z calcd for $C_{32}H_{37}N_6O_5$ $[M+H]^+$ 585.2820, found 585.2835.

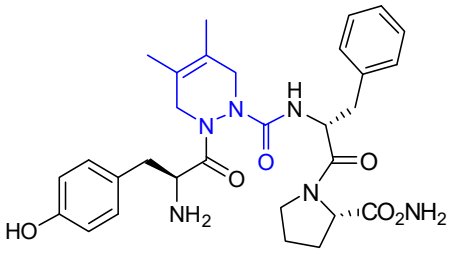

4.19a

Tyr-(4,5-dimethyl-Δ[4])azaPip-D-Phe-Pro-NH$_2$ (4.19a): LC-MS analysis (a) 10-90% of MeOH (0.1% FA) in H_2O (0.1% FA) over 9 min, then 10% MeOH for 5 min, R.T. = 6.70 min; (b) 10-90% MeCN (0.1% FA) in H_2O (0.1% FA) over 9 min, then 5% MeCN for 5 min, R.T. = 4.76 min; HRMS m/z calcd for $C_{30}H_{39}N_6O_5$ $[M+H]^+$ 563.2976, found 563.2964.

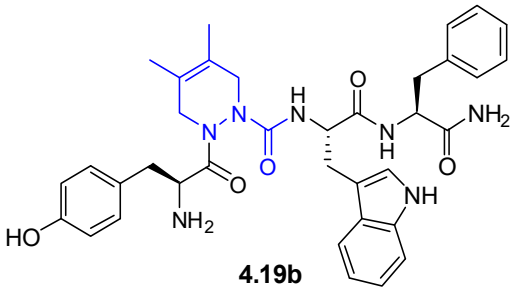

4.19b

Tyr-(4,5-dimethyl-Δ[4])azaPip-Trp-Phe-NH$_2$ (4.19b): LC-MS analysis (a) 10-90% of MeOH (0.1% FA) in H_2O (0.1% FA) over 9 min, then 10% MeOH for 5 min, R.T. = 7.38 min; (b)10-90% MeCN (0.1% FA) in H_2O (0.1% FA) over 9 min, then 10% MeCN for 5 min, R.T. = 5.12 min; HRMS m/z calcd for $C_{36}H_{42}N_7O_5$ $[M+H]^+$ 652.3242, found 652.3234.

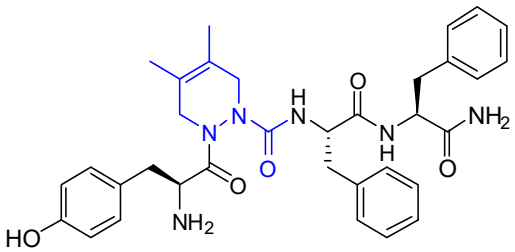

4.19c

Tyr-(4,5-dimethyl-Δ[4])azaPip-Phe-Phe-NH$_2$ (4.19c): LC-MS analysis (a) 10-90% of MeOH (0.1% FA) in H_2O (0.1% FA) over 9 min, then 10% MeOH for 5 min, R.T. = 7.32 min; (b) 10-90% MeCN (0.1% FA) in H_2O (0.1% FA) over 9 min, then 10% MeCN for 5 min, R.T. = 5.18 min; HRMS m/z calcd for $C_{34}H_{41}N_6O_5$ $[M+H]^+$ 613.3133, found 613.3112.

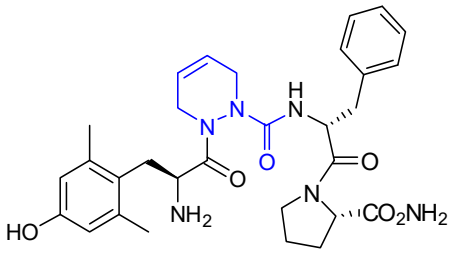

4.20a

Dmt-(Δ[4])azaPip-D-Phe-Pro-NH2 (4.20a): LC-MS analysis (a) 10-90% of MeOH (0.1% FA) in H_2O (0.1% FA) over 9 min, then 10% MeOH for 5 min, R.T. = 6.14 min; (b) 10-90% MeCN (0.1% FA) in H_2O (0.1% FA) over 9 min, then 10% MeCN for 5 min, R.T. = 4.34 min; HRMS m/z calcd for $C_{30}H_{39}N_6O_5$ $[M+H]^+$ 563.2976, found 563.2962.

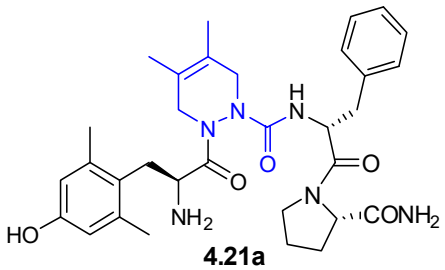

4.21a

Dmt-(4,5-dimethyl-Δ[4])azaPip-D-Phe-Pro-NH$_2$ (4.21a): LC-MS analysis (a) 10-90% of MeOH (0.1% FA) in H_2O (0.1% FA) over 9 min, then 10% MeOH for 5 min, R.T. = 7.01 min; (b) 10-90% MeCN (0.1% FA) in H_2O (0.1% FA) over 9 min, then 10% MeCN for 5 min, R.T. = 4.96 min; HRMS m/z calcd for $C_{32}H_{43}N_6O_5$ $[M+H]^+$ 591.3289, found 591.3284.

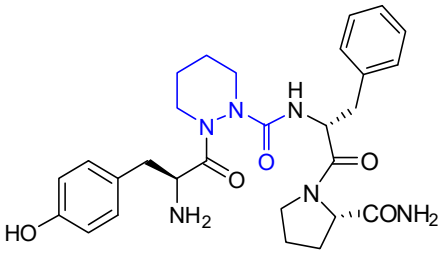

4.22a

Tyr-azaPip-D-Phe-Pro-NH$_2$ (4.22a): LC-MS analysis (a) 10-90% of MeOH (0.1% FA) in H_2O (0.1% FA) over 9 min, then 10% MeOH for 5 min, R.T. = 5.73 min; (b) 10-90% MeCN (0.1% FA) in H_2O (0.1% FA) over 9 min, then 10% MeCN for 5 min, R.T. = 4.07 min; HRMS m/z calcd for $C_{28}H_{37}N_6O_5$ $[M+H]^+$ 537.2820, found 537.2826.

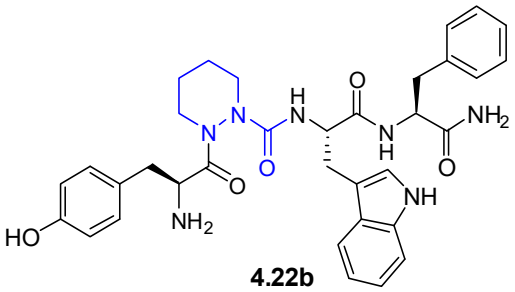

4.22b

Trp-azaPip-Trp-Phe-NH$_2$ (4.22b): LC-MS analysis (a) 10-90% of MeOH (0.1% FA) in H_2O (0.1% FA) over 9 min, then 10% MeOH for 5 min, R.T. = 6.61 min; (b) 10-90% MeCN (0.1% FA) in H_2O (0.1% FA) over 9 min, then 10% MeCN for 5 min, R.T. = 4.68 min; HRMS m/z calcd for $C_{34}H_{40}N_7O_5$ $[M+H]^+$ 626.3085, found 626.3099.

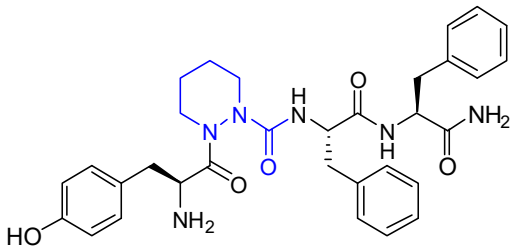

4.22c

Tyr-azaPip-Phe-Phe-NH$_2$ (4.22c): LC-MS analysis (a) 10-90% of MeOH (0.1% FA) in H_2O (0.1% FA) over 9 min, then 10% MeOH for 5 min, R.T. = 6.47 min; (b) 10-90% MeCN (0.1% FA) in H_2O (0.1% FA) over 9 min, then 10% MeCN for 5 min, R.T. = 4.58 min; HRMS m/z calcd for $C_{32}H_{39}N_6O_5$ $[M+H]^+$ 587.2976, found 587.29

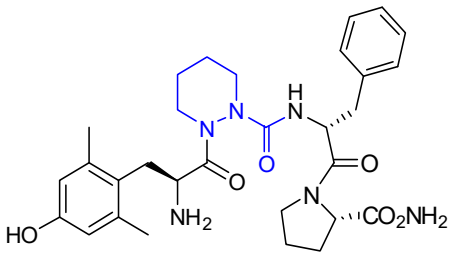

4.23a

Dmt-azaPip-D-Phe-Pro-NH_2 (4.23a): LC-MS analysis (a) 10-90% of MeOH (0.1% FA) in H_2O (0.1% FA) over 9 min, then 10% MeOH for 5 min, R.T. = 6.09 min; (b) 10-90% MeCN (0.1% FA) in H_2O (0.1% FA) over 9 min, then 10% MeCN for 5 min, R.T. = 4.29 min; HRMS m/z calcd for $C_{30}H_{41}N_6O_5$ $[M+H]^+$565.3133, found 565.3138.

4. Analytical LC-MS characterization of purified azapipecolate GHRP-6 analogues (4.27- 4.31).

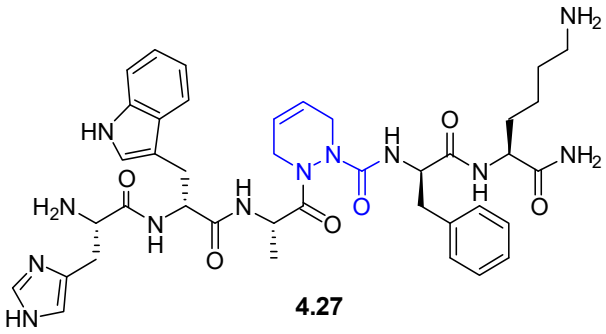

4.27

His-D-Trp-Ala-(Δ^4)azaPip-D-Phe-Lys-NH_2 (4.27): LC-MS analysis (a) 5-50% of MeOH (0.1% FA) in H_2O (0.1% FA) over 9 min, then 5% MeOH over 5 min, R.T. = 4.87 min; (b) 5-50% MeCN (0.1% FA) in H_2O (0.1% FA) over 9 min, then 5% MeCN for 5 min, R.T. = 3.92 min; HRMS m/z calcd for $C_{40}H_{53}N_{12}O_6$ $[M+H]^+$ 797.4206, found 797.4189. LC-MS m/z calcd for $C_{40}H_{53}N_{12}O_6$ $[M+H]^+$ 797.41, found 797.4.

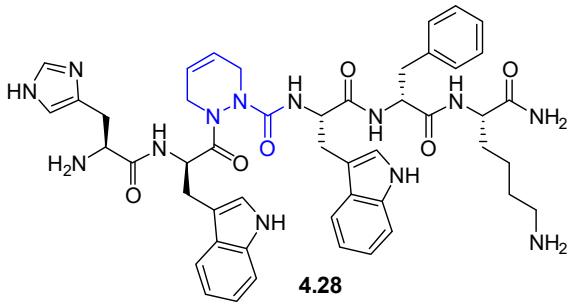

4.28

His-D-Trp-(Δ^4)azaPip-Trp-D-Phe-Lys-NH_2 (4.28): LC-MS analysis (a) 5-50% of MeOH (0.1% FA) in H_2O (0.1% FA) over 9 min, then 5% MeOH for 5 min, R.T. = 5.98 min; (b) 5-

50% MeCN (0.1% FA) in H_2O (0.1% FA) over 9 min, then 5% MeCN for 5 min, R.T. = 5.82 min; HRMS m/z calcd for $C_{48}H_{58}N_{13}O_6$ $[M+H]^+$ 912.46275, found 912.4628. LC-MS m/z calcd for $C_{48}H_{58}N_{13}O_6$ $[M+H]^+$ 912.46, found 912.4.

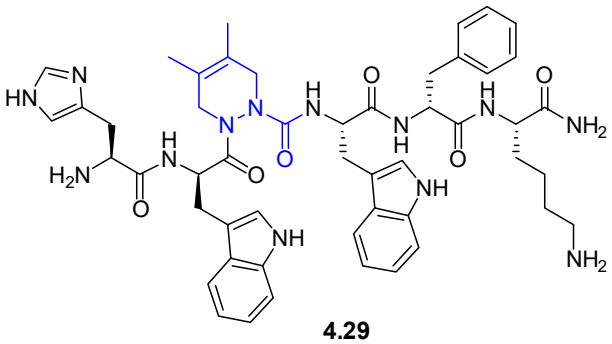

4.29

His-D-Trp-(4,5-dimethyl-Δ[4])azaPip-Trp-D-Phe-Lys-NH_2 (**4.29**): LC-MS analysis (a) 2-98% of MeOH (0.1% FA) in H_2O (0.1% FA) over 11 min, then 2% MeOH for 4 min, R.T. = 4.91 min; (b) 2-50% MeCN (0.1% FA) in H_2O (0.1% FA) over 11 min, then 2% MeCN for 4 min, R.T. = 5.26 min; HRMS m/z calcd for $C_{50}H_{61}N_{13}O_6$ $[M+Na]^+$ 962.4760, found 962.4764. LC-MS m/z calcd for $C_{50}H_{61}N_{13}O_6$ $[M+Na]^+$ 962.49, found 962.52.

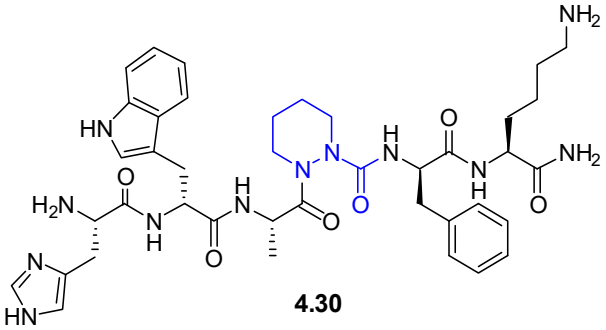

4.30

His-D-Trp-Ala-azaPip-D-Phe-Lys-NH_2 (**4.30**): LC-MS analysis (a) 5-50% of MeOH (0.1% FA) in H_2O (0.1% FA) over 9 min, then 5% MeOH for 5 min, R.T. = 5.15 min; (b) 5-50% MeCN (0.1% FA) in H_2O (0.1% FA) over 9 min, then 5% MeCN for 5 min, R.T. = 3.97 min; HRMS m/z calcd for $C_{40}H_{55}N_{12}O_6$ $[M+H]^+$ 799.4362, found 799.4381. LC-MS m/z calcd for $C_{40}H_{55}N_{12}O_6$ $[M+H]^+$ 799.43, found 799.4.

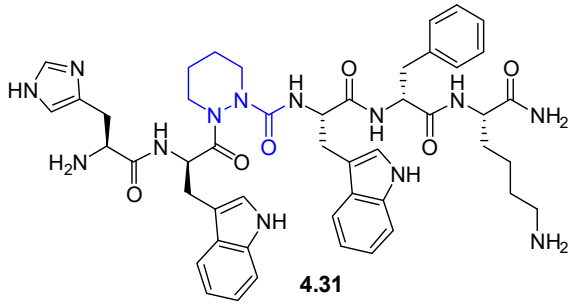

4.31

His-D-Trp-azaPip-Trp-D-Phe-Lys-NH2 (4.31): LC-MS analysis (a) 5-50% of MeOH (0.1% FA) in H_2O (0.1% FA) over 9 min, then 5% MeOH for 5 min, R.T. = 6.07 min; (b) 5-50% MeCN (0.1% FA) in H_2O (0.1% FA) over 9 min, then 5% MeCN for 5 min, R.T. = 4.70 min; HRMS m/z calcd for $C_{48}H_{60}N_{13}O_6$ $[M+H]^+$ 914.4784, found 914.4780. LC-MS m/z calcd for $C_{48}H_{60}N_{13}O_6$ $[M+H]^+$ 914.47, found 914.5.

References

(1) Boeglin, D.; Lubell, W. D., Aza-Amino Acid Scanning of Secondary Structure Suited for Solid-Phase Peptide Synthesis with Fmoc Chemistry and Aza-Amino Acids with Heteroatomic Side Chains. *J. Comb. Chem.* **2005**, *7*, 864-878.

(2) Lubell, W.; Blankenship, J.; Fridkin, G.; Kaul, R., Peptides. *In Science of Synthesis 21.11, Chemistry of Amides;* Thieme: Stuttgart, Germany, **2005**, 713-809.

Annex 4: NMR spectra for chapters 2, 3, and 4

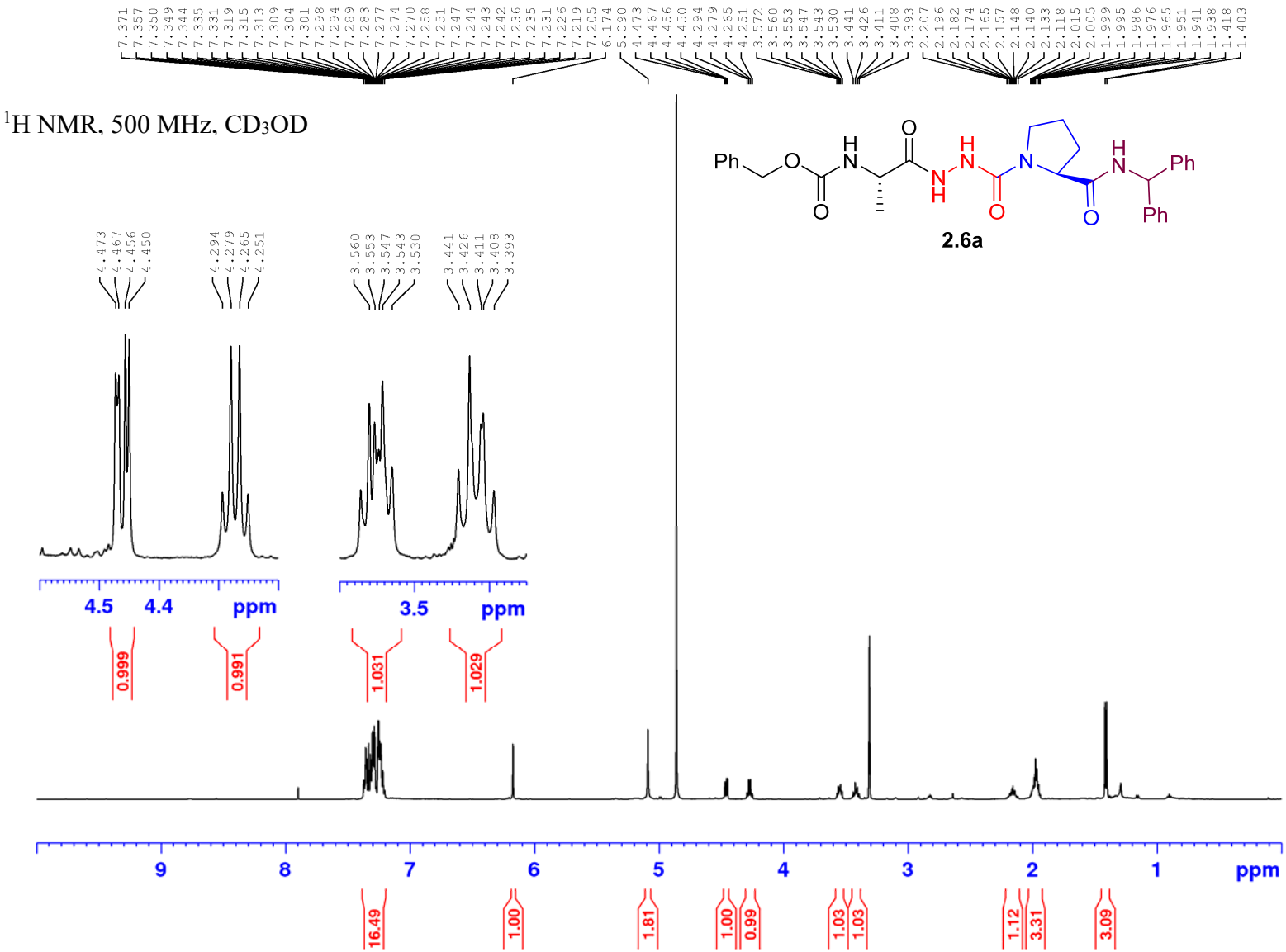
7.371 7.357 7.350 7.349 7.344 7.335 7.331 7.319 7.315 7.313 7.309 7.304 7.301 7.298 7.294 7.289 7.283 7.277 7.274 7.270 7.258 7.251 7.247 7.244 7.243 7.242 7.236 7.235 7.231 7.226 7.219 7.205 6.174 5.090 4.473 4.467 4.456 4.450 4.294 4.279 4.265 4.251 3.572 3.560 3.553 3.547 3.543 3.530 3.441 3.426 3.411 3.408 3.393 2.207 2.196 2.182 2.174 2.165 2.157 2.148 2.140 2.133 2.118 2.015 2.005 1.999 1.995 1.986 1.976 1.965 1.951 1.941 1.938 1.418 1.403
1H NMR, 500 MHz, CD3OD
Ph O O H N O H N N H O N O H N Ph Ph
2.6a
4.5 4.4 ppm
3.5 ppm
0.999 0.991 1.031 1.029
9 8 7 6 5 4 3 2 1 ppm
16.49 1.00 1.81 1.00 0.99 1.03 1.03 1.12 3.31 3.09

^{13}C NMR, 125 MHz, CD_3OD

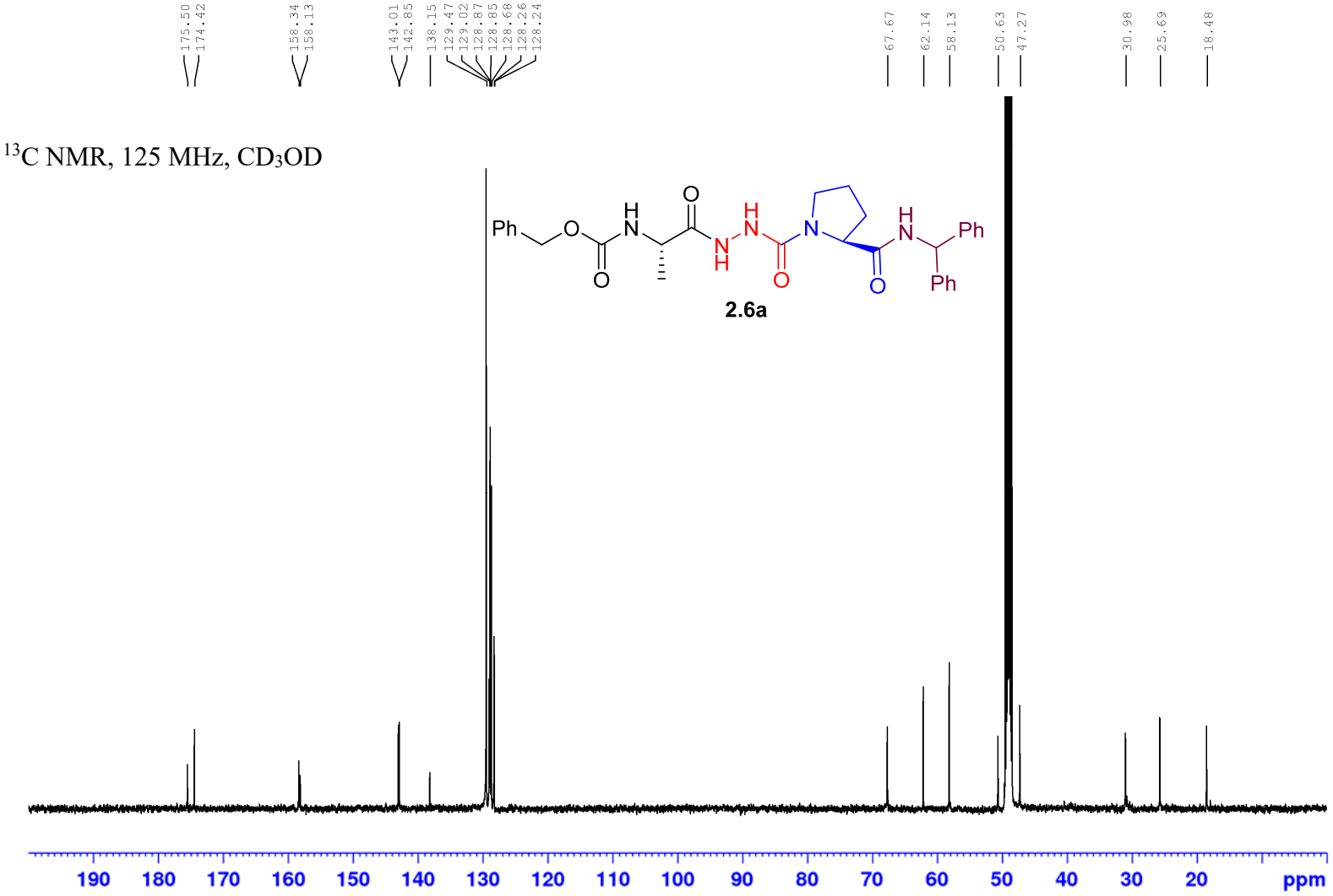

^{1}H NMR, 500 MHz, $CDCl_3$

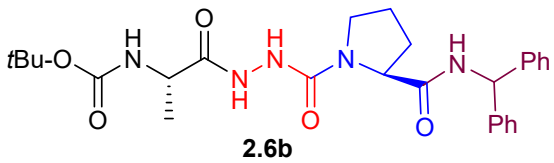

2.6b

^{13}C NMR, 125 MHz, $CDCl_3$

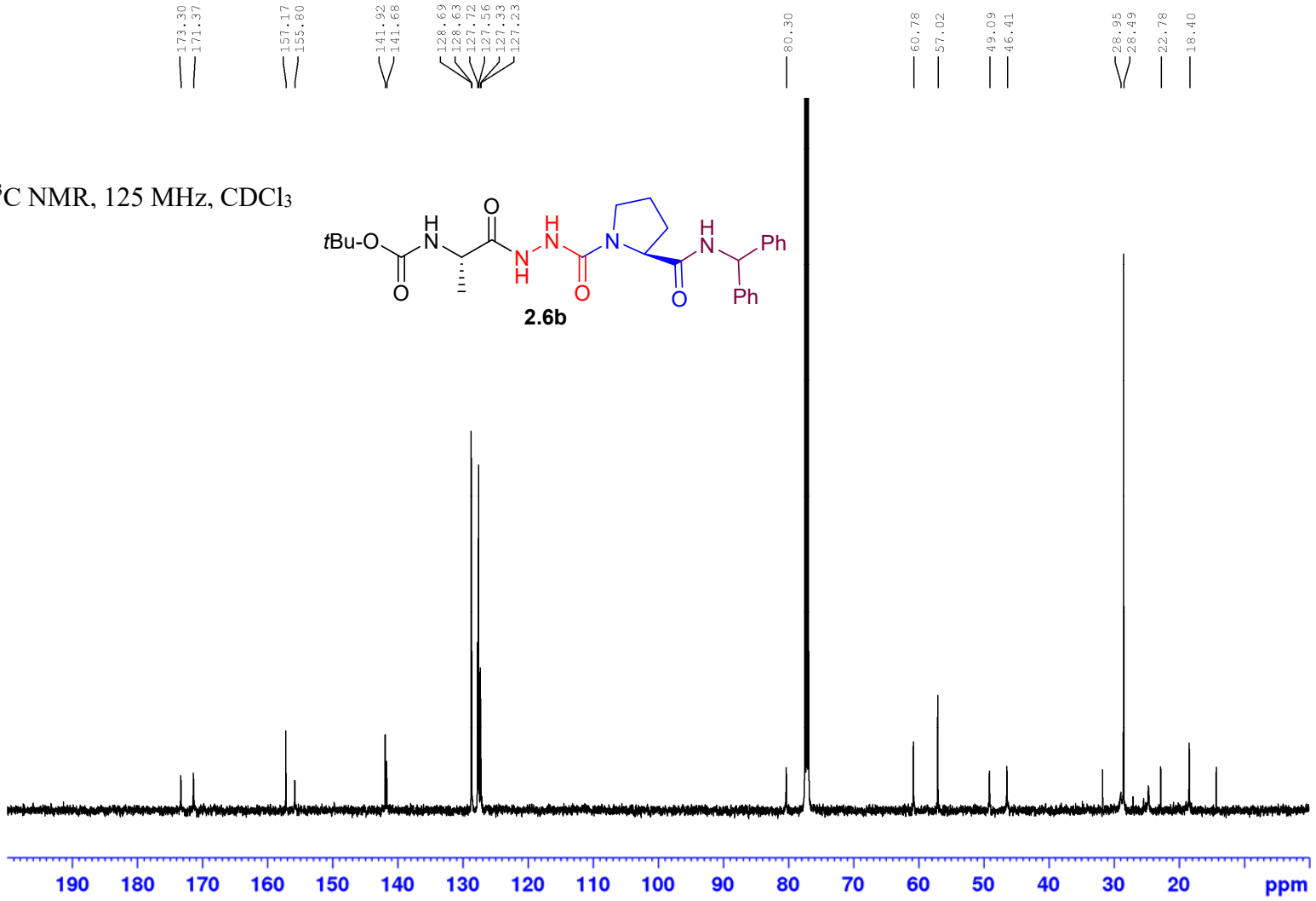

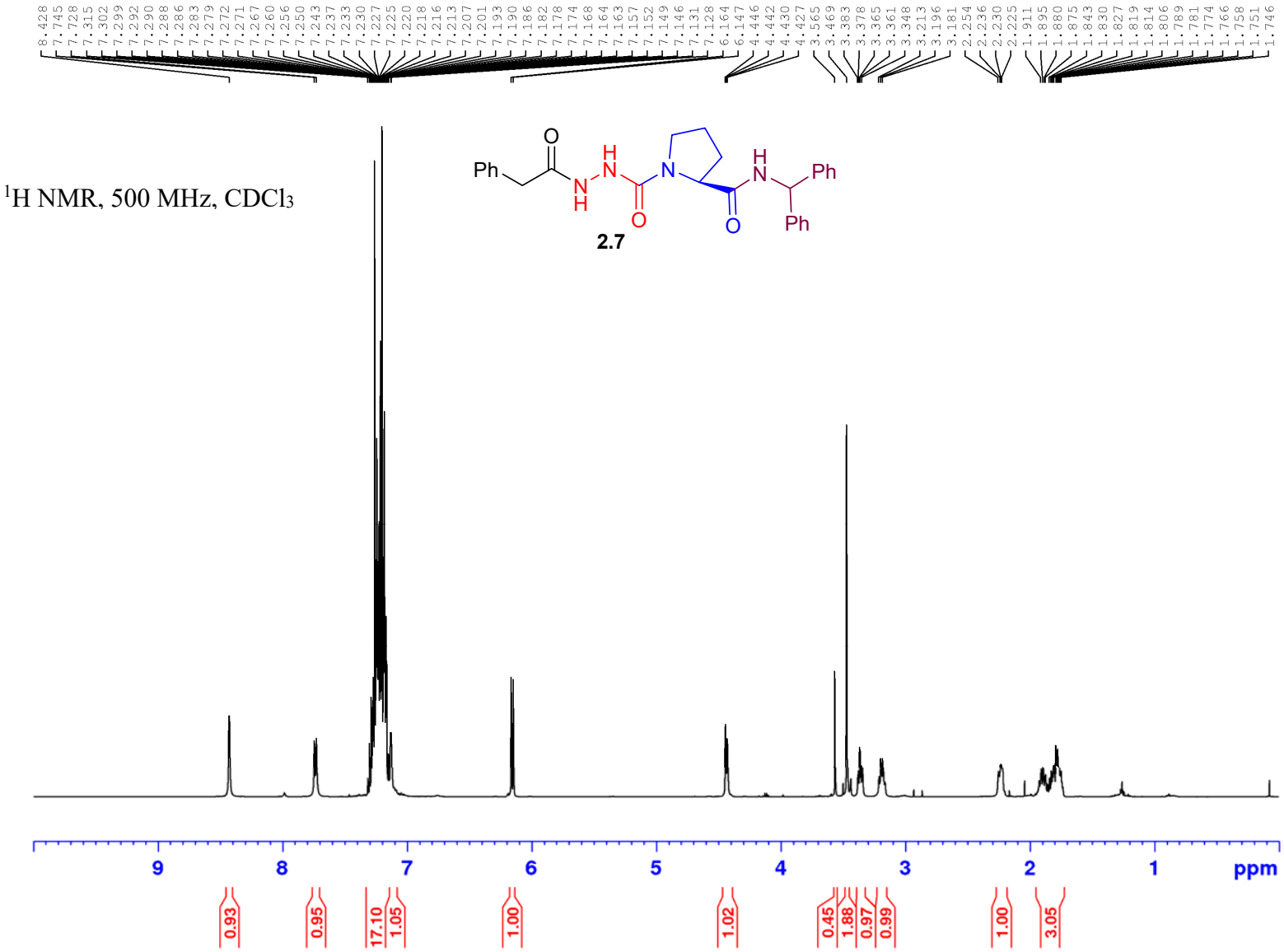
8.428
7.745
7.728
7.315
7.302
7.299
7.292
7.290
7.288
7.286
7.283
7.279
7.272
7.271
7.267
7.260
7.256
7.250
7.243
7.237
7.233
7.230
7.227
7.225
7.220
7.218
7.216
7.213
7.207
7.201
7.193
7.190
7.186
7.182
7.178
7.174
7.168
7.164
7.163
7.157
7.152
7.149
7.146
7.131
7.128
6.164
6.147
4.446
4.442
4.430
4.427
3.565
3.469
3.383
3.378
3.365
3.361
3.348
3.213
3.196
3.181
2.254
2.236
2.230
2.225
1.911
1.895
1.880
1.875
1.843
1.830
1.827
1.819
1.814
1.806
1.789
1.781
1.774
1.766
1.758
1.751
1.746
1H NMR, 500 MHz, CDCl3
Ph
O
H
N
N
H
N
O
N
H
Ph
Ph
O
2.7
9
8
7
6
5
4
3
2
1
ppm
0.93
0.95
17.10
1.05
1.00
1.02
0.45
1.88
0.97
0.99
1.00
3.05

^{13}C NMR, 125 MHz, $CDCl_3$

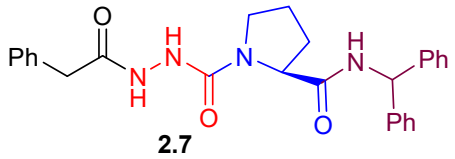

2.7

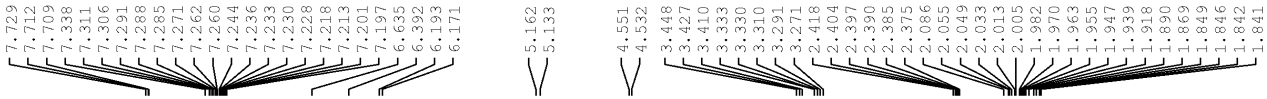

^{1}H NMR, 400 MHz, $CDCl_3$

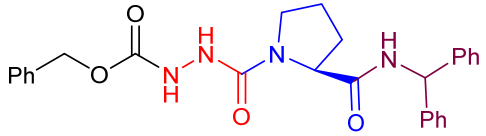

2.8a

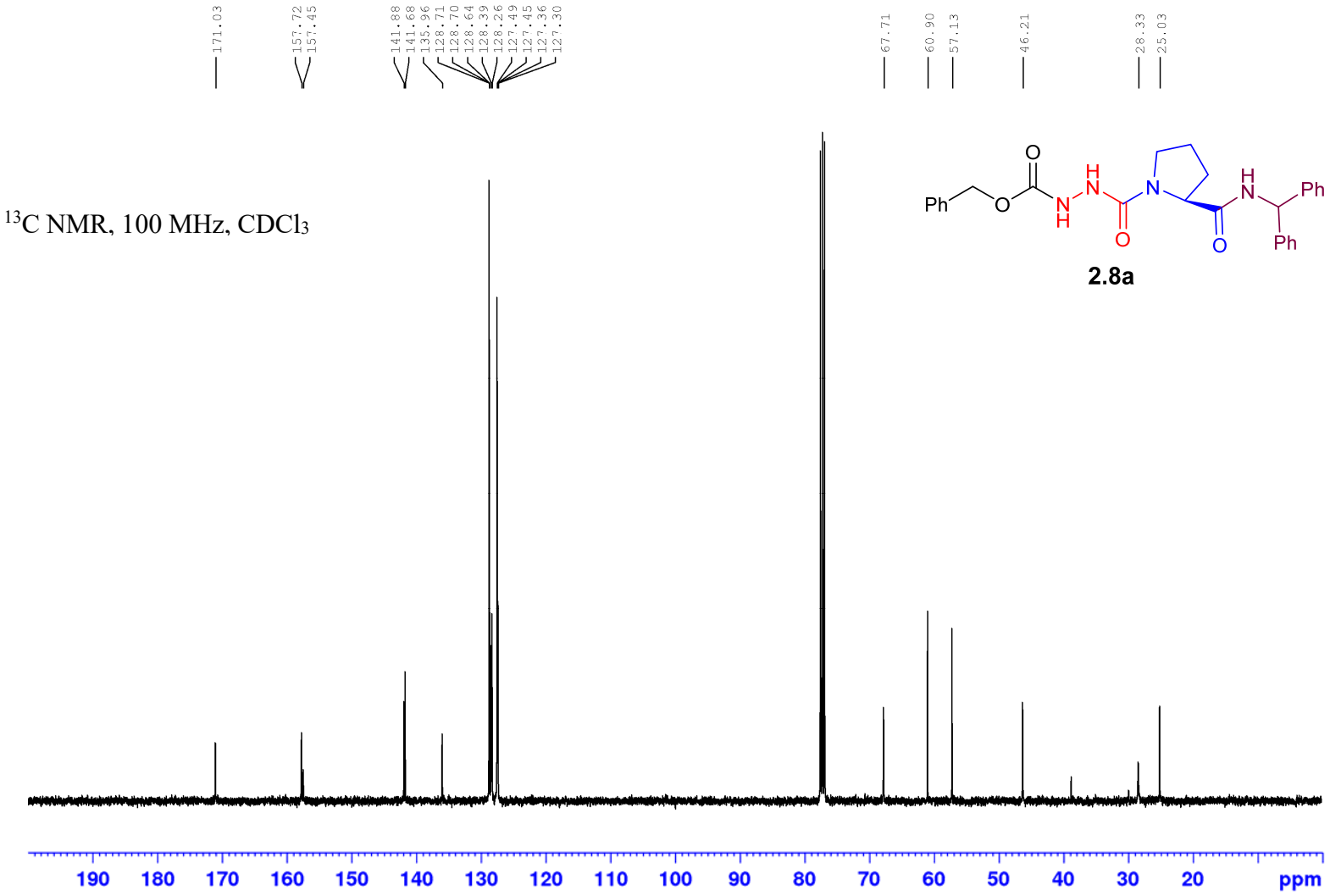
171.03
157.72
157.45
141.88
141.68
135.96
128.71
128.70
128.64
128.39
128.26
127.49
127.45
127.36
127.30
67.71
60.90
57.13
46.21
28.33
25.03
13C NMR, 100 MHz, CDCl3
Ph
O
O
H
N
N
H
N
O
O
H
N
Ph
Ph
2.8a
190
180
170
160
150
140
130
120
110
100
90
80
70
60
50
40
30
20
ppm

^{1}H NMR, 500 MHz, $CDCl_3$

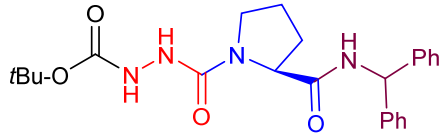

2.8b

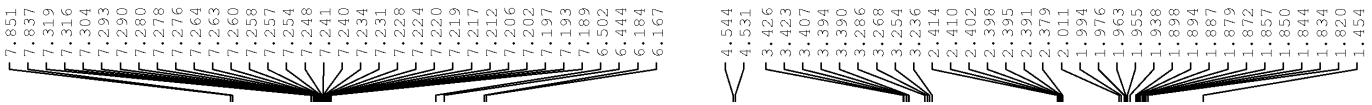

^{13}C NMR, 125 MHz, $CDCl_3$

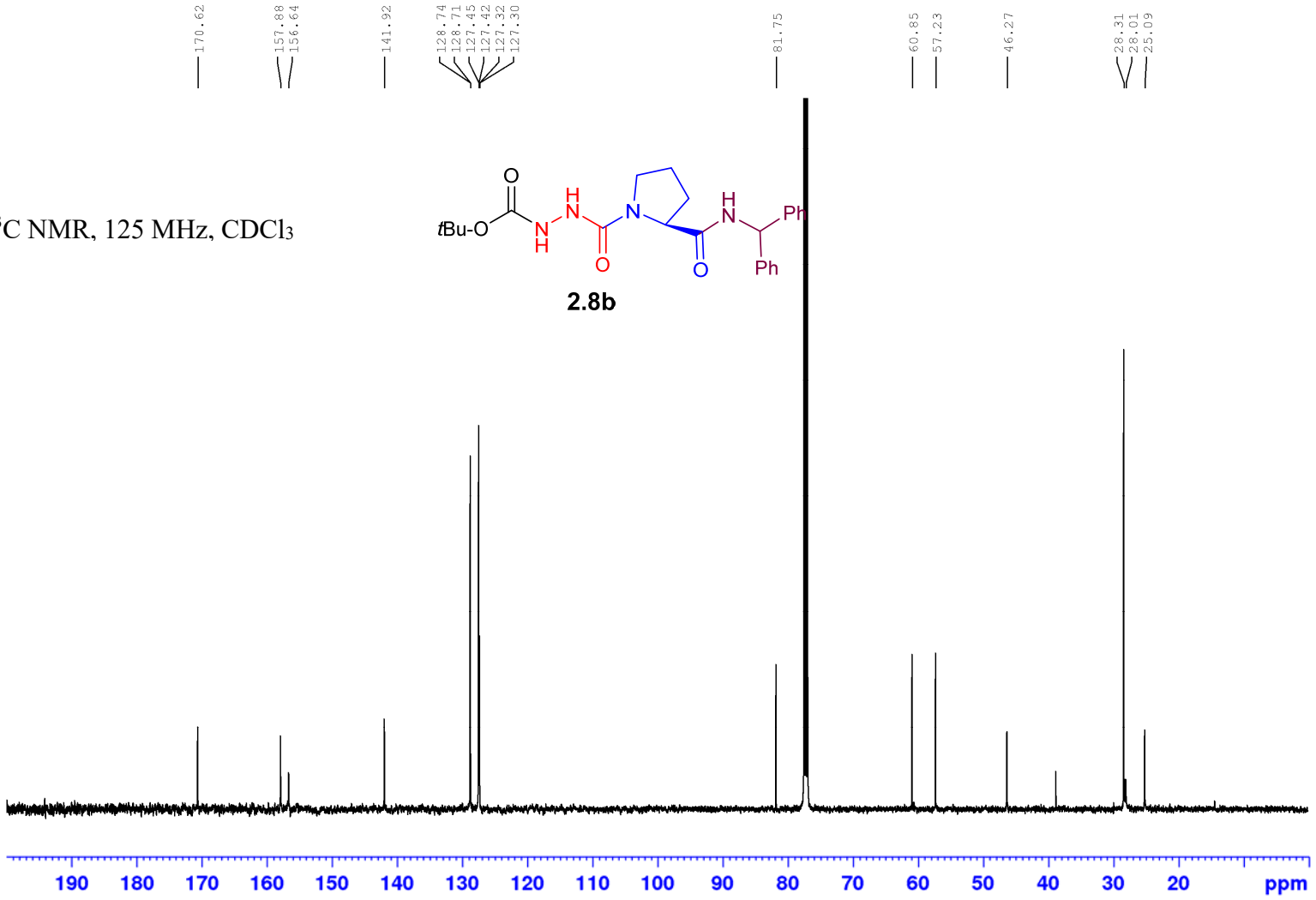

2.8b

^{1}H NMR, 500 MHz, $CDCl_3$

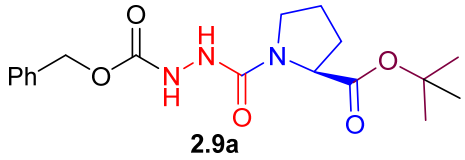

2.9a

^{13}C NMR, 125 MHz, $CDCl_3$

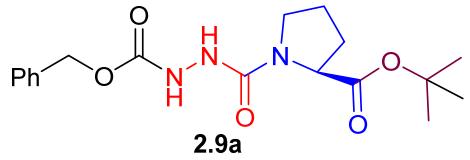

2.9a

^{1}H NMR, 500 MHz, $CDCl_3$

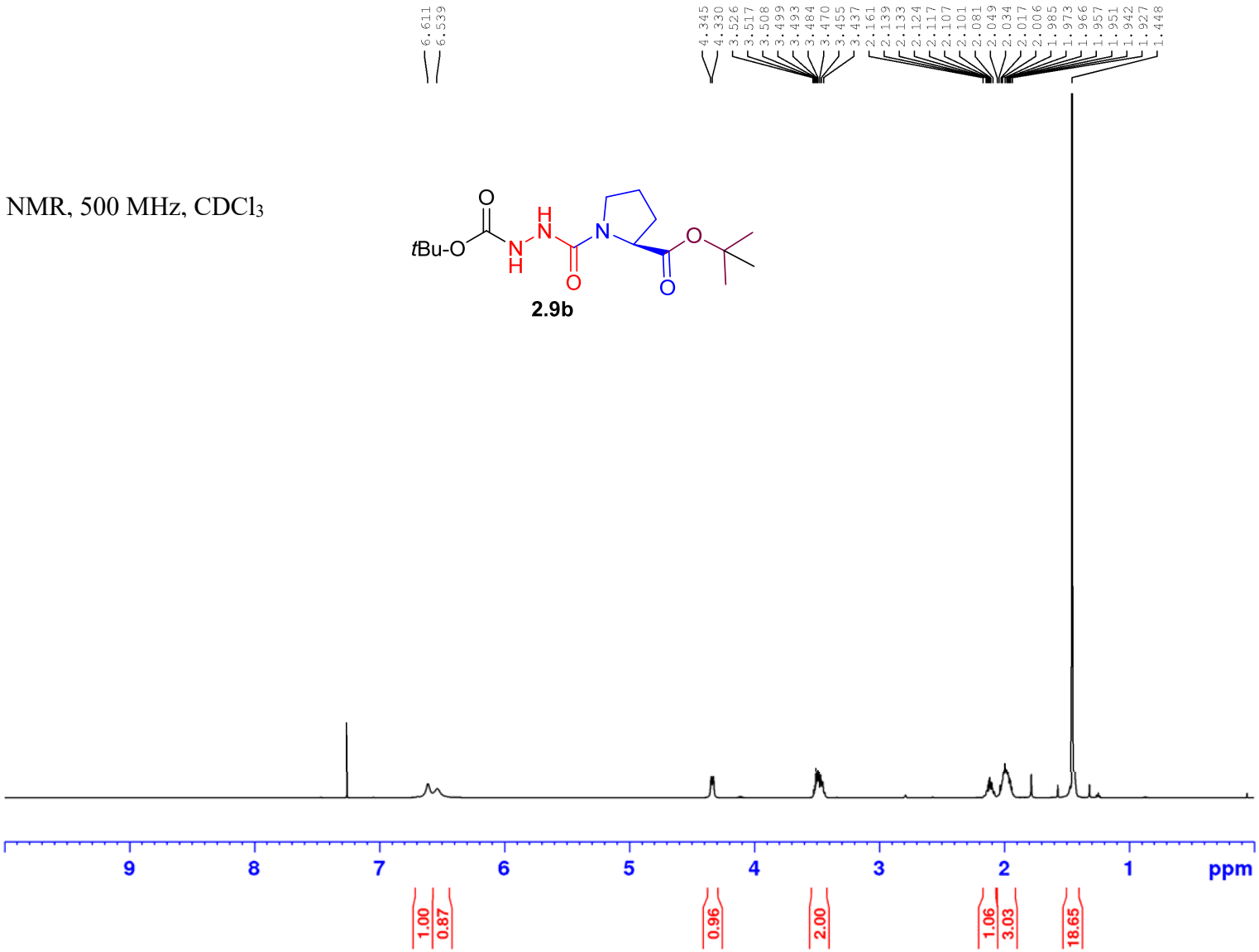

^{13}C NMR, 125 MHz, $CDCl_3$

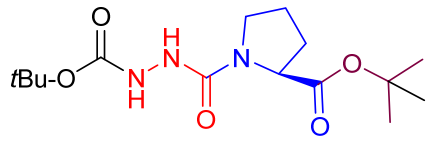

2.9b

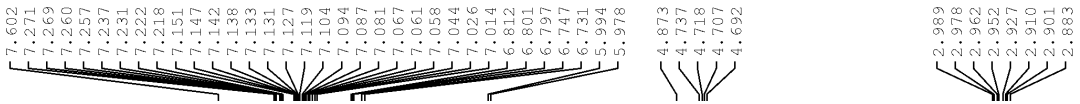

^{1}H NMR, 500 MHz, $CDCl_3$

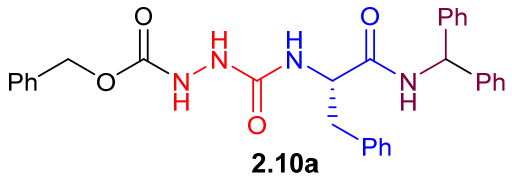

2.10a

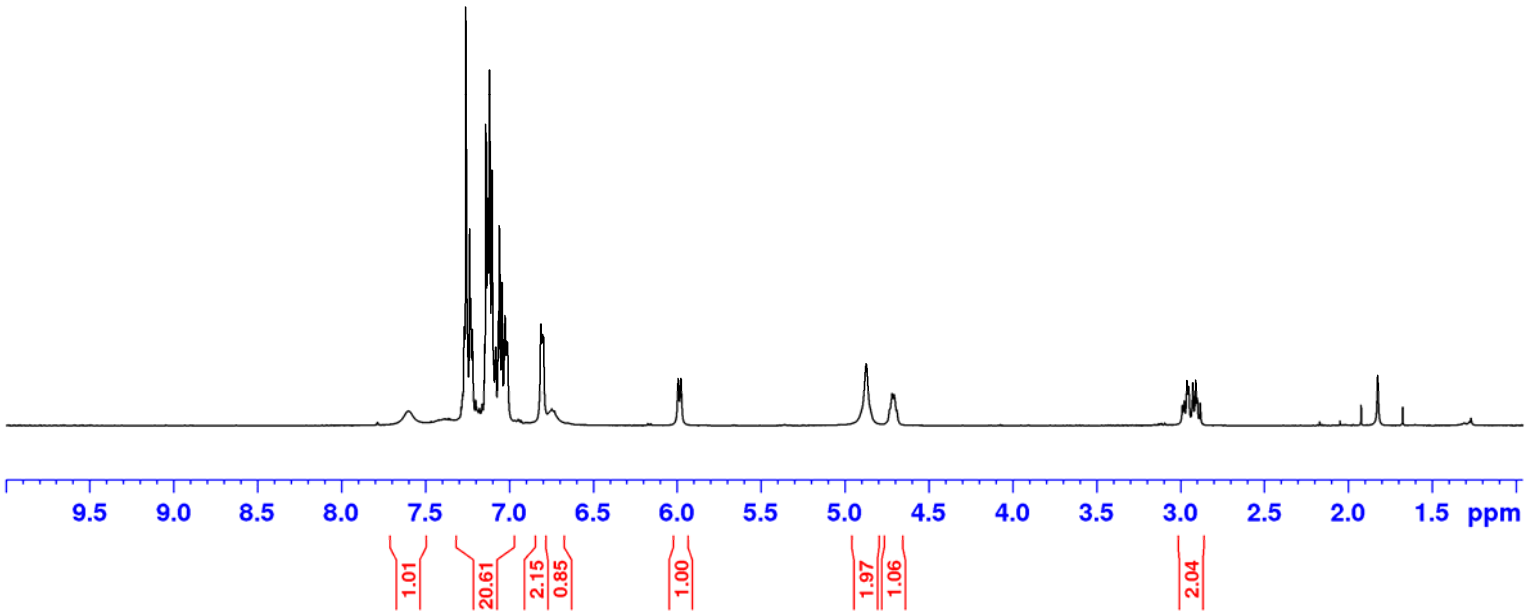

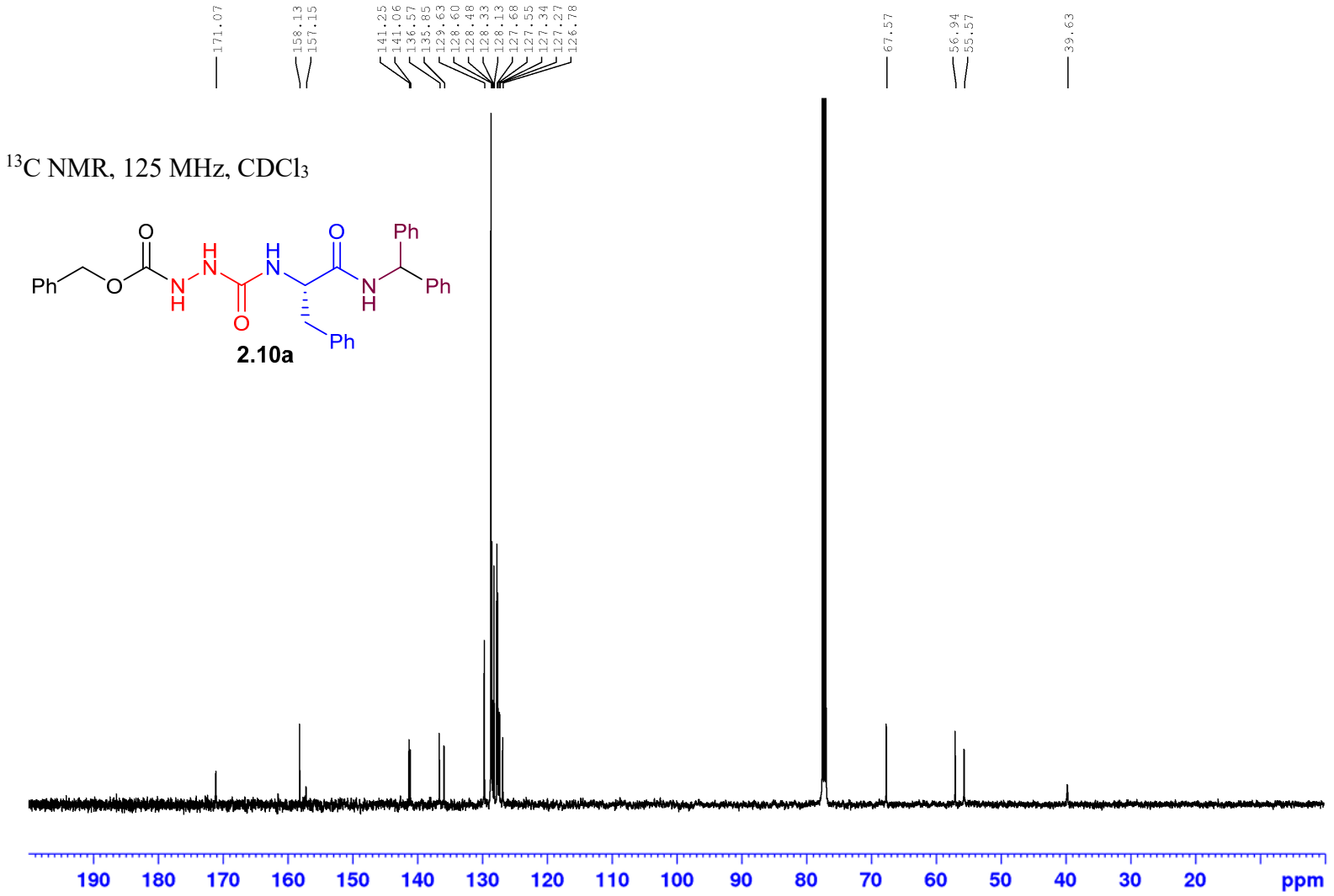

^{13}C NMR, 125 MHz, $CDCl_3$

2.10a

^{1}H NMR, 400 MHz, CD_3OD

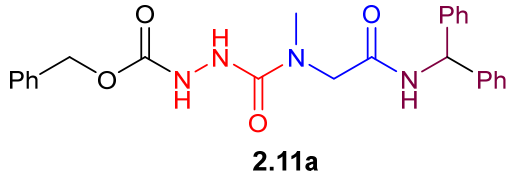

2.11a

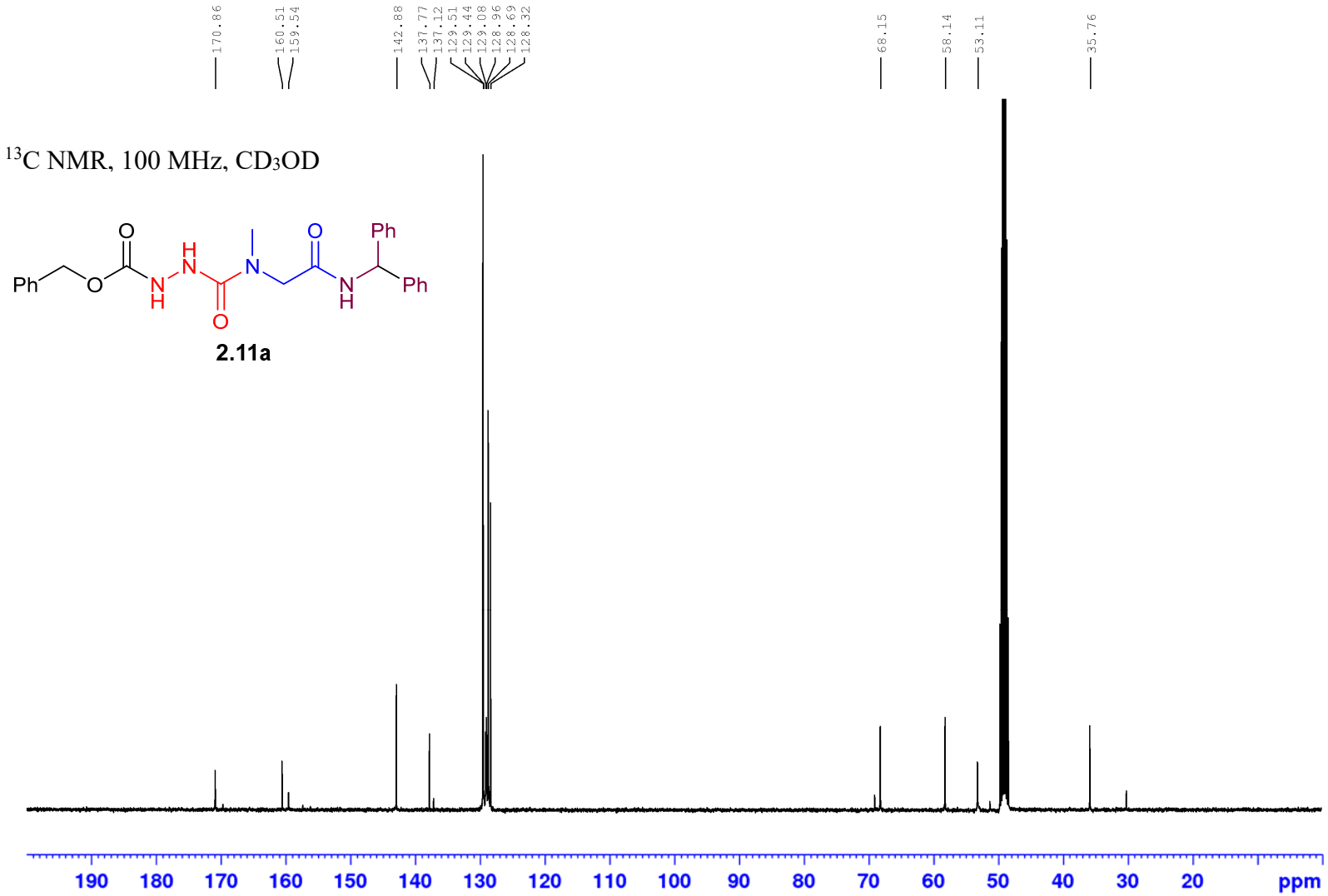
170.86
160.51
159.54
142.88
137.77
137.12
129.51
129.44
129.08
128.96
128.69
128.32
68.15
58.14
53.11
35.76
13C NMR, 100 MHz, CD3OD
Ph
O
O
N
H
N
H
N
O
O
N
H
Ph
Ph
2.11a
190
180
170
160
150
140
130
120
110
100
90
80
70
60
50
40
30
20
ppm

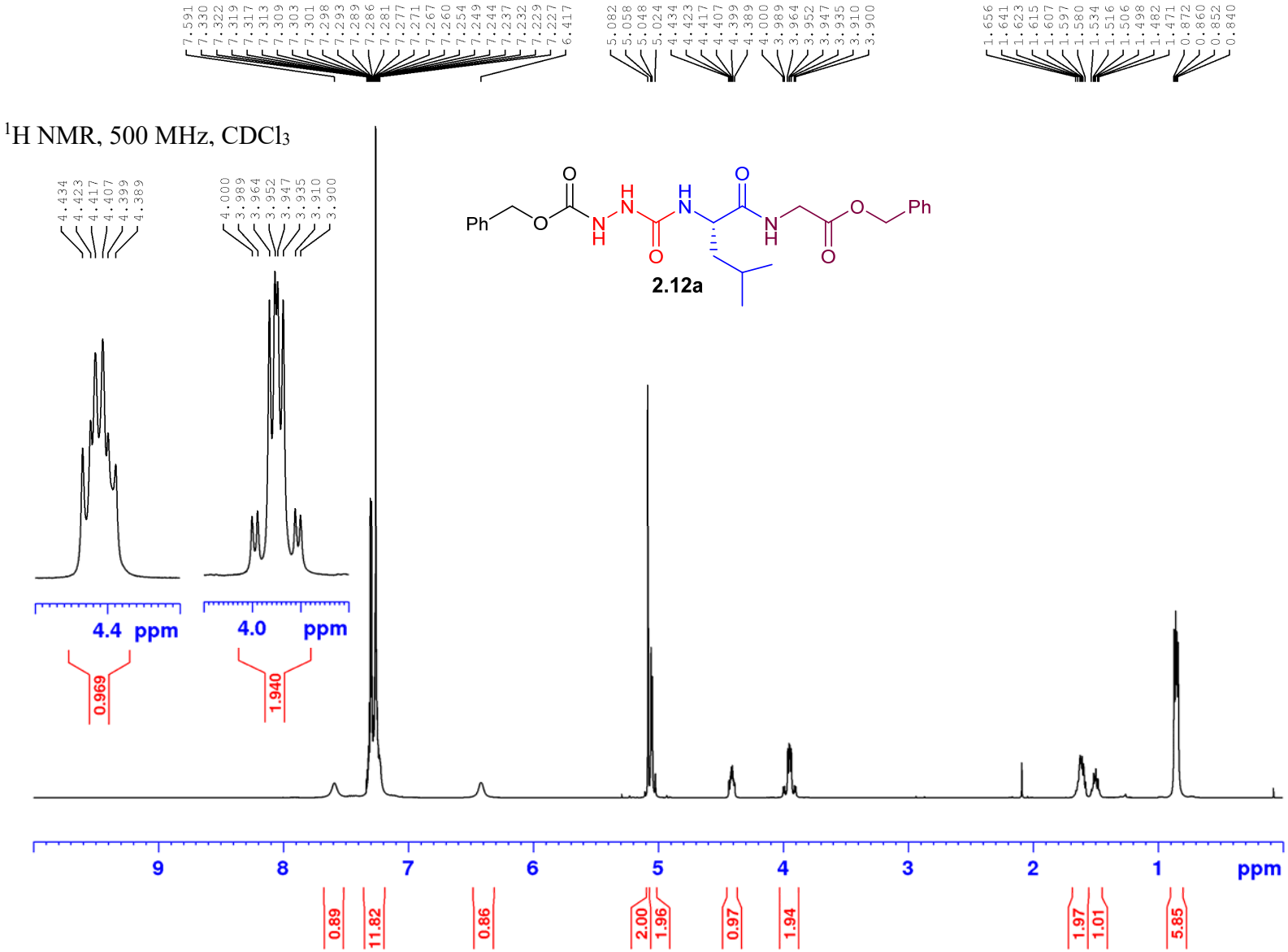
7.591
7.330
7.322
7.319
7.317
7.313
7.309
7.303
7.301
7.298
7.293
7.289
7.286
7.281
7.277
7.271
7.267
7.260
7.254
7.249
7.244
7.237
7.232
7.229
7.227
6.417
5.082
5.058
5.048
5.024
4.434
4.423
4.417
4.407
4.399
4.389
4.000
3.989
3.964
3.952
3.947
3.935
3.910
3.900
1.656
1.641
1.623
1.615
1.607
1.597
1.580
1.534
1.516
1.506
1.498
1.482
1.471
0.872
0.860
0.852
0.840
1H NMR, 500 MHz, CDCl3
Ph
O
O
N
H
H
N
O
H
N
O
N
H
O
O
Ph
2.12a
4.4 ppm
4.0 ppm
0.969
1.940
9
8
7
6
5
4
3
2
1
ppm
0.89
11.82
0.86
2.00
1.96
0.97
1.94
1.97
1.01
5.85

^{13}C NMR, 125 MHz, $CDCl_3$

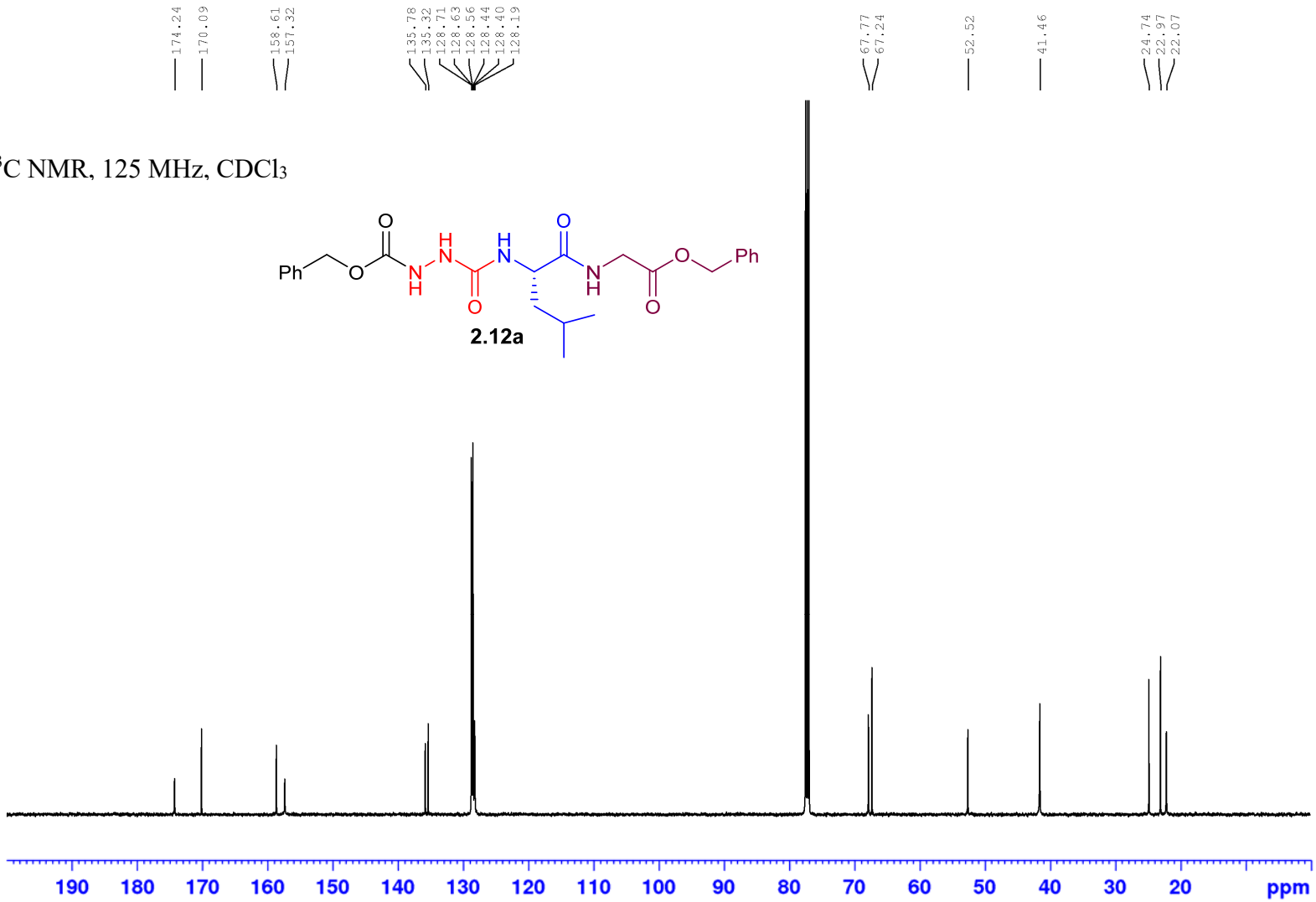

^{1}H NMR, 500 MHz, $CDCl_3$

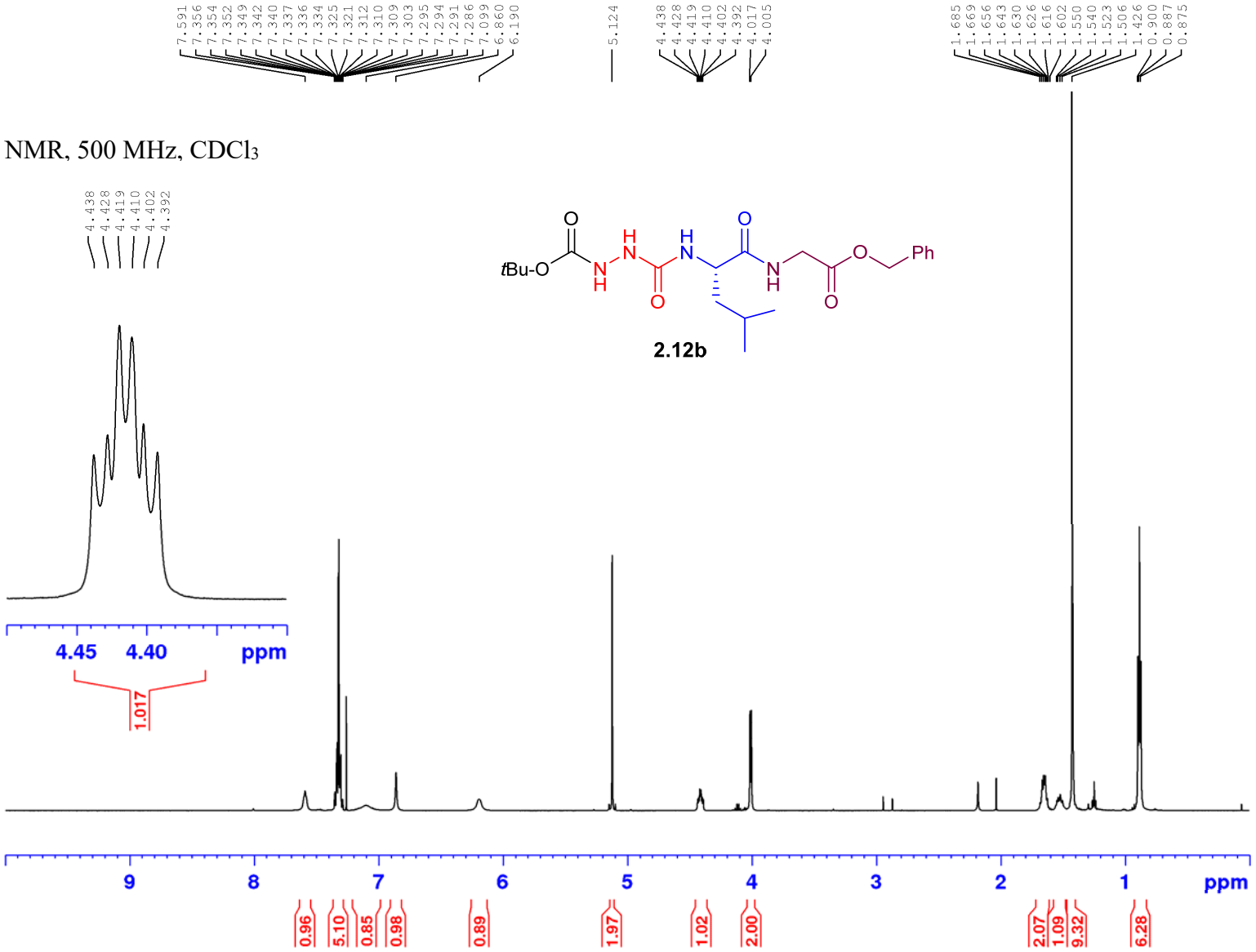

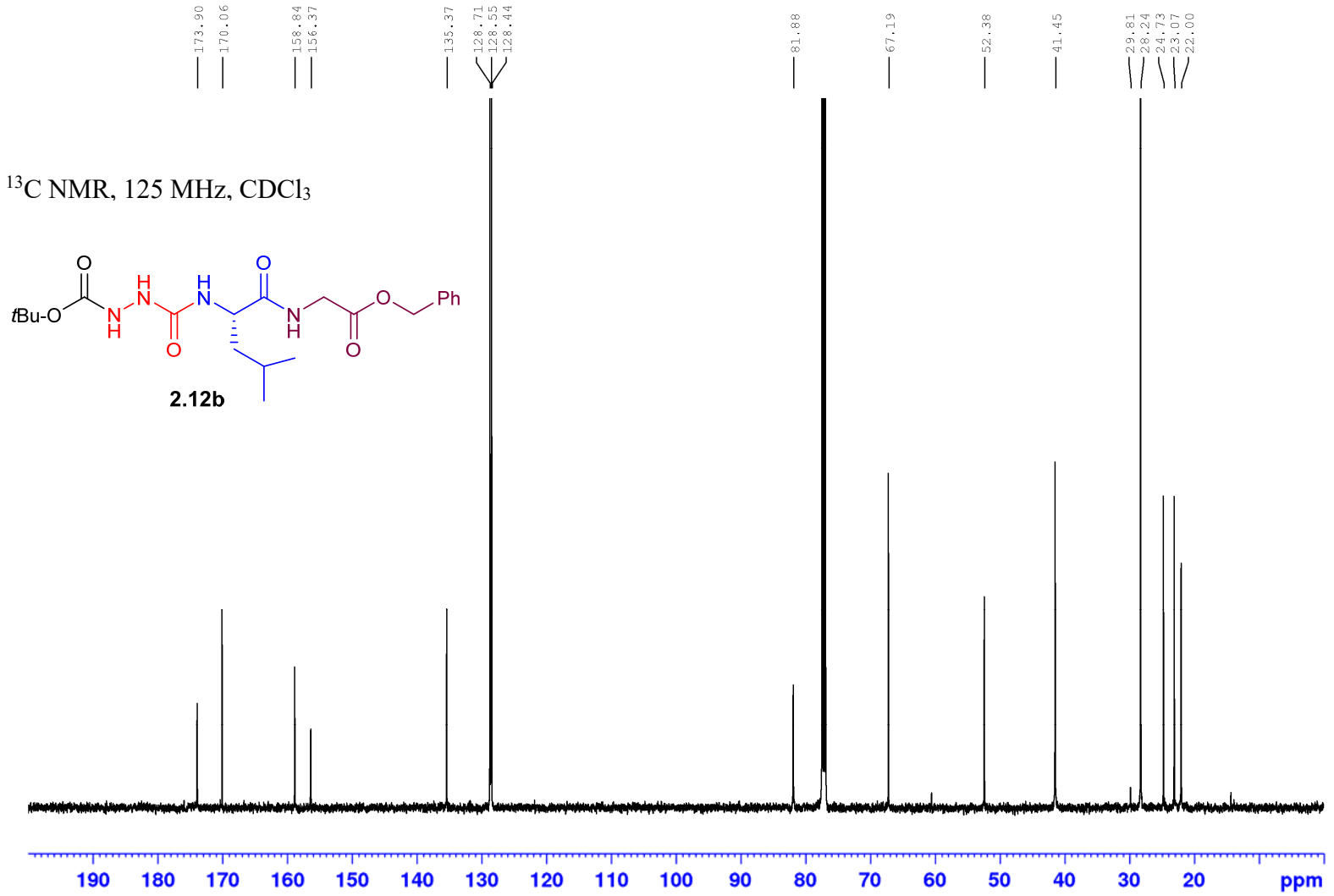

^{13}C NMR, 125 MHz, $CDCl_3$

2.12b

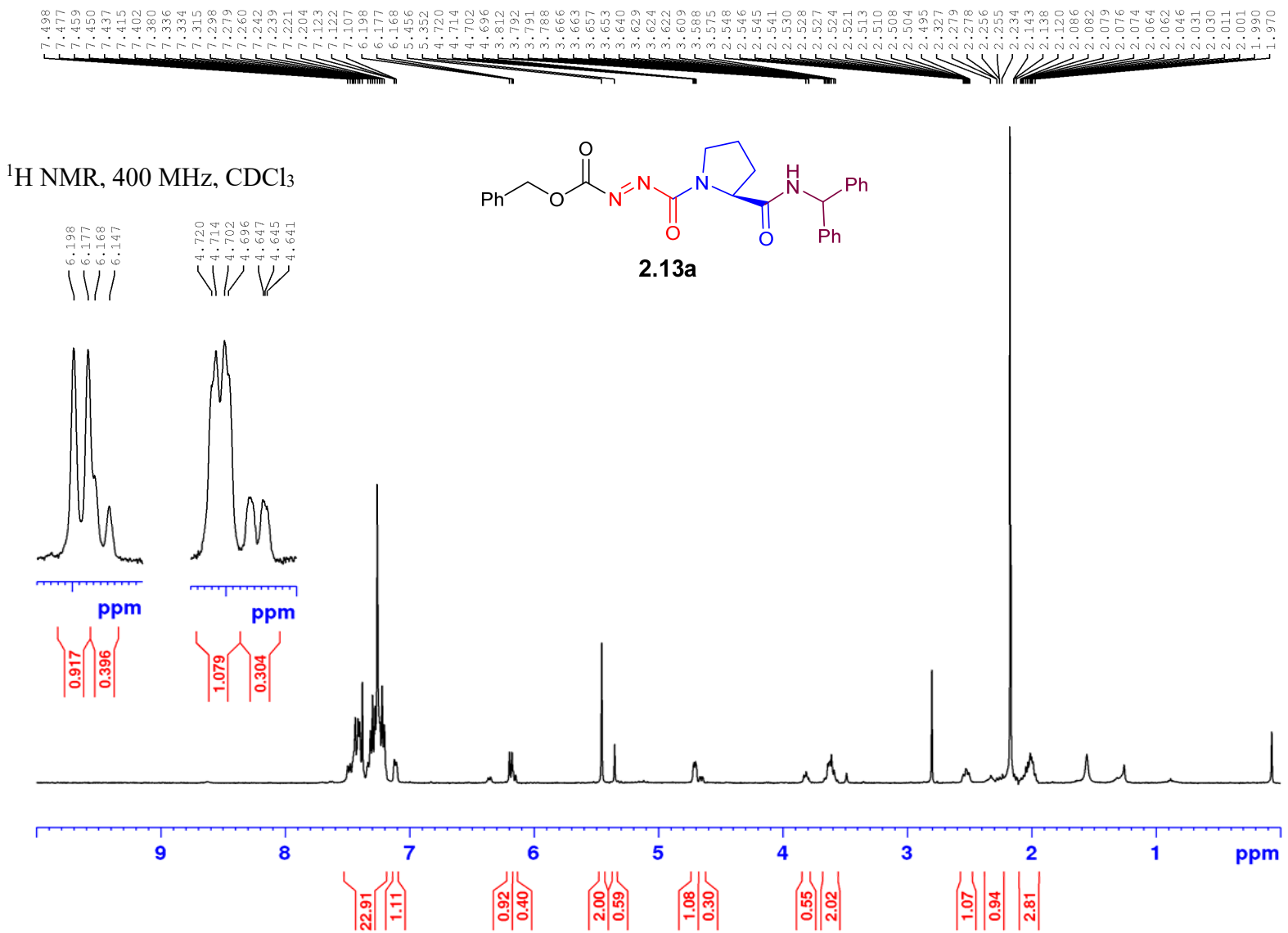
^{1}H NMR, 400 MHz, CDCl$_3$
2.13a
ppm
9
8
7
6
5
4
3
2
1
ppm

^{1}H NMR, 500 MHz, $CDCl_3$

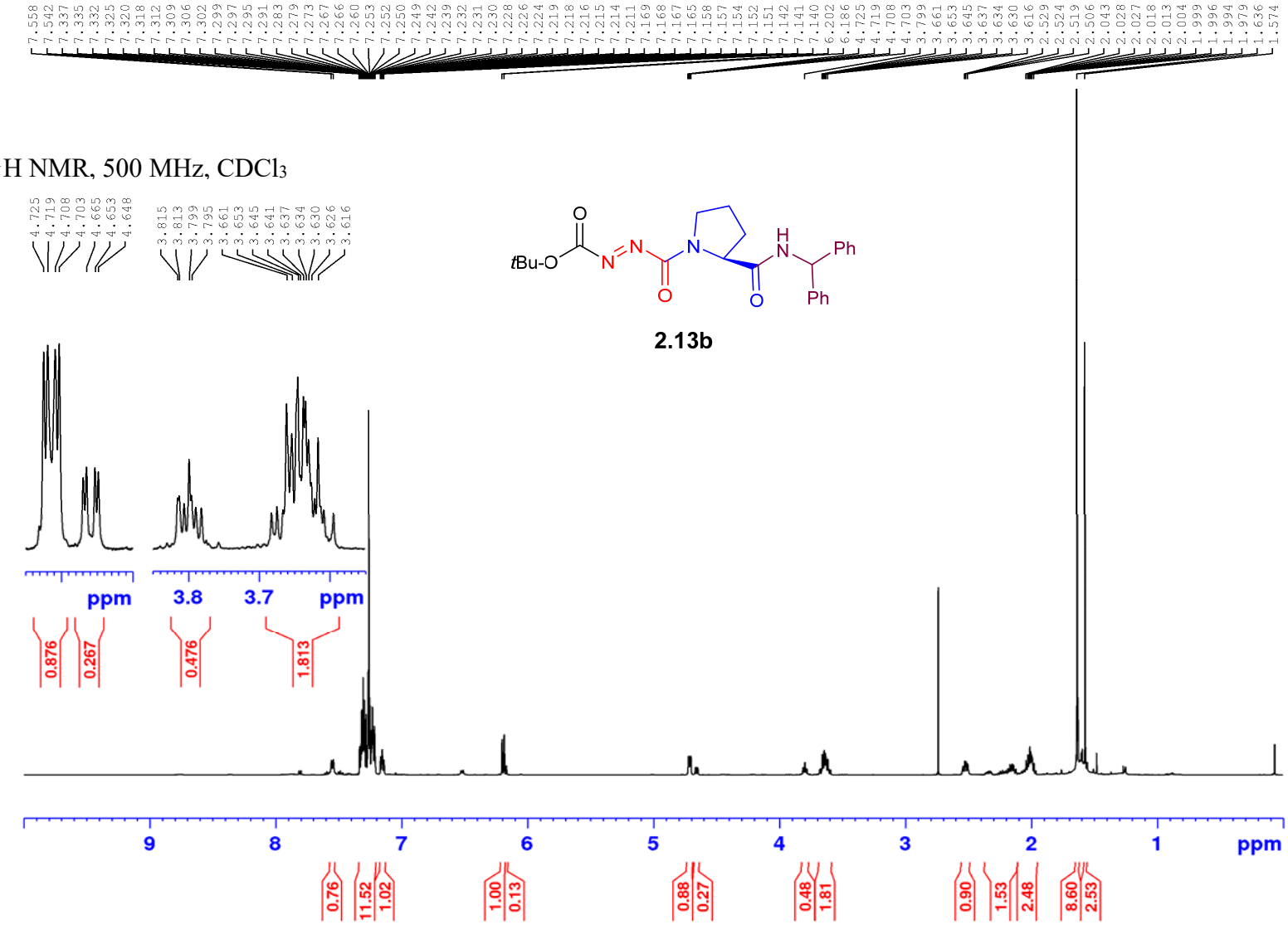

^{1}H NMR, 500 MHz, $CDCl_3$

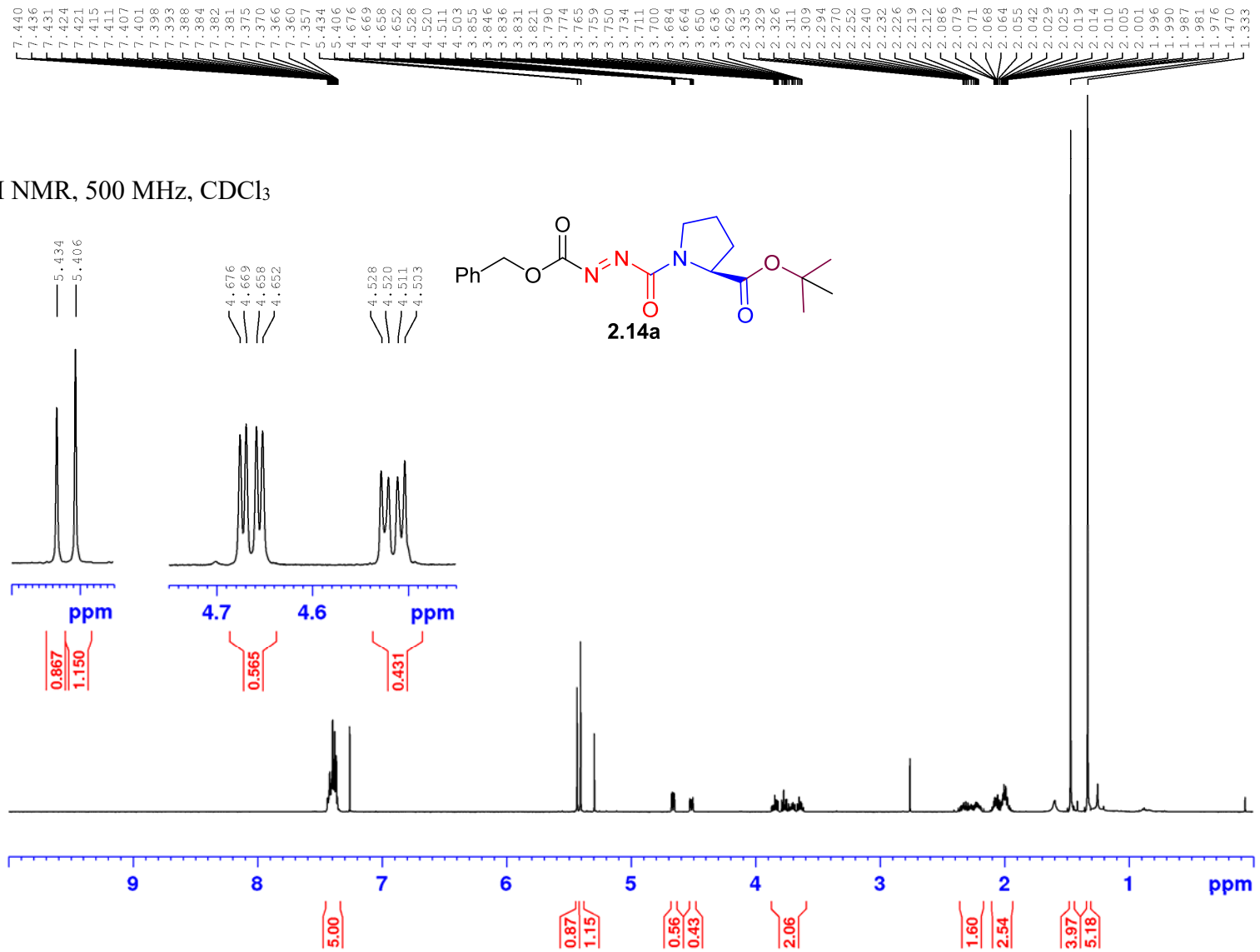

^{13}C NMR, 125 MHz, $CDCl_3$

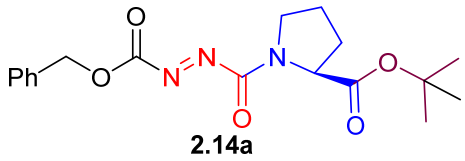

2.14a

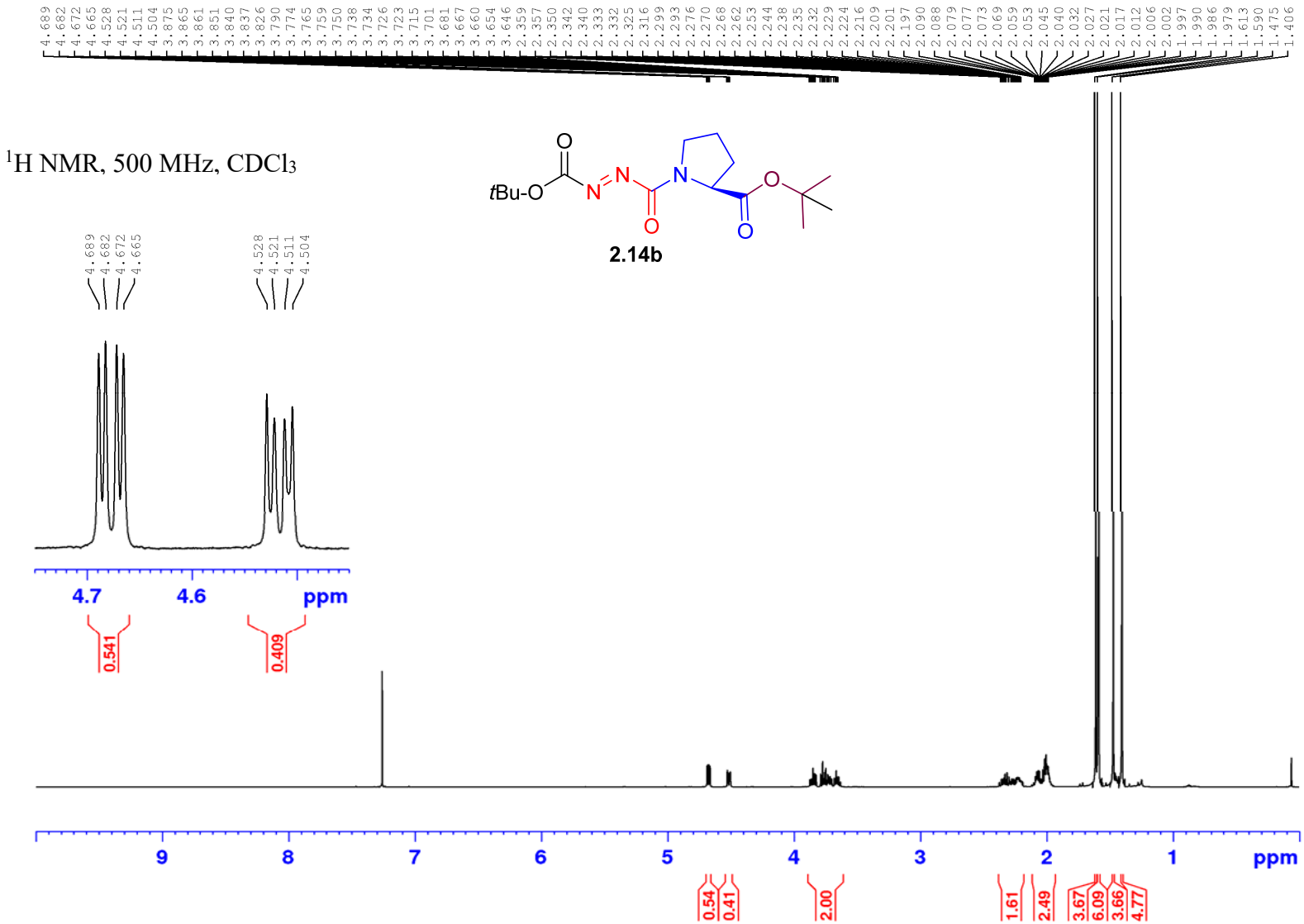
4.689
4.682
4.672
4.665
4.528
4.521
4.511
4.504
3.875
3.865
3.861
3.851
3.840
3.837
3.826
3.790
3.774
3.765
3.759
3.750
3.738
3.734
3.726
3.723
3.715
3.701
3.681
3.667
3.660
3.654
3.646
2.359
2.357
2.350
2.342
2.340
2.333
2.332
2.325
2.316
2.299
2.293
2.276
2.270
2.268
2.262
2.253
2.244
2.238
2.235
2.232
2.229
2.224
2.216
2.209
2.201
2.197
2.090
2.088
2.079
2.077
2.073
2.069
2.059
2.053
2.045
2.040
2.032
2.027
2.021
2.017
2.012
2.006
2.002
1.997
1.990
1.986
1.979
1.613
1.590
1.475
1.406
1H NMR, 500 MHz, CDCl3
tBu-O
2.14b
4.7
4.6
ppm
0.541
0.409
9
8
7
6
5
4
3
2
1
ppm
0.54
0.41
2.00
1.61
2.49
3.67
6.09
3.66
4.77

^{13}C NMR, 125 MHz, $CDCl_3$

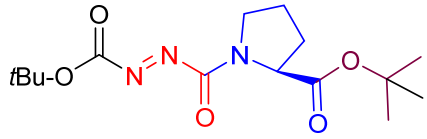

2.14b

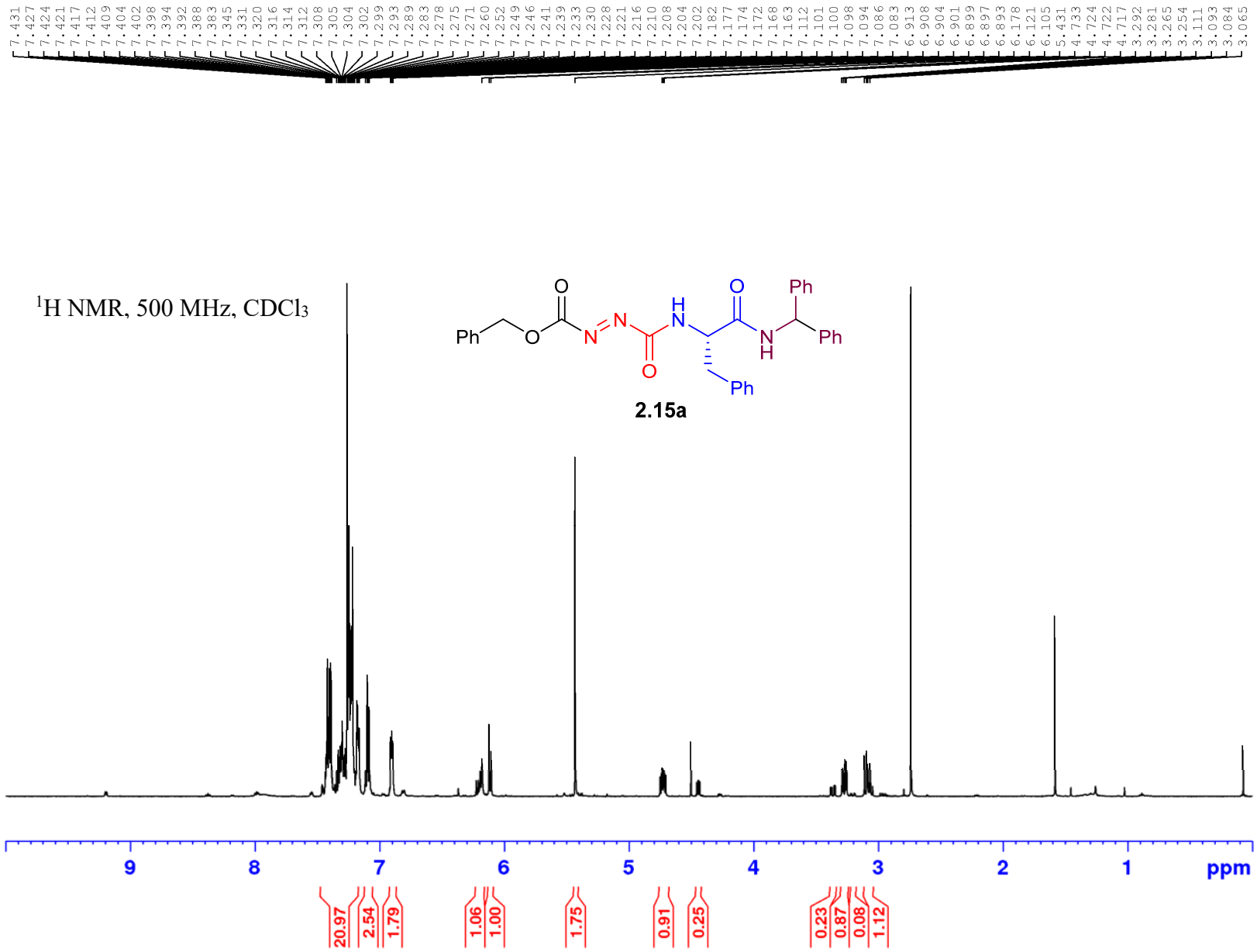
7.431
7.427
7.424
7.421
7.417
7.412
7.409
7.404
7.402
7.398
7.394
7.392
7.388
7.383
7.345
7.331
7.320
7.316
7.314
7.312
7.308
7.305
7.304
7.302
7.299
7.293
7.289
7.283
7.278
7.275
7.271
7.260
7.252
7.249
7.246
7.241
7.239
7.233
7.230
7.228
7.221
7.216
7.210
7.208
7.204
7.202
7.182
7.177
7.174
7.172
7.168
7.163
7.112
7.101
7.100
7.098
7.094
7.086
7.083
6.913
6.908
6.904
6.901
6.899
6.897
6.893
6.178
6.121
6.105
5.431
4.733
4.724
4.722
4.717
3.292
3.281
3.265
3.254
3.111
3.093
3.084
3.065
1H NMR, 500 MHz, CDCl3
Ph
O
O
N
N
O
H
N
O
N
H
Ph
Ph
Ph
2.15a
9
8
7
6
5
4
3
2
1
ppm
20.97
2.54
1.79
1.06
1.00
1.75
0.91
0.25
0.23
0.87
0.08
1.12

^{1}H NMR, 500 MHz, CD_3OD

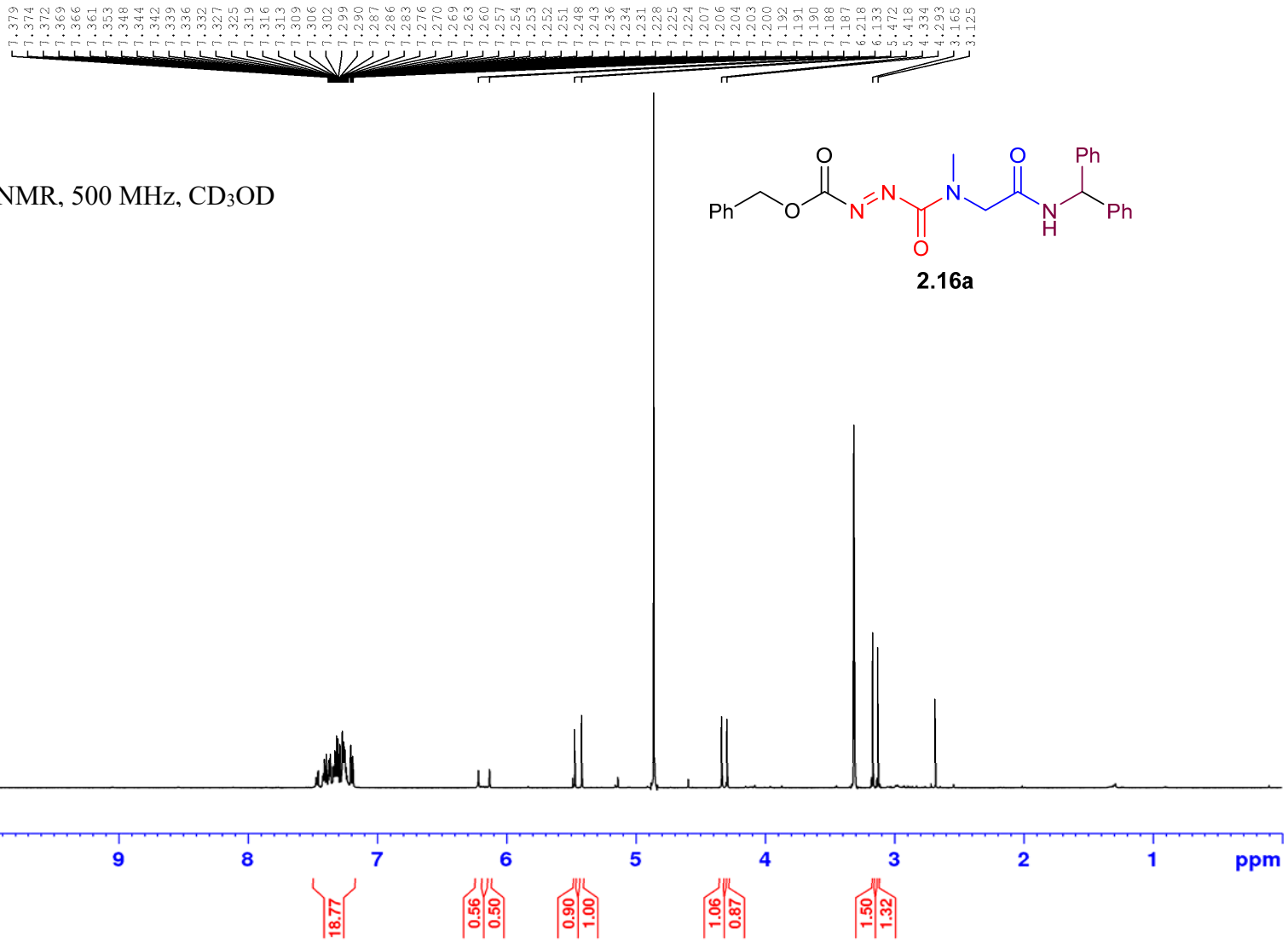

^{13}C NMR, 125 MHz, $CDCl_3$

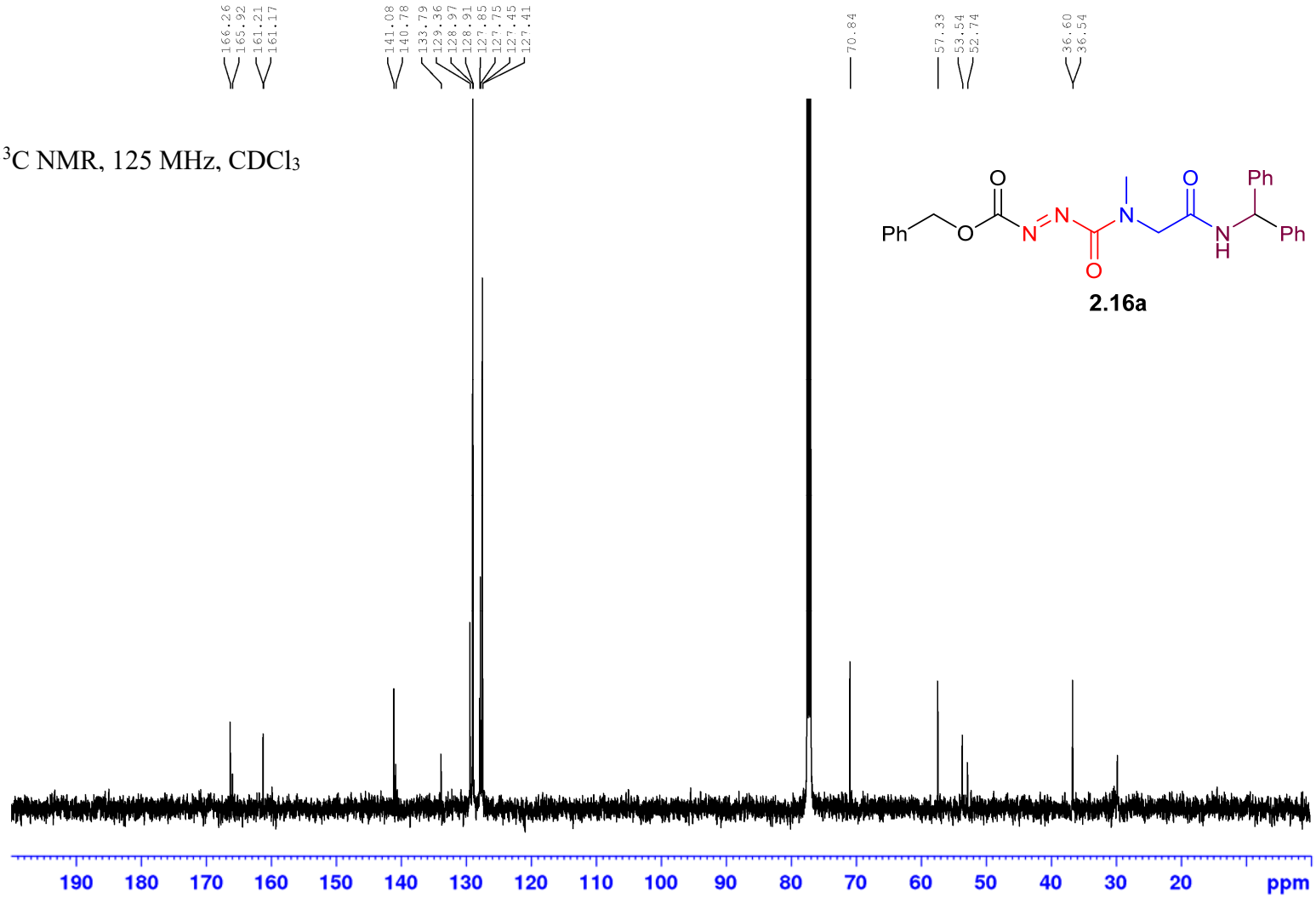

2.16a

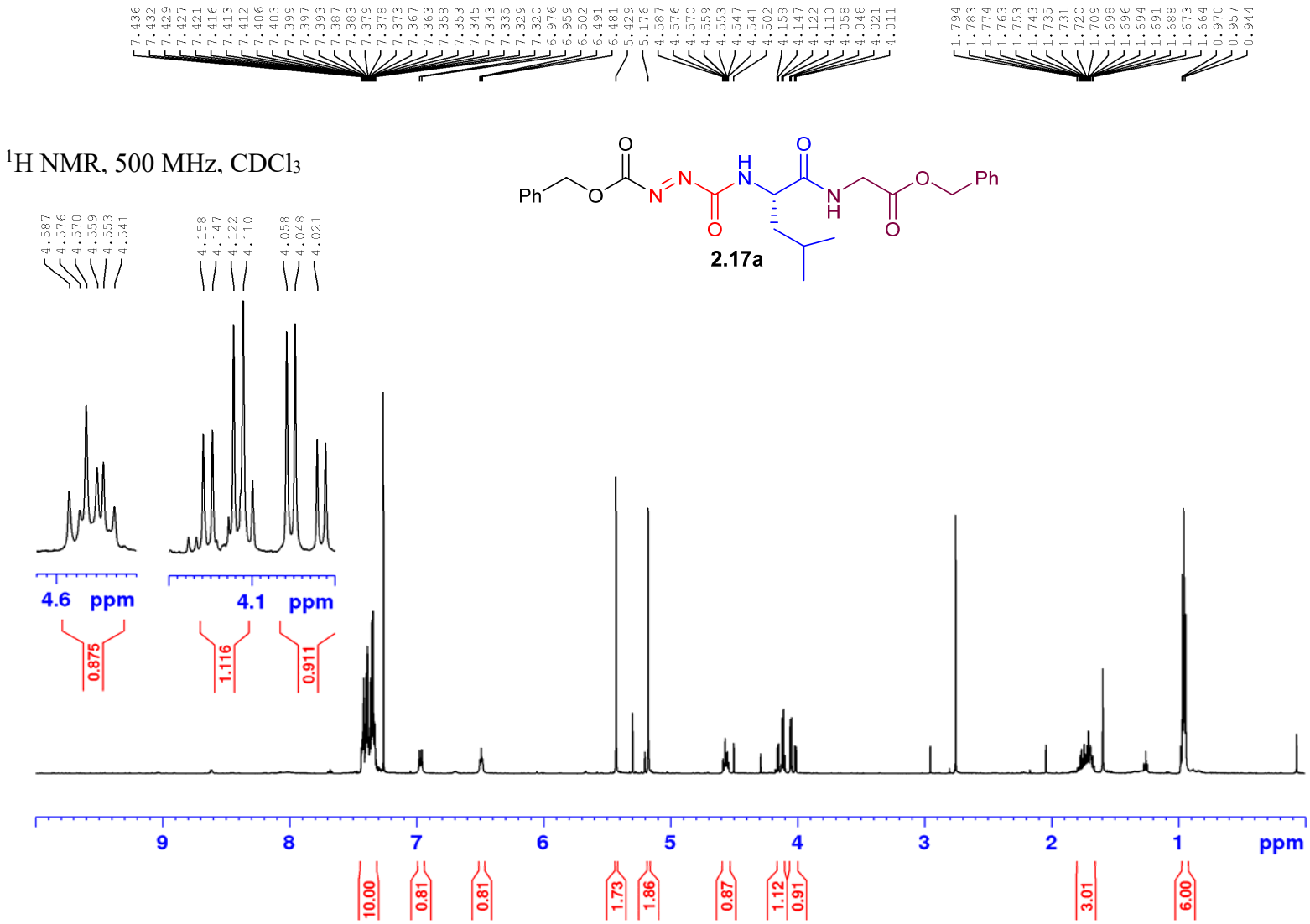
7.436
7.432
7.429
7.427
7.421
7.416
7.413
7.412
7.406
7.403
7.399
7.397
7.393
7.387
7.383
7.379
7.378
7.373
7.367
7.363
7.358
7.353
7.345
7.343
7.335
7.329
7.320
6.976
6.959
6.502
6.491
6.481
5.429
5.176
4.587
4.576
4.570
4.559
4.553
4.547
4.541
4.502
4.158
4.147
4.122
4.110
4.058
4.048
4.021
4.011
1.794
1.783
1.774
1.763
1.753
1.743
1.735
1.731
1.720
1.709
1.698
1.696
1.694
1.691
1.688
1.673
1.664
0.970
0.957
0.944
1H NMR, 500 MHz, CDCl3
Ph
O
O
N
N
H
O
N
H
O
O
O
Ph
2.17a
4.587
4.576
4.570
4.559
4.553
4.541
4.158
4.147
4.122
4.110
4.058
4.048
4.021
4.6 ppm
4.1 ppm
0.875
1.116
0.911
9
8
7
6
5
4
3
2
1
ppm
10.00
0.81
0.81
1.73
1.86
0.87
1.12
0.91
3.01
6.00

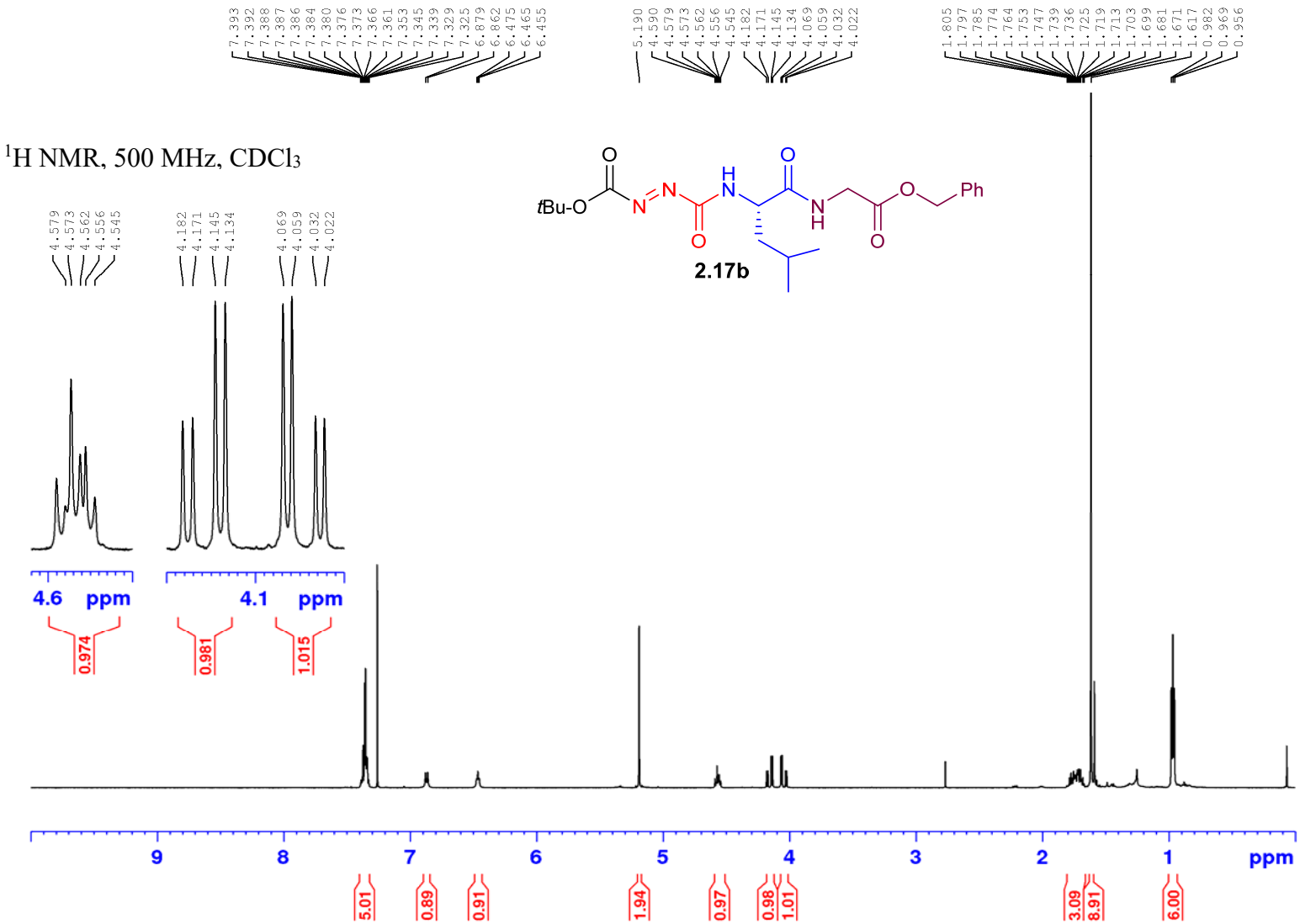
^{1}H NMR, 500 MHz, CDCl$_3$
tBu-O
Ph
2.17b
4.6 ppm
4.1 ppm
9
8
7
6
5
4
3
2
1
ppm

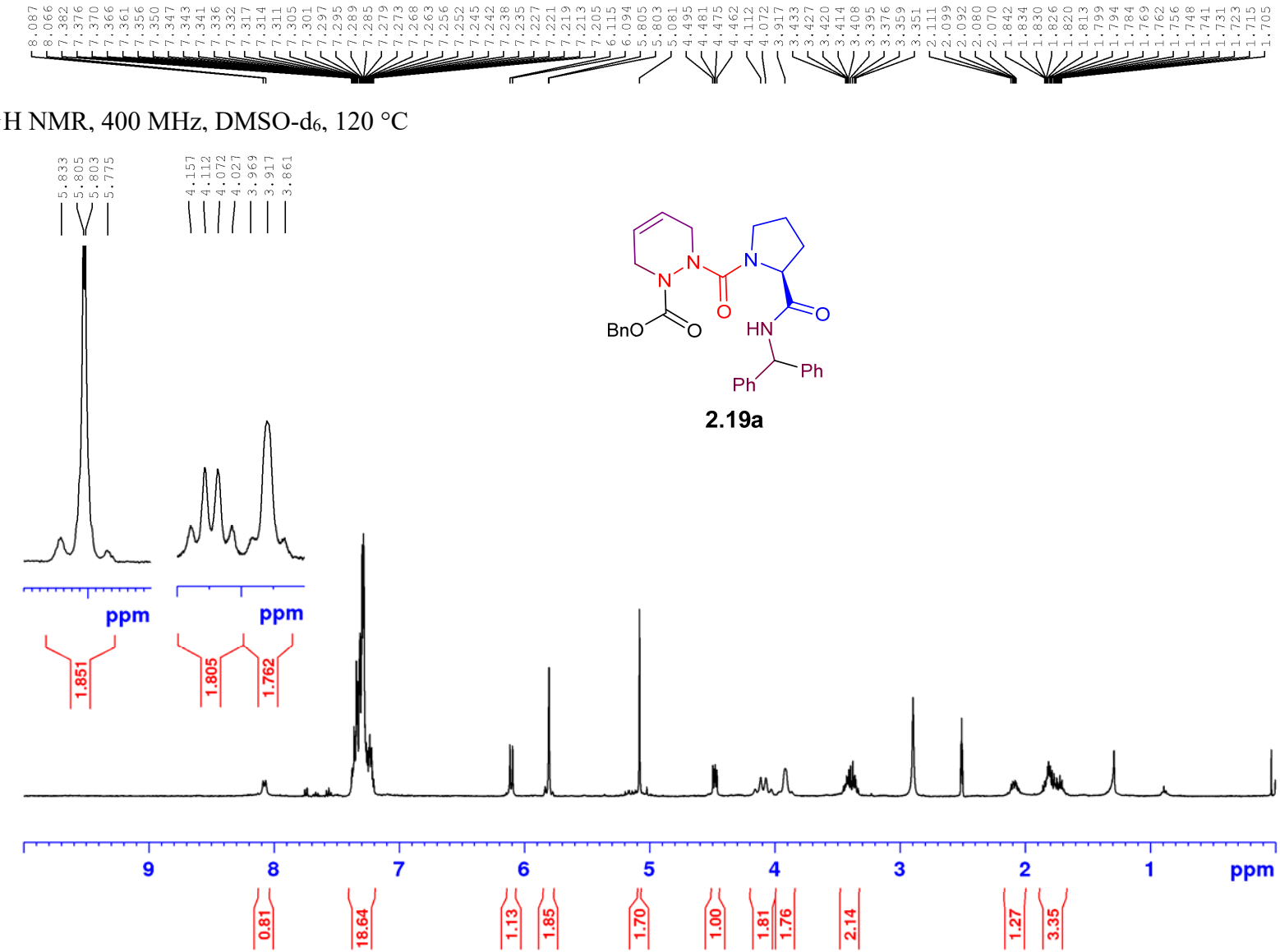

^{1}H NMR, 400 MHz, DMSO-d_6, 120 °C

^{13}C NMR, 100 MHz, DMSO-d_6, 120 °C

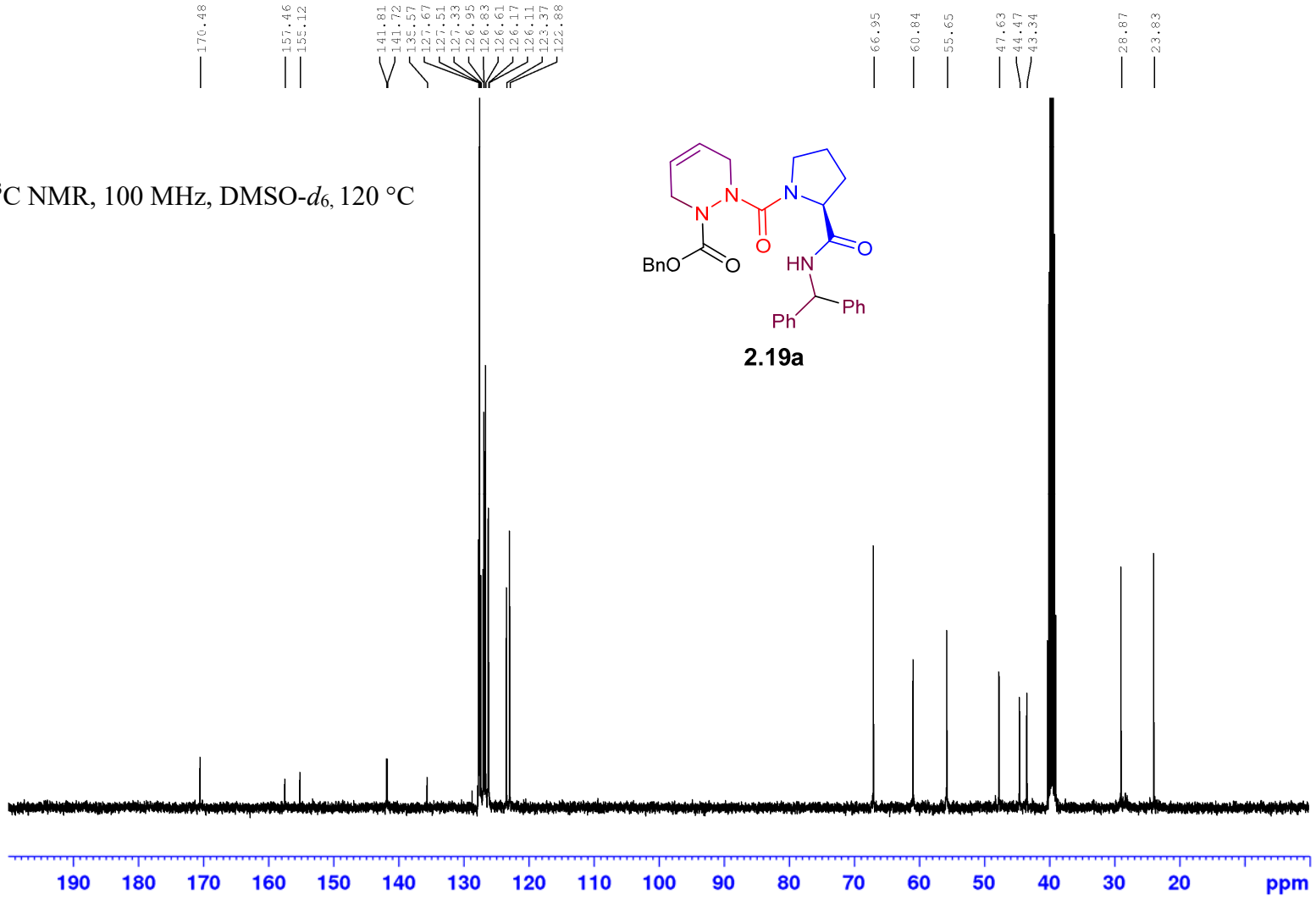

2.19a

^{1}H NMR, 500 MHz, $CDCl_3$

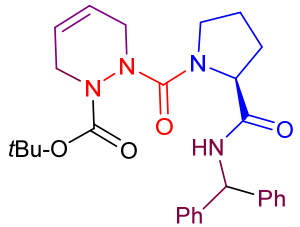

2.19b

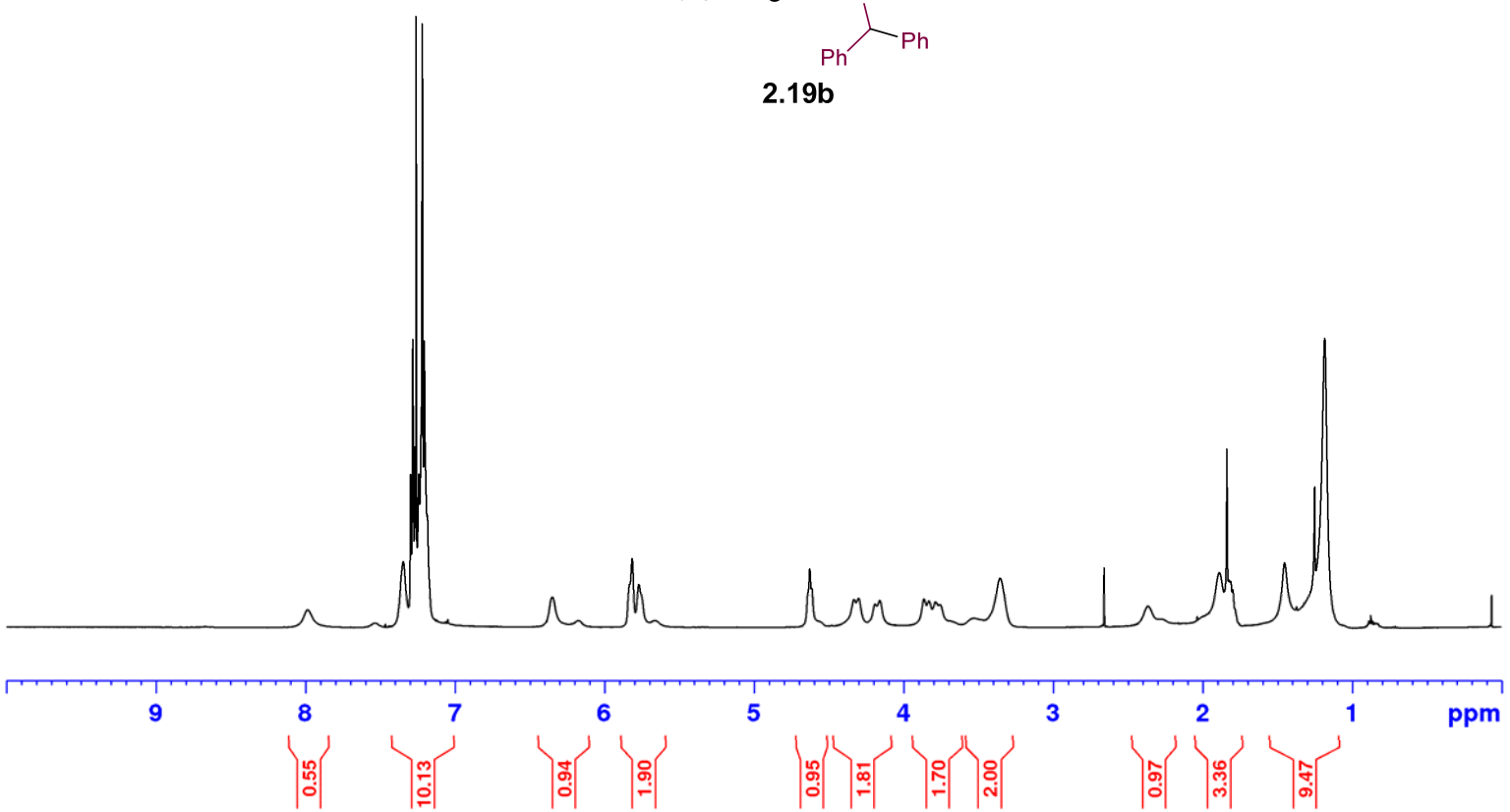

^{13}C NMR, 125 MHz, $CDCl_3$

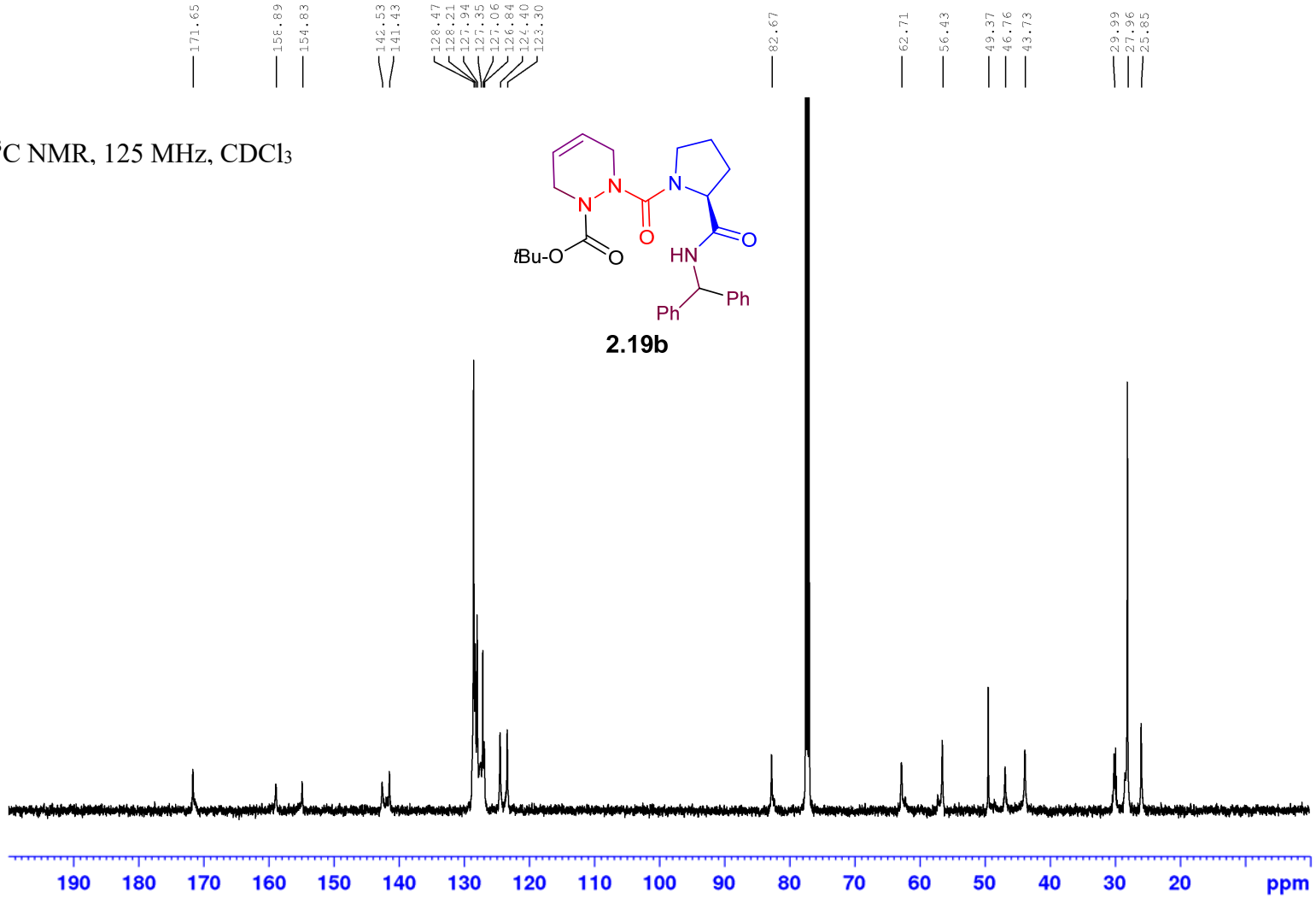

2.19b

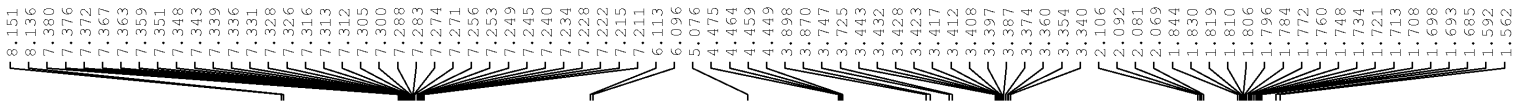

^{1}H NMR, 500 MHz, DMSO-*d*$_6$, 100 °C

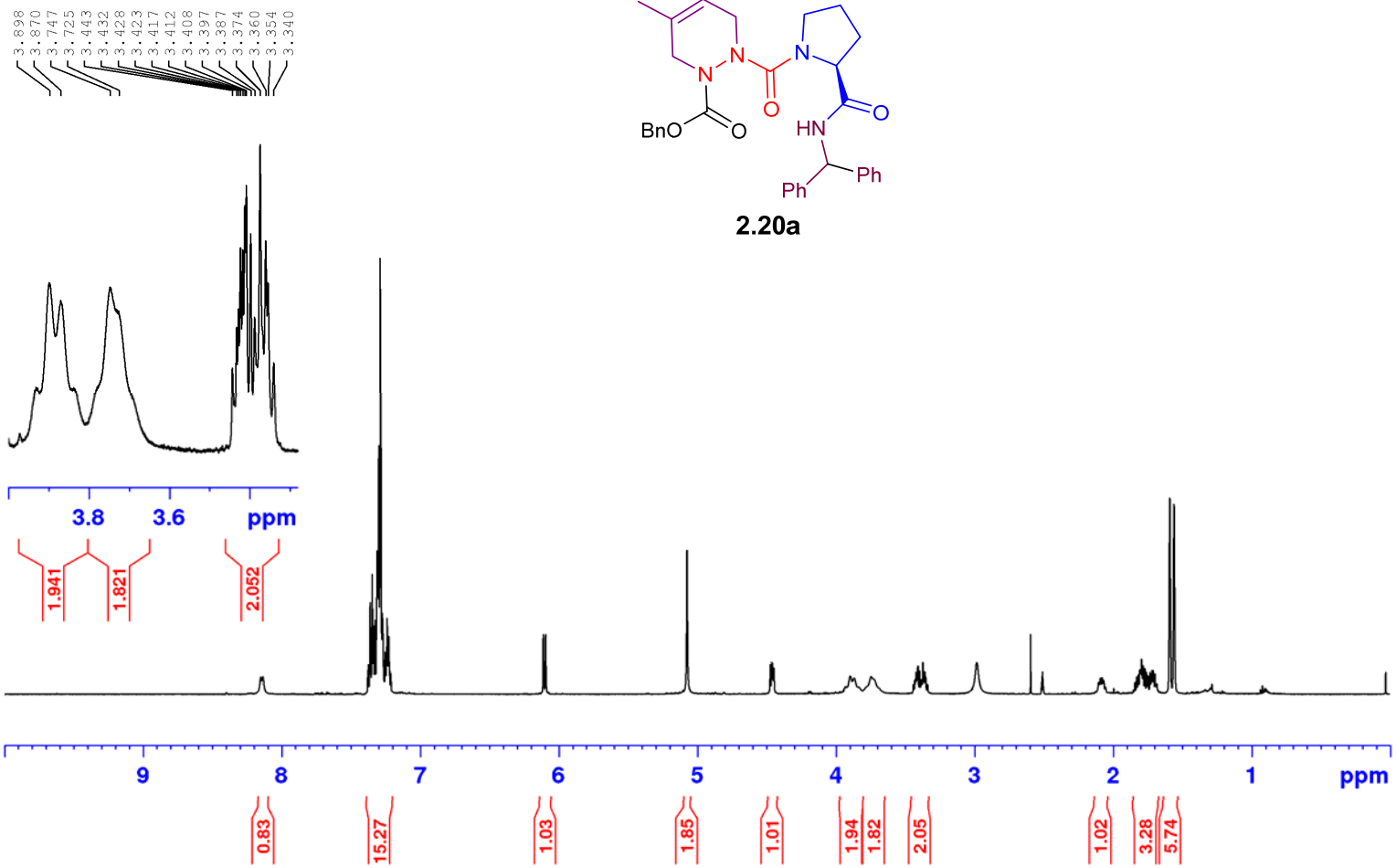

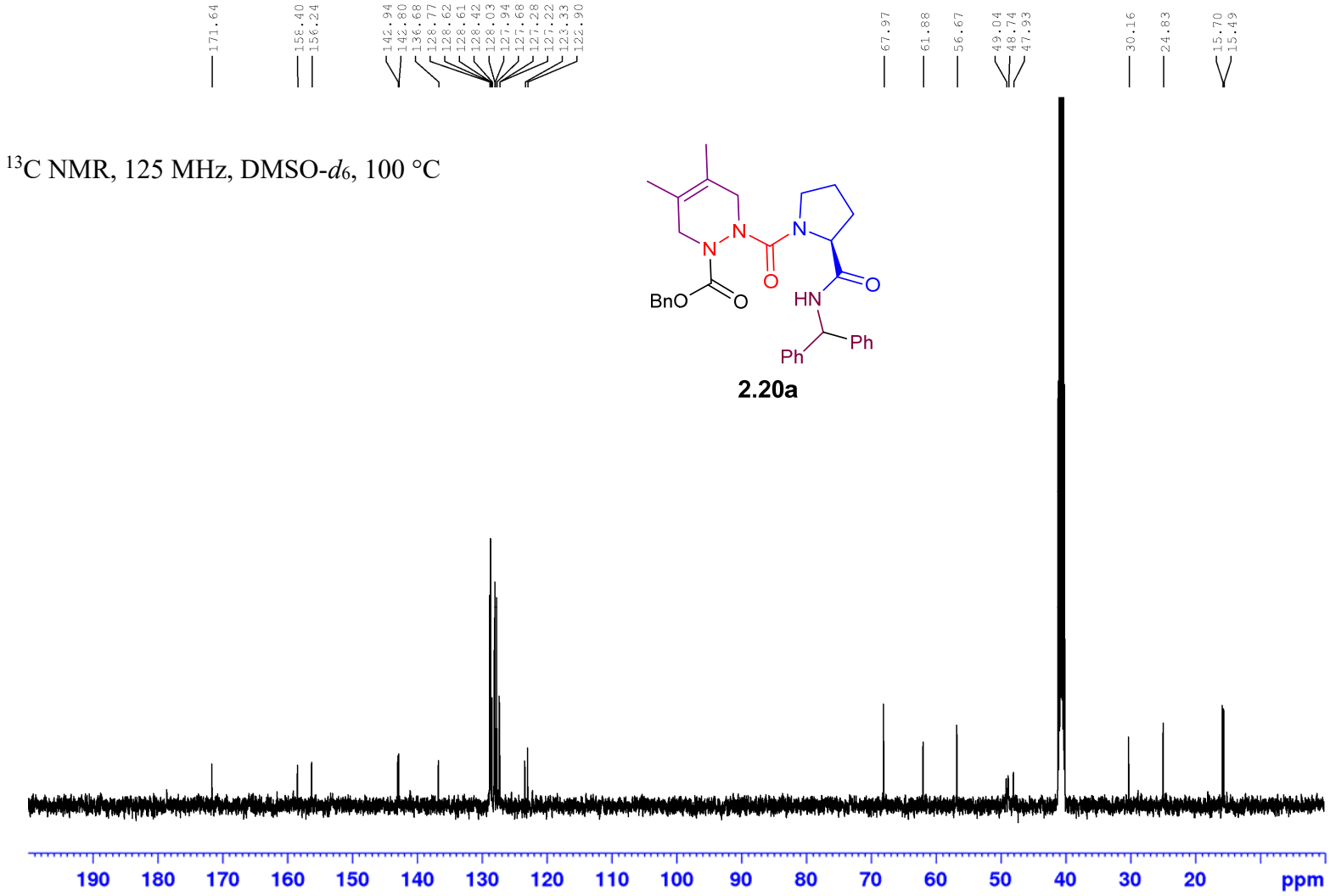

^{13}C NMR, 125 MHz, DMSO-d_6, 100 °C

2.20a

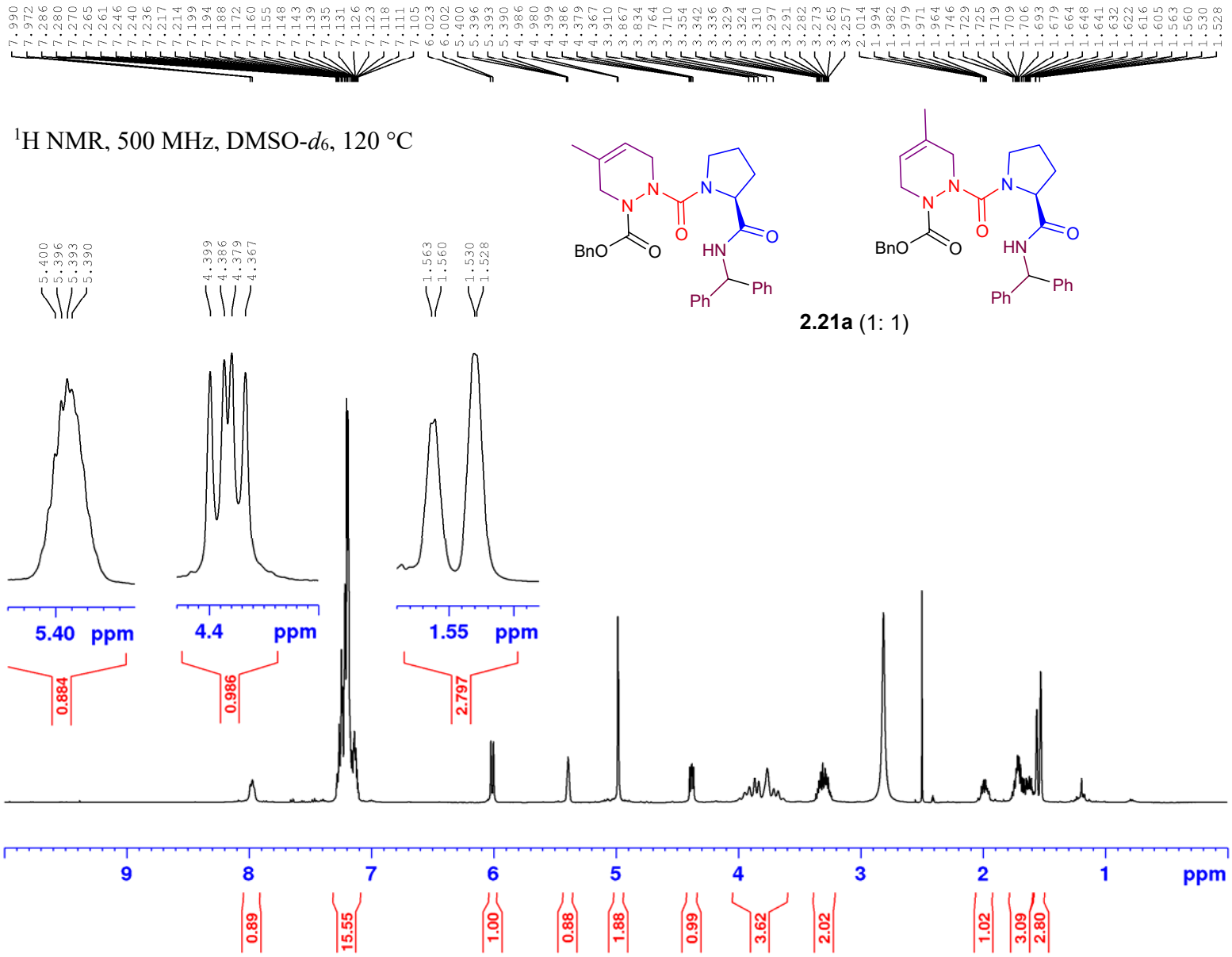

^{1}H NMR, 500 MHz, DMSO-d_6, 120 °C

2.21a (1: 1)

^{13}C NMR, 125 MHz, DMSO-d_6, 120 °C

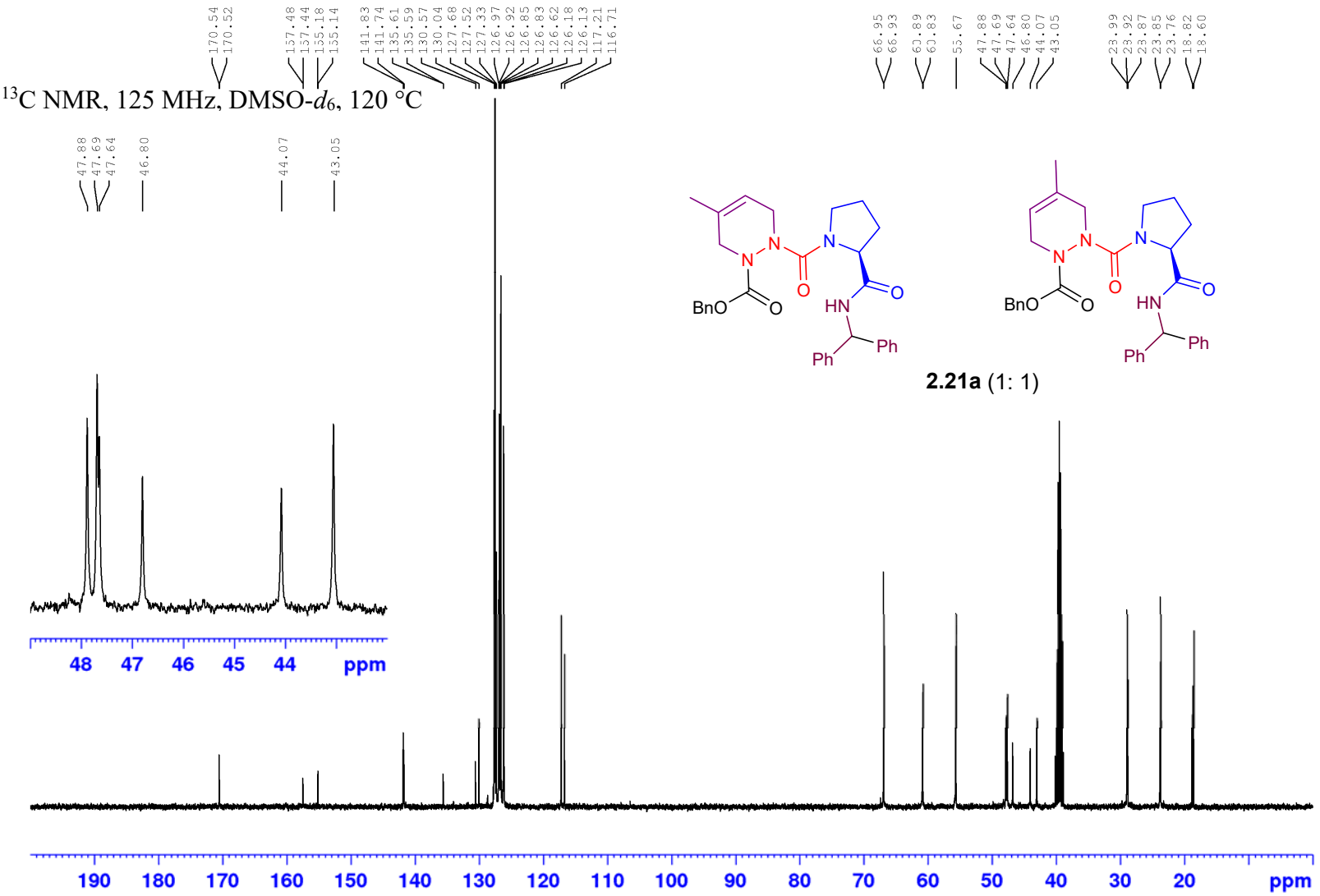

2.21a (1: 1)

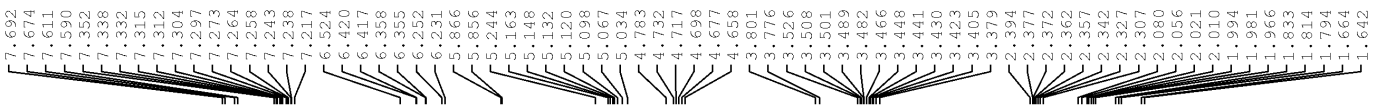

^{1}H NMR, 400 MHz, $CDCl_3$

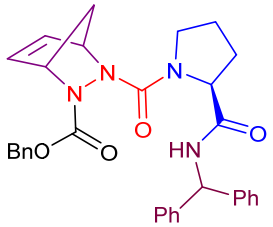

2.22a

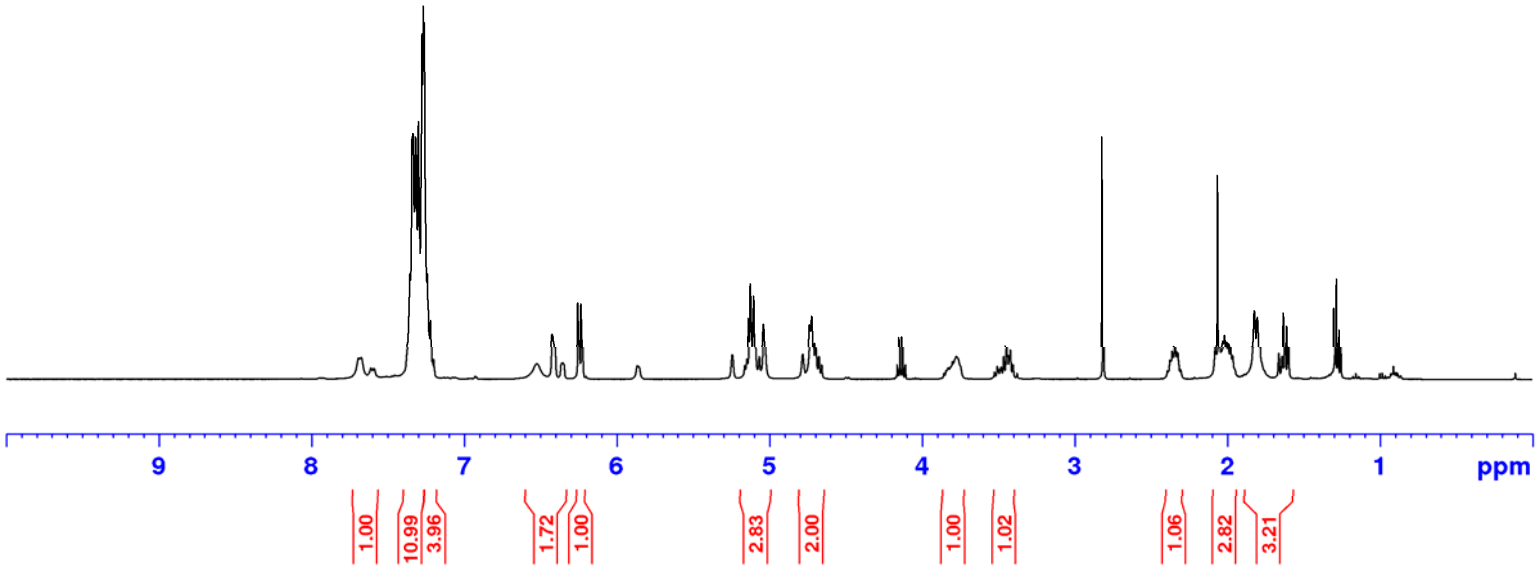

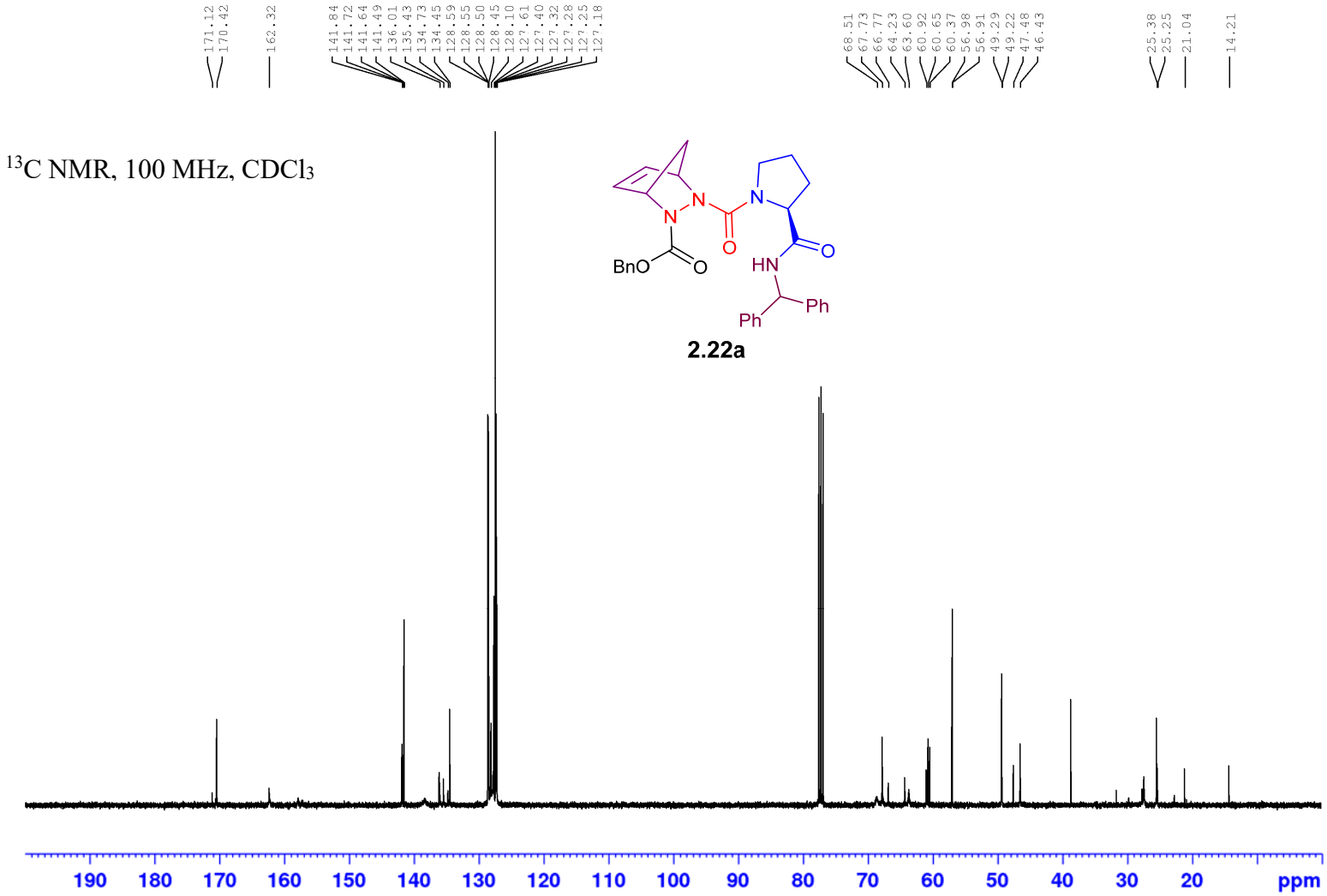

^{13}C NMR, 100 MHz, $CDCl_3$

2.22a

^{1}H NMR, 500 MHz, $CDCl_3$

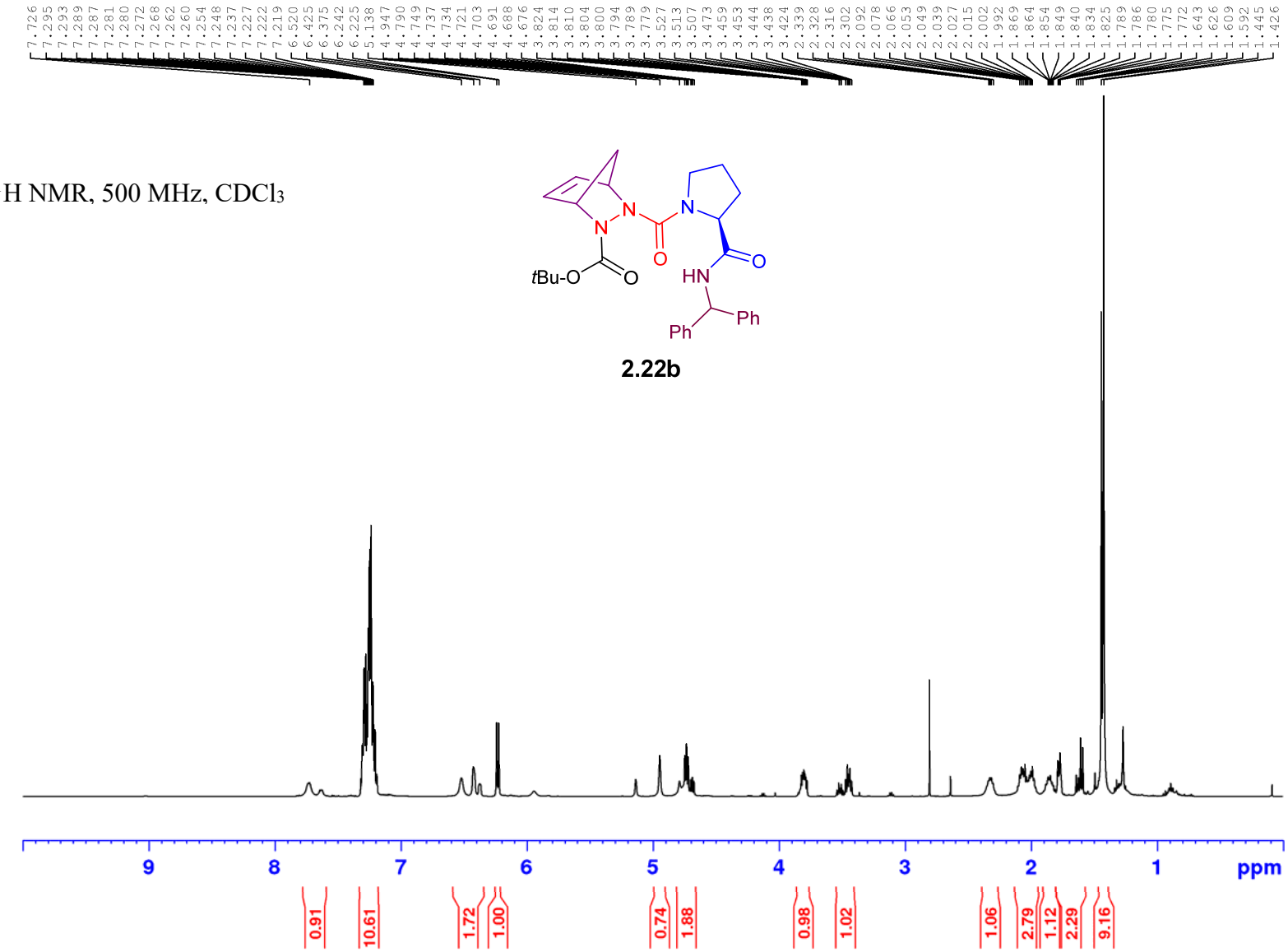

2.22b

^{13}C NMR, 125 MHz, $CDCl_3$

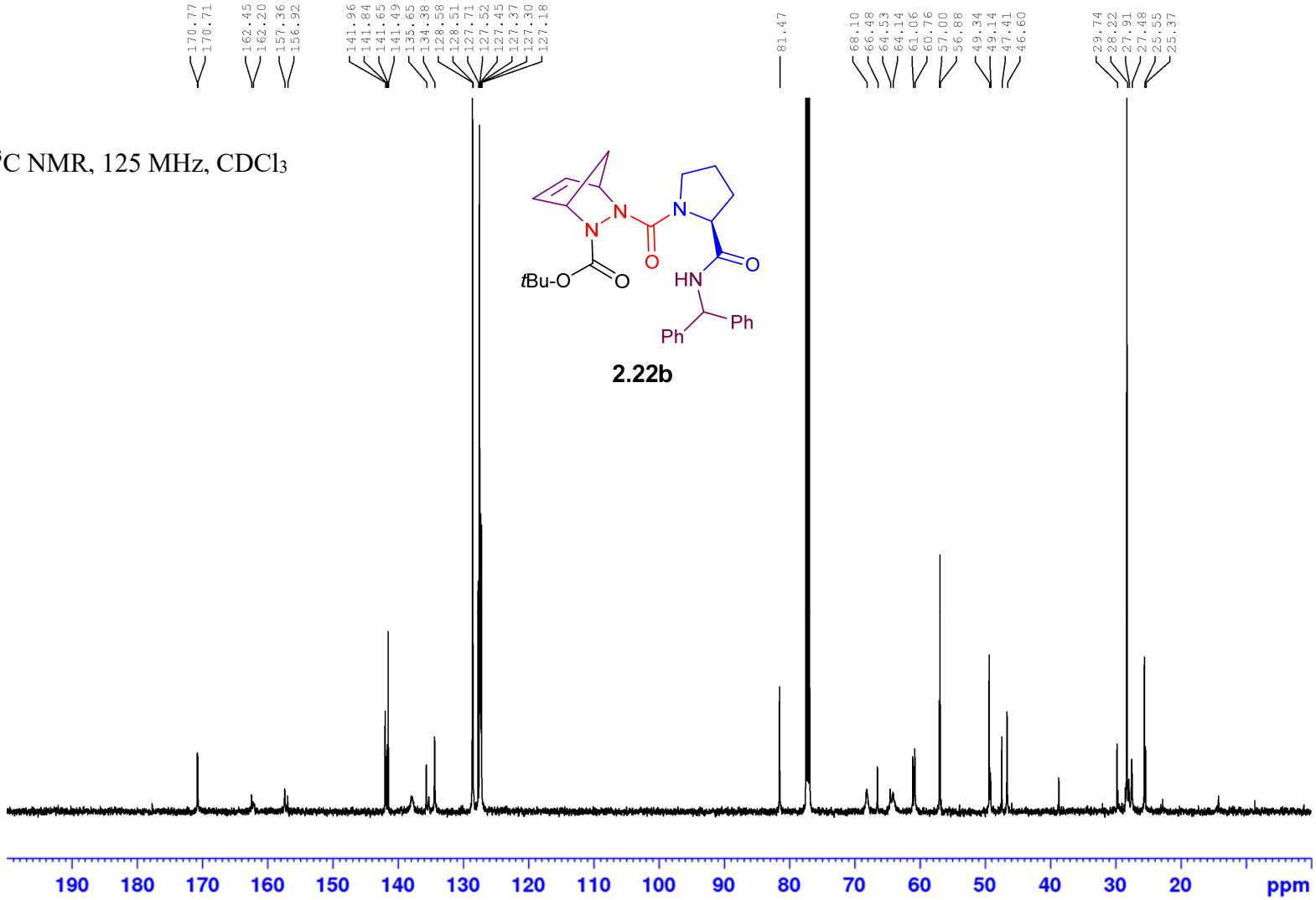

2.22b

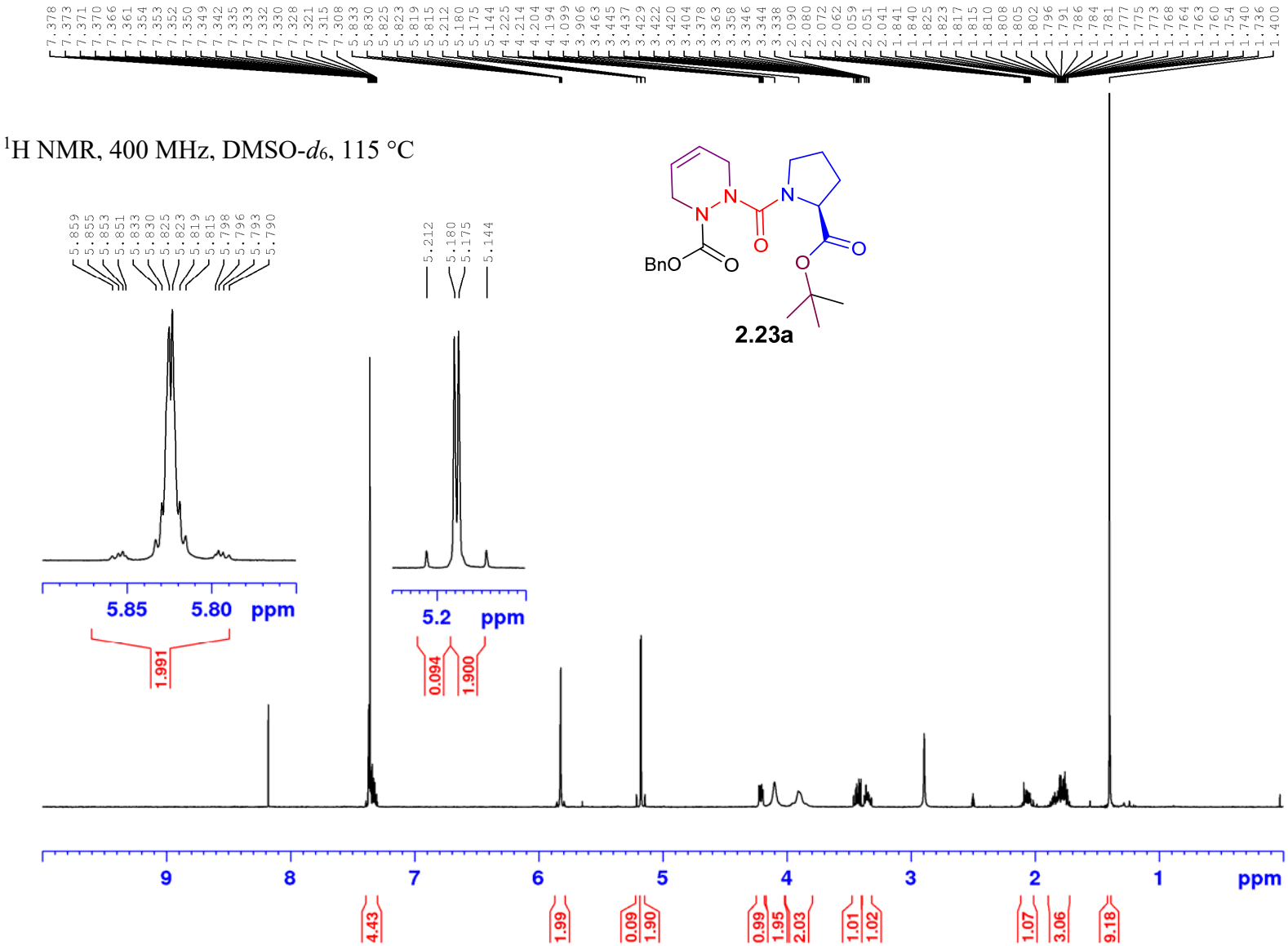

^{1}H NMR, 400 MHz, DMSO-d_6, 115 °C

^{13}C NMR, 100 MHz, DMSO-d_6, 115 °C

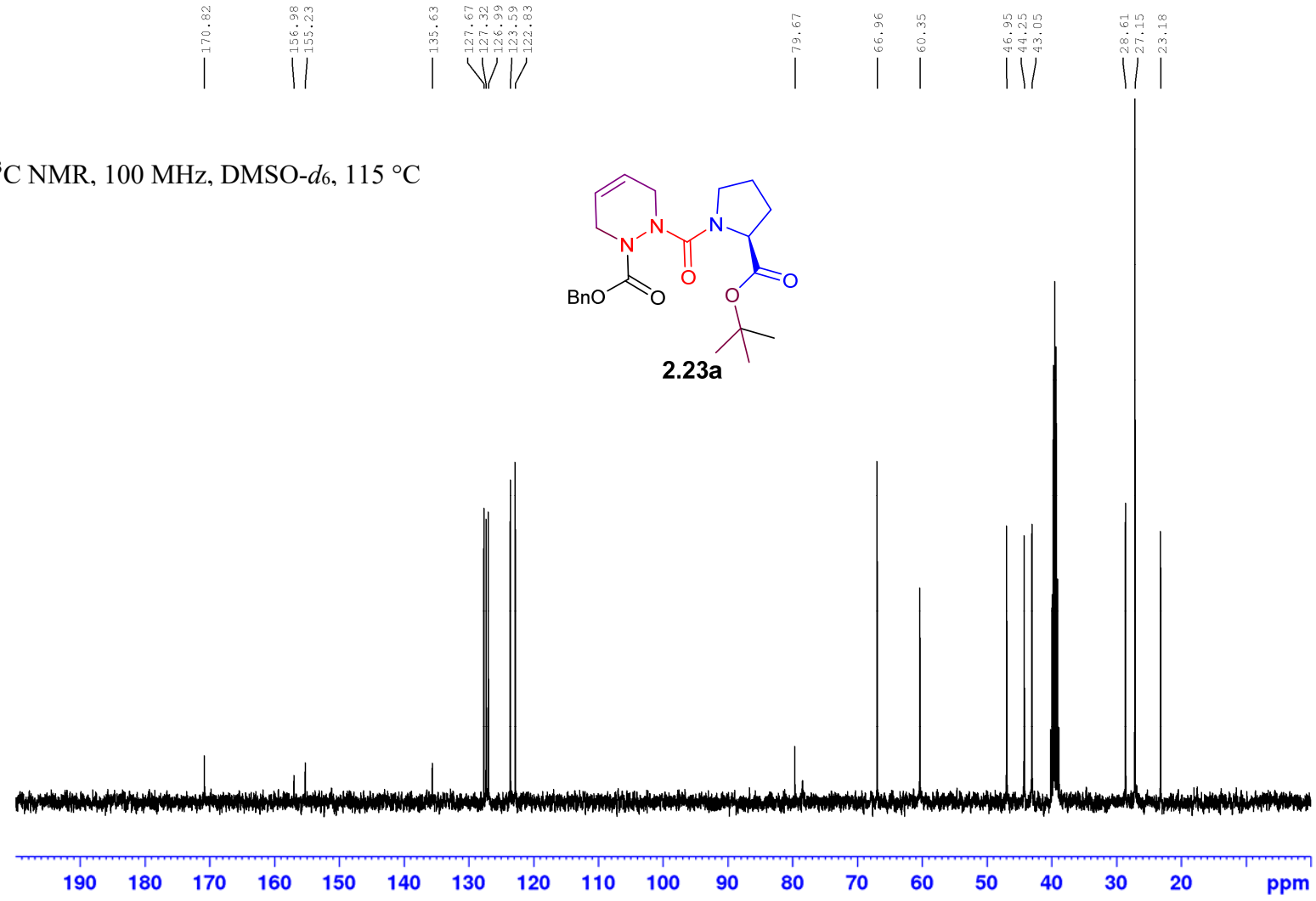

^{1}H NMR, 400 MHz, DMSO-*d*$_6$, 110 °C

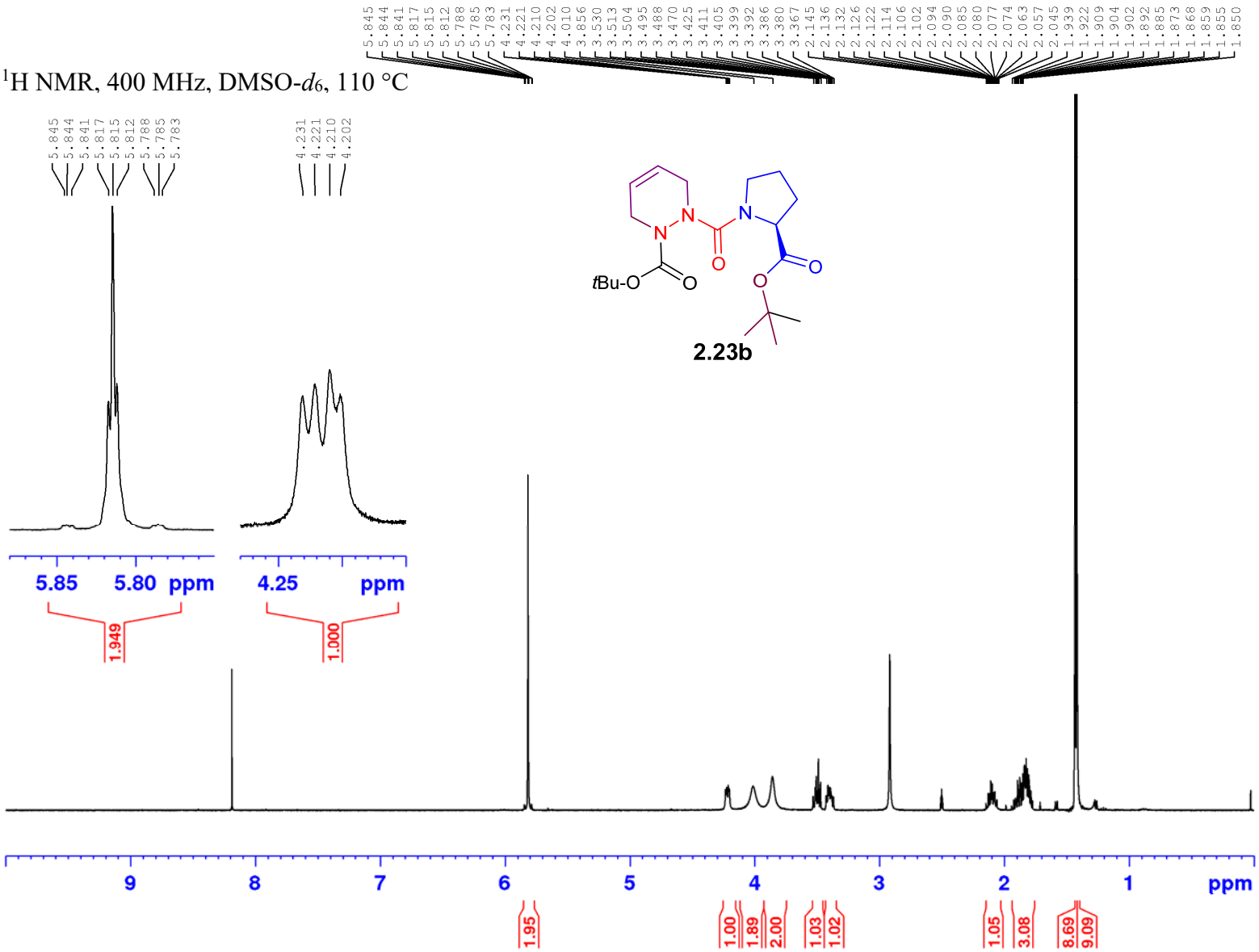

^{13}C NMR, 100 MHz, DMSO-d_6, 110 °C

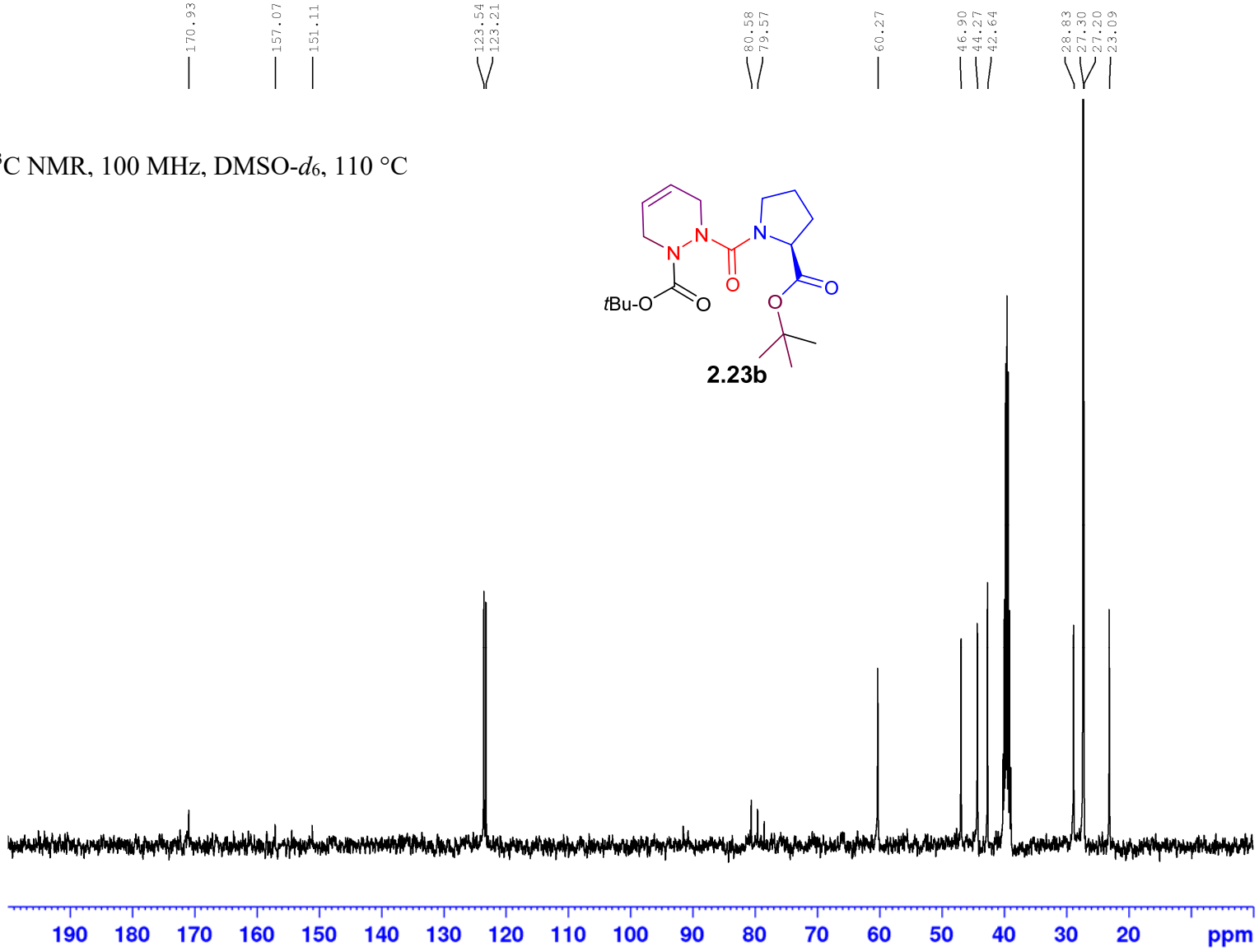

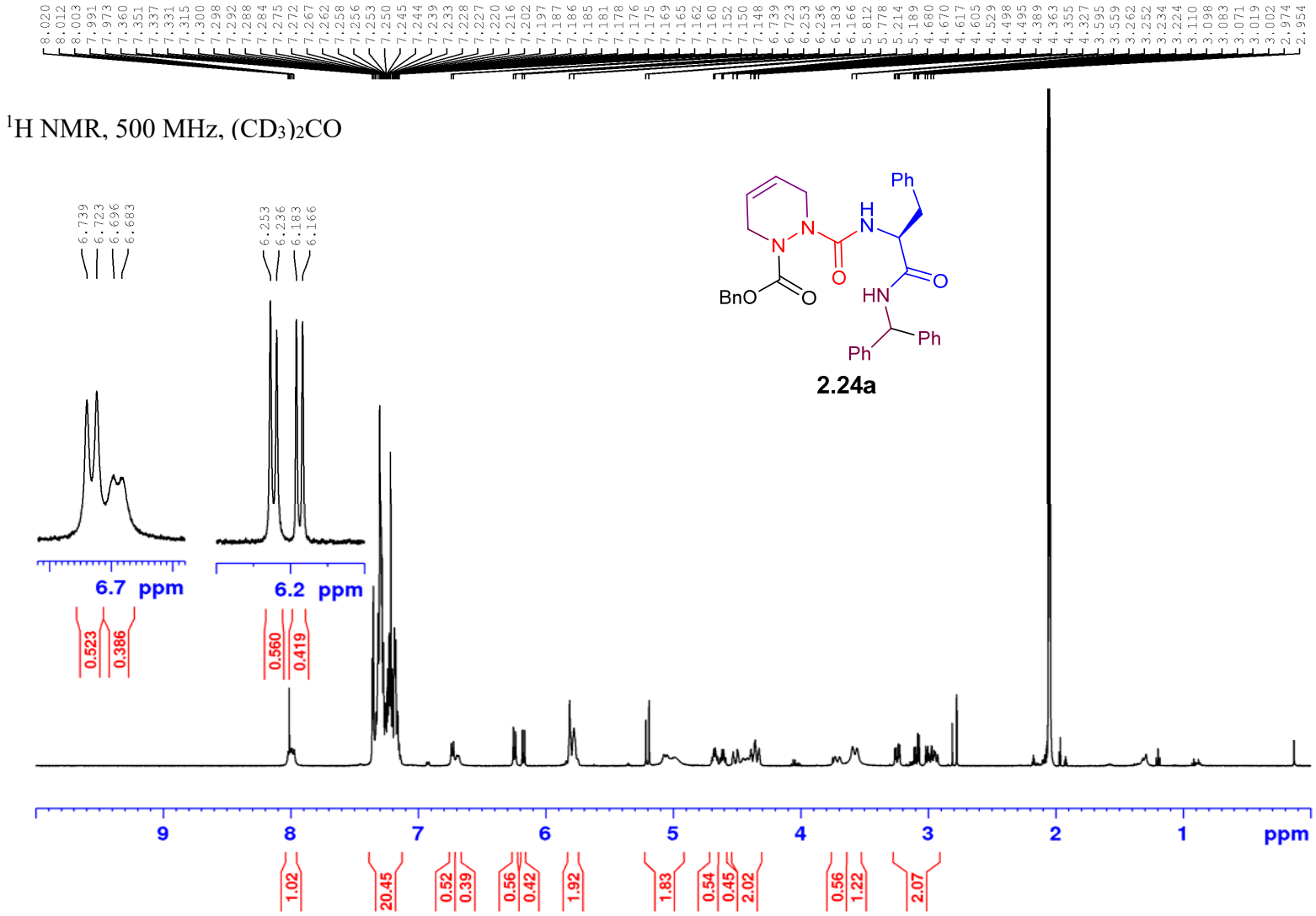

^{1}H NMR, 500 MHz, $(CD_3)_2CO$

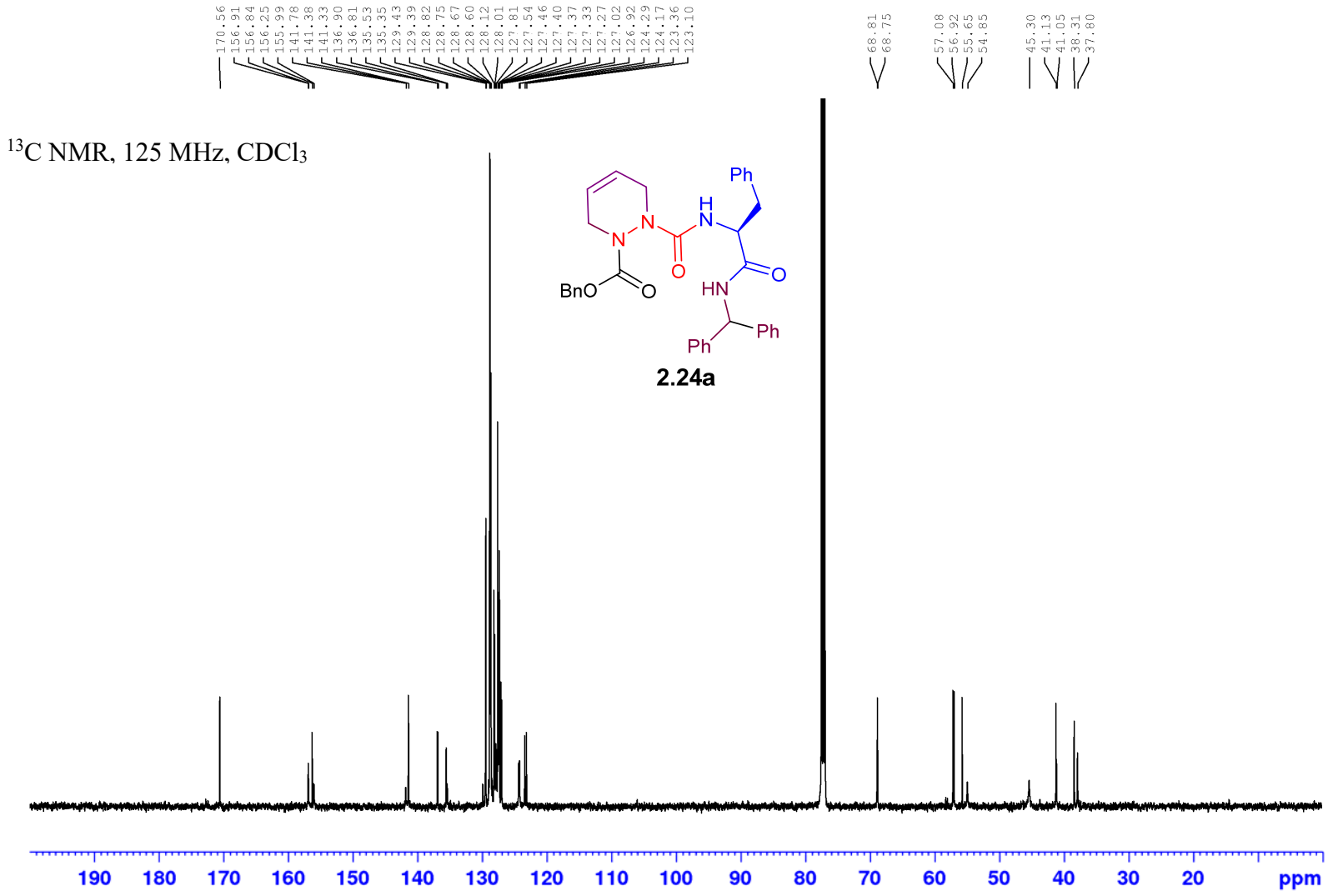

^{13}C NMR, 125 MHz, $CDCl_3$

2.24a

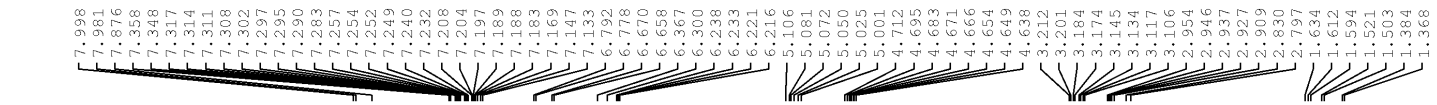

^{1}H NMR, 500 MHz, $(CD_3)_2CO$

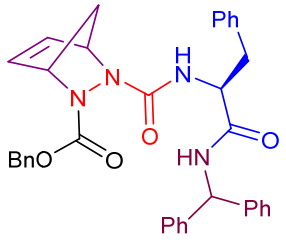

2.25a

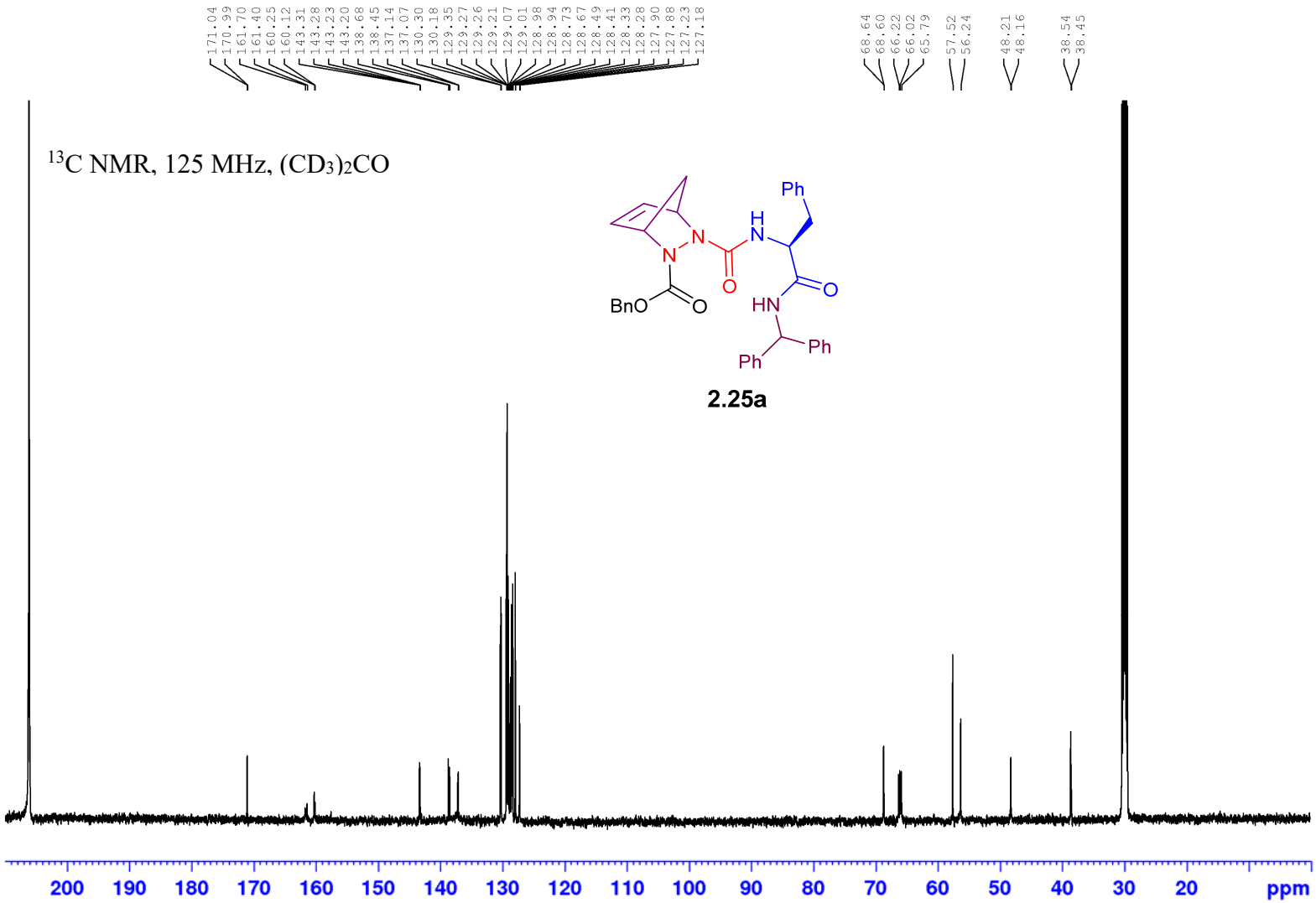
171.04
170.99
161.70
161.40
160.25
160.12
143.31
143.28
143.23
143.20
138.68
138.45
137.14
137.07
130.30
130.18
129.35
129.27
129.26
129.21
129.07
129.01
128.98
128.94
128.73
128.67
128.49
128.41
128.33
128.28
127.90
127.88
127.23
127.18
68.64
68.60
66.22
66.02
65.79
57.52
56.24
48.21
48.16
38.54
38.45
13C NMR, 125 MHz, (CD3)2CO
Ph
H
N
N
N
O
BnO
O
HN
O
Ph
Ph
2.25a
200
190
180
170
160
150
140
130
120
110
100
90
80
70
60
50
40
30
20
ppm

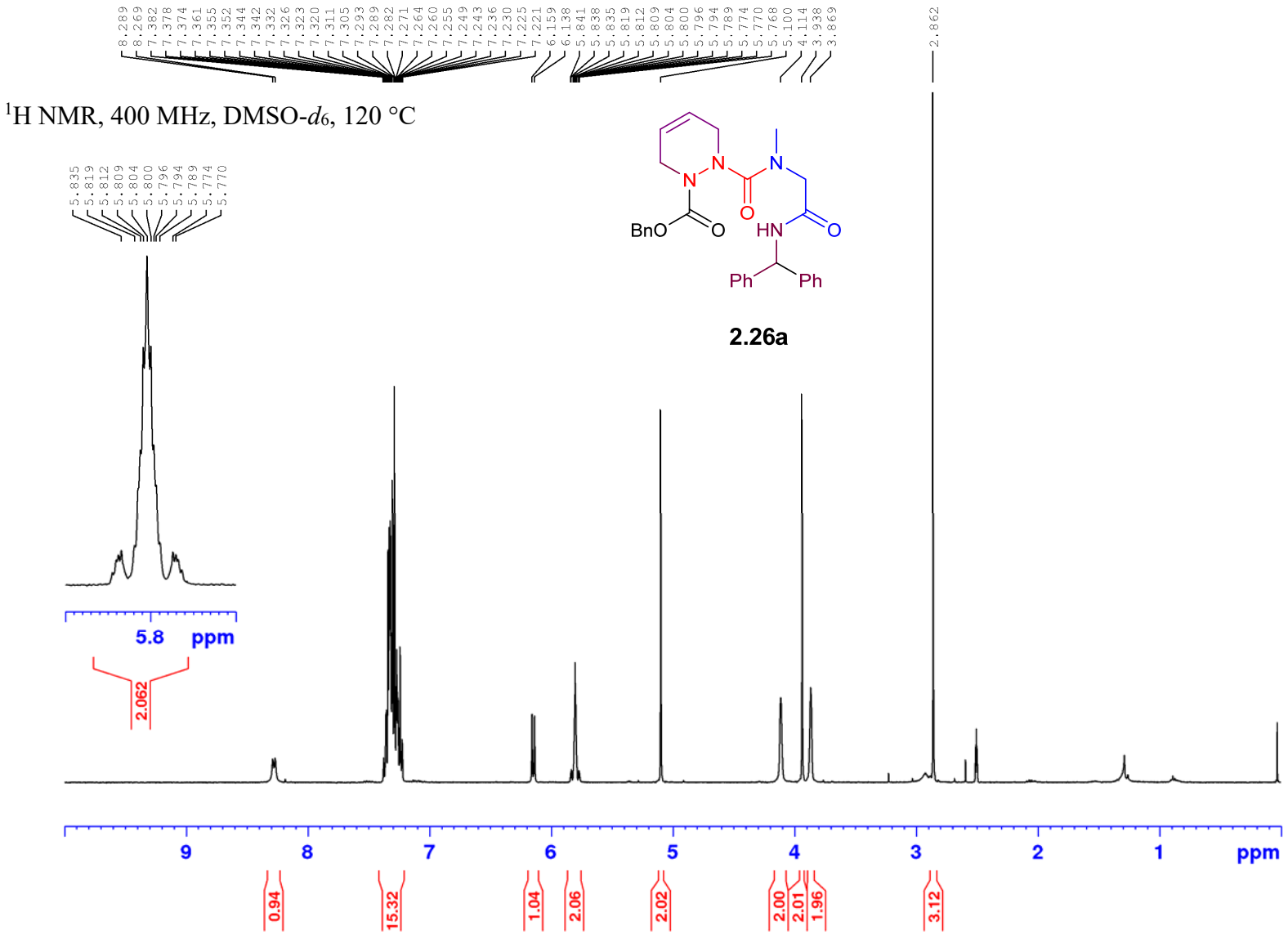

^{1}H NMR, 400 MHz, DMSO-d_6, 120 °C

^{13}C NMR, 100 MHz, DMSO-d_6, 120 °C

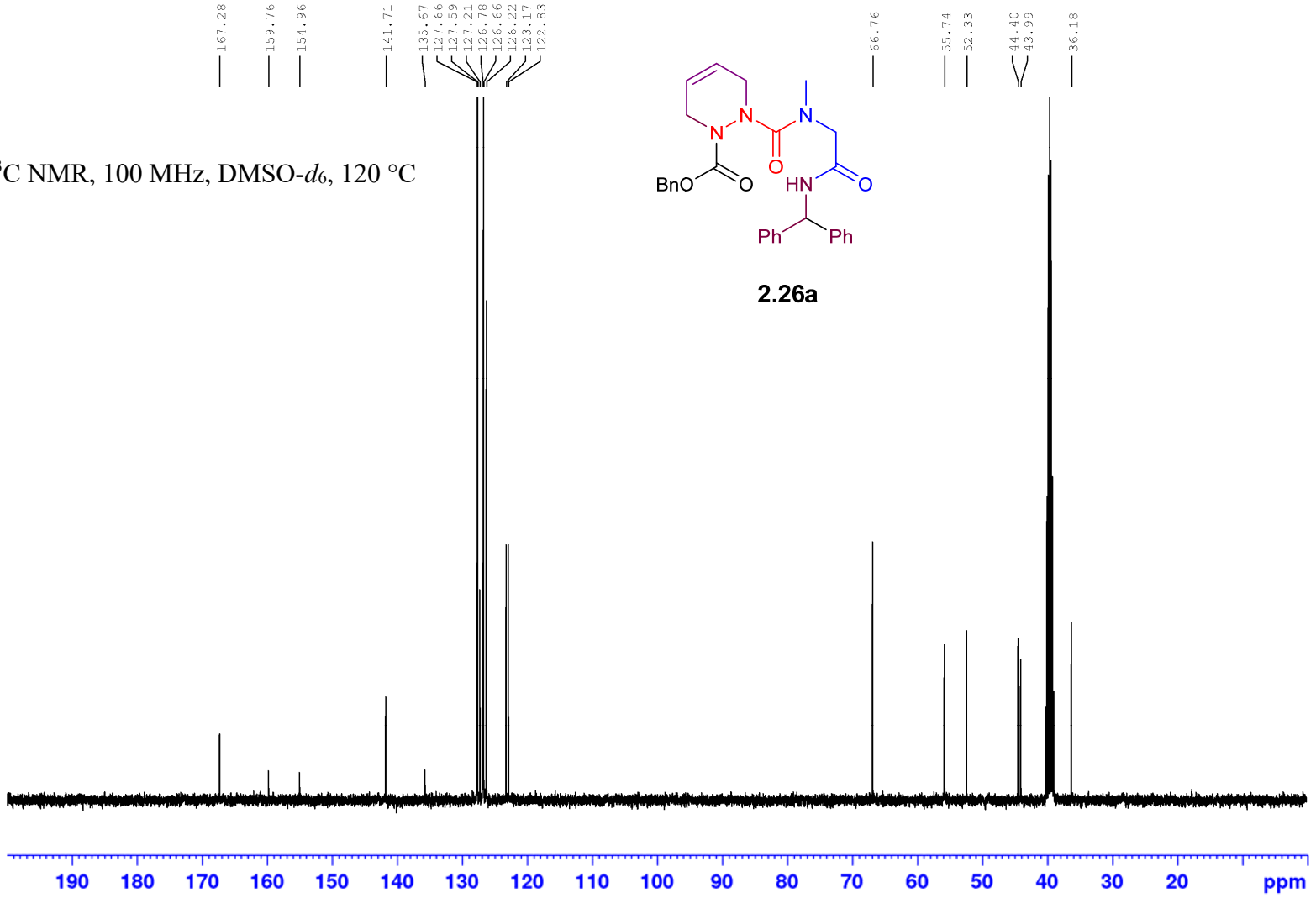

2.26a

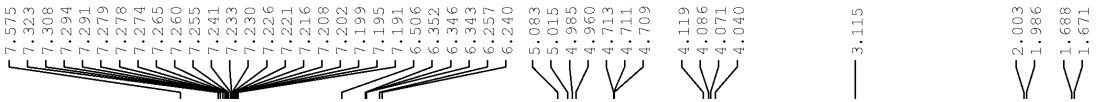

^{1}H NMR, 500 MHz, $CDCl_3$

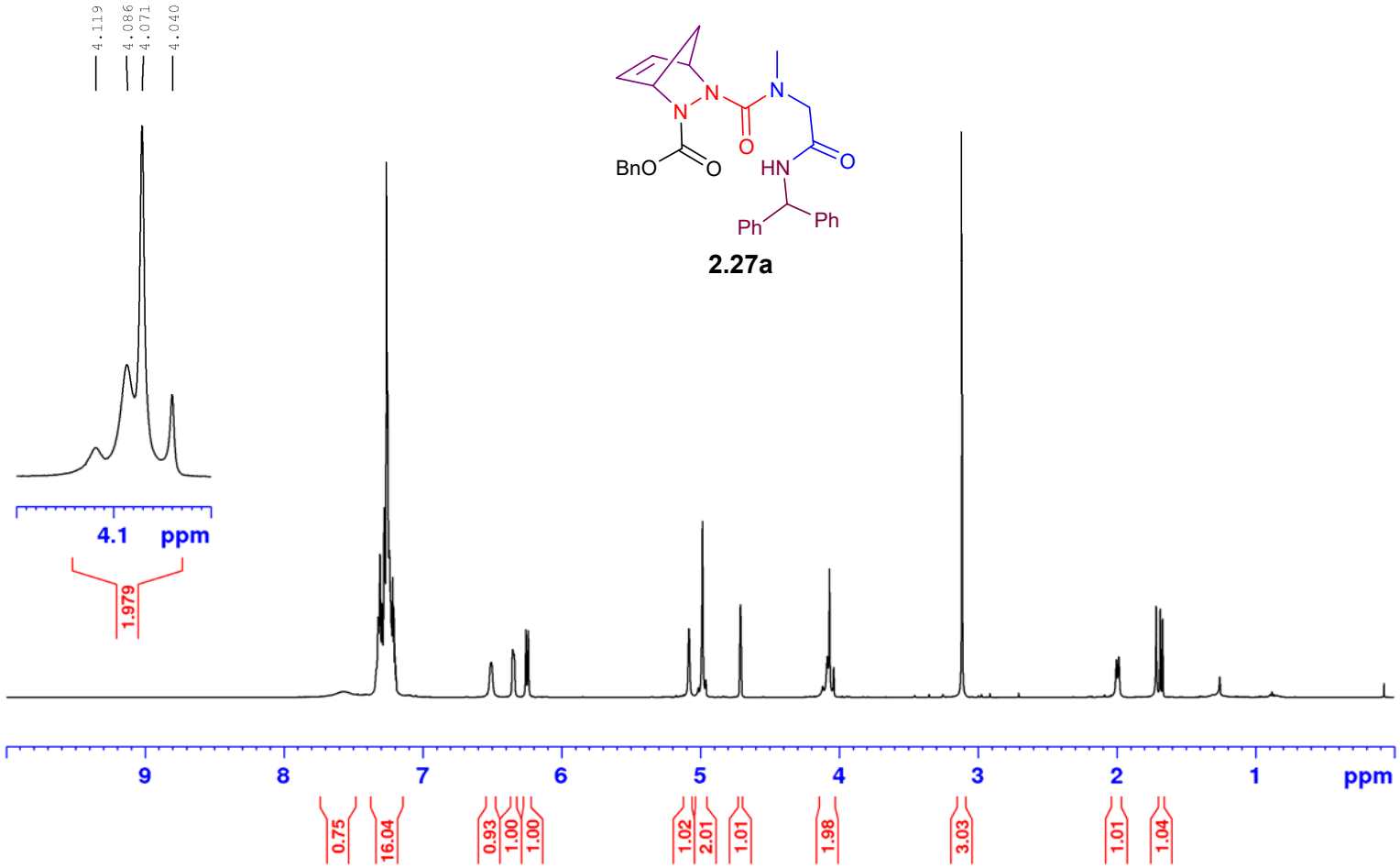

^{13}C NMR, 125 MHz, $CDCl_3$

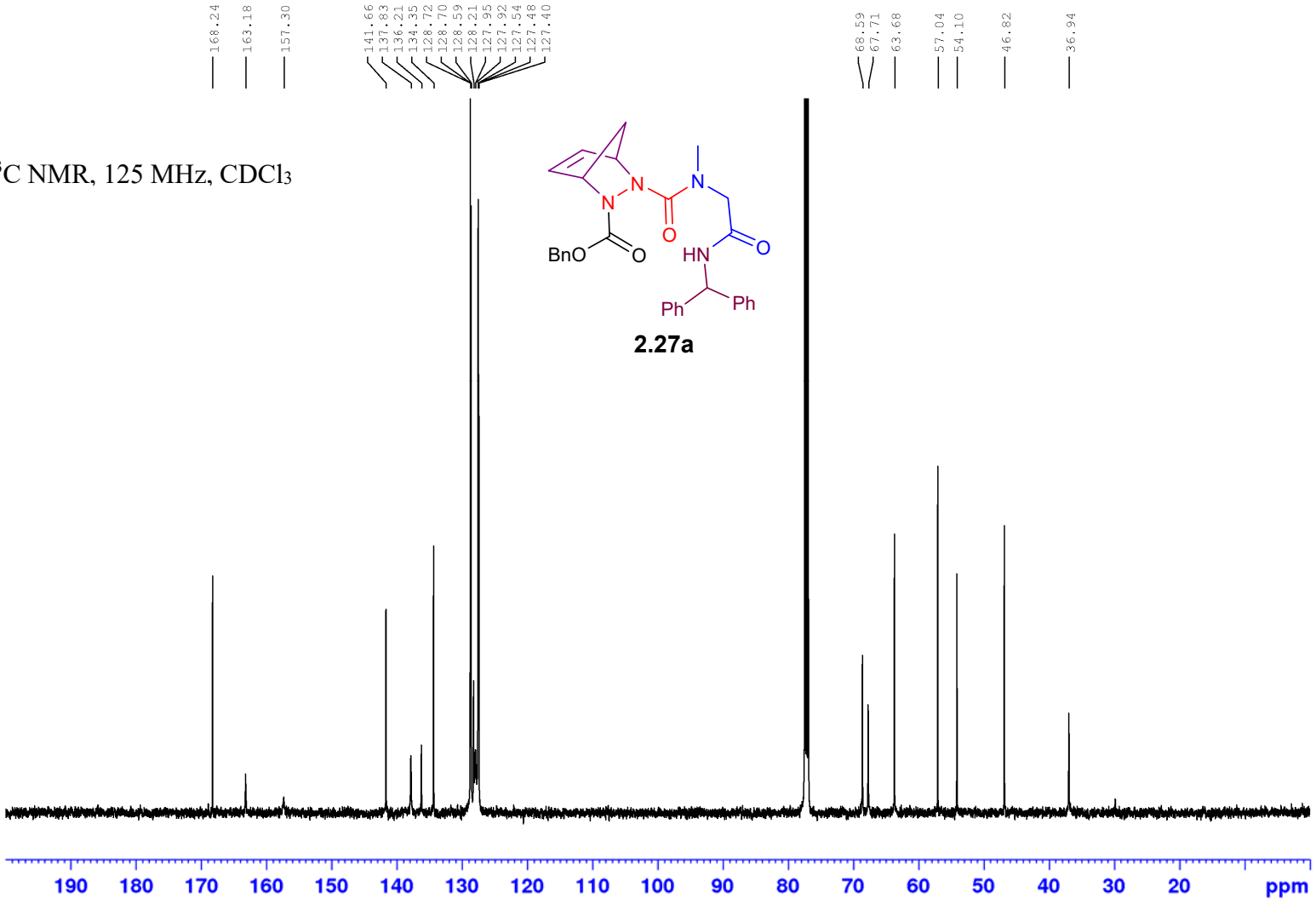

2.27a

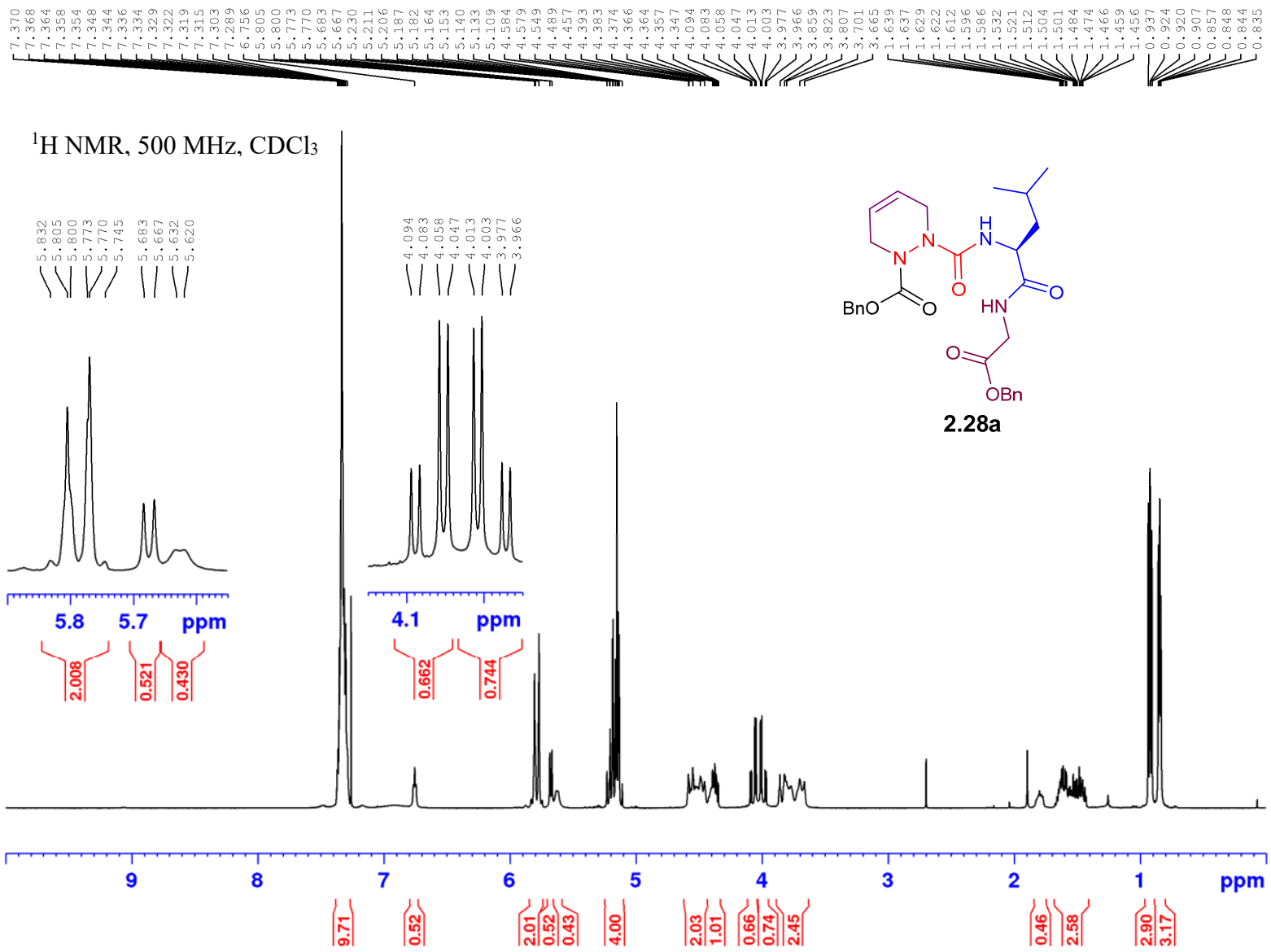
7.370 7.368 7.364 7.358 7.354 7.348 7.344 7.336 7.334 7.329 7.322 7.319 7.315 7.303 7.289 6.756 5.805 5.800 5.773 5.770 5.683 5.667 5.230 5.211 5.206 5.187 5.182 5.164 5.153 5.140 5.133 5.109 4.584 4.579 4.549 4.489 4.457 4.393 4.383 4.374 4.366 4.364 4.357 4.347 4.094 4.083 4.058 4.047 4.013 4.003 3.977 3.966 3.859 3.823 3.807 3.701 3.665 1.639 1.637 1.629 1.622 1.612 1.596 1.586 1.532 1.521 1.512 1.504 1.501 1.484 1.474 1.466 1.459 1.456 0.937 0.924 0.920 0.907 0.857 0.848 0.844 0.835
^{1}H NMR, 500 MHz, CDCl$_3$
5.832 5.805 5.800 5.773 5.770 5.745 5.683 5.667 5.632 5.620
4.094 4.083 4.058 4.047 4.013 4.003 3.977 3.966
5.8 5.7 ppm
4.1 ppm
2.008 0.521 0.430
0.662 0.744
BnO
HN
OBn
2.28a
9 8 7 6 5 4 3 2 1 ppm
9.71 0.52 2.01 0.52 0.43 4.00 2.03 1.01 0.66 0.74 2.45 0.46 2.58 2.90 3.17

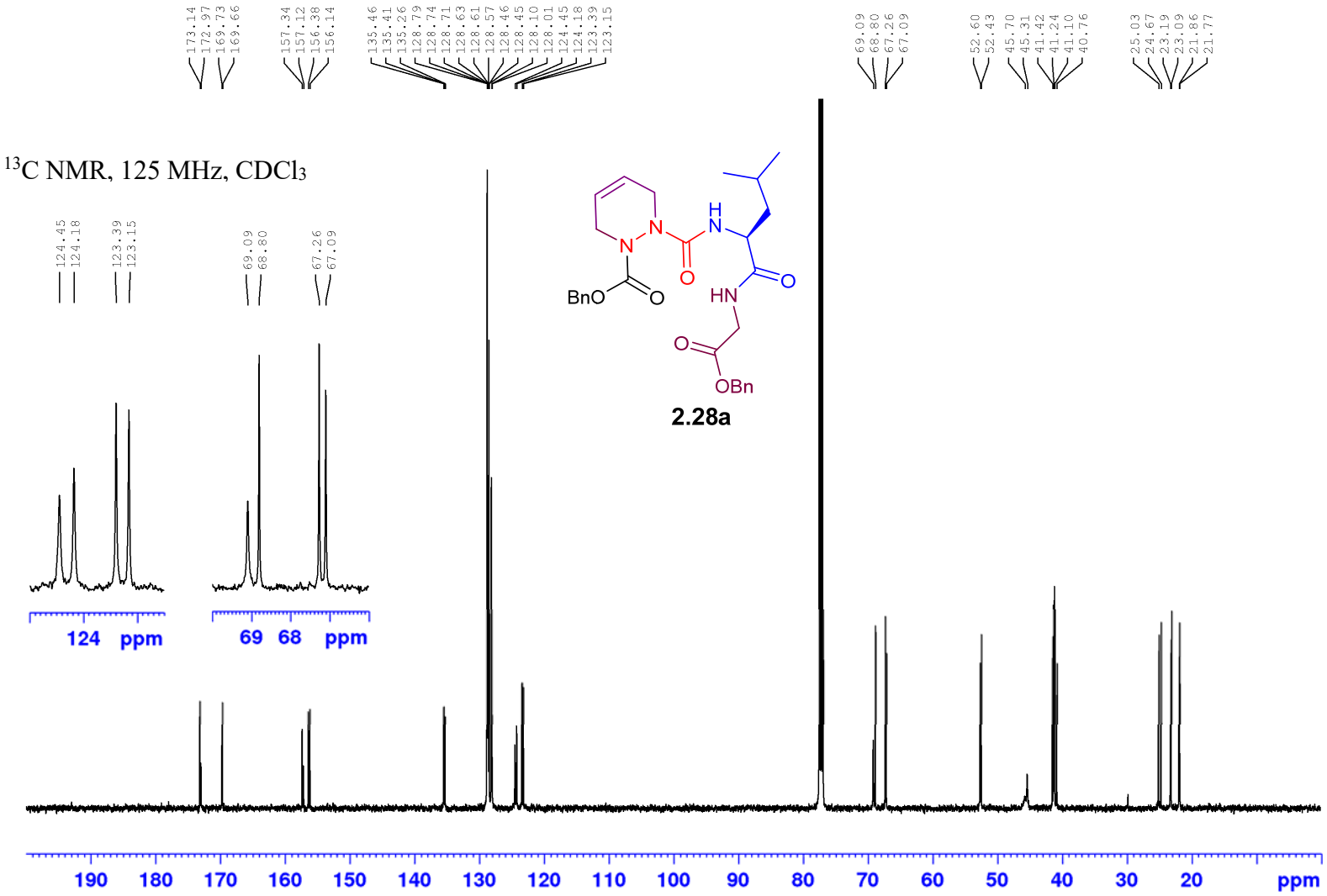
^{13}C NMR, 125 MHz, CDCl$_3$
173.14
172.97
169.73
169.66
157.34
157.12
156.38
156.14
135.46
135.41
135.26
128.79
128.74
128.71
128.63
128.61
128.57
128.46
128.45
128.10
128.01
124.45
124.18
123.39
123.15
69.09
68.80
67.26
67.09
52.60
52.43
45.70
45.31
41.42
41.24
41.10
40.76
25.03
24.67
23.19
23.09
21.86
21.77
124.45
124.18
123.39
123.15
69.09
68.80
67.26
67.09
124 ppm
69 68 ppm
BnO
O
N
N
H
N
O
O
HN
O
O
OBn
2.28a
190 180 170 160 150 140 130 120 110 100 90 80 70 60 50 40 30 20 ppm

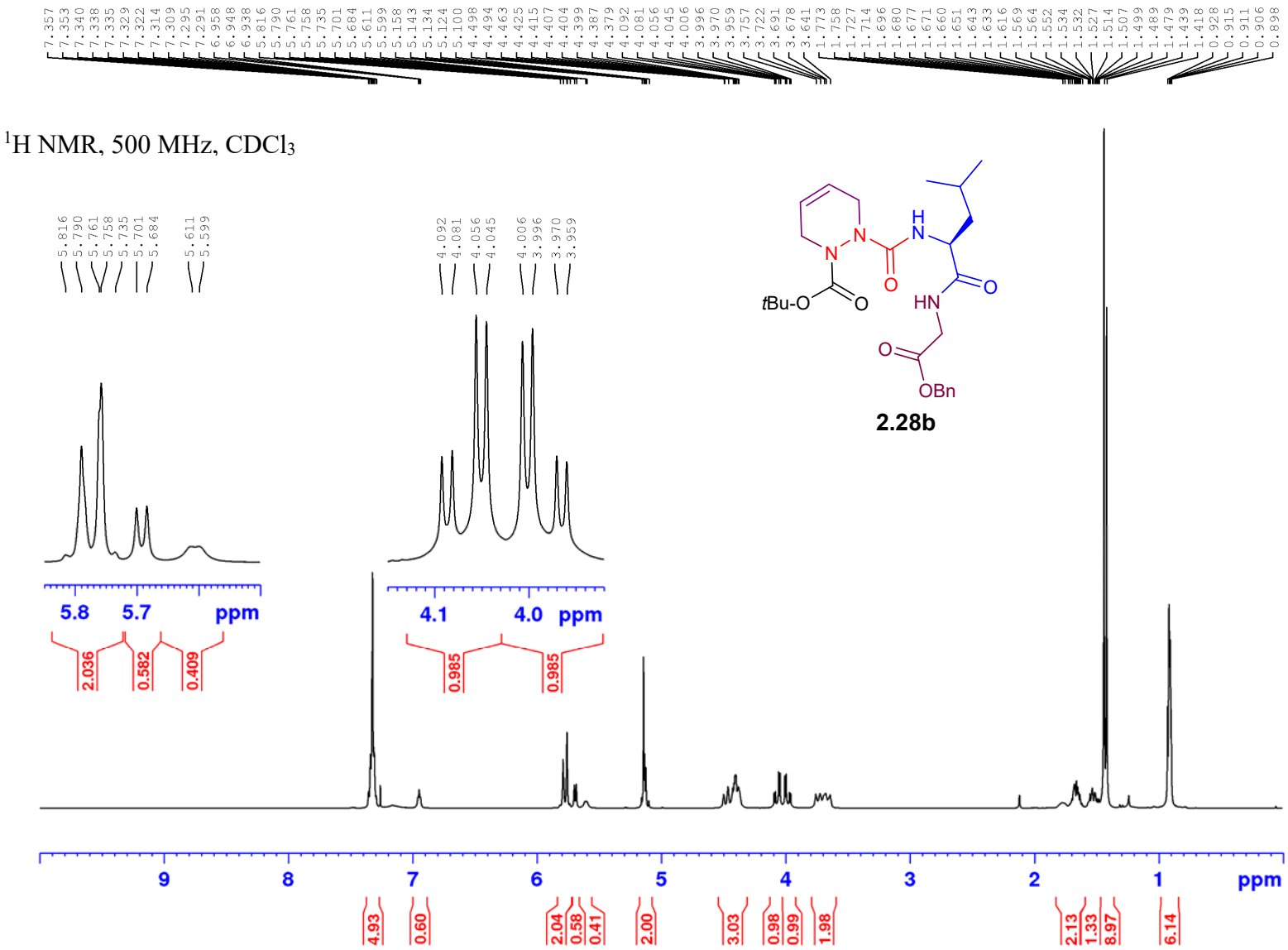
7.357
7.353
7.340
7.338
7.335
7.329
7.322
7.314
7.309
7.295
7.291
6.958
6.948
6.938
5.816
5.790
5.761
5.758
5.735
5.701
5.684
5.611
5.599
5.158
5.143
5.134
5.124
5.100
4.498
4.494
4.463
4.425
4.415
4.407
4.404
4.399
4.387
4.379
4.092
4.081
4.056
4.045
4.006
3.996
3.970
3.959
3.757
3.722
3.691
3.678
3.641
1.773
1.758
1.727
1.714
1.696
1.680
1.677
1.671
1.660
1.651
1.643
1.633
1.616
1.569
1.564
1.552
1.534
1.532
1.527
1.514
1.507
1.499
1.489
1.479
1.439
1.418
0.928
0.915
0.911
0.906
0.898
1H NMR, 500 MHz, CDCl3
5.8
5.7
ppm
2.036
0.582
0.409
4.1
4.0
ppm
0.985
0.985
tBu-O
O
N
N
H
N
O
HN
O
O
OBn
2.28b
9
8
7
6
5
4
3
2
1
ppm
4.93
0.60
2.04
0.58
0.41
2.00
3.03
0.98
0.99
1.98
2.13
1.33
8.97
6.14

^{13}C NMR, 125 MHz, $CDCl_3$

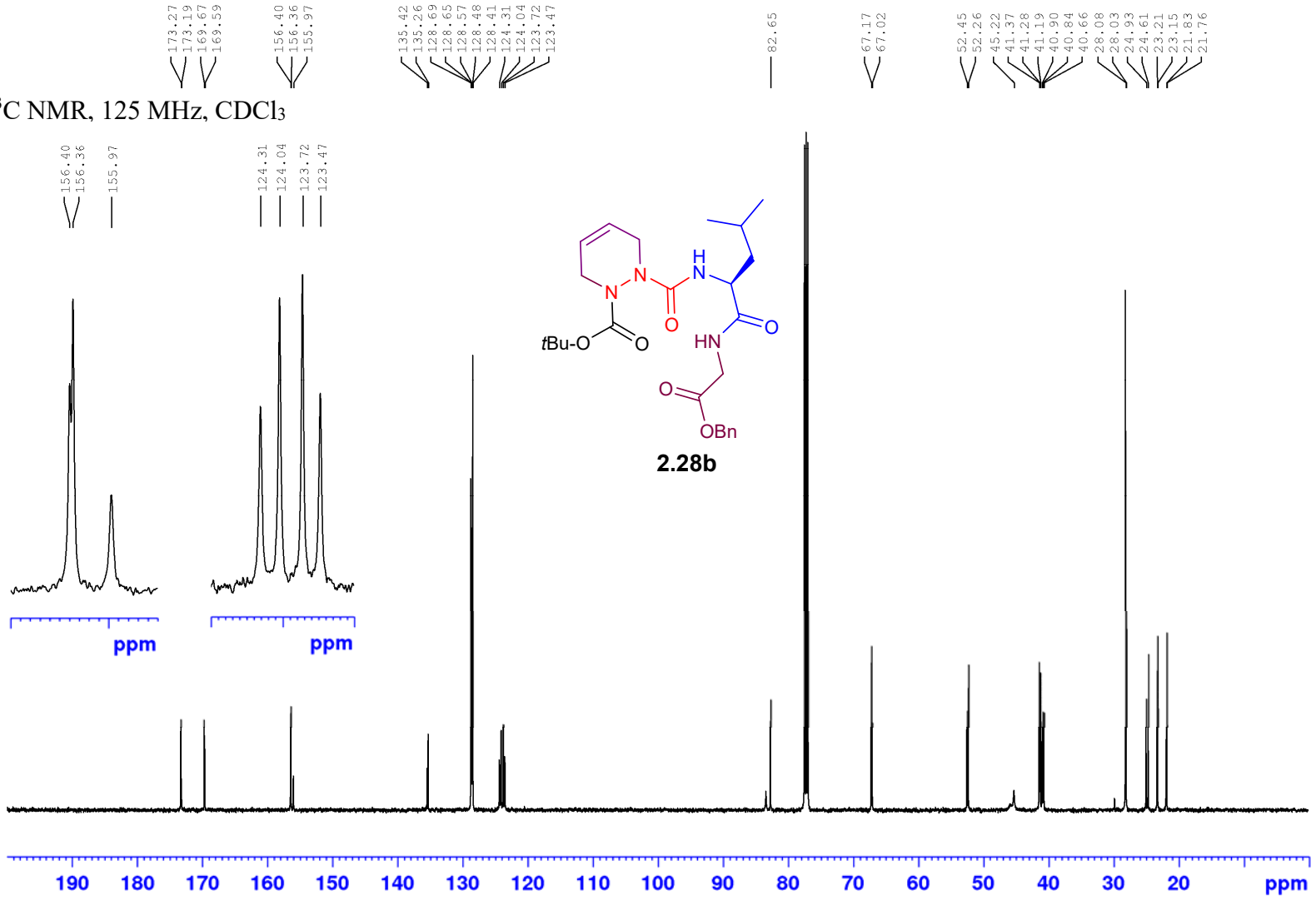

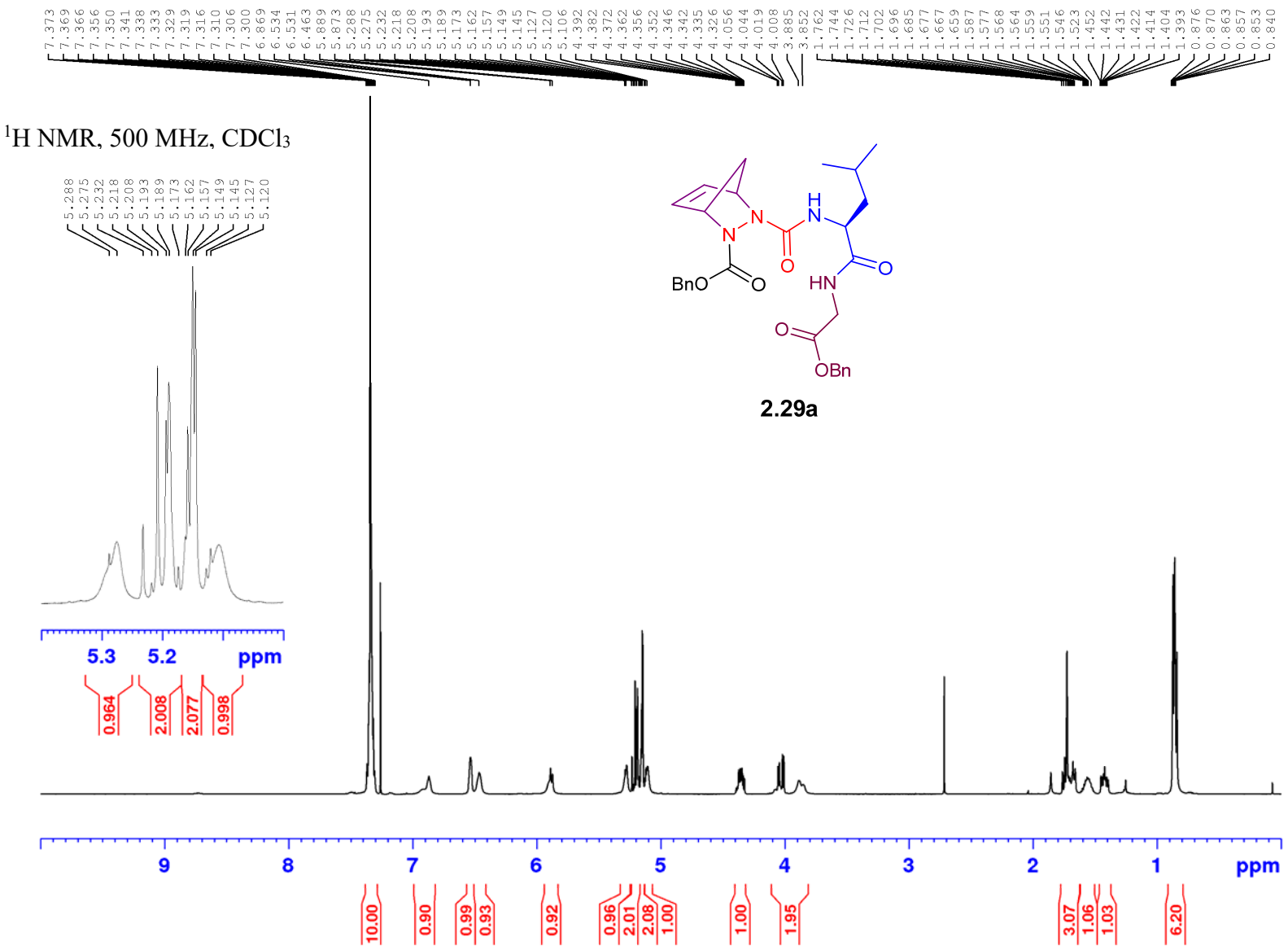
7.373
7.369
7.366
7.356
7.350
7.341
7.338
7.333
7.329
7.319
7.316
7.310
7.306
7.300
6.869
6.534
6.531
6.463
5.889
5.873
5.288
5.275
5.232
5.218
5.208
5.193
5.189
5.173
5.162
5.157
5.149
5.145
5.127
5.120
5.106
4.392
4.382
4.372
4.362
4.356
4.352
4.346
4.342
4.335
4.326
4.056
4.044
4.019
4.008
3.885
3.852
1.762
1.744
1.726
1.712
1.702
1.696
1.685
1.677
1.667
1.659
1.587
1.577
1.568
1.564
1.559
1.551
1.546
1.523
1.452
1.442
1.431
1.422
1.414
1.404
1.393
0.876
0.870
0.863
0.857
0.853
0.840
1H NMR, 500 MHz, CDCl3
BnO
O
N
N
H
N
O
HN
O
O
OBn
2.29a
5.3
5.2
ppm
0.964
2.008
2.077
0.998
9
8
7
6
5
4
3
2
1
ppm
10.00
0.90
0.99
0.93
0.92
0.96
2.01
2.08
1.00
1.00
1.95
3.07
1.06
1.03
6.20

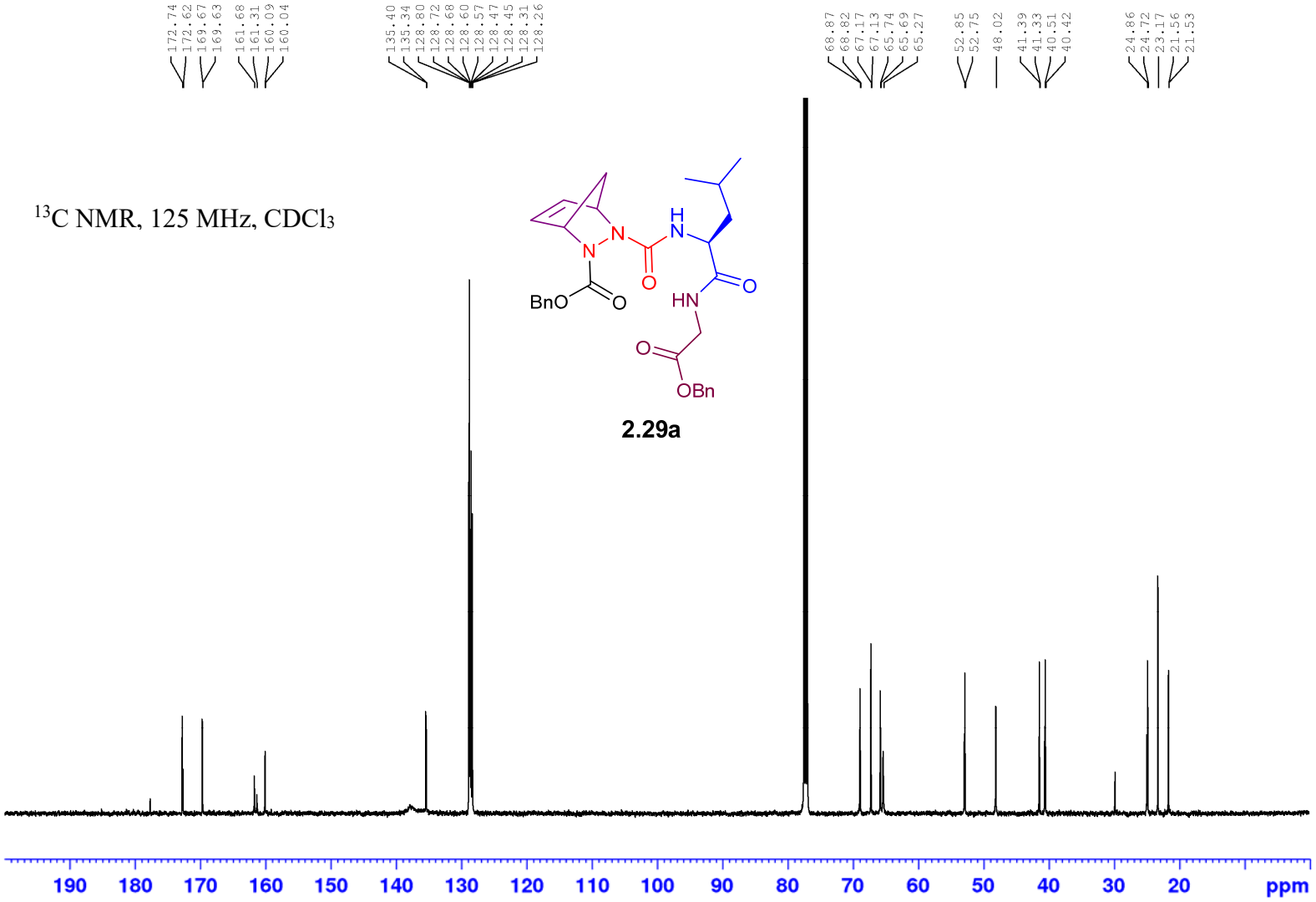

^{13}C NMR, 125 MHz, $CDCl_3$

2.29a

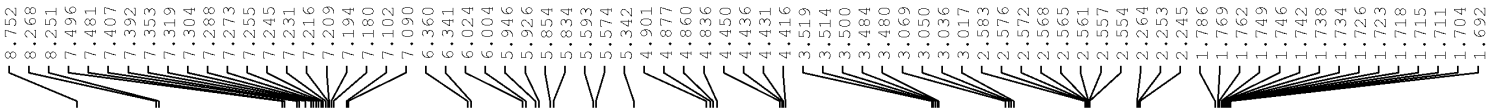

^{1}H NMR, 500 MHz, $(CD_3)_2CO$

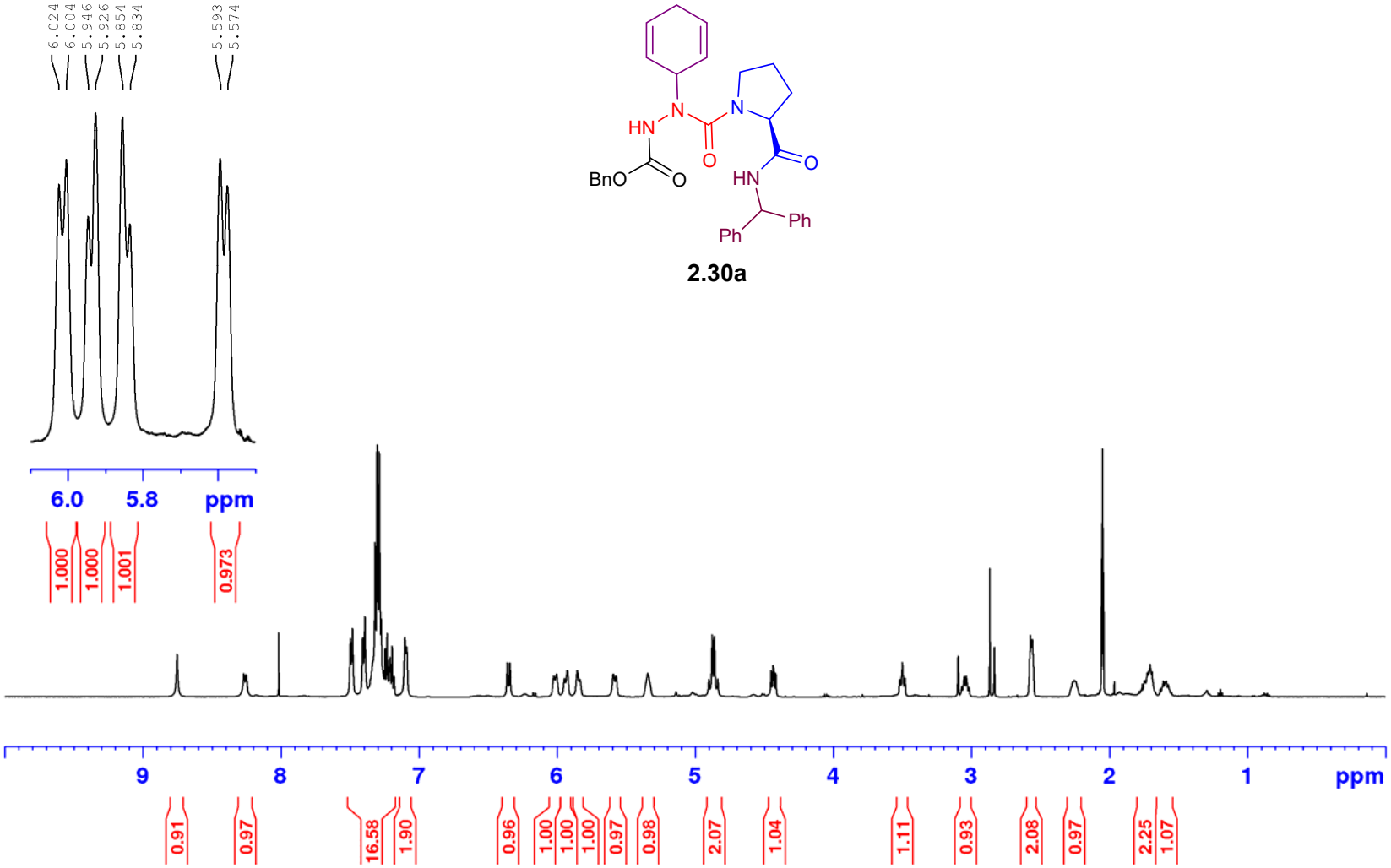

2.30a

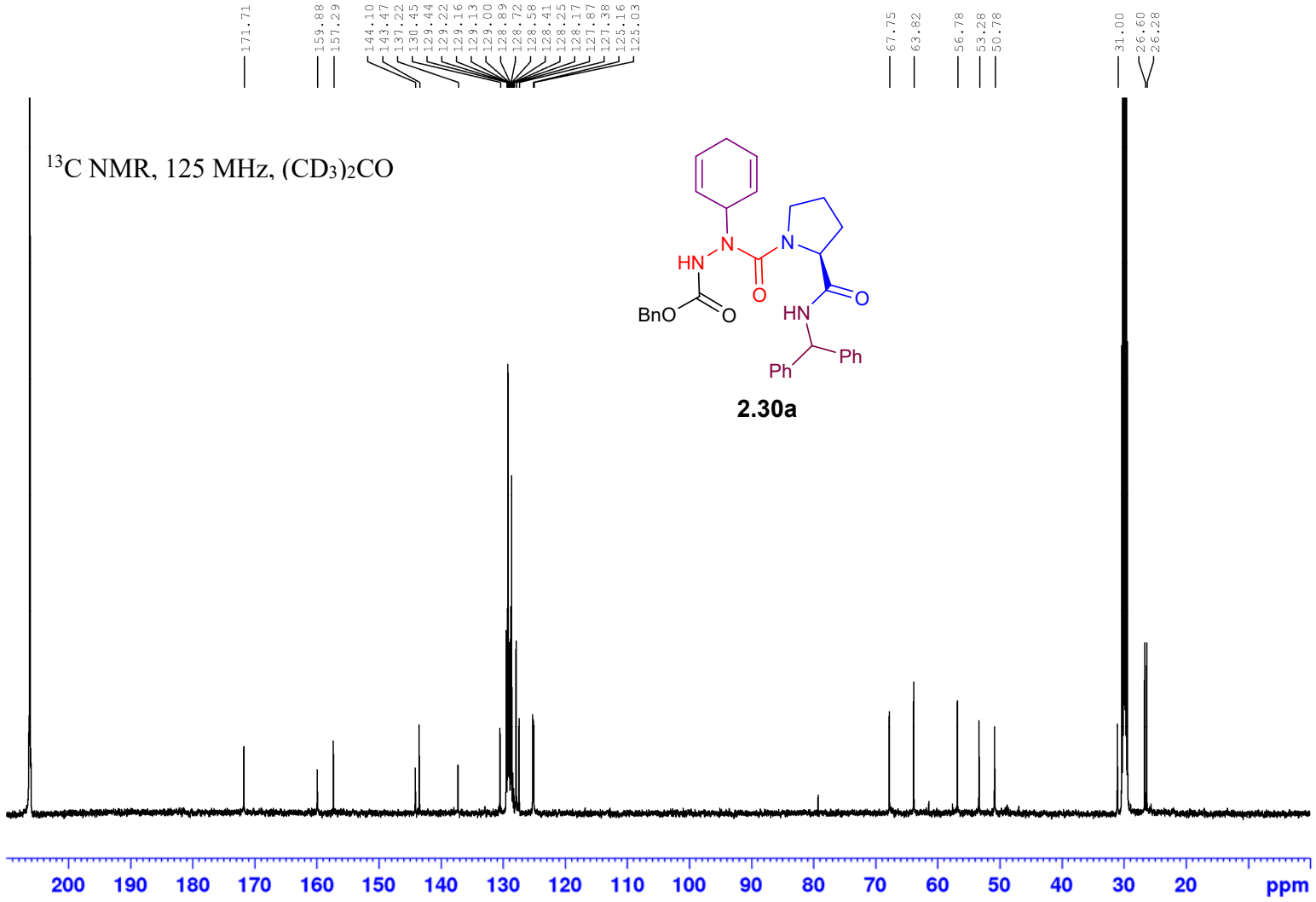
171.71
159.88
157.29
144.10
143.47
137.22
130.45
129.44
129.22
129.16
129.13
129.00
128.89
128.72
128.58
128.41
128.25
128.17
127.87
127.38
125.16
125.03
67.75
63.82
56.78
53.28
50.78
31.00
26.60
26.28
13C NMR, 125 MHz, (CD3)2CO
HN
N
N
O
BnO
O
O
HN
Ph
Ph
2.30a
200
190
180
170
160
150
140
130
120
110
100
90
80
70
60
50
40
30
20
ppm

^{1}H NMR, 400 MHz, DMSO-*d*$_6$, 120 °C

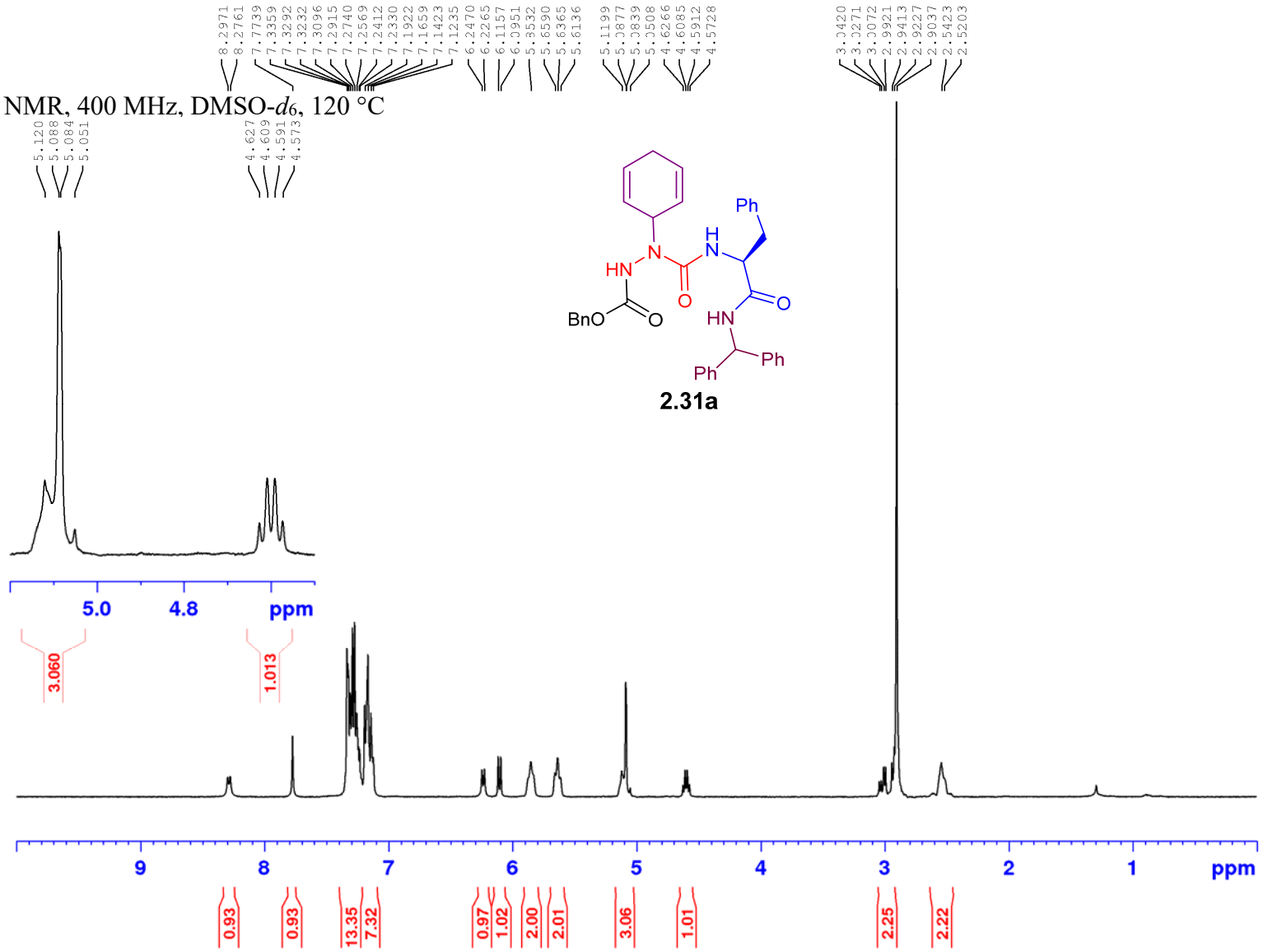

^{13}C NMR, 100 MHz, DMSO-d_6, 120 °C

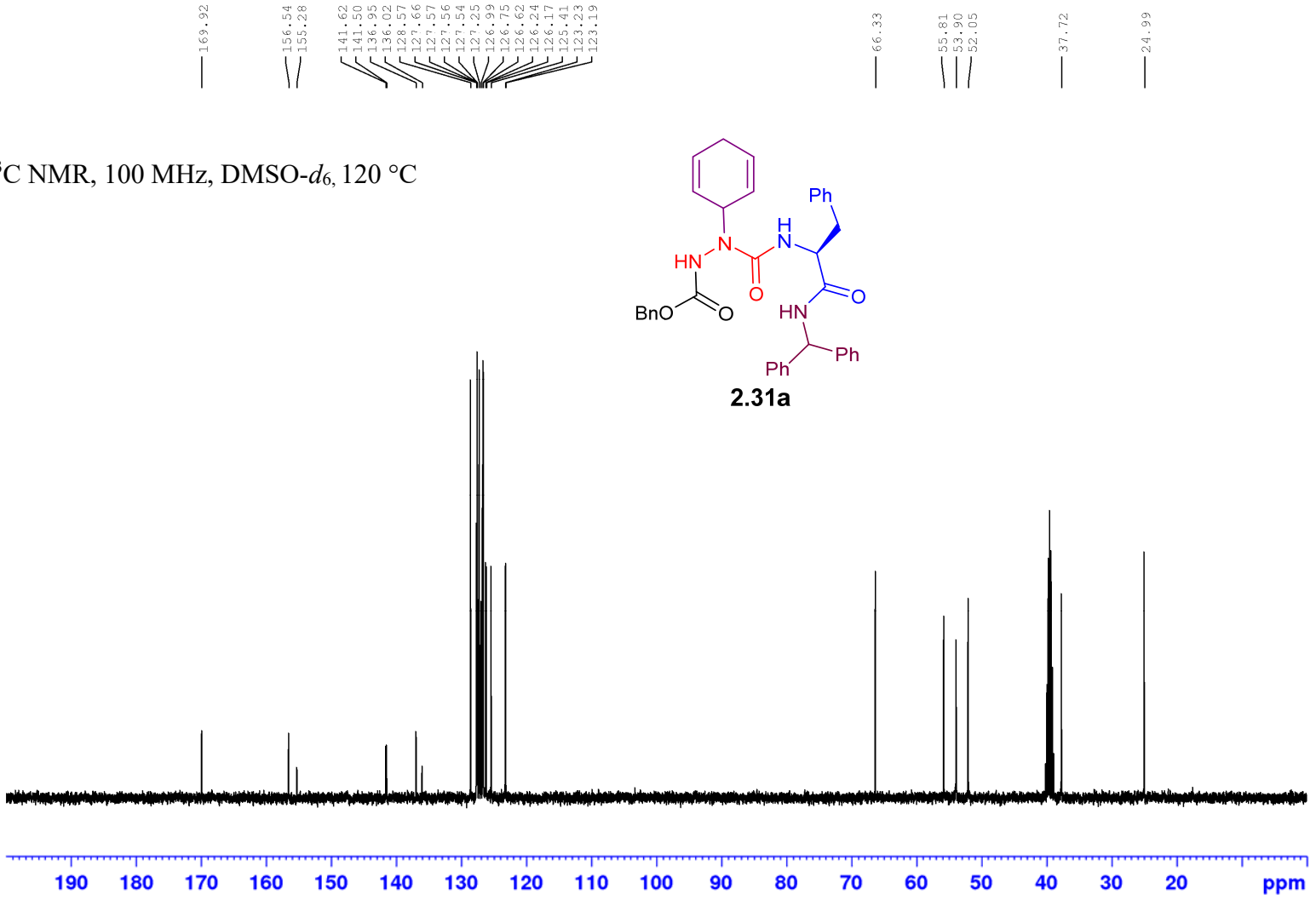

2.31a

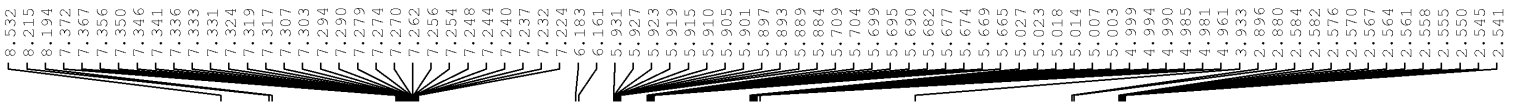

^{1}H NMR, 400 MHz, DMSO-d_6, 120 °C

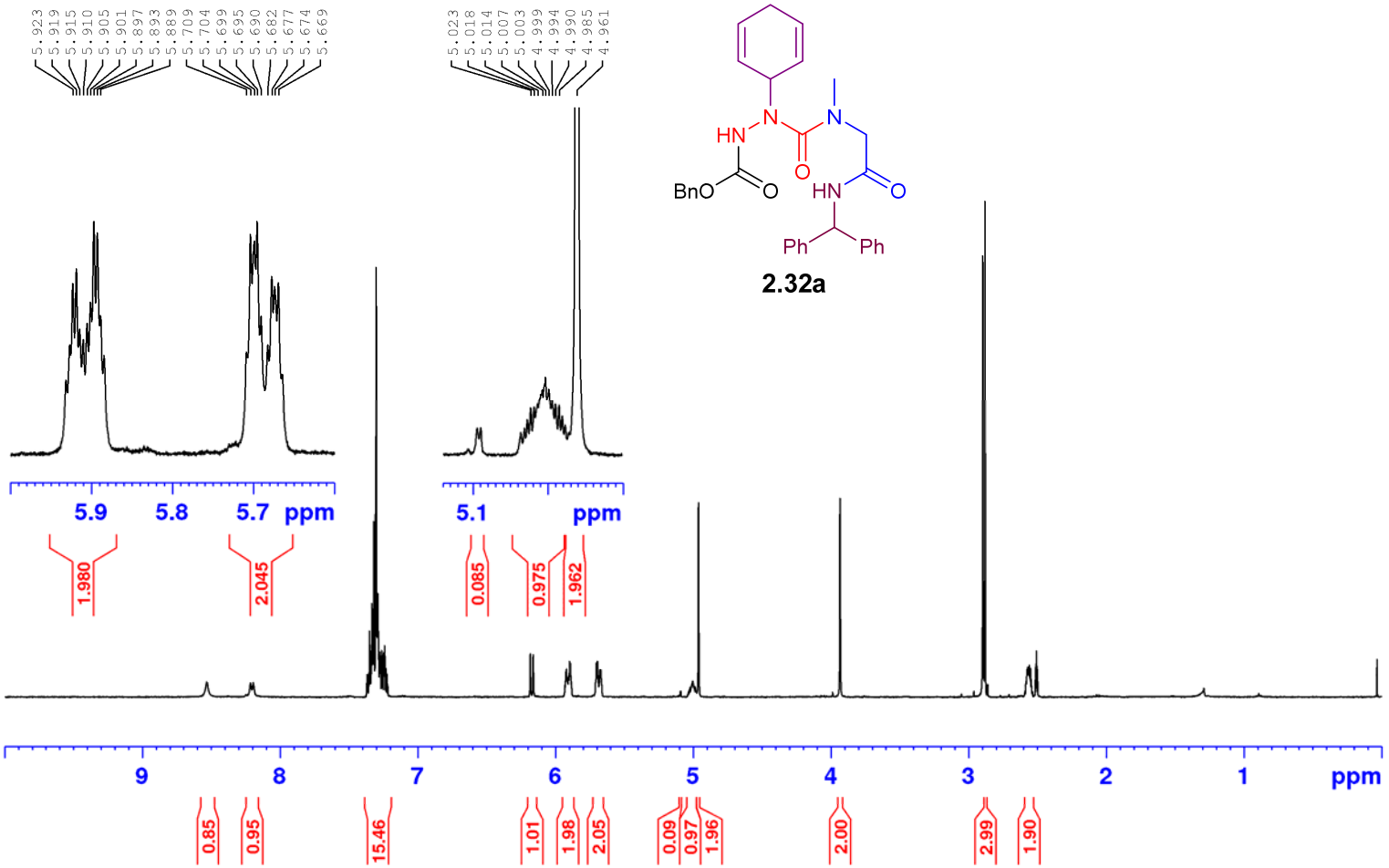

^{13}C NMR, 100 MHz, DMSO-d_6, 120 °C

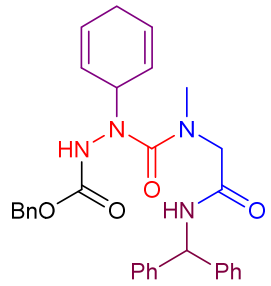

2.32a

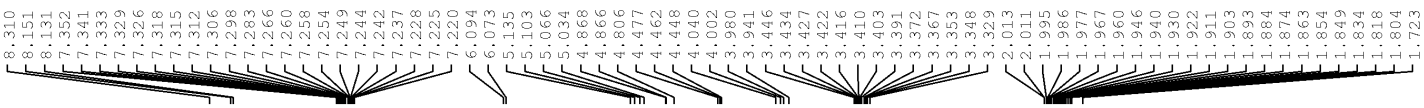

^{1}H NMR, 400 MHz, DMSO-d_6, 120 °C (NUS)

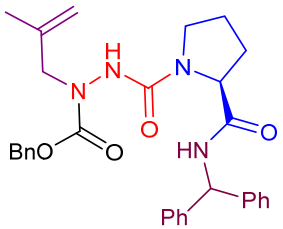

2.33a

^{13}C NMR, 100 MHz, DMSO-d_6, 120 °C (NUS)

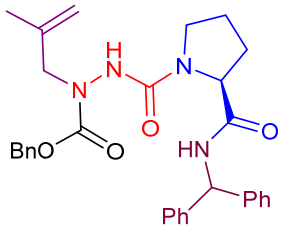

2.33a

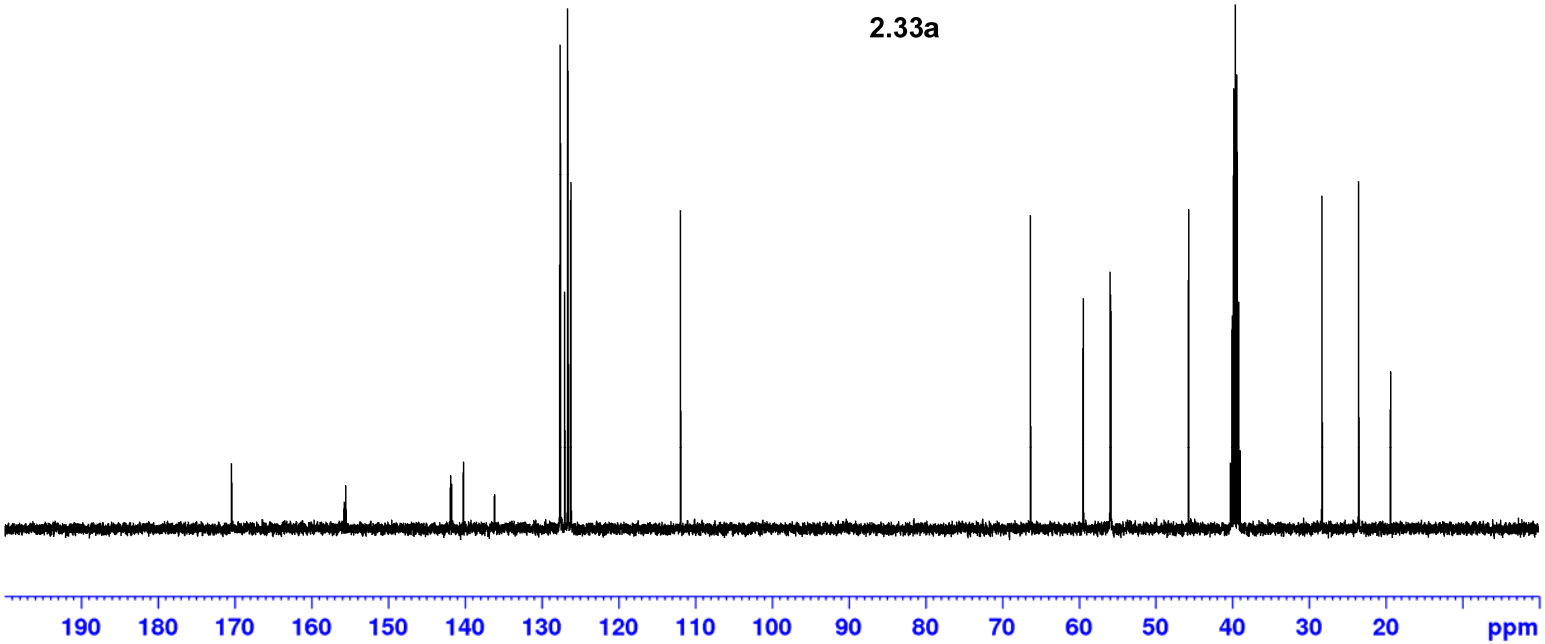

2D HMBC, 100 MHz, DMSO-d_6, 120 °C (NUS)

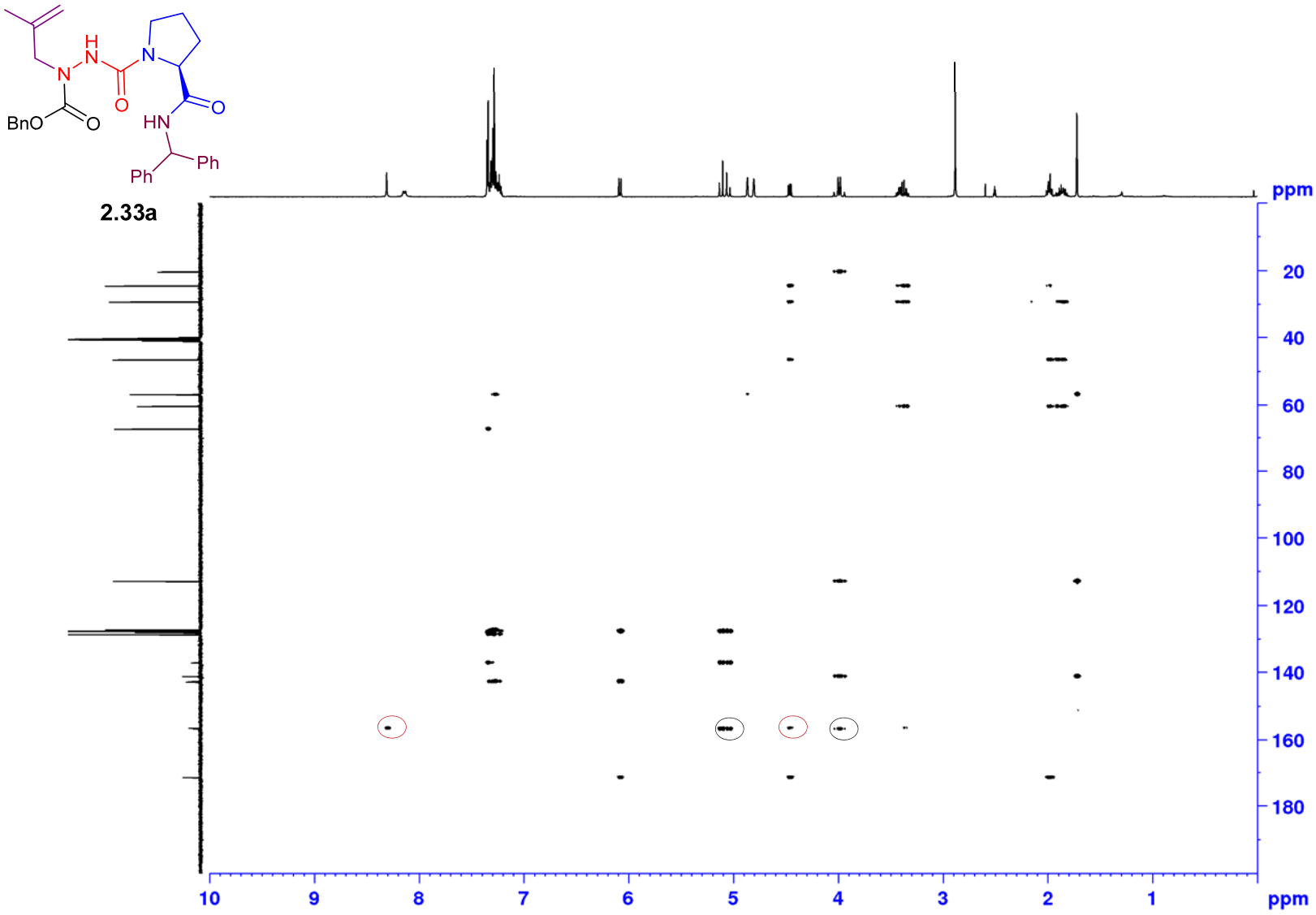

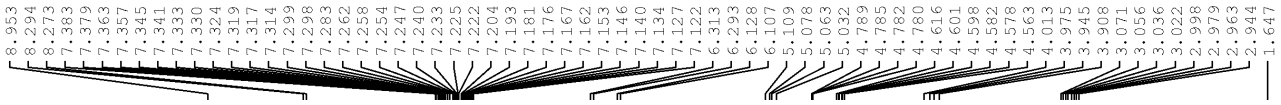

^{1}H NMR, 400 MHz, DMSO-d_6, 120 °C (NUS)

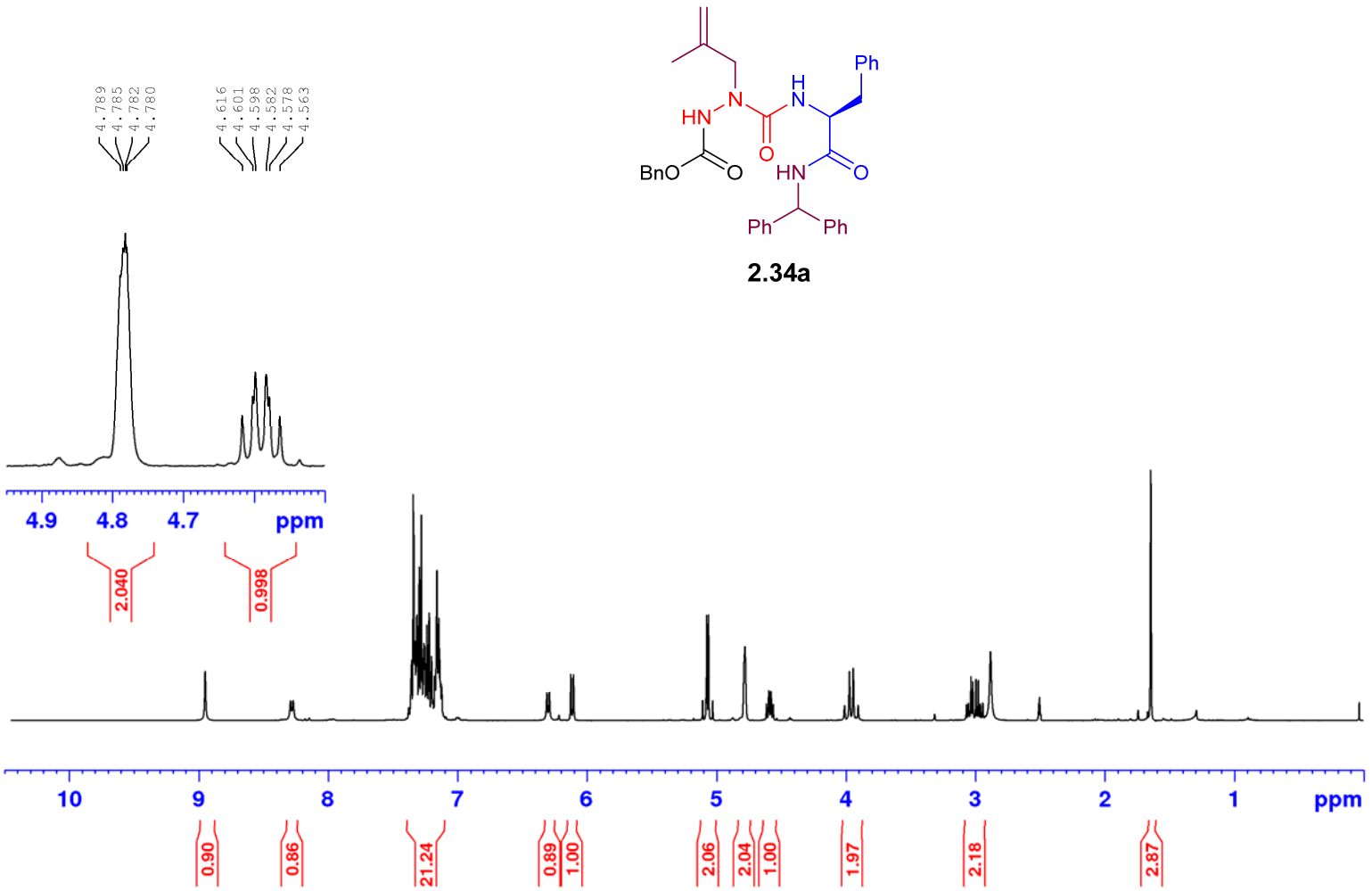

2.34a

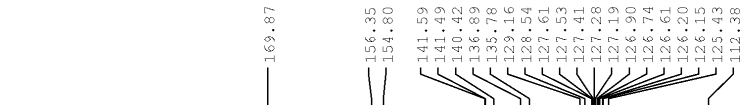

^{13}C NMR, 100 MHz, DMSO-d_6, 120 °C (NUS)

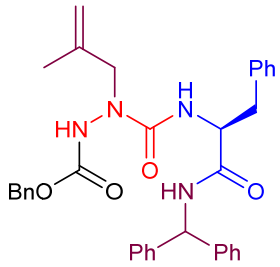

2.34a

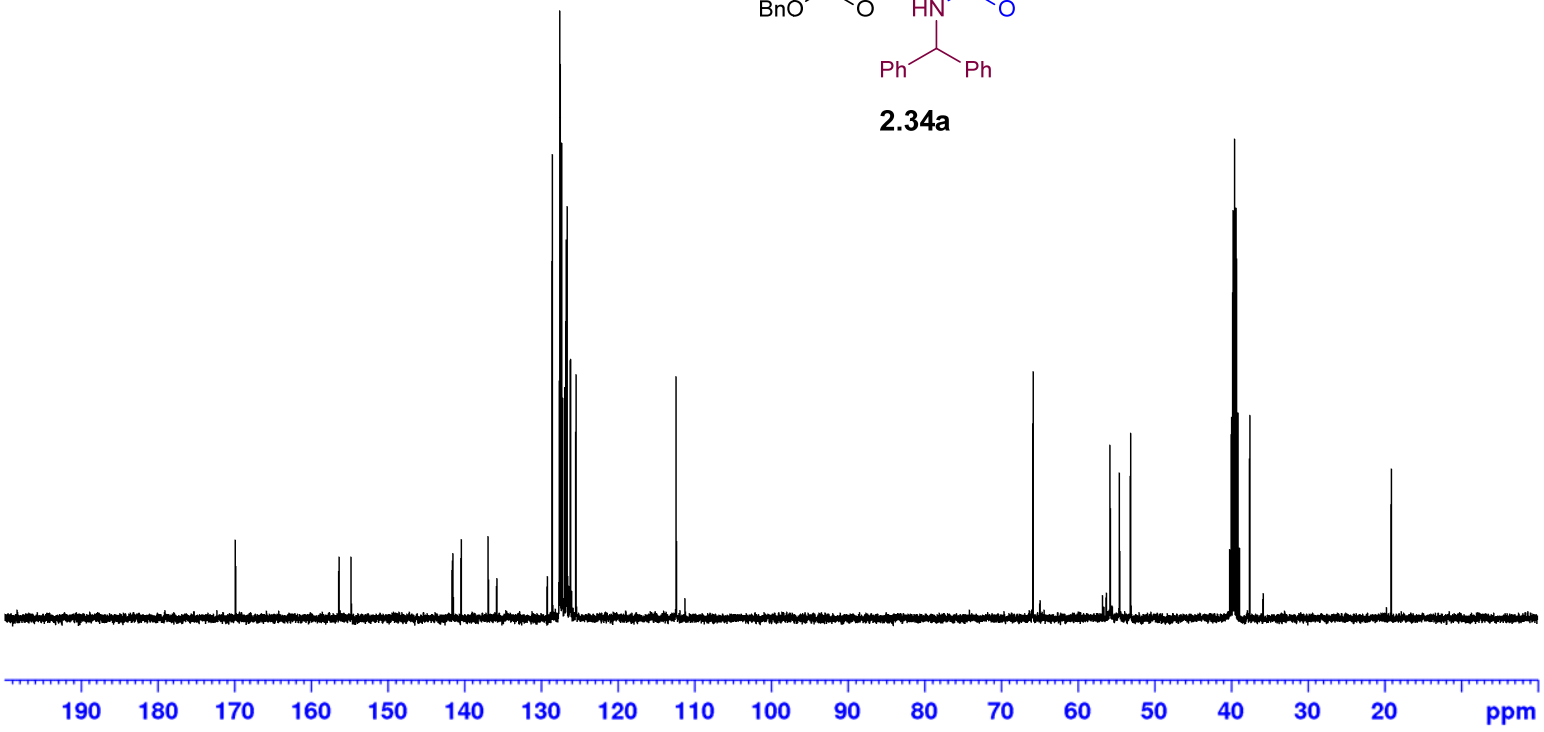

2D HMBC, 100 MHz, DMSO-d_6, 120 °C (NUS)

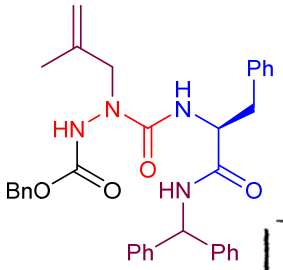

2.34a

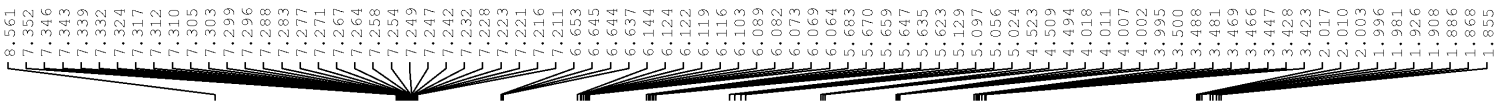

^{1}H NMR, 400 MHz, DMSO-d_6, 120 °C (NUS)

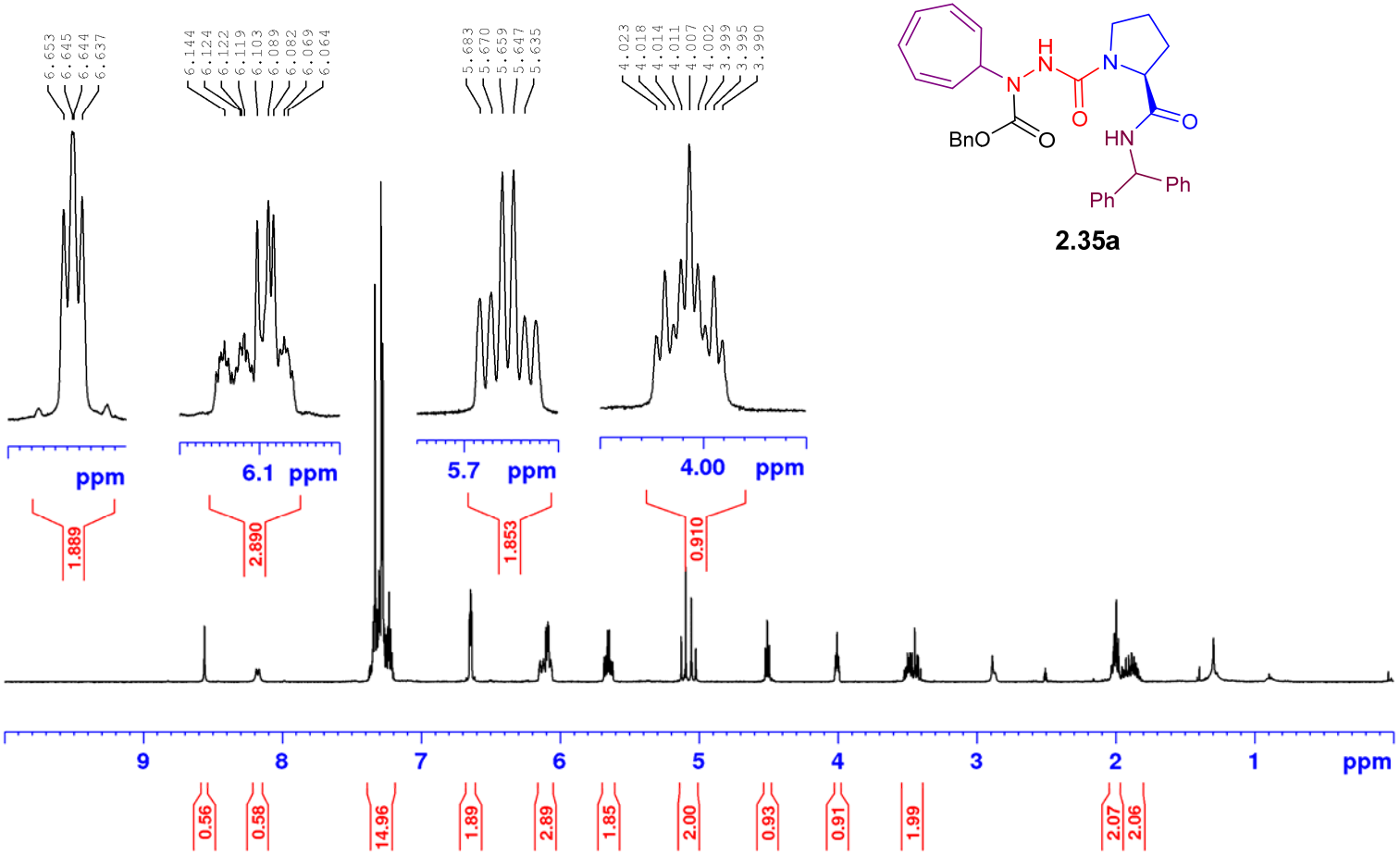

2.35a

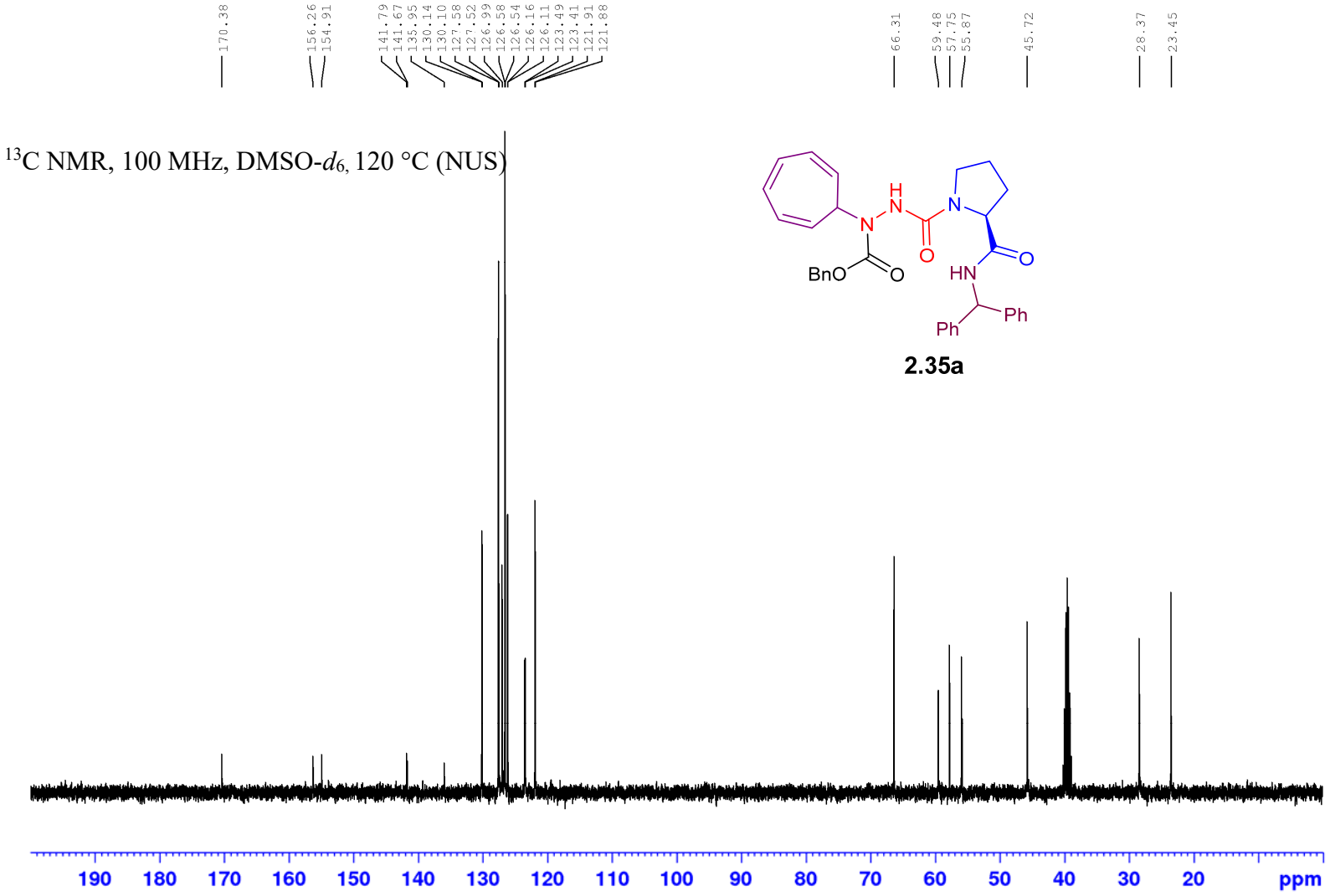
170.38
156.26
154.91
141.79
141.67
135.95
130.14
130.10
127.58
127.52
126.99
126.58
126.54
126.16
126.11
123.49
123.41
121.91
121.88
66.31
59.48
57.75
55.87
45.72
28.37
23.45
13C NMR, 100 MHz, DMSO-d6, 120 °C (NUS)
BnO
O
N
H
N
O
N
O
HN
Ph
Ph
2.35a
190
180
170
160
150
140
130
120
110
100
90
80
70
60
50
40
30
20
ppm

^{1}H NMR, 500 MHz, $CDCl_3$

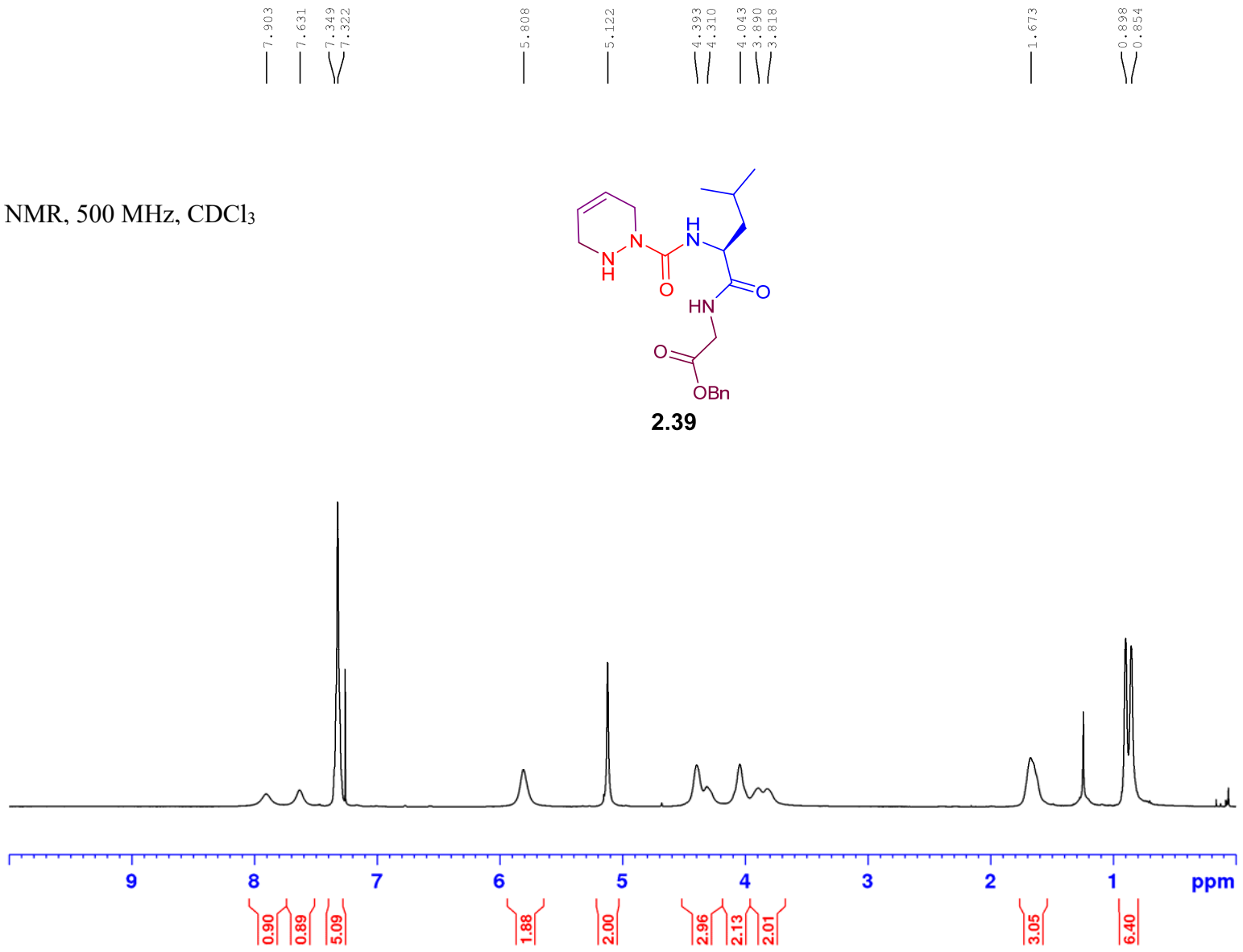

2.39

^{13}C NMR, 125 MHz, $CDCl_3$

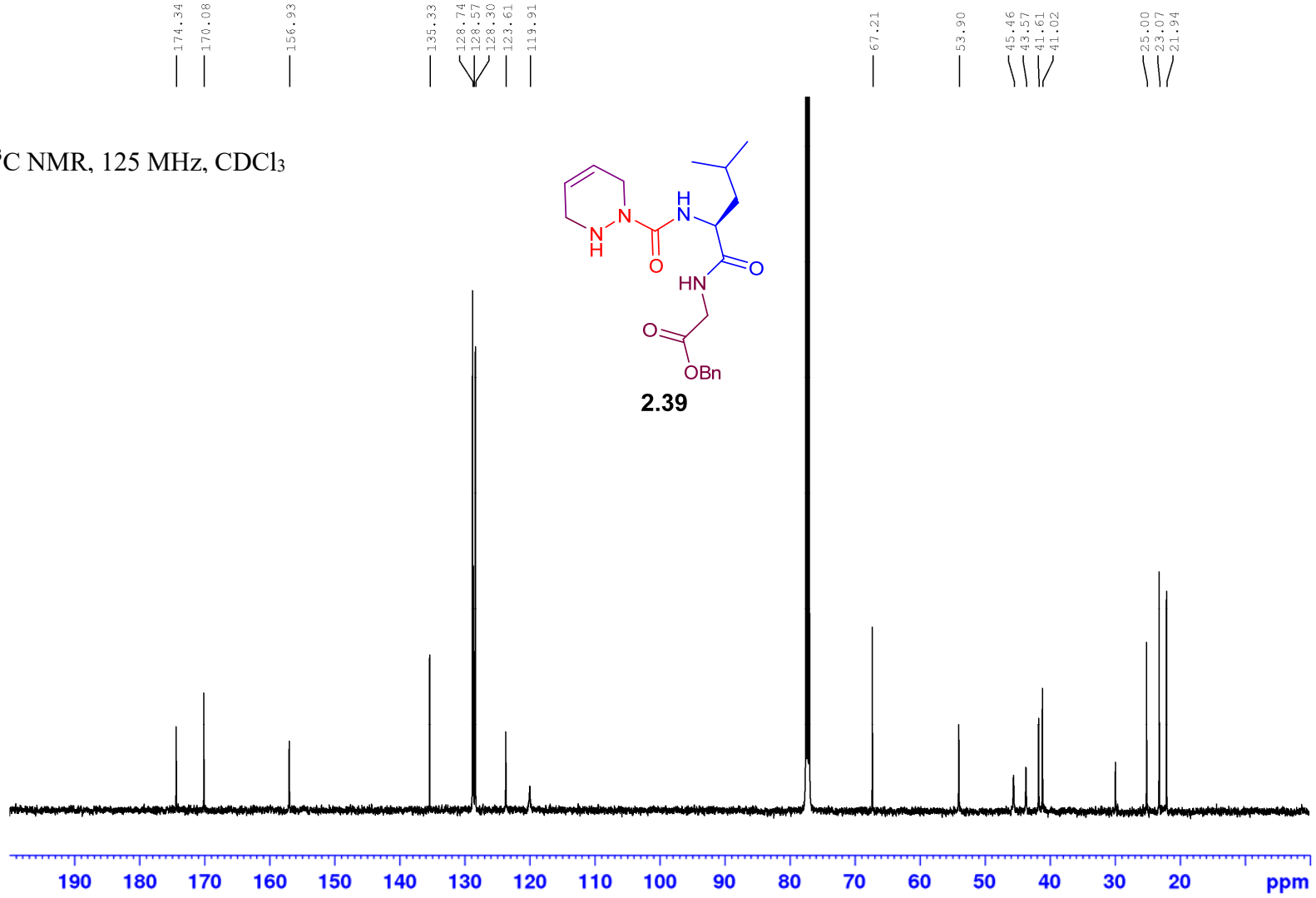

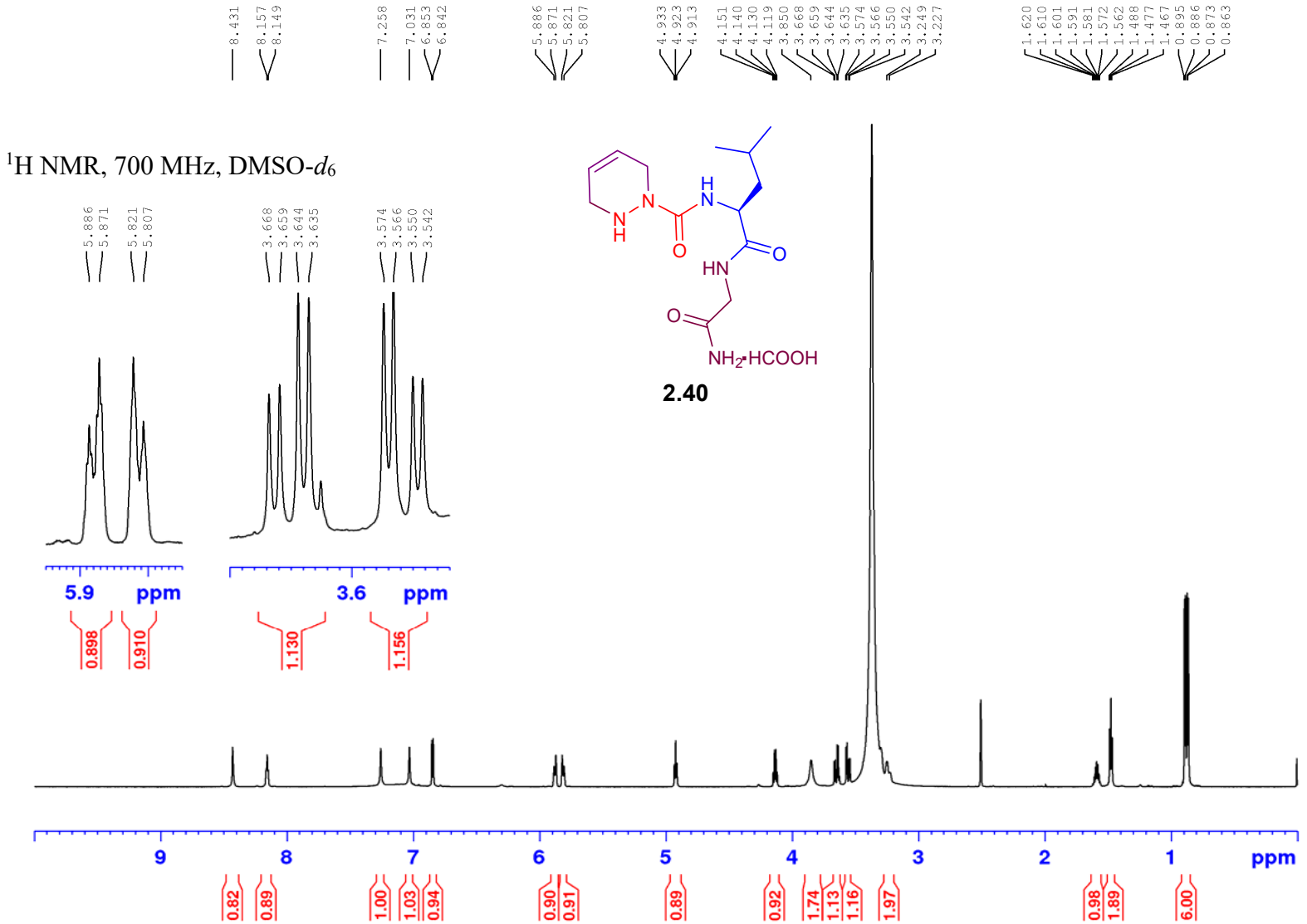
^{1}H NMR, 700 MHz, DMSO-d_6
2.40
NH2•HCOOH
HN
ppm

^{13}C NMR, 175 MHz, DMSO-d_6

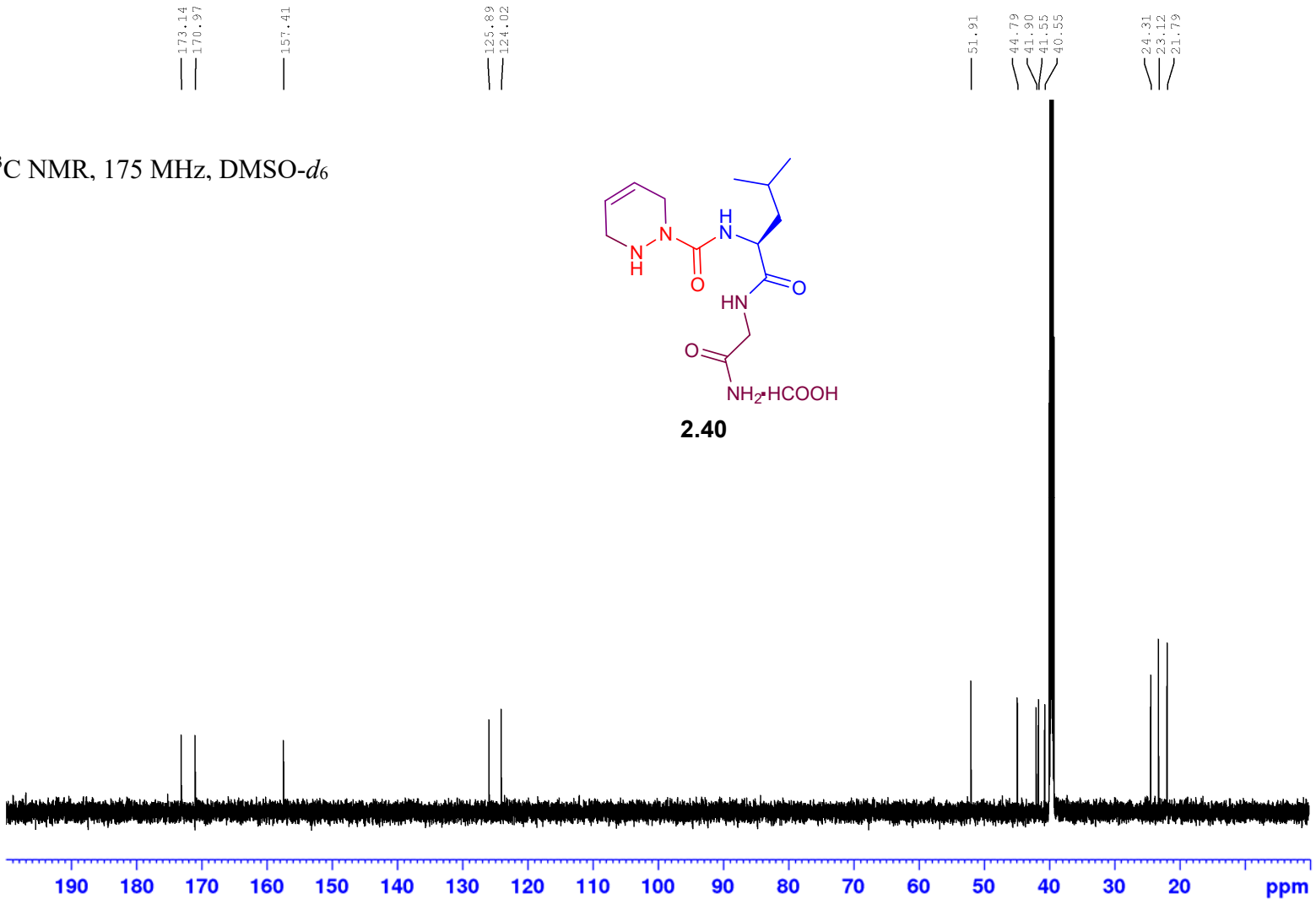

2.40

^{1}H NMR, 700 MHz, DMSO-d_6

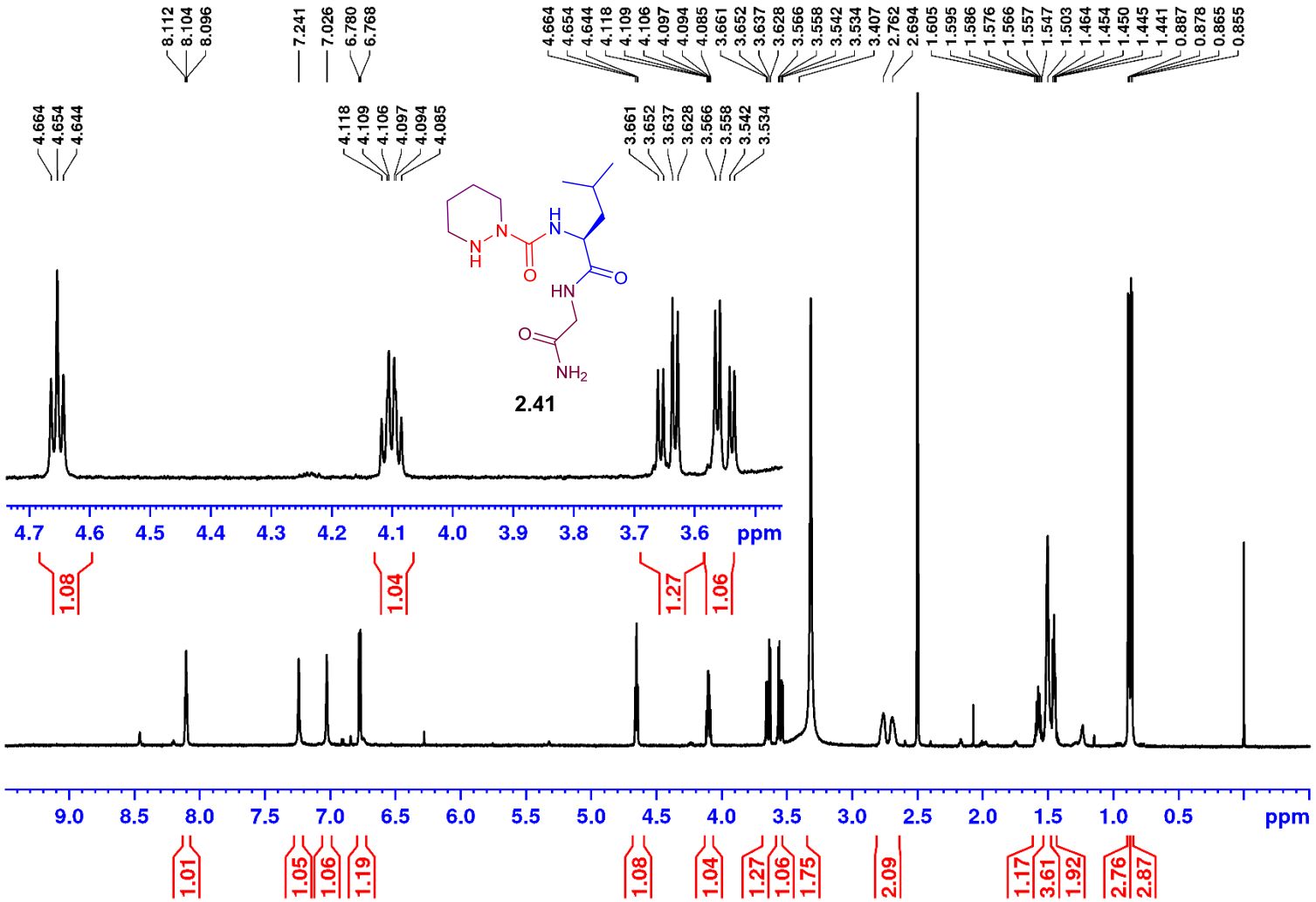

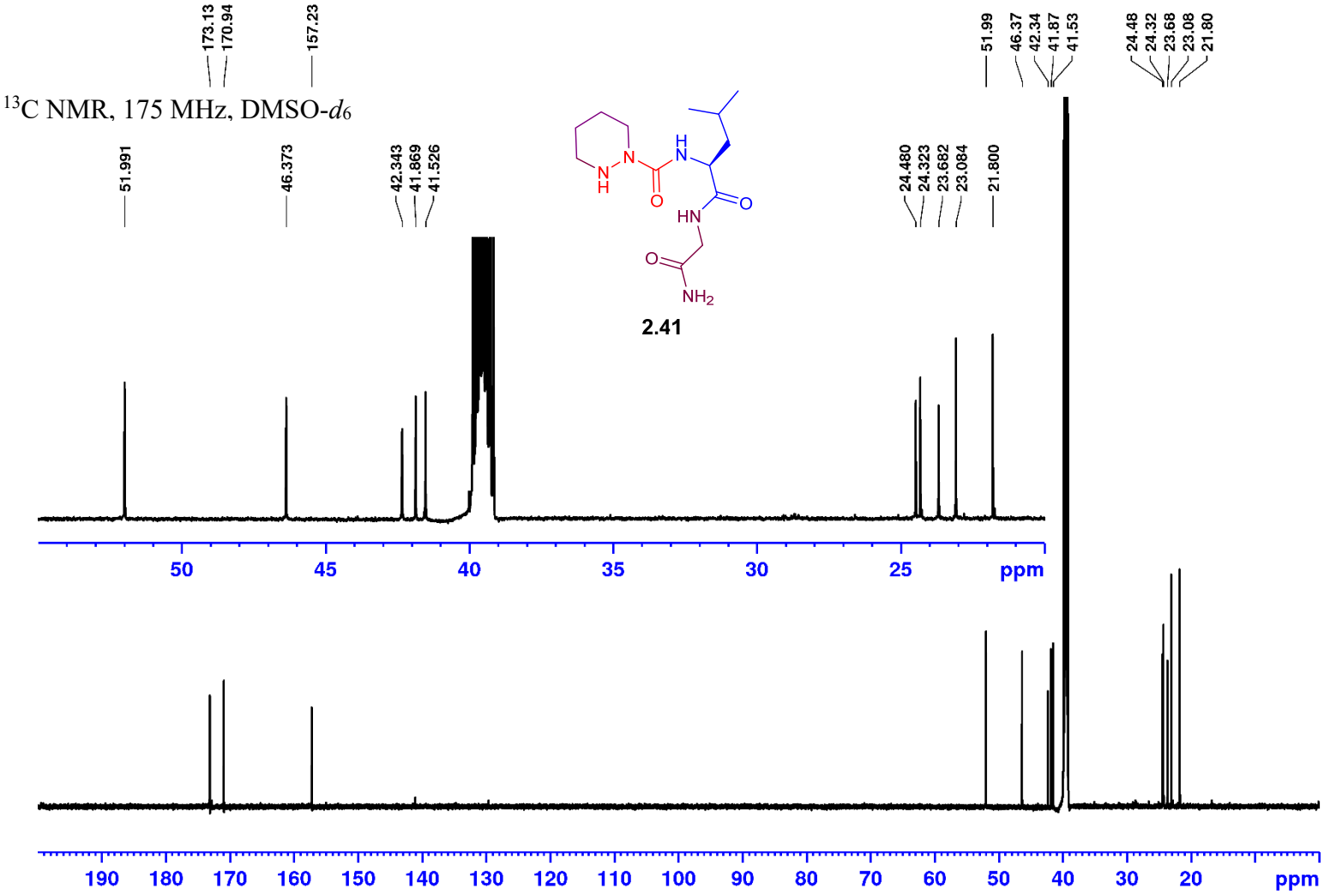
^{13}C NMR, 175 MHz, DMSO-d_6
173.13
170.94
157.23
51.991
46.373
42.343
41.869
41.526
51.99
46.37
42.34
41.87
41.53
24.480
24.323
23.682
23.084
21.800
24.48
24.32
23.68
23.08
21.80
2.41
50
45
40
35
30
25
ppm
190
180
170
160
150
140
130
120
110
100
90
80
70
60
50
40
30
20
ppm

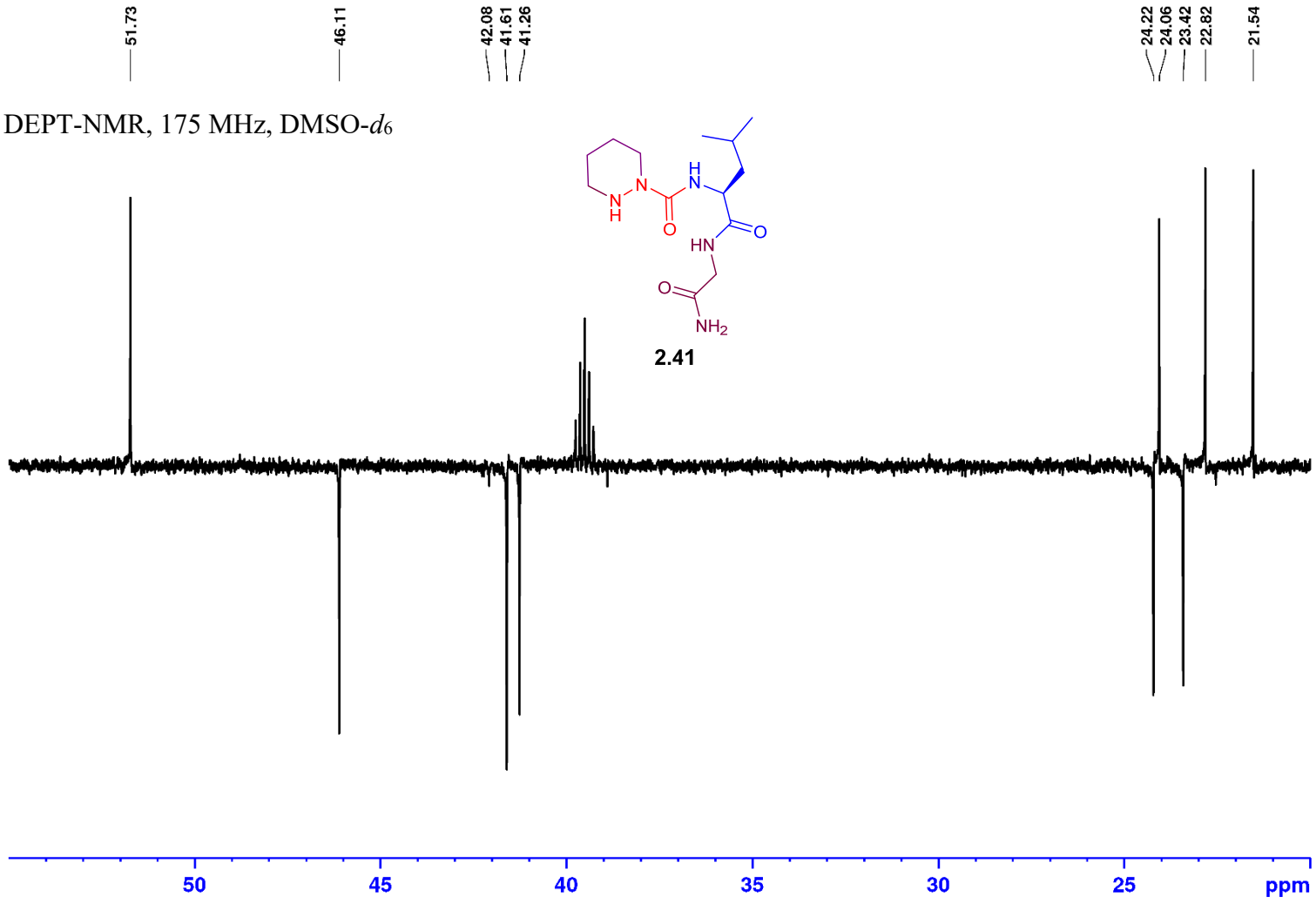
51.73
46.11
42.08
41.61
41.26
24.22
24.06
23.42
22.82
21.54
DEPT-NMR, 175 MHz, DMSO-d6
2.41
50
45
40
35
30
25
ppm

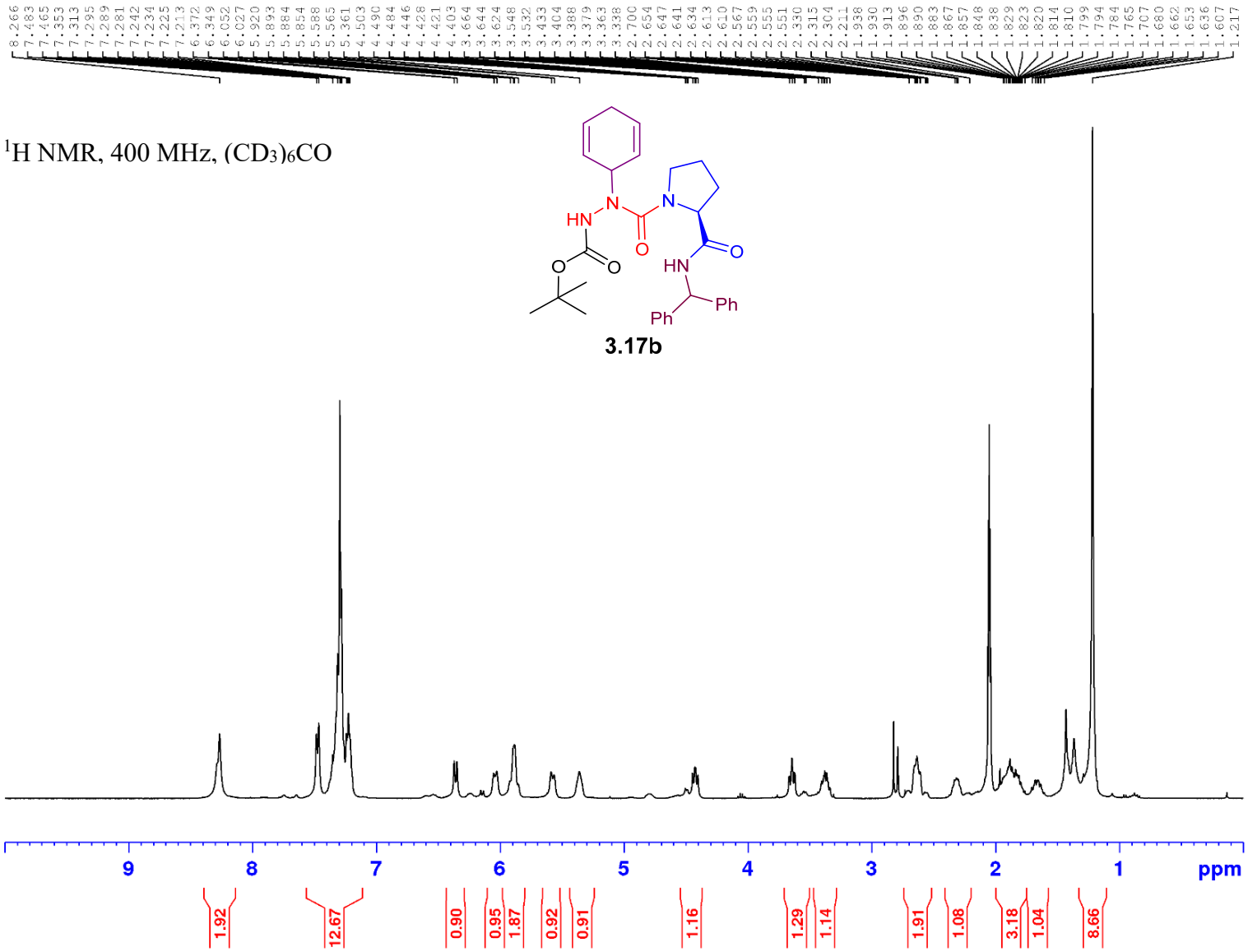
8.266
7.483
7.465
7.353
7.313
7.295
7.289
7.281
7.242
7.234
7.225
7.213
6.372
6.349
6.052
6.027
5.920
5.893
5.884
5.854
5.588
5.565
5.361
4.503
4.490
4.484
4.446
4.428
4.421
4.403
3.664
3.644
3.624
3.548
3.532
3.433
3.404
3.388
3.379
3.363
3.338
2.700
2.654
2.647
2.641
2.634
2.613
2.610
2.567
2.559
2.555
2.551
2.330
2.315
2.304
2.211
1.938
1.930
1.913
1.896
1.890
1.883
1.867
1.857
1.848
1.838
1.829
1.823
1.820
1.814
1.810
1.799
1.794
1.784
1.765
1.707
1.680
1.662
1.653
1.636
1.607
1.217
^{1}H NMR, 400 MHz, $(CD_3)_6CO$
HN
N
N
O
O
O
HN
Ph
Ph
3.17b
9
8
7
6
5
4
3
2
1
ppm
1.92
12.67
0.90
0.95
1.87
0.92
0.91
1.16
1.29
1.14
1.91
1.08
3.18
1.04
8.66

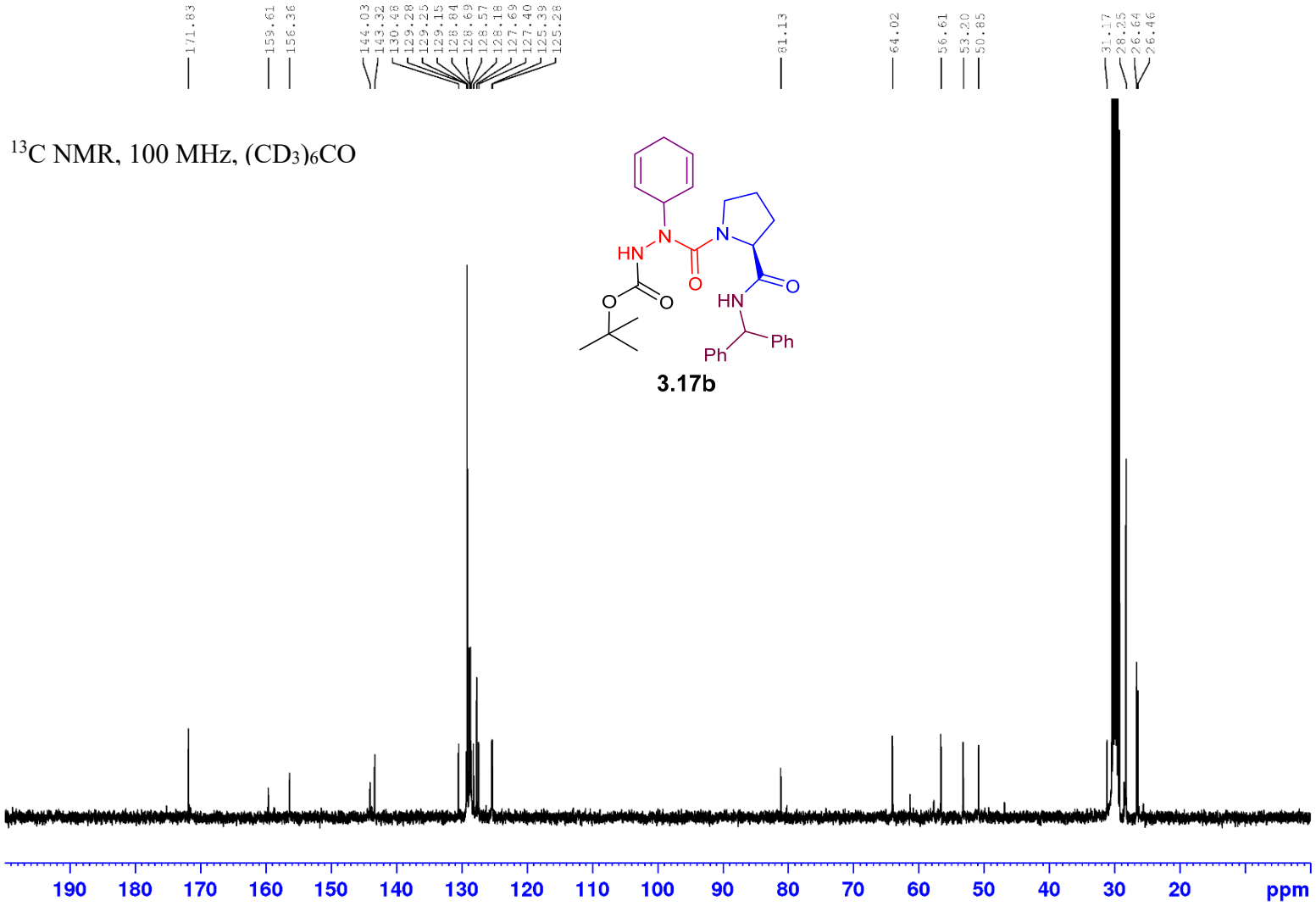

^{13}C NMR, 100 MHz, $(CD_3)_6CO$

3.17b

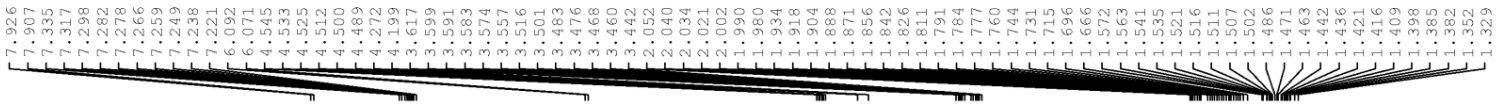

^{1}H NMR, 400 MHz, DMSO-d_6

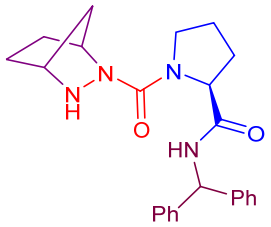

3.18

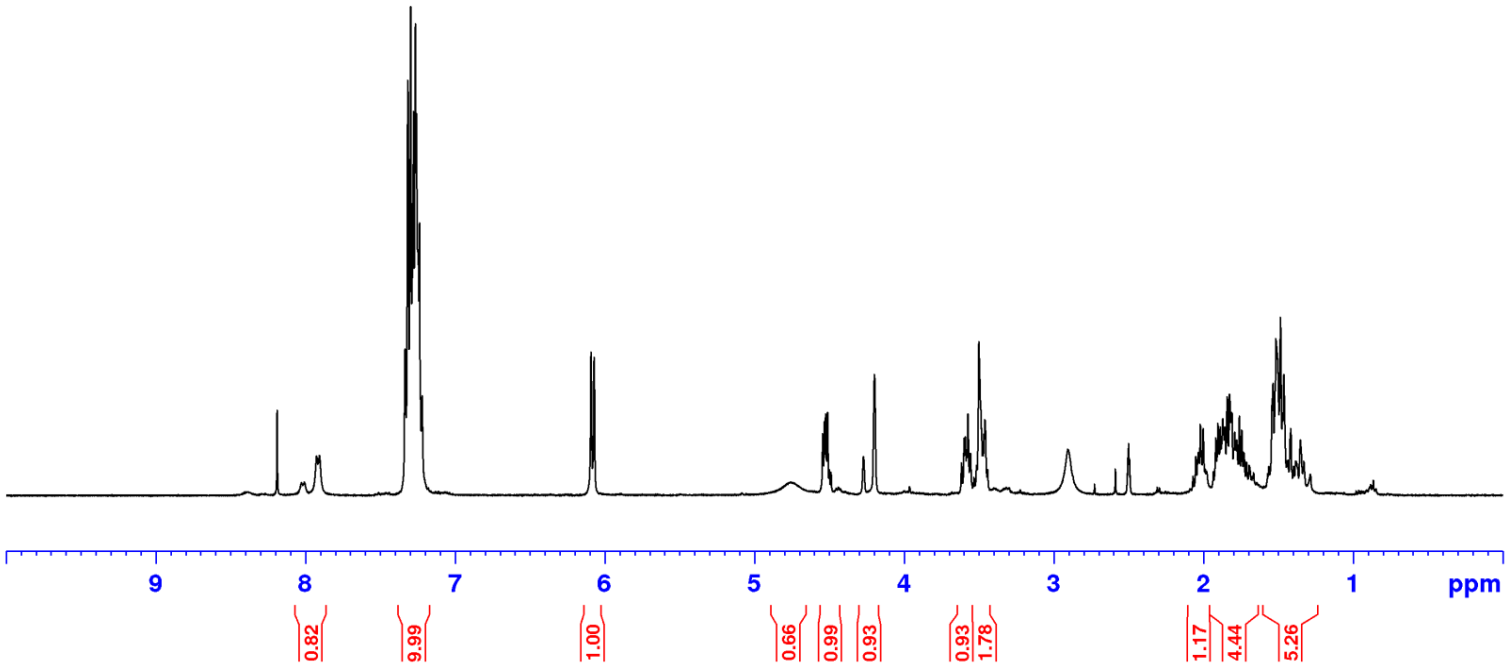

^{13}C NMR, 400 MHz, DMSO-d_6, 120 °C

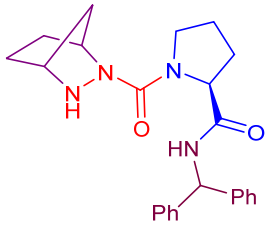

3.18

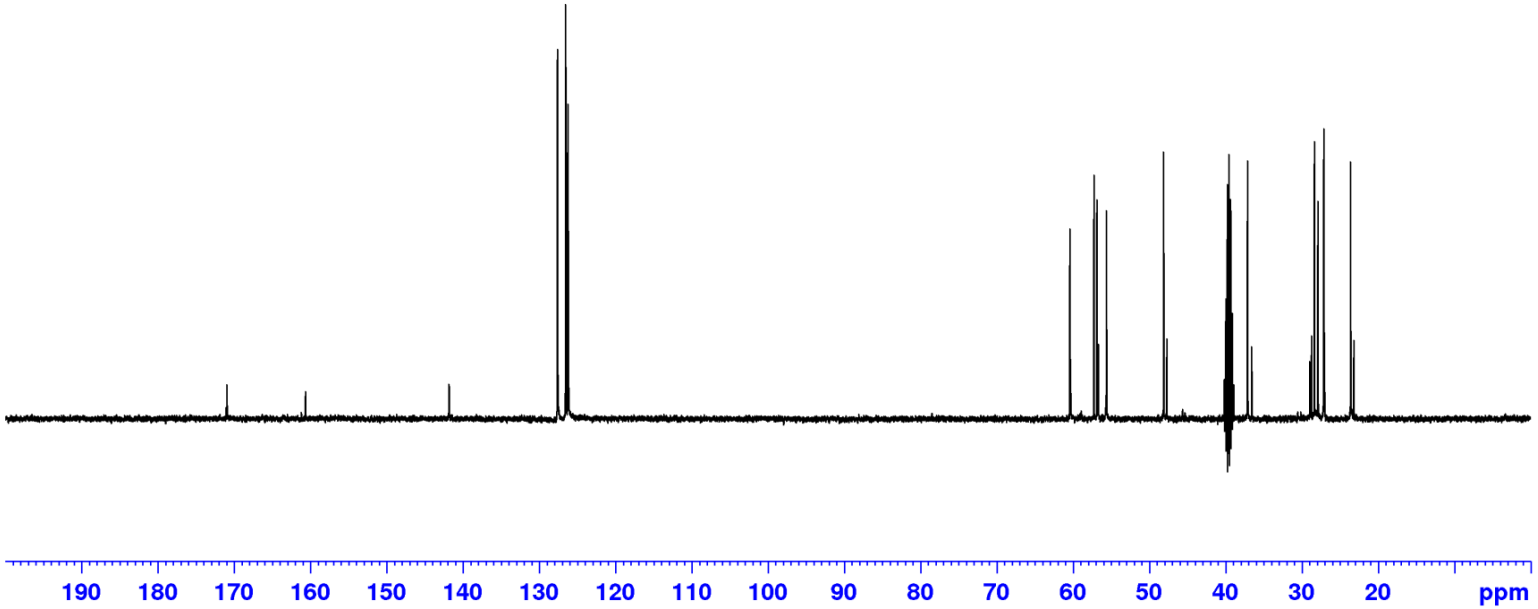

^{1}H NMR, 400 MHz, $CDCl_3$

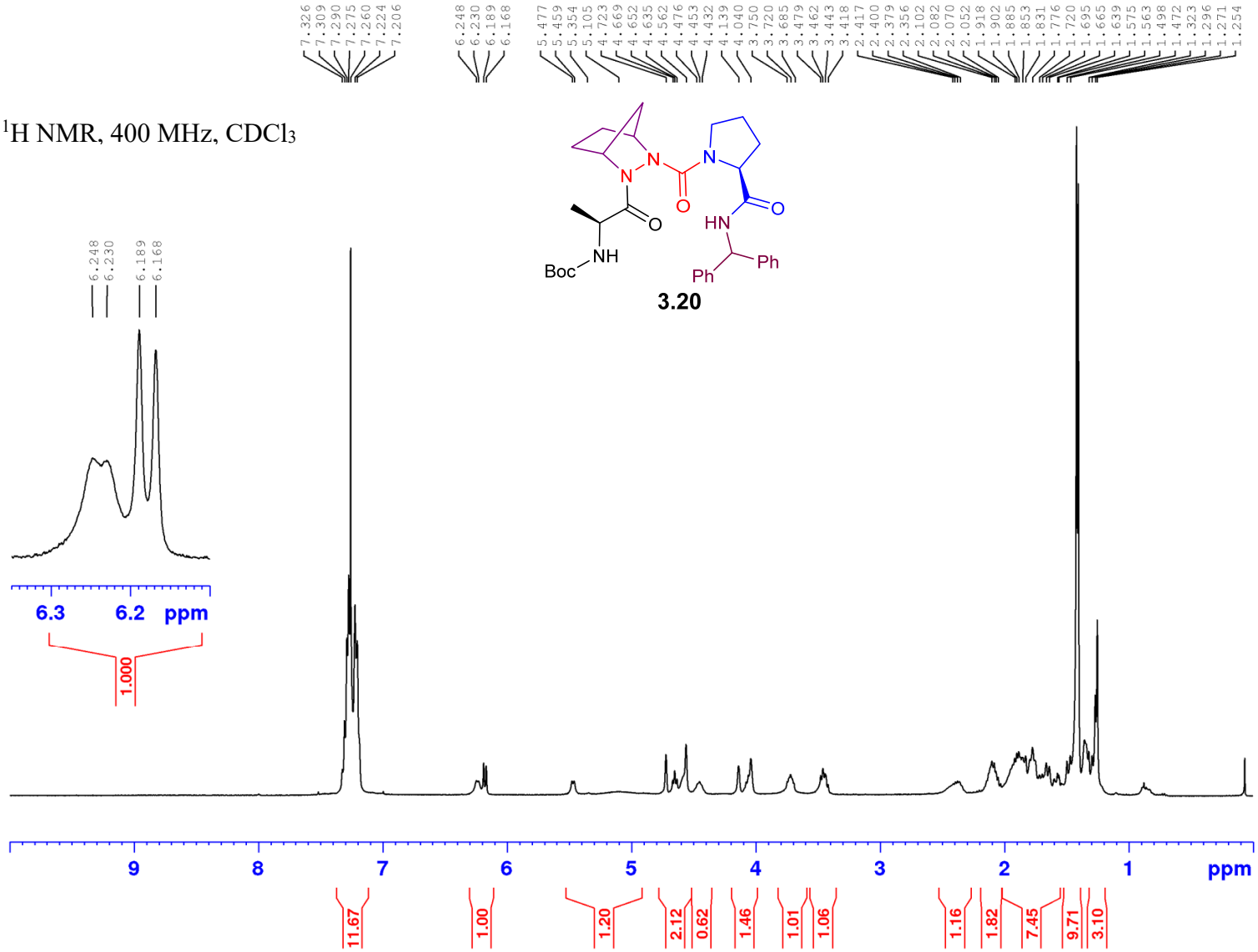

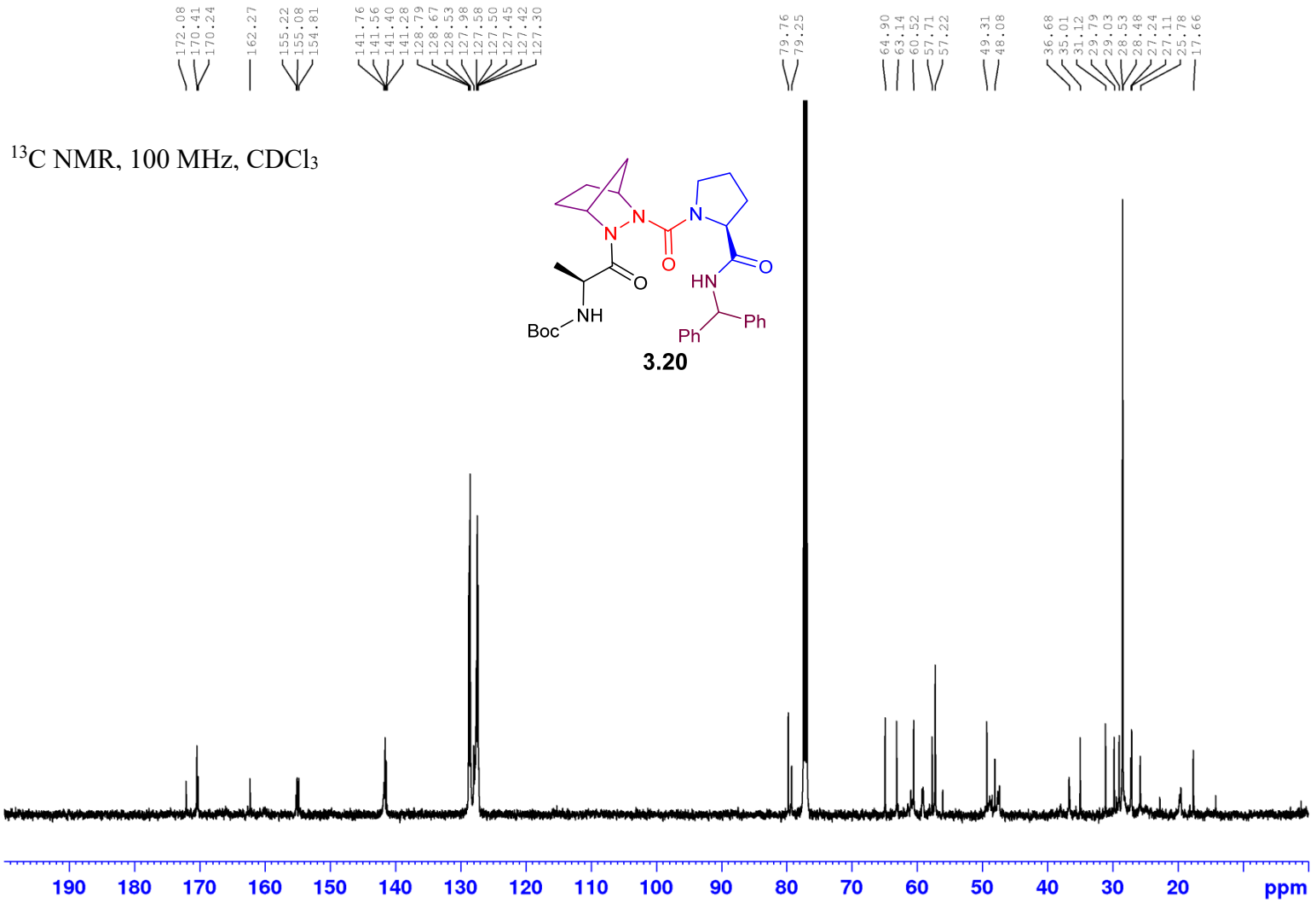

^{13}C NMR, 100 MHz, $CDCl_3$

3.20

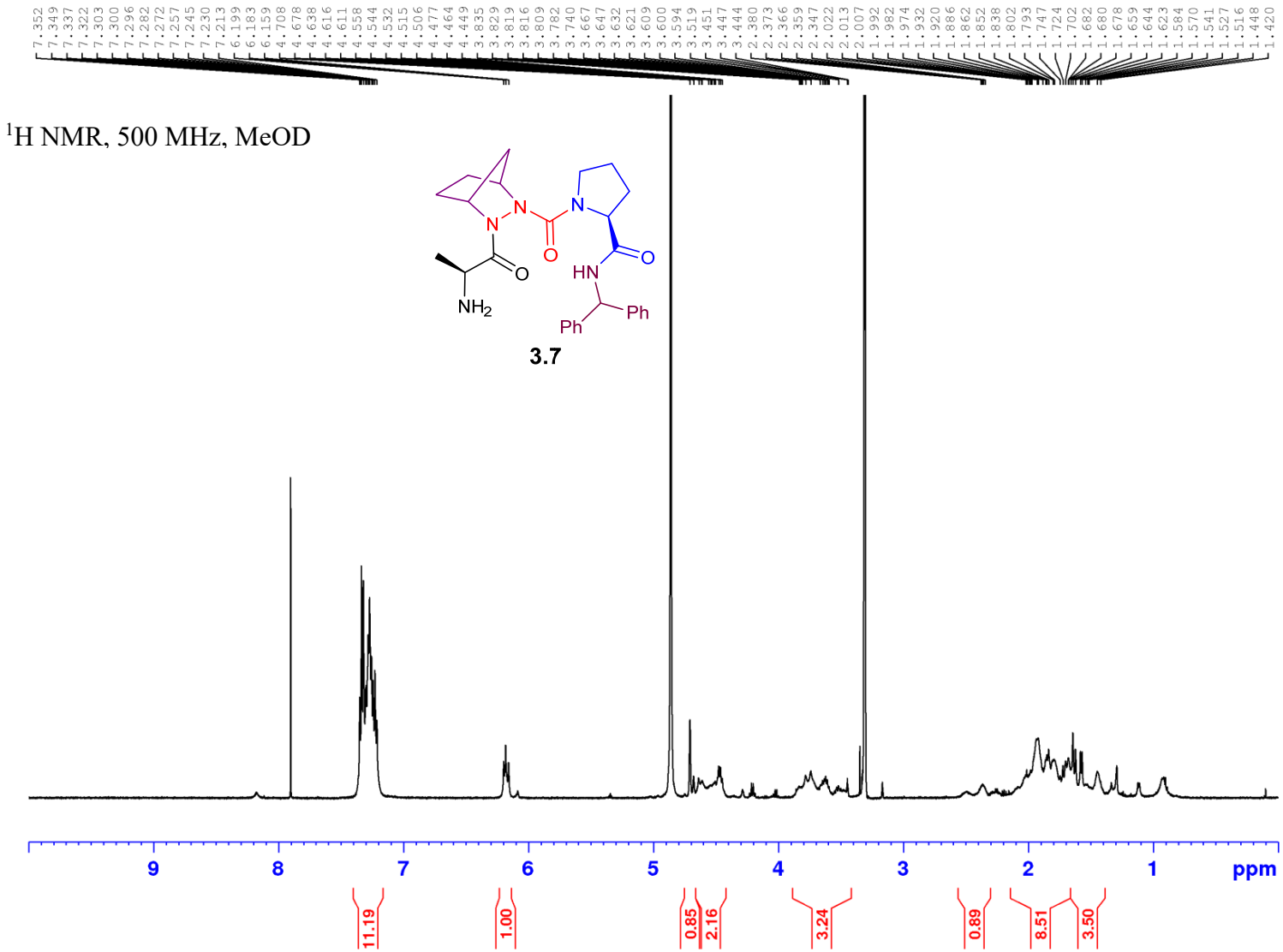
7.352
7.349
7.337
7.322
7.303
7.300
7.296
7.282
7.272
7.257
7.245
7.230
7.213
6.199
6.183
6.159
4.708
4.678
4.638
4.616
4.611
4.558
4.544
4.532
4.515
4.506
4.477
4.464
4.449
3.835
3.829
3.819
3.816
3.809
3.782
3.740
3.667
3.647
3.632
3.621
3.609
3.600
3.594
3.519
3.451
3.447
3.444
2.380
2.373
2.366
2.359
2.347
2.022
2.013
2.007
1.992
1.982
1.974
1.932
1.920
1.886
1.862
1.852
1.838
1.802
1.793
1.747
1.724
1.702
1.682
1.680
1.678
1.659
1.644
1.623
1.584
1.570
1.541
1.527
1.516
1.448
1.420
[1]H NMR, 500 MHz, MeOD
N
N
O
N
O
HN
Ph
Ph
NH2
O
3.7
9
8
7
6
5
4
3
2
1
ppm
11.19
1.00
0.85
2.16
3.24
0.89
8.51
3.50

^{13}C NMR, 125 MHz, MeOD

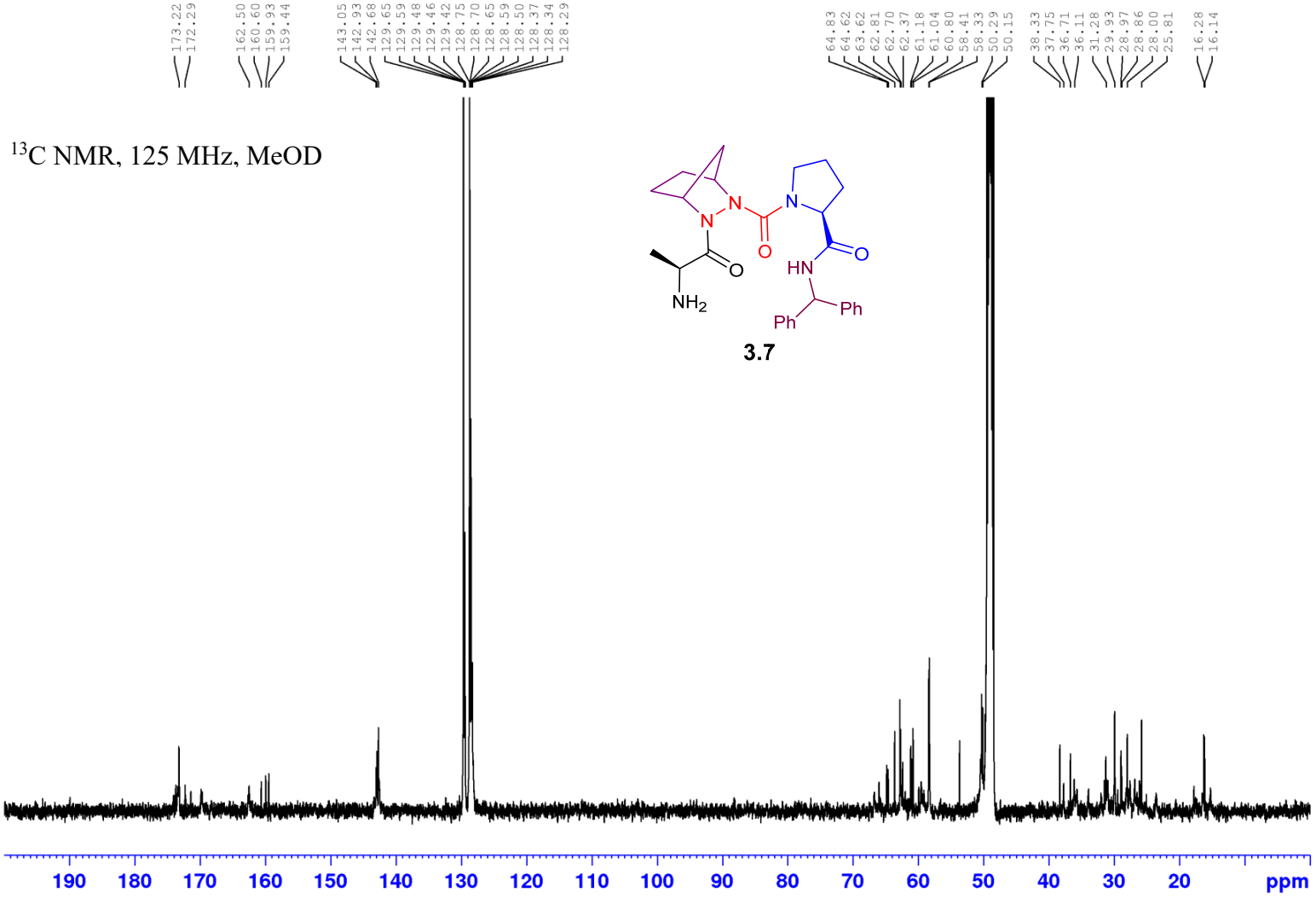

3.7

^{1}H NMR, 500 MHz, MeOD

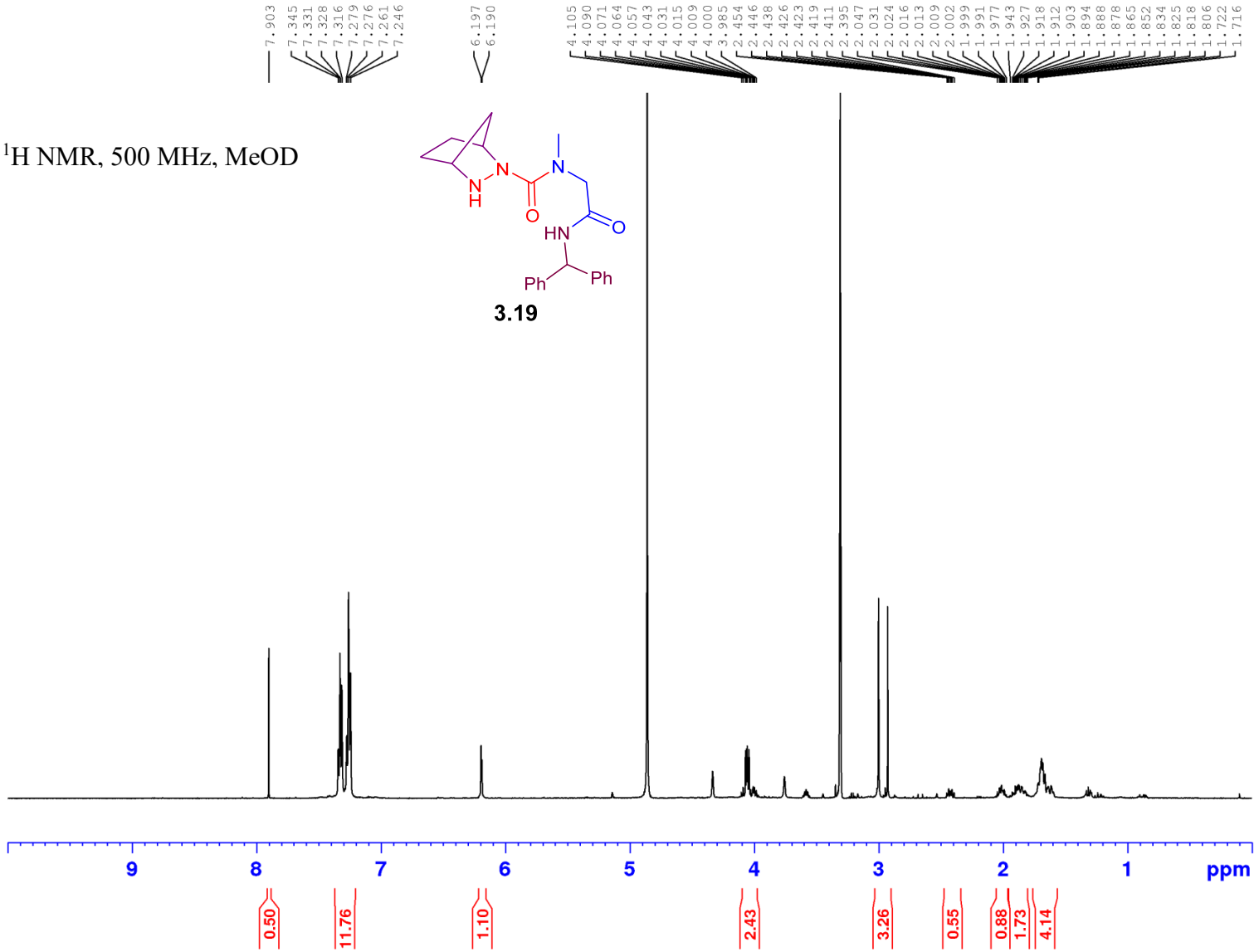

3.19

^{13}C NMR, 125 MHz, MeOD

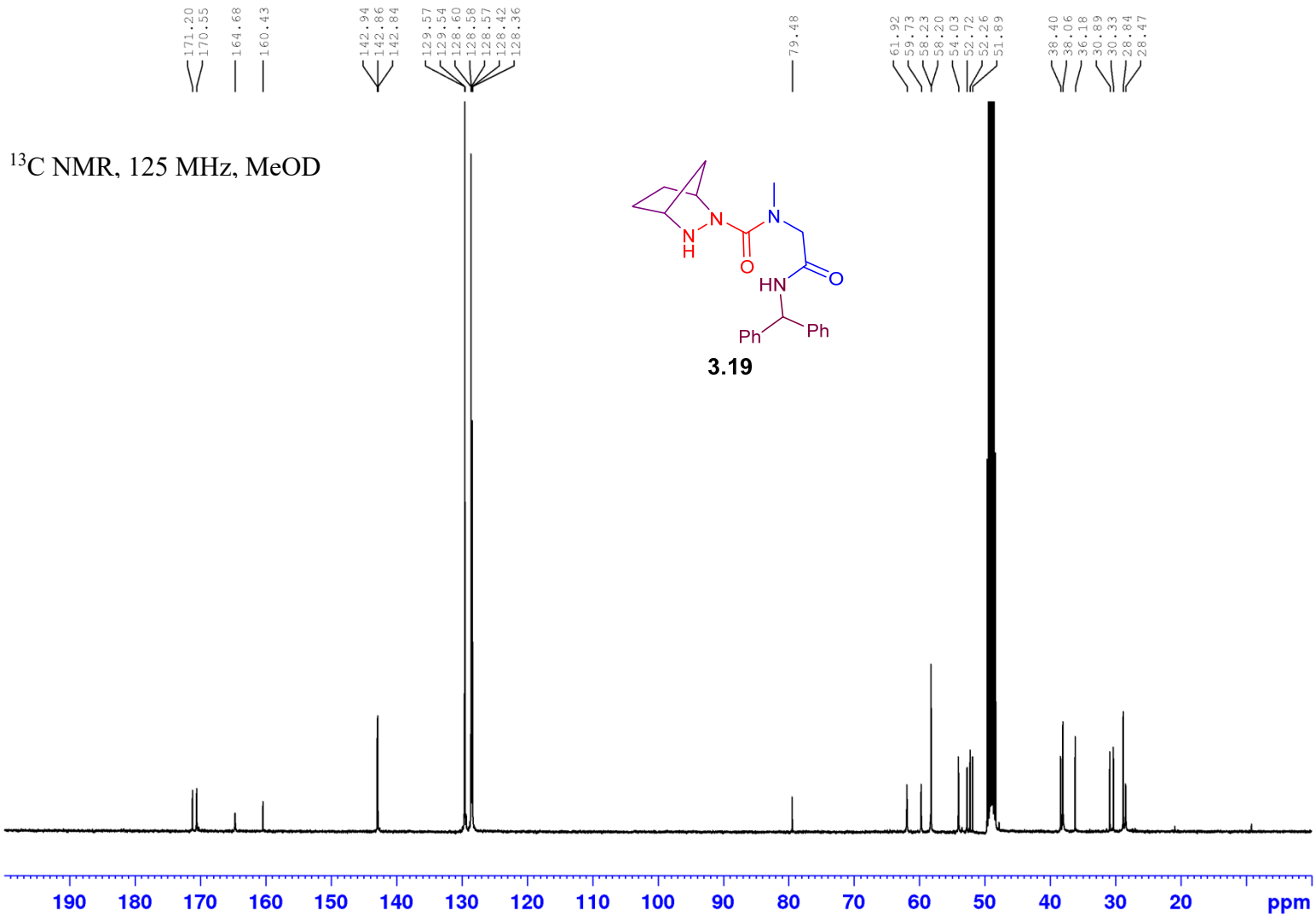

3.19

^{1}H NMR, 500 MHz, MeOD

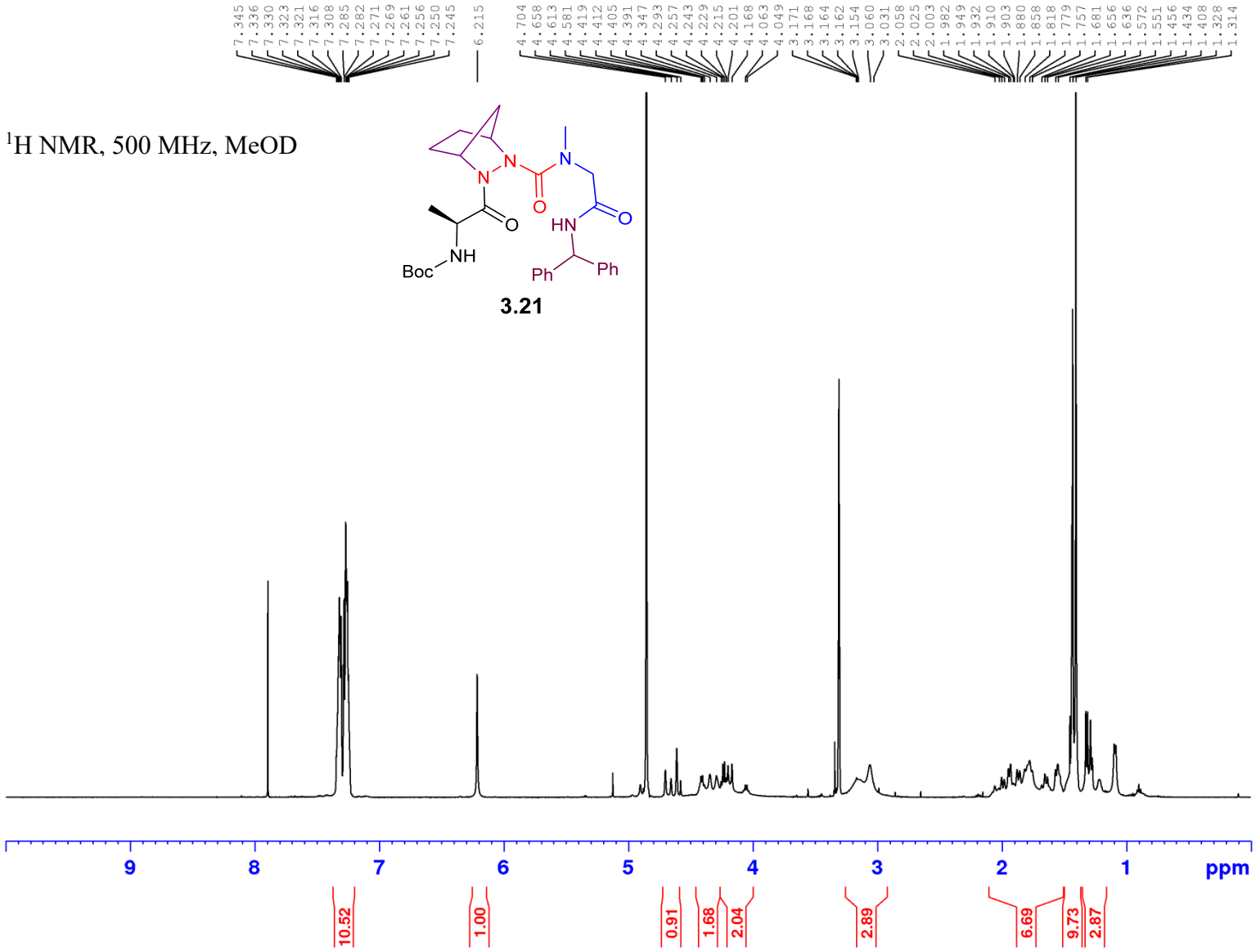

3.21

^{13}C NMR, 125 MHz, MeOD

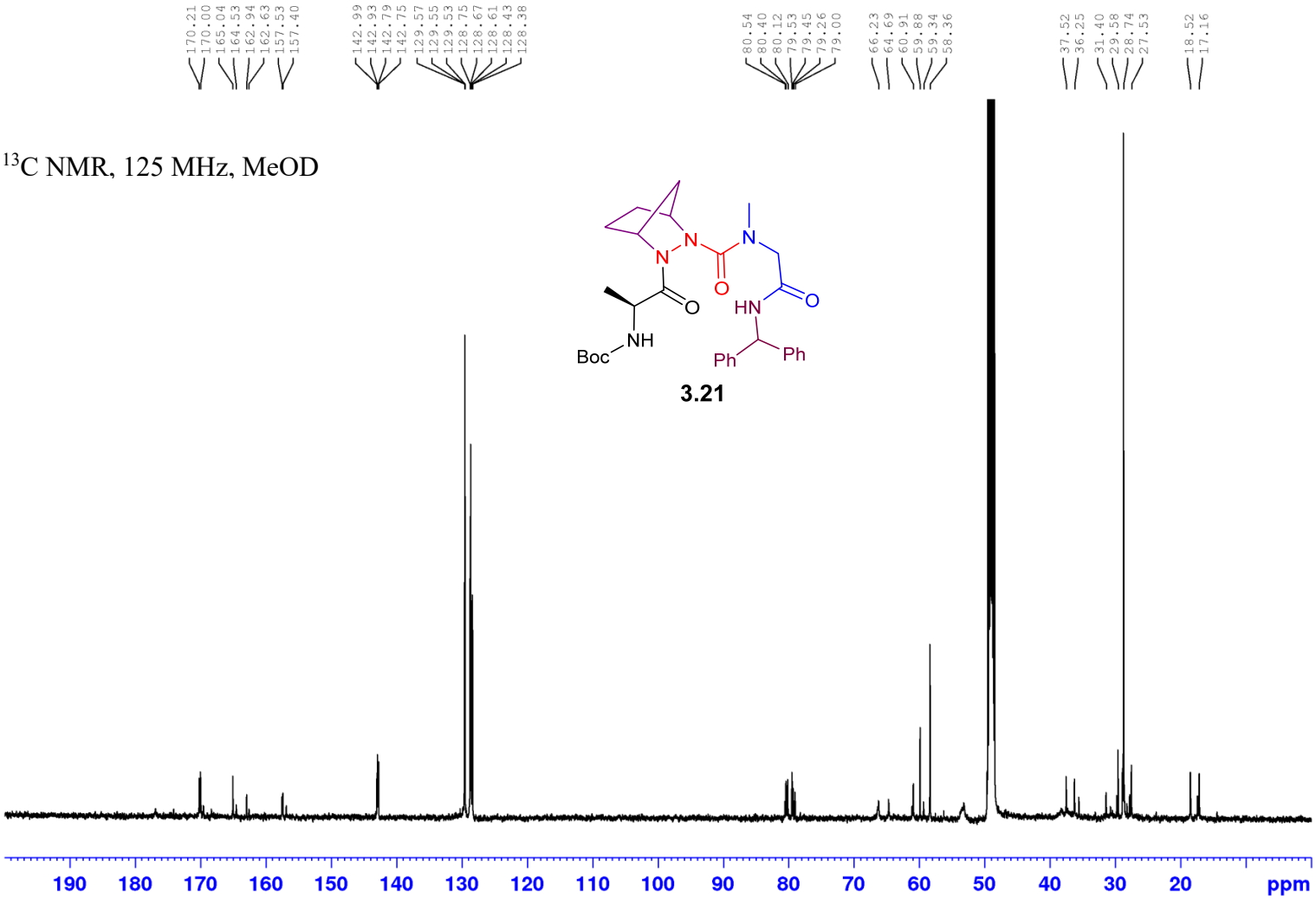

3.21

^{1}H NMR, 700 MHz, DMSO-d_6

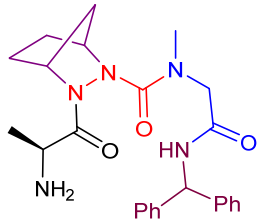

3.8

^{13}C NMR, 175 MHz, DMSO-*d*$_6$

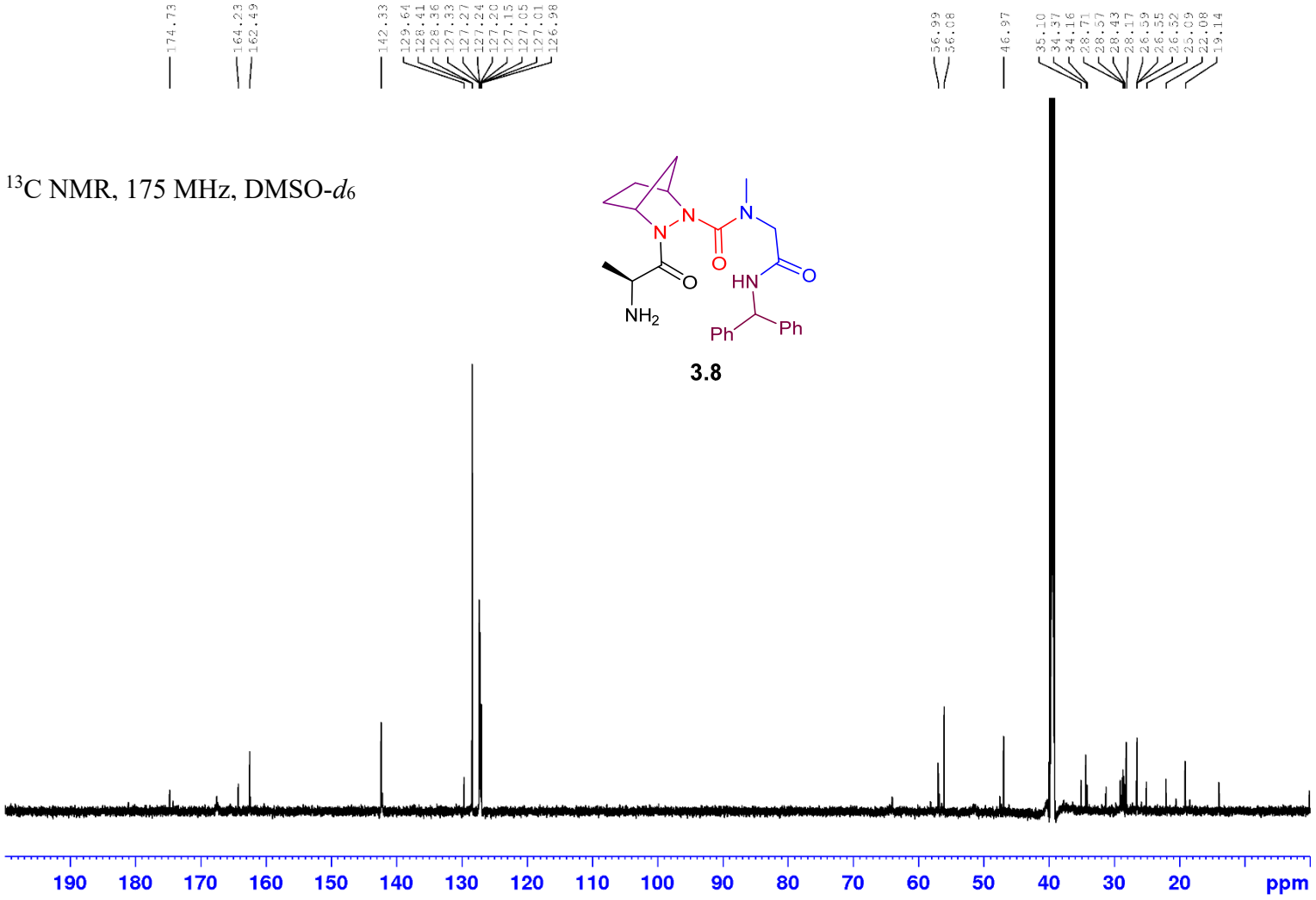

3.8

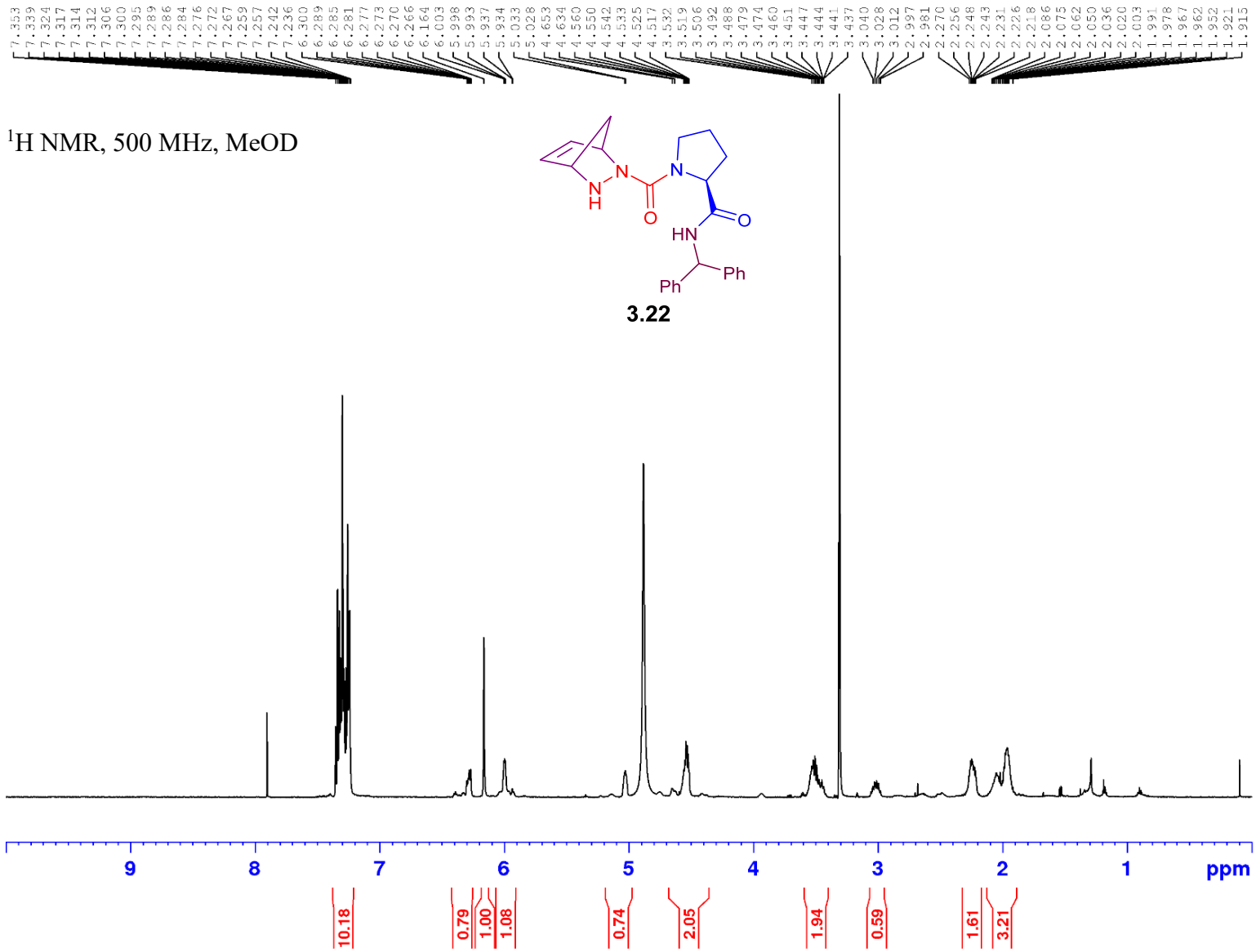
7.353
7.339
7.324
7.317
7.314
7.312
7.306
7.300
7.295
7.289
7.286
7.284
7.276
7.272
7.267
7.259
7.257
7.242
7.236
6.300
6.289
6.285
6.281
6.277
6.273
6.270
6.266
6.164
6.003
5.998
5.993
5.937
5.934
5.033
5.028
4.653
4.634
4.560
4.550
4.542
4.533
4.525
4.517
3.532
3.519
3.506
3.492
3.488
3.479
3.474
3.460
3.451
3.447
3.444
3.441
3.437
3.040
3.028
3.012
2.997
2.981
2.270
2.256
2.248
2.243
2.231
2.226
2.218
2.086
2.075
2.062
2.050
2.036
2.020
2.003
1.991
1.978
1.967
1.962
1.952
1.921
1.915
1H NMR, 500 MHz, MeOD
N
N
H
O
N
O
HN
Ph
Ph
3.22
9
8
7
6
5
4
3
2
1
ppm
10.18
0.79
1.00
1.08
0.74
2.05
1.94
0.59
1.61
3.21

^{13}C NMR, 125 MHz, MeOD

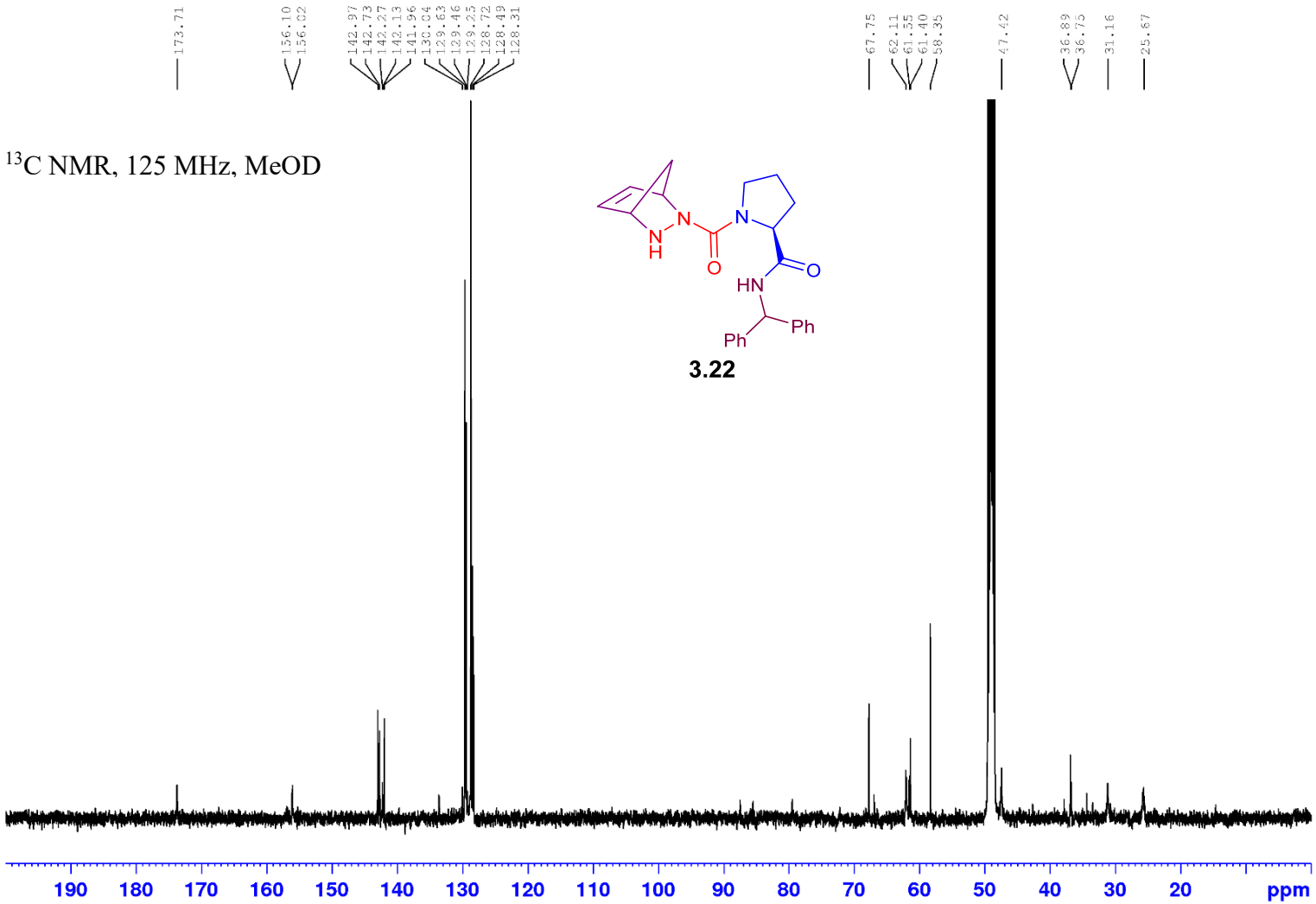

3.22

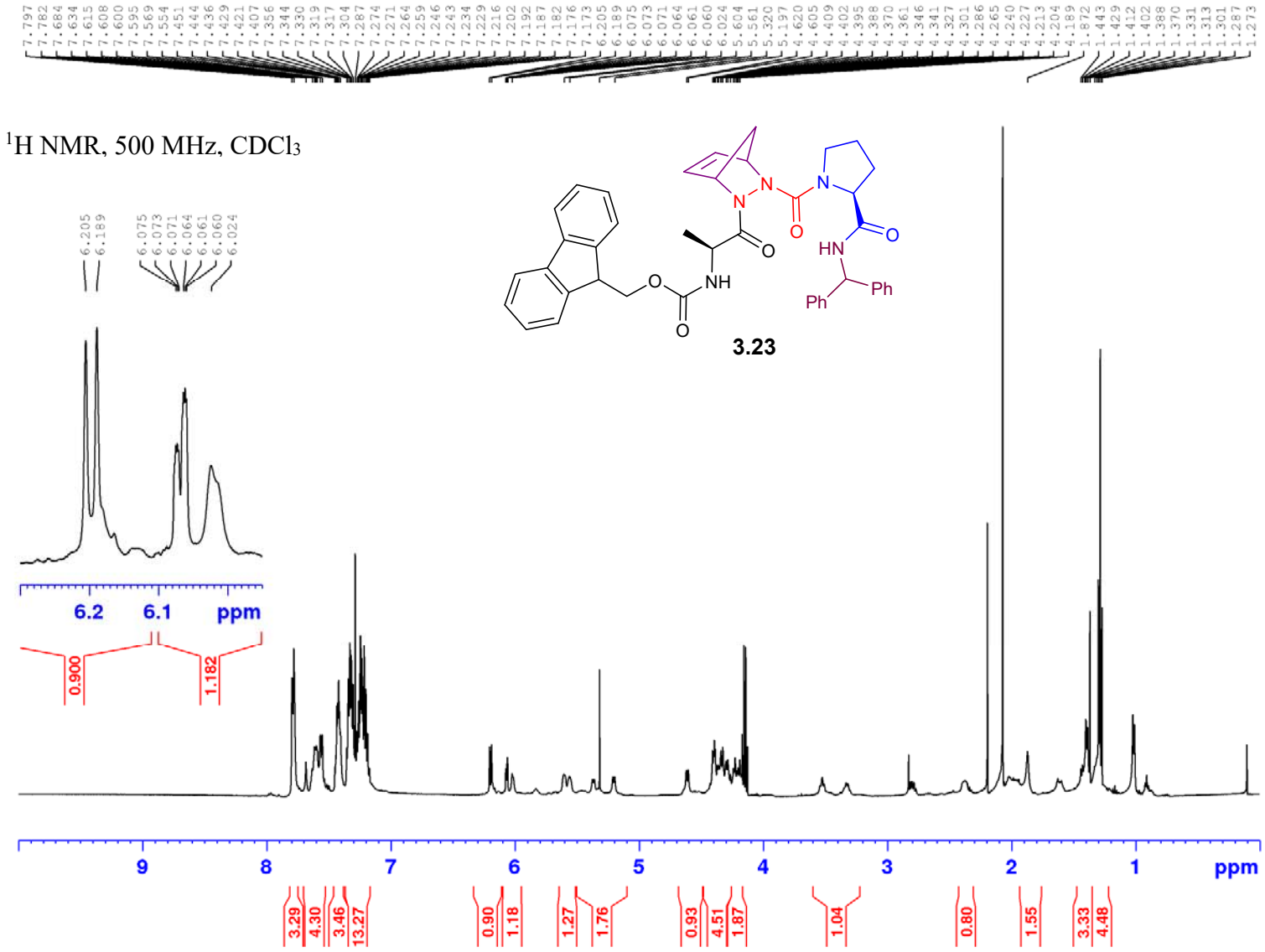
7.797
7.782
7.684
7.634
7.615
7.608
7.600
7.595
7.569
7.554
7.451
7.444
7.436
7.429
7.421
7.407
7.356
7.344
7.330
7.319
7.317
7.304
7.287
7.274
7.271
7.264
7.259
7.246
7.243
7.234
7.229
7.216
7.202
7.192
7.187
7.182
7.176
7.173
6.205
6.189
6.075
6.073
6.071
6.064
6.061
6.060
6.024
5.604
5.561
5.320
5.197
4.620
4.605
4.409
4.402
4.395
4.388
4.370
4.361
4.346
4.341
4.327
4.301
4.286
4.265
4.240
4.227
4.213
4.204
4.189
1.872
1.443
1.429
1.412
1.402
1.388
1.370
1.331
1.313
1.301
1.287
1.273
^{1}H NMR, 500 MHz, CDCl$_3$
N
N
O
N
O
HN
O
NH
O
O
Ph
Ph
3.23
6.2
6.1
ppm
0.900
1.182
9
8
7
6
5
4
3
2
1
ppm
3.29
4.30
3.46
13.27
0.90
1.18
1.27
1.76
0.93
4.51
1.87
1.04
0.80
1.55
3.33
4.48

^{13}C NMR, 125 MHz, $CDCl_3$

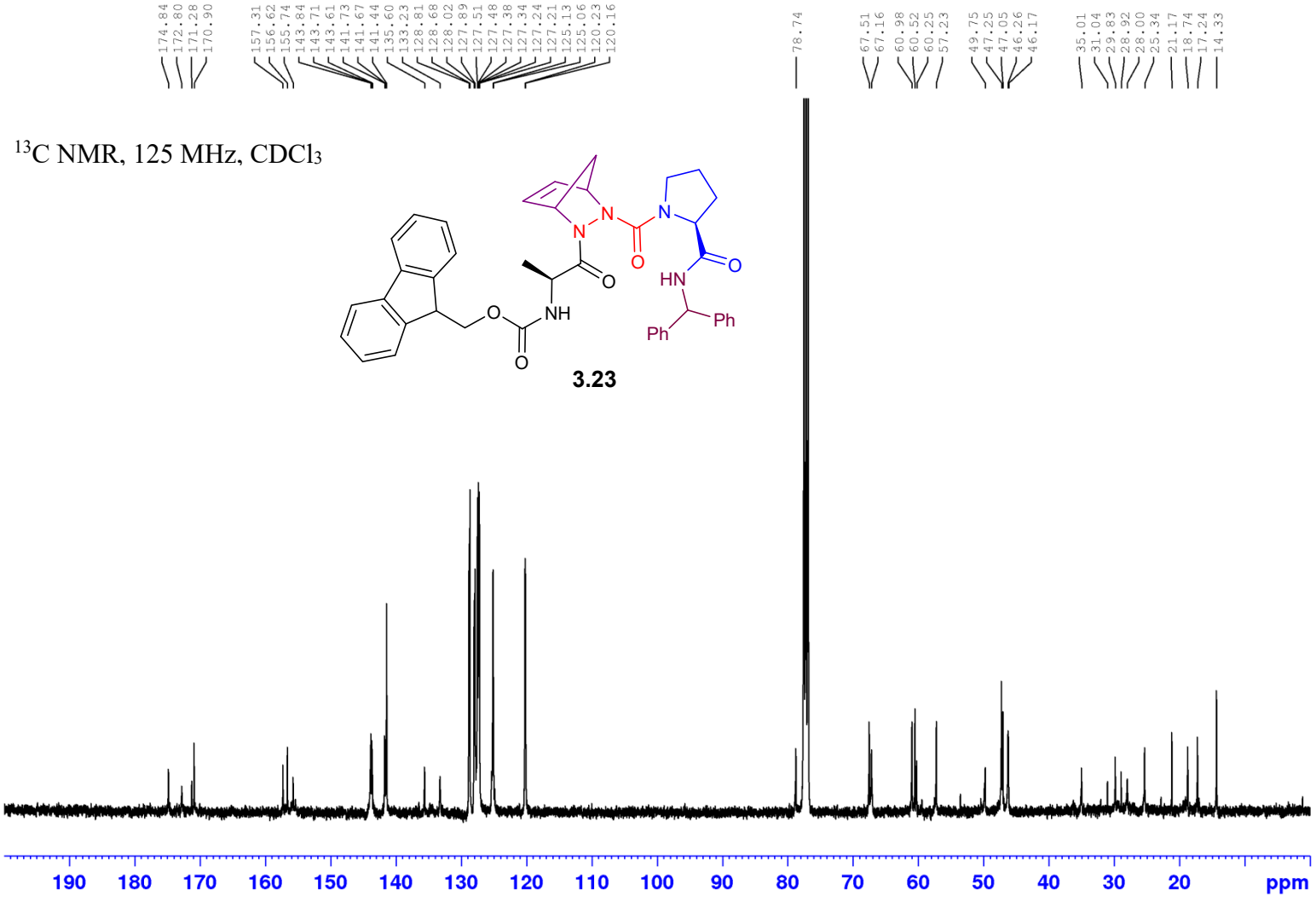

3.23

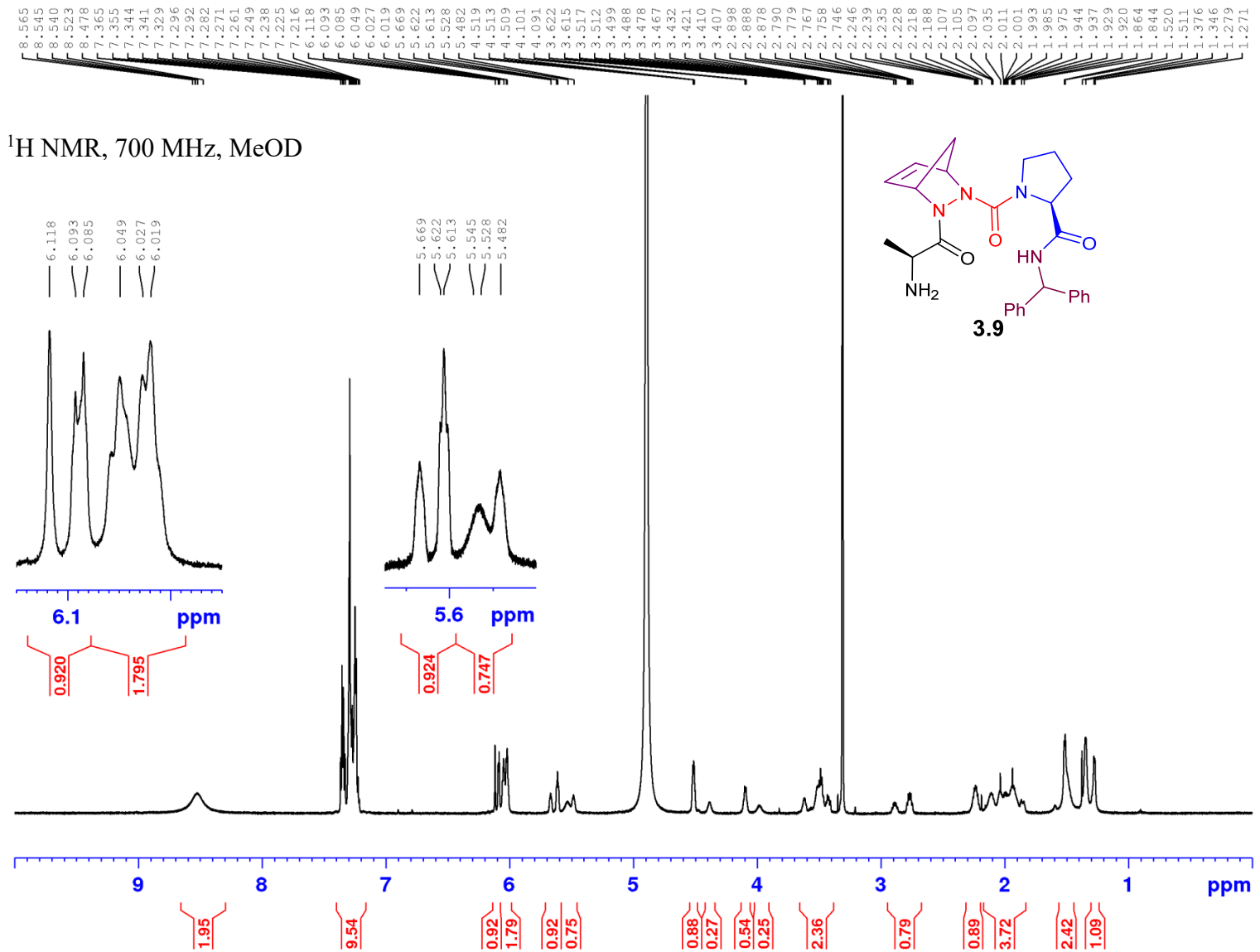
^{1}H NMR, 700 MHz, MeOD
3.9
6.1 ppm
5.6 ppm
9 8 7 6 5 4 3 2 1 ppm

^{13}C NMR, 175 MHz, MeOD

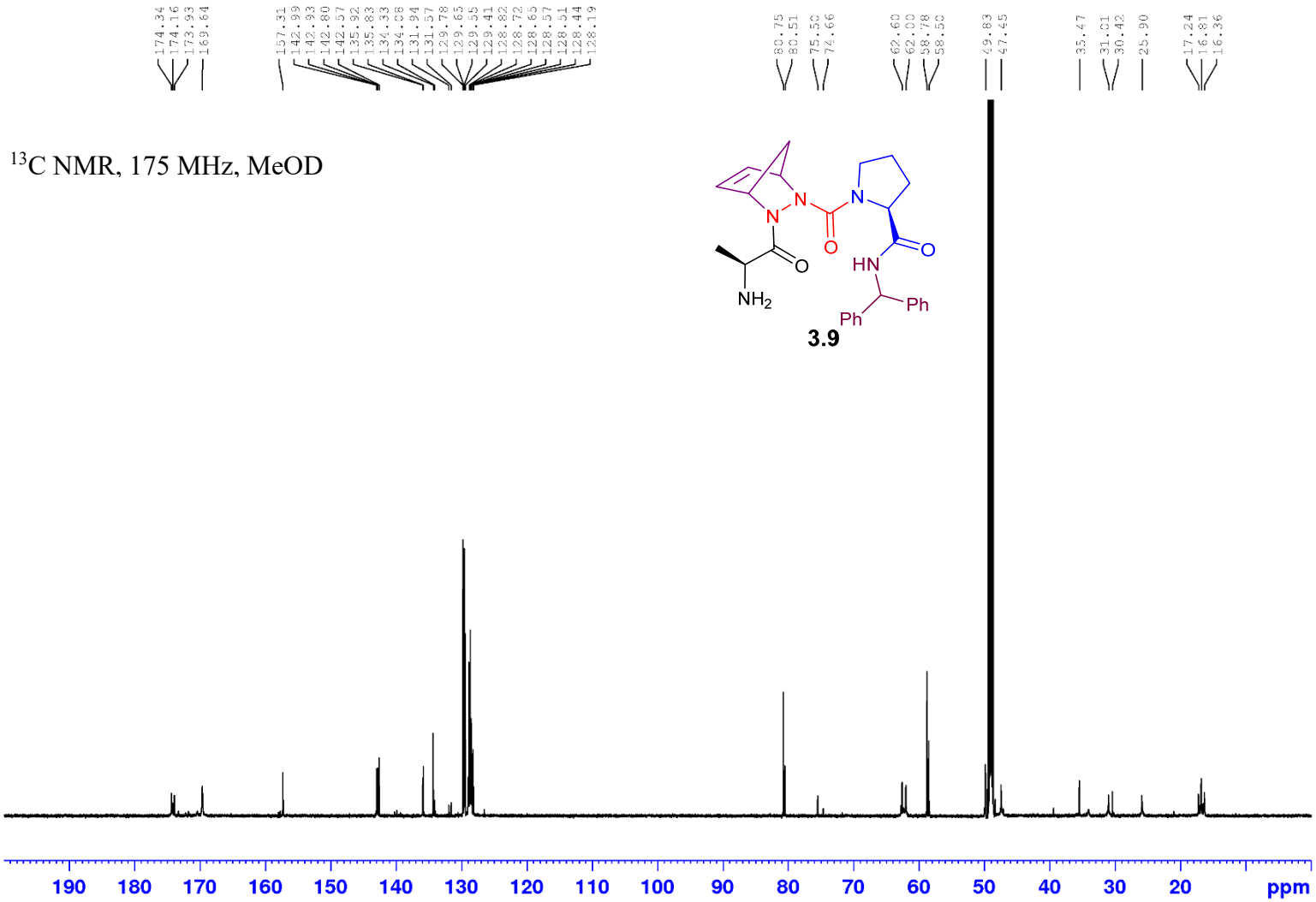

3.9

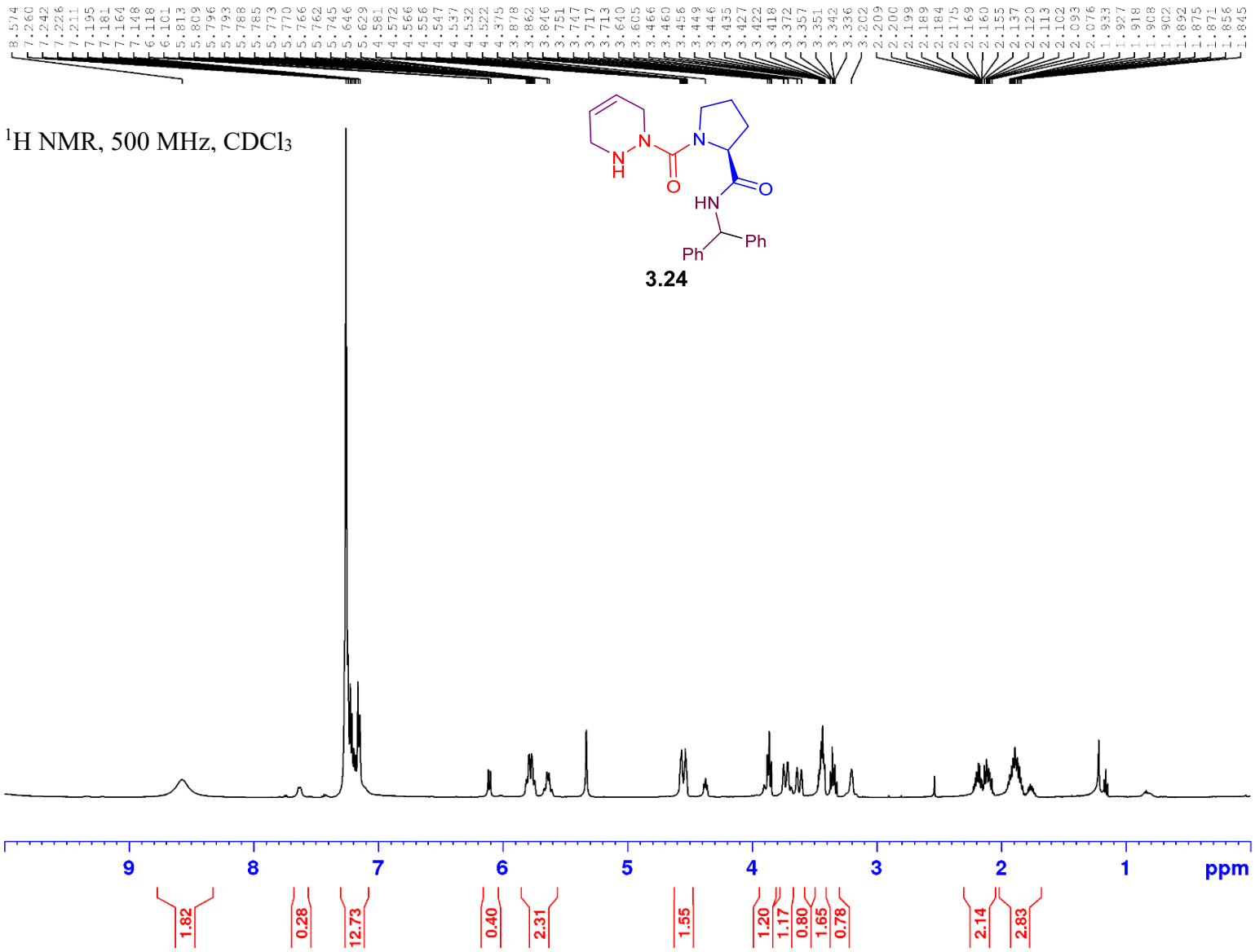
8.574
7.260
7.242
7.226
7.211
7.195
7.181
7.164
7.148
6.118
6.101
5.813
5.809
5.796
5.793
5.788
5.785
5.773
5.770
5.766
5.762
5.745
5.646
5.629
4.581
4.572
4.566
4.556
4.547
4.537
4.532
4.522
4.375
3.878
3.862
3.846
3.751
3.747
3.717
3.713
3.640
3.605
3.466
3.460
3.456
3.449
3.446
3.435
3.427
3.422
3.418
3.372
3.357
3.351
3.342
3.336
3.202
2.209
2.200
2.199
2.189
2.184
2.175
2.169
2.160
2.155
2.137
2.120
2.113
2.102
2.093
2.076
1.933
1.927
1.918
1.908
1.902
1.892
1.875
1.871
1.856
1.845
1H NMR, 500 MHz, CDCl3
N
N
H
O
N
O
HN
Ph
Ph
3.24
9
8
7
6
5
4
3
2
1
ppm
1.82
0.28
12.73
0.40
2.31
1.55
1.20
1.17
0.80
1.65
0.78
2.14
2.83

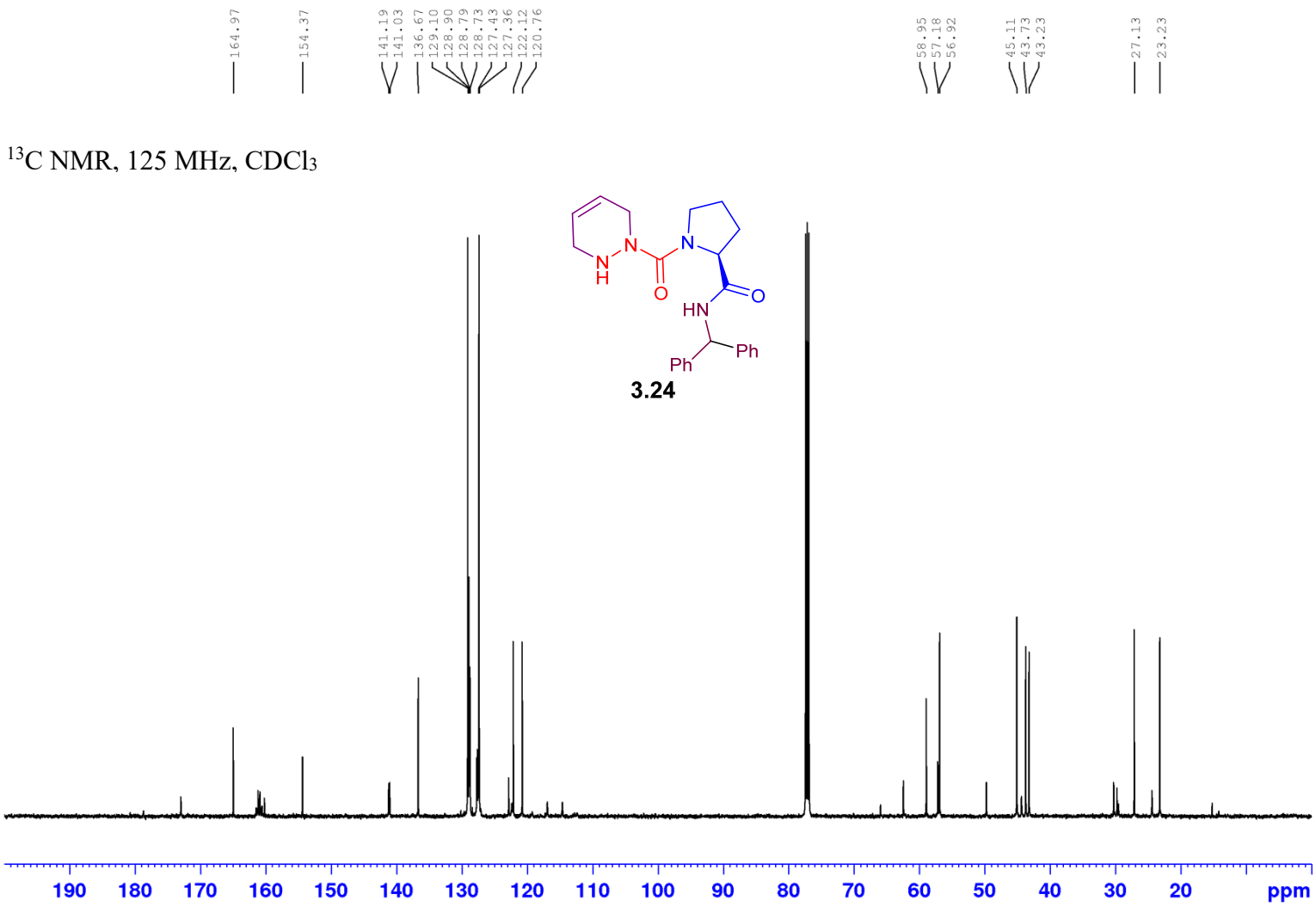

^{13}C NMR, 125 MHz, $CDCl_3$

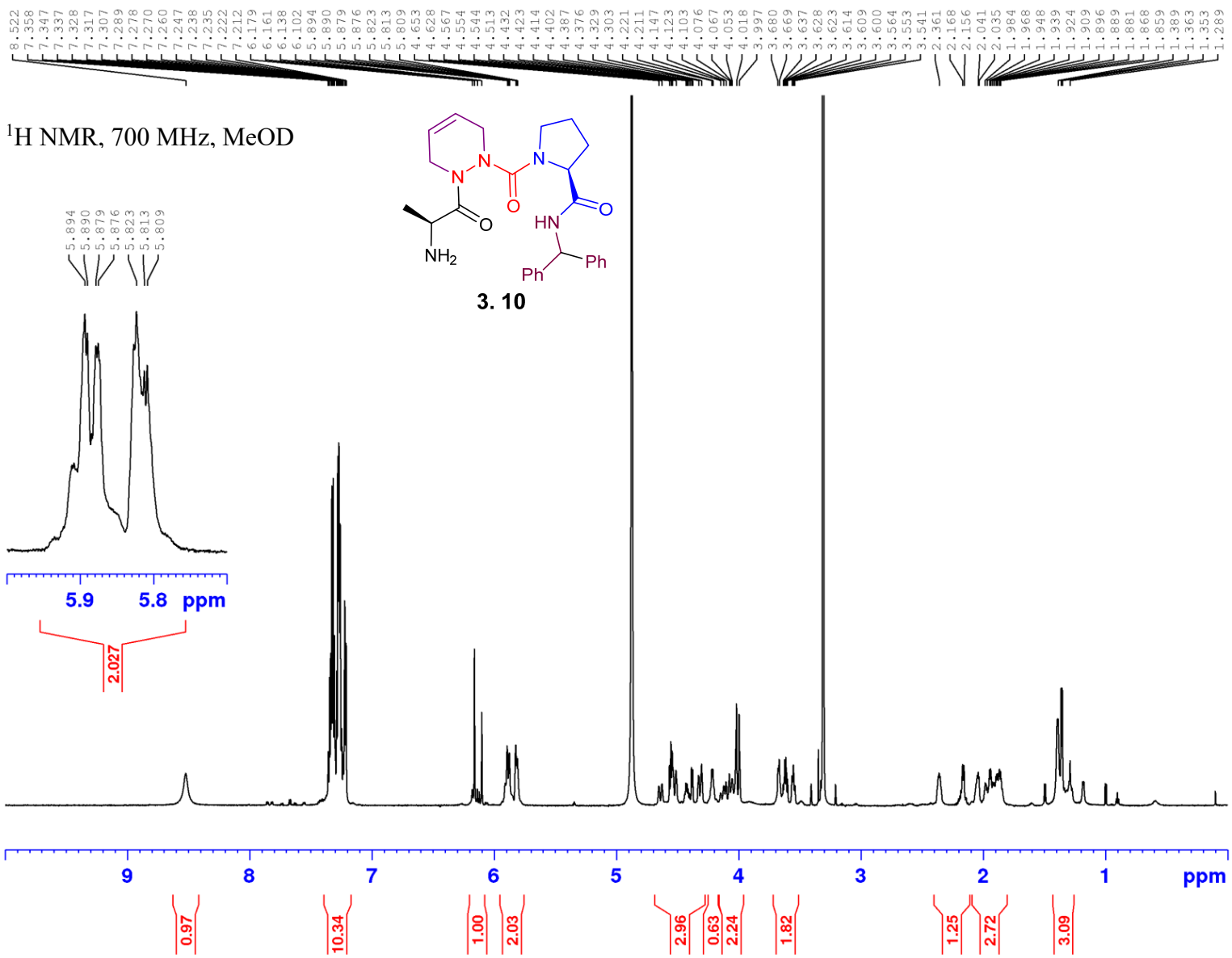
8.522
7.358
7.347
7.337
7.328
7.317
7.307
7.289
7.278
7.270
7.260
7.247
7.238
7.235
7.222
7.212
6.179
6.161
6.138
6.102
5.894
5.890
5.879
5.876
5.823
5.813
5.809
4.653
4.628
4.567
4.554
4.544
4.513
4.432
4.423
4.414
4.402
4.387
4.376
4.329
4.303
4.221
4.211
4.147
4.123
4.103
4.076
4.067
4.053
4.018
3.997
3.680
3.669
3.637
3.628
3.623
3.614
3.609
3.600
3.564
3.553
3.541
2.361
2.168
2.156
2.041
2.035
1.984
1.968
1.948
1.939
1.924
1.909
1.896
1.889
1.881
1.868
1.859
1.389
1.363
1.353
1.289
1H NMR, 700 MHz, MeOD
N
N
O
N
O
HN
O
NH2
Ph
Ph
3. 10
5.894
5.890
5.879
5.876
5.823
5.813
5.809
5.9
5.8
ppm
2.027
9
8
7
6
5
4
3
2
1
ppm
0.97
10.34
1.00
2.03
2.96
0.63
2.24
1.82
1.25
2.72
3.09

^{13}C NMR, 175 MHz, MeOD

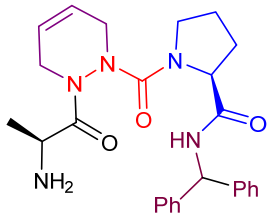

3. 10

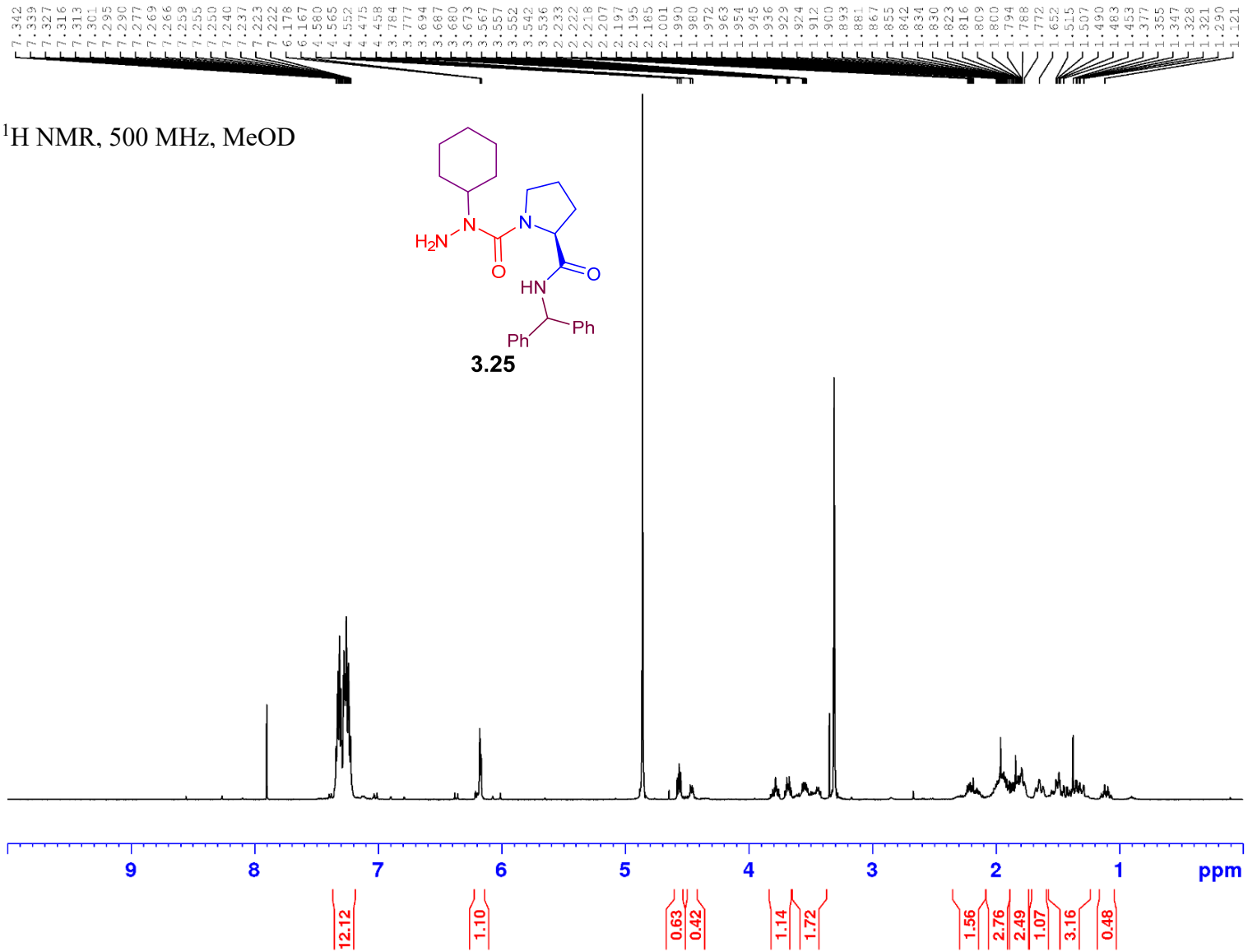
7.342
7.339
7.327
7.316
7.313
7.301
7.295
7.290
7.277
7.269
7.266
7.259
7.255
7.250
7.240
7.237
7.223
7.222
6.178
6.167
4.580
4.565
4.552
4.475
4.458
3.784
3.777
3.694
3.687
3.680
3.673
3.567
3.557
3.552
3.542
3.536
2.233
2.222
2.218
2.207
2.197
2.195
2.185
2.001
1.990
1.980
1.972
1.963
1.954
1.945
1.936
1.929
1.924
1.912
1.900
1.893
1.881
1.867
1.855
1.842
1.834
1.830
1.823
1.816
1.809
1.800
1.794
1.788
1.772
1.652
1.515
1.507
1.490
1.483
1.453
1.377
1.355
1.347
1.328
1.321
1.290
1.121
^{1}H NMR, 500 MHz, MeOD
H2N
N
O
N
O
HN
Ph
Ph
3.25
9
8
7
6
5
4
3
2
1
ppm
12.12
1.10
0.63
0.42
1.14
1.72
1.56
2.76
2.49
1.07
3.16
0.48

^{13}C NMR, 125 MHz, MeOD

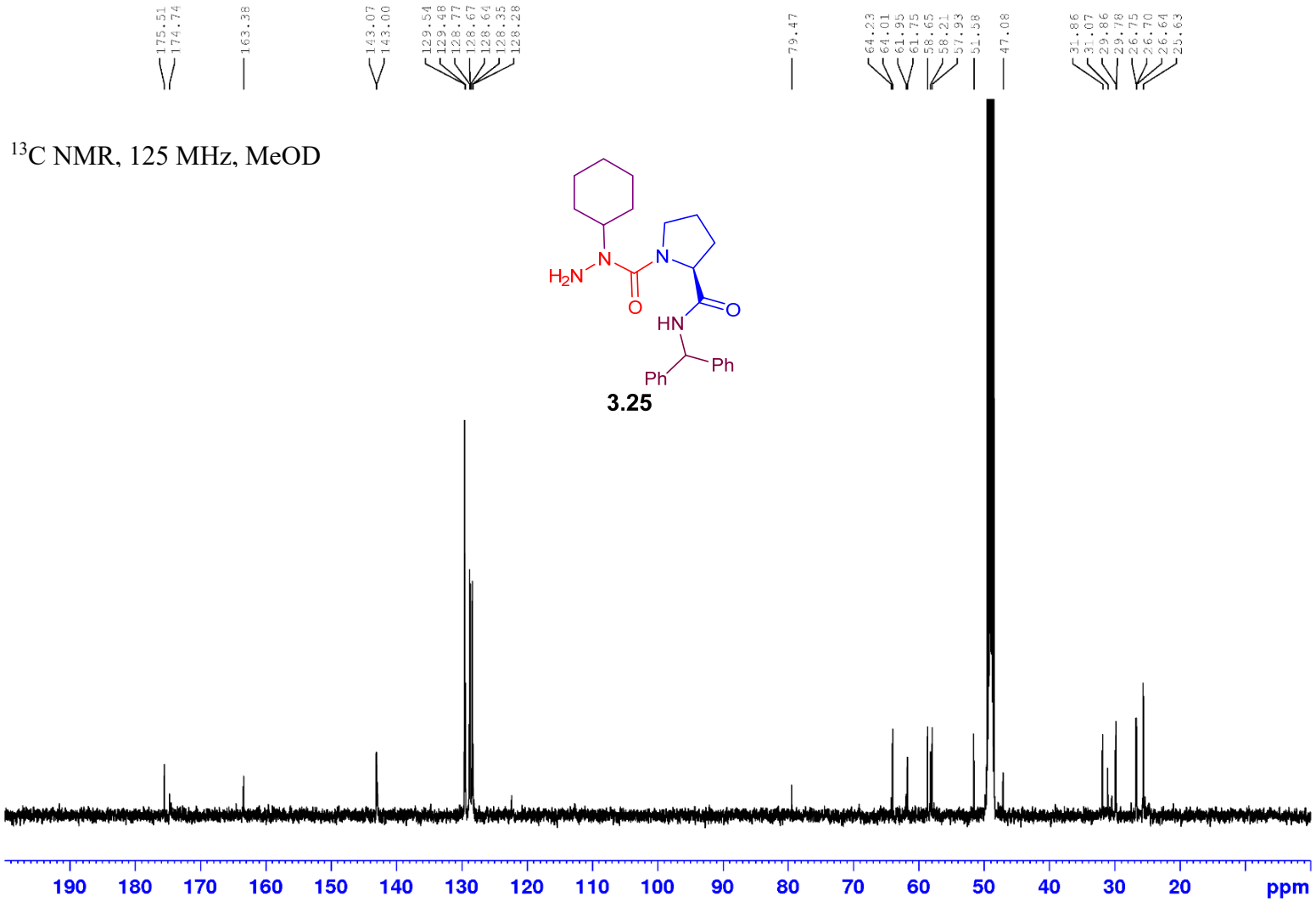

3.25

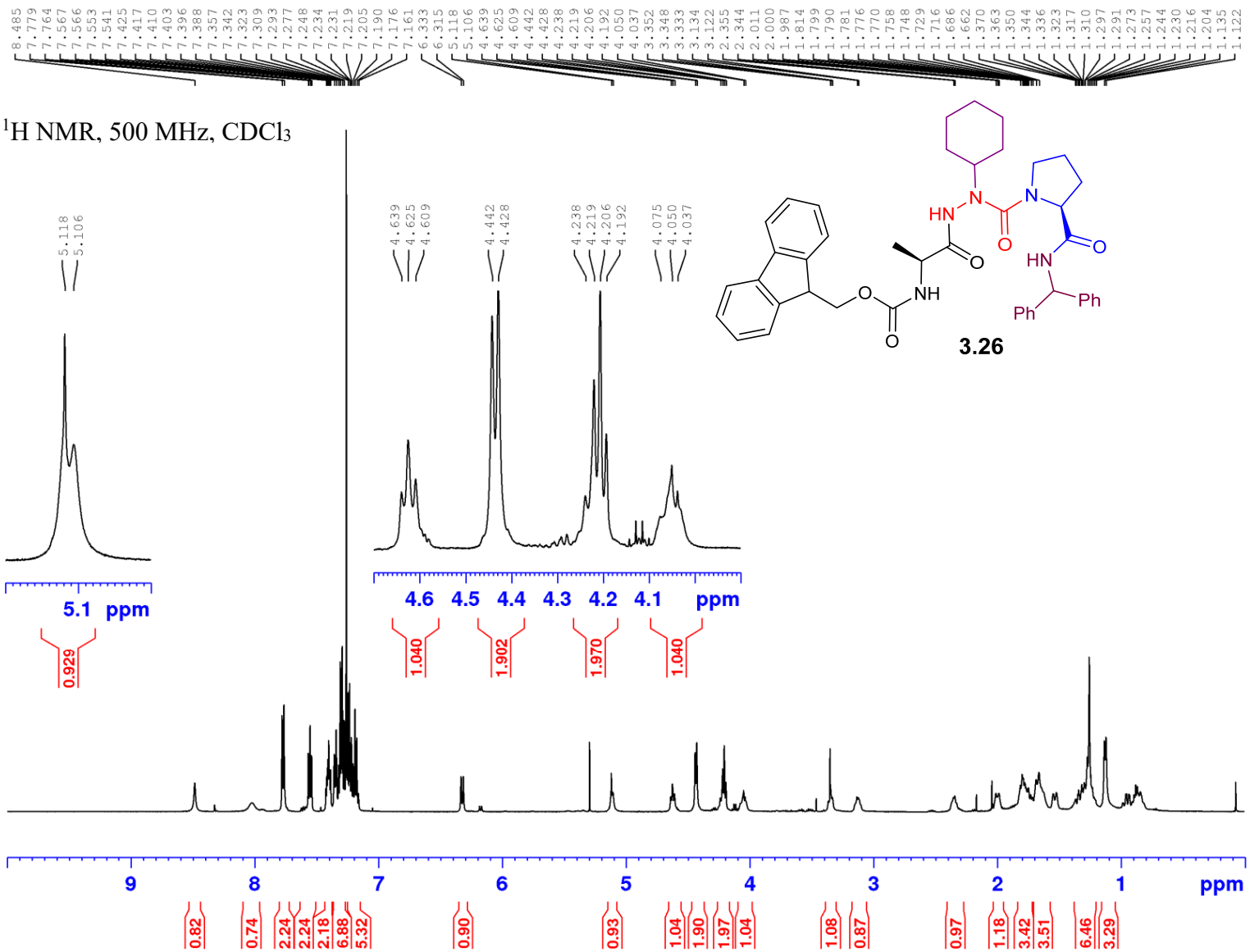
^{1}H NMR, 500 MHz, CDCl$_3$
3.26
5.1 ppm
4.6 4.5 4.4 4.3 4.2 4.1 ppm
9 8 7 6 5 4 3 2 1 ppm

^{13}C NMR, 125 MHz, $CDCl_3$

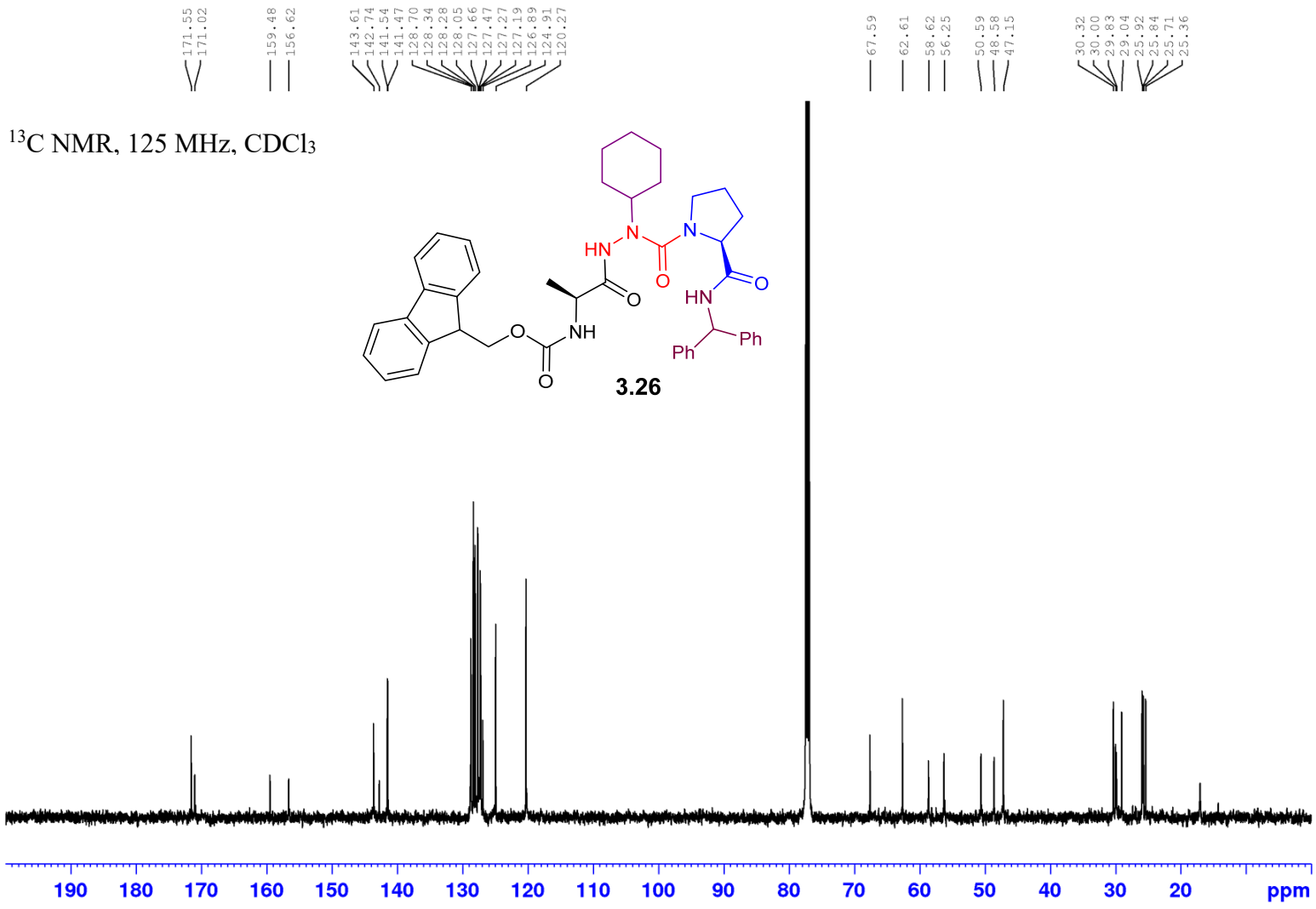

3.26

^{1}H NMR, 700 MHz, DMSO-d_6

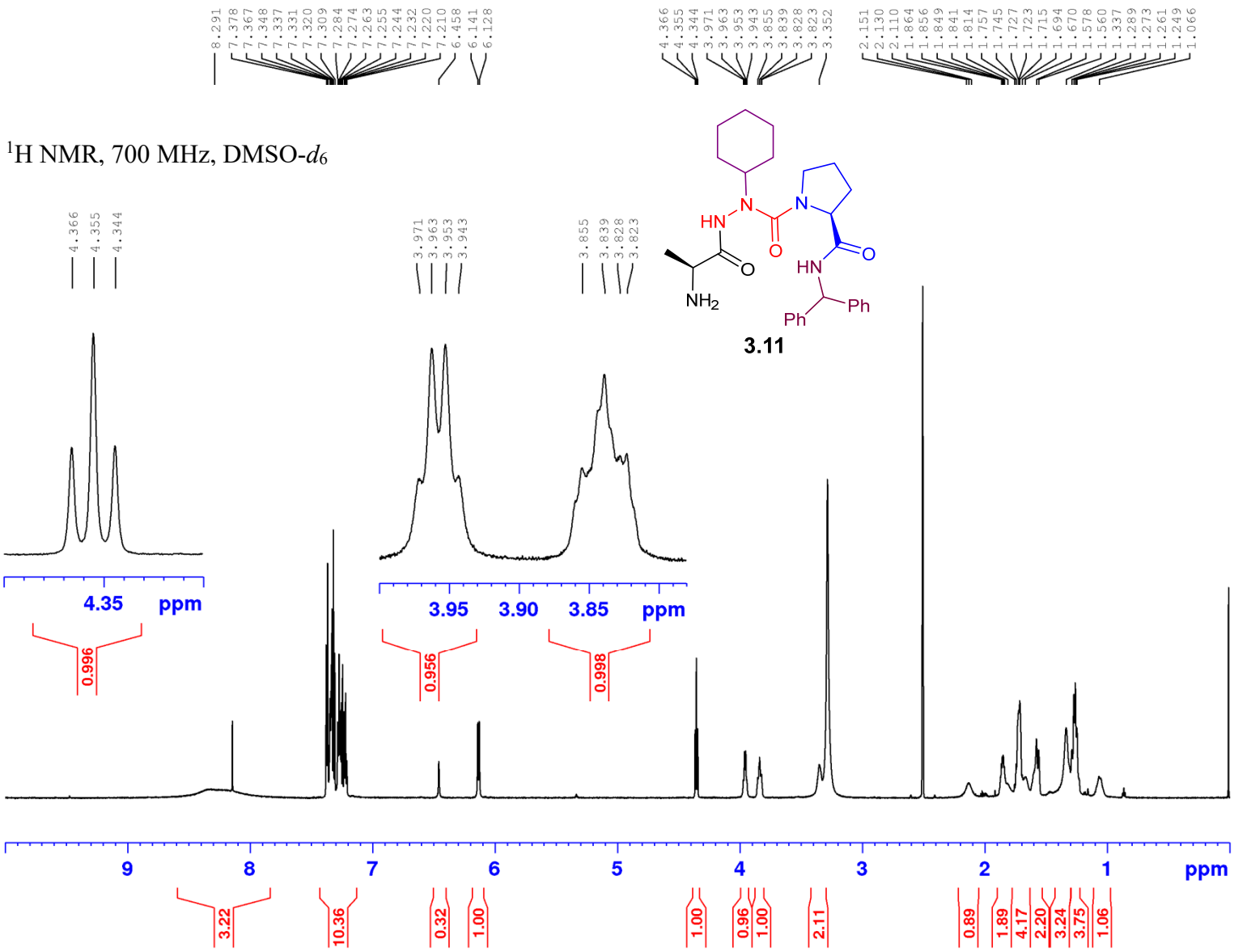

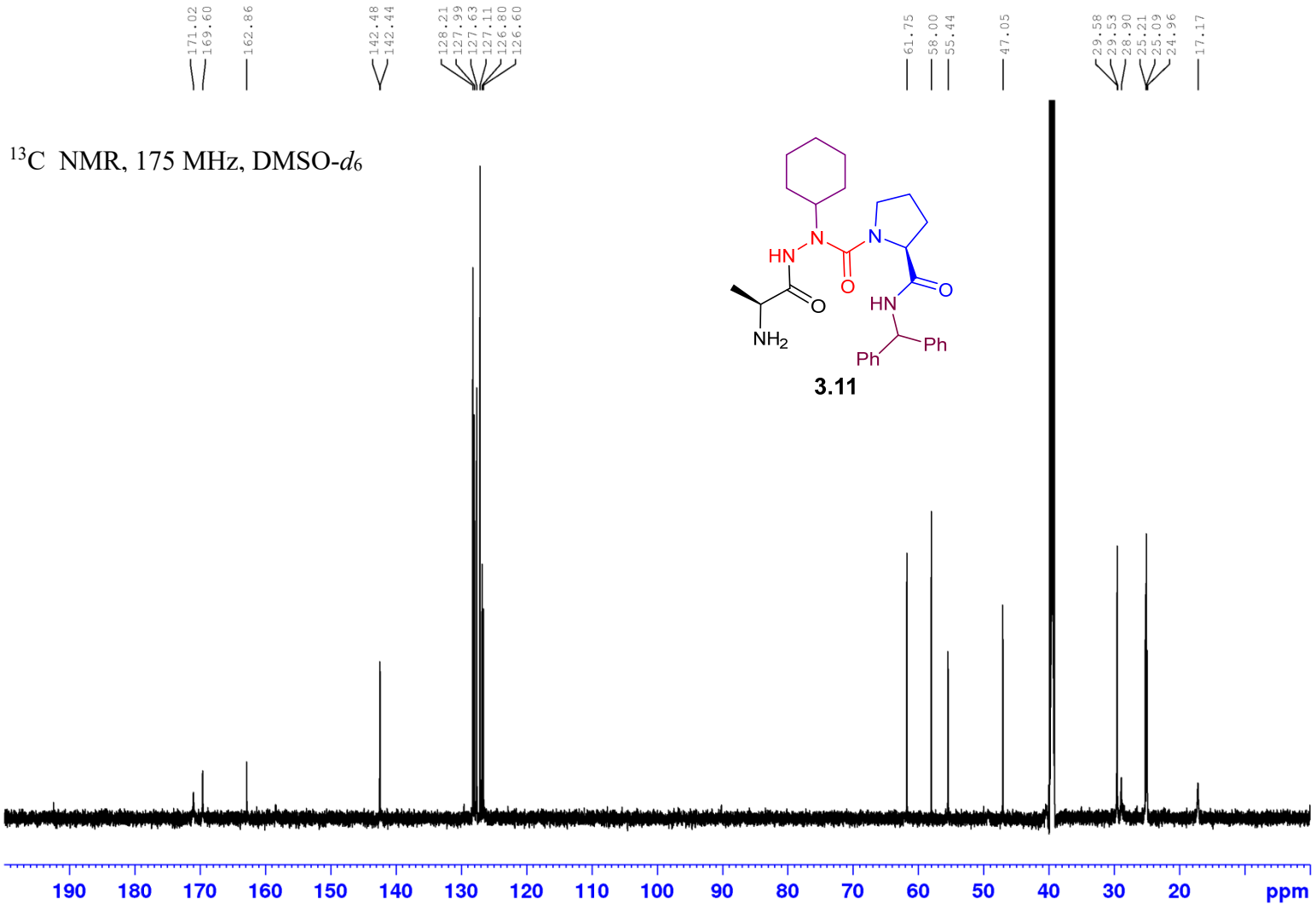

^{13}C NMR, 175 MHz, DMSO-d_6

3.11

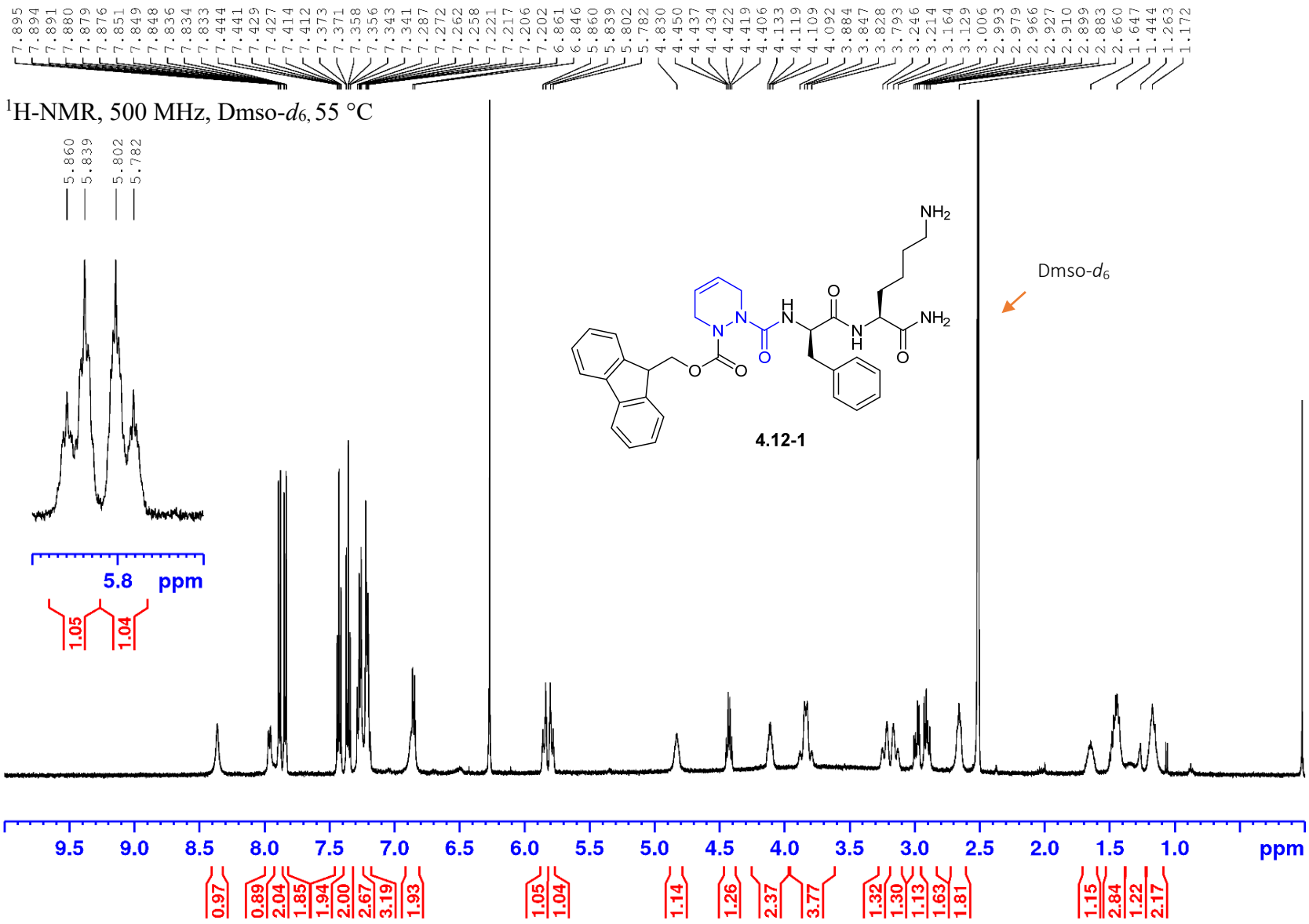
7.895 7.894 7.891 7.880 7.879 7.876 7.851 7.849 7.848 7.836 7.834 7.833 7.444 7.441 7.429 7.427 7.414 7.412 7.373 7.371 7.358 7.356 7.343 7.341 7.287 7.272 7.262 7.258 7.221 7.217 7.206 7.202 6.861 6.846 5.860 5.839 5.802 5.782 4.830 4.450 4.437 4.434 4.422 4.419 4.406 4.133 4.119 4.109 4.092 3.884 3.847 3.828 3.793 3.246 3.214 3.164 3.129 3.006 2.993 2.979 2.966 2.927 2.910 2.899 2.883 2.660 1.647 1.444 1.263 1.172
[1]H-NMR, 500 MHz, Dmso-d6, 55 °C
5.860 5.839 5.802 5.782
5.8 ppm
1.05 1.04
NH2
NH2
Dmso-d6
4.12-1
9.5 9.0 8.5 8.0 7.5 7.0 6.5 6.0 5.5 5.0 4.5 4.0 3.5 3.0 2.5 2.0 1.5 1.0 ppm
0.97 0.89 2.04 1.85 1.94 2.00 2.67 3.19 1.93 1.05 1.04 1.14 1.26 2.37 3.77 1.32 1.30 1.13 1.63 1.81 1.15 2.84 1.22 2.17

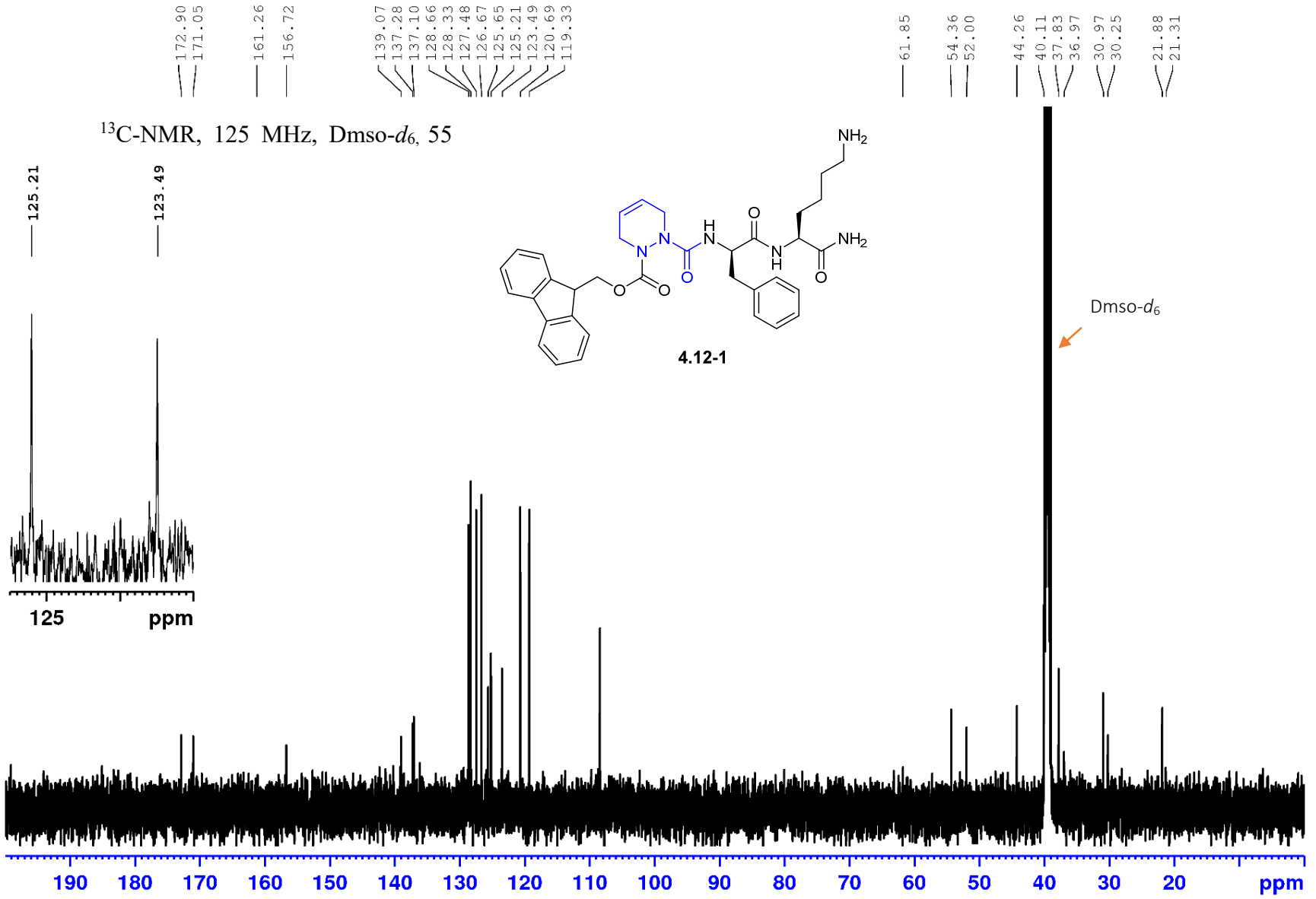
172.90
171.05
161.26
156.72
139.07
137.28
137.10
128.66
128.33
127.48
126.67
125.65
125.21
123.49
120.69
119.33
61.85
54.36
52.00
44.26
40.11
37.83
36.97
30.97
30.25
21.88
21.31
13C-NMR, 125 MHz, Dmso-d6, 55
125.21
123.49
125
ppm
NH2
NH2
Dmso-d6
4.12-1
190
180
170
160
150
140
130
120
110
100
90
80
70
60
50
40
30
20
ppm

bbfo.proton DMSO /d chimie 5

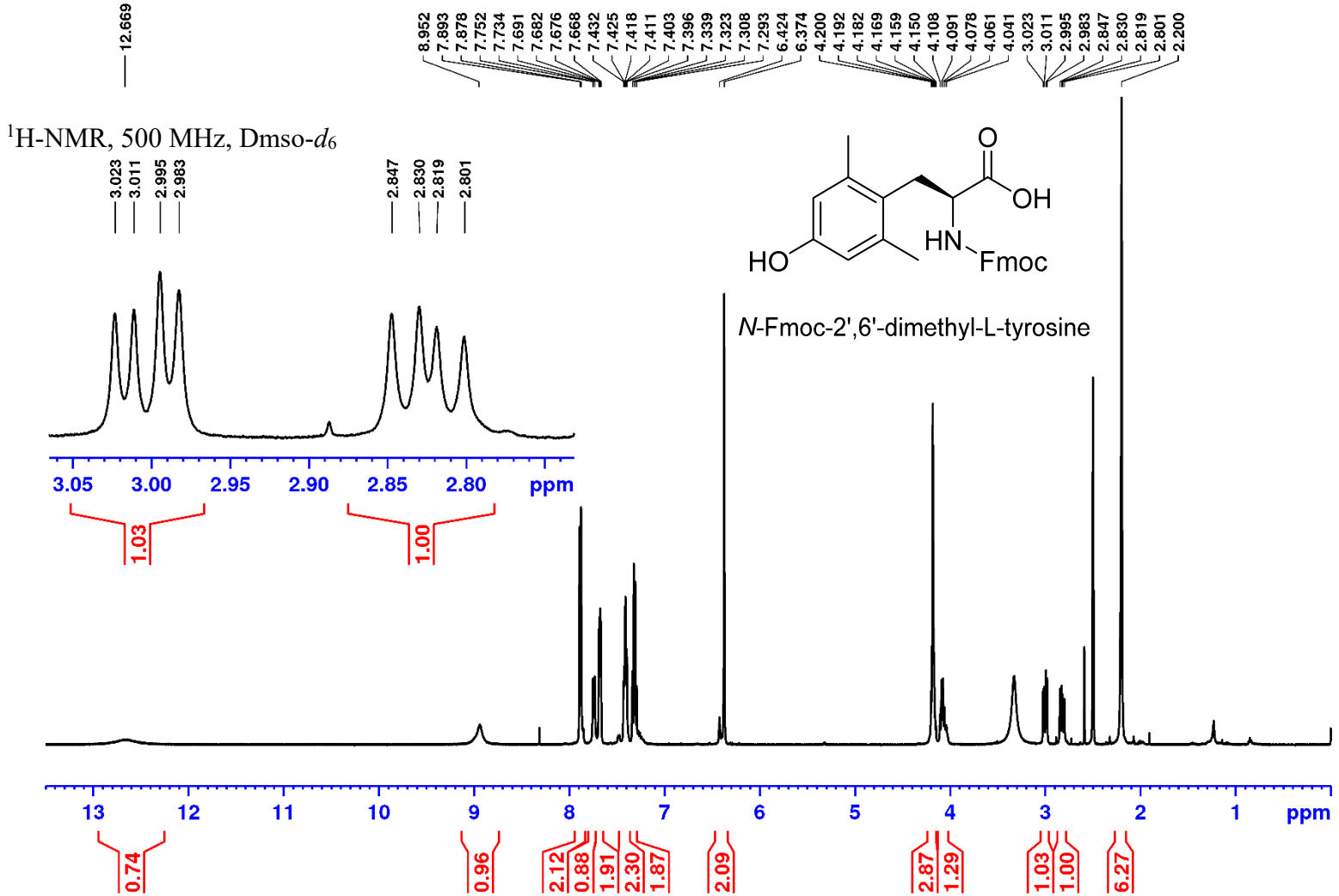

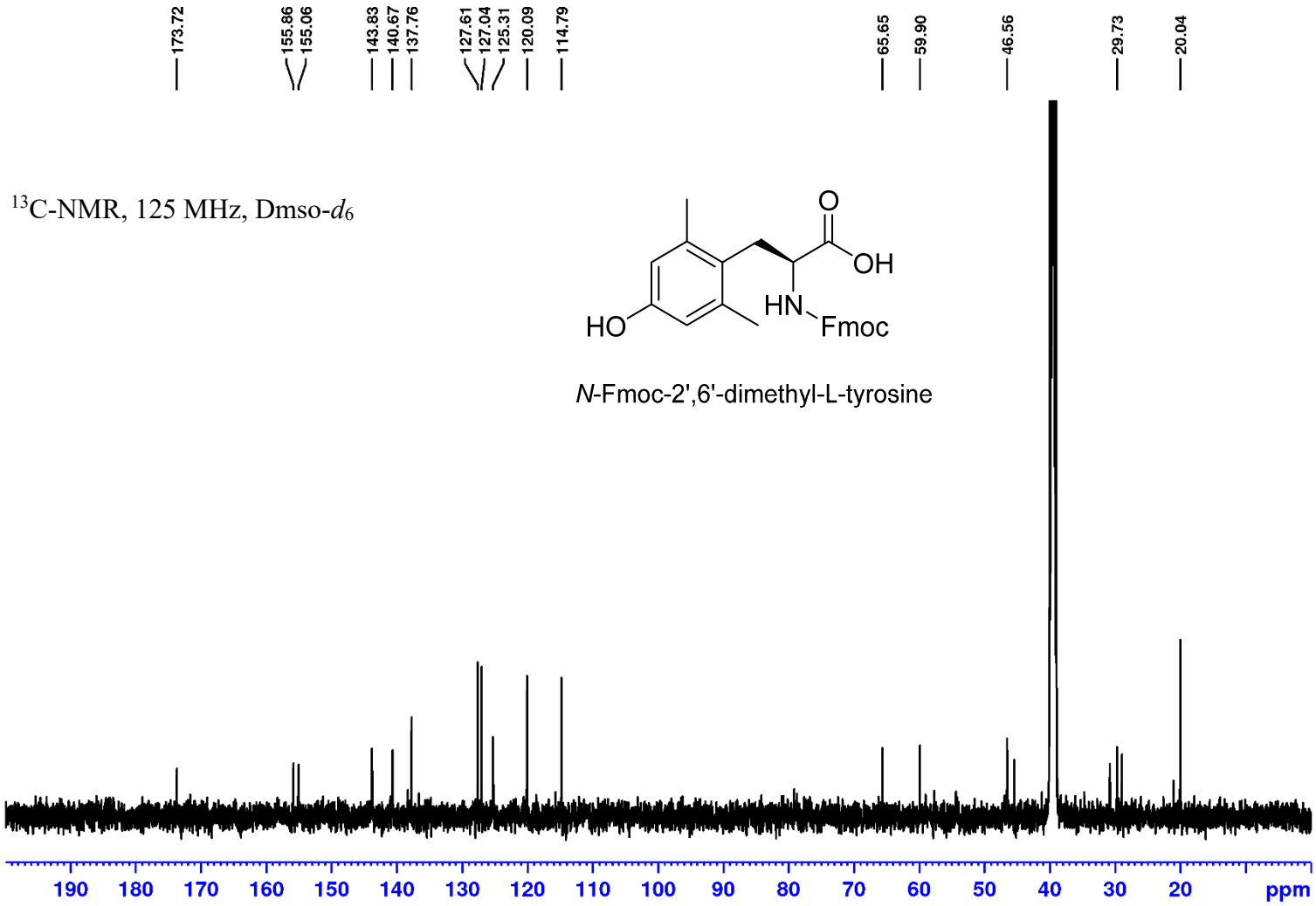

^{13}C-NMR, 125 MHz, Dmso-d_6

N-Fmoc-2',6'-dimethyl-L-tyrosine

DEPT-NMR, 125 MHz, Dmso-d_6,

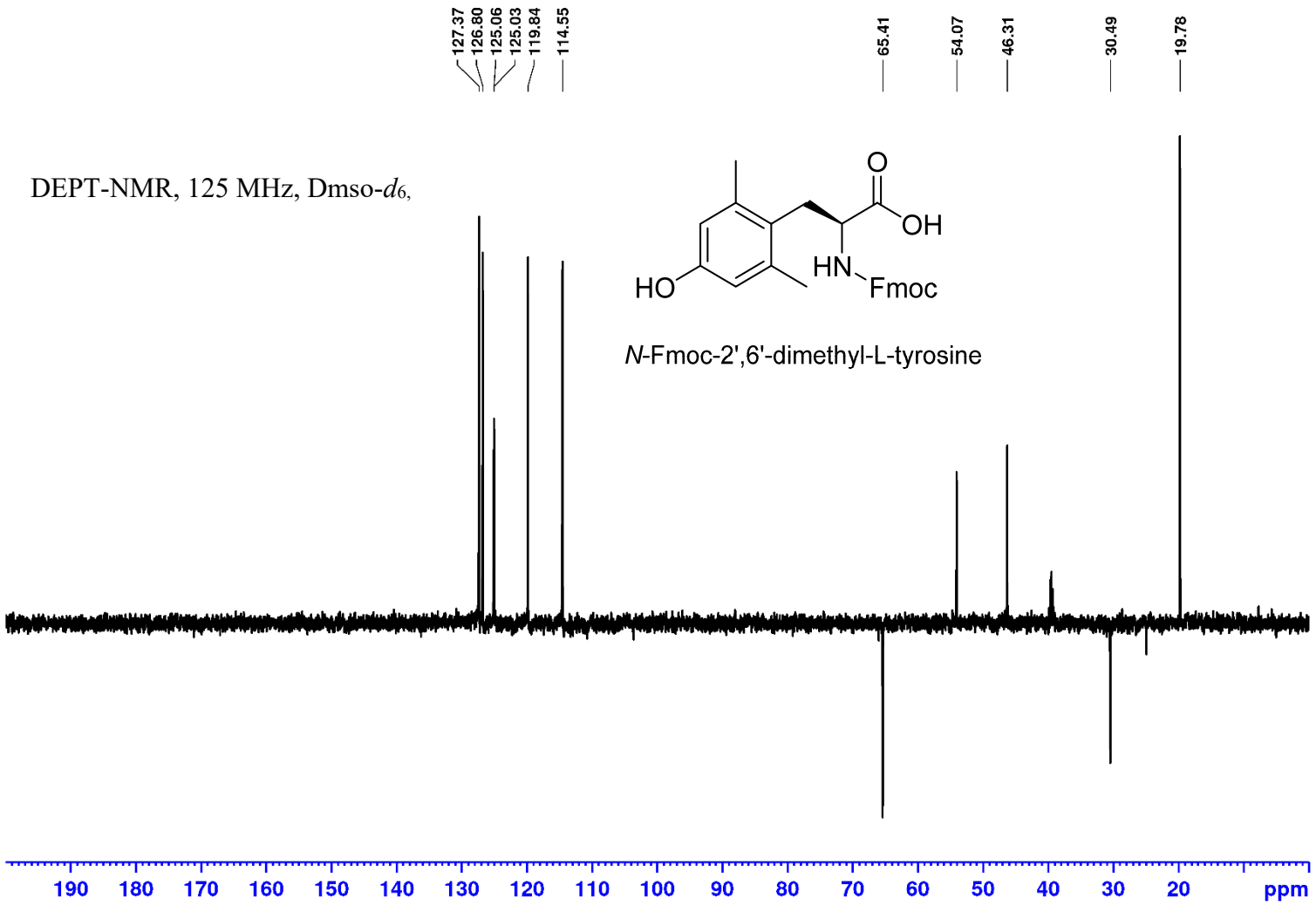

N-Fmoc-2',6'-dimethyl-L-tyrosine

Annex 5: IR spectra for Chapter 4

Fmoc-azaGly-D-Phe-Lys(Boc)-NH-Rink resin **4.8**:

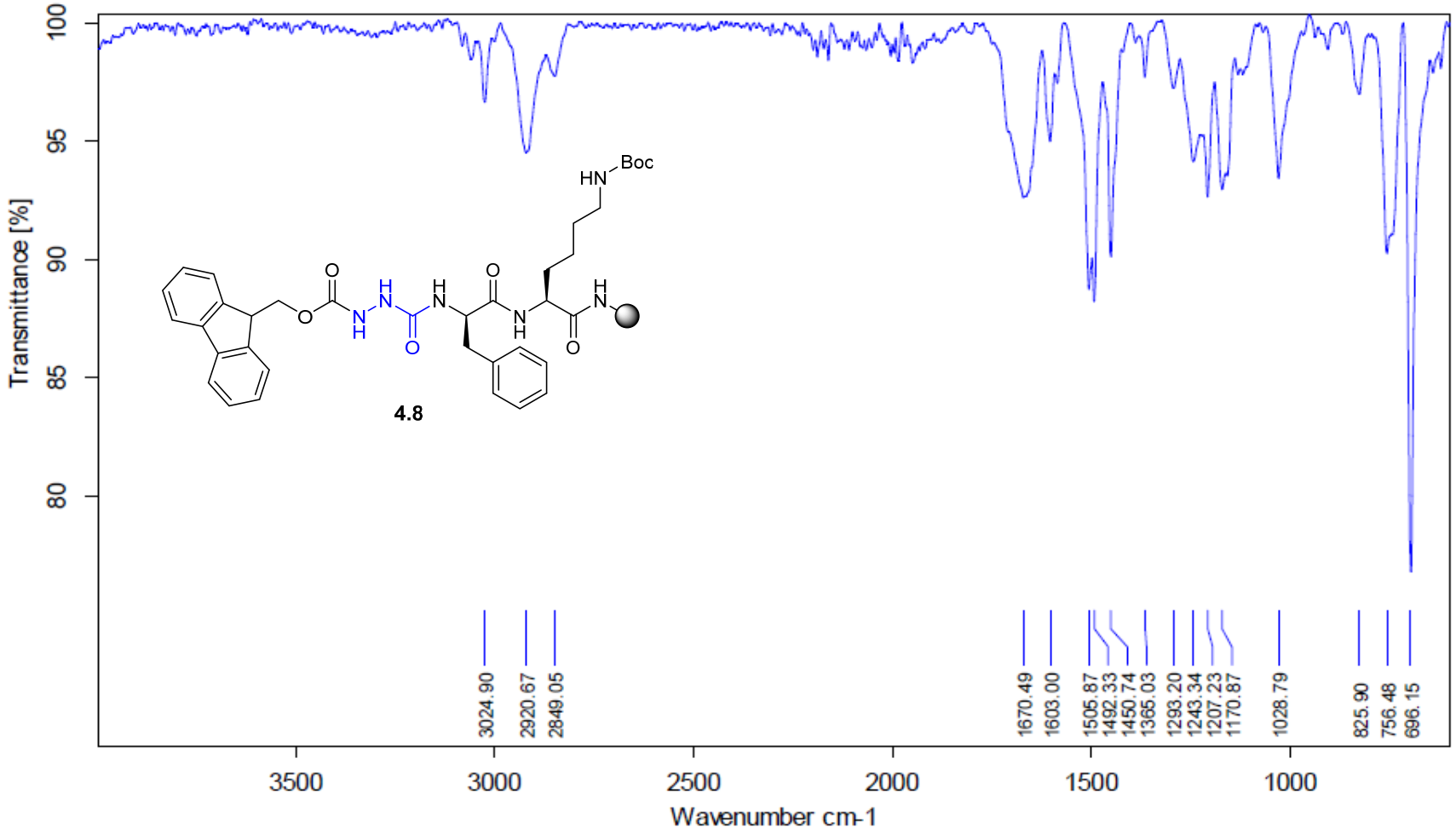

Fmoc-azoGly-D-Phe-Lys(Boc)-NH-Rink resin **4.10**:

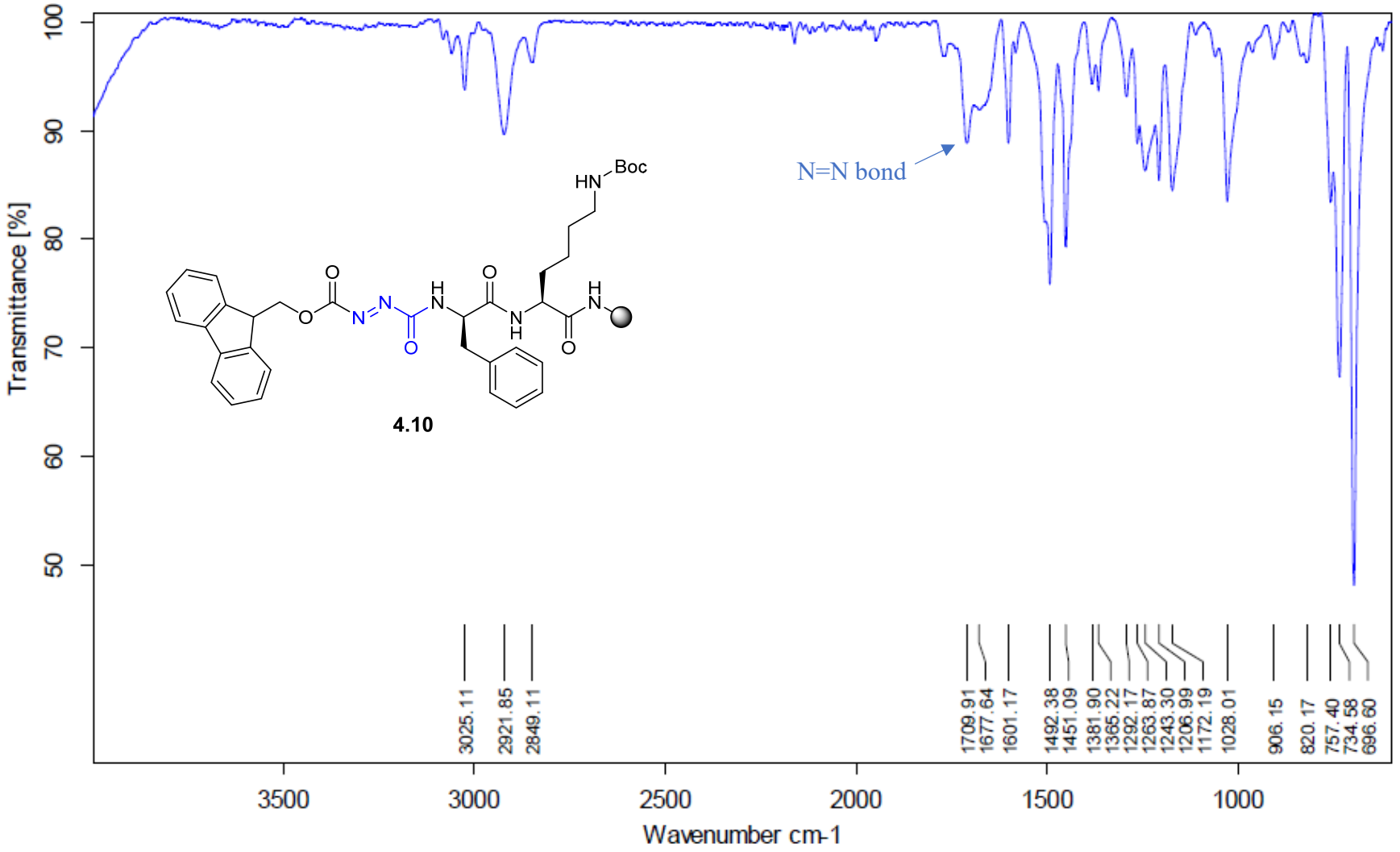

Annex 6: LCMS spectra for Chapter 4

Analytical LC-MS characterization of purified azapipecolyl opioids (4.18-4.23) and GHRP-6 analogues (4.27-4.31).

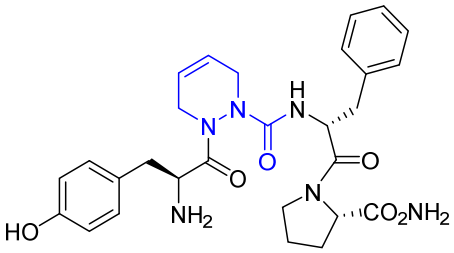

4.18a

Tyr-(Δ^4)azaPip-D-Phe-Pro-NH_2 (4.18a): LC-MS analysis (a) 20-95% of MeOH (0.1% FA) in H_2O (0.1% FA) over 11 min, then 20% MeOH for 4 min, R.T. = 7.55 min; (b) 10-95% MeCN (0.1% FA) in H_2O (0.1% FA) over 11 min, then 10% MeCN for 4 min, R.T. = 6.42 min; HRMS m/z calcd for $C_{28}H_{35}N_6O_5$ $[M+H]^+$ 535.2663, found 535.2679.

a) LCMS in MeOH/H_2O for 4.18a:

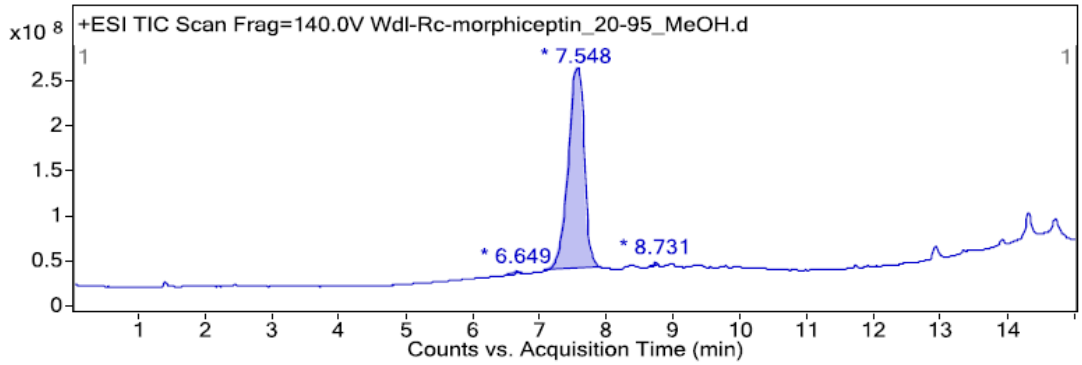

b) LCMS in MeCN/H_2O for 4.18a:

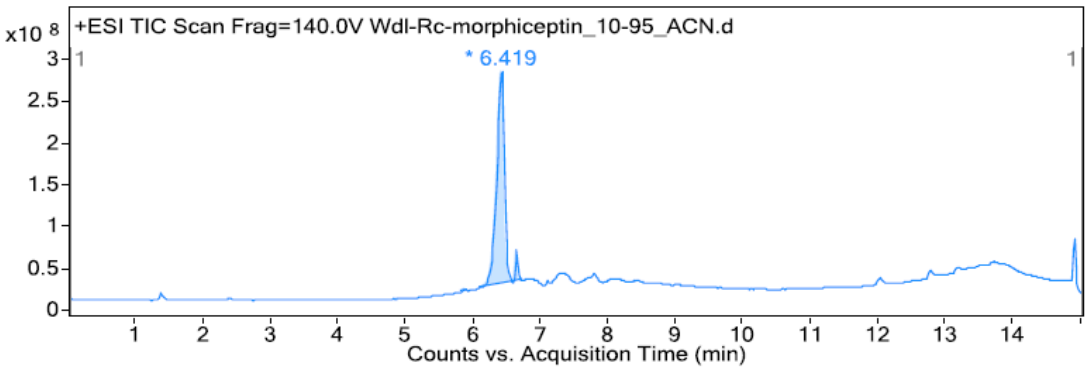

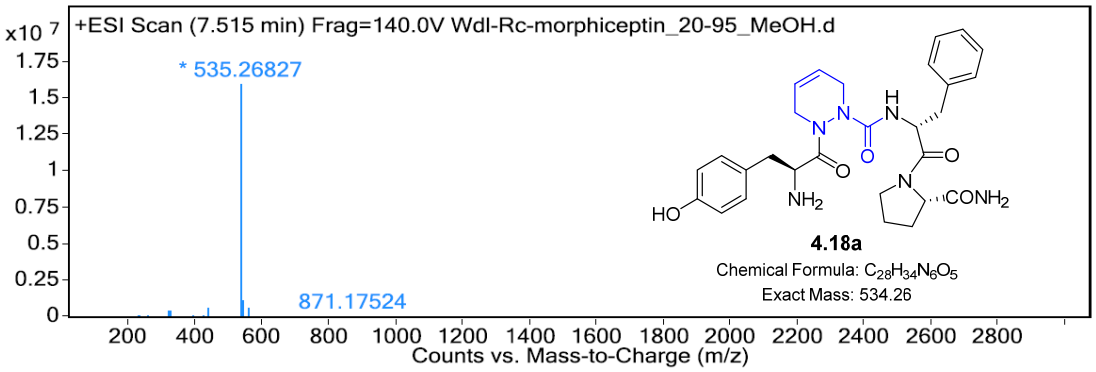

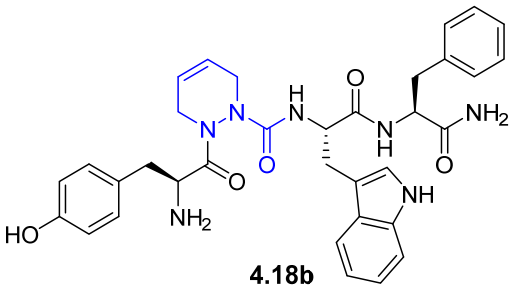

Tyr-(Δ^4)azaPip-Trp-Phe-NH_2 (4.18b): LC-MS analysis (a) 20-95% of MeOH (0.1% FA) in H_2O (0.1% FA) over 11 min, then 20% MeOH for 4 min, R.T. = 8.37 min; (b) 20-95% MeCN (0.1% FA) in H_2O (0.1% FA) over 15 min, then 20% MeCN for 3 min, R.T. = 6.61 min; HRMS m/z calcd for $C_{34}H_{38}N_7O_5$ $[M+H]^+$ 624.2929, found 624.2944.

a) LCMS in MeOH/H_2O for 4.18b:

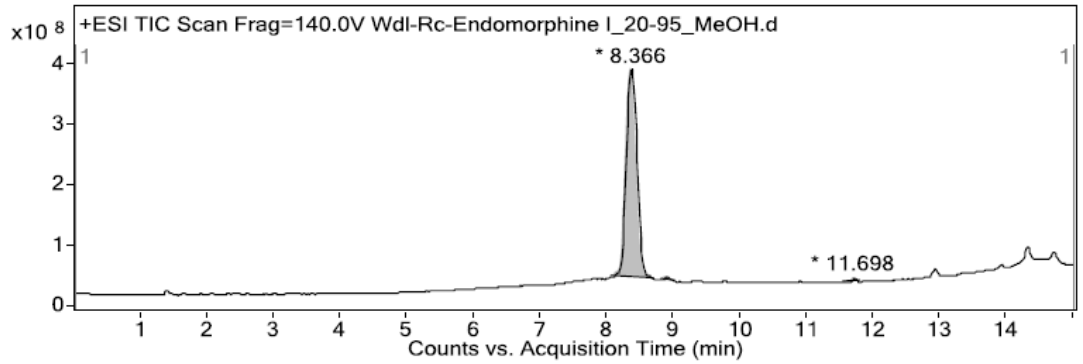

b) LCMS in MeCN/H_2O for 4.18b:

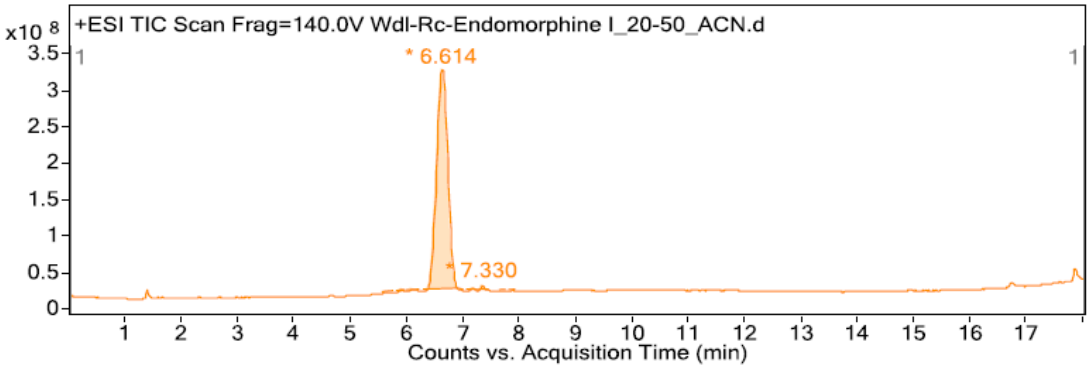

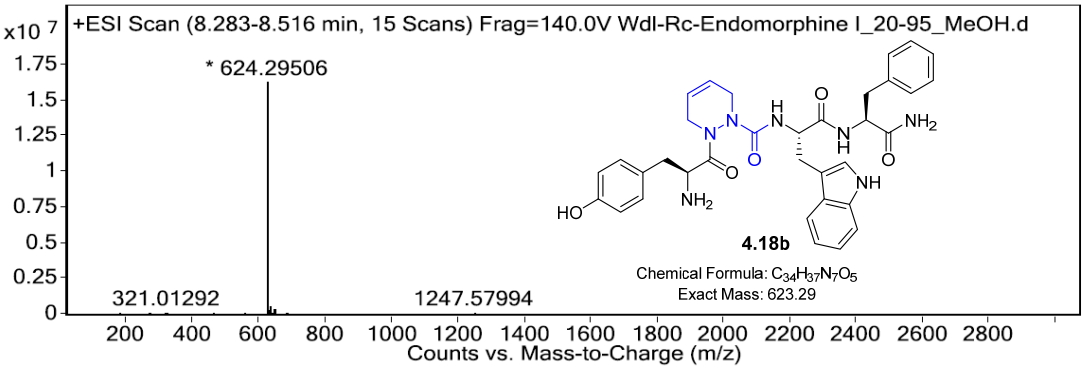

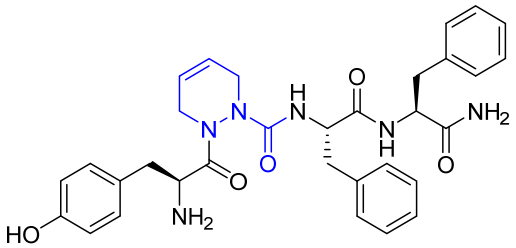

4.18c

Tyr-(Δ^4)azaPip-Phe-Phe-NH_2 (4.18c): (a) LC-MS analysis (a) 20-95% of MeOH (0.1% FA) in H_2O (0.1% FA) over 11 min, then 20% MeOH for 4 min, R.T. = 8.25 min; (b) 20-95% MeCN (0.1% FA) in H_2O (0.1% FA) over 11 min, then 20% MeCN for 4 min, R.T. = 5.60 min; HRMS m/z calcd for $C_{32}H_{37}N_6O_5$ $[M+H]^+$ 585.2820, found 585.2835.

a) LCMS in MeOH/H_2O for 4.18c:

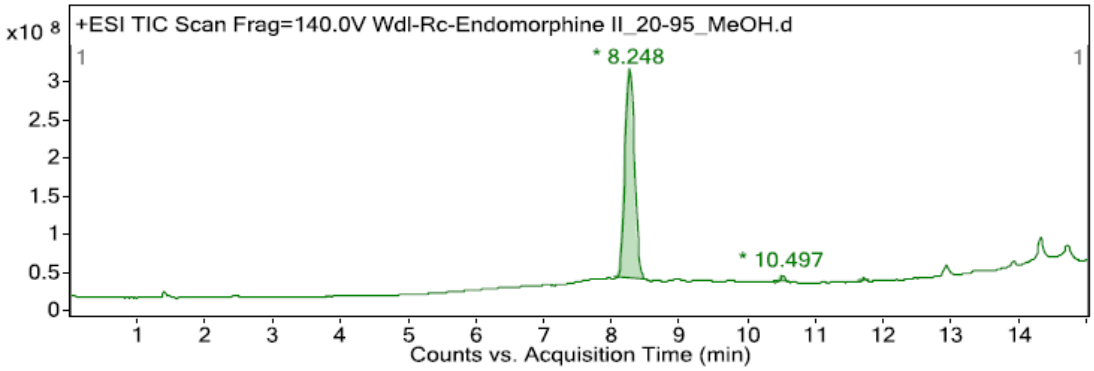

b) LCMS in MeCN/H_2O for 4.18c:

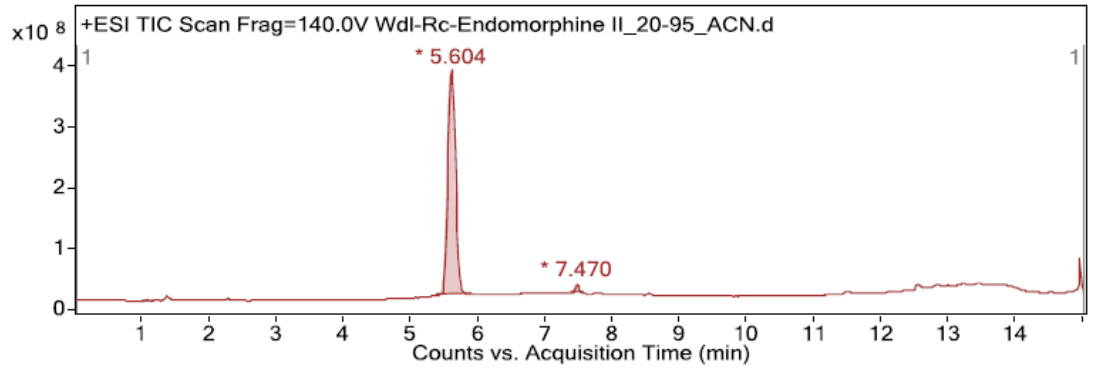

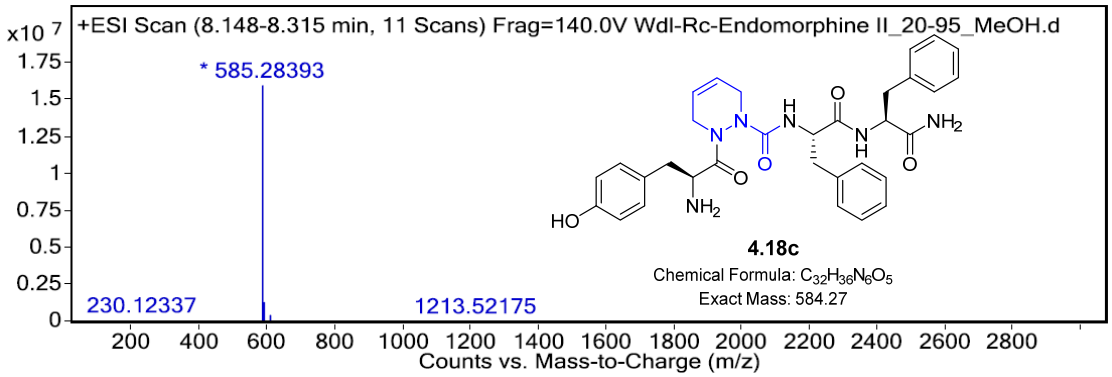

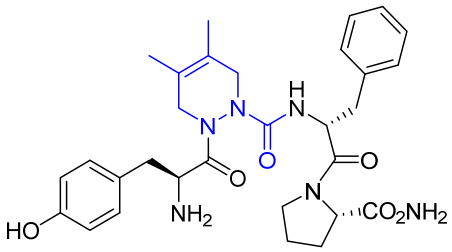

4.19a

Tyr-(4,5-dimethyl-Δ[4])azaPip-D-Phe-Pro-NH$_2$ (4.19a): LC-MS analysis (a) 10-90% of MeOH (0.1% FA) in H_2O (0.1% FA) over 9 min, then 10% MeOH for 5 min, R.T. = 6.70 min; (b) 10-90% MeCN (0.1% FA) in H_2O (0.1% FA) over 9 min, then 5% MeCN for 5 min, R.T. = 4.76 min; HRMS m/z calcd for $C_{30}H_{39}N_6O_5$ $[M+H]^+$ 563.2976, found 563.2964.

a) LCMS in MeOH/H_2O for 4.19a:

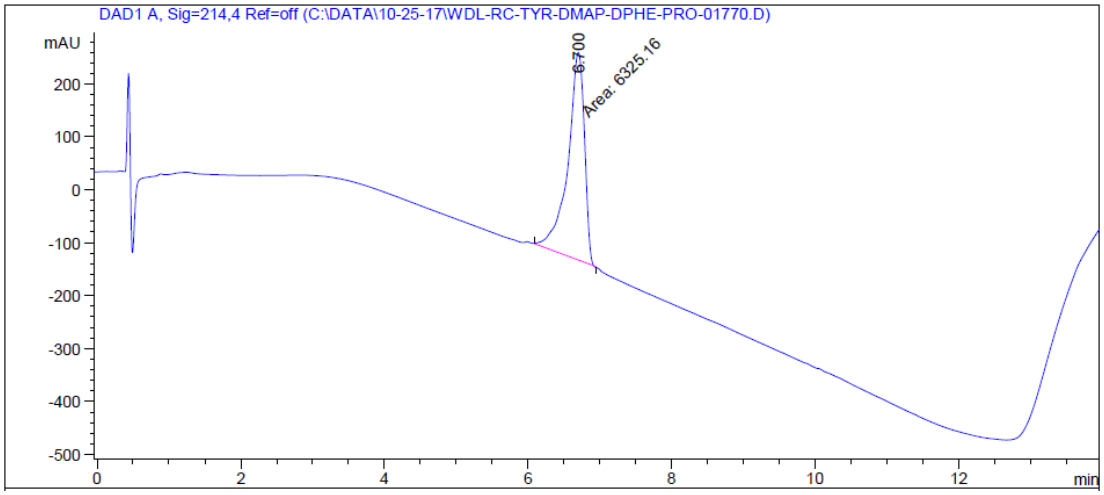

b) LCMS in MeCN/H_2O for 4.19a:

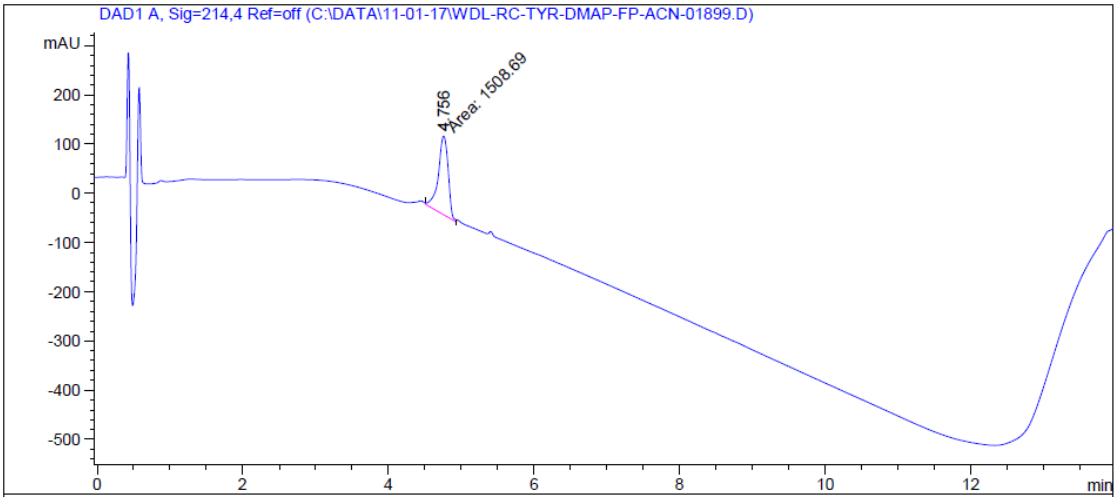

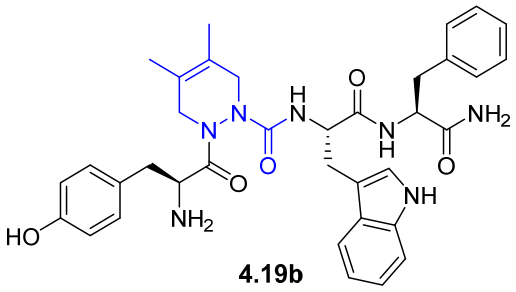

4.19b

Tyr-(4,5-dimethyl-Δ[4])azaPip-Trp-Phe-NH$_2$ (**4.19b**): LC-MS analysis (a) 10-90% of MeOH (0.1% FA) in H_2O (0.1% FA) over 9 min, then 10% MeOH for 5 min, R.T. = 7.38 min; (b)10-90% MeCN (0.1% FA) in H_2O (0.1% FA) over 9 min, then 10% MeCN for 5 min, R.T. = 5.12 min; HRMS m/z calcd for $C_{36}H_{42}N_7O_5$ $[M+H]^+$ 652.3242, found 652.3234.

a) LCMS in MeOH/H_2O for 4.19b:

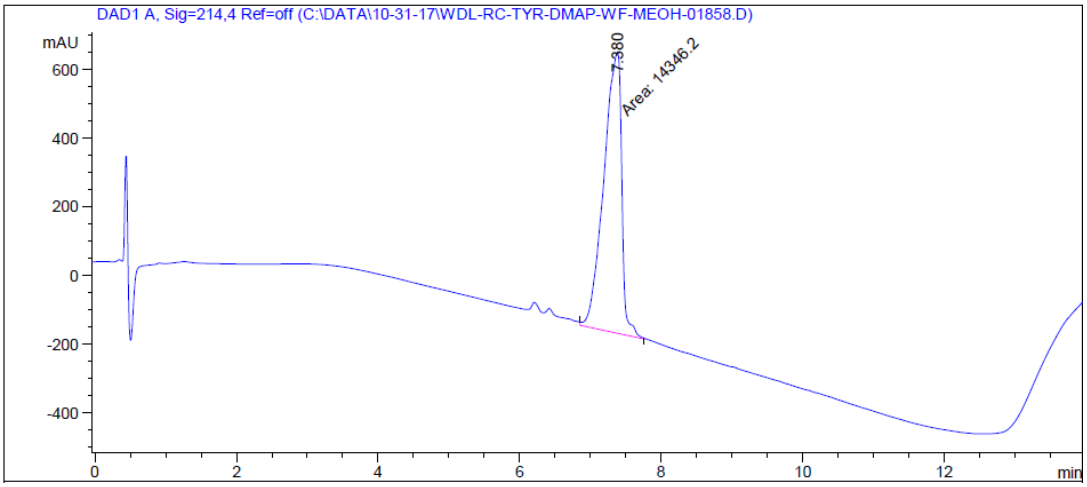

b) LCMS in MeCN/H_2O for 4.19b:

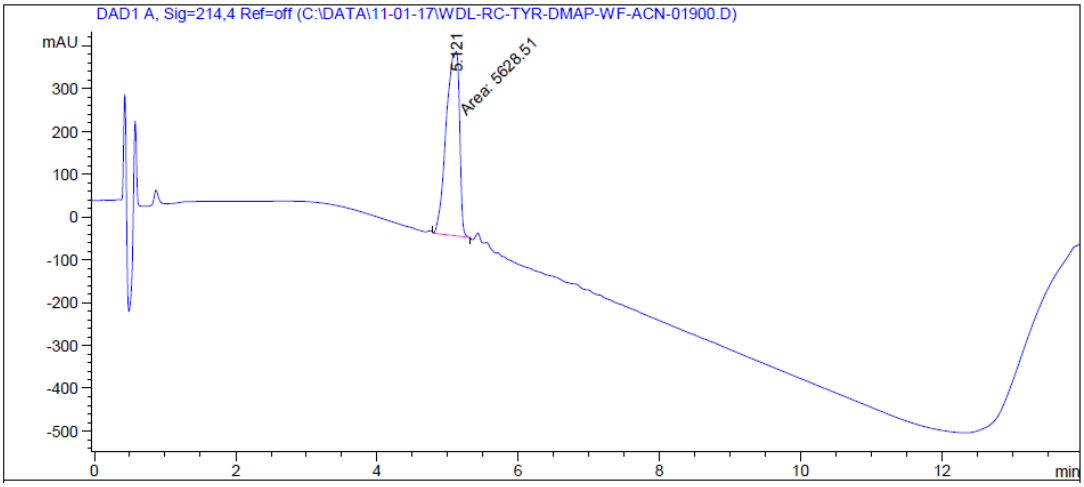

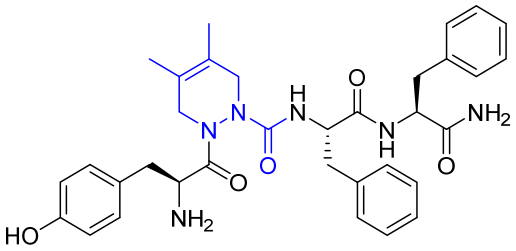

4.19c

Tyr-(4,5-dimethyl-Δ[4])azaPip-Phe-Phe-NH$_2$ (4.19c): LC-MS analysis (a) 10-90% of MeOH (0.1% FA) in H_2O (0.1% FA) over 9 min, then 10% MeOH for 5 min, R.T. = 7.32 min; (b) 10-90% MeCN (0.1% FA) in H_2O (0.1% FA) over 9 min, then 10% MeCN for 5 min, R.T. = 5.18 min; HRMS m/z calcd for $C_{34}H_{41}N_6O_5$ $[M+H]^+$ 613.3133, found 613.3112.

a) LCMS in MeOH/H_2O for 4.19c:

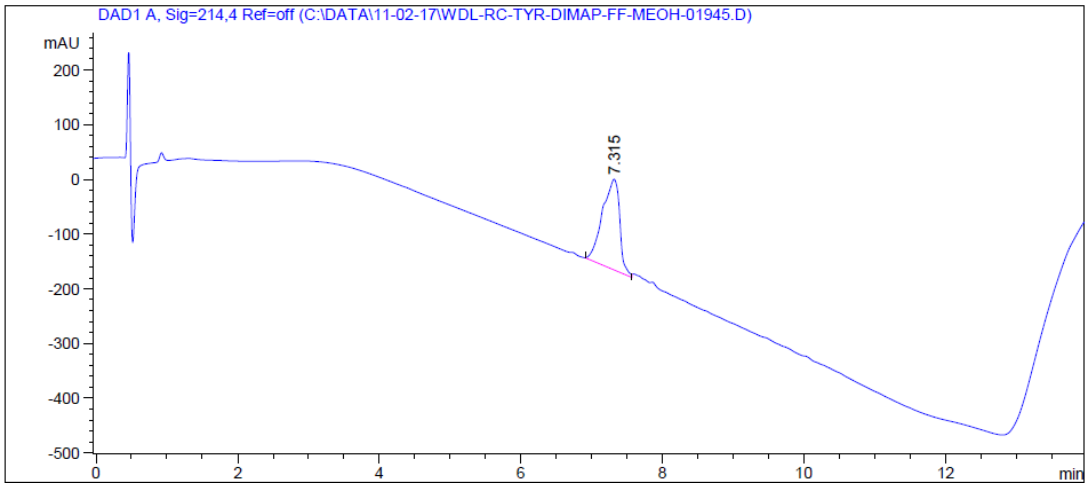

b) LCMS in MeCN/H_2O for 4.19c:

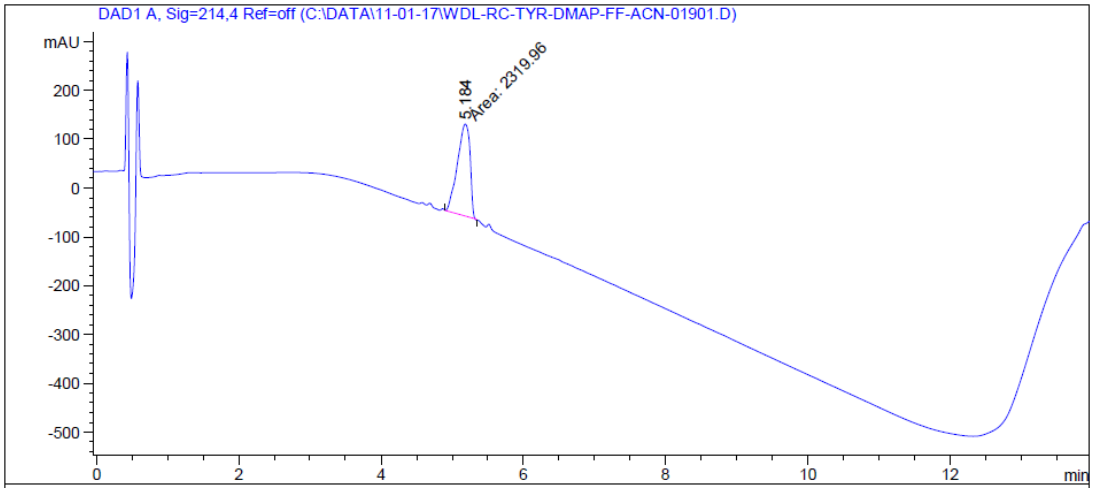

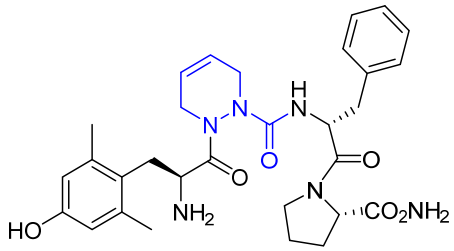

4.20a

Dmt-(Δ[4])azaPip-D-Phe-Pro-NH2 (4.20a): LC-MS analysis (a) 10-90% of MeOH (0.1% FA) in H_2O (0.1% FA) over 9 min, then 10% MeOH for 5 min, R.T. = 6.14 min; (b) 10-90% MeCN (0.1% FA) in H_2O (0.1% FA) over 9 min, then 10% MeCN for 5 min, R.T. = 4.34 min; HRMS m/z calcd for $C_{30}H_{39}N_6O_5$ $[M+H]^+$ 563.2976, found 563.2962.

a) LCMS in MeOH/H_2O for 4.20a:

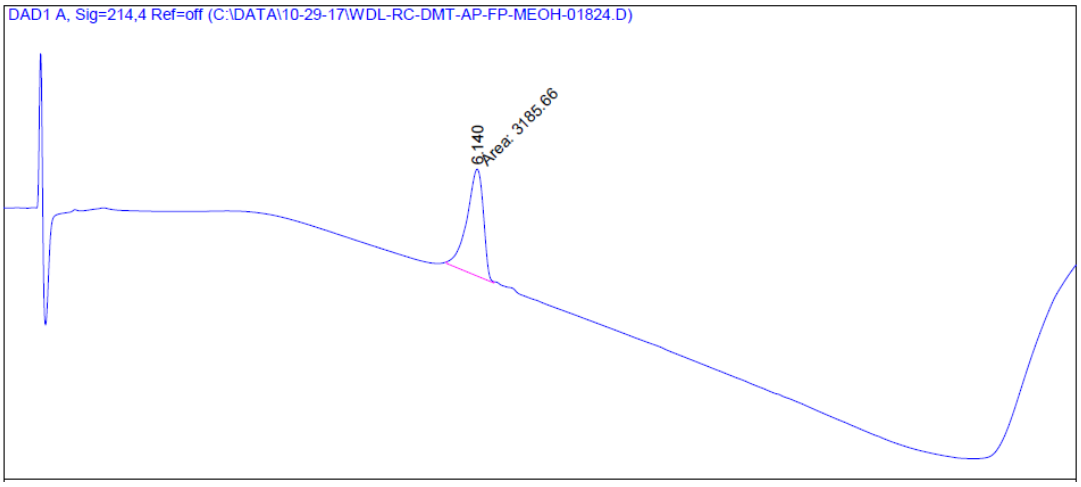

b) LCMS in MeCN/H_2O for 4.20a:

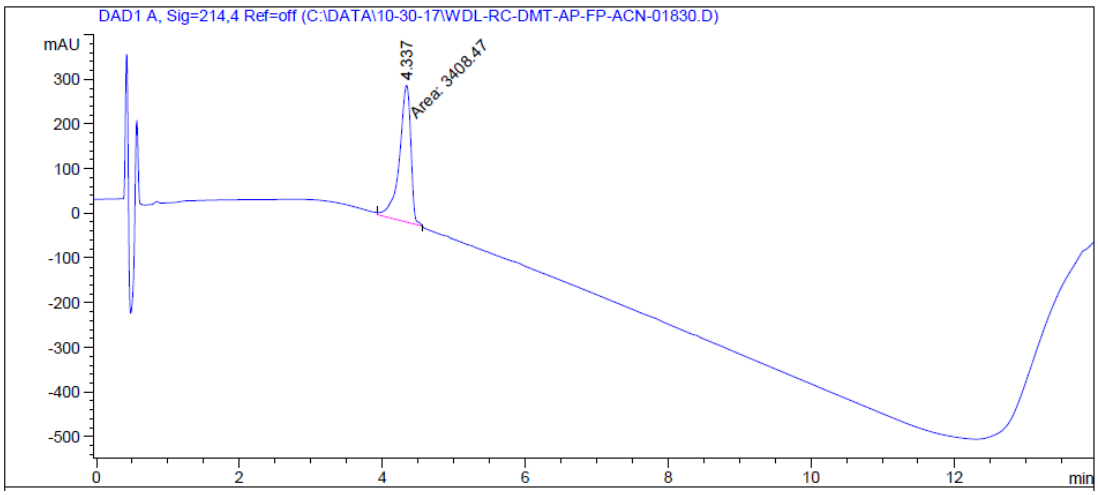

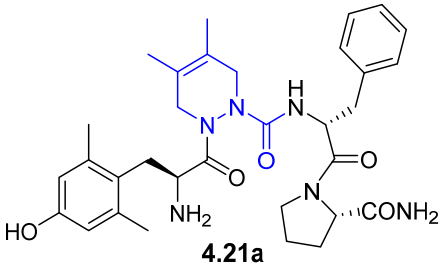

4.21a

Dmt-(4,5-dimethyl-Δ[4])azaPip-D-Phe-Pro-NH$_2$ (4.21a): LC-MS analysis (a) 10-90% of MeOH (0.1% FA) in H_2O (0.1% FA) over 9 min, then 10% MeOH for 5 min, R.T. = 7.01 min; (b) 10-90% MeCN (0.1% FA) in H_2O (0.1% FA) over 9 min, then 10% MeCN for 5 min, R.T. = 4.96 min; HRMS m/z calcd for $C_{32}H_{43}N_6O_5$ $[M+H]^+$ 591.3289, found 591.3284.

a) LCMS in MeOH/H_2O for 4.21a:

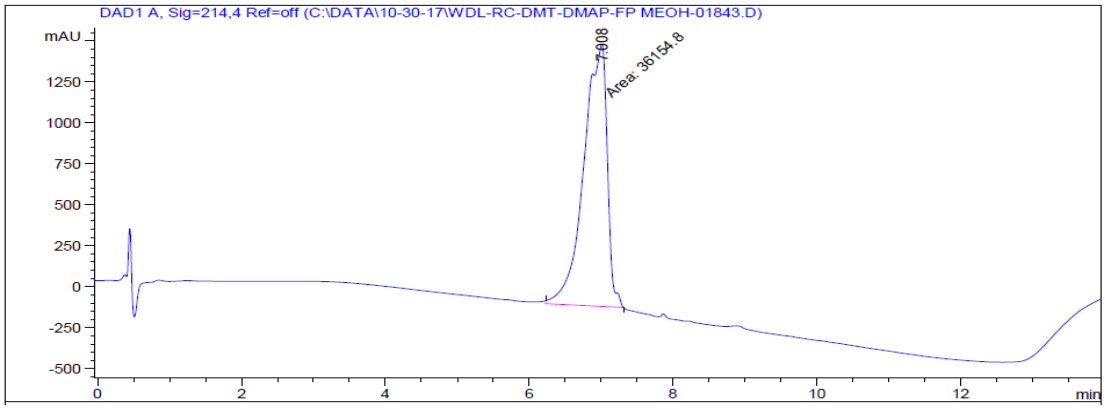

b) LCMS in MeCN/H_2O for 4.21a:

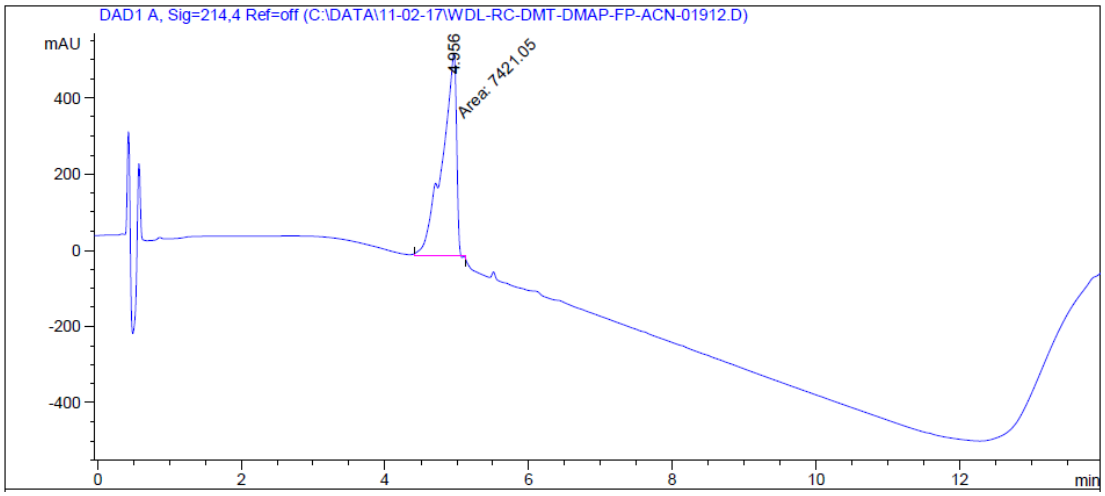

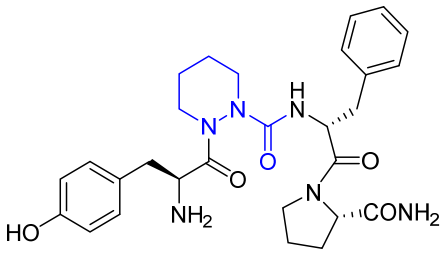

4.22a

Tyr-azaPip-D-Phe-Pro-NH_2 (4.22a): LC-MS analysis (a) 10-90% of MeOH (0.1% FA) inH_2O (0.1% FA) over 9 min, then 10% MeOH for 5 min, R.T. = 5.73 min; (b) 10-90% MeCN (0.1% FA) in H_2O (0.1% FA) over 9 min, then 10% MeCN for 5 min, R.T. = 4.07 min; HRMS m/z calcd for $C_{28}H_{37}N_6O_5$ $[M+H]^+$ 537.2820, found 537.2826.

a) LCMS in MeOH/H_2O for 4.22a:

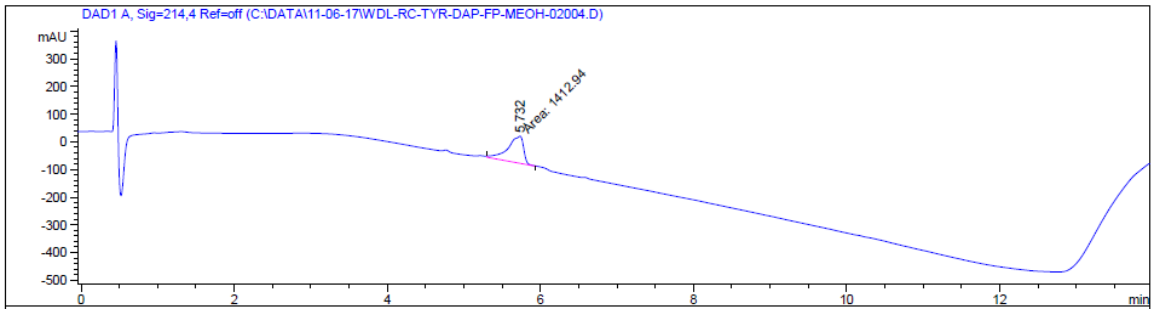

b) LCMS in ACN/H_2O for 4.22a:

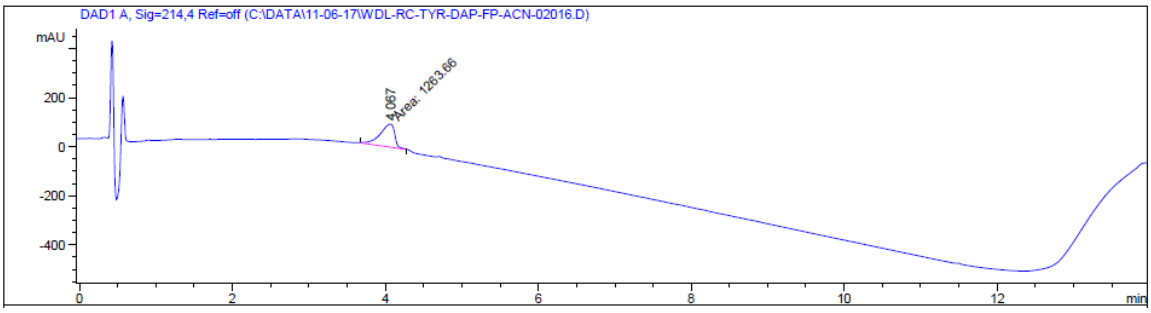

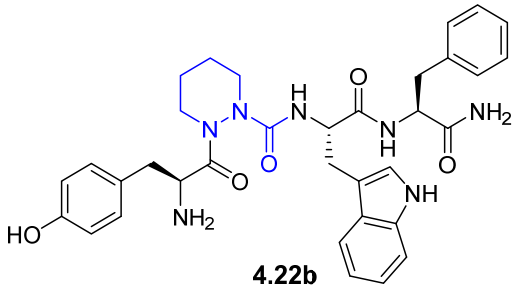

4.22b

Trp-azaPip-Trp-Phe-NH_2 (**4.22b**): LC-MS analysis (a) 10-90% of MeOH (0.1% FA) in H_2O (0.1% FA) over 9 min, then 10% MeOH for 5 min, R.T. = 6.61 min; (b) 10-90% MeCN (0.1% FA) in H_2O (0.1% FA) over 9 min, then 10% MeCN for 5 min, R.T. = 4.68 min; HRMS m/z calcd for $C_{34}H_{40}N_7O_5$ $[M+H]^+$ 626.3085, found 626.3099.

a) LCMS in MeOH/H_2O for 4.22b:

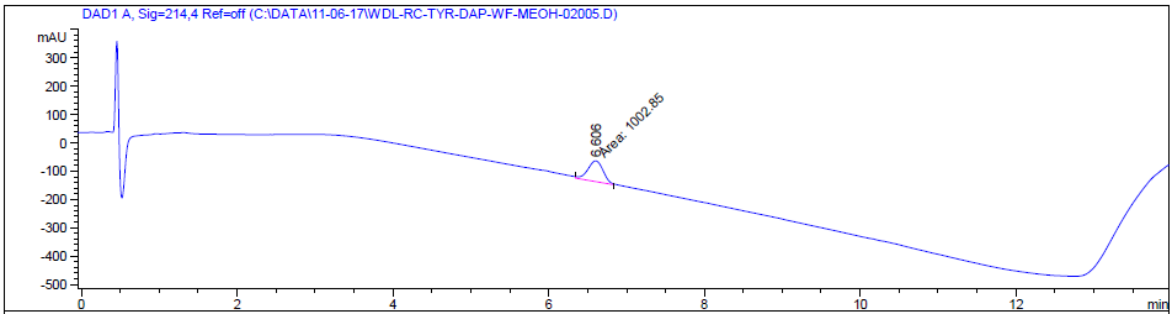

b) LCMS in ACN/H_2O for 4.22b:

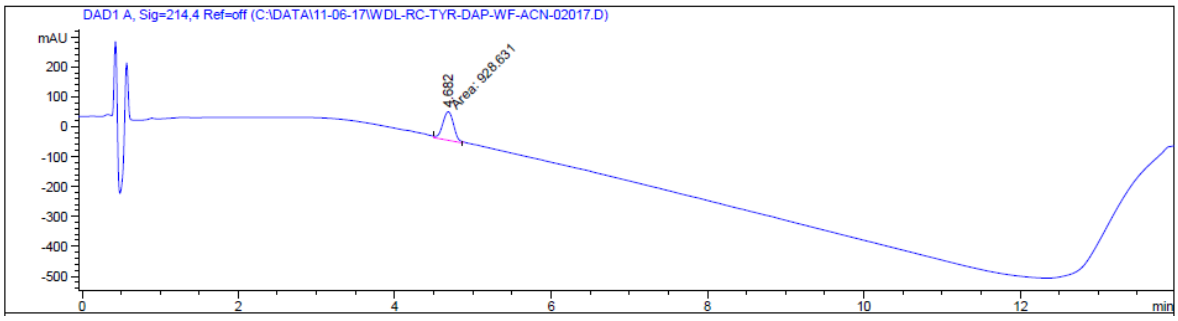

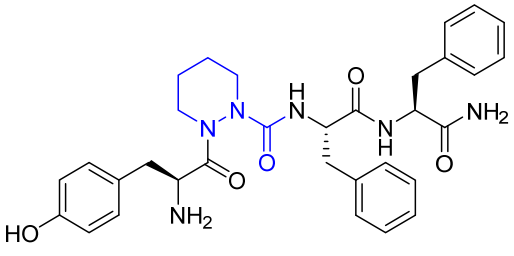

4.22c

Tyr-azaPip-Phe-Phe-NH$_2$ (4.22c): LC-MS analysis (a) 10-90% of MeOH (0.1% FA) in H_2O (0.1% FA) over 9 min, then 10% MeOH for 5 min, R.T. = 6.47 min; (b) 10-90% MeCN (0.1% FA) in H_2O (0.1% FA) over 9 min, then 10% MeCN for 5 min, R.T. = 4.58 min; HRMS m/z calcd for $C_{32}H_{39}N_6O_5$ $[M+H]^+$ 587.2976, found 587.2991.

a) LCMS in MeOH/H$_2$O for 4.22c:

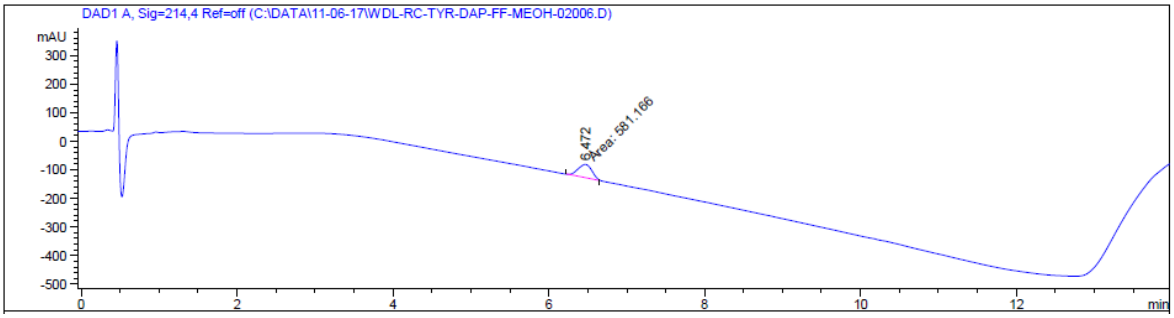

b) LCMS in MeCN/H$_2$O for 4.22c:

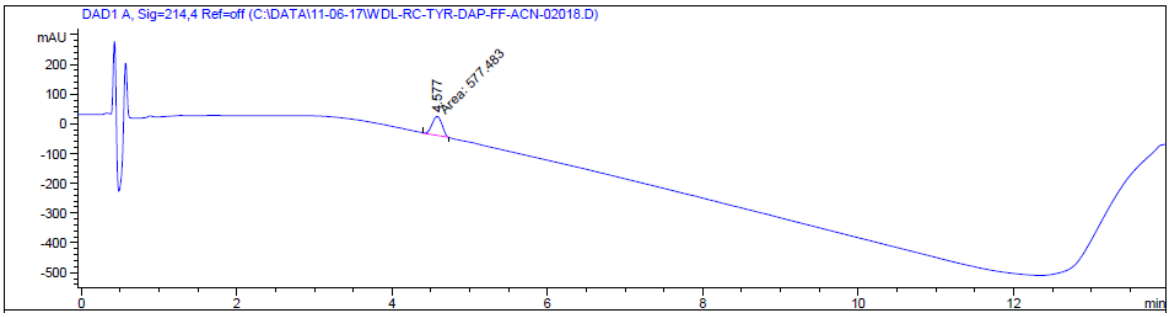

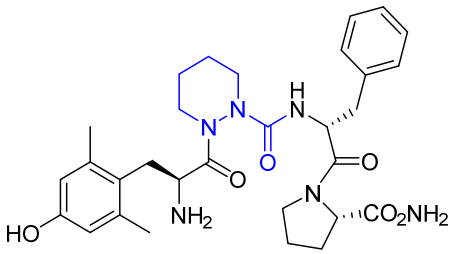

4.23a

Dmt-azaPip-D-Phe-Pro-NH_2 (4.23a): LC-MS analysis (a) 10-90% of MeOH (0.1% FA) in H_2O (0.1% FA) over 9 min, then 10% MeOH for 5 min, R.T. = 6.09 min; (b) 10-90% MeCN (0.1% FA) in H_2O (0.1% FA) over 9 min, then 10% MeCN for 5 min, R.T. = 4.29 min; HRMS m/z calcd for $C_{30}H_{41}N_6O_5$ $[M+H]^+$565.3133, found 565.3138.

a) LCMS in MeOH/H_2O for 4.23a:

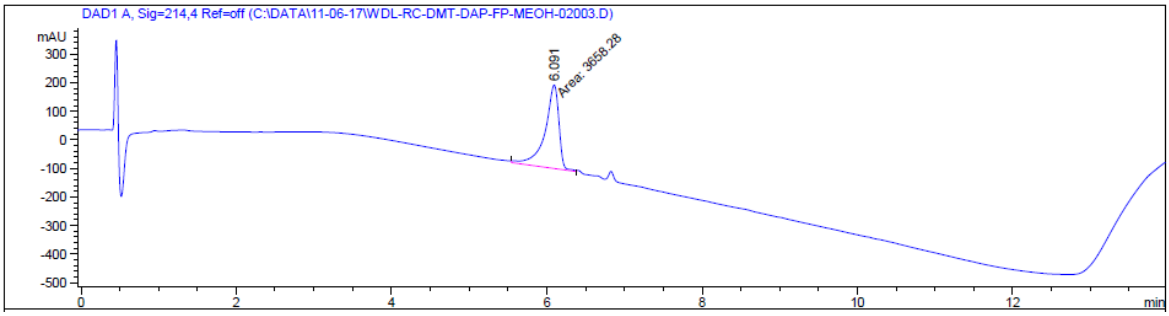

b) LCMS in MeCN/H_2O for 4.23a:

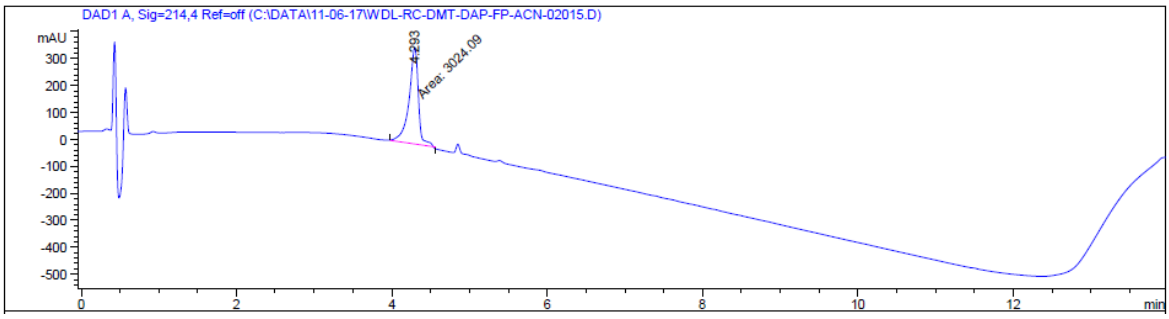

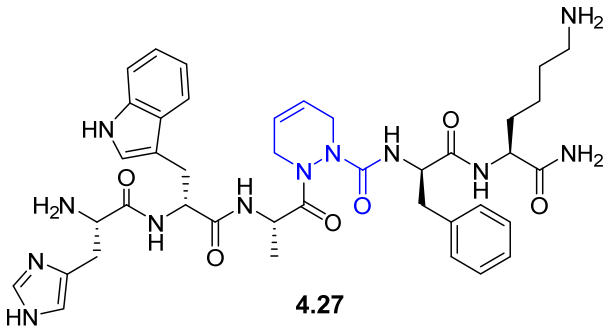

4.27

His-D-Trp-Ala-(Δ^4)azaPip-D-Phe-Lys-NH_2 (4.27): LC-MS analysis (a) 5-50% of MeOH (0.1% FA) in H_2O (0.1% FA) over 9 min, then 5% MeOH over 5 min, R.T. = 4.87 min; (b) 5-50% MeCN (0.1% FA) in H_2O (0.1% FA) over 9 min, then 5% MeCN for 5 min, R.T. = 3.92 min; HRMS m/z calcd for $C_{40}H_{53}N_{12}O_6$ $[M+H]^+$ 797.4206, found 797.4189. LC-MS m/z calcd for $C_{40}H_{53}N_{12}O_6$ $[M+H]^+$ 797.41, found 797.4.

LCMS for crude 4.27:

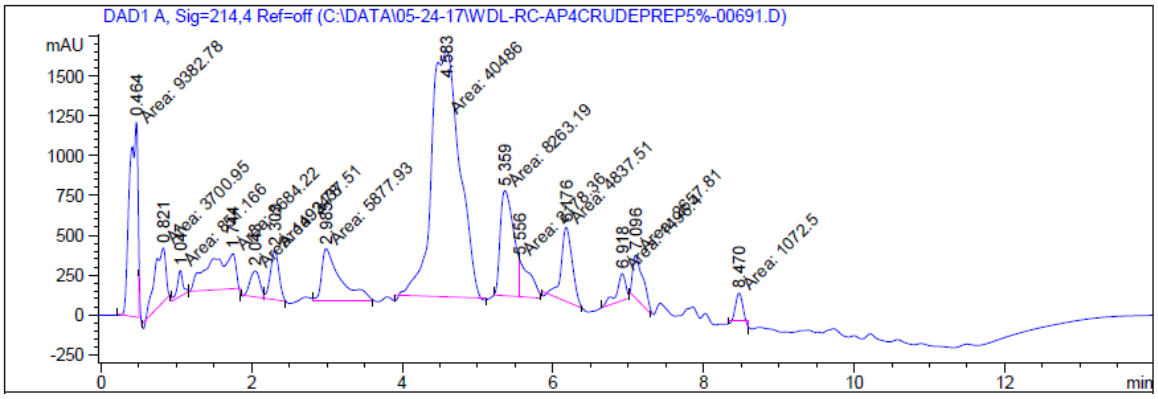

LC-MS analysis of crude **4.27** on a Sunfire™ column with a gradient of 5-50% MeOH (0.1% FA) in water (0.1% FA) over 9 min then at 5% MeOH (0.1% FA) in water (0.1% FA) over 5 min, R.T. = 4.58 min. ESI-MS m/z calcd for $C_{40}H_{53}N_{12}O_6$ $[M+H]^+$ 797.41, found 797.4.

a) LCMS in MeOH/H_2O for 4.27:

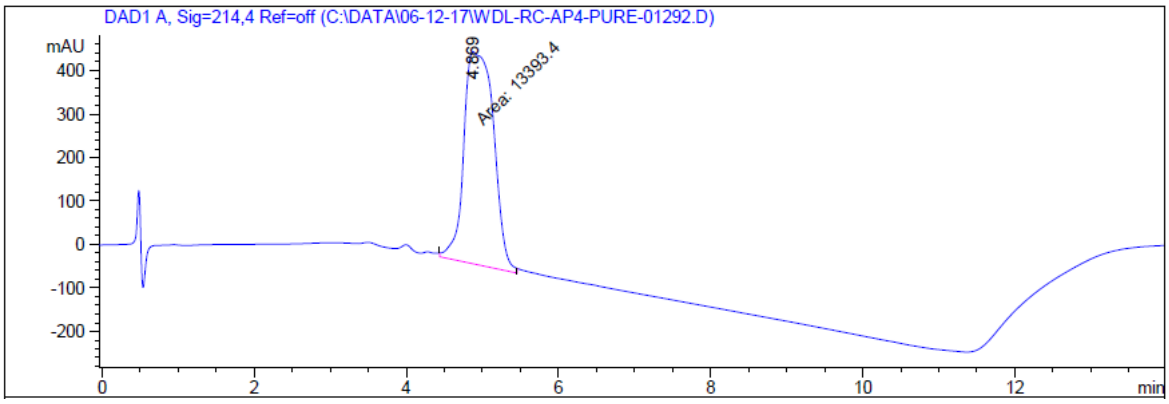

b) LCMS in ACN/H_2O for 4.27:

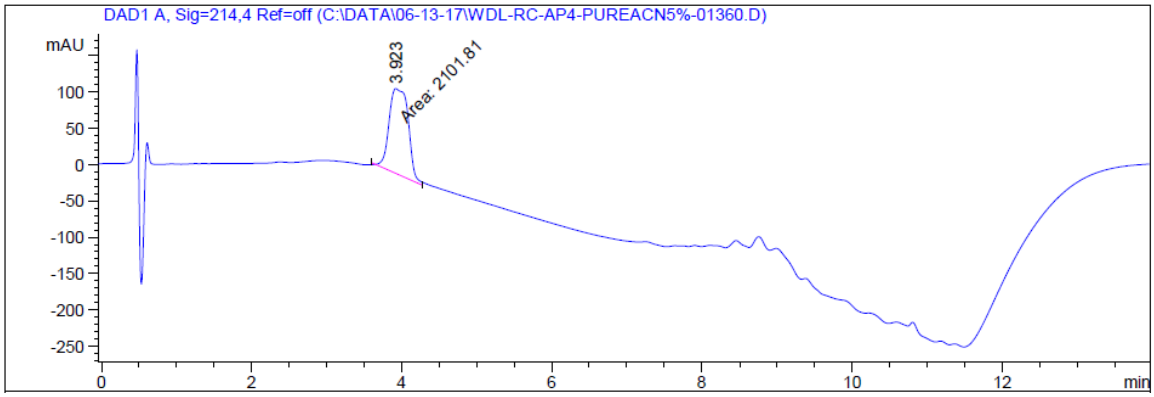

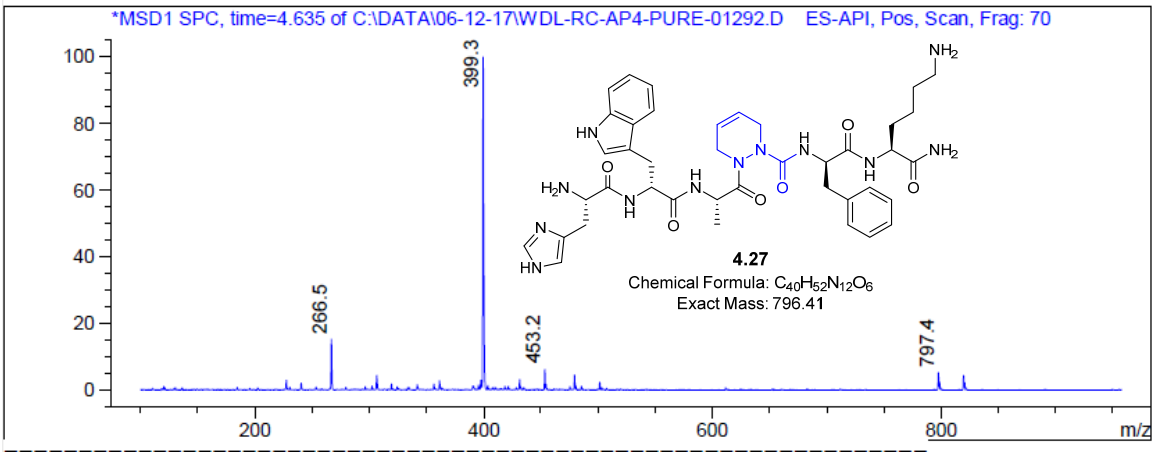

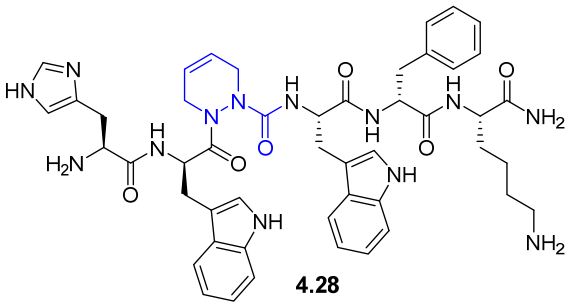

4.28

His-D-Trp-(Δ^4)azaPip-Trp-D-Phe-Lys-NH_2 (4.28): LC-MS analysis (a) 5-50% of MeOH (0.1% FA) in H_2O (0.1% FA) over 9 min, then 5% MeOH for 5 min, R.T. = 5.98 min; (b) 5-50% MeCN (0.1% FA) in H_2O (0.1% FA) over 9 min, then 5% MeCN for 5 min, R.T. = 5.82 min; HRMS m/z calcd for $C_{48}H_{58}N_{13}O_6$ $[M+H]^+$ 912.46275, found 912.4628. LC-MS m/z calcd for $C_{48}H_{58}N_{13}O_6$ $[M+H]^+$ 912.46, found 912.4.

LCMS for crude **4.28**:

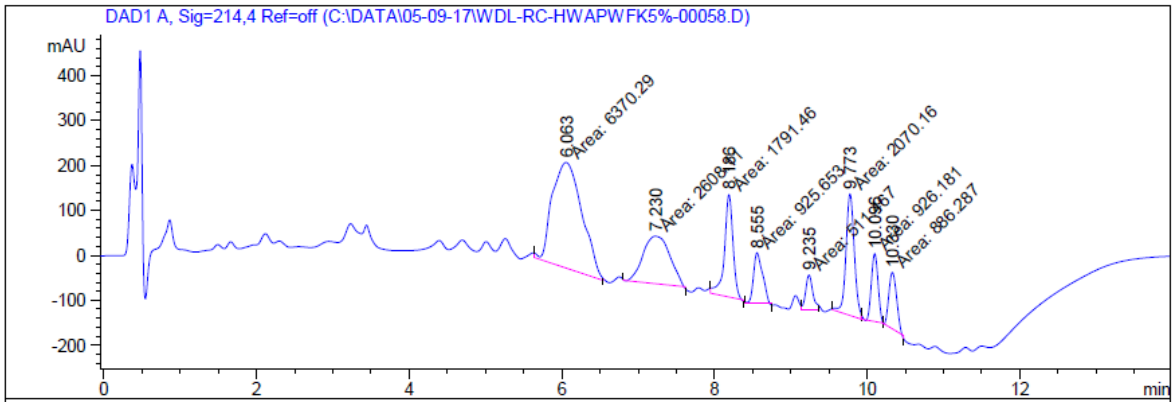

LC-MS analysis of crude **4.28** on a Sunfire™ column with a gradient of 5-50% MeOH (0.1% FA) in water (0.1% FA) for 9 min then at 5% MeOH (0.1% FA) in water (0.1% FA) for 5 min, R.T. = 6.06 min. ESI-MS m/z calcd for $C_{48}H_{58}N_{13}O_6$ $[M+H]^+$ 912.46, found 912.4.

a) LCMS in MeOH/H_2O for 4.28:

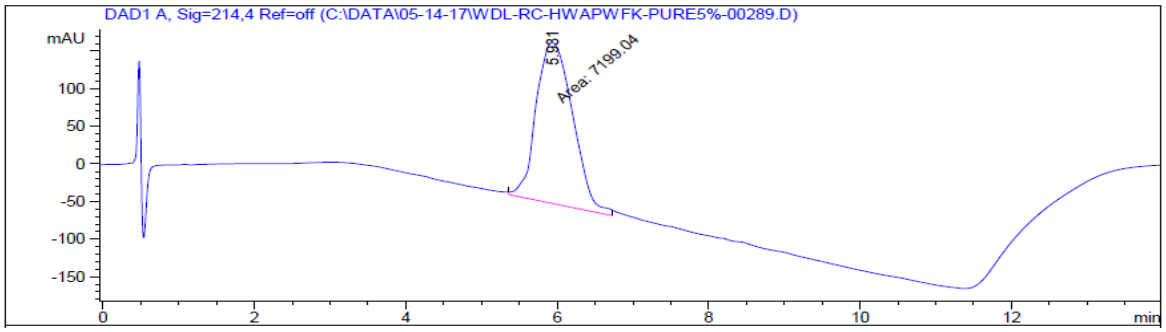

b) LCMS in ACN/H_2O for 4.28:

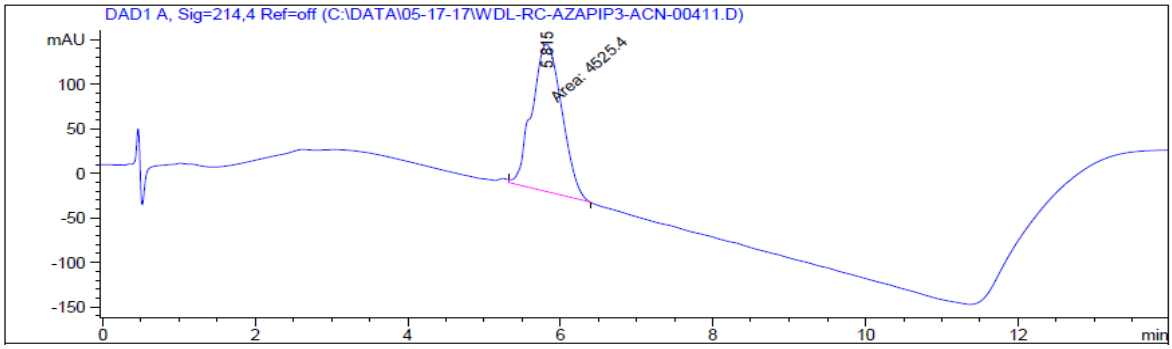

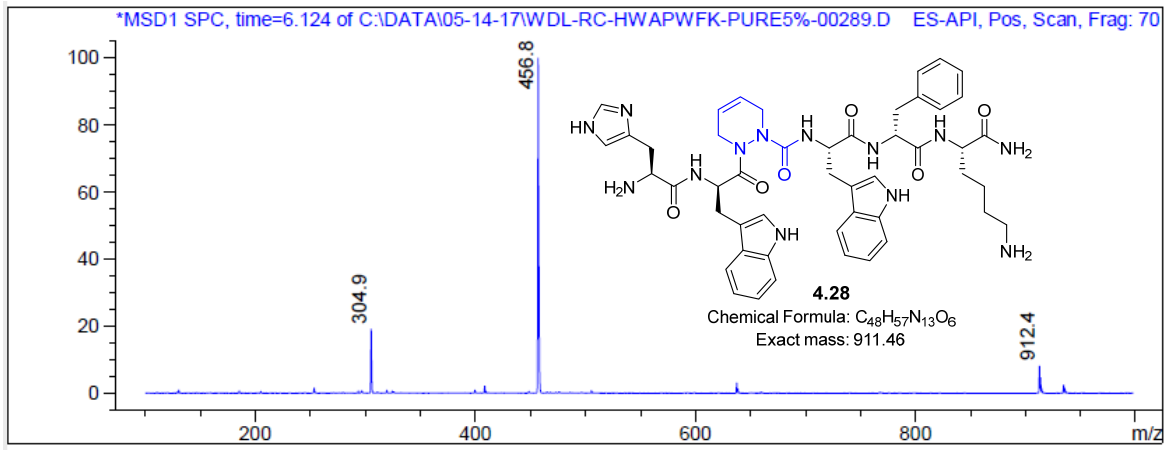

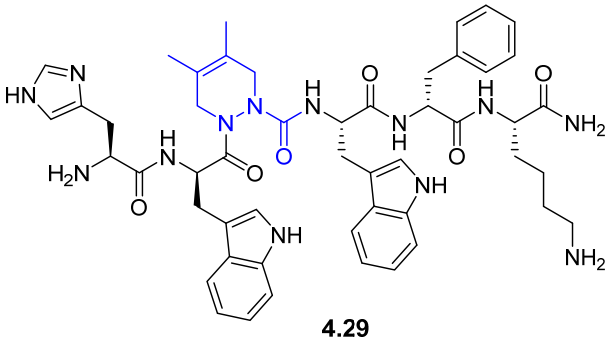

4.29

His-D-Trp-(4,5-dimethyl-Δ[4])azaPip-Trp-D-Phe-Lys-NH₂ (4.29): LC-MS analysis (a) 2-98% of MeOH (0.1% FA) in H_2O (0.1% FA) over 11 min, then 2% MeOH for 4 min, R.T. = 4.91 min; (b) 2-50% MeCN (0.1% FA) in H_2O (0.1% FA) over 11 min, then 2% MeCN for 4 min, R.T. = 5.26 min; HRMS m/z calcd for $C_{50}H_{61}N_{13}O_6$ $[M+Na]^+$ 962.4760, found 962.4764. LC-MS m/z calcd for $C_{50}H_{61}N_{13}O_6$ $[M+Na]^+$ 962.49, found 962.52.

LCMS for crude 4.29:

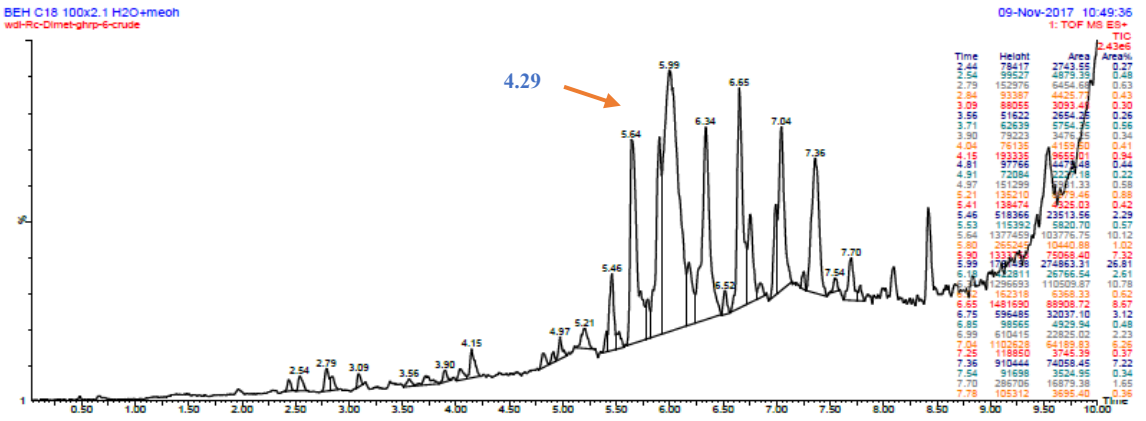

LC-MS analysis of crude **4.29** on a BEH C18, 2.1 x 100mm, 1.7um column with a gradient of 2-50% MeOH (0.1% FA) in water (0.1% FA) for 11 min then at 2% MeOH (0.1% FA) in water (0.1% FA) for 4 min, R.T. = 5.99 min. ESI-MS m/z calcd for $C_{50}H_{61}N_{13}O_6$ $[M+Na]^+$ 962.49, found 962.52.

a) LCMS in MeOH/H_2O for 4.29:

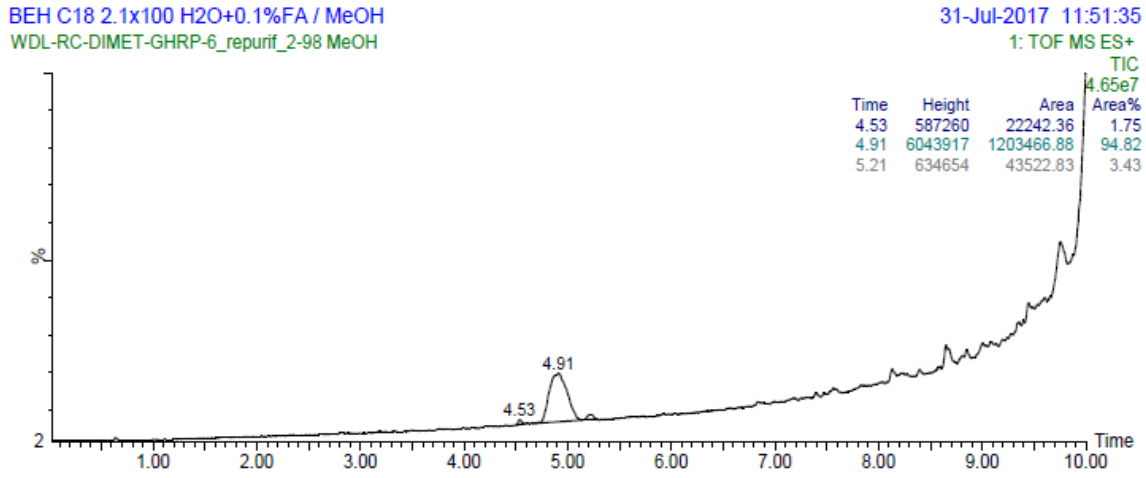

b) LCMS in ACN/H_2O for 4.29:

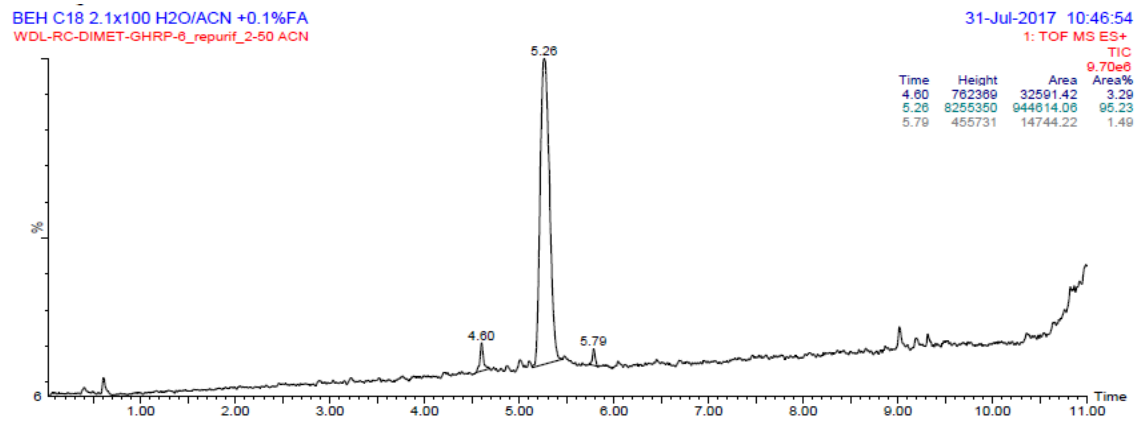

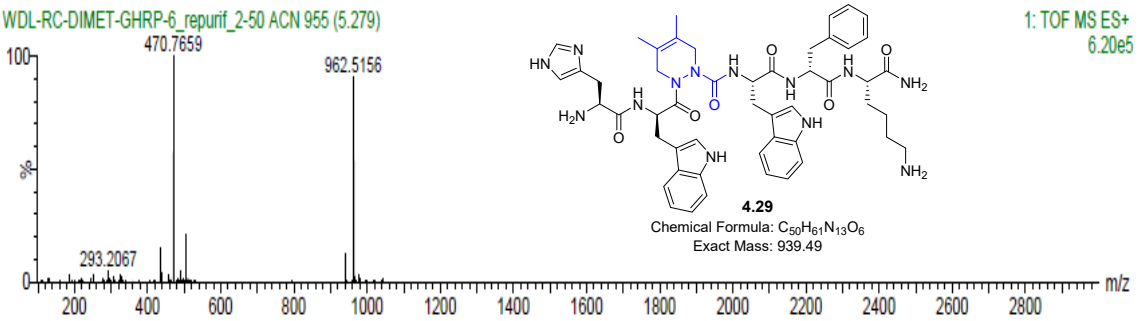

4.29

Chemical Formula: $C_{50}H_{61}N_{13}O_6$

Exact Mass: 939.49

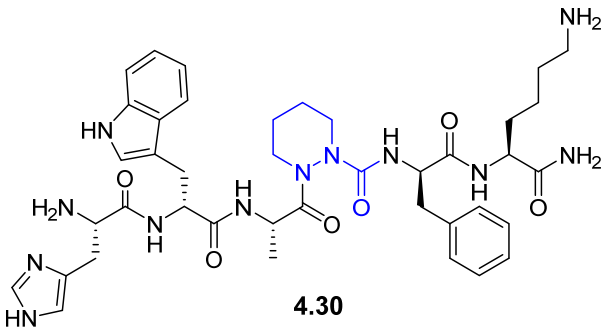

4.30

His-D-Trp-Ala-azaPip-D-Phe-Lys-NH_2 (**4.30**): LC-MS analysis (a) 5-50% of MeOH (0.1% FA) in H_2O (0.1% FA) over 9 min, then 5% MeOH for 5 min, R.T. = 5.15 min; (b) 5-50% MeCN (0.1% FA) in H_2O (0.1% FA) over 9 min, then 5% MeCN for 5 min, R.T. = 3.97 min; HRMS m/z calcd for $C_{40}H_{55}N_{12}O_6$ $[M+H]^+$ 799.4362, found 799.4381. LC-MS m/z calcd for $C_{40}H_{55}N_{12}O_6$ $[M+H]^+$ 799.43, found 799.4.

a) LCMS in MeOH/H_2O for 4.30:

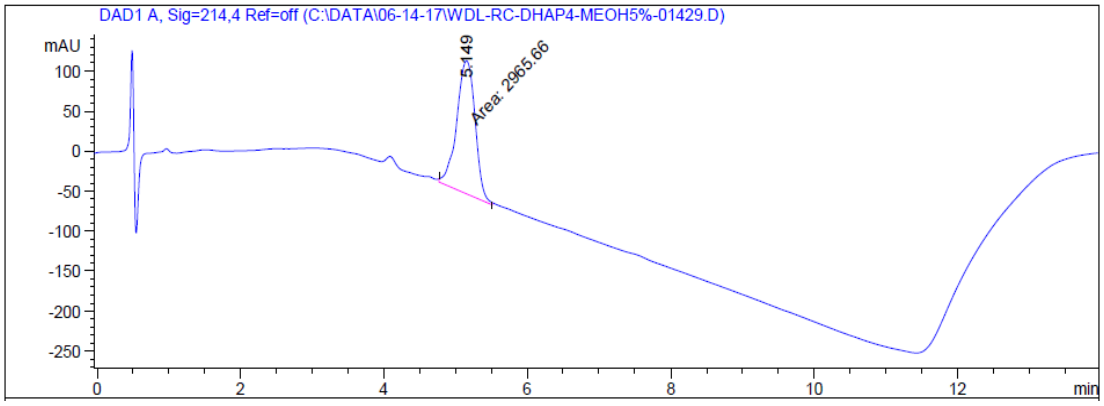

b) LCMS in ACN/H_2O for 4.30:

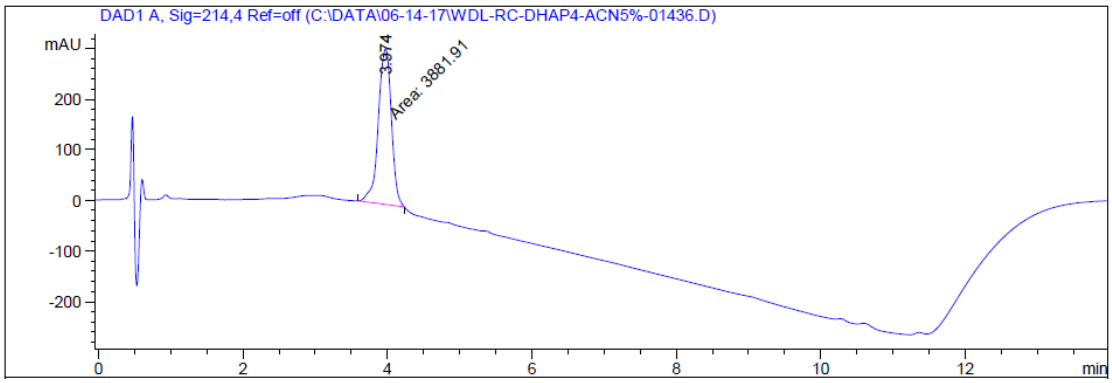

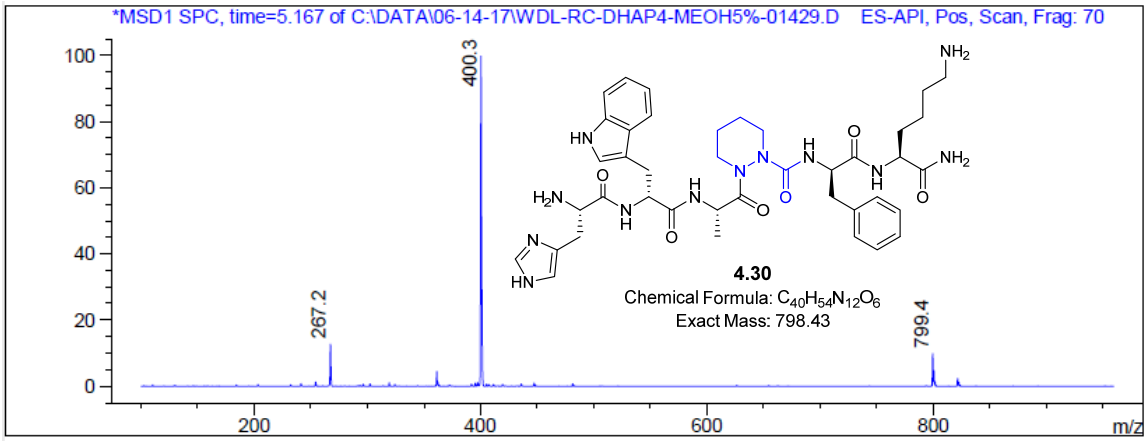

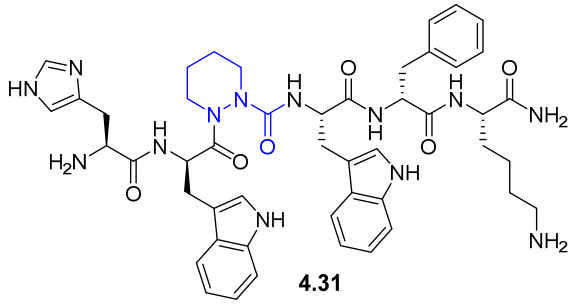

His-D-Trp-azaPip-Trp-D-Phe-Lys-NH2 (4.31): LC-MS analysis (a) 5-50% of MeOH (0.1% FA) in H_2O (0.1% FA) over 9 min, then 5% MeOH for 5 min, R.T. = 6.07 min; (b) 5-50% MeCN (0.1% FA) in H_2O (0.1% FA) over 9 min, then 5% MeCN for 5 min, R.T. = 4.70 min; HRMS m/z calcd for $C_{48}H_{60}N_{13}O_6$ $[M+H]^+$ 914.4784, found 914.4780. LC-MS m/z calcd for $C_{48}H_{60}N_{13}O_6$ $[M+H]^+$ 914.47, found 914.5.

a) LCMS in MeOH/H_2O for 4.31:

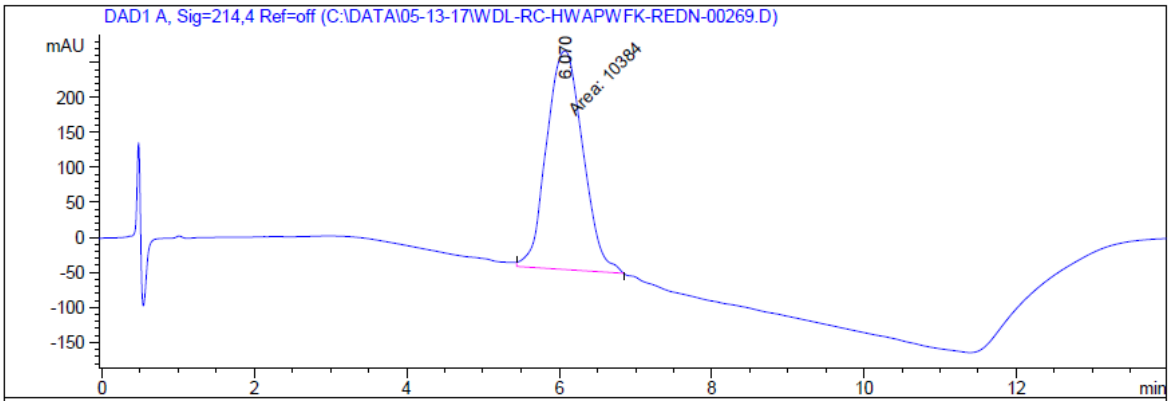

b) LCMS in ACN/H_2O for 4.31:

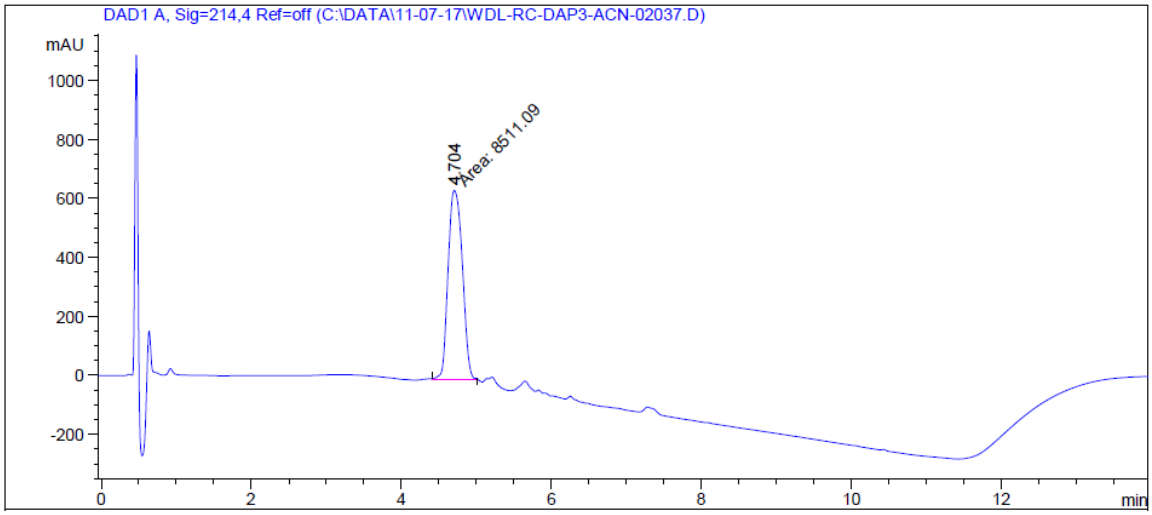

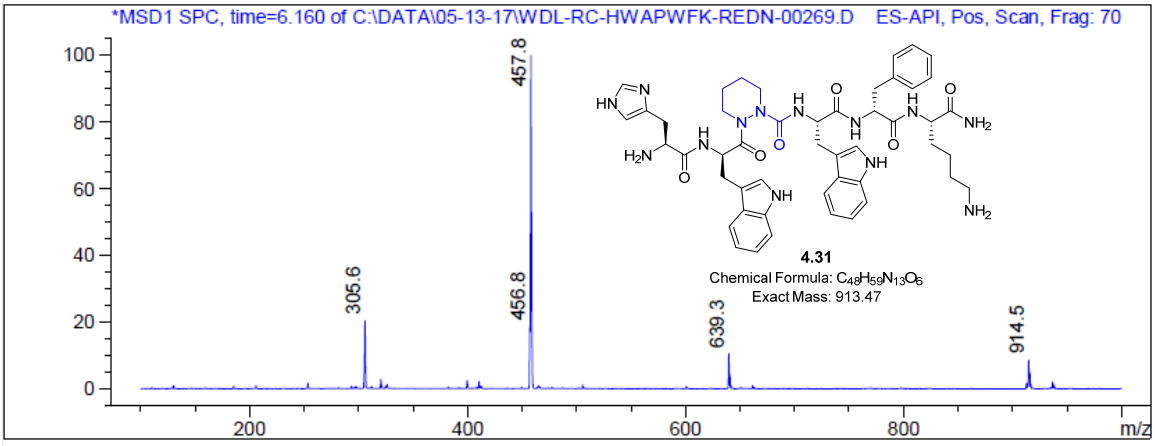

Filename: Chingle_Ramesh_2018_these.pdf.docx
Directory: C:\Users\Windows10\Documents
Template: C:\Users\Windows10\AppData\Roaming\Microsoft\Templates\Normal.dotm
Title:
Subject:
Author: Ramesh Chingle
Keywords:
Comments:
Creation Date: 23-May-18 5:44:00 PM
Change Number: 3
Last Saved On: 24-May-18 1:18:00 AM
Last Saved By: Chingle Ramesh
Total Editing Time: 385 Minutes
Last Printed On: 24-May-18 1:20:00 AM
As of Last Complete Printing
Number of Pages: 436
Number of Words: 108,703 (approx.)
Number of Characters: 619,608 (approx.)